Aspects of mineralogical variation in the Western A Lode, N.B.H.C. Mine, Broken Hill, New South Wales, Australia

Author:
Bottrill, Ralph Stephen

Publication Date:
1984

DOI:
https://doi.org/10.26190/unsworks/11188

R. S. BOTTRILL

M.Sc.

1984

UNSW

Aspects of Mineralogical Variation in the Western A Lode, N.B.H.C. Mine, Broken Hill, New South Wales, Australia.

A thesis submitted by

Ralph Stephen Bottrill, Bsc (Hons.) Adel.

for the degree of

Master of Science

in the

School of Applied Geology

University of New South Wales

in

September 1984

Form 1
WAIVER

THE UNIVERSITY OF NEW SOUTH WALES

DECLARATION RELATING TO DISPOSITION OF THESIS

This is to certify that I Ralph Stephen Bottrill being a candidate for the degree of Master of Science am fully aware of the policy of the University relating to the retention and use of higher degree theses, namely that the University retains the copies of any thesis submitted for examination, "and is free to allow the thesis to be consulted or borrowed. Subject to the provisions of the Copyright Act (1968) the University may issue the thesis in whole or in part, in photostat or microfilm or other copying medium."

In the light of these provisions I grant the University Librarian permission to publish, or to authorise the publication of my thesis, in whole or in part, as he deems fit.

I also authorize the publication by University Microfilms of a 600 word abstract in Dissertation Abstracts International (D.A.I.).

Signature .....

Witness .....

Date 16/4/84

DECLARATION

I declare that this thesis is my own work and has not been submitted in any form for another degree or diploma at any university or other institution of tertiary education. Information derived from other sources, published and unpublished, has been acknowledged in the text.

R.S Bottrill

CONTENTS

CONTENTS (cont.)

CONTENTS (cont.)

CONTENTS (cont.)

TABLES

FIGURES

FIGURES (cont.)

FIGURES (cont.)

FIGURES (cont.)

Abstract

The Western A Lode (WAL), an extension of the zinc - rich A lode at Broken Hill, NSW, shows a gradation between manganese silicate - rich sulphide ores and the pelitic metasediments of the wallrocks. This sequence can be subdivided petrographically into four broad zones, approximately symmetric about the centre of the lode. Passing from the pelitic wallrocks these zones are: a sillimanite gneiss, a gahnite - rich zone, a garnet quartzite and an amphibole - pyroxenoid zone. This latter zone may be further subdivided into amphibole and pyroxenoid subzones.

Sulphides occur throughout the WAL sequence, and commonly are concentrated in the gahnite - rich zone and in the lower garnet quartzite, stratigraphically immediately below the lower amphibole subzone, but the principal concentration is in the pyroxenoid subzone. Distinct geochemical trends parallel the mineralogical variations: approaching the centre of the WAL from the wallrocks there is a distinct increase in Ca, Mn, P, S and base metals, and a corresponding decrease in Al, Ti, K and Mg/Mg + Fe. Some minerals reflect these trends in their composition: biotite shows a decrease in Al, and garnet a decrease in Mg and an increase in Ca and Mn towards the lode centre.

The sillimanite gneiss is considered to have been deposited as an argillaceous sediment in an anoxic basin. The other WAL rocktypes are consistent with having originally contained accessory to dominant Mn/Fe/Ca carbonate, silica and sulphides, chemically precipitated from exhaled hydrothermal solutions. These chemical sediments gradually overwhelmed the detrital input, but became overwhelmed again by detrital sediments as the exhalation waned.

Metamorphism of the lode to lower granulite facies resulted in almost complete decarbonation and dehydration, and partial desulphurisation, and was followed by extensive but variable retrogression. The prograde and retrograde metamorphic events have both contributed to a complex range of mineral assemblages, compositions and textures with minor sulphide remobilization. They have also instigated sulphide - silicate reactions, especially between gahnite, sphalerite, staurolite and phyllosilicates.

Chapter 1. Introduction and Previous Work.

1.1 The Nature of this Investigation.

The Broken Hill silver-lead-zinc deposit occurs in high grade metamorphic rocks of the Lower Proterozoic Willyama Complex, in the Barrier Ranges of far western New South Wales (Fig's 1.1, 1.2, and 1.3). The deposit comprises a number of distinct ore-bearing lenses, of which the A-lode is economically one of the most important (Fig. 1.4). The western A-lode (WAL) (Figs. 1.4 and 1.5), has, so far, been left largely untouched in mining operations. It occurs mainly in the New Broken Hill Consolidated (NBHC) and Zinc Corporation (ZC) mines.

The main components of the lode are quartz, garnet, sphalerite and pyrrhotite, with galena, pyroxmangite, biotite, feldspar, gahnite and amphiboles locally abundant, but generally the distribution of minerals in the lode is extremely heterogenous particularly for the sulphides. The structure is very complex and highly deformed, but mesoscopic layering is sometimes present.

The origin of the Broken Hill ore deposit has been the subject of controversy for some time but it is now generally agreed to have been deposited as a chemical sediment and subsequently isochemically metamorphosed (Johnson & Klinger, 1975; Stanton, 1976a, b, c, d; Plimer, 1979) The original nature of some rock-types, e.g. quartz-gahnite rocks, pegmatoids, and garnet-rich rocks, is still poorly understood, despite intensive study by many workers (e.g. Stanton, 1976a, b, c, d; Spry, 1978; Billington, 1979; and Plimer, 1979). A number of peculiarities about the ore bodies have not been satisfactorily explained, such as the complete lack of pyrite, the

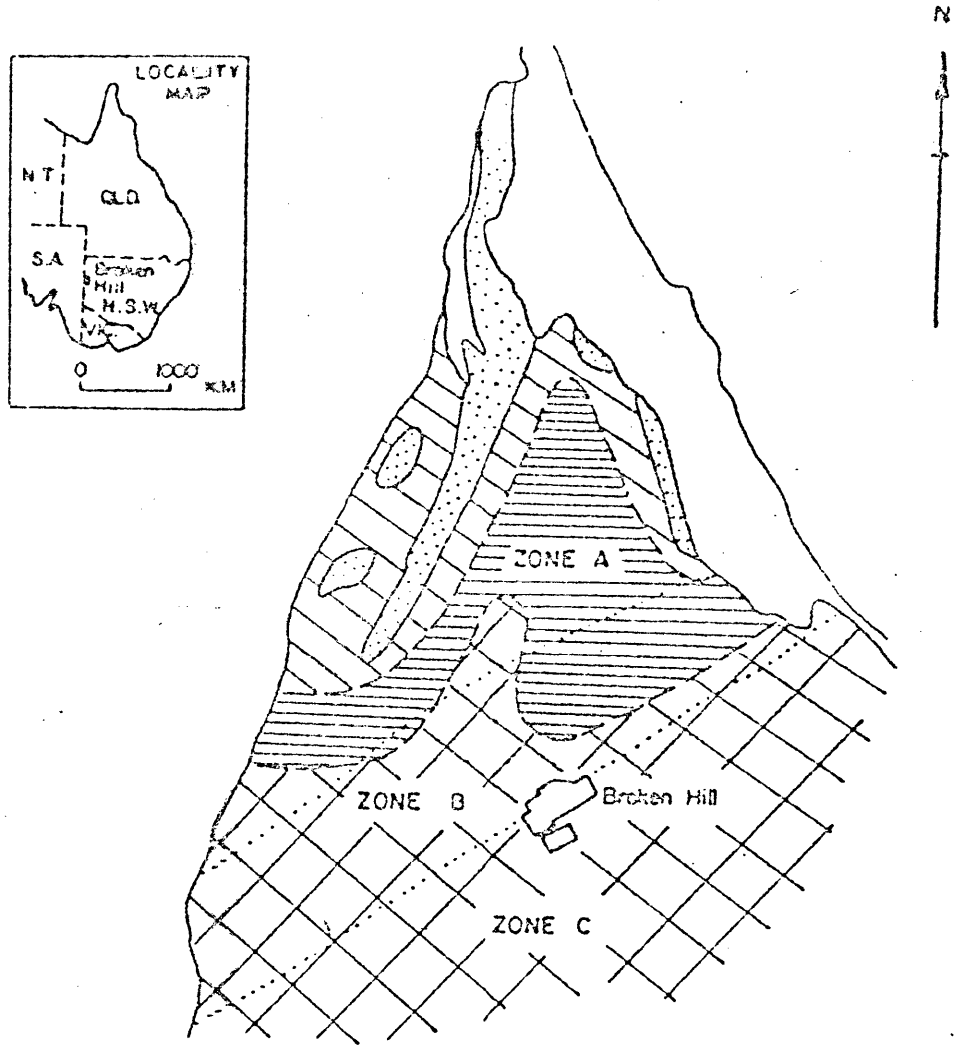

REFERENCE

After Phillips (1978)

Zone 1

Zone 2

Zone 3

Zone 4

After Binns (1964)

Zone A

Zone B

Zone C

Fig. 1.1 Prograde metamorphic zones of the Broken Hill Block. For explanation of zones see Table 1.1 (after Elliott, 1979).

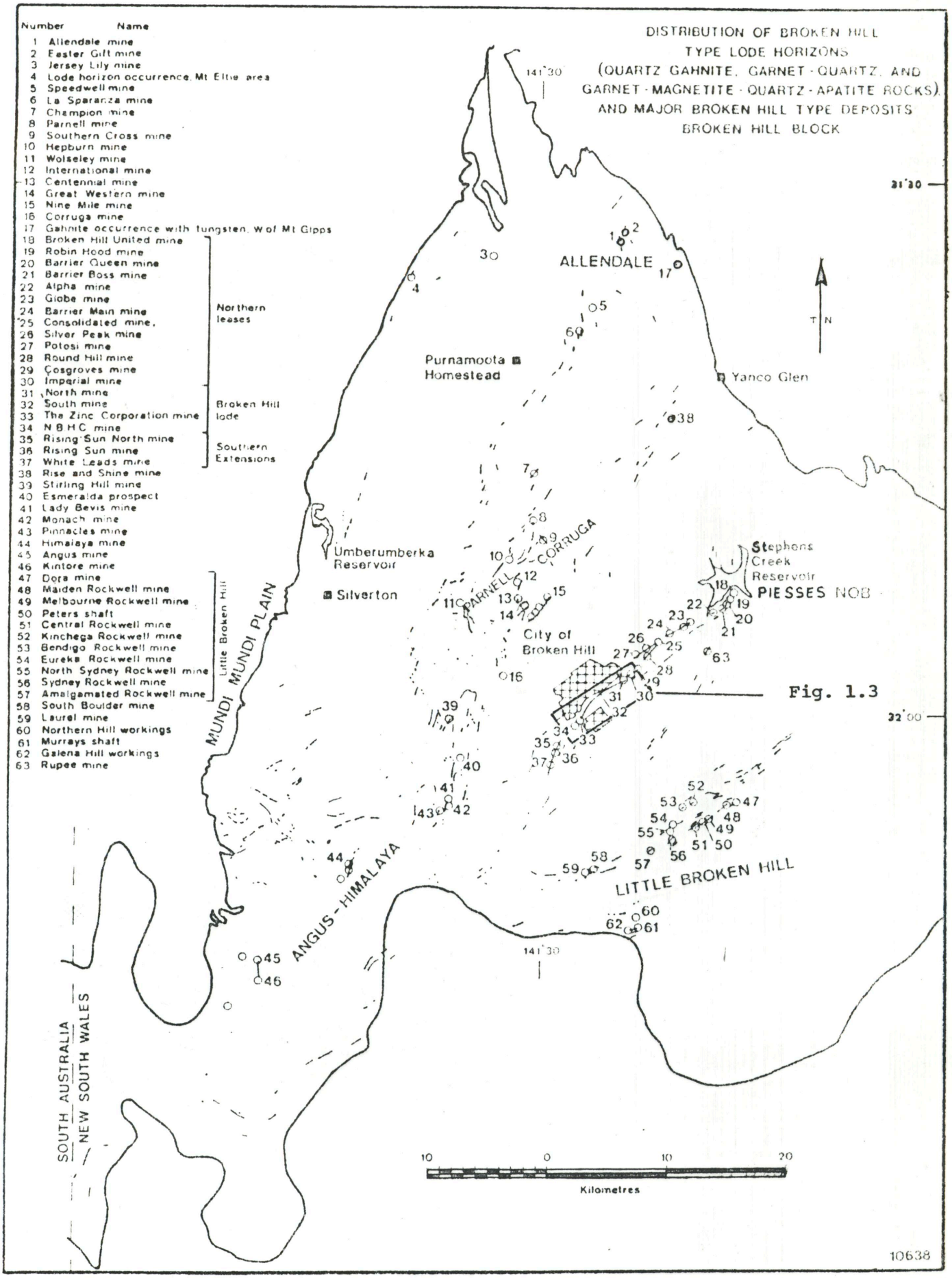

Fig. 1.2 (showing position of Fig. 1.3) from Barnes (1980).

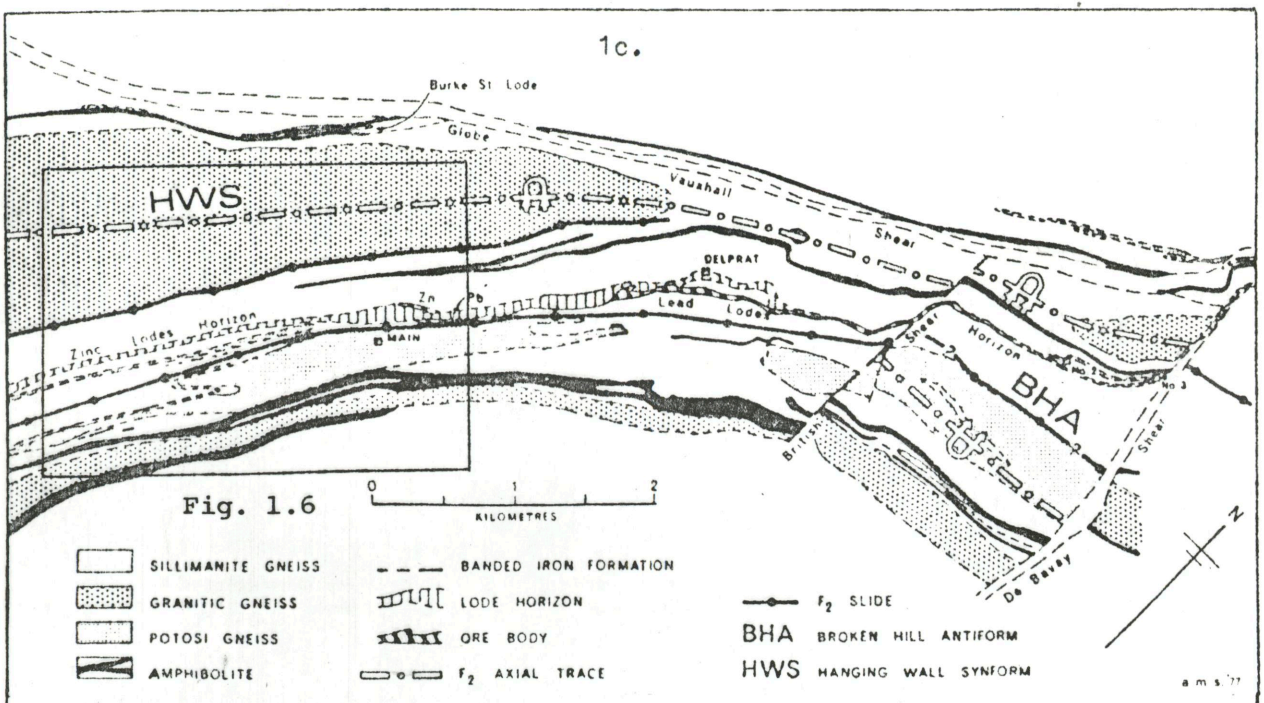

Fig. 1.6

A. Simplified geological map of the Broken Hill mines area after Johnson and Klingner (1976). The inferred trace of the Broken Hill antiform is also shown.

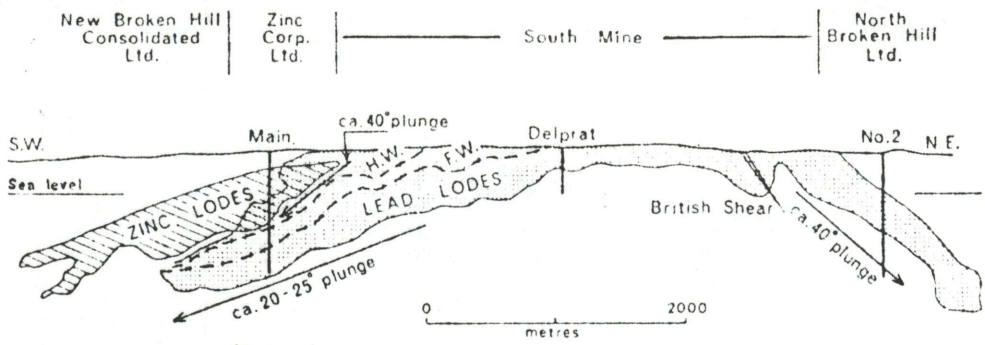

H.W. Hanging Wall hinge line of No.3 Lens in Western Anticline
F.W. Foot Wall hinge line of No.3 Lens in Western Anticline

B.

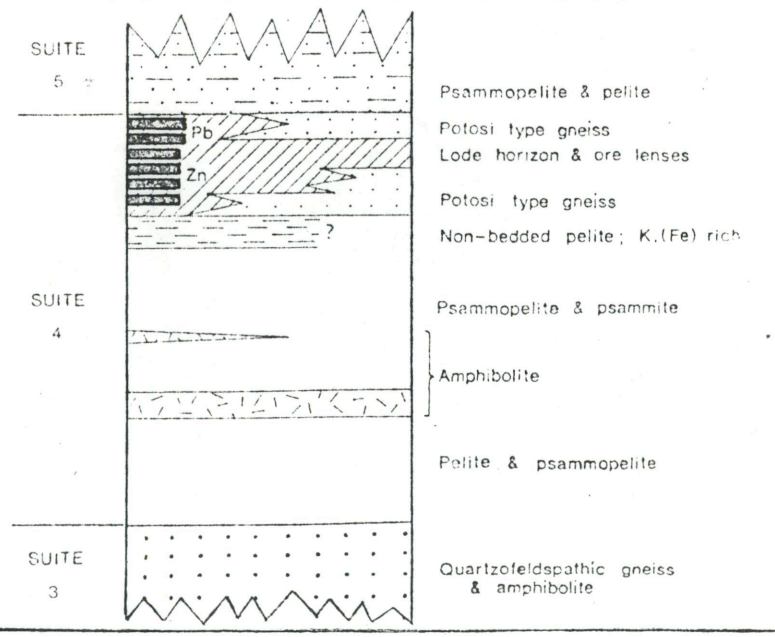

C.

Fig. 1.3 A. Geological Map (Laing, et al, 1978), showing Fig. 1.6
B. Longitudinal cross section, looking NW (Laing et al, 1978)
C. Stratigraphic sequence in mines area (Laing et al, 1980).

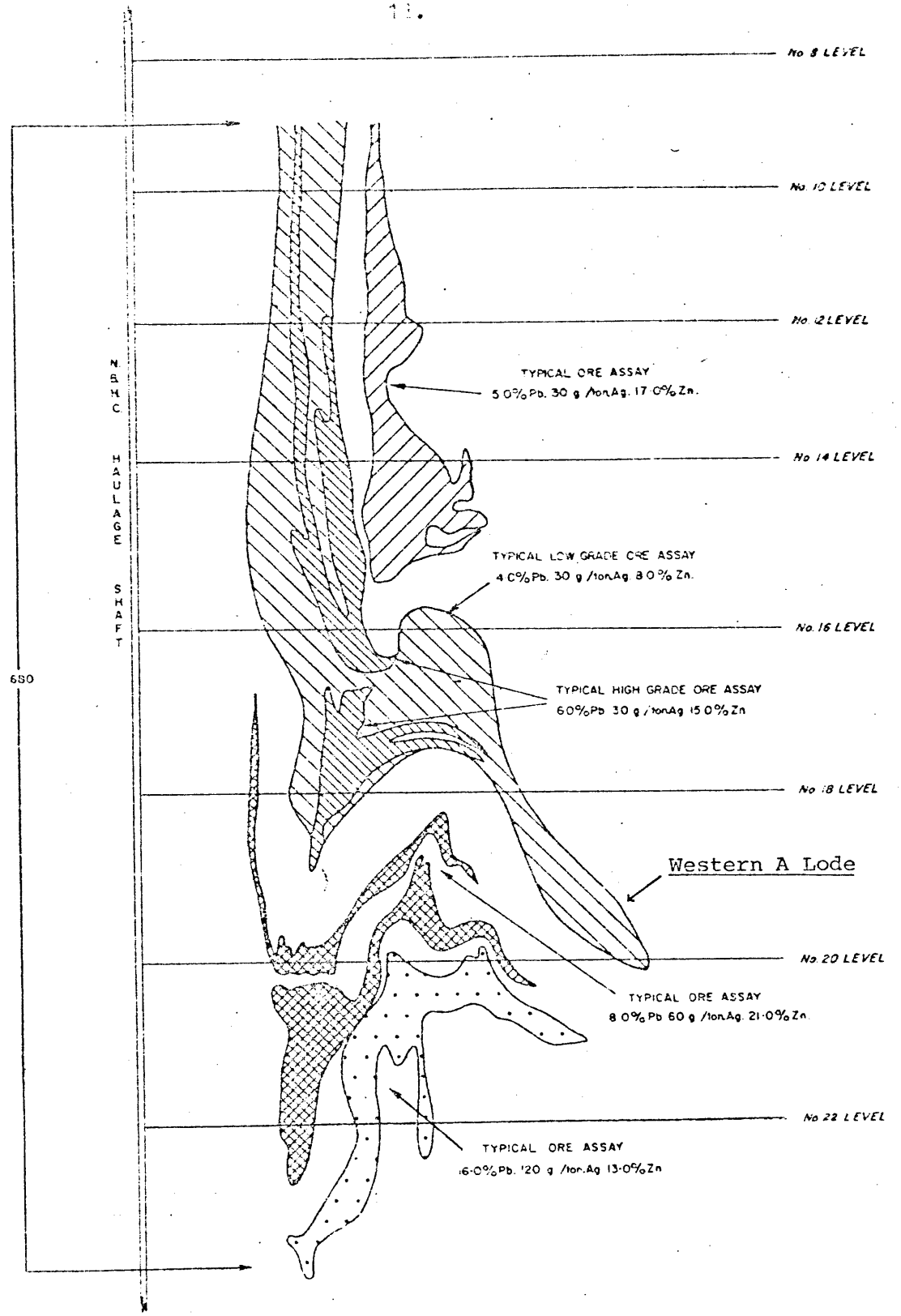

LEGEND

- B Lode
- Low Grade A Lode
- Medium Grade A Lode
- No 1 Lens Upper B Lower
- Lead Lode Nos 2 & 3 Lenses

NEW BROKEN HILL CONSOLIDATED LIMITED

Fig. 1.4 GEOLOGICAL CROSS SECTION No. 62

(LOOKING SOUTH 19° EAST)

SCALE 0 50 100 150 METRES

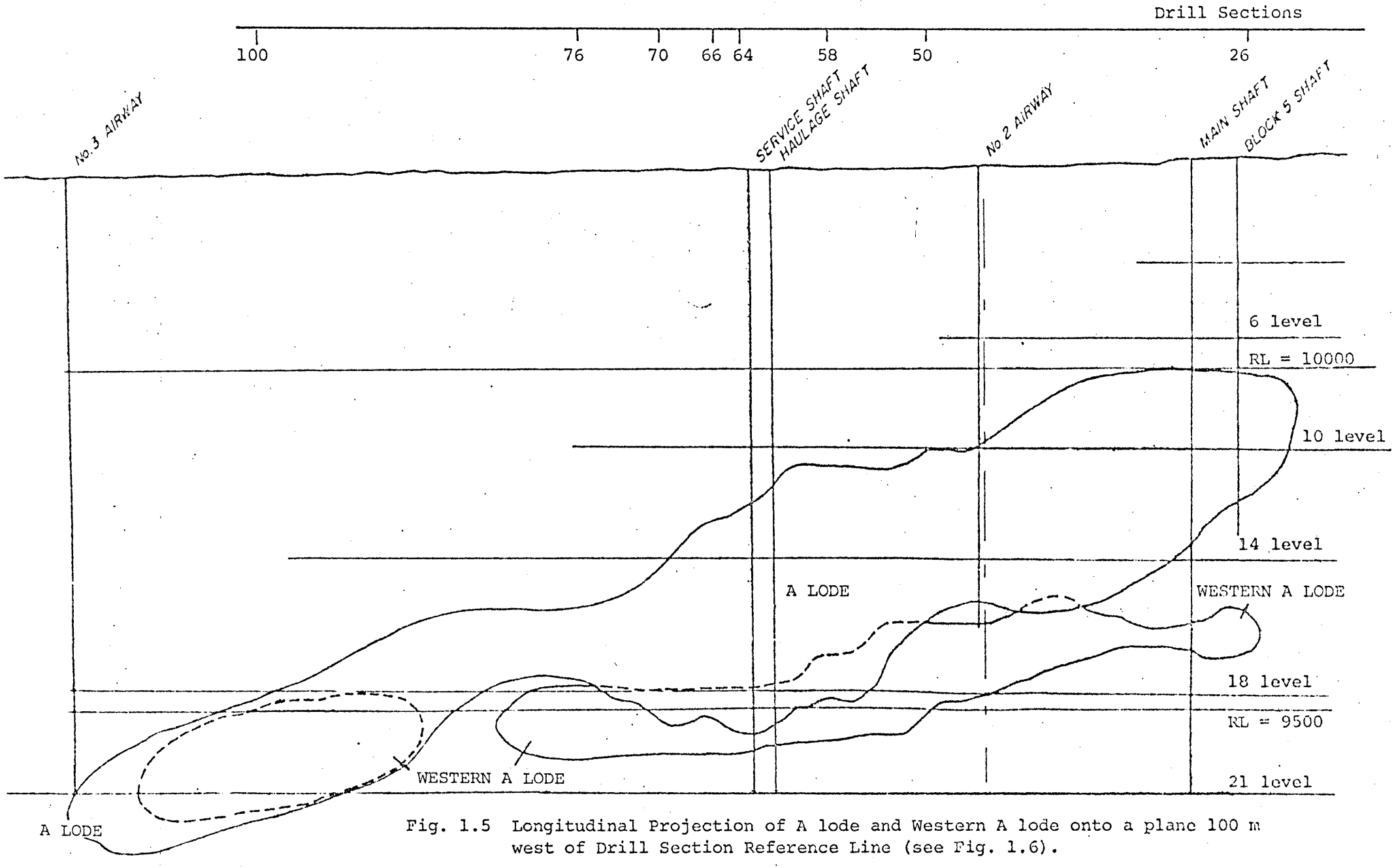

Fig. 1.5 Longitudinal Projection of A lode and Western A lode onto a plane 100 m west of Drill Section Reference Line (see Fig. 1.6).

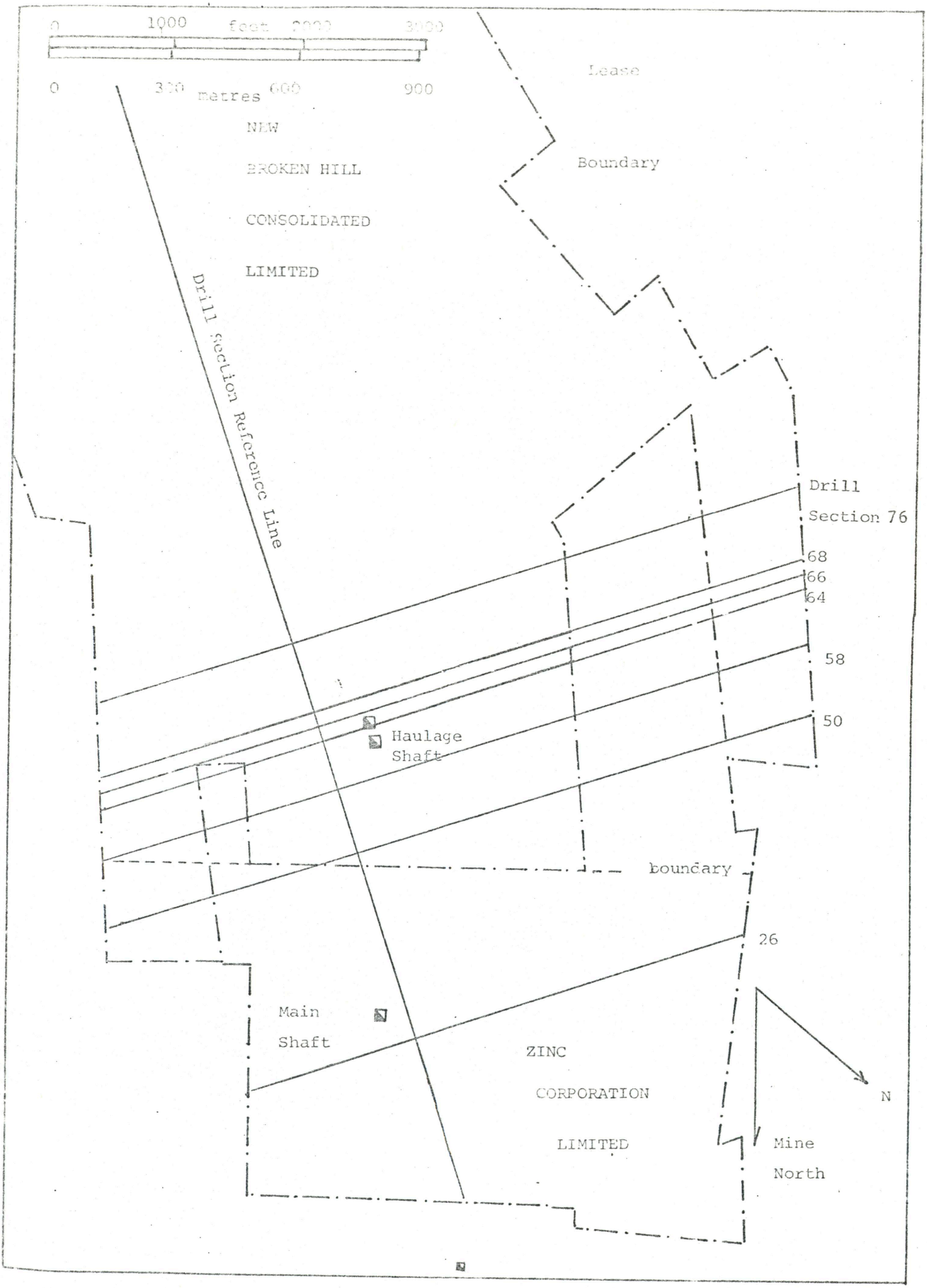

Figure 1.6: Z.C. and N.B.H.C. leases, showing drill sections used.

TABLE 1.1 A comparison of mineral assemblages used to define metamorphic zones in the Broken Hill Block (from Elliott, 1979).

Binns (1964)			Phillips et al. (1976)		
ZONE	MAFIC ROCKS	PELITIC ROCKS	ZONE	MAFIC ROCKS	PELITIC ROCKS
A	Amphibolite with green or blue-green hornblende	Sillimanite-muscovite	1	Hornblende-Plagioclase	Andalusite-muscovite
B	Amphibolite with brown or brown-green hornblende	Sillimanite-orthoclase	2	As above	Sillimanite-muscovite ± garnet
C	Hornblende-orthopyroxene-clinopyroxene granulite	As above	3	Hornblende-Plagioclase ± orthopyroxene	Sillimanite-muscovite (± garnet, cordierite)
			4	Orthopyroxene-clinopyroxene-(± hornblene, garnet)	

high zinc content of many non-sulphide phases (gahnite, staurolite, ilmenite, biotite, etc.), and the unusual compositions of some rock-types.

This study endeavours principally to elucidate the mineralogical variation in the Western A-lode.

An attempt is made to determine from the lode's mineralogy:
i) whether the variability is principally sedimentological or deformational in character;
ii) the effect of retrogression on the lode;
iii) constraints on the genesis of the ores and wallrocks.

This investigation will assist the mining companies by:
i) defining mineralogical criteria which may be useful in helping outline the WAL.
ii) provide information regarding the distribution of various sulphides within the WAL.

1.2 General Geology

The metamorphosed stratabound Broken Hill ore deposit occurs in the Broken Hill Group of the Lower Proterozoic Willyama Supergroup (formerly Willyama Complex; Willis et al. 1983). The suites defined in the Willyama Supergroup by Willis, 1983, from earliest to latest, are:

i) Clevedale Migmatites.
ii) Thorndale Composite Gneiss.
iii) Thackaringa Group: quartzofeldspathic gneisses and quartz-albite rocks.
iv) Broken Hill Group: pelitic metasediments, basic gneisses, garnetiferous quartzofeldspathic rocks and lode rocks.
v) Sundown Group: pelitic to psammitic metasediments.

vi) Paragon Group: graphitic metasediments and quartzites.

Stevens et al. (1980) suggested that this stratigraphic sequence, lacking obvious unconformities, represents a variation from immature sandy sediments (suites 1-3) to more shaley sediments (suite 4), shaley and mature sandy sediments (suite 5), and shallow water silty to clayey sediments (suites 6-7). Volcanism reached a maximum intensity in suites 3-4 and then virtually ceased with deposition of the principal stratiform ore-bearing rocks. Stevens et al. (1980) postulated that the sequence represents deposition with decreasing depth and increasing maturity in a shelf environment.

This complex of highly deformed metasediments and metavolcanics has been subjected to varying grades of metamorphism ,the peak of which has been dated at about 1700 Ma (Pigeon, 1967; Shaw, 1968; Reynolds, 1971) with deposition of the original rocks postulated at 1800 Ma ago (Shaw, 1968). A more recent comparitive study of various isotopic dating methods by Gulson (1983) dated the two metamorphic peaks at 1580 and 1660 Ma.

The metamorphic history is complex and Binns (1962, 1964) defined four major deformations. The structural analysis of Laing et al. (1978), however, seems more generally accepted at present, and they recognised M1 and M2 as two prograde deformations of similar grade, and M3 as a retrograde deformation. They suggested that these may be all part of the one orogeny, the "Olarian Orogeny", with M3 probably commencing soon after M2, and continuing until about the emplacement of the Mundi Mundi granite at about 1500 Ma (Pigeon, 1967). The range in metamorphic conditions, according to Phillips (1980) is from 500°, 3kbar, P_{H2O} = 1, to 800°, 6kbar and P_{H2O} = 0.5 +_ 0.2. (Table 1.2).

Partial melting is often well developed, with migmatites being

Table 1.2 Summary of estimated metamorphic conditions at Broken Hill (adapted from Elliott, 1979)

HIGH GRADE METAMORPHISM

Reference	Metamorphism event after Laing 1977	$P_T$kb	T°C	P_{H_2O}	Method of Calculation
Binns, 1964	M_{1-2}	5-10	750-800	$P_{H_2O} << P_T$	Reaction curves
Chenhall, 1973	M_{1-2}	3-5	680-800	$P_{H_2O} << P_T$	Reaction curves
Hewins, 1975	M_{1-2}	-	780-843	-	Mg-Fe partitioning between orthopyroxene and clinopyroxene
S. Lee (pers. comm., 1976)	M_{1-2}	> 6	700-800	$P_{H_2O} < P_T$	Mg-Fe partitioning between cordierite and garnet.
Scott et al. 1977	M_{1-2}	7.8 av. max.	650-800	-	Partitioning of FeS, between sphalerite and hexagonal pyrrhotite
Laing, 1977	M_1	5.2 - 6.9	650-750	$P_{H_2O} < P_T$	Reaction curves
Laing, 1977	M_2	5.5 - 7.0	600-750	$P_{H_2O} < P_T$	Reaction curves
Phillips, 1978, 1980	M_{1-2}	4.9 - 5.5	710-770	a_{H_2O}= 0.25 $\pm$ 0.1	Reaction curves, Opx-garnet, & cordierite-garnet partitioning, melting & dehydration reactions.
Elliott, 1979	M_1 & M_2	5.5 - 7.0	650-800	$P_{H_2O} < P_T$	Reaction curves, geobarometry & geothermometry studies listed above.

REGIONAL RETROGRADE METAMORPHISM

Chenhall, 1973	M_3	6.0 - 4.5	600-480	$P_{H_2O} = P_T$	Reaction curves
Laing, 1977	M_3	6.0 - 3.0	750-450	variable	Reaction curves
Elliott, 1979	M_3	5.5 - 3.0	650-450	" but high	Reaction curves.

common in the higher-grade metamorphic facies (Corbett and Phillips (1981)). Phillips and Wall (1981) found evidence that CO2-induced crustal dehydration preceded the formation of the granulite facies terrain, and like Stevens et al. (1980) thought the high thermal gradient to result from upwelling of basic magma or mantle material. There is a general trend of increasing metamorphic grade from northwest to southeast, first described by Binns (1962, 1964), and more accurately defined by Phillips (1978 & 1980) (Fig. 1.1 and Table 1.1). The latter author mapped four metamorphic zones, showing that the isograds were both folded and faulted by later retrograde deformational events, and considered that the Broken Hill ore bodies had been subjected to metamorphism of the two - pyroxene zone of the granulite facies.

The Complex is transected by numerous M3 retrograde shear zones (RSZ) as described by Vernon and Ransom (1971), Corbett and Phillips (1981) and Etheridge and Cooper (1981). These also increase in metamorphic grade to the southeast and, as noted by Chenhall (1973), and Corbett and Phillips (1981), the presence of kyanite and staurolite in some RSZ is indicative of comparatively high pressure. Kyanite is unknown in the Willyama Complex outside of the two-pyroxene zone (Corbett and Phillips, 1981). Fine-grained muscovite, biotite, garnet and sillimanite are typical minerals of the RSZ. Widespread incipient migmatization was thought by Corbett and Phillips to be accompanied by incipient retrogression in surrounding rocks, but the RSZ seem unrelated to migmatites (Etheridge and Cooper, 1981). The latter workers explain the retrogression in RSZ as being due to meteoric fluids penetrating down to about 10 km !, and exceptionally large amounts of fluid (1,000-10,000 x rock volume) were postulated to

account for the large amount of muscovite/sericite, and loss of silica. Isotopic evidence shows that the RSZ probably represent a long series of deformational events during and following M3, from about 1490 to about 460 Ma (Etheridge and Cooper, 1981).

Stevens et al. (1980) postulated a rift-environment origin for the ore deposit, associated with hotspots and, although neither modern continental or island arc settings are strictly compatible, favoured a frontal - arc basin setting similar to the Green Tuff region of Japan. Willis et al. (1983) similarly inferred a setting within an active rift zone in a subsiding extensional shelf-like environment, but noted the lack of evidence for pre-existing continental crust to the east, and the absence of coarse pyroclastics and conglomerates in the sequence. They suggest that the Broken Hill Block lay towards the continental margin, and postulate a broad, marine, ensialic back-arc basin behind a continental margin as a possible setting.

1.3 Geology of the Mines Area

1.3.1 Lithology

Carruthers and Pratten (1961), recognized a sequence of rocks in these Broken Hill Mines area which they termed the "Mine Sequence" (Fig. 1.3). This has been discussed in detail by Johnson and Klingner, (1975), Laing et al. (1978) and Laing, (1980). In their recent subdivision of the Willyama Supergroup, Willis et al. (1983) placed most of the Mine Sequence within the Broken Hill Group, and the major mineralisation within the Hores Gneiss, Purnamoota Sub-group. Johnson and Gow (1975) have shown that most other major Broken Hill-type mineralization in the Willyama Complex is associated with this

sequence. It should be noted however, that the Pinnacles Mine (the second largest deposit within the Willyama Complex c.f. Turner, 1927) and numerous small stratiform deposits, occur within the Thackaringa Group, slightly older than the Broken Hill Group, and are of Broken Hill-type (Barnes, 1980; Leyh & Larsen, 1983).

The Mine Sequence consists principally of a range of pelitic to psammitic and feldspathic gneisses, commonly migmatized. Concordant iron-rich amphibolite horizons are common, but minor, units. An essentially massive, coarse-grained, leucocratic, quartzo-feldspathic gneiss has been termed the "Granite Gneiss" (Carruthers and Pratten, 1961), "Felsic Gneiss" (Plimer, 1979) and Rasp Ridge Gneiss (Willis et al. 1983). Several units of a distinctive garnet-plagioclase-orthoclase-biotite gneiss, within the Hores Gneiss (Willis et al. 1983) are termed the "Potosi Gneiss" (Carruthers & Pratten, 1961) and have a close relationship to the orebodies.

The Mine Sequence probably originated as a mixed volcano-sedimentary succession (Johnson and Klingner, 1975). Plimer (1979), using field relationships, relict textures and structures, and geochemical data, showed that the felsic gneiss, Potosi Gneiss and amphibolites are probably of igneous origin. The progenitors were suggested to be an altered acid pyroclastics, a rhyodacitic tuff, and a basaltic tuff, respectively. Willis et al. (1983), suggested that the associated metasediments were derived by subaerial weathering, erosion and redeposition of this volcanic material.

The orebodies consist of a series of lenses, conformable with the general stratigraphy, known as the "lode horizon" (Carruthers and Pratten, 1961) (Figures 1.3 and 1.4). These lodes have a complex and variable composition (Tables 1.3 and 1.4), and are separated by a

TABLE 1.3 PRINCIPAL ORE LENSES AT ZC/NBHC MINES

Lead Lodes	3 lens	(stratigraphic top/structural base)
	2 lens	
Zinc Lodes	1 lens upper	
	1 lens lower	
	A lode	
	B lode	(stratigraphic base/structural top)

TABLE 1.4 PRINCIPAL GANGUE MINERALOGY AND TYPICAL MINING GRADES OF THE BROKEN HILL OREBODIES (adapted from Johnson and Klingner, 1976; Plimer, 1979).

Orebody	Gangue	Typical mining grade		
		%Pb	g/t Ag	%Zn
3 lens (NE end)	rhodonite, fluorite, quartz, garnet, gahnite, apatite pyroxmangite, amphiboles.	15	300	13
3 lens (SW end)	quartz, fluorite, rhodonite, garnet.	11	200	15
2 lens	calcite, rhodonite, bustamite, manganoan hedenbergite, tephroite, quartz, garnet, orthoclase, micas.	14	100	11
1 lens	quartz, calcite, bustamite. orthoclase, apatite, gahnite.	8	50	20
A lode	rhodonite, pyroxmangite, quartz, manganoan hedenbergite, garnet. gahnite, calcite, apatite, orthoclase.	4	40	10
B lode	quartz, orthoclase, garnet, apatite.	5	40	17

siliceous sillimanite gneiss which commonly shows some interlayering and gradation with lode rocks, and may contain layers rich in quartz, garnet, sulphides and/or other lode-indicative minerals. Feldspathic and/or migmatitic layers are common.

Quartz, sulphides, garnet, gahnite, calcite, fluorite, pyroxenoids, pyroxenes, orthoclase, plagioclase, fluorapatite, amphiboles and micas are all locally abundant, and most are widely distributed throughout the lodes. Most of these can be major phases, sometimes locally forming almost monominerallic rocks. Many different lode rock types were described and classified by Spry (1978) and Billington (1979), the most persistent being "quartz-gahnite", which occurs along about 300 km strike-length (Plimer (1979) and Fig 1.2), but "garnet quartzite" is also common. These rocktypes were thought by Spry (1978) to have formed from zinc and manganese oxide rich sediments respectively. The lode horizon has great lateral continuity despite the discontinuous nature of component rock bodies, and occurs in nearly all parts of the Willyama Complex (Stevens, 1980).

"Banded Iron Formation" (BIF) is a term given by Carruthers and Pratten (1961) to well-layered horizons consisting principally of garnet, quartz, magnetite and apatite with sulphides and gahnite as common accessories. Eight such horizons have been recognized.

1.3.2 Stratigraphy and Environment of Deposition of the Orebodies

There are six principal lodes at Broken Hill (Tables 1.3 and 1.4) and also some weak stringer mineralization stratigraphically below the B lode at ZC, which has been referred to as "C lode" (Spry, 1978). Typical cross-sections of the lodes in the ZC-NBHC area are shown in Figures 1.3 and 1.4.

The reference lines and coordinates used in these sections are an arbitary but well established system unique to Broken Hill and developed by the Broken Hill mining companies. The base line is defined as 0 = 10,000 metres below sea level, and ground level at Broken Hill is thus at about 10,280 metres on these coordinates. The mine levels are about 50 metres apart.

The felsic gneiss lies stratigraphically above the orebodies, while units of Potosi Gneiss may lie above, below and stratigraphically equivalent to the ore lenses in the east (Hawkins, 1968a; Plimer, 1979). The BIF's lie above or in stratigraphically equivalent horizons on opposite sides of Potosi Gneiss bodies to the sulphides lenses (Plimer, 1979). In general, thinning of Potosi Gneiss bodies is related to the deposition of the major sulphide bodies (MacKenzie and Gow, 1970). The latter authors suggested that ridges of Potosi Gneiss separated the reducing environment of sulphide deposition from the oxidizing environment of BIF deposition. Eight principal BIF's (1-3 metres thick) are present in the mine area, but only four show significant continuity, with the principal horizon extending for 15 km.

Facies variations in the Willyama Complex are very common (Thomas, 1960), and especially so within the mines sequence (Hawkins, 1968; Plimer, 1979). The ore lenses occur within relatively homogenous sillimanite gneiss, but influxes of chemical sediments (now largely represented by quartz, garnet and sulphide-rich rocks) produced extremely rapid facies variations. Billington (1979) suggested that changes from oxide to silicate to sulphide facies occurred during deposition.

Penecontemporaneous faulting probably occurred during deposition of

the Broken Hill Group sediments and Leyh (1982) indicated that retrograde shear zones may have been active during sedimentation in an area 18 km NE of Broken Hill. Evidence of the latter also exists near the main NBHC shaft and in the southern extensions of the orebody (Johnson and Klingner, 1975), and may result in a dramatic cut-off in sulphide thickness (T. Jackson, pers. comm.). The orebody lies near the intersection of two major lineaments, and lies parallel to the Darling Lineament (O'Driscoll, 1968, 1983).

Despite some structural attenuation, the orebodies have a length/breadth ratio of about 8:1. MacKenzie (1968) and Johnson and Klingner (1975) postulated a long, narrow, fault-bounded sea-floor depression and Plimer (1979) additionally envisaged distal volcanic centres.

Stevens et al. (1980) thought the mine sequence to have been deposited following a period of rifting-induced volcanism in a deep, but shallowing, basin with low detrital influx.

1.3.3 Structure in the region of the Orebodies

The structure of the mines area is very complex and is still in some dispute with different structural models having been proposed by Hobbs (1966), Johnson and Klingner (1975), Hodgson (1975a) and Laing et al. (1978). The model of Laing et al. is perhaps the one most generally favoured, and these workers were the first to prove that the orebodies have been overturned and recognized an earlier deformation event to that which produced the prominent structures of the Broken Hill area. Aspects of this model are shown in Figure 1.7.

The first generation of folding is represented by very large scale, commonly recumbent, folds throughout the area, and the orebodies occur

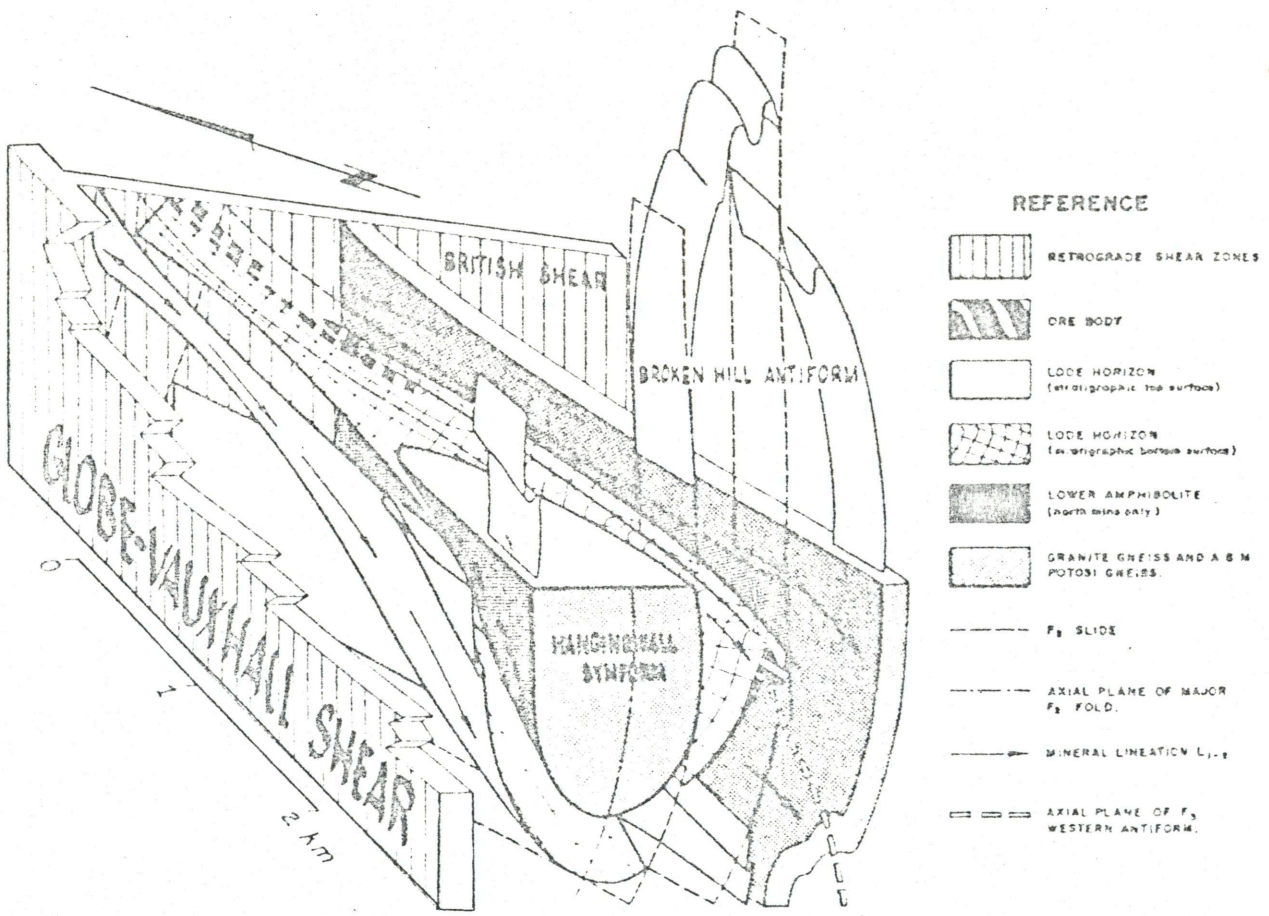

Fig. 1.7 Block diagram of the southern mines area, showing interpreted relationships between the main marker units and the main structures. For simplicity the Globe-Vauxhall shear and British shear are shown dipping vertically and the Broken Hill synform is omitted. (Laing et al, 1978).

on the overturned limb of one of these. This folding (F1) was synchronous with the first high-grade metamorphism (M1); the second high grade metamorphism (M2) was associated with large scale tight F2 folding. The third major deformation (F3), responsible for small scale folds and crenulations in the orebody, was synchronous with retrograde metamorphism (M3). F2 and F3 folds are frequently coaxial (Johnson and Klingner, 1975).

Shearing is common in the area, and the principal retrograde shear zones are shown in Figures 1.3 and 1.7. These commonly are oriented NNE, often parallel to S3. Incipient retrogression outside these zones is very common, and frequently seems related spatially, and perhaps also genetically, to migmatization (Corbett and Phillips, 1981).

The orebodies are apparently thickened in F3 fold hinges in the NBHC and ZC mines, and Laing et al. (1978) suggested that some movement of sulphides into F2 and F3 fold hinges may have occurred. Hopwood (1978) showed that intrafolial folds were common in orebodies, and are perhaps due to syntectonic hydrothermal activity, related to metamorphism or mineralization. Vokes (1968, 1971) described how sulphides can be mobilized to a few metres under high grade regional metamorphism, and such mobilization at Broken Hill was described by Maiden (1975). The consistency of stratigraphic relations was used by Matthias (1973), Stanton (1976) and Plimer (1979) as evidence for the overall insignificance of such movement or transposition. The orebody therefore seems to have had an original linear shape.

1.3.4 Wallrock Alteration

Wallrock alteration at Broken Hill is generally assumed to be minor

and insignificant (Johnson and Klingner, 1975) and Plimer (1975 and 1979), Stanton (1976d) and Elliott (1979) describe geochemical variations that indicate that premetamorphic hydrothermal alteration probably did occur on a small scale. Plimer (1979) suggested that the geochemical variations principally represent premetamorphic sericitization shown mainly by areas of high K, Si and Rb. Sericite-schist zones bordering sulphides were suspected of being an alteration feature, but probably just indicate differential movement of sulphide ore with respect to the surrounding rocks (Plimer, 1979).

1.3.5 Metamorphism and synmetamorphic metasomatism in the lodes

The orebodies have been metamorphosed to the 2-pyroxene zone of lower granulite facies (Phillips, 1980) during M1 and M2, along with the enclosing rocks (Maiden, 1975). Partial melting of silicates and sulphides was probably contemporaneous (Plimer, 1976a and Lawrence, 1967).

Most geologists have assumed that essentially isochemical metamorphism occurred in these rocks, as sedimentary structures and chemical stratigraphy have been preserved - locally at least (Matthias, 1974, Glen and Laing, 1975, Stanton and Williams, 1978 and Plimer, 1977 and 1979). There is, however, considerable evidence for allochemical reactions in many rocktypes. Garnet and/or biotite-rich rims on amphibolite dykes (Stillwell and Edwards, 1956; Segnit, 1961; Plimer, 1979), and garnet-rich alteration rims to orebodies (Jones, 1968; Maiden, 1972; Spry, 1978; Billington, 1979) are common, indicating significant element mobility. The abundance of anhydrous silicates, including garnets, pyroxenes, pyroxenoids and sillimanite, indicate the loss of volatiles, principally H_2O and CO_2 (Plimer,

1979). Ahmad and Wilson (1982) proposed hydrogen metasomatism to explain fibrolite formation and movement of U and B in sillimanite gneisses at Broken Hill. Quartz-rich veins have also been interpreted to be indicative of metasomatism (Dewar, 1968; Phillips, 1980).

Desulphurization has been proposed by Wall et al. (1976) and Plimer (1977a) to account for the lack of pyrite and abundance of gahnite in these lodes, but Spry (1978) and Plimer (1977b) found no evidence for sulphur loss, and suggested that the lodes were originally sulphur-poor. Wall and England (1979) showed that sphalerite should re-equilibrate at high temperature and pressure with Fe-Mg-Al silicates, producing gahnite in equilibrium with H2S-rich fluid.

Saxby (1981) thought that the rarity of graphite at Broken Hill (Ramdohr, 1950) resulted from synmetamorphic oxidation by H20 or Fe203. Synmetamorphic oxidation and reduction seems, however, poorly understood at present (Mueller, 1967, Klein, 1973, Speer, 1981 and Haase, 1982). Methane leaks out of the Broken Hill ore (I. Plimer, pers. comm.) and thus may be an important component of intergranular fluids and may have been derived from original graphite (Saxby, 1981).

The low permeability of various rocktypes may preclude metamorphic equilibration (Rumble et al. 1982), and may explain the lack of element mobility in BIF's (Stanton and Williams, 1978).

1.3.6 Retrogression of the Orebodies

Despite the early recognition of the presence and significance of the RSZ (The Geological Subcommitee of the late Scientific Society of Broken Hill, 1910; Andrews, 1922) little detailed study of the effects of retrogression on the lodes has been undertaken. Scott et al. (1977) suggested that the sulphides had undergone post-metamorphic or

retrograde re-equilibration. This is most important for pyrrhotite, which exhibits several breakdown reactions from the original hexagonal pyrrhotite, including exsolution of troilite, and formation of monoclinic pyrrhotite, pyrite and marcasite. Spry (1978) noted some retrograde zoning in garnet, gahnite and loellingite, and breakdown of loellingite to arsenopyrite.

The retrogression appears to have significantly mobilized a number of elements, some on quite a large scale. Silver, lead, copper, iron, manganese, mercury, arsenic and antimony are among the most important of these and their mobilization into RSZ apparently resulted from an influx of aqueous fluid (Ryall, 1979a; Plimer, 1980c). Jones (1968), thought that the garnet sandstones resulted from large scale manganese metasomatism related to the RSZ.

1.3.7 Zoning and Variability in the Orebodies

The lode horizon appears to be quite continuous throughout the Willyama Complex (Johnson and Klingner, 1975) but, as described above, can have a very variable lithology. A number of attempts have been made to study the variation within this formation, and especially within the sulphide-rich rocks, mostly involved relating any apparent zoning to various origins.

Burrell (1943), Garretty (1943), Gustafson et al. (1950), Hawkins (1968a) and Stanton and Richards (1961) described the variations in base metal ratios in the lodes. Each lode has comparatively constant and characteristic ratios, enabling distinction of lodes even in close contact. King and O'Driscoll (1953), King and Thompson (1953) and Carruthers (1965) cited these ratios in support of a syngenetic origin, but they could not provide a satisfactory explanation for

their variation.

Plimer (1968) studied the variability of the lodes, and concluded that the complexity was due to both original depositional variability, and several types of tectonic mineral redistribution.

Burford (1972) studied the B lode, and found evidence for a weakly defined lateral zoning, as indicated by variations in Cu, Pb, Zn, Ag and Bi, all opposite in trend to other volcanogenic deposits, and which he thought to indicate overturning of this orebody. The copper-rich zone on the hanging wall was also noted by Hawkins (1968).

Mackenzie (1968) noted that a pyrrhotite-rich zone envelops the lead lodes but could find no explanation for it.

Stanton (1976a, b, c, d) and Stanton et al. (1978) discussed the geochemical variation within the lodes and the BIF's and the interrelations of various components. A general zonation was not found in the sulphide lodes but the BIF's show consistent zoning down to fine bands. This latter fact was used as evidence for isochemical metamorphism and for lack of any mobilization in the area, although Rutland et al. (1979) thought this conclusion very debatable, the BIF being an unusual lithology. Stanton (1976a,b,c,d) thought of the BIF as an oxide facies variant of the sulphide lodes, deposited in the closing stages of ore deposition.

Plimer (1975) detected a minor alteration zone, potassium-rich and sericitized, about the ore deposit, and he ascribed this to retrograde alteration. Fluid ascent along sulphide-silicate boundaries was thought to be responsible.

Stanton (1976c) compared the vertical distribution of the major metal in these lodes with other stratiform sulphide orebodies, where Cu-Zn-Pb-Ag is the usual order of deposition. The opposite trend

appears in the Broken Hill orebodies, both within each lode and over the whole lode sequence, and this he interpreted as indicating inversion of the lodes, a hypothesis supported by the structural work of Laing et al. (1978) and now generally accepted.

Plimer (1977 and 1979) reconsidered the alteration zone and showed that most aspects of it could have been due to pre-metamorphic hydrothermal alteration. Similarities were shown between this alteration zone and those near known submarine exhalative ore deposits. In the latter paper Plimer proposed that elemental zoning (Fig. 1.8) within and between the lodes is related to this alteration. Elliott (1979) discussed these geochemical haloes in greater detail and found them to be stratigraphically controlled originating from primary chemical precipitation as well as hydrothermal alteration.

Billington (1979) discussed variations within the orebodies and associated quartzites, which suggested variation from oxide to silicate to sulphide facies.

Ryall (1979a) noted a general increase in mercury towards the stratigraphic tops of most lodes, but no relation between lodes. This vertical variation is consistent with other stratiform ore deposits (Ryall, 1979b), but is complicated by mobilization due to partial melting, plastic flow and retrograde shear zones. It was shown that a much greater number of samples would be required for adequate determination of distribution of any components. Most studies of geological and geochemical variability at Broken Hill have similarly been on a broad scale, with indefinite results.

1.4 Methods of Investigation used in this study.

The Western A lode is not exposed on the surface and at present has

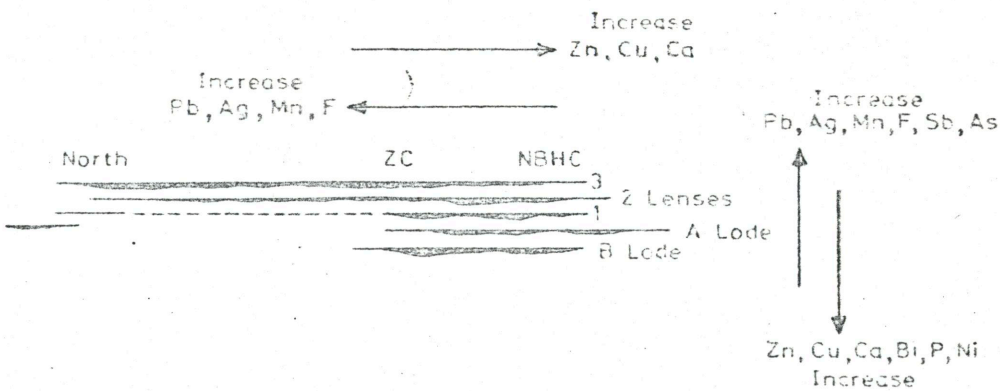

Fig. 1.8 Schematic unfolded longitudinal section of Broken Hill orebodies from northern to southern (ZC and NBHC mines) part of field showing elemental zonation observed along and across strike (from Plimer, 1979).

only minor exposures in underground workings. There has, however, been extensive diamond drilling of the lode, as 23mm diameter core. Most sampling was thus done on this core, aided by several trips underground.

Significant sections of selected drill holes were logged, and the resulting cross-sections are described in Chapter 2. The results are generally similar to the NBHC core logs, despite some incompatibility in style due mainly to more detailed logging with somewhat different aims.

Samples have been taken at various intervals, depending on lithology and mineralogy, in order to obtain representative samples of major units or rocktypes, as well as of many anomalous units and unusual assemblages. Sampling sometimes was needed at 10 cm intervals or less due to the extremely patchy nature of much of the lode.

Logging likewise was initially attempted at 1 m intervals, determining average mineralogical compositions, but has reverted to logging of rocktypes, from 10 cm thickness upwards. This fine-scale logging has still not produced a well defined correlation between holes, although some trends are obvious. Several hundred samples have thus been gathered, and polished thin sections were made of most, for the study of sulphides and oxides as well as silicates, and for microprobe analysis.

Mineral phases were analysed by X-ray Diffractometry to positively confirm their identity. This proved to be a necessity for many of the pyroxenoids.

About 500 Electron Microprobe analyses were conducted on most important silicate and oxide phases.

NBHC has provided access to their analytical data, which usually

comprised Pb, Zn, Ag and Cu with occasional Fe, As and Bi analyses. Whole-rock and some trace element analyses were also provided by NBHC for selected sections of one drillhole. A large number of whole-rock analyses of most common units around the lodes are available from other sources, so this aspect was not stressed in this thesis; particular aspects of whole rock chemical variation have been described in great detail by Stanton (1972), Plimer (1979) and Elliott (1979).

Chapter 2. Stratigraphy & Structure

2.1 Introduction

The WAL is a western extension of the A lode (Tables 1.3, 1.4; Fig 1.4), being overturned and dipping steeply to the Northwest. The A lode proper is similar in nature and complexity to the WAL but, due to sulphide concentration in an F2 fold hinge, has a higher economic grade. Examples of the mineral distributions on which the lode is subdivided for this study are shown on Fig. 2.10.

Relogging of WAL drillcore has produced good evidence for broad zoning into several distinct horizons (Fig. 2.1 - 2.6). The boundaries between the various zones are often difficult to define however, due to frequent intercalation, intergradation and shearing. Microscopic investigation was necessary to define most boundaries, although the major parts of most zones are easily identified mesoscopically. The various zones are discussed below.

2.2 Sillimanite Gneiss

The lode is enclosed within a pelitic gneiss, locally termed the sillimanite gneiss. This is principally a siliceous biotite-sillimanite gneiss, but may include minor lenses of garnet, quartz, biotite and feldspar-rich gneisses and quartzites, rarely more than a few metres thick. Minor patches of lode rocks, e.g. garnet quartzite or gahnite-rich rock, often sulphide-bearing, may occur. Quartzo-feldspathic zones are probably principally anatectic, and are described in section 3.4.4.

The gneiss is commonly retrogressed, resulting in a sericite gneiss or sericite schist where this has been most extensive.

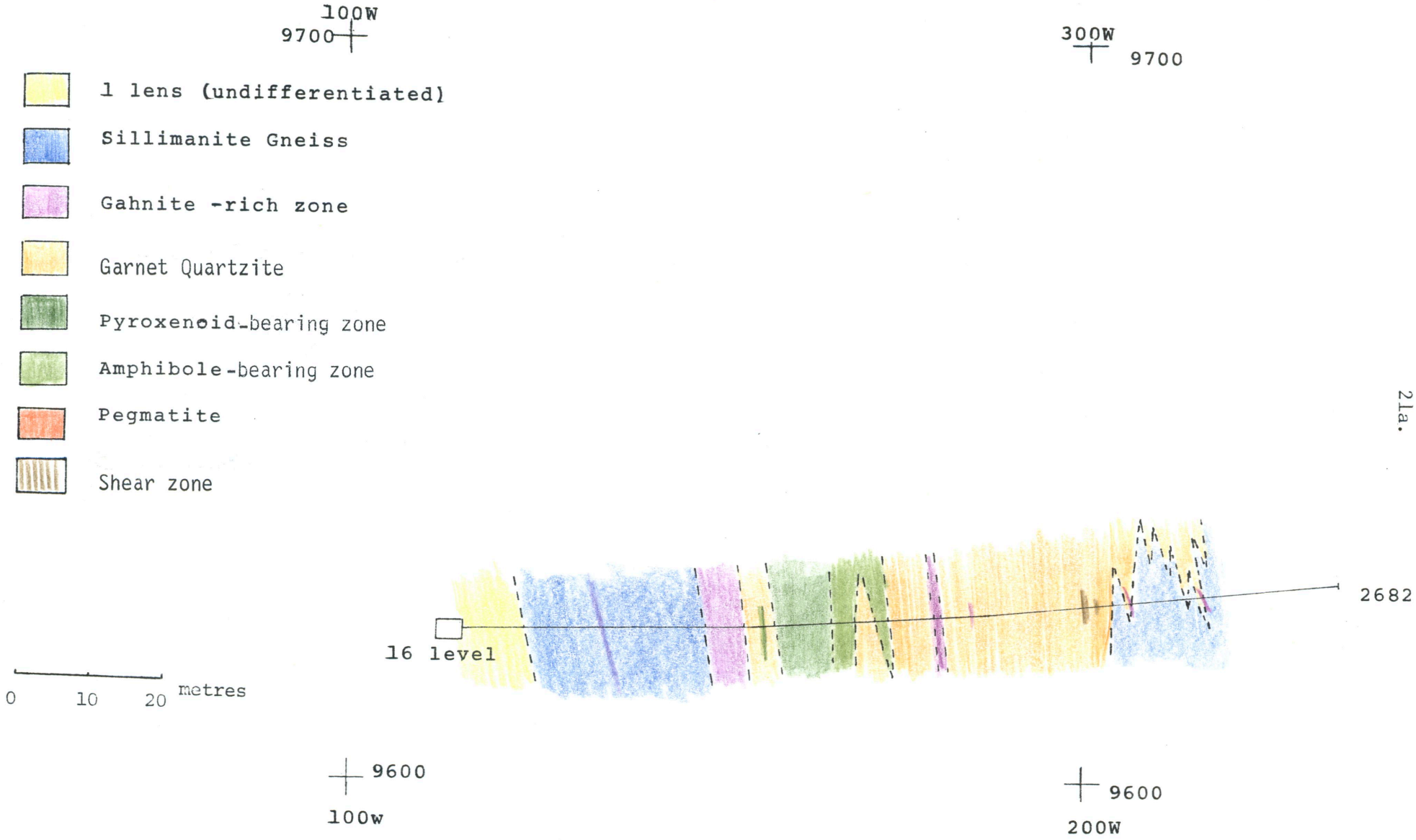

Figure 2.1 Drill section 26 (Z.C.) (grid coordinates in metres - see figures 1.5 and 1.6 for position)

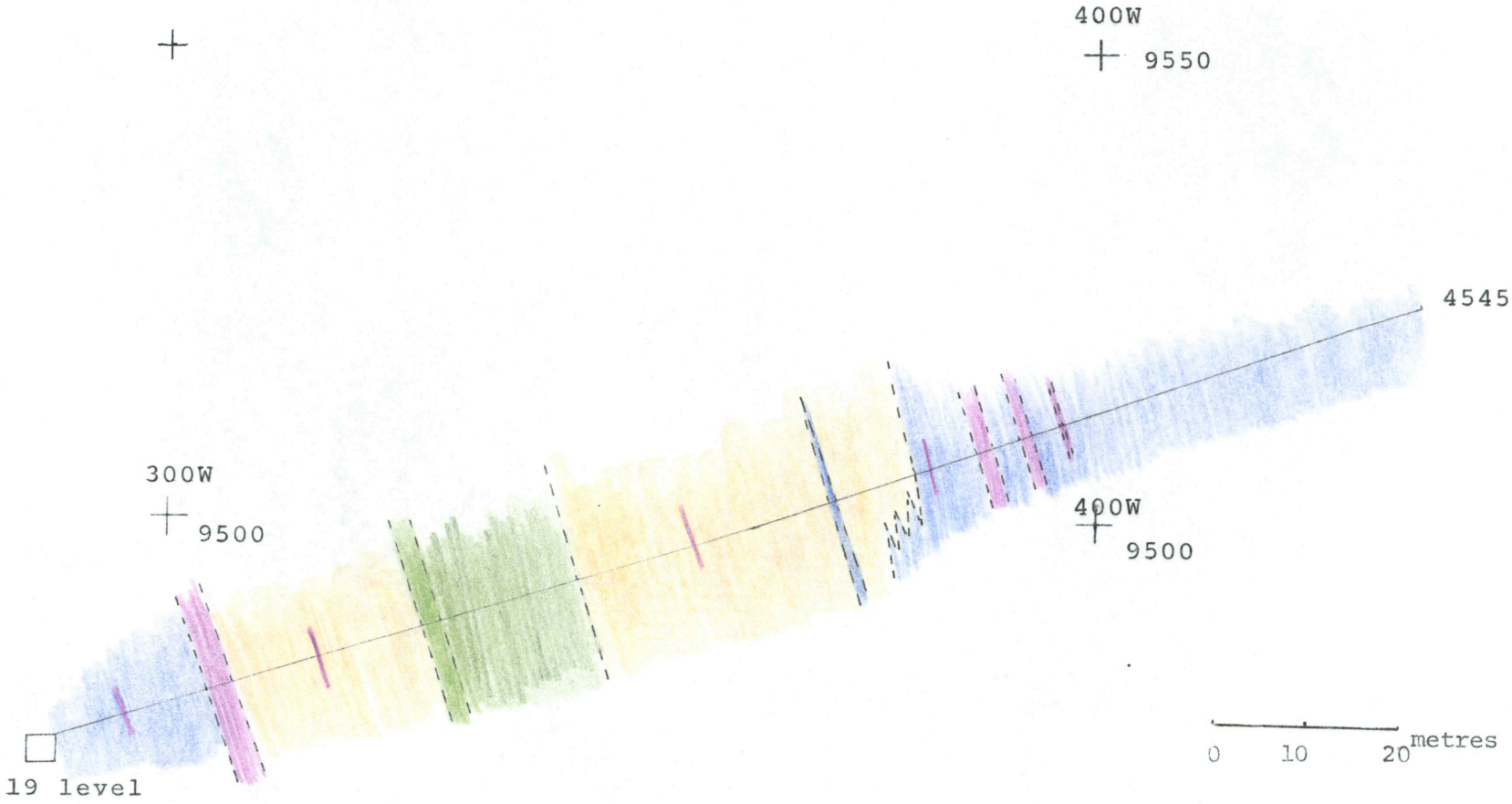

Figure 2.2 Drill Section 50, NBHC. Legend as for Figure 2.1

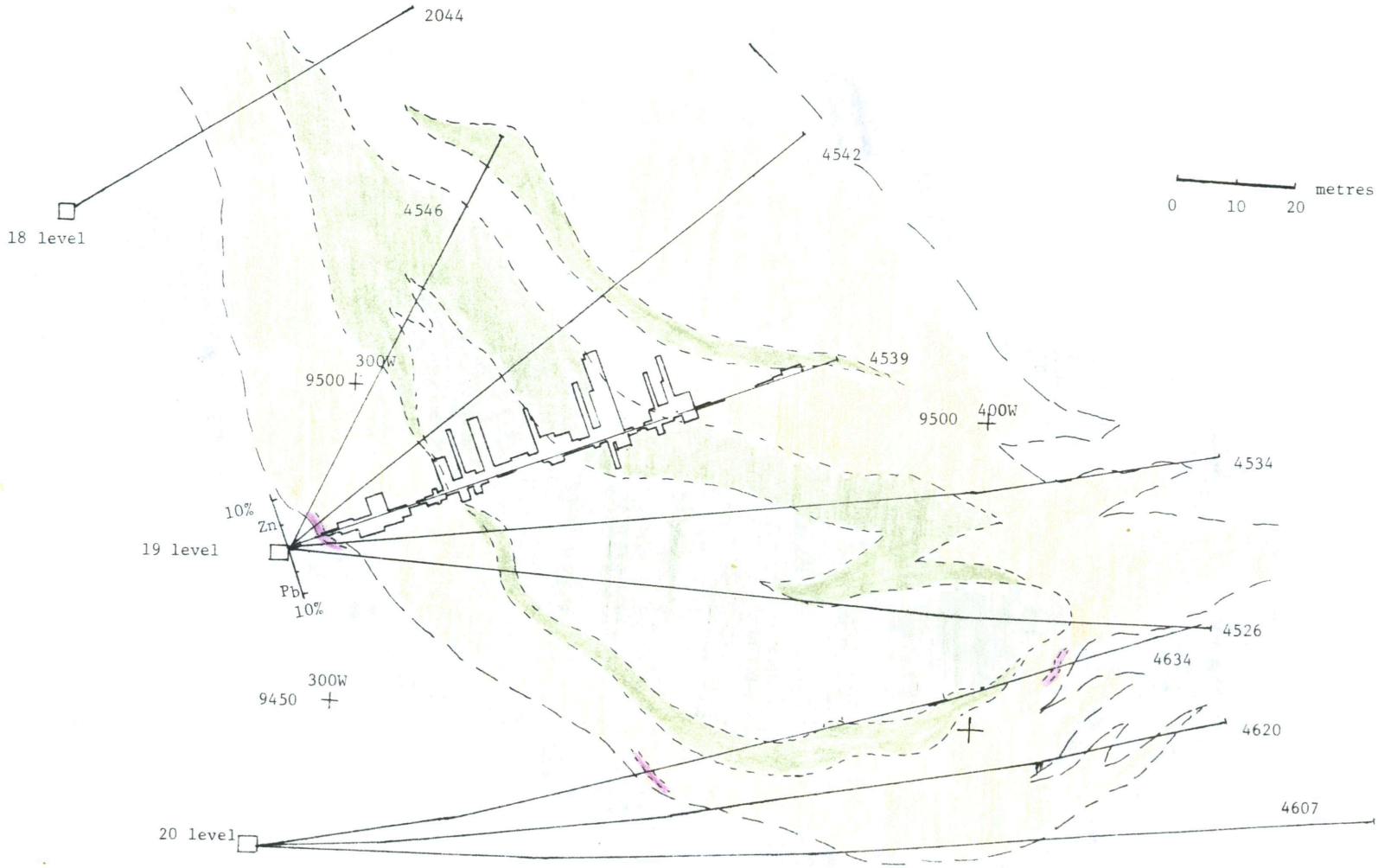

Fig. 2.3. Drill section 58, NBHC, showing interpreted structure.

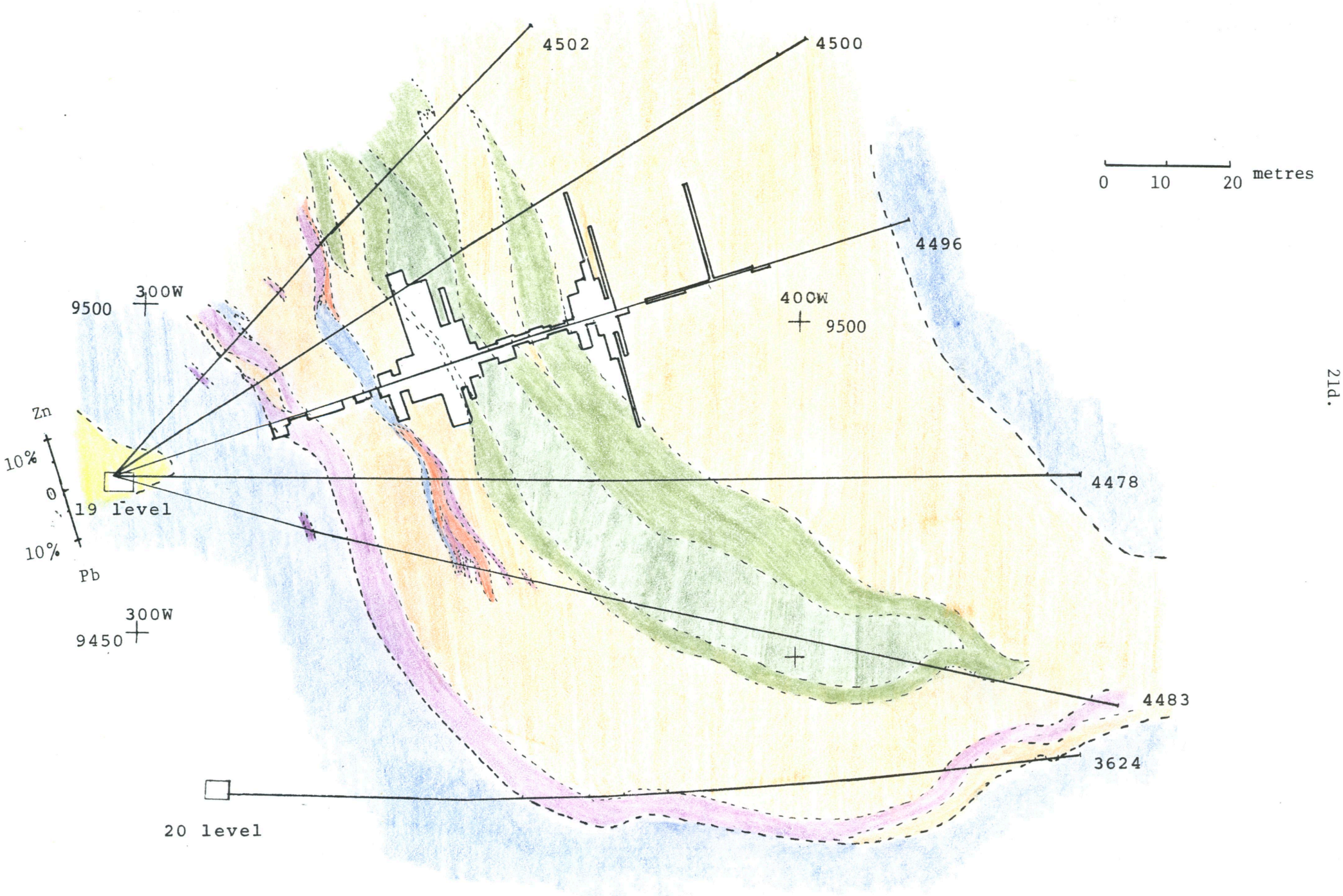

Figure 2.4 Drill section 64,NBHC, showing interpreted structure.

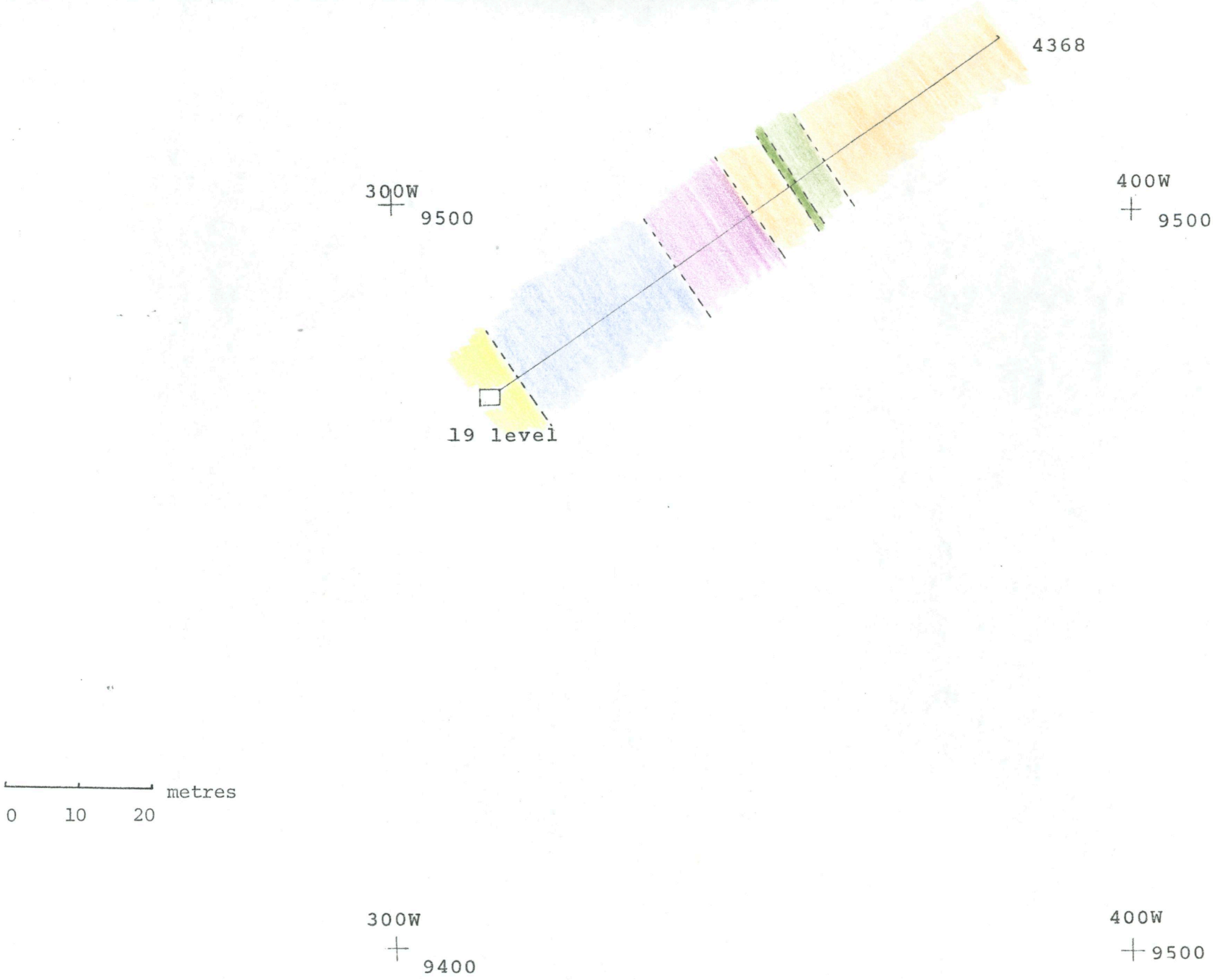

Figure 2.5 Drill section 66, NBHC

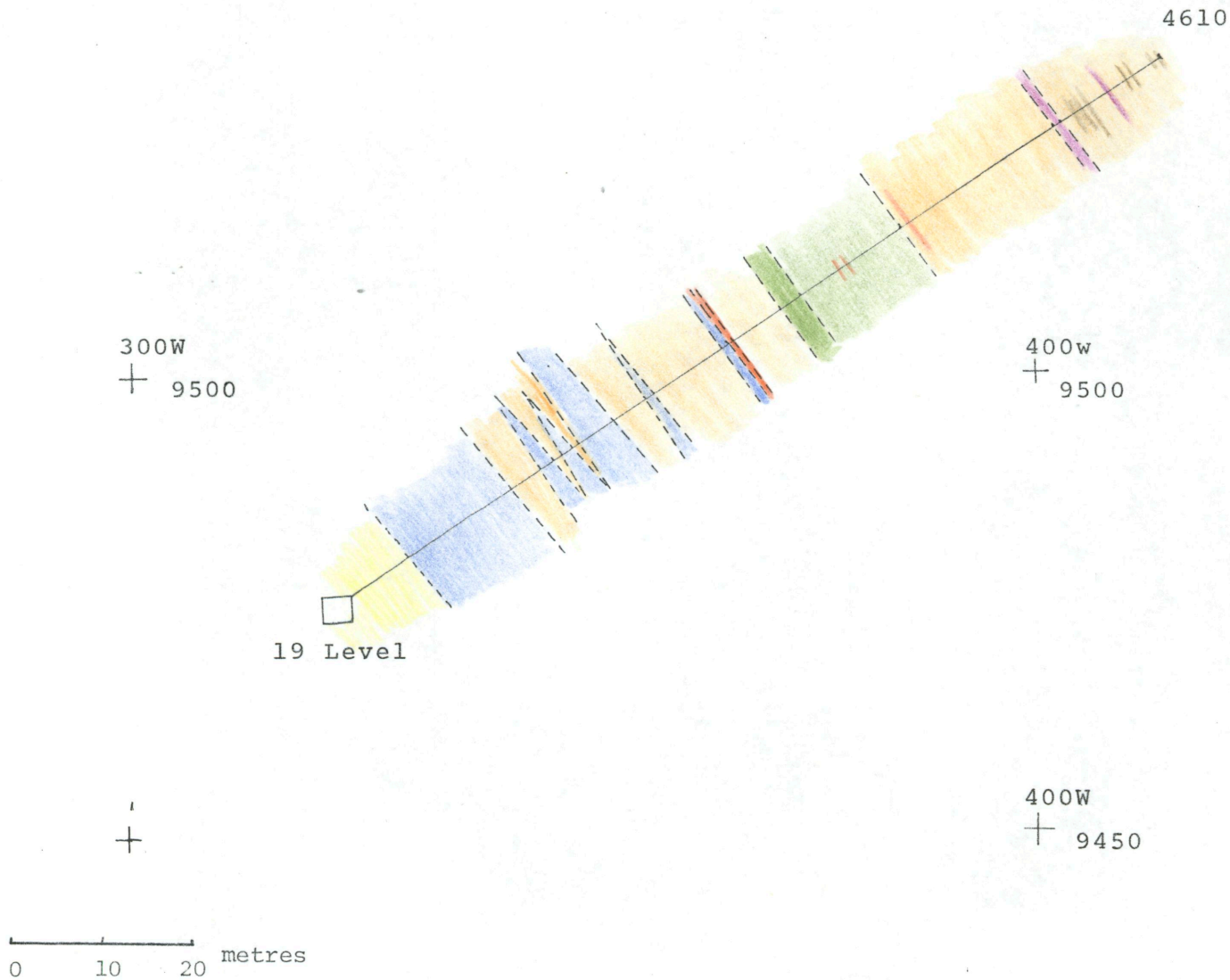

Figure 2.6 Drill section 68 , NBHC

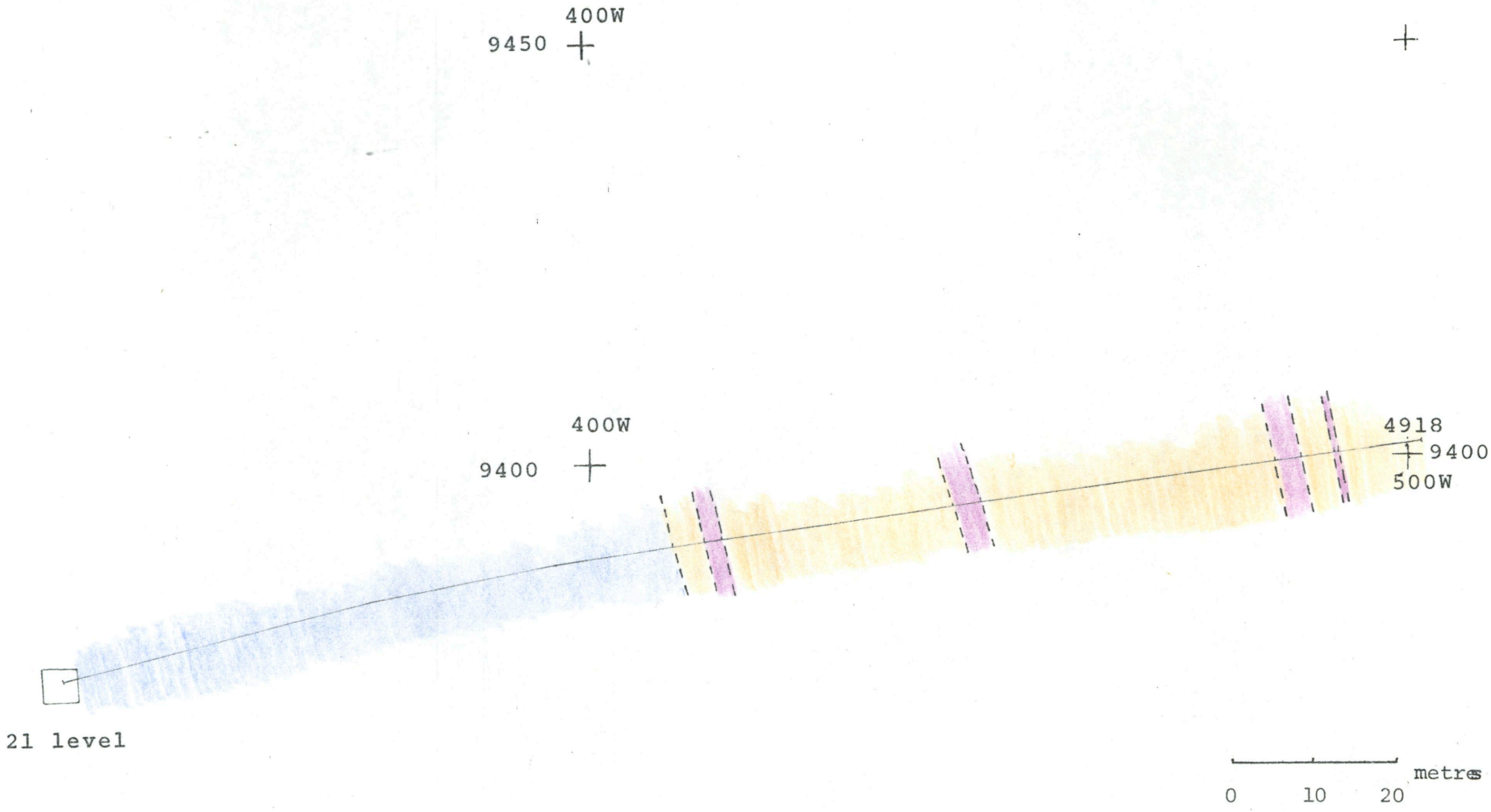

Figure 2.7 Drill Section 70, NBHC

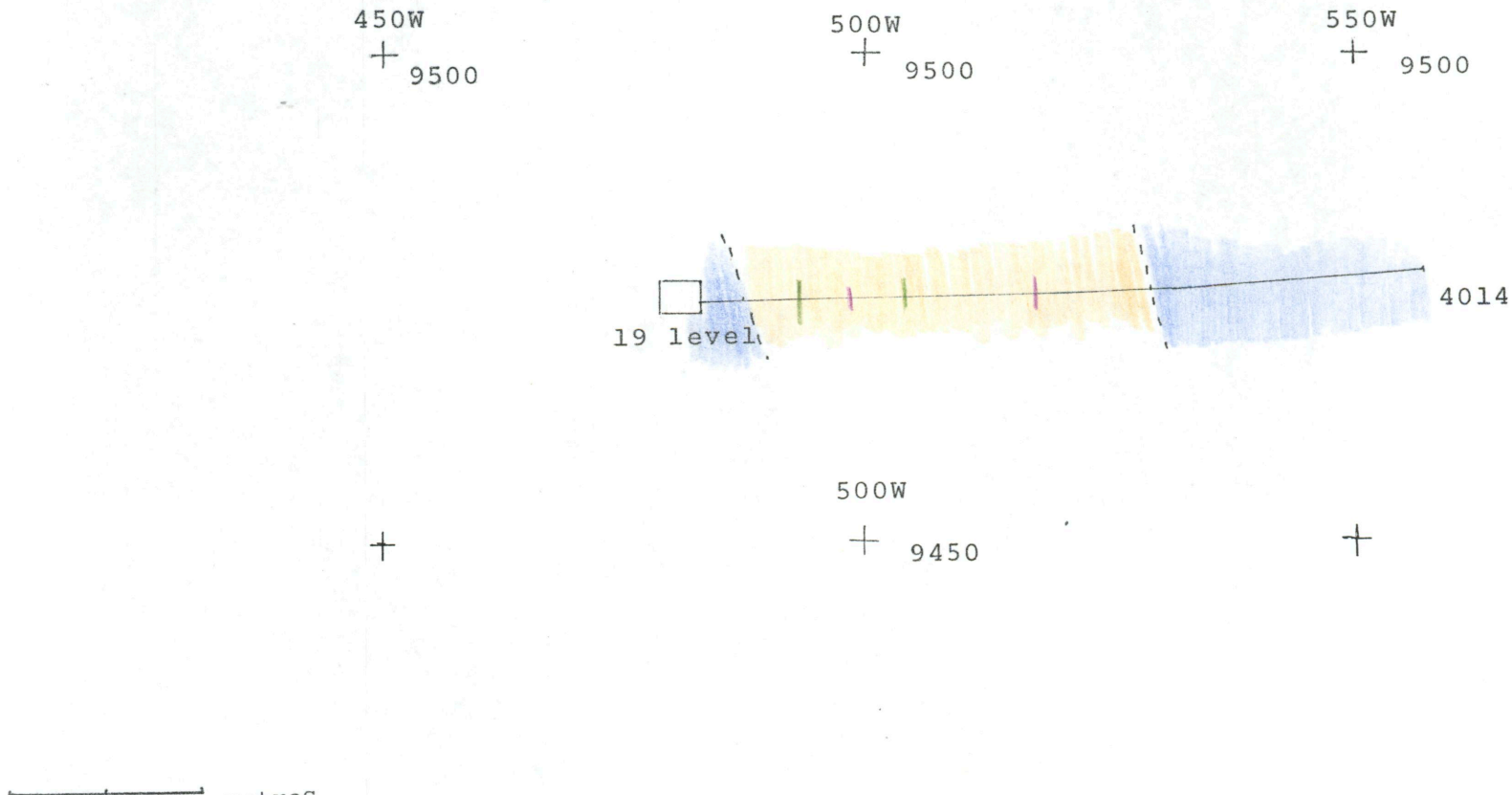

Figure 2.8 Drill Section 76, NBHC

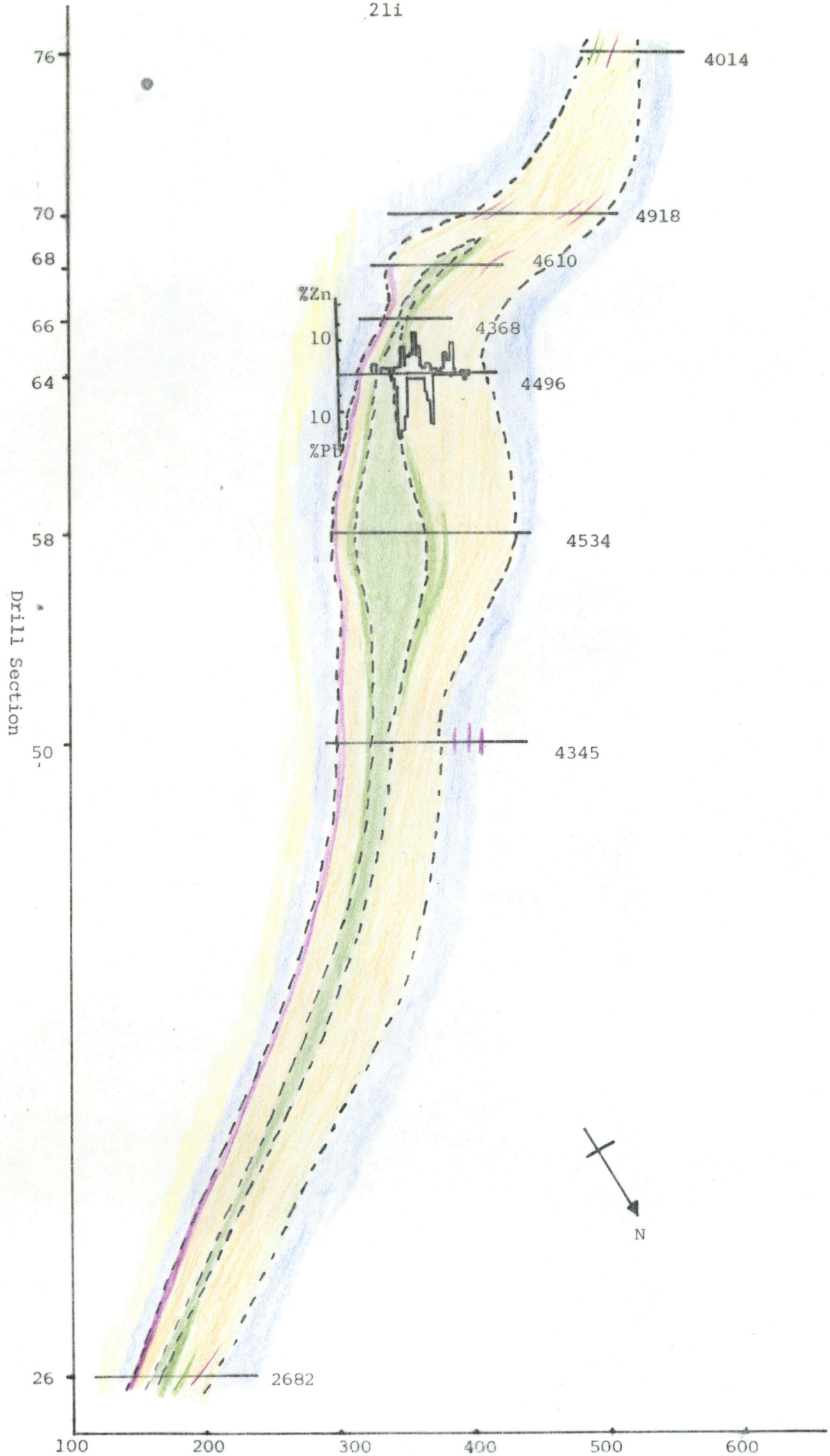

Figure 2.9: Approximate Projection of WAL onto the 19 Level (see Figure 2.1 for legend) Scale = 1: 4000

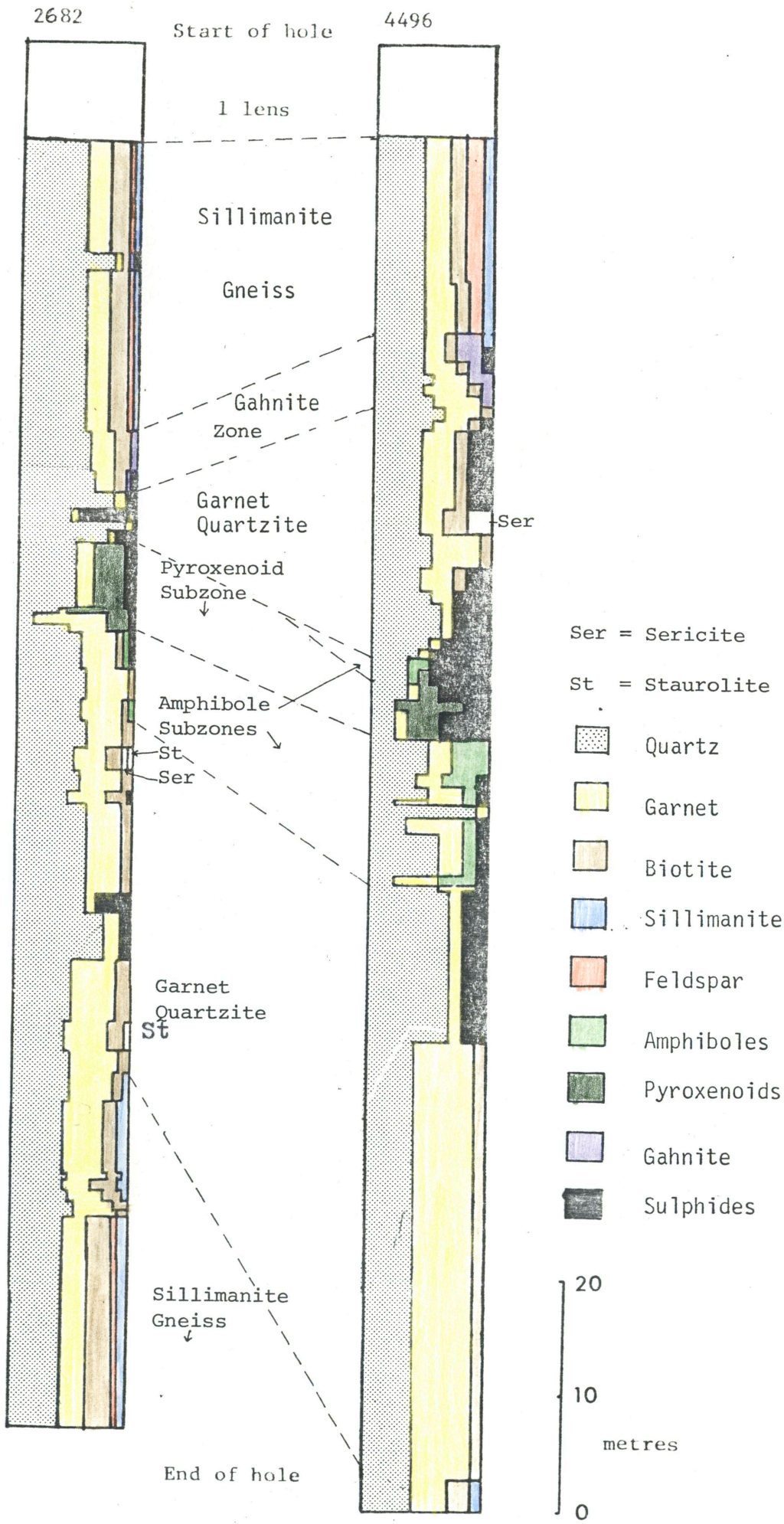

Fig. 2.10 Schematic Mineral Distribution in Drillholes 2682 and 4496

2.3 Gahnite-rich Zone

This subdivision is normally the uppermost zone in the WAL stratigraphy. Gahnite is not uncommon in the garnet quartzites or sillimanite gneisses, but is volumetrically insignificant there. This zone is defined to average more than 5 vol.% of gahnite, which is not always visible in hand specimen. This zone has a high variability, comprising lithologies varying from gneisses to garnet quartzites, with abundant, but erratically distributed, sulphides and gahnite. Quartzo-feldspathic rocks may occur, but are minor. Spinels (gahnite and hercynite), biotite, garnet (almandine), quartz, pyrrhotite, and galena are the most common phases.

Coarse-grained blue quartz ± gahnite veins are common in this zone, and these may also contain biotite or garnet (seldom both).

This zone has a variable size and gahnite content, apparently related to the sulphide content and as it is insignificant in some sulphide-poor areas it has not been shown on all sections. It normally separates the gneiss from the garnet quartzites but may occasionally lie within either lithology. Banerjee (1974) described a similar gahnite-rich selvage (also containing quartz-gahnite veins) between zinc-rich sulphide ore and aluminous wallrocks in the Geco Mine, Canada, as being of metamorphic origin.

2.4 Upper Garnet Quartzite

Stratigraphically below the major gahnite-rich zone are quartzites of widely variable composition (the 'quartzite envelope' of Billington, 1979). In the WAL they are principally garnet quartzites with variable sulphide and biotite contents, but minor gahnite-bearing, and staurolite-bearing horizons may occur. A zone of

quartzofeldspathic rocks ± sillimanite gneiss ± quartz - gahnite rocks, all commonly extensively sericitized, is widespread but cross cutting in this zone (Figure 2.4), and is related to shearing and pegmatite intrusion. Blue and white quartz veins, breccias (garnet quartzite in quartz veins) and coarse-grained garnet - sulphide - quartz patches are probably related to the "remobilized garnet quartzites" of Spry (1978) and occur throughout the garnet-rich lithologies. Quartz and sulphides tend to show a general antipathetic relation to garnet and biotite, giving rise to the "biotite - garnet quartzites" and "sulphide quartzites" of Billington (1979), the latter lithology being most common near the base, and the former near the top of this zone (Fig. 2.7).

2.5 Pyroxenoid-Amphibole Zone

This zone lies approximately in the central, most sulphide-rich, part of the lode and is defined to include all pyroxenoid and most of the significant amphibole occurrences (>5 vol.%) of the MAL. The major minerals include pyroxmangite, rhodonite, spessartine, quartz, amphiboles, sphalerite, pyrrhotite and galena. Bustamite, frequently mentioned in N.B.H.C. mine logs, is a misidentification of cummingtonite - group amphiboles or other pyroxenoids. Clinopyroxenes (principally manganoan hedenbergite) are locally abundant.

The pyroxmangite usually occurs in irregularly - shaped coarse-grained, almost monominerallic pods several metres across, (similar structures in the Broken Hill lodes were described by Maiden (1975) as boudins). Amphibole - rich garnet quartzites tend to envelope these pyroxenoid - rich rocks with little overlap, and thus amphibole and pyroxenoid subzones may be recognised.

Sulphide-rich quartzites are common in this zone, and grade into pyroxmangite and/or garnet-rich rocks.

"Garnet Sandstone" (a local term for a fine - grained spessartine - rich rock, c.f. Andrews,1922), is present in small patches throughout, but rarely outside, this zone. Jones (1968) and Hodgson (1975c) considered these rocktypes to be metasomatic in origin, however the genesis is unclear.

Garnet quartzites, amphibole - garnet quartzites and, rarely, biotite - garnet quartzites occur towards the outer parts of this zone. Fluorapatite - rich quartzites are minor but intriguing lithologies often present in this zone. These litholigies can be either massive or layered, and presumably indicate original sedimentary phosphate accumulations.

2.6 Lower Garnet Quartzite

Stratigraphically this is the lowermost, and most westerly, zone of the WAL. It closely resembles the upper garnet quartzite, but is usually considerably thicker, with biotite perhaps less common. Gahnite may be locally abundant near the stratigraphic base, but the gahnite - rich zone is discontinuous.

A fracture zone, up to 5m thick may occur here,and grades from vughs filled with unconsolidated sandy and clayey material, through chlorite + calcite veins to chloritized garnet quartzites.

2.7 Sillimanite Gneiss

This gneiss, stratigraphically underlying the lodes, appears similar to the overlying gneiss, but little data is available on it due to insufficient drillhole intersections.

Chapter 3. Petrography

3.1 Introduction

The WAL has undergone a complex metamorphic history, as described for the general area in Chapter 1. The present textures are usually at least partly retrograde in nature but there seems evidence for greater retrogression in gahnite-bearing and amphibole-bearing rocks than in other rocktypes. The major mineralogical constituents and grainsizes are shown in Tables 3.1 and 3.2. The rocktypes described below are related to, but not necessarily equivalent to, the zones described in Chapter 2, which usually comprise many different lithologies.

3.2 Textures

Throughout most of the lode rocks there is a tendency towards a granoblastic texture due to contemporaneous recrystallization of silicates, sulphides and oxides at high metamorphic grade (Lawrence, 1973). Lawrence (1973) showed that polygonization in sulphides may also occur during recrystallisation following retrograde metamorphism and shearing and is particularly evident at Broken Hill. This tendency towards polygonization, dependent on relative surface energies (Spry, 1969) has also been described in these rocks by Stanton (1964).

A linear fabric may be present, due to alignment of prismatic minerals such as sillimanite and amphibole with fold axes or shear directions. Pyroxmangite may also rarely show a weak alignment in recrystallised fractures in pyroxenoid bodies.

A strong planar fabric is occasionally present within schistose biotite or muscovite-rich horizons and is common in RSZ, due to sericitization. Gneissic biotite and/or sillimanite-rich layers are

Table 3.1: Approximate Grainsize Ranges (mm)

Mineral	Prograde	Remobilized/Pegmatitic	Retrograde
Quartz	0.5 - 2	0.5 - 20	0.1 - 0.5
Garnet	0.1 - 1	0.5 - 20	0.1 - 0.5
Biotite	0.1 - 5	-	0.1 - 1
Sillimanite	0.2 - 2	-	0.02 - 0.4
Staurolite	-	-	0.1 - 4
Gahnite	0.1 - 2.5	0.5 - 15	-
Muscovite	-	0.1 - 1	0.01 - 1.5
Orthoclase	0.5 - 10	10 - 100	-
Plagioclase	0.1 - 1	0.1 - 0.5	-
Chlorite	-	-	0.01 - 1.5
Cummingtonite series	-	-	0.1 - 10
Actinolite	-	-	0.1 - 2
Rhodonite/ Pyroxmangite	1 - 15	5 - 50	-
Manganoan Hedenbergite	1 - 10	-	-
Fluorapatite	0.1 - 0.5	-	-
Ilmenite	0.01 - 0.2	-	<0.02
Sphalerite	0.1 - 10	0.2 - 50	<0.1
Galena	0.1 - 10	0.2 - 50	<0.2
Pyrrhotite	0.1 - 10	0.2 - 50	-
Chalcopyrite	0.1 - 2	0.2 - 5	-
Arsenopyrite/ Loellingite	0.2 - 5	-	0.2 - 2

Table 3.2: AVERAGE MODAL COMPOSITIONS OF IMPORTANT ROCK TYPES

(Visual estimates from polished thin sections)

Rock type	Sillimanite Gneiss	Gahnite-rich rocks	Garnet Quartzite	Amphibole-Garnet Quartzite	Pyroxenoid -rich rocks	Sulphide Quartzite
No. of thin sections used	6	27	31	20	23	13
Quartz	48 (21*)	36 (27)	65 (23)	48 (31)	23 (22)	59 (17)
Garnet	20 (10)	9 (10)	26 (16)	30 (25)	13 (14)	9 (9)
Biotite	14 (6)	11 (16)	5 (6)	tr	tr	4 (6)
Sillimanite	3 (5)	1	tr	-	-	tr
Staurolite	3 (4)	4 (10)	tr	-	-	-
Gahnite	tr	22 (20)	tr	-	-	1
Muscovite	12 (2)	4 (11)	1	-	-	3 (5)
Orthoclase	tr	3 (9)	tr	-	-	-
Cummingtonite series	-	-	tr	13 (11)	5 (10)	tr
Pyroxenoids	-	-	-	-	45 (30)	tr
Mn-Hedenbergite	-	-	-	-	6 (15)	-
Sphalerite	-	1	1	5 (8)	3 (5)	12 (10)
Galena	-	2 (3)	tr	tr	1	1
Pyrrhotite	tr	7 (8)	1	4 (8)	3 (6)	11 (13)
Arsenopyrite/Loellingite	-	2 (4)	tr	tr	tr	1

* Standard Deviation

often present in the sillimanite gneiss, gahnite-rich zone, and garnet quartzites.

Local remobilization is indicated by quartz - rich veins and pegmatite veins (which can be either quartzofeldspathic or sulphide rich). Late stage shearing is indicated by microfaulting in garnet and gahnite (Fig. 3.1), as well as by amphibole-rich and sericite-rich veins.

3.3 Petrography of Principal Rock types.

3.3.1 Pelites (Sillimanite Gneiss).

The principal prograde assemblage in this lithology is quartz-sillimanite- biotite - garnet - orthoclase. Orthoclase, and rarely minor plagioclase, occur in quartzo-feldspathic segregations which grade into pegmatites. Orthoclase is also commonly present as poikiloblastic porphyroblasts or 'augen', especially stratigraphically immediately below the WAL. Sillimanite, garnet, biotite, and quartz - rich layers are all locally abundant.

Chloritic alteration of biotite is common, but such replacement rarely goes to completion. Sericitisation along grain boundaries and cleavages is common in sillimanite and feldspars, and rare about garnet and biotite.

3.3.2 Gahnite-rich rocks.

This zone is complex and variable, but the stable prograde assemblage is usually quartz - gahnite - biotite $\pm$ garnet $\pm$ sillimanite $\pm$ galena $\pm$ pyrrhotite. Similar rock types have been described from Broken Hill by Segnit (1961). Sillimanite segregations

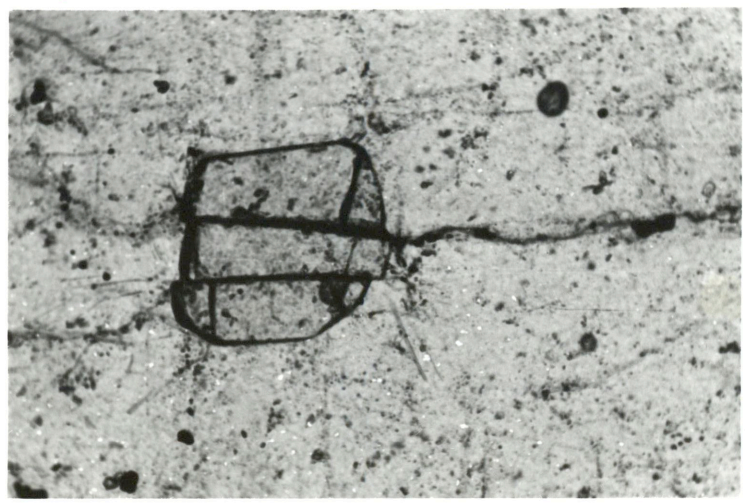

Fig. 3.1 Microfaulted garnet in quartz (4502/62.8). PPL.

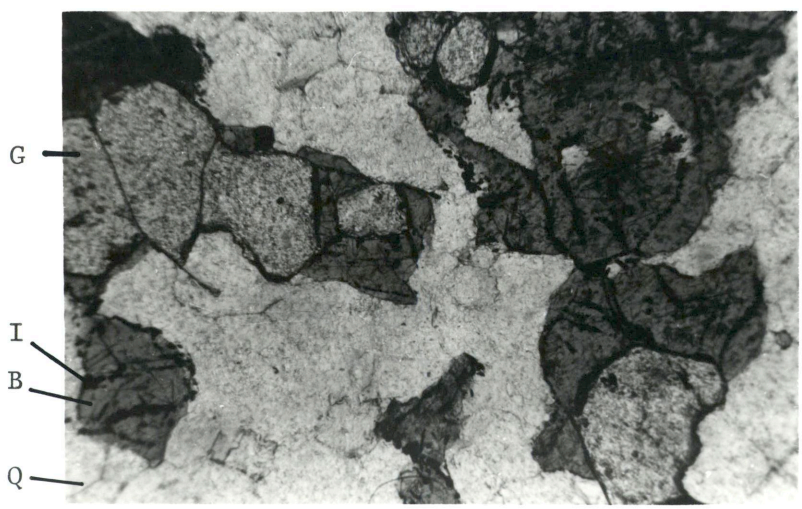

Fig. 3.2 Exsolution of ilmenite and rutile in and about biotite (4502/36.4)
Q = quartz, B = biotite, G = garnet, I = ilmenite. PPL.
Rutile closely resembles ilmenite in this photograph.

and garnet layers occur and, with biotite, define a weak foliation. Quartzo-feldspathic segregations are locally present, but commonly transect this foliation. Gahnite-quartz veins, similar to those described by Banerjee (1974), are locally abundant.

Biotite is commonly present as a selvage about gahnite, although not normally appearing to replace it, and they may be genetically related. Where intergrown with fine staurolite about gahnite (c.f. Sections 4.7 and 4.10), it may however be a reaction product. Most biotite is partly chloritized, and may show exsolution lamellae or coronas of rutile and ilmenite (Figure 3.2). This corona may be partly incorporated within the biotite grain, indicating retrograde recrystallization. It resembles the coronas produced by partial fusion of biotite, but lacks the glass, magnetite, and anhydrous silicates usually formed from such breakdown (Le Maitre, 1973; Busch et al., 1974; Brown, 1979).

Staurolite commonly replaces gahnite, as described in sections 4.7 and 4.10, but is usually in textural equilibrium with muscovite, garnet, biotite and sillimanite, indicating complete retrograde recrystallisation of these rocks.

3.3.3 Garnet Quartzite

The general prograde assemblage of this rocktype is quartz - garnet - biotite +_ sphalerite +_ galena +_ pyrrhotite +_ sillimanite +_ gahnite +_ amphibole but is commonly almost pure quartz and garnet. Where biotite and/or gahnite are abundant, these rock types may grade into the gneissic or gahnite-rich units, or with incresing sulphides into sulphide quartzites. Amphiboles (mainly of the cummingtonite group, but also actinolites) are rare, and are usually restricted to near the

amphibole subzones. They do not coexist with sillimanite or gahnite but rarely coexist with biotite. Small anhedral grains of monazite, rutile and allanite are local accessories and euhedral ilmenite is frequently abundant. Minor scheelite has been recently noted in garnet quartzites from the A-lode (D. Milton, pers. comm.) but was not found in this study.

Macro and meso-bands, down to about 2mm thick, are defined mainly by variations in contents of quartz, garnet, biotite and /or sulphides, and are not uncommon.

Retrogression has not greatly affected this rocktype, except for partial chloritization of biotite, locally abundant staurolite (sometimes as fine cross-cutting veinlets) in the outer parts of this zone (Figure 3.3), and minor amphiboles present in the inner parts of this zone.

3.3.4 Pyroxenoid-rich rocks

The common prograde assemblage is quartz - garnet - pyroxmangite - rhodonite - sphalerite - pyrrhotite - galena $\pm$ chalcopyrite $\pm$ manganoan hedenbergite $\pm$ fluorapatite $\pm$ loellingite $\pm$ biotite. By definition the pyroxenoids are restricted to, and biotite practically absent from, the pyroxenoid subzone which may, in places, be almost monominerallic.

The pyroxenoids in the WAL are pyroxmangite and rhodonite, both (Mn, Fe, Ca)SiO3, which are present in approximately equivalent amounts (see Appendix for analyses). Any pyroxmangite discussed below may, in part, be rhodonite, as they are very difficult to distinguish (see Section 4.9). Manganoan clinopyroxenes, near hedenbergite in composition, but with significant but variable johannsenite

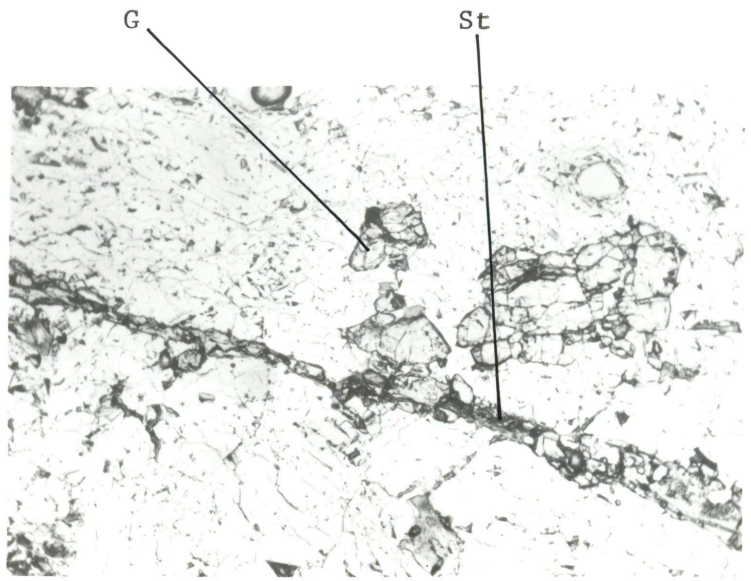

Fig. 3.3 Staurolite (St) vein in quartzite with garnet (G). (4918/85.3). PPL.

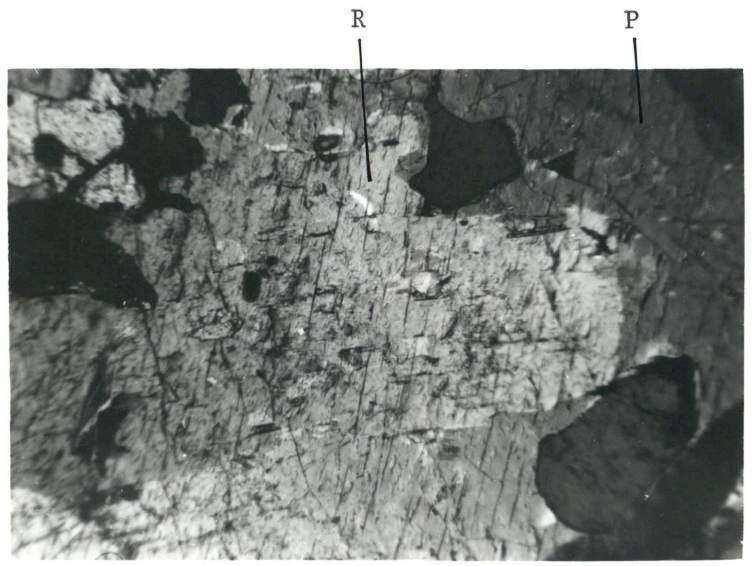

Fig. 3.4 Intergrowth of rhodonite (R) and pyroxmangite (P). (2/9A). XPL.

($CaMnSi_2O_6$), diopside and kanoite ($MnMgSi_2O_6$) components, are locally common and, being closely associated with the pyroxenoids are, for simplicity, commonly included as such in this thesis.

The pyroxenoids commonly occur in massive granoblastic aggregates, sometimes quite pure but usually with some interstitial sulphides, garnet and quartz. Intergrowths of rhodonite, pyroxmangite and hedenbergite are quite common (Figures 3.4 & 3.5). Occasional subplanar zones of finer pyroxmangite seem to represent healed fractures in massive pyroxenoids.

Fine to coarse-grained amphiboles* (cummingtonite and actinolite groups) are common as a direct replacement of pyroxmangite (Figures 3.6 & 3.7), preferentially along grain boundaries and cleavages, but are not always directly associated.

Pyrosmalite and manganpyrosmalite are less common retrograde alteration products of pyroxmangite, usually closely associated with very fine to coarse, apparently remobilised, galena (Figures 3.8 & 3.9). 'Sturtite', a poorly defined, non-crystalline, neotocite-like phase (Hodge-Smith, 1930; Portnov et al. 1978; Clark et al. 1978), is a much later stage alteration product of pyroxmangite.

Manganoan stilpnomelane is another uncommon retrograde phase found intergrown with sulphides within massive pyroxenoids (Figure 3.10). Allanite, sphene and biotite are other rare accessories in this zone.

3.3.5 Amphibole-rich units

The amphiboles are uncommon within garnet quartzites and pyroxenoid - rich rocks, but are most abundant in the selvage (amphibole subzones) between these two lithologies. The amphibole frequently occurs as patches, veins and small aggregates in garnet quartzites.

* Dannemorite ($Mn_2Fe_5Si_8O_{22}(OH)_2$) is usually the dominant end-member

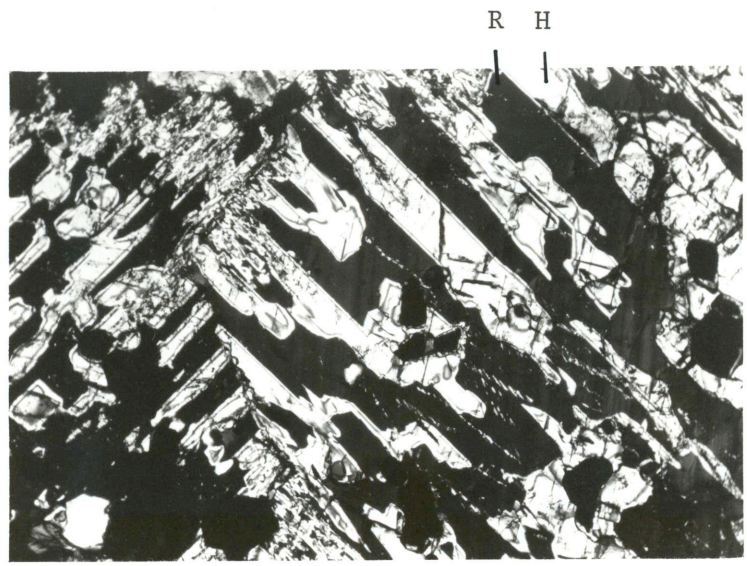

Fig. 3.5 Intergrowth of rhodonite (R) and hedenbergite (H) (4478/68.1) XPL.

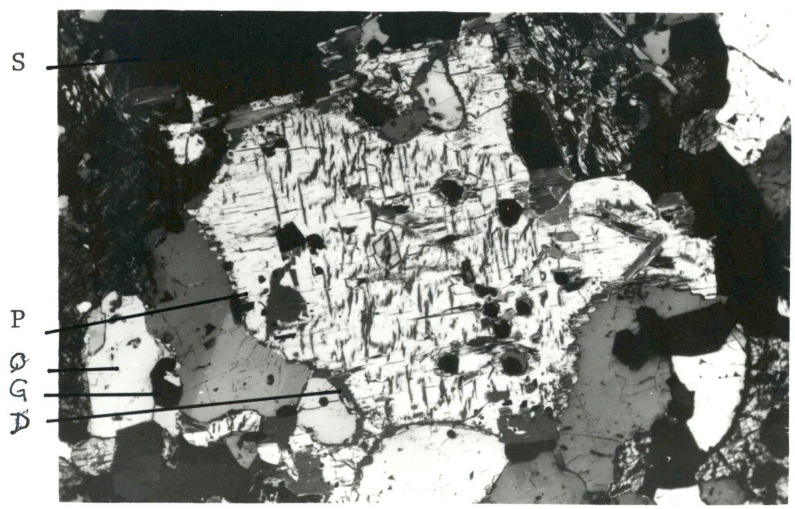

Fig. 3.6 Dannemorite (D) replacing pyroxenoid (P) along grain boundaries, fractures and cleavages, with quartz (Q), garnet (G) and sulphides (S). (4634/73.0). XPL.

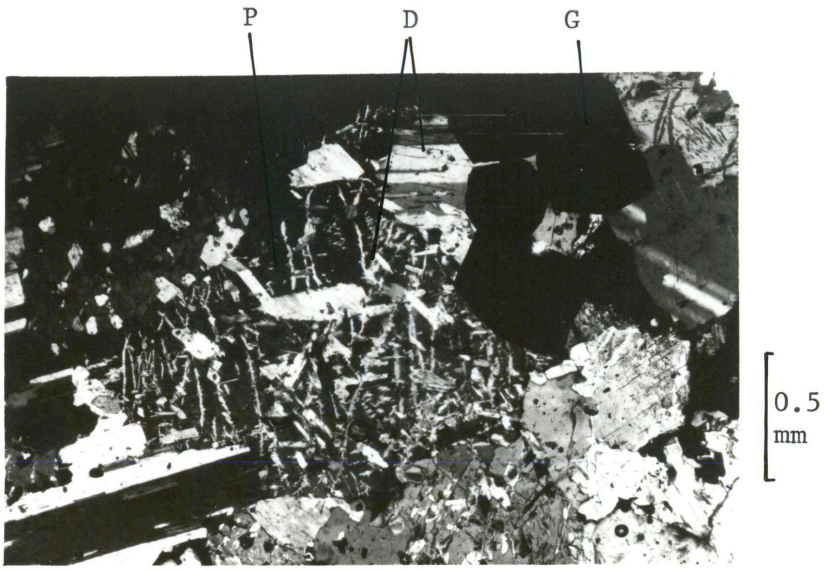

Fig. 3.7 Dannemorite (D) replacing pyroxenoid (P) along fractures and cleavages, with coarse dannemorite and garnet (G). (2/1B). XPL.

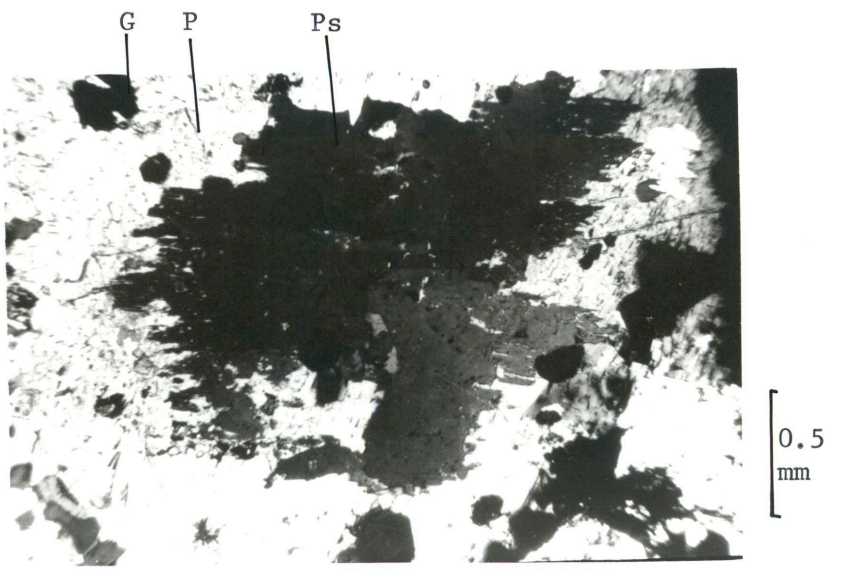

Fig. 3.8 Ragged pyrosmalite (Ps) crystal replacing pyroxenoid (P) with garnet (G) and sulphides (S). (2/9B). XPL.

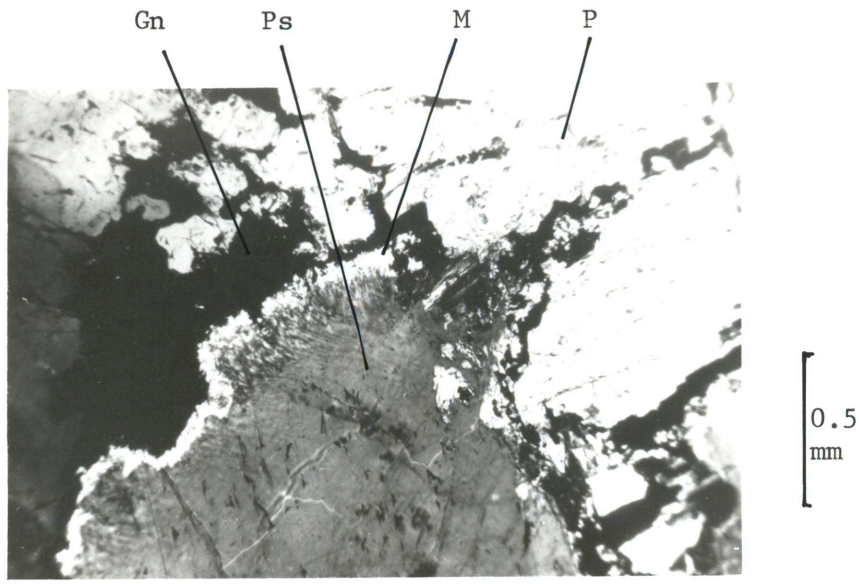

Fig. 3.9 Alteration of pyroxenoid (P) to pyrosmalite (Ps) with a fine-graded selvage of manganpyrosmalite (M) and galena (Gn). (2/9BA). XPL.

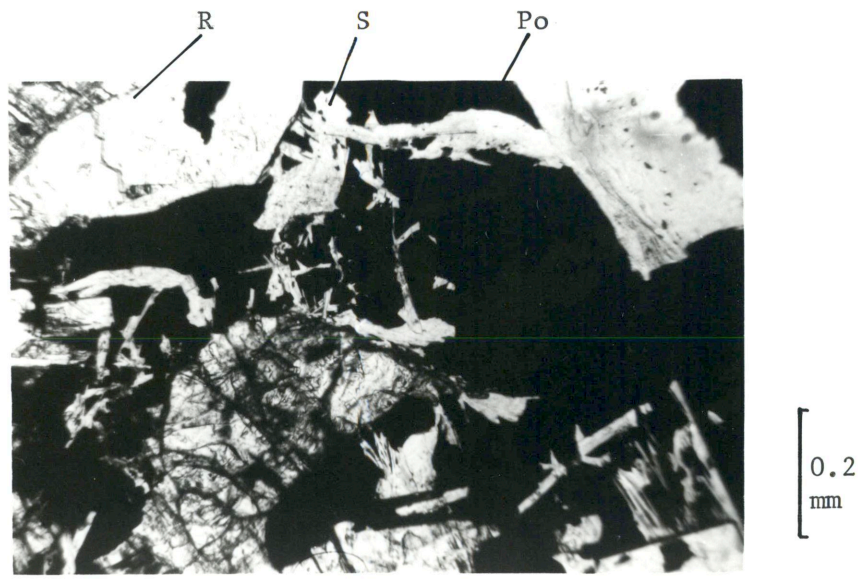

Fig. 3.10 Manganoan stilpnomelane (S) in pyrrhotite (Po) with rhodonite (R) (4483/116.1). PPL.

Garnet, biotite and rarely chlorite occur locally in equilibrium with the amphiboles but pyroxenoids are rare, and are usually highly altered, within this rock type. Amphiboles may occur in 'tension gashes' as fibrous aggregates with sulphides, which probably indicate late stage metasomatic activity related to shearing and fracturing (Figure 3.11). These associated sulphides are predominately sphalerite and pyrrhotite, but include minor galena and chalcopyrite. Small amphibole selvages separating garnet - rich and quartz - rich lithologies could also represent zones of shearing. Some irregularly shaped amphibole-sulphide (mainly sphalerite and pyrrhotite) aggregates in quartz are possible replacements of original pyroxmangite grains (Fig.3.13). Some amphiboles appear to have also replaced sulphides (predominantly sphalerite and pyrrhotite) (Figures 3.14 & 3.15). Some exhibit several generations of formation (Figures 3.16 - 3.18), as is shown by a variation in colour, grainsize or number of inclusions.

3.3.6 Sulphide Quartzite

These lithologies comprise the major sulphide bearing rocks of the A lodes and are most common in, or near, the amphibole - pyroxenoid zone. The most economically viable sections of the lode are thus dependant on the abundance of these sulphide quartzites. The major assemblage is quartz - sphalerite - galena - pyrrhotite $\pm$ garnet $\pm$ arsenopyrite / loellingite. They show signs of remobilisation into coarse grained veins and "pegmatites", as described by Lawrence (1967) and Maiden (1975), and are extremely inhomogenous. They grade into garnet quartzites, amphibole - rich or pyroxenoid - rich units, with increasing garnet, amphibole and pyroxenoid contents respectively.

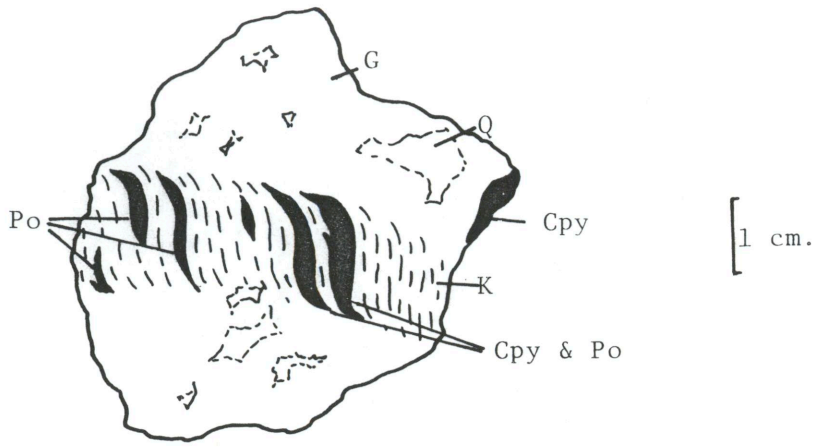

Fig. 3.11. Vein of cummingtonite/dannemorite (K), with chalcopyrite (Cpy) and pyrrhotite (Po), in coarse grained, remobilised garnet (G) and quartz (Q).

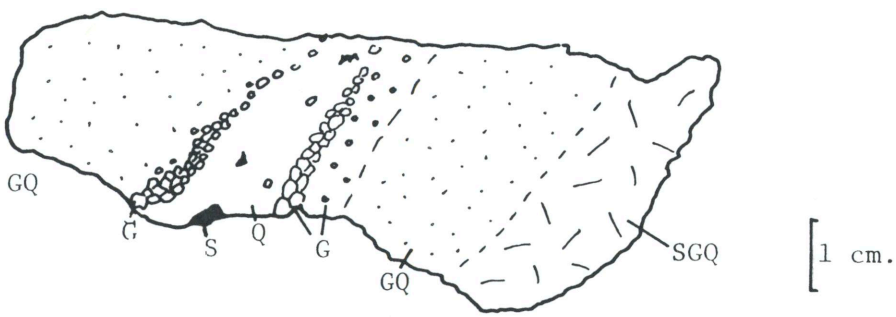

Fig. 3.12. Quartz vein (Q) with remobilised sulphides (S) and coarse grained garnet-rich selvages, in garnet quartzite (GQ), with sulphide--garnet quartzite (SGQ).

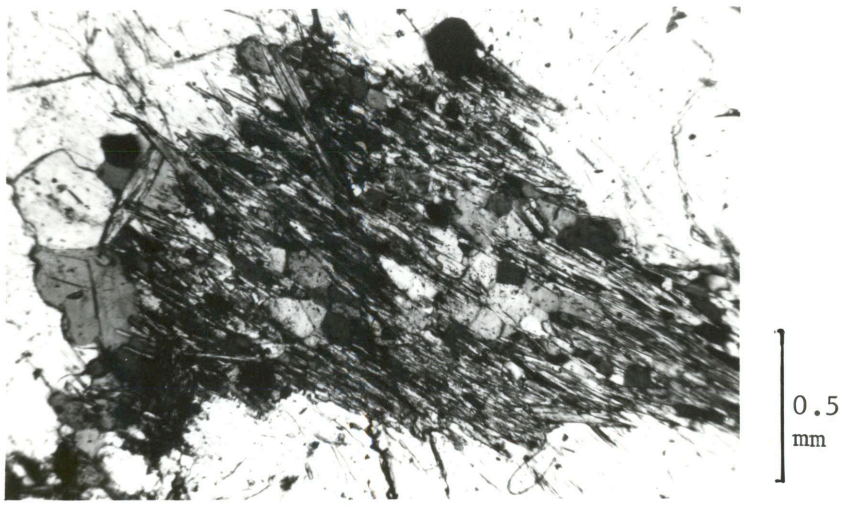

Fig. 3.13 Aggregate of dannemorite in quartz. (2/4A). XPL.

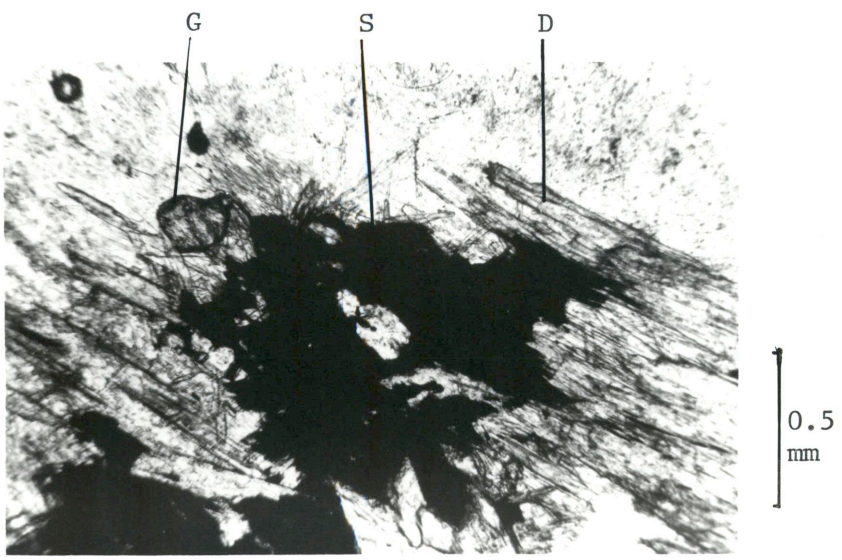

Fig. 3.14 Dannemorite (D) replacing sphalerite (S) with garnet (G). (2/3A). PPL.

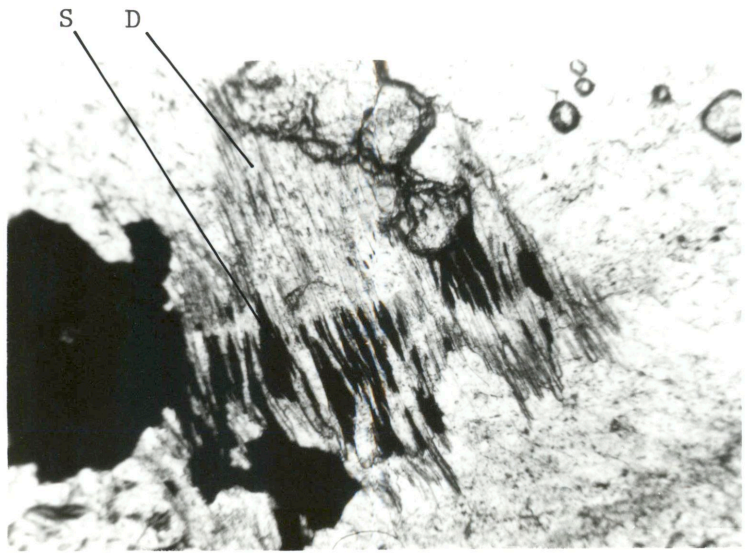

Fig. 3.15 Sphalerite (S) intergrown with dannemorite (D). (2/3A). PPL.

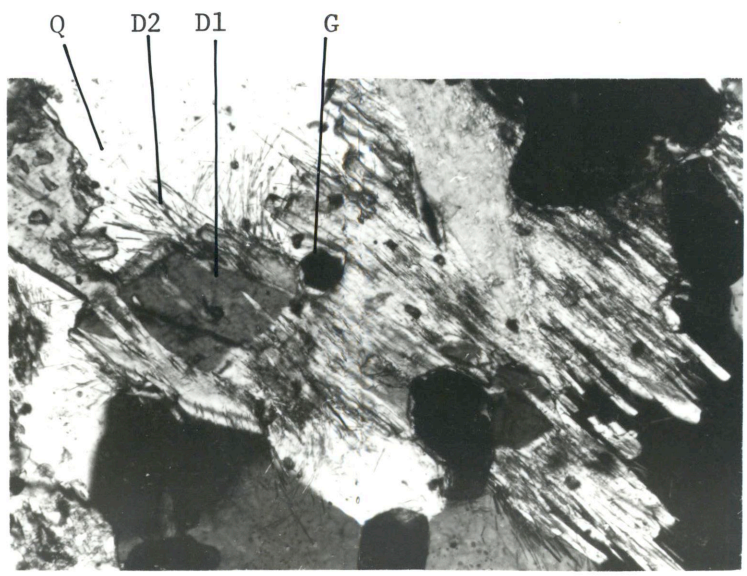

Fig. 3.16 2 generations of dannemorite (D1 and D2) with garnet (G) and quartz (Q). (4502/65.1A). XPL.

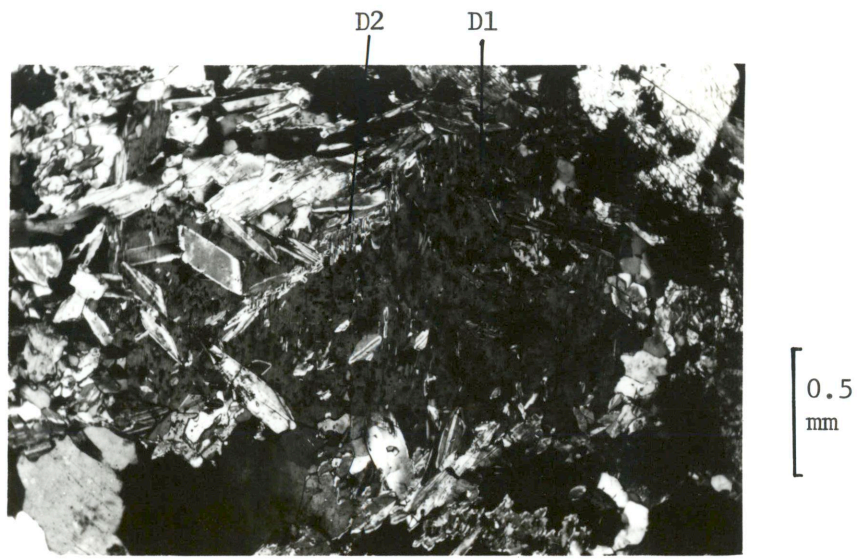

Fig. 3.17 2 generations of dannemorite (D1 and D2) with quartz (Q) and sphalerite (S). (4502/65.1B). XPL.

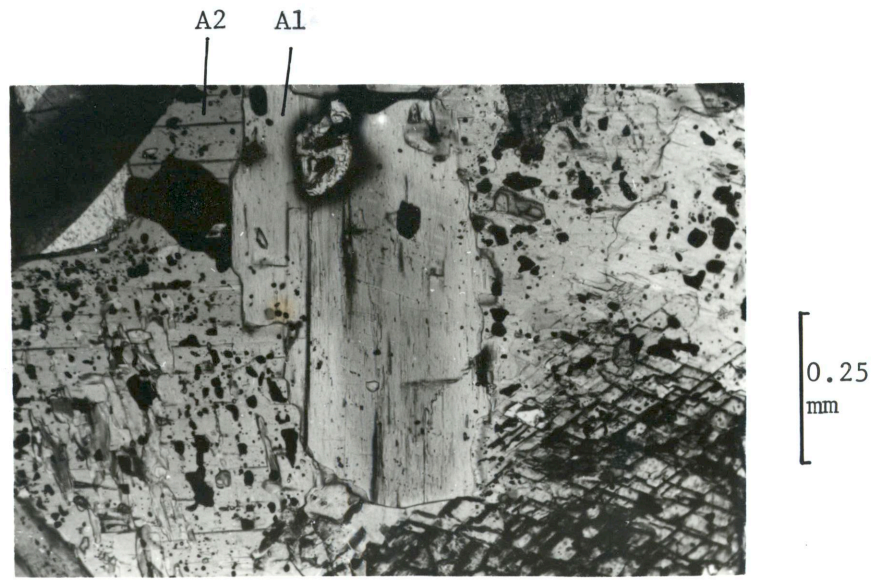

Fig. 3.18 2 generations of actinolite (A1 and A2) with sulphide inclusions and a pleochroic halo about allanite (top centre). (4478/85.8). PPL.

These rocktypes show good polygonal textures, indicative of annealing after high-grade metamorphism. Stanton (1964) and Lawrence (1973) have discussed the textures of the Broken Hill sulphide minerals, of which these are quite typical, in some detail.

3.4 Petrography of Minor Rocktypes

3.4.1 Introduction

Although few geologists still favour an epigenetic, hydrothermal origin for the orebodies (Johnson and Klingner, 1975) a limited amount of metasomatism is known to have occurred in close spatial association with them (Segnit, 1968; Hodgson, 1975; Phillips, 1978; Plimer, 1979). Many of the following minor rock types may result from such local metasomatism.

Pegmatoid rocktypes are a common, but minor, phase in these rocks. They appear to be principally anatectic in origin, but some metasomatism was probably involved in their formation (Plimer, 1976a).

Retrogressive lithologies, probably also partly metasomatic, are also discussed here.

3.4.2 Quartz-rich veins

Small veins rich in quartz (generally bluish, but sometimes white) are common throughout the lodes. They are mentioned by Dewar (1968), who found them to grade into the pegmatites and described them as metasomatic. These veins may be pure quartz, but commonly contain coarse sulphides $\pm$ gahnite $\pm$ garnet. Quartz-gahnite veins (Phillips, 1980) and "remobilised garnet quartzites" (Spry, 1978) are varieties. Blue and white quartz veins cutting garnet quartzites may result in

coarse garnet at the vein edges (Figure 3.12) (a phenomenon discussed by Walther and Orville, 1982) but these veins do not appear to have remobilised material to any great extent. Blue quartz is common in most lode rocks at Broken Hill, and was thought by some geologists to represent original chert (D. Milton, pers. comm.). Dewar (1968) however, showed blue quartz veins to be remobilised some distance from lode rocks, and found them to transect the stratigraphy. The blue and white forms of quartz are discussed in section 4.2.

3.4.3 Garnet Sandstone

'Garnet Sandstone' (see also section 2.5) consists of between 50 -95 vol.% garnet, with quartz, sulphides and amphiboles, and grades into garnet quartzite. This rocktype is not nearly as well developed in they WAL as in the lead lodes, where its abundance is related to the higher Ca and Mn there, and where it is correspondingly richer in Ca and Mn (Spry, 1978). Scheelite was not noted in garnet sandstones from the WAL, despite its abundance in garnet sandstones of the lead lodes and minor presence in the A lode garnet quartzites (D. Milton, pers. comm.).

Banding is usually absent, but quartz veins may be present. The rock is frequently quite friable. The lithology is restricted within, or close to, the sulphide - pyroxenoid - amphibole zone and varies from 5 cm to 1 m thick.

3.4.4 Quartzo-feldspathic rocks

This rock type, also termed lode pegmatite by mine geologists, migmatite or pegmatoid rock, is present in most drillholes in this lode. It most frequently occurs in the sillimanite gneiss and gahnite

rich rocks, but may occur in the garnet quartzites. Plimer (1976a) described similar lithologies, including veins, lenses, concordant and irregular masses, as being anatectic in origin, although Billington (1979) considered that they derived, in part, from acid pyroclastics. Phillips (1978) considered that this anatectic fluid resulted from biotite breakdown, perhaps instigated by an influx of CO_2 - rich fluid (Phillips and Wall,1982) and Plimer (1976a) suggested that the sulphides may form an impermeable barrier to these pegmatite fluids, localizing the pegmatite into "stratigraphic" horizons. Dewar (1968) and Hodgson (1975b) found that some of the pegmatites graded into quartz veins, but there is no evidence for this in the WAL.

The pegmatites found in this study show cross-cutting relationships to the WAL and thus it is postulated that the pegmatites derive from anatexis in the garnet - quartzite and sillimanite gneiss, the anatectic fluid being somewhat localized by the relatively impermeable sulphide-rich rocks.

3.4.5 Apatite - rich Rocks.

These unusual rock types are occasionally found as small bodies within the pyroxenoid-amphibole zone. They are quite variable in composition but a common assemblage is quartz - garnet - fluorapatite $\pm$ pyroxenoids $\pm$ biotite $\pm$ galena, and they closely resemble garnet quartzites.

Their genesis is uncertain, but Stanton (1976e) found a strong correlation between P and S in the Broken Hill lodes. Fluorapatite is quite common throughout the WAL (Birch et al. 1983), and is considered to represent sedimentary apatite accumulations derived from phosphate-rich ore - bearing fluids.

3.4.6 Remobilised Sulphides

This is a minor, but important and widespread, rock type throughout the WAL. It is usually coarse grained, and has galena - sphalerite - pyrrhotite - quartz ± garnet ± pyroxmangite ± chalcopyrite as a common assemblage.

Macroscopic structures and textures indicate that this rocktype derived from metamorphic remobilization (principally mechanical but aided by fluid activity) of disseminated sulphides similar to the process described by Rui and Bakke (1973).

3.5 Petrography of Retrograde Lithologies

The effect of retrogression is highly dependent on the nature and composition of the various rock types. Small shear zones may be present throughout the lode, but seldom completely obliterate the original mineral assemblage or texture. They grade from chlorite ± calcite ± pyrite in joints, to highly sericitized or amphibolitized zones up to 3 m thick (section 3.3.5). Attempts by mine geologists and the author to define the limits of a RSZ in the western part of the WAL, and relate it to the mineralogical zones defined here, proved inconclusive. Retrogression is quite pervasive through the WAL, however, and can be identified in practically all major rocktypes, as described above.

The pegmatites are extensively sheared and sericitized, and are commonly closely related to shear zones. Partial melts could conceivably exploit such intermittently active zones of weakness, or alternatively, shearing could be promoted by the locally high fH_2O (Griggs, 1967) present during cooling and crystallization of the

pegmatites. Various breccias, often associated with these quartzo-feldspathic rocktypes, were thought by Billington (1979) to have a sedimentary or pyroclastic origin but no evidence was found in this study for such an origin, and they seem more likely to be syn-deformational, formed by brittle deformation and metasomatism during shearing.

Gahnite rich rocks may be almost completely retrogressed to quartz - sericite - chlorite over a few metres. Large thicknesses of amphibole-rich rock appear to originate from retrogressed pyroxmangite, and some gradations can be seen on a macroscopic scale.

The patchy retrogression with partial replacement of prograde minerals is typical of retrograde metamorphism (Yardley, 1981a) and is due to widely variable fH_2O.

Chapter 4. Mineralogy.

4.1 Introduction.

The mineralogy of the major gangue minerals in the WAL was studied by transmitted and reflected light microscopy, electron microprobe analysis, and x-ray diffraction. Methods of chemical analysis are described in Appendix I, the microprobe analyses are listed in Appendix II, and average analyses are listed in Table 4.1.

All Fe determined in the microprobe analyses was calculated as Fe^{2+}, as Fe^{3+} was assumed to be negligible. Fe^{2+}/Fe^{3+} varies from about 20 to 60 in WAL garnets, if the assumptions described in Section 4.3 are considered to be valid. Fe^{2+}/Fe^{3+} was shown by Plimer (1977b) to average 19 in metasediments between the Broken Hill lodes, 12.9 in wallrock metasediments, 8.7 in wallrock biotites and 11.5 in wallrock garnets.

All percentages are quoted as weight percent unless otherwise stated.

4.2 Quartz.

Quartz is the most abundant mineral present in the WAL and surrounding rocktypes. It can be subdivided into blue and white varieties by appearance in hand specimen.

Most of the coarser, prograde quartz tends toward an opalescent blue colour, with a waxy or greasy lustre. The blue colour can only be observed in reflected light but, in thin section, undulose extinction and microfracturing are seen to be very abundant. A fine, diffuse cross - hatching is commonly seen, indicating a mosaic structure to be present, with domains of about 10 to 50 microns (Figure 4.1). This

Table 4.1 Average analyses of various mineral phases in the WAL

Mineral	Ilmenite	Chlorite	*Green Biotite	Muscovite / Phengite	Paragonite	Pyrosmalite	Manganpyrosmalite	Greenalite	?Berthierine	Sturtite/ Hisingerite	Stilpnomelane
No. analyses	4	5	6	4	2	5	2	1	2	4	2
SiO_2	.01	23.38	33.24	47.64	45.88	34.34	32.05	29.35	28.09	40.34	45.68
TiO_2	51.95	.03	.09	.17	.01	.00	.00	.00	.00	.01	.03
Al_2O_3	.00	22.11	18.26	32.81	36.67	.02	.03	8.91	16.13	.10	4.66
FeO	44.55	32.95	26.15	2.88	2.42	28.24	22.64	35.90	33.44	22.40	30.73
MnO	2.70	.34	.25	.09	.18	23.27	26.88	.90	.74	18.89	9.88
MgO	0.41	7.80	5.62	.77	.17	.46	.25	3.97	6.84	.31	1.12
CaO	.00	.01	.00	.01	.18	.08	.14	.53	.16	0.43	.00
Na_2O	.00	.01	.10	.12	6.51	.04	.00	.02	.03	4.62	.04
K_2O	.00	.01	8.80	10.53	1.39	.01	.00	.10	.07	.12	4.15
ZnO	.12	.24	.00	.16	.10	.01	.01	.05	.13	.03	.04
Total	99.74	86.89	93.83	95.17	93.52	86.47	82.01	79.73	85.63	87.24	96.33
Si	.003	5.208	5.367	6.387	6.058	6.083	6.026	1.837	1.588	.969	11.908
Ti	.991	.004	.011	.018	.001	.000	.000	.000	.000	.000	.007
Al	.000	5.818	3.476	5.169	5.709	.003	.007	.657	1.075	.003	1.431
Fe	.945	6.180	3.532	.333	.265	4.185	3.545	1.879	1.581	.458	6.699
Mn	.058	.068	.035	.010	.020	3.494	4.290	.048	.035	.379	2.182
Mg	.016	2.551	1.353	.154	.034	.122	.071	.370	.576	.013	.434
Ca	.000	.003	.001	.002	.026	.016	.029	.035	.010	.011	.000
Na	.000	.002	.032	.032	1.692	.006	.001	.003	.003	.096	.021
K	.000	.002	1.813	1.816	.236	.001	.000	.008	.005	.002	1.381
Zn	.001	.039	.000	.016	.010	.001	.002	.002	.005	.001	.008
O	3	28	22	22	22	20	20	7	7	3	36
No. atoms	5.014	47.875	37.992	35.935	36.051	33.908	33.970	11.840	11.879	4.932	60.071

* Includes 0.74% Cl_2O, 0.58% F_2O, 0.166 atoms Cl, 0.208 atoms F

Table 4.1 (Cont.)

Mineral	*Fluorapatite	Sphene	Calcite	Almandine	Spessartine	Biotite	Sillimanite	Orthoclase	Anorthite	Gahnite
No. analyses	2	5	2	14	14	14	5	5	5	26
SiO_2	.74	30.82	.04	36.81	37.02	37.35	37.33	63.57	43.44	.02
TiO_2	.00	33.92	.00	.01	.04	1.42	.12	.00	.03	.04
Al_2O_3	.00	2.45	.01	20.34	20.37	14.43	61.83	19.57	35.39	56.55
FeO	.00	2.24	1.28	33.65	12.73	18.71	.37	.02	.02	12.12
MnO	.56	.74	6.22	4.99	24.16	.82	.01	.00	.06	.18
MgO	.32	.27	.11	2.65	.38	11.83	.00	.00	.08	1.30
CaO	52.03	27.61	47.65	.75	5.04	.01	.01	.04	19.96	.00
Na_2O	.20	.10	.01	.01	.05	.12	.01	0.45	.38	.39
K_2O	.00	.01	.00	.00	.01	9.30	.00	15.59	.05	.00
ZnO	.00	.01	.01	.05	.03	.12	.02	.00	.00	28.82
Total	92.98	98.17	55.33	98.66	99.82	94.11	99.70	100.99	99.41	99.41
Si	.062	1.028	.001	3.017	3.016	5.765	1.012	2.946	2.028	.001
Ti	.000	.848	.000	.001	.003	.165	.001	.000	.001	.001
Al	.000	.096	.000	1.962	1.957	2.629	1.974	1.069	1.946	1.985
Fe	.000	.044	.019	2.286	.868	2.417	.008	.000	.001	.302
Mn	.042	.020	.091	.343	1.669	.107	.000	.000	.003	.005
Mg	.042	.013	.003	.324	.046	2.722	.000	.000	.006	.058
Ca	4.744	.983	.886	.063	.439	.001	.000	.002	.978	.000
Na	.051	.008	.000	.002	.007	.036	.000	.041	.035	.011
K	.000	.000	.000	.000	.001	1.833	.000	.922	.003	.000
Zn	.000	.000	.000	.003	.002	.014	.000	.000	.000	.634
O	12	5	1	12	12	22	5	8	8	4
No. atoms	19.773	8.040	1.999	20.002	20.007	37.689	7.995	12.980	13.001	6.995

* (includes 38.97% P_2O_5, 0.06% Cl, 2.809 atoms P, 0.010 atoms Cl)

** (includes 1.75% PbO)

Table 4.1 (Cont.)

Mineral	*Hercynite	Cummingtonite & Dannemorite	Actinolite	Tirodite	Low - Mg Pyroxmangite	Magnesian Pyroxmangite	Rhodonite	Hedenbergite	Kanoite	Staurolite
No. analyses	5	12	7	5	6	5	10	11	6	8
SiO_2	.03	48.33	50.44	52.48	47.48	49.05	46.54	49.54	49.60	27.90
TiO_2	.00	.02	.09	.01	.01	.01	.01	.01	.01	.31
Al_2O_3	57.45	.10	1.22	.20	.01	.01	.01	.11	.09	51.84
FeO	22.19	29.46	21.65	17.41	21.14	17.81	16.94	17.70	17.79	11.29
MnO	.14	9.31	2.60	10.39	26.13	27.16	27.80	8.22	19.62	.13
MgO	1.44	6.07	8.92	12.93	1.44	2.88	.65	4.88	10.00	1.38
CaO	.00	1.37	10.66	3.30	3.78	4.31	6.82	18.19	2.61	.00
Na_2O	.00	.03	.06	.07	.02	.01	.01	.04	.04	.10
K_2O	.01	.01	.12	.02	.00	.00	.01	.01	.01	.00
ZnO	18.02	.14	.23	.21	.20	.22	.20	.11	.27	3.54
Total	99.40	94.86	95.98	97.03	100.21	101.45	99.00	98.79	100.03	96.49
Si	.001	7.915	7.808	7.949	1.009	1.014	1.002	2.008	1.999	7.909
Ti	.000	.002	.010	.001	.000	.000	.000	.000	.000	0.067
Al	1.985	.020	.216	.037	.000	.000	.000	.005	.005	17.326
Fe	.546	4.094	2.824	2.205	.376	.308	.305	.604	.600	2.676
Mn	.004	1.291	.347	1.335	.471	.476	.507	.283	.670	.032
Mg	.063	1.457	2.034	2.919	.046	.089	.021	.290	.601	.583
Ca	.000	.239	1.767	.537	.086	.095	.158	.793	.113	.000
Na	.000	.006	.009	.010	.000	.000	.000	.001	.001	.055
K	.000	.001	.012	.002	.000	.000	.000	.000	.000	.000
Zn	.390	.028	.026	.023	.003	.003	.003	.003	.008	.745
O	4	23	23	23	3	3	3	6	6	46
No. atoms	6.989	38.053	38.053	38.019	4.991	4.986	4.997	4.988	9.997	75.393

* includes 0.12% Cr_2O_3 (0.003 atoms Cr)

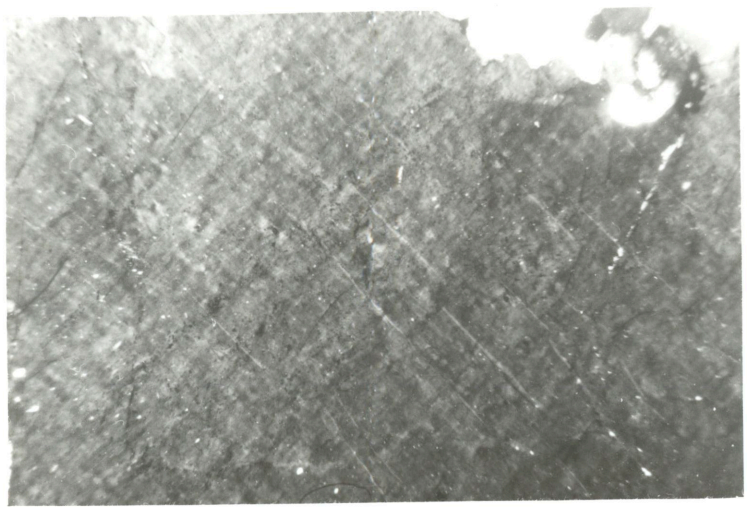

Fig. 4.1 Blue quartz, showing a fine cross-hatching, and some recrystallisation (top right). XPL.

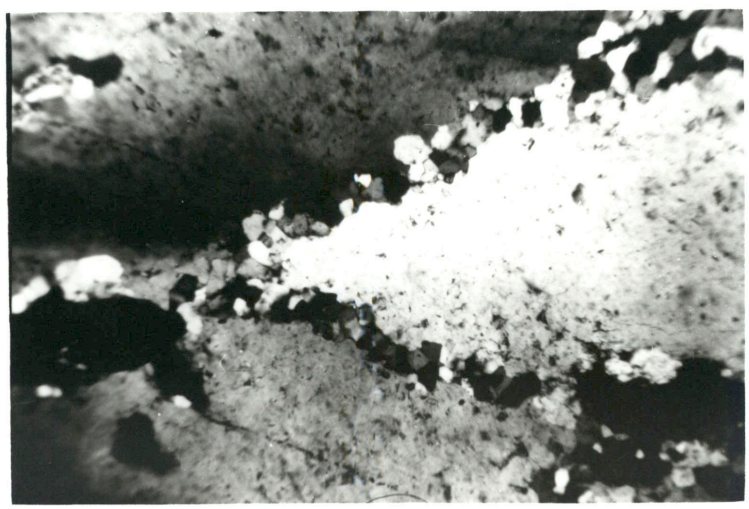

Fig. 4.2 Blue quartz (with inclusions) recrystallised along grain boundaries (4502/20.4).

could be related to fine twinning resulting from inversion of α to β quartz during cooling (similar textures were observed by the author in some volcanic quartz). Various inclusions are commonly abundant but are usually difficult to identify due to their size - usually less than 5 microns and often less than 1 micron, but also up to 250 microns. These appear to include rutile, sulphides (principally pyrrhotite and sphalerite), biotite, amphiboles, gahnite, garnet, sericite and, most abundantly, fluid inclusions. Stringers or planar zones of inclusions, often sulphides, probably represent Boehm lamellae (Dietrich, 1971), and are locally common. These lamellae are due to movement of material into small fractures or cleavages in quartz, followed by the healing of these structures. The blue quartz commonly shows signs of retrograde recrystallization along fractures and grain boundaries to white quartz (Figure 4.2).

White quartz is finer grained (Table 3.1), less strained, and has fewer inclusions. It varies from milky to clear, depending upon the abundance of fluid incusions.

Wise (1981) attributed the colour of blue quartz to three principal causes :

I. Scattering of light by closely spaced microfractures.

II. Scattering or partial reflection from inclusions.

III. Colouration by titanium.

i) Jayaraman (1939) showed that the size of the domains produced by microfracturing must be of similar orders of magnitude to the wavelength of light (ie. 0.2 to 0.5 microns) in order to produce scattering or partial reflection of light (the Tyndall effect).

ii) Colloidal sized inclusions of rutile, tourmaline, ilmenite, magnetite, zoisite, apatite and bubbles have all been cited as

possible causes of colouration by scattering or partial reflection of light (Dietrich, 1971). Rutile is usually one of the most abundant inclusions, and has been noted in much blue quartz from Broken Hill by Ramdohr (1950), Stillwell (1957), Segnit (1961) and Spry (1978) although little blue quartz studied by the author contained rutile. Some white quartz was also found to contain fine rutile and other similar inclusions to those found in blue quartz.

iii) At high temperatures quartz may contain considerable titanium in solid solution (Ramdohr, 1950), and this is largely exsolved on cooling, often as reticulated needles of rutile (Wise, 1981). Plimer (pers. comm. to Billington (1979)) and the author failed to detect Ti in quartz by electron microprobe analysis. Fe, in contrast, is variable but can be up to 0.1% FeO in blue quartz, suggesting the possibility of blue colouration by Fe2+ - Fe3+ charge transfer, as in blue kyanite (Faye & Nickel, 1969), and blue sillimanite (Rossman et al. 1982).

As no evidence exists for Ti in the lattice, and inclusions are not ubiquitous, an origin either from scattering of light by microfractures, or from an Fe-doped colour centre, is feasible.

4.3 Garnet

The garnets in and around the WAL are basically solid solutions of almandine and spessartine, with relatively small grossular and pyrope contents (Figs. 4.3 & 4.4 & Table 4.1). Average analyses indicate a small Al deficiency and, assuming : i) that this is not a systematic error in calculation, ii) that stoichiometry should be perfect, iii) that this deficiency is all due to Fe3+ substitution for Al, then

Fig. 4.3 Composition of Garnets. Triangles represent samples from the pyroxenoid subzone, asterisks the amphibole subzone, circles the garnet quartzite, squares the gahnite zone and crosses the sillimanite gneiss. Molecular %.

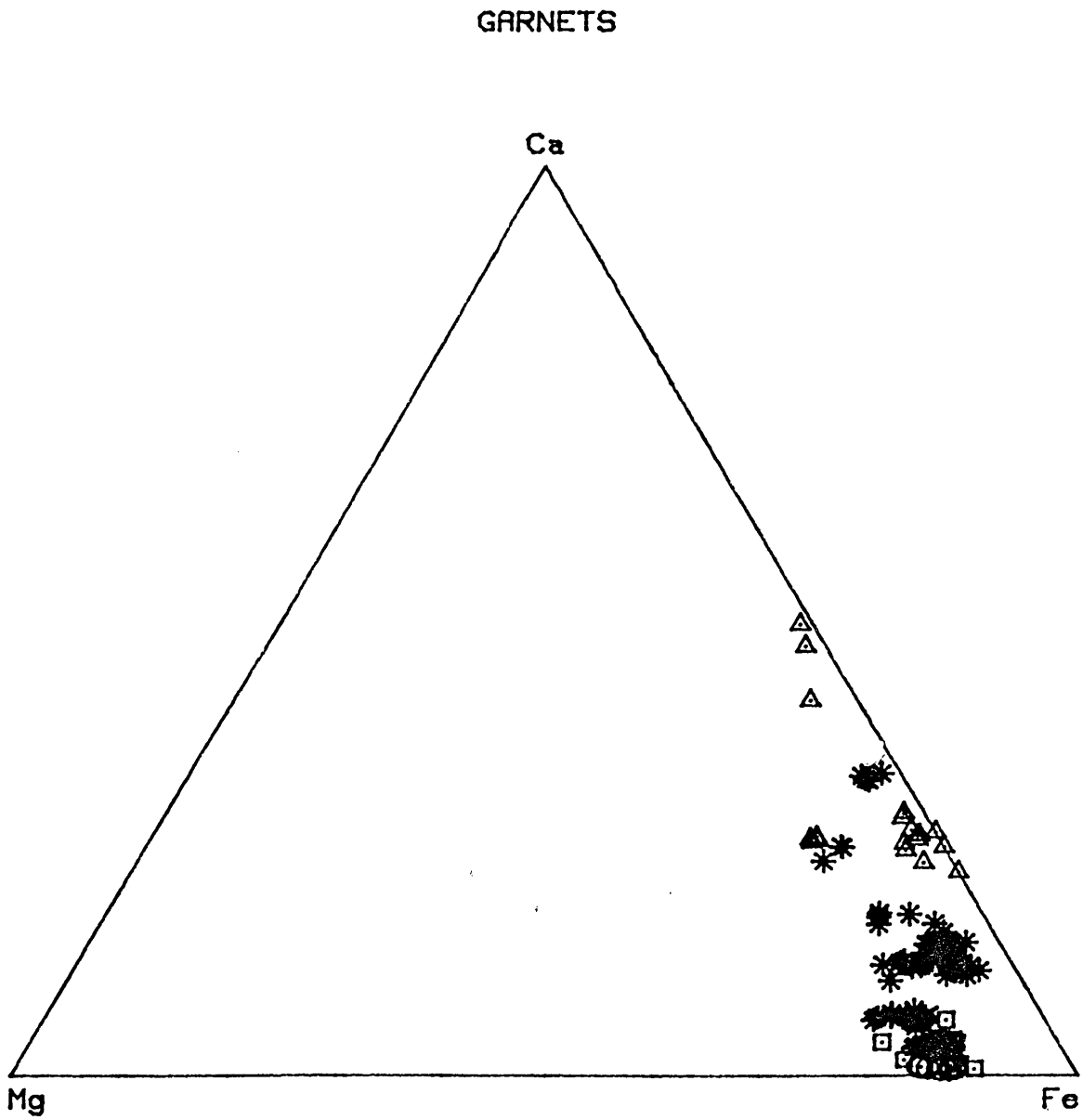

Fig. 4.4 Composition of Garnets. Triangles represent samples from the pyroxenoid subzone, asterisks the amphibole subzone, circles the garnet quartzite, squares the gahnite zone and crosses the sillimanite gneiss. Molecular %.

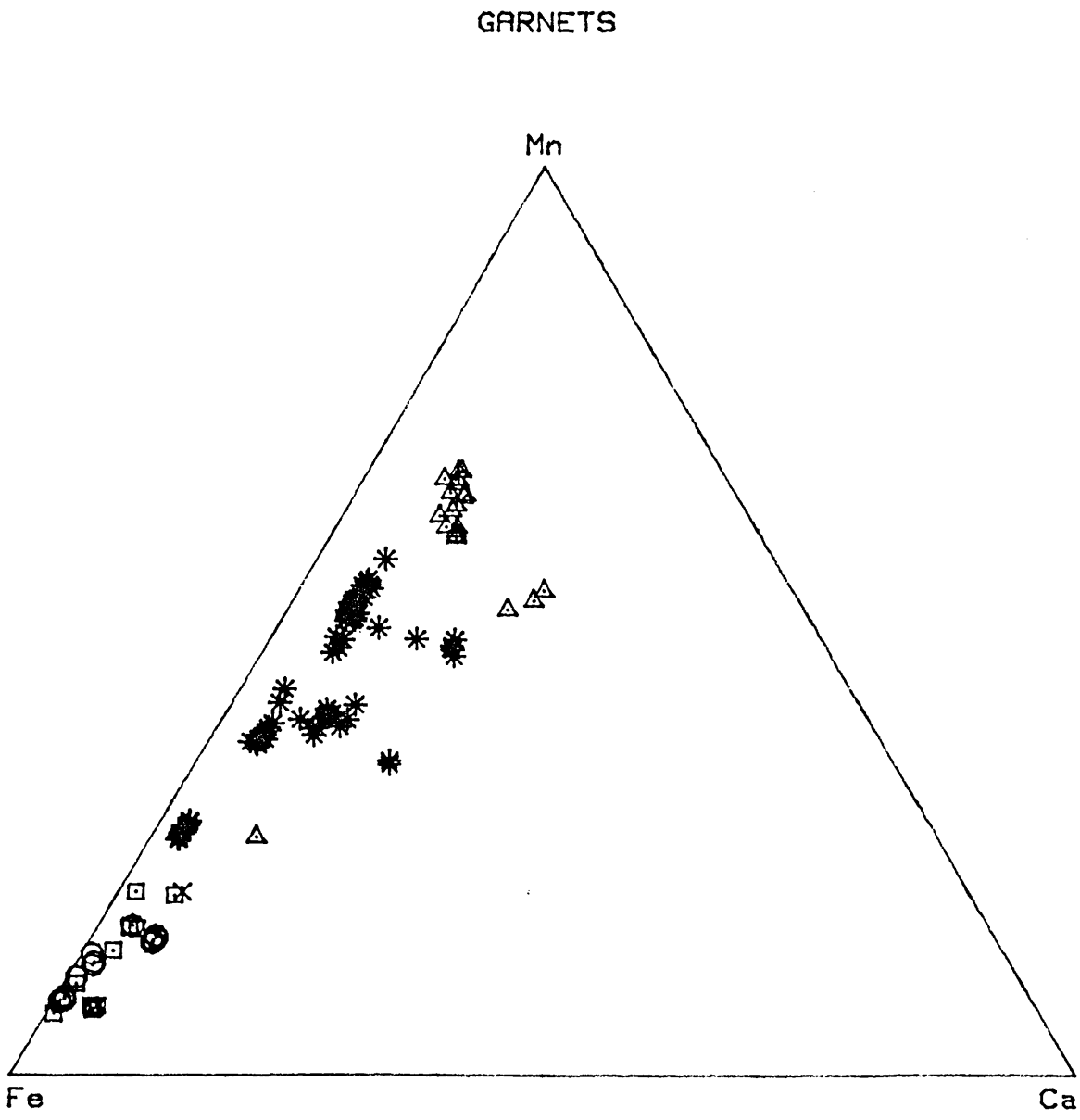

Fe^{2+}/Fe^{3+} could be calculated as c.60 in almandine and 20 in spessartine. Mn^{3+} was assumed to be negligible, as Mn has a lower oxidation potential than Fe, and thus the calderite ($Mn_3Fe_2(SiO_4)_3$) component was ignored. Using the method of Rickwood (1968), almandine was found to be the major component of most WAL garnets, comprising up to 90 mol%, but spessartine can be up to 68 mol%, grossular up to 23 mol% and pyrope up to 18 mol%. Figures 4.3 and 4.4 indicate almost constant ratios of Mn/Ca and Mg/Fe. A small schorlomite component, indicated by a minor Ti content, is locally present, but Cr and the uvarovite component was not detected in the few samples tested. A small amount of Zn, up to .14 wgt% ZnO is present in some garnets.

Zoning is a common feature of these garnets and an example of the chemical variation is shown in Fig. 4.5. Mn is nearly always enriched in the garnet rims, while Mg shows a corresponding depletion. Mg-rich rims were found only once. Ca and Fe are more variable, but most commonly show depletion in garnet rims. This zoning, with high Mn rims, is typical of that termed reverse, retrograde growth, or diffusion zoning, and is commonly found in garnets of high metamorphic grades (Bethune et al. 1975 ; Tracy, 1982). It usually indicates homogenization of original garnet growth zoning (normal zoning, (Hollister, 1966)), followed by later diffusion of components between the garnet rim and adjacent minerals (Grant & Wieblen, 1971; Tracy, 1982). In the WAL this reverse zoning appears to be better developed in amphibole - bearing rocks, and was probably formed by Mn - metasomatism and/or partial retrograde re-equilibration of garnets with amphiboles.

The garnets vary from pinkish orange to purplish pink in hand specimen and pale pink to colourless in thin section. Some garnets

Fig. 4.5 Composition zoning in a garnet from the amphibole subzone (4502/65.1A).

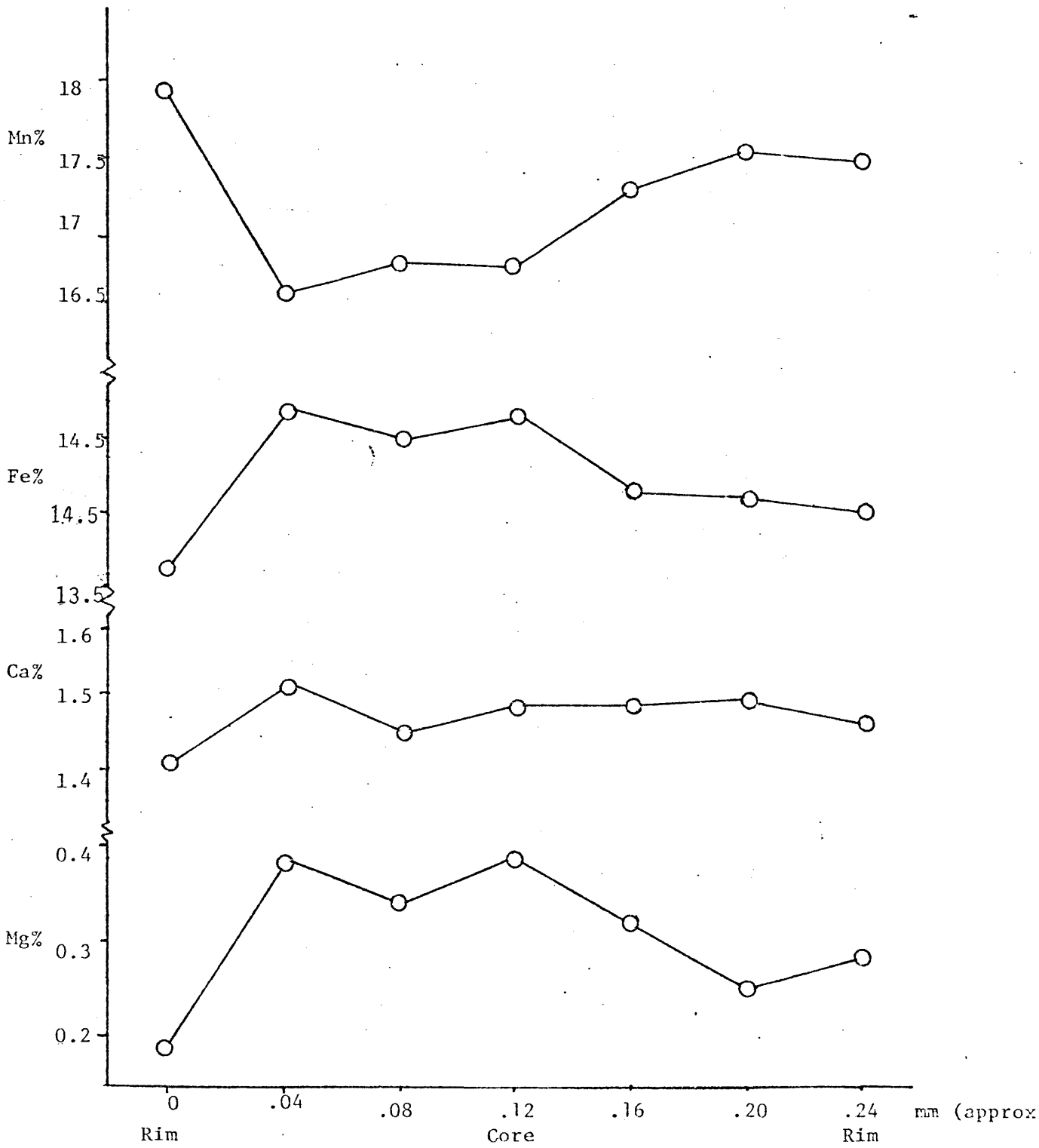

exhibit colour zoning, but microprobe analysis failed to indicate consistent chemical correlation with this and so variations in oxidation states or trace elements may be involved.

The cores of medium to large garnets are commonly highly poikiloblastic, with a less poikiloblastic overgrowth formed more slowly than the cores (Spry, 1969). These garnets usually show slight reverse zoning, and this may indicate either: i) the overgrowth formed during retrogression or ii) the overgrowth formed during the second of the two high grade metamorphic events, with homogenization and later overprinting of reverse zoning during retrograde re-equilibration.

The presence of fine ilmenite inclusions within some garnet is indicative of replacement of Ti-rich biotite (Figure 4.32).

The garnets are usually euhedral to subhedral, but may be quite amoeboid in texture when highly poikiloblastic, and fracturing and microfaulting, due to retrograde shearing, is common (Figure 3.1).

In contrast to most other ferromagnesian phases of the lode, garnet very rarely shows any alteration, but instances of breakdown to chlorite and minor replacement by amphiboles and sericite were noted.

4.4 Biotites

Plots of trioctahedral micas indicate that they nearly all fall within the field of biotite, as defined in Deer et al (1966), although some are phlogopite (Figure 4.6). Some, including the phlogopites, fall slightly outside the normal range, showing less than 2 Al / formula unit (22 oxygens), but most have a high siderophyllite ($K_2Fe_4Al_6Si_4O_{20}(OH)_4$) content. An average biotite analysis is shown in Table 4.1. The manganese and zinc contents (indicative of a

Fig. 4.6 The relation between Fe/Fe + Mg and Al (atoms/22 oxygen) in biotites, showing the biotite field as defined by Deer et al. (1966). Crosses represent biotites from the sillimanite gneiss, squares are from the gahnite zone, circles the garnet quartzite, asterisks the amphibole subzone, triangles the pyroxenoid subzone and the five-pointed stars are green biotite.

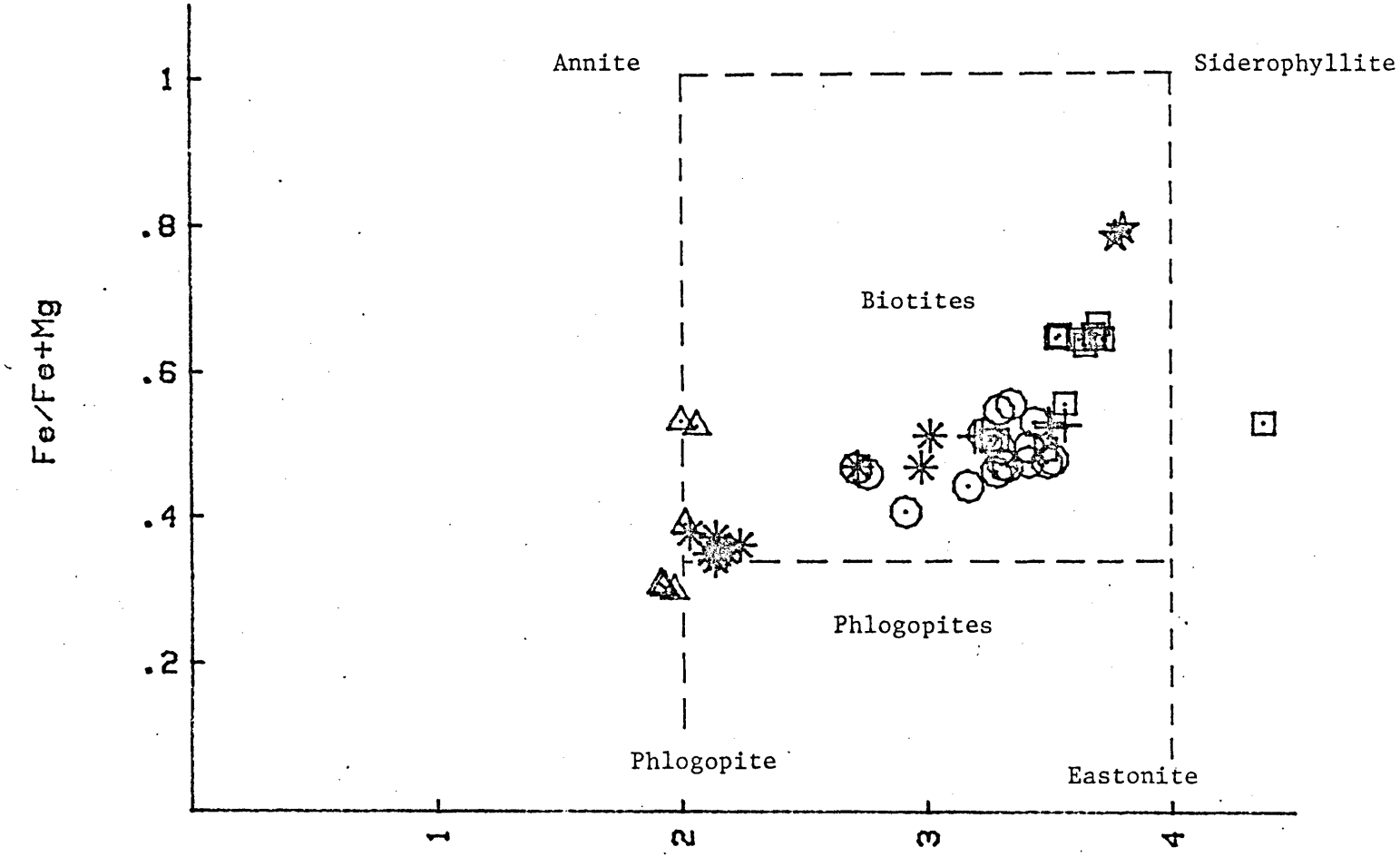

hendricksite ($K_2(Zn,Mn)_6Al_2Si_4O_{20}(OH)_4$) component (Frondel & Ito, 1966)) are usually very low (up to 2.4% MnO and 0.33% ZnO). The Fe and Al contents show a positive correlation (Figs. 4.6 and 4.7), in contrast to whole-rock trends (Section 5.2.1). This could be due, in part, to instability of the annite component (Wones et al. 1977), but sulphurization of biotite, discussed further in Section 5.3.2, appears more important. Most biotite with Al < 2.5 is Mg-rich and coexists with amphiboles, into which Fe may be preferentially partitioned.

TiO_2 is variable, ranging from 0 to 3.2% TiO_2, and this is reflected strongly in the colour and pleochroism. Ti-rich biotites are deep red-brown and strongly pleochroic, while Ti-poor biotites are pale yellow-brown, or rarely green, with slight pleochroism (green biotite is distinguished from chlorite by its higher birefringence). The Ti content is closely related to Fe/Mg + Fe (Figure 4.8), in contrast to the whole-rock trends (Section 5.2.1), and is discussed further in Section 5.3.2.

Halogens were not routinely determined by the microprobe analysis programme used but the result of a few selected separate analyses are shown in Table 4.2. Fluorine is usually quite high, up to 3.0% F, while Cl is usually much lower, but the rare green biotites contain up to 0.8% Cl.

The low alkali contents of most of these biotites may be due to either volatilization under the electron beam, or perhaps some mixed layering of chlorite in biotite (Mohr & Newton, 1983). One such low alkali biotite contains 1.4 atoms of K per 22 oxygen and 1.3 wgt.% ZnO and still appears homogenous. Bachinski & Simpson (1984) found that this is not uncommon in even quite pure and homogenous Si-deficient biotite, due to substitution of divalent cations for K.

Ilmenite and rutile are very common as exsolution products in, and as coronas about, biotite grains (Figure 3.2) and they result from

Fig. 4.7 Relation between Mg, (Fe & Mn) and Al in trioctahedral micas, showing the compositional limits from Foster (1960). Biotites from the sillimanite gneiss are represented as crosses, from the gahnite-rich zone as squares, the garnet quartzite as circles, the amphibole subzone as asterisks and the pyroxenoid subzone as triangles. Green (retrograde) biotites are represented by diamonds. Molecular %.

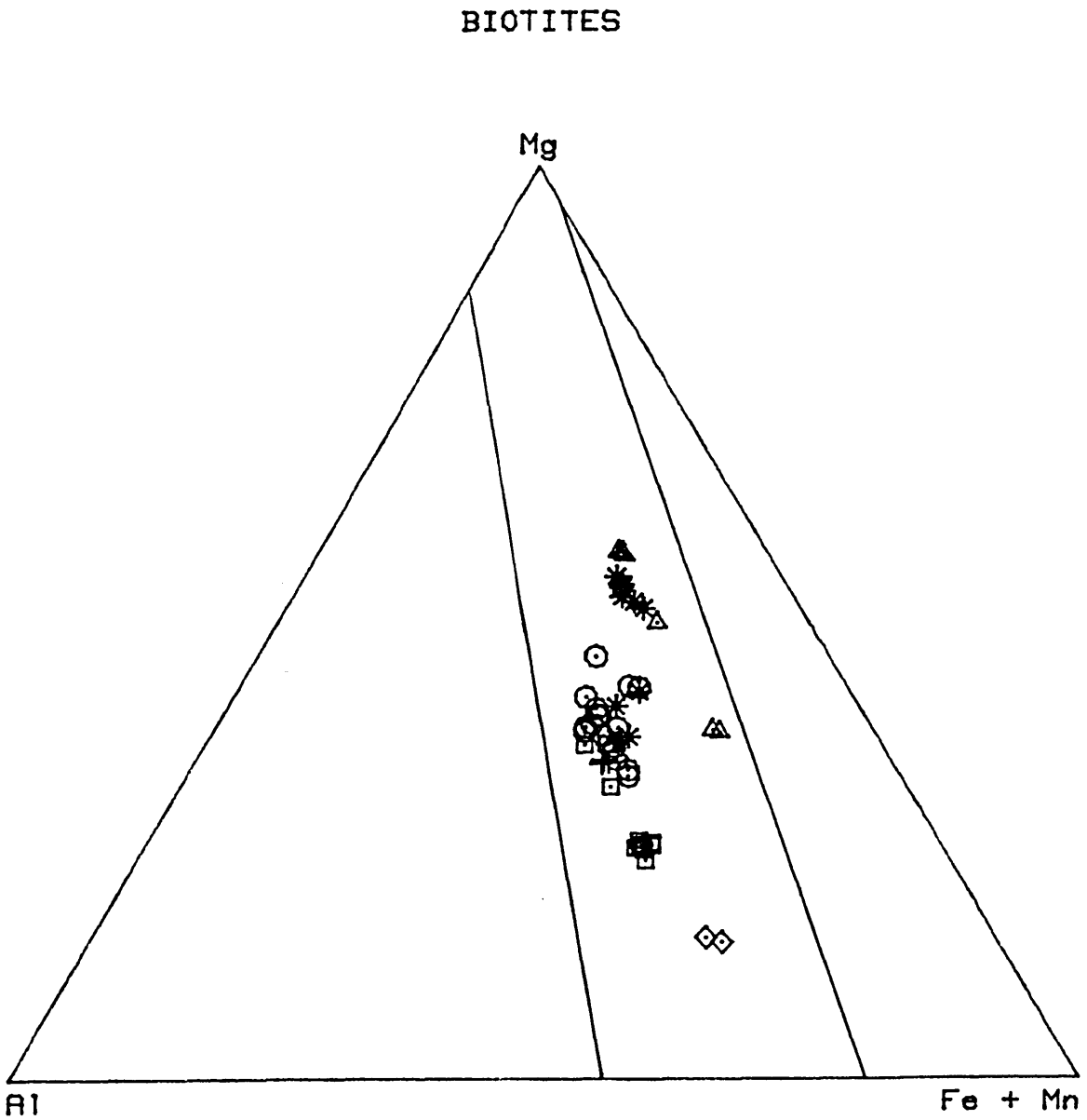

Fig. 4.8 The relation between Fe/Fe + Mg and TiO_2 in biotites. Biotite from sillimanite gneiss is indicated by crosses, from the gahnite zone by squares, from the garnet quartzites by circles, from the amphibole subzone by asterisks, and from the pyroxenoid zone by triangles.

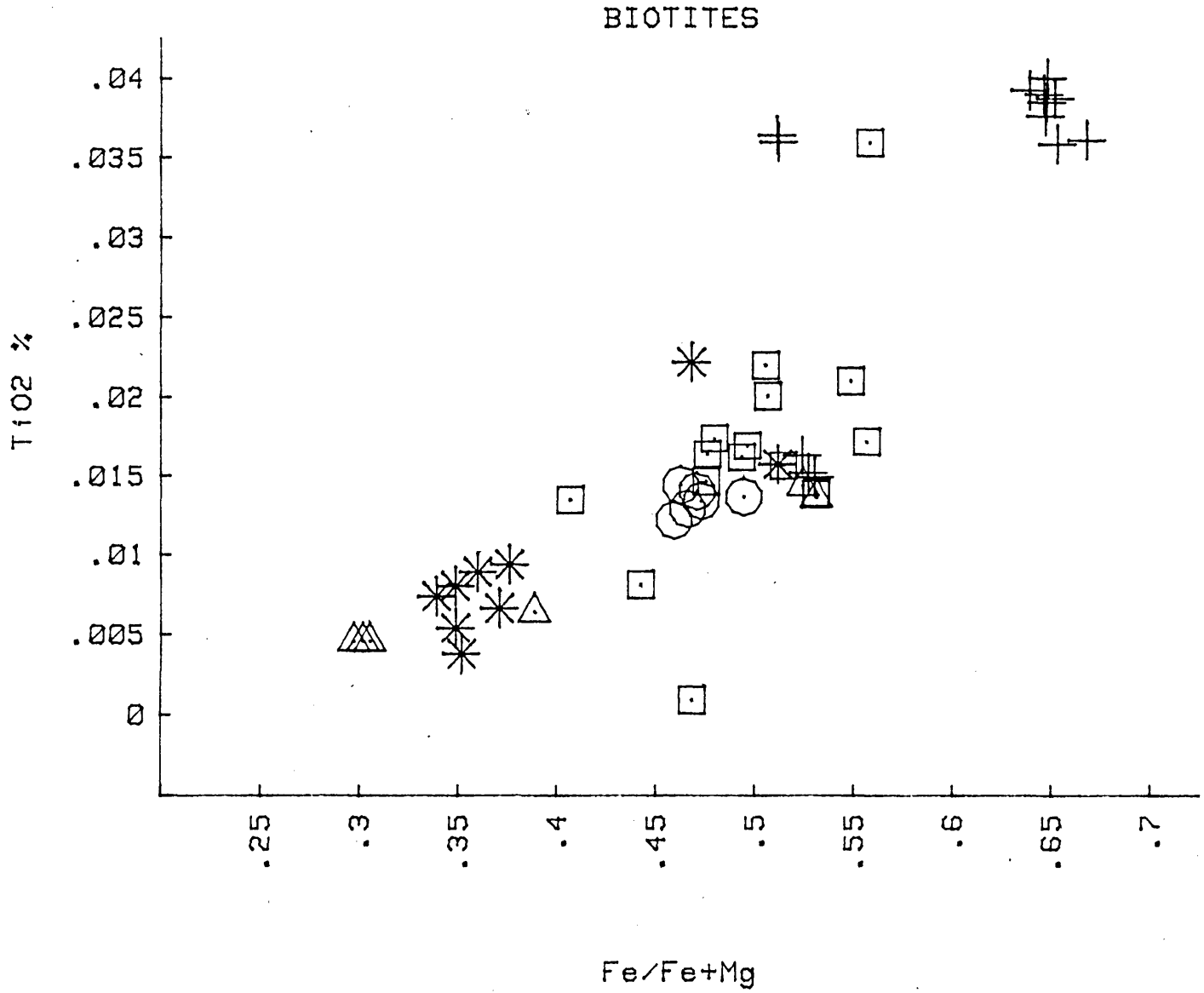

Table 4.2 : Fluorine and chlorine in various phases

SAMPLE	MINERAL		% F	% Cl
4502 / 52.9	Biotite	1	0.790	0.182
		2	0.697	0.215
		3	0.833	0.168
		4	0.812	0.187
		5	1.469	0.626
		6	1.446	0.617
4502 / 47.1	Biotite	1	0.233	0.764
	(green)	2	0.216	0.769
4502 / 65.1A	Biotite	1	0 *	0.068
		2	0.045	0.077
4545 / 42.8	Biotite	1	2.951	0.354
		2	2.951	0.354
	Actinolite	1	0.638	0
		2	0.846	0.111
2 / 9BA	Actinolite	1	0.122	0.063
		2	0	0.033
	Dannemorite	1	0	0.059
		2	0.031	0.038
4502 / 65.1A	Dannemorite	1	0	0
	(coarse)	2	0	0.072
	(fine)	1	0	0
		2	0	0.076
4502 / 47.1C	Muscovite	1	0	0
		2	1.63	0

* 0 = below limits of detection

retrograde recrystallization of biotite (the biotite lattice can accomodate more Ti at higher temperature: Serdyuchenko, 1948). The corona is commonly incorporated within the new biotite grain (Figure 3.2) or, not uncommonly, is some distance (<0.1mm.) from the present biotite grain. The coronas are not considered to represent prograde breakdown, which probably did occur to some extent (Phillips, 1980) as the other likely breakdown phases: magnetite, amphiboles, pyroxenes and olivines (Le Maitre, 1979; Busch et al., 1974; Brown, 1979) were not observed in the association. This fine ilmenite may however be incorporated into garnet, indicating some prograde biotite breakdown i.e. garnetization of biotite (Figure 4.32).

Retrograde chlorite commonly interleaves with, or partly envelops, many biotites and the enveloping chlorite may contain fine galena inclusions (Figure 4.9), indicating some sulphide remobilization during retrogression.

4.5 Sillimanite

An analysis of sillimanite (Table 4.1), indicates a small but significant Fe content (0.18% FeO). This could be present as Fe3+ substituting for Al (Plimer, 1977a). Sillimanite frequently shows partial replacement by sericite. As well as coarse prisms, some minor fibrolitic sillimanite is also present, indicative of Al mobility in late stage fluids (Ahmad & Wilson,1981).

4.6 Feldspars.

Five feldspars from the WAL were analysed by electron microprobe (Table 4.1), and three were found to be orthoclase ($Or_{93}Ab_7$ to $Or_{97}Ab_2An_1$) while two were anorthite ($An_{97}Ab_3$).

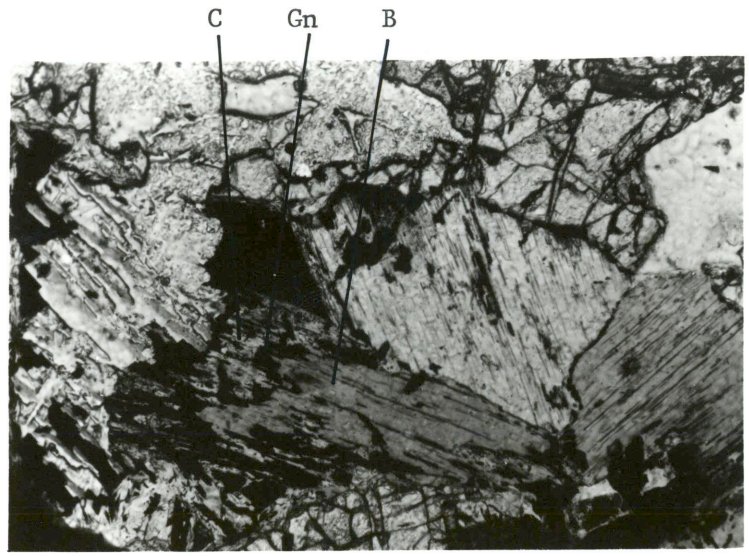

Fig. 4.9 Chlorite (C) and galena (Gn) replacing biotite (B). (4502/25.4). PPL.

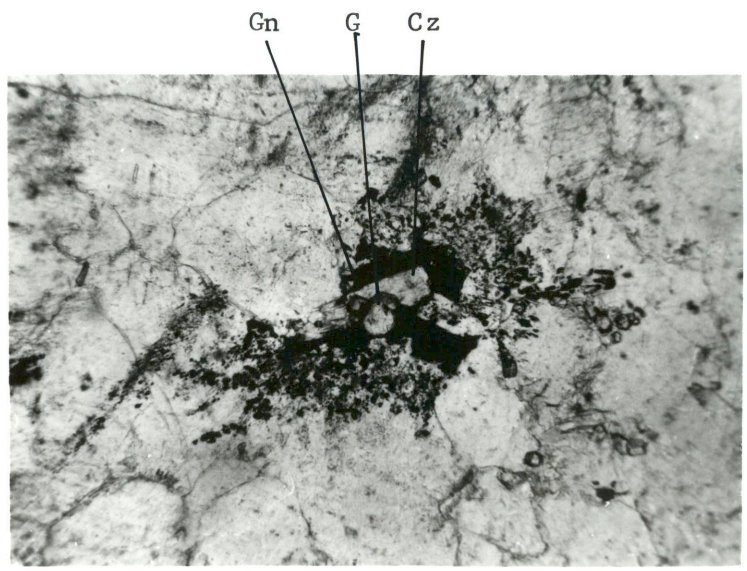

Fig. 4.10 Fine galena (Gn) inclusions in orthoclase, with a core of coarser galena about garnet (G) and clinozoisite (Cz). (4502/46.7B). PPL.

The structural states of five alkali feldspars were determined by the high resolution X-ray diffraction method of Wright (1968), to range between orthoclase and intermediate microcline (Figure 4.11). The values of 2θ, and thus the position of feldspars on this diagram, are probably affected by substitution of Pb for K in the feldspar lattice. Optical examination revealed no evidence for the presence of the 'tartan twinning' characteristic of microclines and it is considered that most alkali feldspar from Broken Hill should be called orthoclase.

Plimer (1976a) found the green alkali feldspar from Broken Hill to be intermediate microcline, in contrast to Čech et al. (1971) who identified only orthoclase, Phillips (1978, 1980), who showed that the Broken Hill area was above the orthoclase isograd, and Fitzgerald and McLaren (1982) who, using transmission electron microscopy, found Broken Hill orthoclase to have only minor microcline inversion lamellae. Binns (1964), however, noted the occurrence of microcline in retrogressed rocks above the orthoclase isograd.

The feldspars range in colour from white to green to dark grey, or rarely pinkish. Lead is usually present, up to 1.2 % PbO (Čech et al. 1971; Plimer, 1976a), and was thought by Čech et al. (1971) to cause the green amazonite - like colouration common in hand specimens of Broken Hill alkali feldspar. Partial sulphurization of the lead during crystallization from anatectic melts is thought by G. Moh (pers. comm.) to cause a common fine graphic intergrowth of galena in orthoclase (Plate 4.10), giving the orthoclase a grey colour. Myriads of minute galena inclusions are centred about coarse galena $\pm$ pyrrhotite $\pm$ sphalerite $\pm$ epidote / clinozoisite $\pm$ gahnite $\pm$ sericite, indicating either complex sulphide - silicate reactions during late -

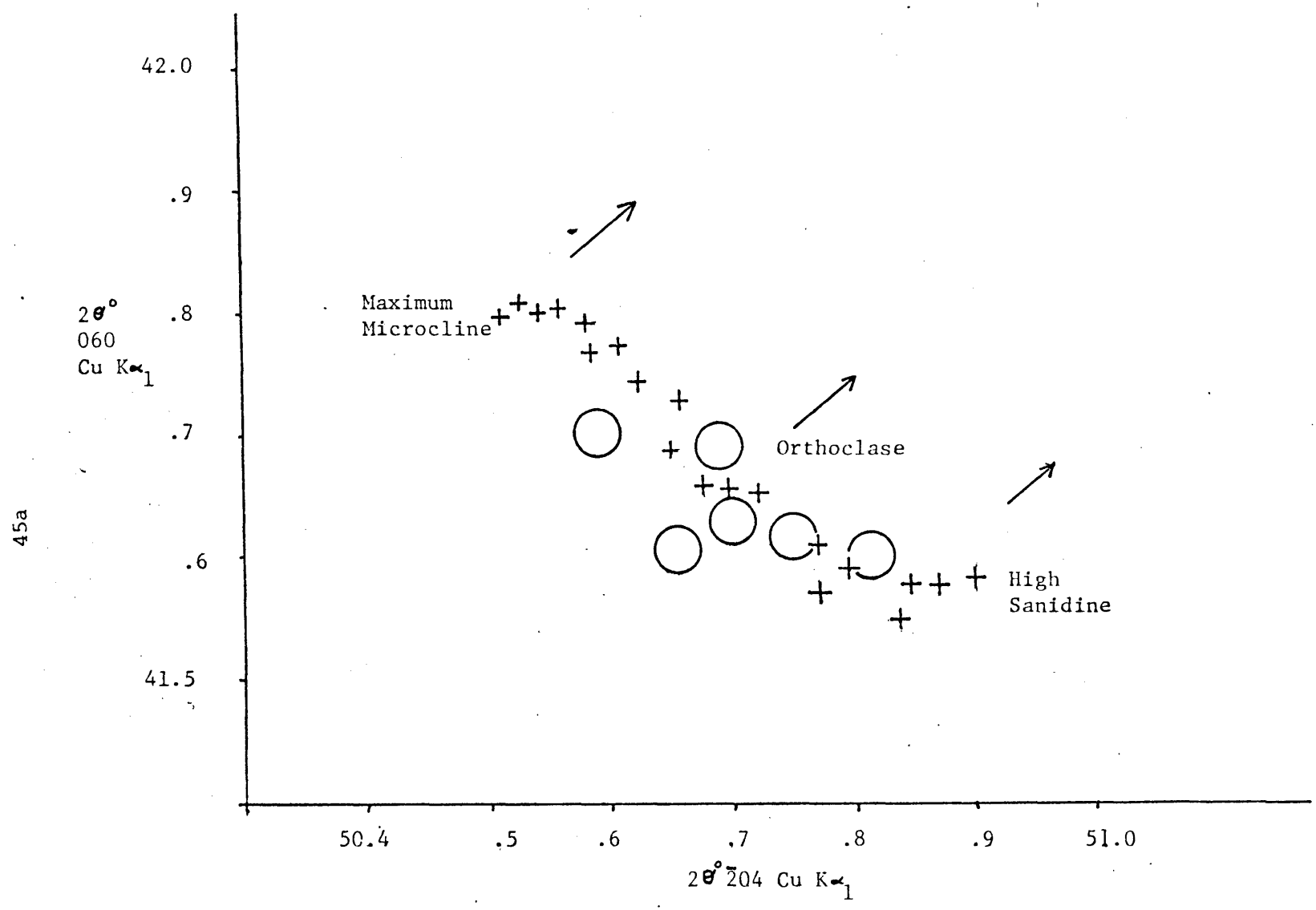

Fig. 4.11 Plot of structural states of WAL potash feldspars (circles), showing some near-end members feldspars from Wright (1968) (crosses) for comparison. The arrows indicate solid solution towards albite.

stage crystallization, or perhaps simply a nucleation effect. Graphic intergrowths of orthoclase with quartz are also common, and gahnite, garnet and biotite are locally abundant as inclusions.

Replacement of orthoclase by sericite along grain boundaries and cleavage planes is very common, but replacement by myrmekite, noted with other, Broken Hill orthoclases (Phillips et al. 1972), was not found in the WAL. Coarse muscovite - quartz - galena $\pm$ sphalerite aggregates locally replace orthoclase.

The anorthite is colourless to white and is commonly sericitized. It is unusually Ca-rich, and may have originated from breakdown of calcite in clay, or perhaps from an original calcic zeolite such as laumontite (see Section 6.2.2).

4.7 Spinels.

The spinel is a green to greenish-black colour in hand specimen and a light to medium green colour in thin section. It is usually poikiloblastic, and is sometimes amoeboid in texture but may also be euhedral, especially when fine grained. It may contain inclusions of quartz, biotite, sulphides or rarely sillmanite and may have a biotite rim in apparent equilibrium.

Most analyses of the spinels from the WAL plot well within the gahnite field (Zn>Fe), but some are zincian hercynite (Fig. 4.12 and Table 4.1). The zincian hercynite has a cell dimension of 8.119 Å (refined from XRD powder data). The magnetite, galaxite ($MnAl_2O_4$) and spinel ($MgAl_2O_4$) components are low. Magnetite and jacobsite have been noted from Broken Hill by Segnit (1977) and Bottrill (pers. comm. (1981) in Birch et al. 1982), but have not been identified in the WAL.

Microprobe analysis indicates that chemical zoning is common in

Fig. 4.12 The Composition of Zincian Spinels (Gahnites and Hercynite). Molecular %.

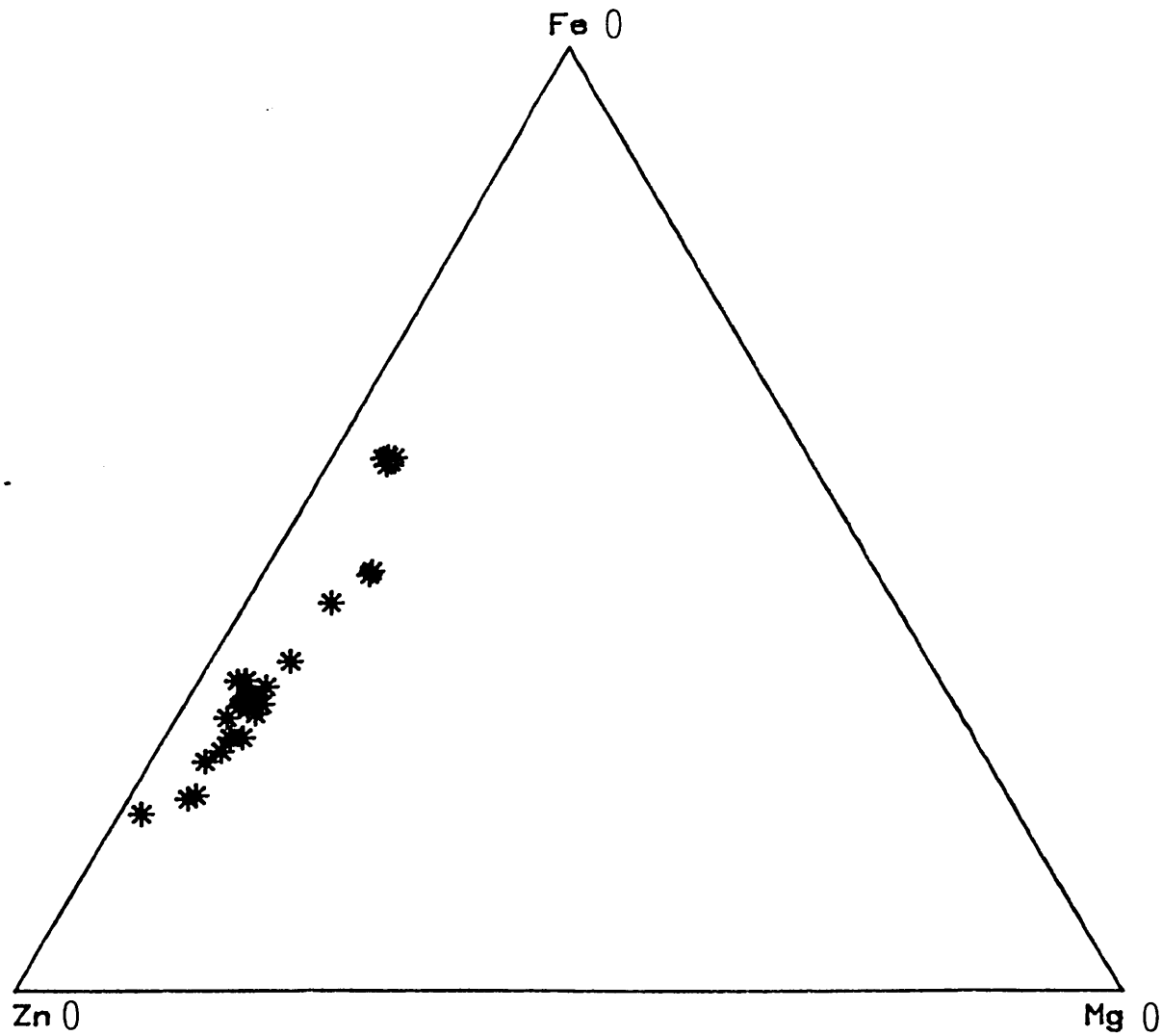

these spinels and, as with garnet, may have normal and reverse trends, the normal zoning indicated by zinc-poor rims and reverse zoning by zinc-rich rims (Spry, 1978). Reverse zoning is more prominent where the spinel has been partly replaced by retrograde phases (e.g. staurolite), as zinc is preferentially retained in gahnite during retrogressive breakdown (Bottrill, 1983a). A similar process occurs in other regions during the breakdown of zincian staurolite, as few other common rock-forming minerals can normally accomodate significant zinc (Kwak, 1974), so Mg and Fe are preferentially partitioned into other phases while Zn accumulates in staurolite. Some of the Fe in the gahnite rims has been sulphurized, perhaps also during retrograde re-equilibration, causing an outer zone rich in fine pyrrhotite (Figure 4.18). Similar partial sulphurization during retrogression affects leollingite (Section 4.12).

The gahnite shows almost ubiquitous, but highly variable, alteration to muscovite, chlorite, staurolite, paragonite, biotite or berthierine ($(Fe,Mg)_{2-3}(Si,Al)_2O_5(OH)_4$). (Figures 4.13 - 4.17). Some of the most likely reactions are:

$$3ZnAl_2O_4 + 6SiO_2 + 2K^+ + 4H^+ = 2KAl_3Si_3O_{10}(OH)_2 + 3Zn^{2+} \qquad (4.1)$$

gahnite quartz muscovite

$$3FeAl_2O_4 + 6SiO_2 + 2K^+ + 4H^+ = 2KAl_3Si_3O_{10}(OH)_2 + 3Fe^{2+} \qquad (4.1a)$$

hercynite quartz muscovite

$$3ZnAl_2O_4 + 6SiO_2 + 2Na^+ + 4H^+ = 2NaAl_3Si_3O_{10}(OH)_2 + 3Zn^{2+} \qquad (4.1b)$$

gahnite quartz paragonite

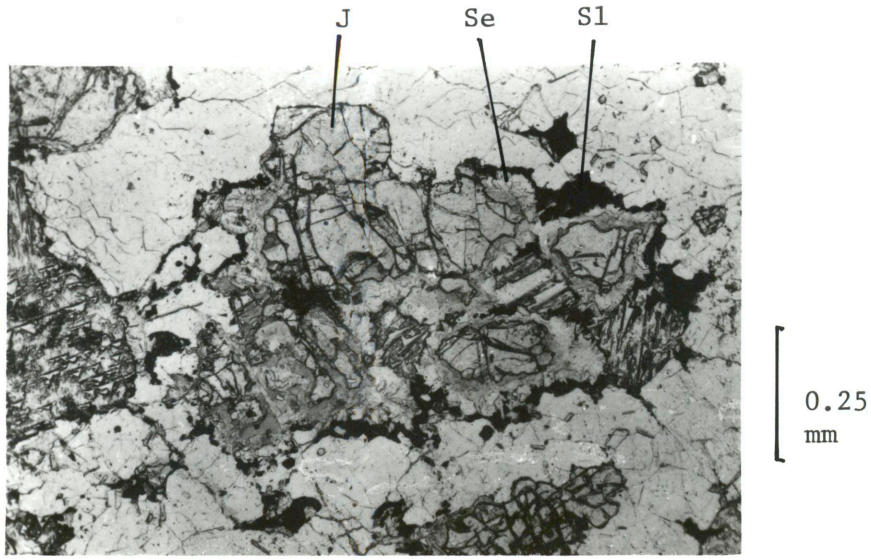

Fig. 4.13 Alteration of gahnite (J) to sericite (Se) with a sphalerite (S1) rim. (4502/91.6). PPL.

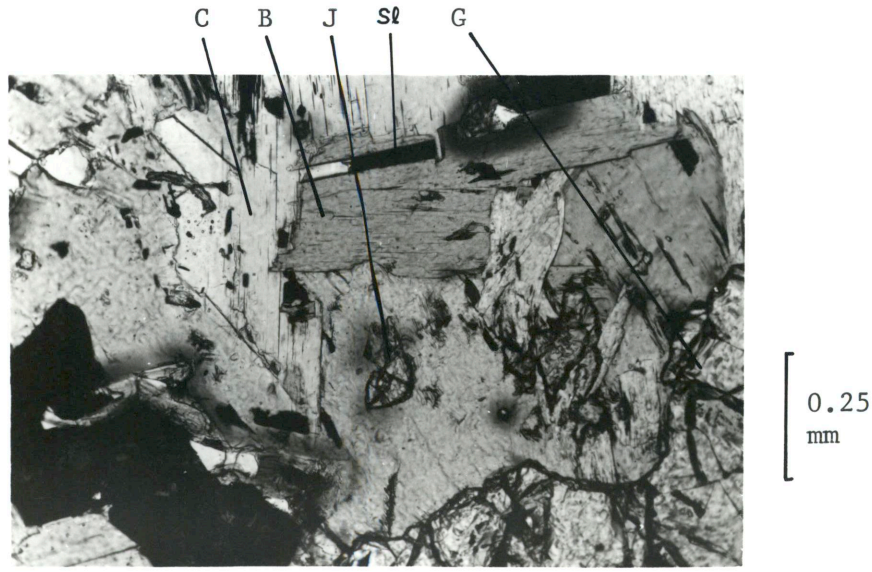

Fig. 4.14 Alteration of biotite (B) and gahnite (J) to chlorite (C), with sphalerite (S1) and garnet (G). (2/13C). PPL.

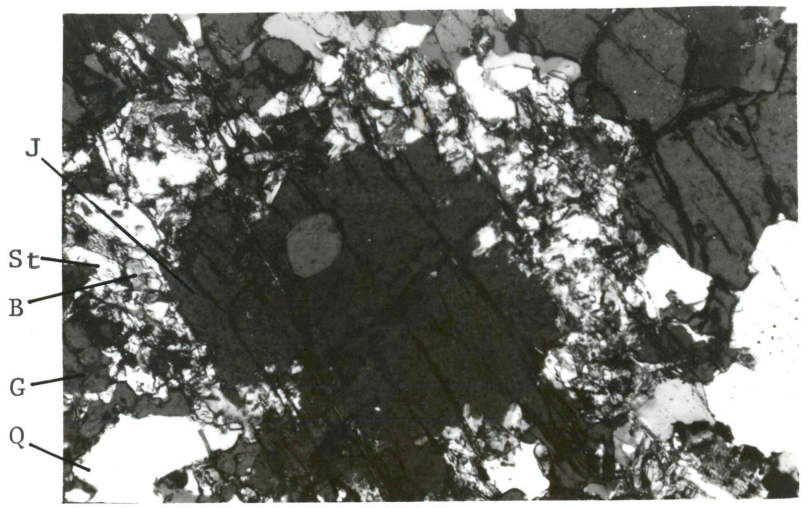

Fig. 4.15 Staurolite (St) alteration rim about gahnite (J), with garnet (G), biotite (B) and quartz (Q). (4500/2502). PXPL.

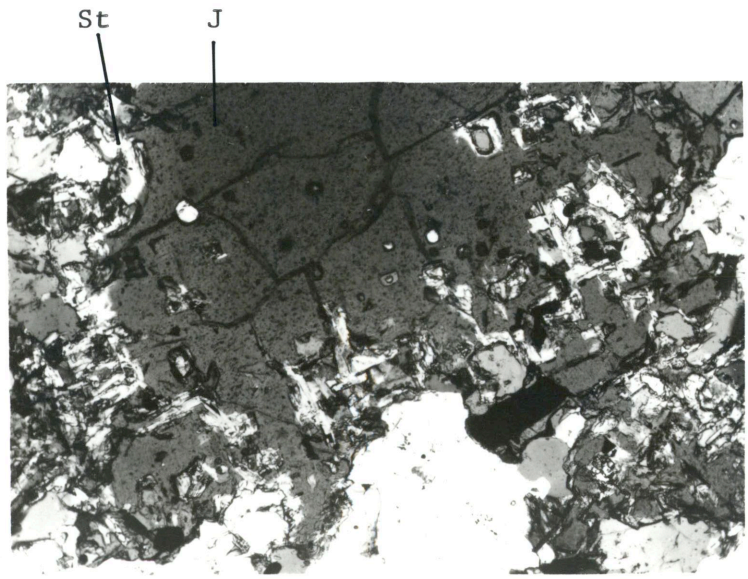

Fig. 4.16 Oriented replacement of gahnite (J) by staurolite (St). (4500/2502). PXPL.

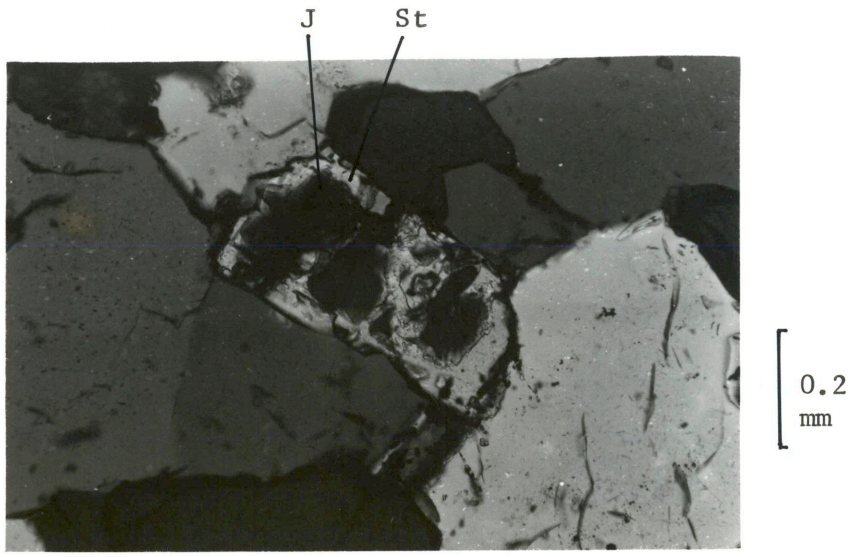

Fig. 4.17 Gahnite (J) partly replaced by a single crystal of staurolite (St). (4500/28.0). XPL.

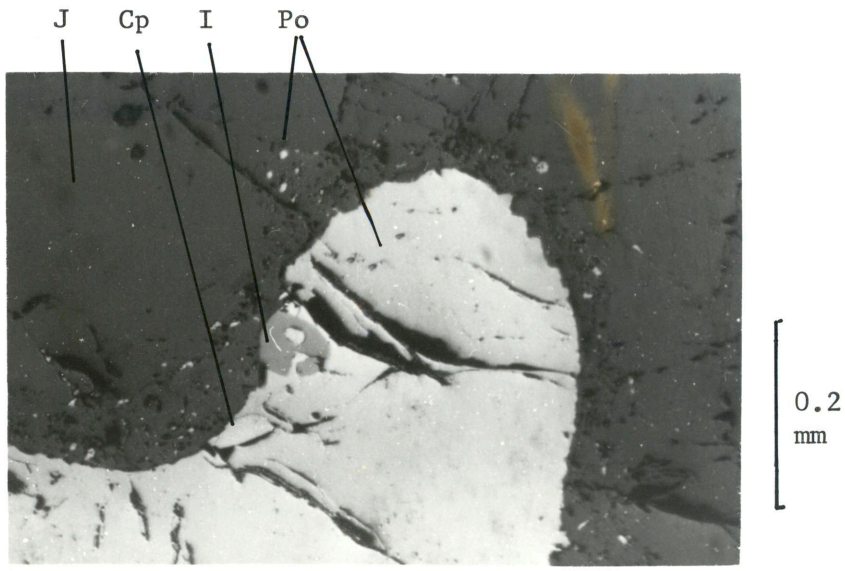

Fig. 4.18 Fine pyrrhotite (Po) inclusions in gahnite (J) adjacent to coarse pyrrhotite, with ilmenite (I) and chalcopyrite (Cp). (1/3). Reflected light, XPL.

$$3ZnAl_2O_4 + 6SiO_2 + 2K^+ + 4H^+ + 3FeS = 2KAl_3Si_3O_{10}(OH)_2 + 3ZnS + 3Fe^{2+}$$

gahnite quartz pyrrhotite muscovite sphalerite

(4.1c)

$$3FeAl_2O_4 + 5.5SiO_2 + 13H_2O + 5Fe^{2+} = Fe_8Al_6Si_{5.5}O_{20}(OH)_{16} + 10H^+ \quad (4.2)$$

hercynite quartz chamosite/berthierine

$$2FeAl_2O_4 + K_2Fe_6Al_2Si_6O_{20}(OH) + 7H_2O = Fe_8Al_6Si_{5.5}O_{20}(OH)_{16} +$$

hercynite annite chamosite/berthierine

$$.5SiO_2 + 2K^+ + 2OH^-$$

quartz (4.2a)

$$8.7(Fe,Zn)Al_2O_4 + H_2O = (Fe,Zn)_4Al_{17.3}Si_8O_{46}(OH)_2 + 4.7FeO \quad (4.3)$$

hercynite staurolite

$$8.7FeAl_2O_4 + 3.2KFe_2Al_3Si_2O_{10}(OH)_2 + 14.1SiO_2 + 1.4H_2O =$$

hercynite siderophyllite quartz

$$1.4Fe_4Al_{17.3}Si_8O_{46}(OH)_2 + 3.2KFe_3AlSi_3O_{10}(OH)_2 \quad (4.3a)$$

staurolite annite

$$4FeAl_2O_4 + 4.7Al_2SiO_5 + H_2O + 3.4SiO_2 = Fe_4Al_{17.3}Si_8O_{46}(OH)_2 \quad (4.3b)$$

hercynite sillimanite quartz staurolite

$$3FeAl_2O_4 + 4SiO_2 + Fe^{2+} + 2K^+ + 4OH^- = 2KFe_2Al_3Si_2O_{10}(OH)_2 \quad (4.4)$$

hercynite quartz siderophyllite

These reactions are seldom simple, as they represent only a part of the retrograde re-equilibration of the mineral assemblages, which

have not always behaved as closed systems. The compositions shown in reactions 4.1 - 4.4 generally represent end-member components, but the Al/Si/O ratios approximate the compositions found in the WAL. The spinel is represented by hercynite in most of these reactions as that component was less stable than the gahnite component during the retrogression as described above.

Gahnite appears particularly unstable in association with pyrrhotite, which is partly replaced by sphalerite. Complete breakdown of gahnite has occurred in some areas, resulting in rounded aggregates of sericite and chlorite (Figure 4.19), although small gahnite inclusions in unfractured crystals of nearby garnet or quartz may remain unaltered. Fine sphalerite is common in the fine sericite - chlorite alteration rim around gahnite, especially when in contact with, or close to, pyrrhotite grains. Some staurolite replaces the gahnite topotactically (Figure 4.16).

Sundblad (1982) suggested that the breakdown of iron silicates rather than sphalerite produces most iron - rich gahnite, and as the WAL gahnite is very iron - rich, grading to hercynite, this was a major factor in its formation. The wide Zn / Fe range suggests that reaction of sphalerite with aluminosilicates was an additional factor (Wall & England, 1979).

4.8 Amphiboles.

Quite a wide variety of amphibole compositions occur within the WAL - most within the cummingtonite series and some within the actinolite series (Figs.4.21, 4.22 and 4.22a ; Table 4.1).

The cummingtonite series amphiboles are pale pinkish-brown in hand specimen, resembling bustamite and often described by mine geologists

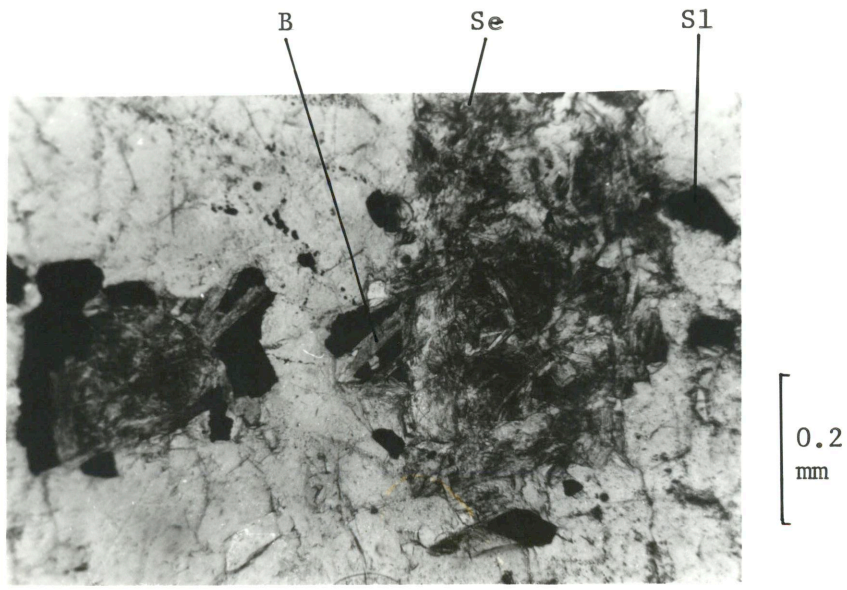

Fig. 4.19 Aggregates of sericite (Se) biotite (B) and sphalerite (S1), pseudomorphous after gahnite. (4502/47.0). PPL.

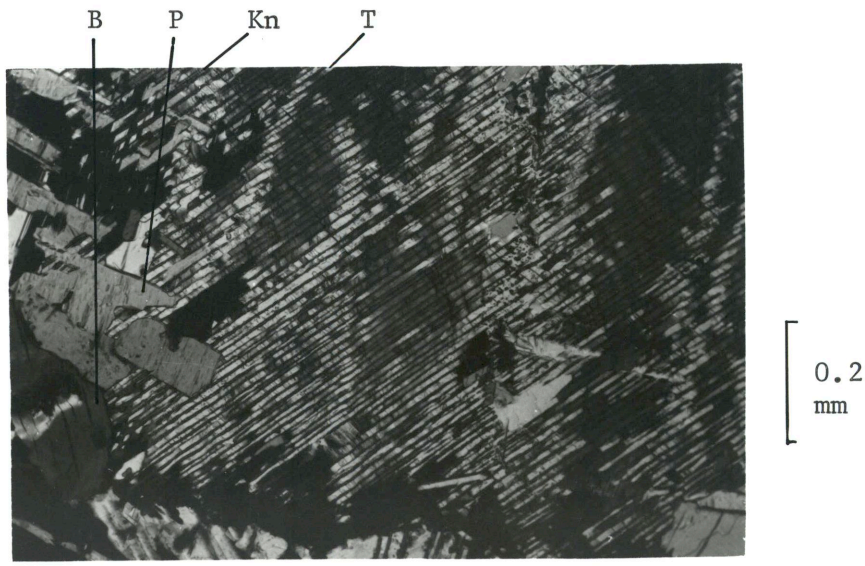

Fig. 4.20 Fine exsolution of kanoite (Kn) in tirodite (T), with Mn-biotite (B) and pyroxmangite (P). (4526/90.6). XPL.

Fig. 4.21 Composition of Amphiboles, showing the compositional fields for cummingtonite group as defined by Leake (1978). Stars represent cummingtonite group minerals, and triangles actinolite group minerals. Molecular %. Dotted lines join coexisting phases.

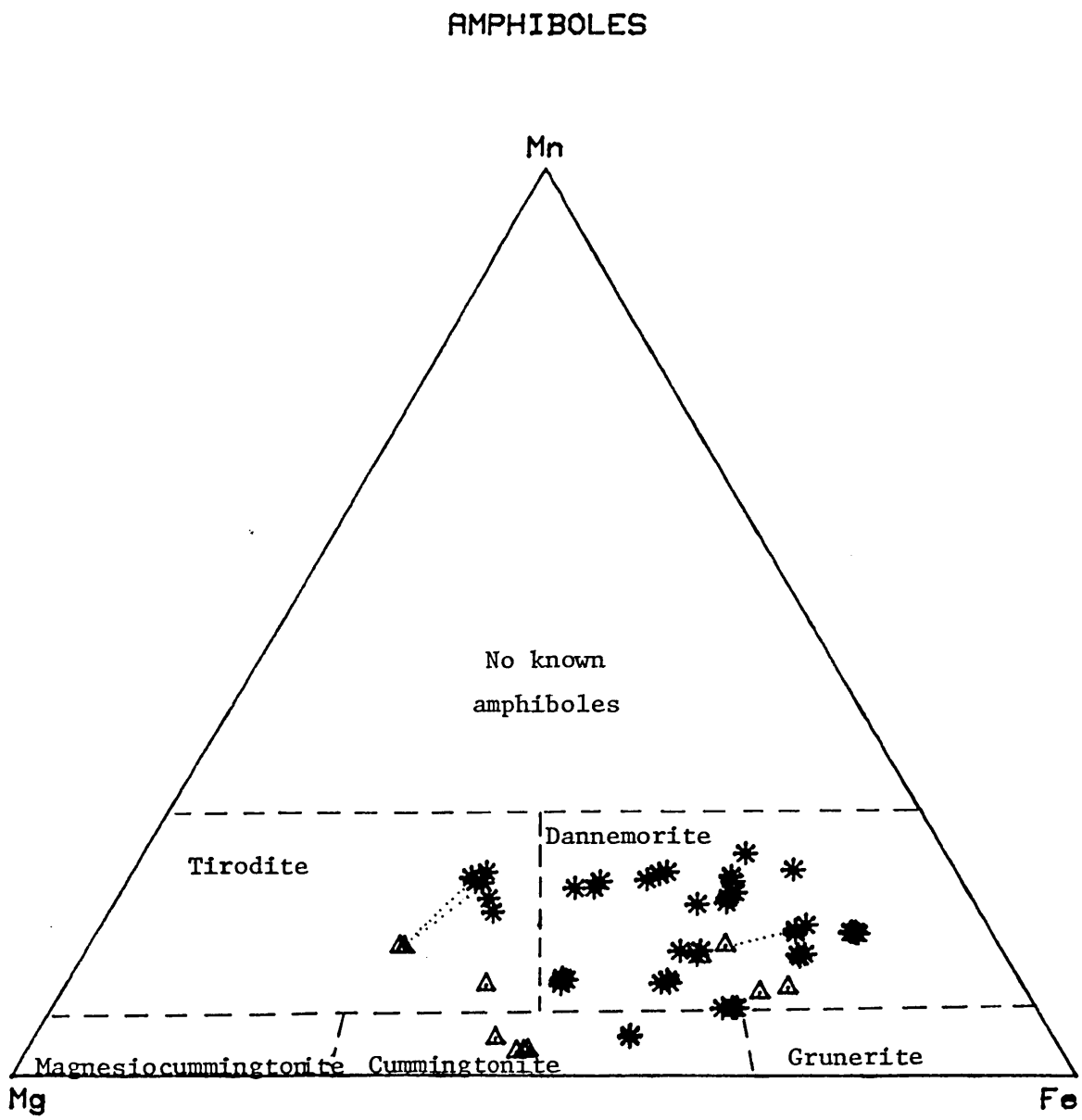

Fig. 4.22 Compositions of Amphiboles, showing the compositional fields for the actinolite group as defined by Leake (1978). Triangles represent actinolite group minerals, stars represent cummingtonite group minerals (those in the actinolite field are tirodites), and circled stars are fine aggregates, perhaps mixtures. Dotted lines join coexisting phases. Molecular %.

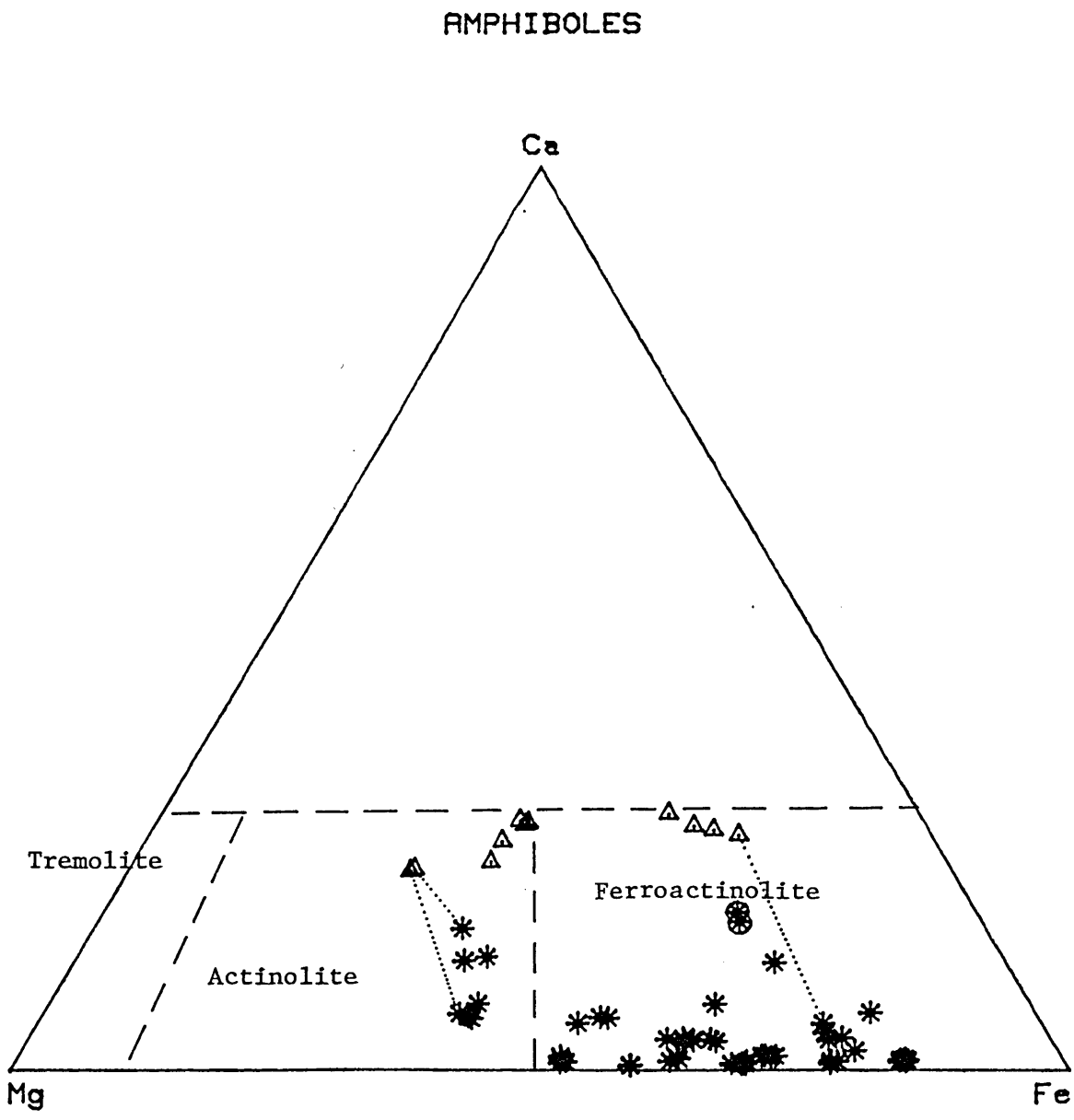

Fig. 4.22a. Composition of Amphiboles (showing theoretical maximum limit of (Ca + Mn) (Robinson et al., 1982). Triangles represent actinolite group minerals and stars represent cummingtonite group minerals. Molecular %.

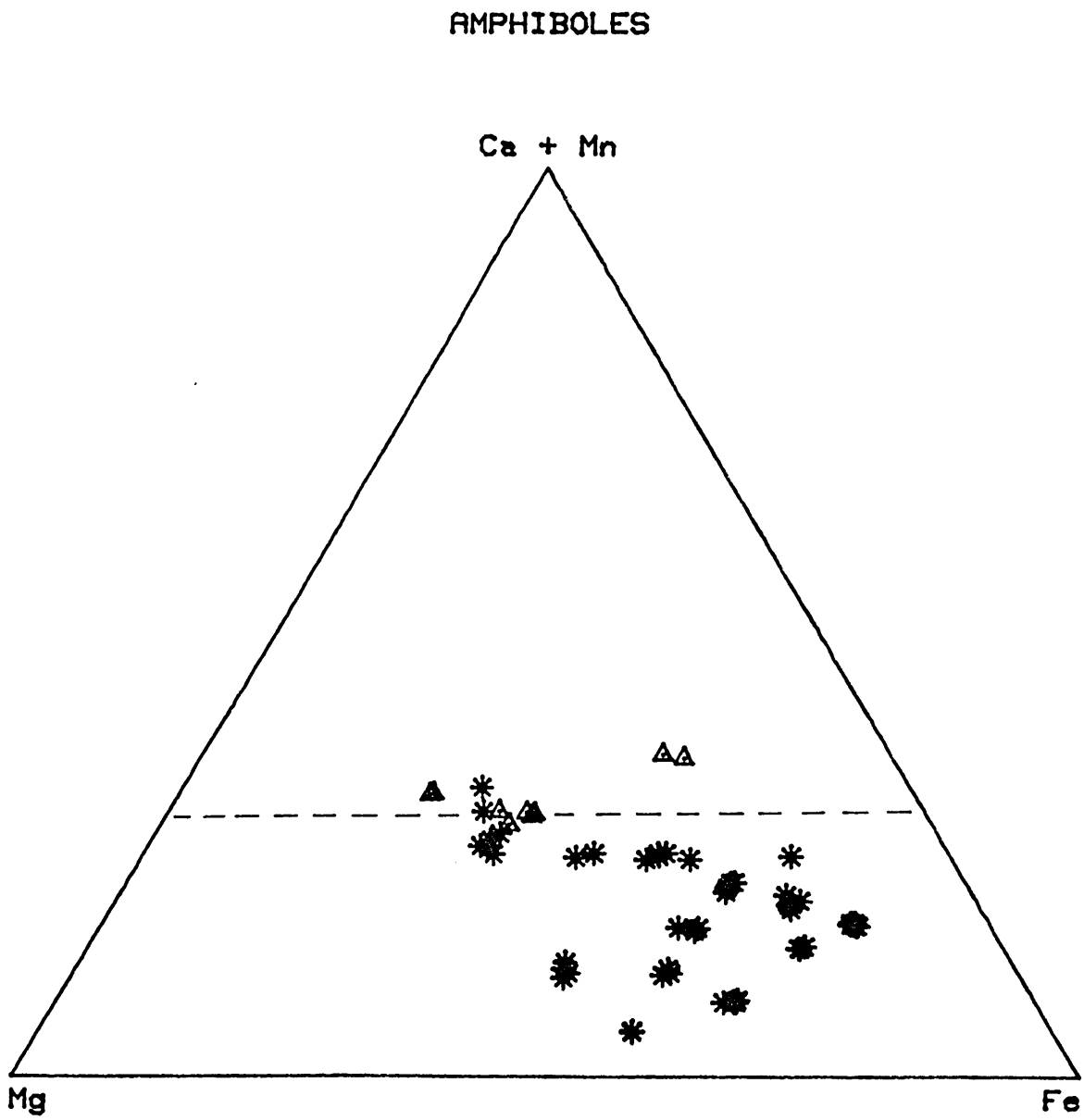

as such, and they are colourless in thin section. Actinolite group minerals are pale green to greenish-black in hand specimen, and are colourless to deep green in thin section. Multiple twinning is almost ubiquitous in cummingtonite series minerals, but is uncommon in actinolites. Tirodite is pale olive green in handspecimen and is almost colourless in thin section. It sometimes shows a bluish 'schillerization', due to diffraction of light by very fine exsolution lamellae.

The actinolite series amphiboles range from actinolite to ferroactinolite (Fe/(Fe + Mg) = 0.35 to 0.75) and are usually Mn - rich (up to 6.4 % MnO) and contain up to 3.3% Al_2O_3. Some analyses approach the actinolitic hornblende compositional field of Leake (1978). Robinson et al. (1982) indicate that in amphiboles, using their crystallographic notation, the site preferences for Ca are M4> M1-2-3> A, for Mn are M4>M1-2-3 and for Fe and Mg are M1-2-3 > M4, and Ca is preferred to Mn in M4 sites. Thus Mn in WAL amphiboles must be partly distributed through M1-2-3 as well as M4 sites, as (Ca + Mn)/(Ca + Mn + Fe + Mg) may be > 2/7 while Ca/(Ca + Mn + Fe + Mg) may be < 2/7 (the theoretical maximum for Ca + Mn in amphiboles) (Figures 4.21-4.23). These amphiboles may have some lattice distortion from accomodating these large ions in the small sites.

The cummingtonite series minerals are usually Mn-rich and fall principally within the dannemorite ($Mn_2Fe_5Si_8O_{22}(OH)_2$) and cummingtonite ($(Mg,Fe)_7Si_8O_{22}(OH)_2$) fields, while tirodite ($Mn_2Mg_5Si_8O_{22}(OH)_2$) was a dominant component of amphiboles in one specimen only. Many members of this series were found to be slightly calcic (Fig 4.22) and this is possibly due to intergrowth with actinolite in some fine aggregates, but up to 2.5% CaO is present in

coarse grained, homogenous dannemorite. Small amounts of Ca are typical of cummingtonite group minerals, and may be necessary for nucleation (Layton & Phillips, 1960; Cameron, 1975), but a maximum of only 2.2 % CaO has been previously recorded in cummingtonite series minerals (Vernon, 1962; Robinson et al. 1982), making this above mentioned specimen the most calcic cummingtonite group described. As in actinolites Ca + Mn/(Ca + Mn + Fe + Mg)may be > 2/7, indicating the presence of minor Mn in M1-2-3 sites. The tirodite contains fine exsolution lamellae of pyroxenoids and pyroxenes (Figure 4.20) which contribute to the spread in tirodite analyses.

Some amphiboles were analysed for halogens (Table 4.2), and the cummingtonites are quite halogen poor (<.03 % F, <.08 %, Cl) while the actinolites have up to .85 % F and .06 % Cl. High halogen contents are typical of high grade amphiboles (Petersen et al. 1982).

Zn is only minor, (up to 0.27 and 0.65 % ZnO in cummingtonites and actinolites respectively) in contrast to the manganoan amphiboles of Franklin, New Jersey (Klein & Ito, 1968), containing up to 10.8 % ZnO. This is due to the much higher sulphide content of the Broken Hill lodes compared with the Franklin Pb-Zn deposits (Squiller and Sclar, 1980), causing most Zn in Broken Hill to be present as sphalerite (sulphides are almost ubiquitous in amphibole rich areas of the WAL).

Na, Ti and Al are usually very low, although some coarse actinolite has up to 3.3 % Al_2O_3.

Overgrowths of amphiboles were noted in a number of cases (Figures 3.16 - 3.18) although consistent chemical differences could not be detected. Some coarse grained actinolite is overgrown by actinolite richer in fine sulphide blebs (Figure 3.18). This could be due to either:

I. Increased growth rate.

II. Sulphurization of pre-existing grains.

III. Sulphur influx into the fluid phase during retrograde growth.

The lack of distinct chemical difference between the core and rims supports the first hypothesis, but it is also quite possible that the amphibole grains re-equilibrated during retrogade metamorphism, and zoning was not preserved. Two distinct generations of cummingtonite series amphiboles may be present - the second generation commonly being very fine grained. As for the actinolites, no consistent chemical variation was detected.

Co-existing actinolite series and cummingtonite series minerals are rare, but one pair is plotted in Figure 4.22. The actinolite has a slightly greater Mg/Mg + Fe than the dannemorite, as Immega and Klein (1976) found to be general for most similar assemblages.

The amphiboles frequently occur as replacements of the pyroxenoids, principally along cleavage planes and grain boundaries (Figures 3.6-3.7) and some aggregates in quartz may represent completely replaced pyroxenoids (Figure 3.13). Some amphiboles, however are found in shear zones (Figure 3.11) and other areas with no direct relationship to pyroxenoids. Some occurrences within pyrosmalite appear to have nucleated about sphene.

Pleochroic haloes were found about allanite inclusions in some actinolites (Figure 3.18).

4.9 Pyroxenes & Pyroxenoids.

The principal pyroxenoids present in the WAL are rhodonite and pyroxmangite both $(Mn,Ca,Fe)SiO_3$, (Figures 4.24 - 4.27; Table 4.1).

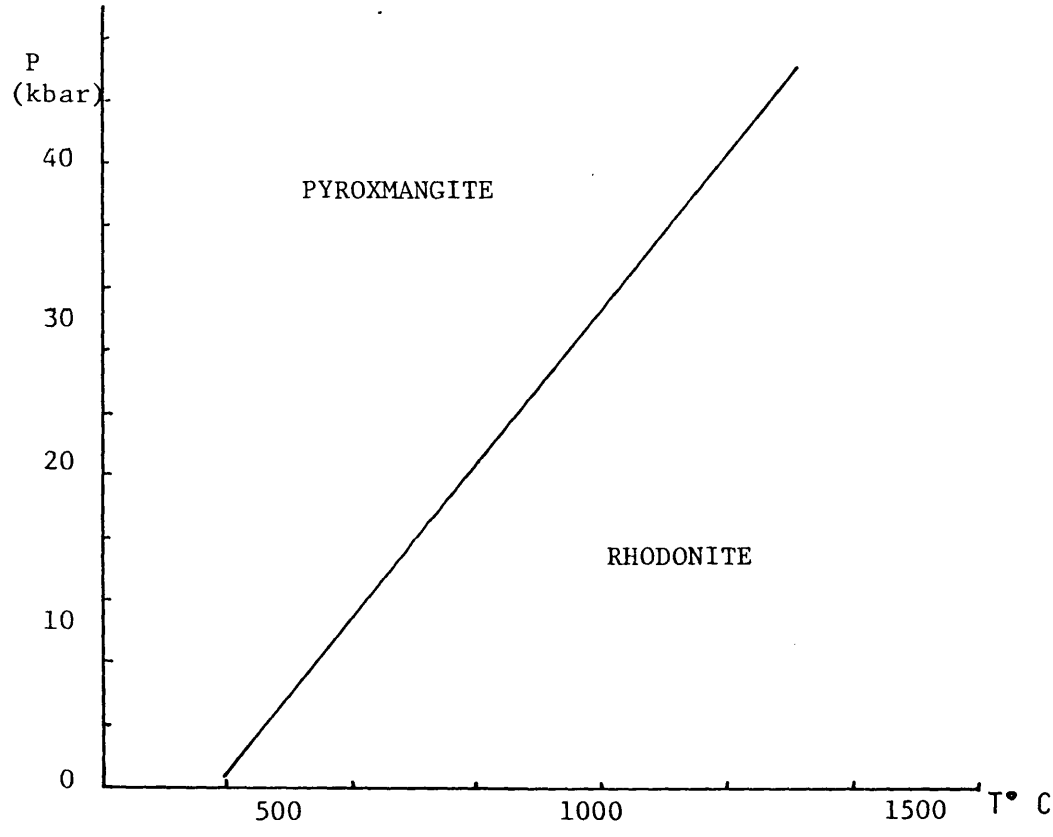

Fig. 4.23 Pressure-temperature curve for the rhodonite/ pyroxmangite transformation, for pure $MnSiO_3$, adapted from Maresch & Mottana (1976).

Fig. 4.24 Composition of Pyroxenoids and Pyroxenes in Mg-poor samples, with approximate moderate to high temperature compositional fields adapted from Hodgson (1975) Peacor (1978), Brown et al. (1980) and Winter et al. (1981) Rhodonites are shown by Δ, pyroxmangites by X, and hedenbergites by ⊡. Molecular %.

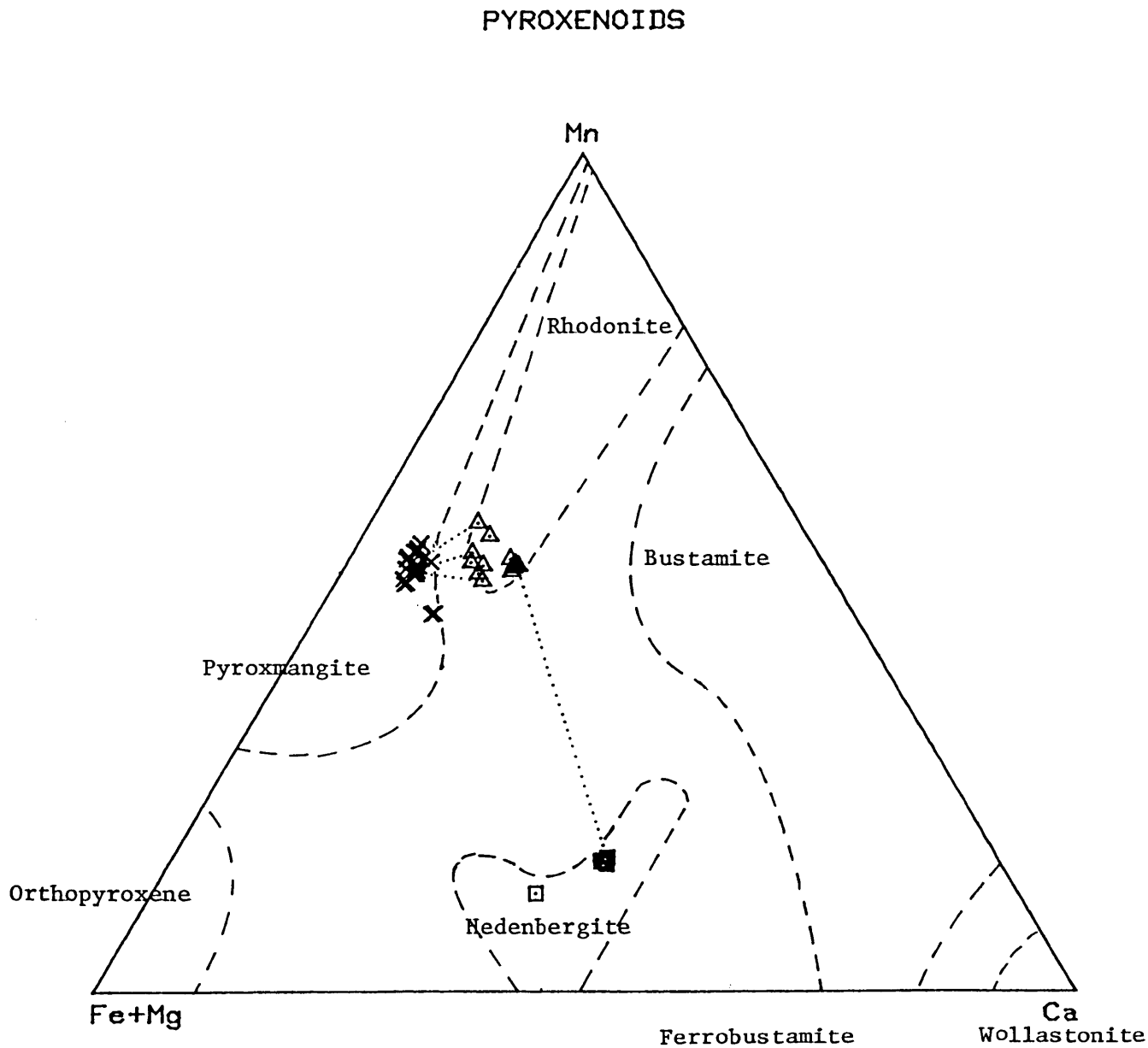

Fig. 4.25 Composition of pyroxenoids, pyroxenes and amphiboles in Mg-rich samples, with approximate compositional fields are adapted from Brown et al. (1980) and Leake (1978). Amphiboles are shown by asterisks, hedenbergite by squares, kanoites by triangles and pyroxmangites by crosses. Molecular %.

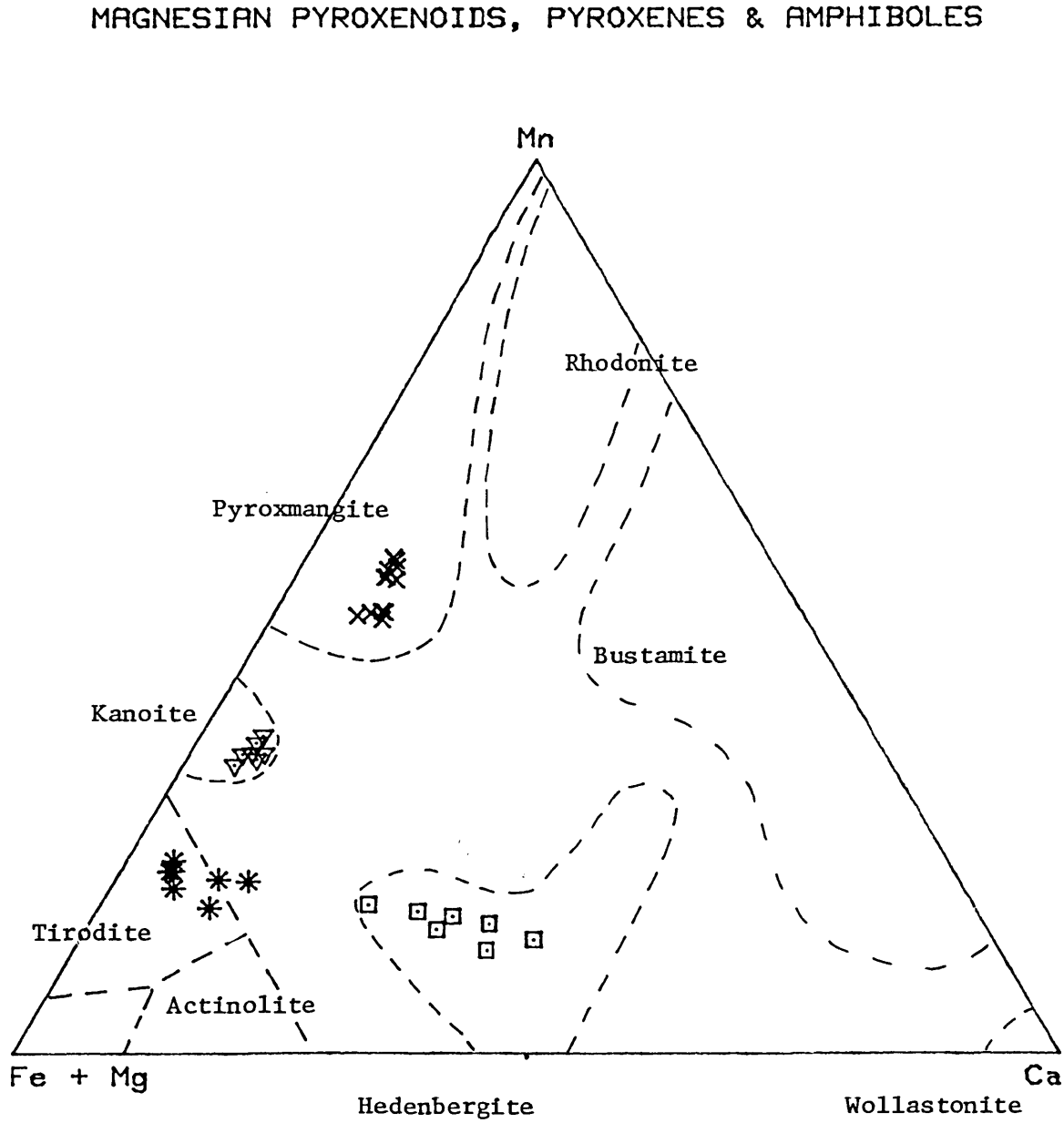

Fig. 4.26 Compositions of pyroxenoids, pyroxenes and amphiboles in Mg-rich samples, showing compositional fields adapted from Brown et al. (1980). Hedenbergites are shown as squares, tirodites as asterisks, kanoites as triangles and pyroxmangite as crosses. Molecular %.

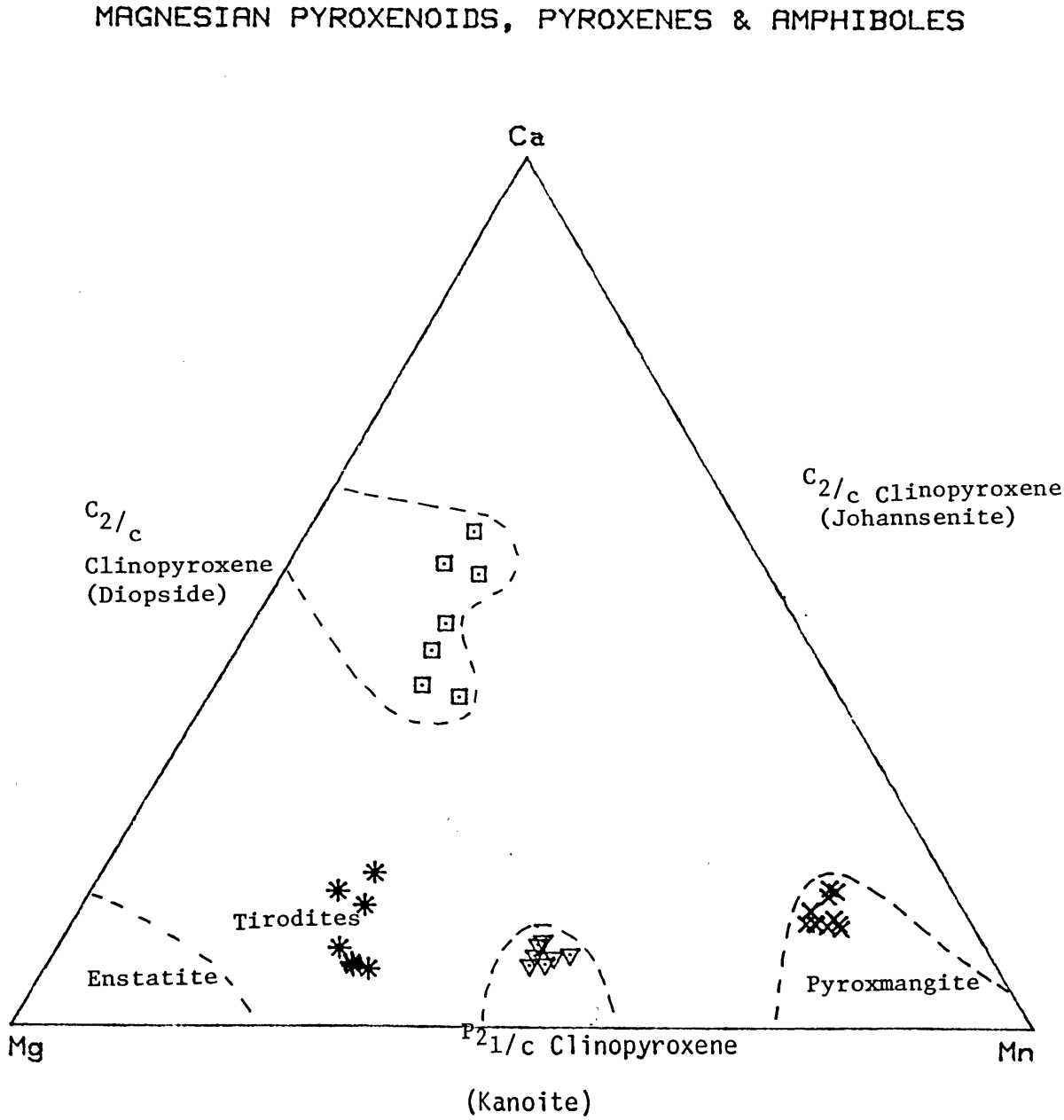

Fig. 4.27 Compositions of Pyroxenes and Pyroxenoids. Rhodonites are represented by Δ, pyroxmangite by X and kanoite by ∇. Compositional fields adapted from Petersen et al. (1984) Molecular %.

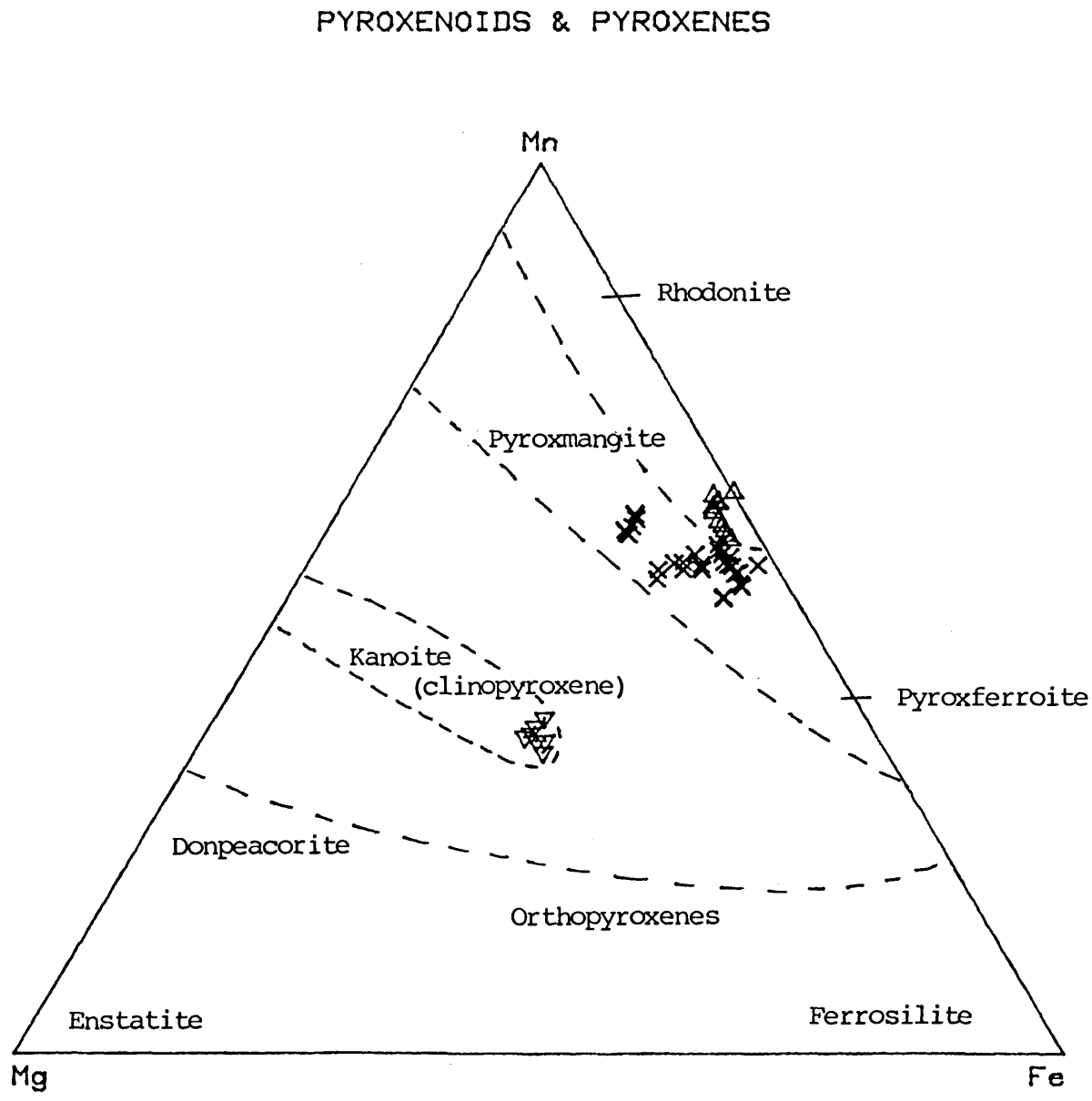

TABLE 4.3: COMPARISON OF RHODONITE AND PYROXMANGITE

(Data from Roberts et al. 1974)

	PYROXMANGITE	RHODONITE
Composition	$(Mn,Fe,Mg,Ca)SiO_3$	$(Mn,Ca,Fe,Mg)SiO_3$
Crystal system	Triclinic	Triclinic
Space group	P1	P1
Z	14	10
3 Strongest	2.95(100)	2.772(100)
Diffraction	2.18(70)	2.980(65)
Lines (Å)	3.12(60)	2.924(65)
Optical consts.		
α	1.726 - 1.748	1.711 - 1.738
β	1.728 - 1.750	1.716 - 1.741
γ	1.744 - 1.764	1.724 - 1.751
2V	35 - 46° (+)	63 - 76° (+)
Colour	Pale pink to dk. brown	Pale pink to brown - red
Hardness	5.5 - 6	5.5 - 6.5
Specific	3.6 - 3.8 (meas.)	3.6 - 3.8 (meas.)
Gravity	3.91 (calc.)	3.73 (calc.)
Cleavage	{110} Perfect	{110} Perfect
	{110} Perfect	{110} Perfect
	{010} Good	{001} Good
	{001} Good	
Twinning	rare; lamellar & simple	not noted

X-ray Diffraction analyses indicate that pyroxmangite may be slightly more abundant than rhodonite in the WAL (Appendix 5), although Burrell (1942) found pyroxmangite to be unimportant in the A lode compared with rhodonite. They are very difficult to distinguish and very detailed optical studies or X-ray analyses are necessary to confirm their identifications (Table 4.3). Maresch and Mottana (1979) showed that pyroxmangite is the high pressure equivalent of, and may invert to, rhodonite (Figure 4.23), but this is also composition-dependant.

Coexisting rhodonite and pyroxmangite were found in the WAL as relatively coarse exsolution intergrowths and are not uncommon (Burrell, 1942; Hodgson, 1975b; Maresch and Mottana, 1979; Aikawa, 1979 and Brown et al. 1980). Their compositions indicate stable coexistence of the two phases in a divariant field. The immiscibility gap is very limited, but shifts with changing temperature and pressure (Maresch and Mottana, 1979), and thus exsolution may occur. Plotting of analyses of the WAL pyroxenoids indicates clustering into two principal groups, (Figs 4.24 - 4.27) and thus the immiscibility gap is fairly well defined over a small compositional range in these samples. The rhodonite - pyroxmangite immiscibility gap is poorly defined at present (Mason, 1973; Aikawa, 1979; Brown et al. 1980; Winter et al. 1981), and is pressure and temperature dependent (Maresch & Mottana, 1979). Zn may be present up to 0.32 % ZnO in both pyroxmangite and rhodonite in the WAL.

Manganoan hedenbergite (often termed manganhedenbergite) is a less common phase in the WAL than rhodonite and pyroxmangite but is locally abundant. The composition is quite variable (Figure 4.24 - 4.27), but the hedenbergite ($CaFeSi_2O_6$) component is always greater than the johannsenite ($CaMnSi_2O_6$), kanoite ($MnMgSi_2O_6$) and diopside ($CaMgSi_2O_6$)

components. The Ca/(Fe + Mg + Mn) is quite variable also, showing that a large amount of Mn, Fe and perhaps Mg can substitute for Ca, and up to 0.3 % ZnO has been found in some hedenbergite. The large amount of Mn substitution for Ca is not typical of manganoan hedenbergite (Mason, 1973; Hodgson, 1975b), and indicates a kanoite component ($MnMgSi_2O_6$). The spread of analyses (Figure 4.25) is partly due to the fine nature of some of the exsolution lamellae of hedenbergite in tirodite, making accurate analysis difficult.

The little work that has been done on the pressure - temperature dependence of Mn - pyroxenes and pyroxenoids indicates that with calibration they would probably make good geobarometers and/or geothermometers (Brown, 1980; Abrecht & Peters, 1980).

A kanoite-like phase ($MnMgSi_2O_6$, a recently described clinopyroxene: Kobayashi, 1977) was found coexisting with tirodite in one sample from 90.6 metres, DH4526. The average formula is about $Mn_{0.7}Mg_{0.6}Fe_{0.6}Ca_{0.1}Si_2O_6$, or $(Mn_{0.7}Fe_{0.2}Ca_{0.1})(Mg_{0.6}Fe_{0.4})Si_2O_6$, similar to some of the kanoite described by Brown et al.(1980) but with a much higher iron content. In several kanoite analyses Fe>Mg, suggesting the presence of an as yet undescribed $MnFeSi_2O_6$ endmember, but deficiencies in Ca and Mn indicate that Fe substites for these elements in the large A site (due to its smaller size Mg is unlikely to substitute in this site) and thus no conclusive evidence can be presented here for the existence of a new mineral. Kanoite occurs in the WAL as fine exsolution lamellae (<40 microns width) in tirodite (Plate 4.20). A similar habit is seen in its other two reported occurrences: as fine intergrowths with manganoan diopside (Brown et al. 1980) and as fine intergrowths with manganoan cummingtonite (Kobayasni, 1977). Further study, including x-ray diffraction and

transmission electron microscopy, is necessary to confirm the identity of this and other phases in this sample.

The pyroxenoids and pyroxenes are commonly euhedral (short prismatic) when enclosed in quartz or feldspar, but more commonly form massive granoblastic aggregates. In handspecimen hedenbergite is dark green, while rhodonite and pyroxmangite are deep red to orange - brown, and both are almost colourless in thin section. The pyroxenoids commonly show alteration to amphiboles (Figures 3.6-3.7), or less commonly pyrosmalite or manganpyrosmalite. The amphiboles preferentially replace pyroxenoids along cleavages, fractures and grain boundaries, while pyrosmalite appears to replace pyroxenoids more completely, and this is probably related to the difficulty in incorporating large amounts of manganese into the amphibole structure (Robinson et al. 1982).

4.10 Staurolite.

Staurolite occurs as euhedral to subhedral, prismatic crystals, light to medium brown in colour and is fine to medium grained. It may exist in equilibrium with muscovite, garnet, biotite and sillimanite, indicating complete retrograde recrystallization of these rocks, but locally shows signs of sericitization. It is commonly poikiloblastic, with inclusions of quartz (commonly fine and vermicular) and rarely fine ilmenite, which probably indicates that this staurolite has replaced biotite. Much staurolite has replaced gahnite, which occurs as relics within some euhedral staurolite crystals (Figure 4.17) or within fine staurolite aggregates (Figures 4.15 - 4.16). Some staurolite has replaced gahnite topotactically (Figure 4.16).

Staurolites in the WAL have all been found to be zincian, with

between 2.5 and 4.3%ZnO (Bottrill, 1983a). Up to 1.6% MgO, 0.15% MnO and 0.52% TiO_2 may also be present and the relation between Fe, Zn and Mg is shown in Figure 4.28. The Fe/Al/Si ratios are variable, and the formula is not simple, but can be represented on average as $(Fe_{2.7}Zn_{0.7}Mg_{0.6})_4 Al_{17.3}Si_{7.9}O_{44}(OH)_2$ (Table 4.1), closer to ($Fe_4 Al_{17.3} (Si,Al)_8 O_{48}H_2$: Griffen, 1981) than that of ($Fe_4Al_{18}Si_{7.5}O_{44}(OH)_4$: Yardley, 1981b). Staurolite is one of the few common rock forming minerals to readily accommodate significant Zn, as the element prefers Fe accomodating sites of tetrahedral coordination, as in spinels, or sites of octahedral coordination with hydroxyl ligands (Wedepohl, 1972).

The breakdown reaction of gahnite to staurolite is complex (Reaction 4.3) with preferential retention of Zn in gahnite, and a common association of fine grained biotite with the staurolite indicates that this may be another product of the reaction. Biotite may, however, surround gahnite without staurolite, and is commonly in equilibrium. The biotite may help balance the gahnite-staurolite reaction by FeSi = Al2 equilibria (Reaction 4.3a). Sillimanite may also be involved in the reaction as it is a not uncommon associate of gahnite and staurolite (Reaction 4.3b).

4.11 Ilmenite.

Ilmenite is fine grained and usually opaque, but where it has exsolved from biotite (Figure 3.2) it is very fine grained, translucent and dark brown in transmitted light. This very fine grained ilmenite can be incorporated into garnet (Figure 4.32), indicating garnetization of biotite.

Microprobe analyses on a number of the coarser ilmenite crystals

Fig. 4.28 Compositions of Staurolites (Molecular %)

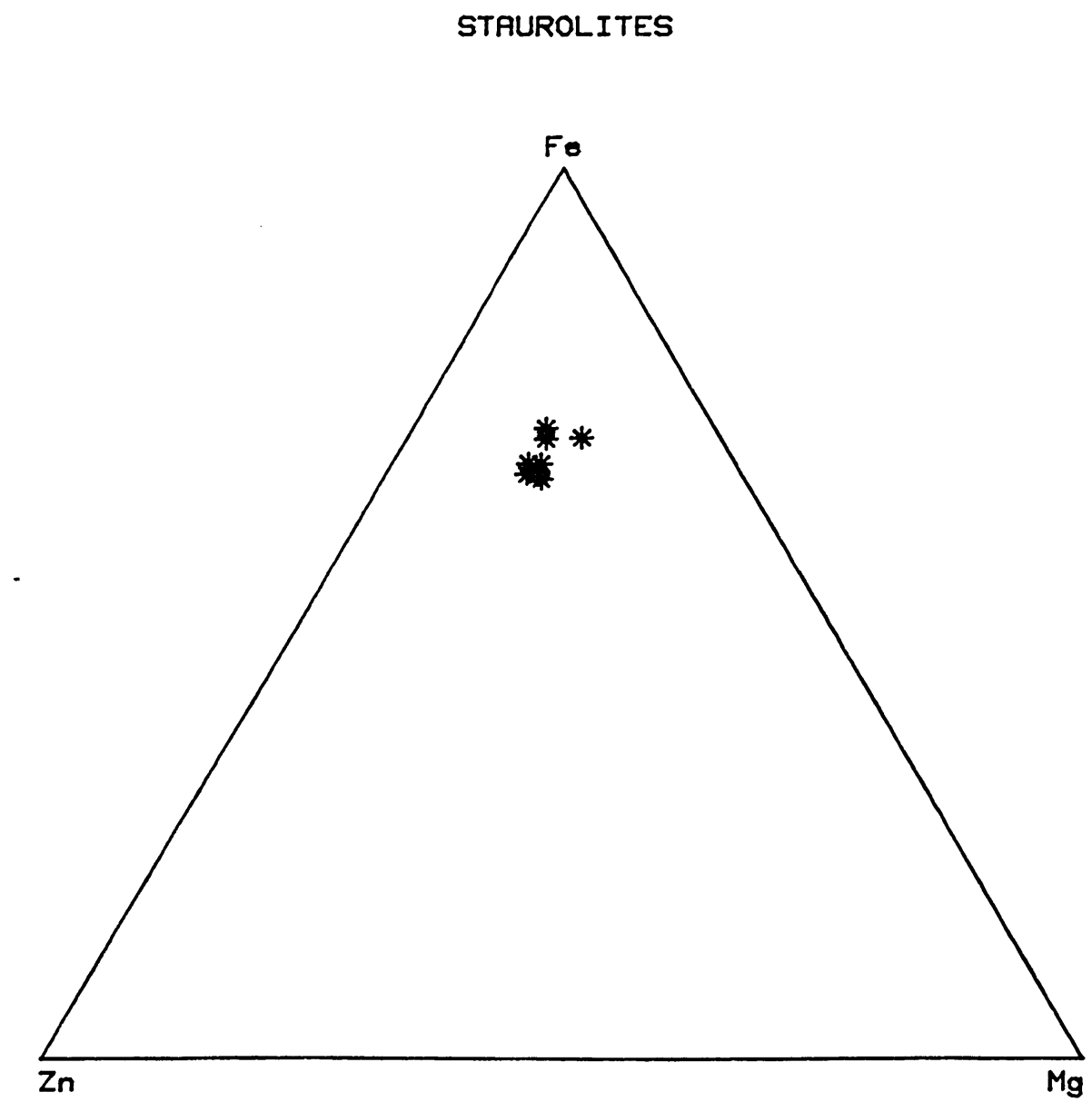

show that they are all manganese - bearing, with between 0.6 and 4.4% MnO (Figure 4.29 and Table 4.1), and small amounts of MgO (< 1.3%) are also present. ZnO was <.05% in all ilmenites analysed, so no significant solid solution towards the zinc analogue of ilmenite, found at Broken Hill by Brown et al. (1970) was detected.

4.12 Sulphides.

Sphalerite, galena, cubanite ($CuFe_2S_3$), pyrrhotite, chalcopyrite, gudmundite (FeSbS), pyrite, arsenopyrite and loellingite were are all noted in polished sections and confirmed by qualitative electron microprobe analyses. Many detailed studies have been published on Broken Hill sulphide chemistry and petrology, including those by Ramdohr, 1950; Stillwell, 1953; Ramdohr, 1972; Lawrence, 1973; Both, 1973; Scott et al. 1977 and Spry, 1978. Most sulphides of the WAL seem little different to those described in these studies, thus only some of the most important factors are mentioned here.

Most sulphide minerals in the WAL are anhedral (except arsenopyrite and loellingite), tending towards coarse - grained polygonal aggregates with balanced surface tensions (Lawrence, 1973), and most inclusions have been forced towards grain boundaries. Many sulphides, especially galena and chalcopyrite, appear to have been squeezed into fractures and small shear zones. Sphalerite is rarely brecciated and cemented by chalcopyrite and galena. Most sulphides can be found as inclusions, often very fine, in some garnet and spinel. Arsenopyrite and loellingite, being more refractory than most sulphides, usually occur in well-formed euhedral crystals.

Some exsolution textures are present, and those noted in the WAL include troilite in hexagonal pyrrhotite (Figure 4.30), cubanite in

Fig. 4.29 Composition of Ilmenites (Molecular %)

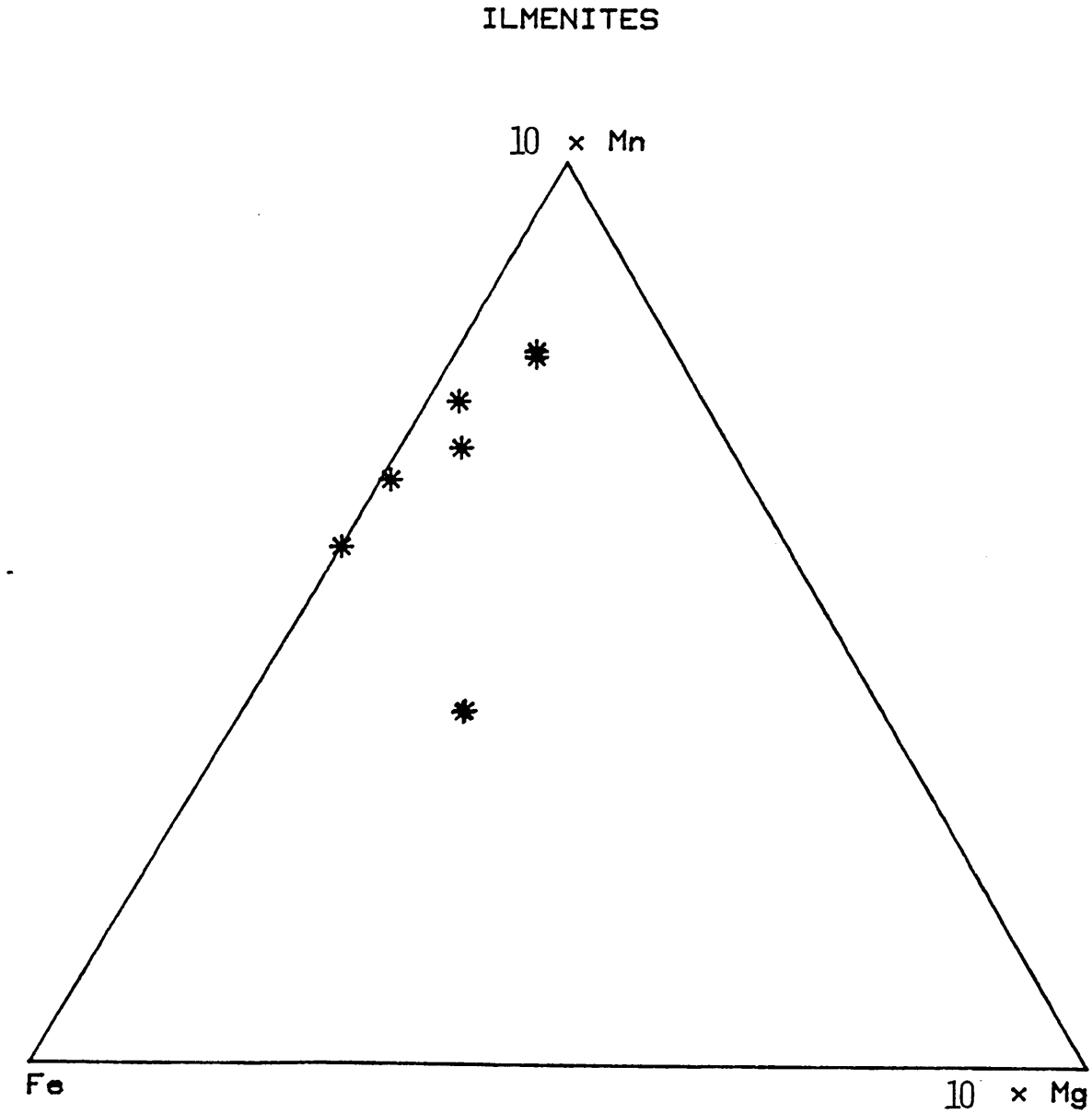

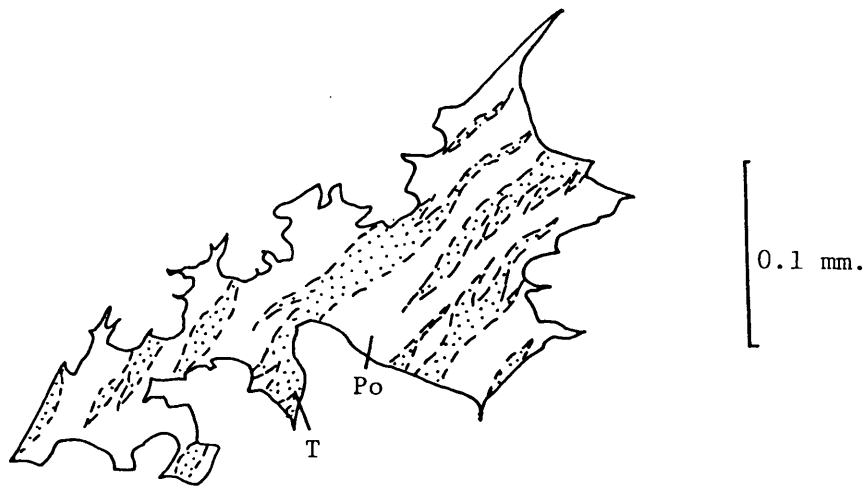

Fig. 4.30 : Pyrrhotite (Po) grain, enclosed in dannemorite, showing typical flame-like exsolution lamellae of troilite (T). (2/1B)

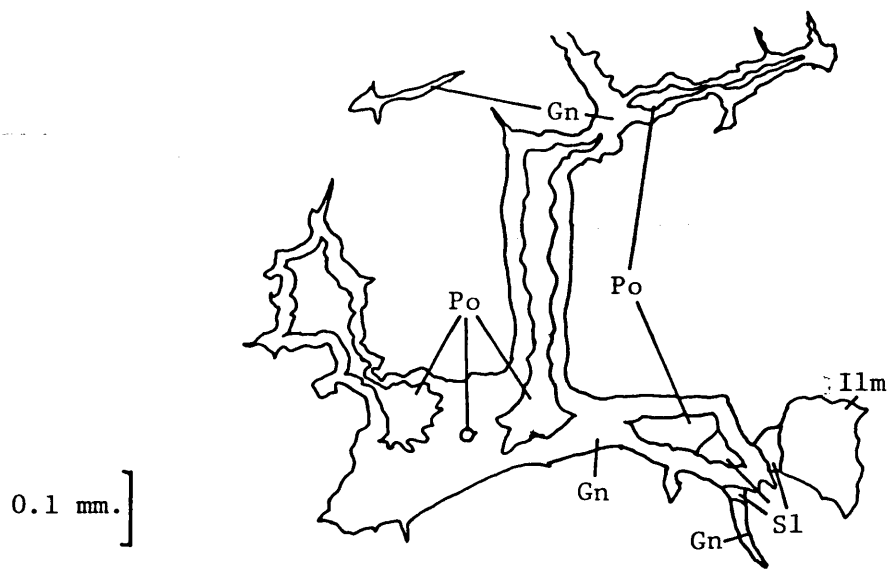

Fig. 4.31: Late stage sulphide vein in garnet quartzite, showing galena (Gn) replacing pyrrhotite (Po), with sphalerite (Sl) and ilmenite (Ilm).

pyrrhotite, chalcopyrite in cubanite and gudmundite in chalcopyrite.

The only definite evidence of alteration or replacement reactions observed were small aggregates of prismatic pyrite on pyrrhotite, and loellingite being replaced by arsenopyrite (Figure 4.34). The arsenopyrite has slightly lower Co and Ni than the loellingite, due to dilution by introduced Fe (e.g from FeO in silicates):

$$\underset{\text{loellingite}}{FeAs_2} + FeO + H_2S = \underset{\text{arsenopyrite}}{2FeAsS} + H_2O \qquad (4.5)$$

There is some evidence for replacement of pyrrhotite by galena in some late-stage veins (Figure 4.31).

Sulphides participate in retrograde replacement of some non-sulphide phases, noticeable in at least three intimate associations:

I. Fine galena within chlorite replacing biotite (Figure 4.9).

II. Fine galena within manganpyrosmalite replacing pyroxenoids (Figure 3.9).

III. Fine sphalerite with sericite and chlorite replacing gahnite (Figs. 4.13, 4.14 and 4.19).

Many sulphides, especially sphalerite and pyrrhotite, are intimately associated with the amphiboles (Figures 3.14-3.15), and it is difficult to determine whether this is an original association or whether it represents a later chemical replacement or mechanical emplacement of more ductile sulphides into brittle silicates. Stilpnomelane also appears most abundantly within sulphide aggregates (Figure 3.10), and has a similar genetic relationship.

4.13 Retrograde Phyllosilicates.

A number of retrograde phyllosilicates occur in the WAL, including

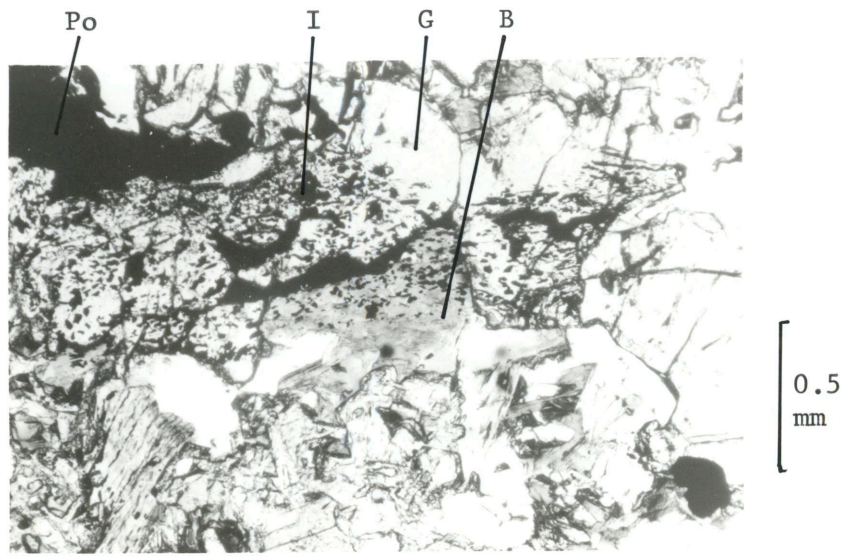

Fig. 4.32 Garnetisation of biotite (B), as evidenced by the presence of fine ilmenite (I) in both biotite and garnet (G), with coarse grained pyrrhotite (Po). (4500/25.2). PPL.

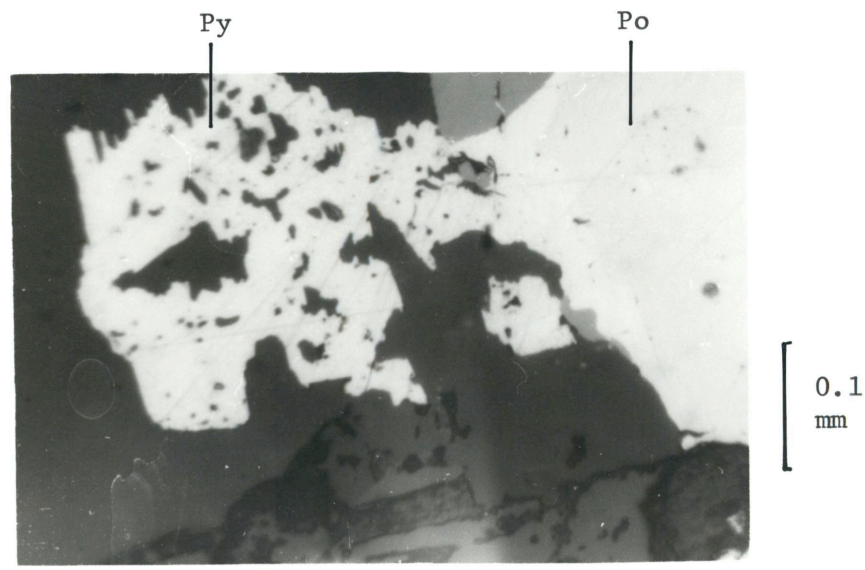

Fig. 4.33 Pyrite (Py) overgrowth on pyrrhotite (Po). (2/5B). Reflected light, PPL.

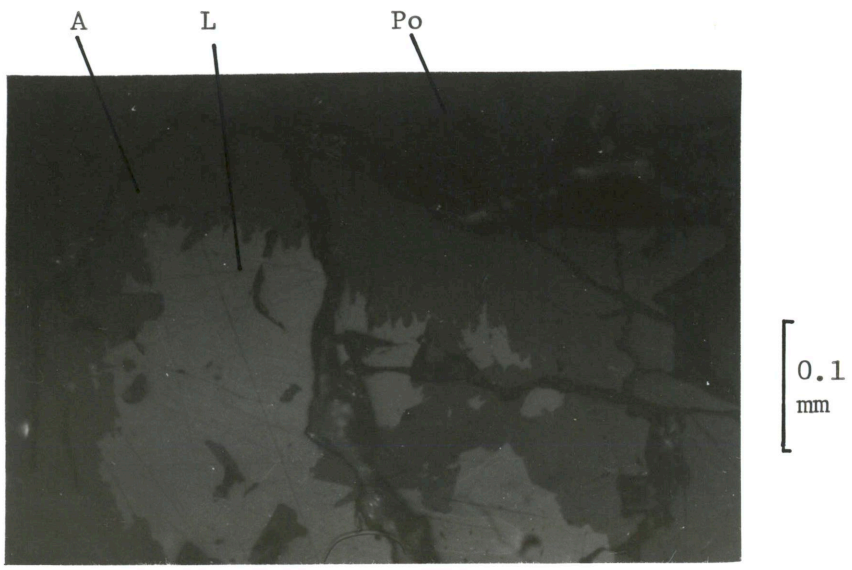

Fig. 4.34 Replacement of loellingite (L) by arsenopyrite (A), in pyrrhotite (Po). (2/5A). Reflected Light, XPL.

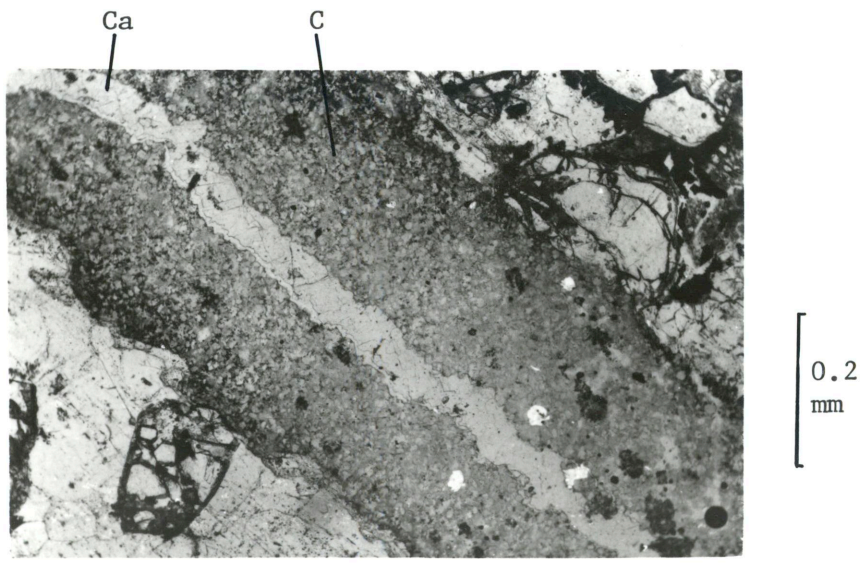

Fig. 4.35 Chlorite (C) - Calcite (Ca) vein in garnet quartzite. White spots indicate probe damage. (4502/48.7). PPL. Fine berthierine is interstitial to chlorite.

chlorite, some green biotites, sericite/muscovite, paragonite, pyrosmalite-group minerals, greenalite (?), berthierine, 'sturtite', and stilpnomelane. Average compositions are given in Table 4.4.

Chlorite is most commonly found replacing biotite, sometimes gahnite, and rarely garnet but some chlorite occurs in veinlets with manganoan calcite and berthierine (Figure 4.35). The chlorites vary from very fine to coarse grained, are green to greenish yellow in thin section, and commonly show the anomalous 'Berlin Blue' interference colours, typical of most Fe-rich chlorites and other chlorites where $2V \simeq 0^{0}$ (Saggerson and Turner, 1982).

The chlorites are widely variable in composition, even on a microscopic scale. Using the nomenclature of Bayliss (1975) for chlorites, most are chamosite, and a few are clinochlore. Using the nomenclature of Hey (1954) or Foster (1962) most are ripidolite but some are daphnite or brunsvigite (Fig.4.36). Plots of coexisting chlorite and biotite (Fig.4.37) show variable non-equilibrium relationships, unlike the assemblages in equilibrium with iron sulphides described by Mohr & Newton (1983), where they are almost equal in Fe /Mg+Fe. The WAL chlorite usually has a higher Fe/Fe + Mg than the coexisting biotite, as a result of the release of Fe by simultaneous gahnite breakdown. The pennantite ($Mn_6Si_4O_{10}(OH)_8$) component is low (<1.1% MnO), and shows a slight negative correlation with Al (Figure 4.38), and the Zn chlorite component (Radke et al. 1978) is even smaller (<0.4% ZnO).

The sericite is usually found replacing gahnite, orthoclase, plagioclase or, rarely garnet and is generally very fine grained and colourless. Sericite (fine - grained muscovite) in the WAL has a small but variable celadonite component, but some has Mg + Fe ~ 1, and Si =

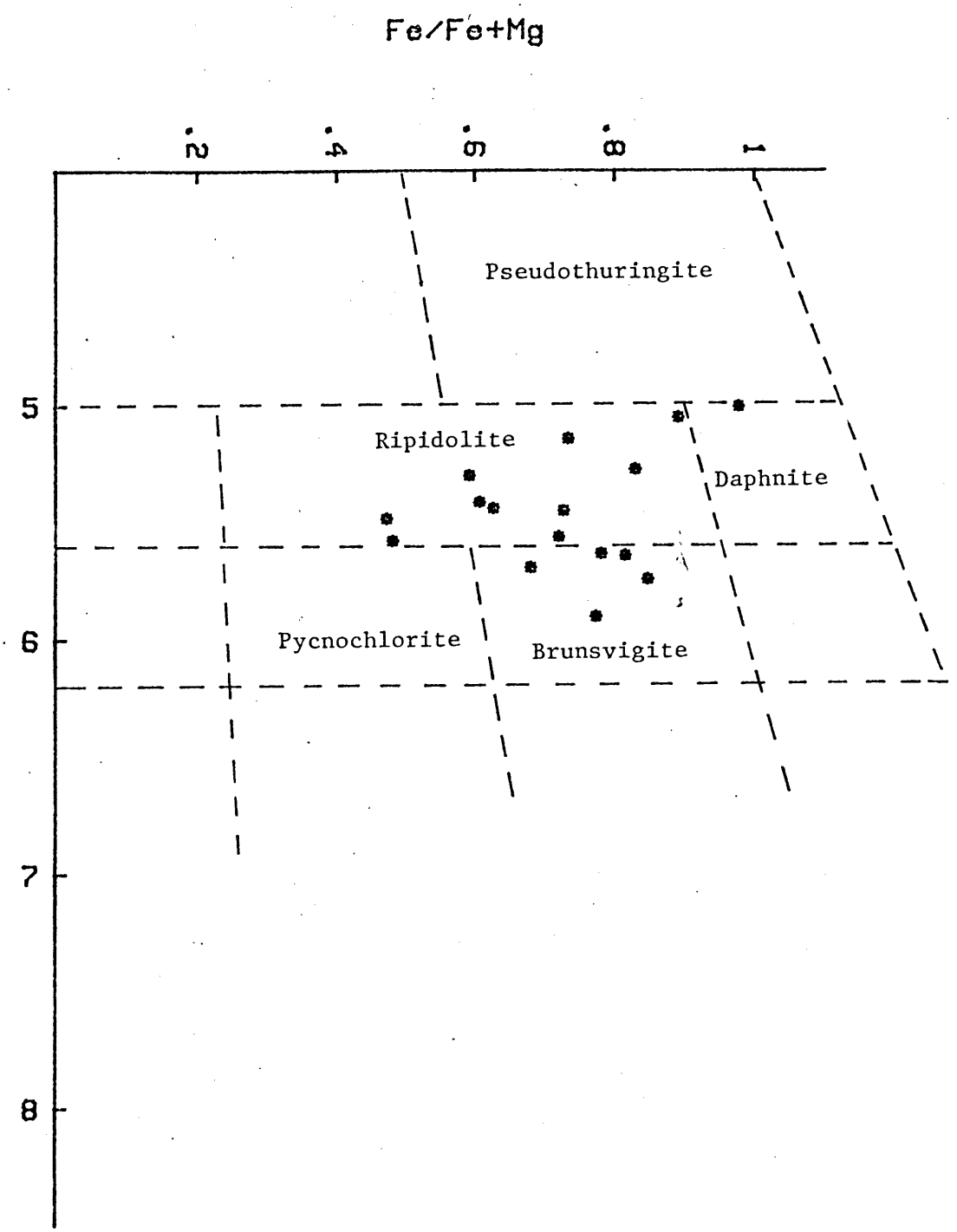

Fig. 4. 36 Composition of Chlorites, showing the composition fields of Hey (1954).

Fig. 4.37 Relations between Coexisting chlorites (triangles) and biotites (crosses).

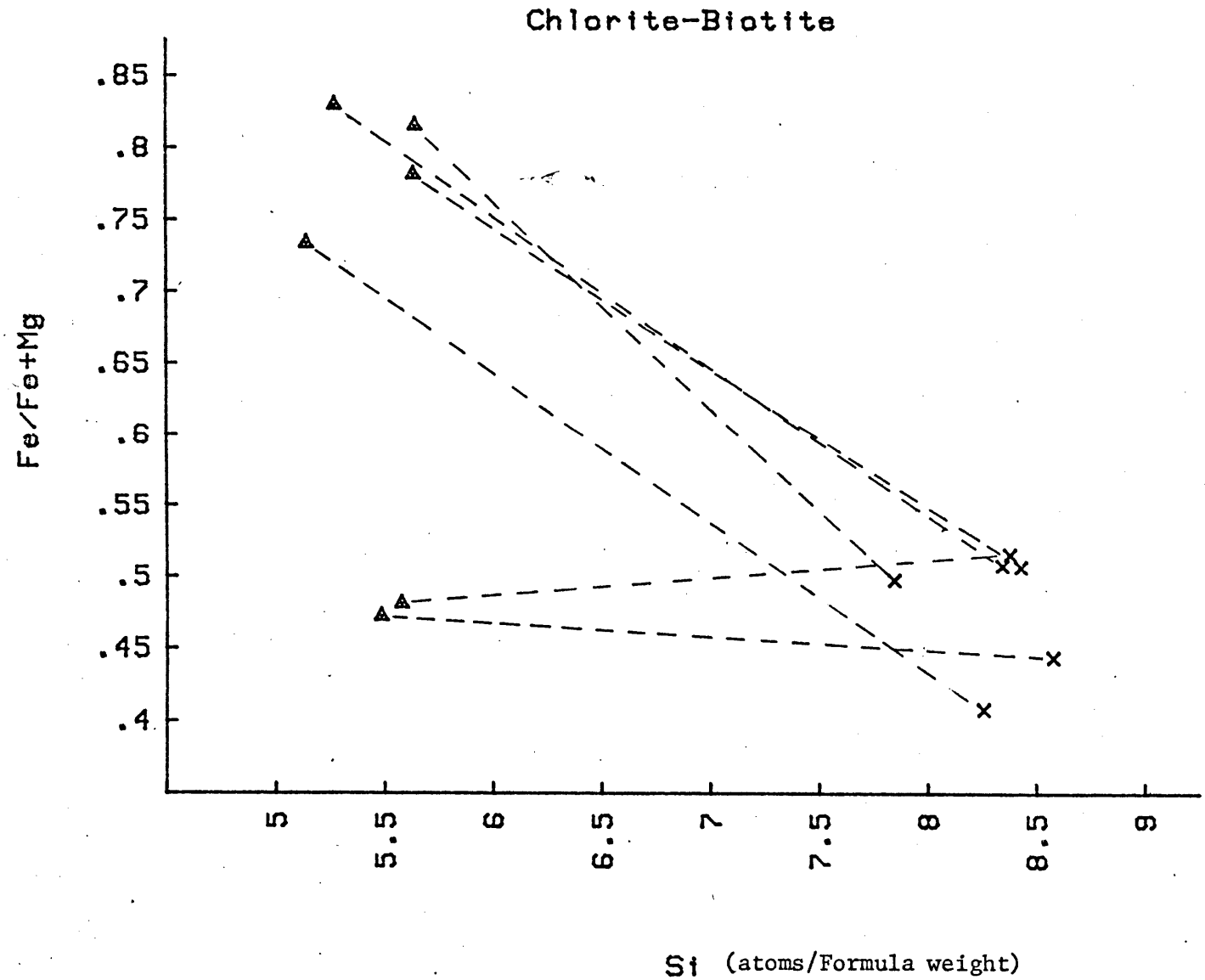

Fig. 4.38 Relations between Mn and Al in chlorites.

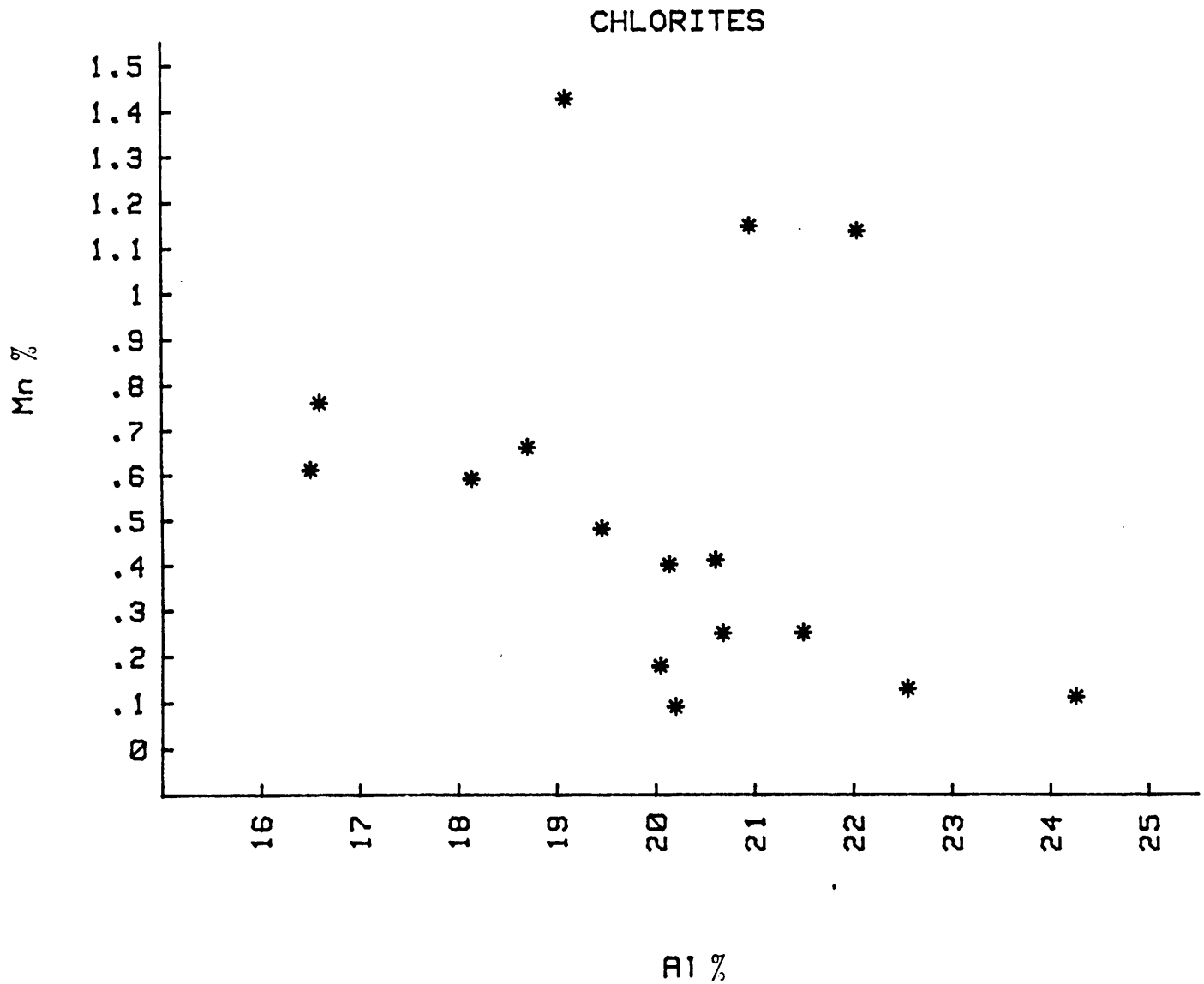

6.6 (for 22 oxygens) and could be classified as either phengite (Crowley & Roy, 1964), or ferrimuscovite (if all Fe is present as Fe^{3+}). The paragonite component is low, and TiO_2 is quite variable.

Two paragonites analysed have variable but high muscovite contents, (about 12%) and moderate Fe and Mg contents (about 0.3 and .15 % respectively). The paragonite was found with chlorite and sphalerite in a replacement rim about gahnite.The sericite is commonly found replacing gahnite, orthoclase, plagioclase or, rarely, garnet, and is usually very fine and colourless.

Pyrosmalite was found in a few samples as replacements of rhodonite and pyroxmangite. The Mn / Mn + Fe ratio is about .45. A fine grained phase, intergrown with galena, is commonly found as a selvage (Figure 3.9) separating pyrosmalite from the pyroxenoids and Electron microprobe analysis indicated a composition like manganpyrosmalite, with Mn/Mn + Fe about 0.69. Friedelite, and other members of the pyrosmalite group, have much higher Mn/Mn + Fe ratios and extra X-ray diffraction lines (Donnay et al. 1980) which were not detected in any WAL samples.

A completely amorphous, black, hydrous, Fe-Mn-silicate is not uncommon as a late-stage alteration product of pyroxenoids, in joints, fractures and calcite veins in massive, quartz-poor pyroxenoid-rich rocks. Very similar material is widespread in other similar parts of the Broken Hill lodes, and was described by Hodge-Smith (1930) as 'sturtite', although this has Mn>Fe while the material analysed from the WAL has Fe>Mn. Fleischer (1980) equated 'sturtite' with neotocite ($MnSiO_3.nH_2O$: Clark et al. 1978) although Portnov et al. (1978) found them to have a different structure. The material is probably hisingerite ($FeSiO_3.nH_2O$: Whelan and Goldich, 1961; Lindqvist and

Jansson, 1962). Hisingerite and neotocite were considered by Whelan and Goldich (1961) and Brigatti (1981) to be smectite group minerals, but Lindqvist and Jansson (1962) thought that hisingerite could be a trioctahedral mica, as Portnov et al. (1978) suggested for 'sturtite'. The nature of these phases is in need of further study by Transmission Electron Microscopy, Differential thermal analysis and Thermogravimetric analysis.

Very fine - grained, brown, iron silicate phases are locally found as alteration products of gahnite or late-stage vein-fillings. Some have chlorite - like compositions, but also coexist with chlorite, and may thus be the septechlorite polymorph, i.e. berthierine ('chamosite'). Some are low in Al, and may be interlayered chlorite - greenalite (Gole, 1980). Some are K-rich, and may be 'hydrobiotite' or consist of disordered interlayered chlorite $\pm$ mica $\pm$ stilpnomelane $\pm$ greenalite, similar to some phases found by Gole (1980). One coarse grained 'biotite' is very low in K (7.1% K_2O) and contains 1.3% ZnO, and may be incipiently chloritized, although this was not obvious in thin section.

Manganoan stilpnomelane is an occasional alteration product of pyroxenoids in the WAL (Figure 3.10). It occurs up to 0.3 mm. in size, is usually intimately associated with sulphides, and is colourless to pale brown in thin section. The pale colour is atypical for stilpnomelanes and is probably due to the unusually low Fe^{3+} and/or Ti, or perhaps less defects in its crystal lattice.

4.14 Other minerals.

Fluorapatite is common in the WAL, as in the rest of the Broken Hill lode (Harada et al. (1974); Lawrence, 1968), and analyses

indicate up to 0.14% MnO. Pleochroic haloes about apatites in some biotites indicate local enrichment in U and/or Th. Plimer (1981) noted the presence of U in apatites from BIFs at Broken Hill and found a linear relationship between F and U.

Allanite is a minor phase in many specimens, and qualitative microprobe scans indicate high Ce and Nd, with lesser Sm, La and other rare earth elements. It is medium to dark brown, non-metamict and moderately pleochroic in thin section.

Clinozoisite/epidote type minerals were identified optically as inclusions within orthoclase. They are colourless to very pale yellow, have anomalous blue interference colours, and probably derive from retrograde breakdown of the anorthite component of the feldspar.

Sphene was found in only a few thin sections of WAL rocks, and is rich in Al and Fe with minor Mn, Mg and Zn. Al - enrichment of sphenes has been taken to indicate high pressure formation (Smith, 1980) but Barron & Barnes (1981) have shown that Al - rich sphenes from the Broken Hill area were formed at only moderate pressure, and were probably stabilized by F. Controls for substitution are complex (Coombs et al., 1976) and the principal substitution is (Al,Fe)(OH,F) = TiO with only minor substitution of Mn, and perhaps Mg, for Ca. The average composition is Ca(Ti0.8,Fe0.1,Al0.1)Si(OH,F)5. Dannemorite may nucleate about sphene.

Rutile is a common, very fine grained accessory, mainly occuring as exsolution in and about biotite.

Monazite and zircon are infrequent, minor, fine grained accessories.

Carbonates are uncommon but two were analyzed - one with chlorite as a vein filling (Ca 0.85 Mn 0.13 Fe 0.12CO3) (Figure 4.35), and one with hedenbergite, actinolite and dannemorite as either a primary or

early retrograde phase ($Ca_{0.85}Mn_{0.13}Fe_{0.12}CO_3$).

Rhodochrosite was verified by X-ray diffraction from a late-stage association with a 'sturtite'-like phase.

Chapter 5. Mineral and whole - rock chemical variability.

5.1 Introduction.

In this chapter the major chemical trends (whole-rock and mineral variation) across the WAL are discussed. Detailed studies of whole-rock variations in and around the Broken Hill lodes have been conducted by Walker (1964), Plimer (1975c & 1979), Stanton (1976a) and Elliott (1979) and Plimer (1977a) studied the mineral chemistry in the wallrocks within about 500 metres of the orebodies. This study attempts to combine both approaches, but differs in scale - being restricted to a detailed investigation of part of one lode (the WAL) and the wallrocks within about 30 metres of this. It was thought that a more detailed study was necessary to properly define the present and original nature and variation within the lode.

5.2 Whole - rock chemistry.

Nine samples of split core from NBHC drill hole DH4502, intersecting the WAL, were selected as representatively as possible, and analysed for the major and some minor elements. Twenty-one elements were determined: Si, Ti, Al, Fe, Mg, Mn, Ca, K, Na, Ba, Pb, Cu, Ni, Zn, S and P by XRF, Rb and Sr by AAS, and B, Ga and Li by Emission Spectroscopy. Analytical techniques are described in Appendix 1. In accordance with the assumptions discussed in Section 4.1, all Fe is assumed to be present as FeO. The results are shown in Table 5.1, down hole variations are illustrated in Appendix IV, summarized in Figure 5.1, and are discussed below.

NBHC Sample No.	293055	293056	293060	2293069	293071	293079	293095	293168
Mineralogical zone	Sillimanite Gneiss	Gahnite zone	Garnet Quartzite	Pyroxenoid-amph. zone	Pyroxenoid subzone	Amphibole subzone	Garnet Quartzite	Sillimanite Gneiss
Interval (m)	21.7-24.7	24.7-27.1	33.6-36.8	53.6-56.5	58.0-58.8	72.2-73.5	98.1-100.7	124.3-125.6
Si %	29.09	25.92	31.14	17.85	19.72	33.28	35.18	35.67
Al %	10.05	7.91	5.17	1.043	1.062	2.48	3.08	5.35
Fe %	6.91	11.87	12.65	8.11	9.99	9.64	10.28	6.92
Mg %	0.738	0.815	0.998	0.273	0.269	0.653	0.632	0.748
Ca %	0.129	0.199	0.107	1.098	1.073	0.450	0.140	0.105
Na %	0.131	<0.01	<0.01	<0.01	<0.01	<0.01	<0.01	<0.01
K %	3.94	1.810	0.258	0.063	0.033	0.018	0.159	0.804
Ti %	0.453	0.329	0.220	<0.01	<0.01	0.071	0.136	0.226
P %	<0.01	0.024	<0.01	0.301	0.180	0.019	<0.01	<0.01
Mn %	0.441	0.646	0.811	3.89	6.43	4.29	0.756	0.498
S %	0.166	2.85	0.892	13.06	11.42	2.32	2.38	0.138
Pb %	0.219	3.36	1.884	11.91	7.81	0.667	0.124	0.081
Zn %	0.299	1.263	0.348	16.71	13.84	1.207	0.934	0.067
Cu %	<0.01	0.101	0.025	0.081	0.073	0.083	0.028	<0.01
Ba %	0.052	0.031	<0.01	<0.01	<0.01	<0.01	<0.01	0.021
Rb ppm	300	190	45	130	75	7	16	70
Sr ppm	22	15	6	12	7	<2	<2	4
Li ppm	30	15	20	<1	<1	<1	8	15
B ppm	3	<3	<3	<3	<3	<3	<3	<3
Ga ppm	25	30	30	10	7	15	25	25

Table 5.1: Whole-rock analyses of drillcore intervals through typical rocktypes of the WAL, from drillhole 4496.

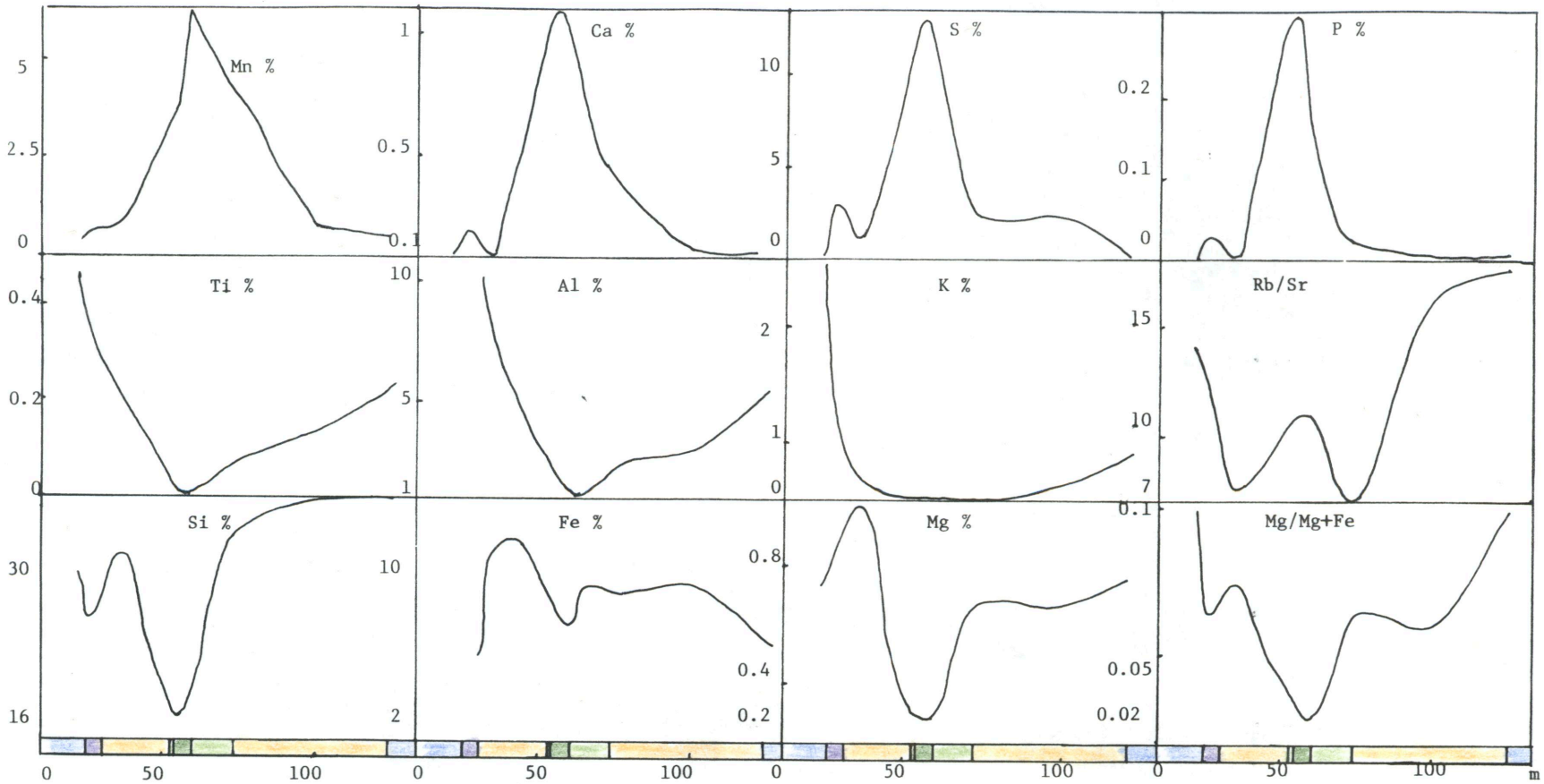

Fig. 5.1 Whole rock geochemical trends for drillhole 4496.

Legend: Sillimanite gneiss, Gahnite-rich zone, Garnet quartzite
Amphibole subzone, Pyroxenoid subzone

The centre of the WAL is approximately the pyroxenoid subzone on this and following figures.

5.2.1 Chemical Variation.

Considerable local depletion towards, or within, the WAL, is shown by Al, Ti, Mg and K (Figure 5.1). Al shows a particularly well - defined trend, varying from about 10% in the sillimanite gneiss and gradually decreasing to about 1% near the centre of the WAL and is closely parallelled by Ti (0.45% to 0.005%). The K concentrations, in contrast, drop rapidly from about 4% in the sillimanite gneiss to below 0.5% within the garnet quartzite envelope but intermediate values occur in the gahnite - bearing zone. K appears to be lower below than above the centre of the WAL, which does not conform with the potassic hydrothermal footwall alteration hypothesis of Plimer (1979) although the difference in scale of these studies makes meaningful assessment difficult. The Mg trend is less well defined, but has comparitively low values (c.0.3% cf. c.0.8%) within the pyroxenoid subzone. The Mg/Mg+Fe trend is, however, better defined, and is more closely related to the Al and Ti trends. There is no obvious relation between Mg and Fe (Figure 5.2). The Si content is relative low (c.19%) within the amphibole-pyroxenoid zone and is moderately constant elsewhere (c.30%), although the slight increase from east to west (hangingwall to footwall) conforms to the footwall silicification hypothesis of Plimer (1979). This increase has a significance of about 90% in Spearman and Kendall correlations (Section 5.2.2). Other elements depleted within the WAL include Ba, Li and Ga.

Many elements are strongly enriched within the WAL, including Ca, Mn, P, S and, of course, the chalcophile elements, especially Pb, Zn and Cu. Ca is most abundant within the pyroxenoid subzone and, except for some enrichment within the amphibole subzone, is comparatively low

Fig. 5.2 Relation between Mg and Fe in whole-rock analyses from drillhole 4496.

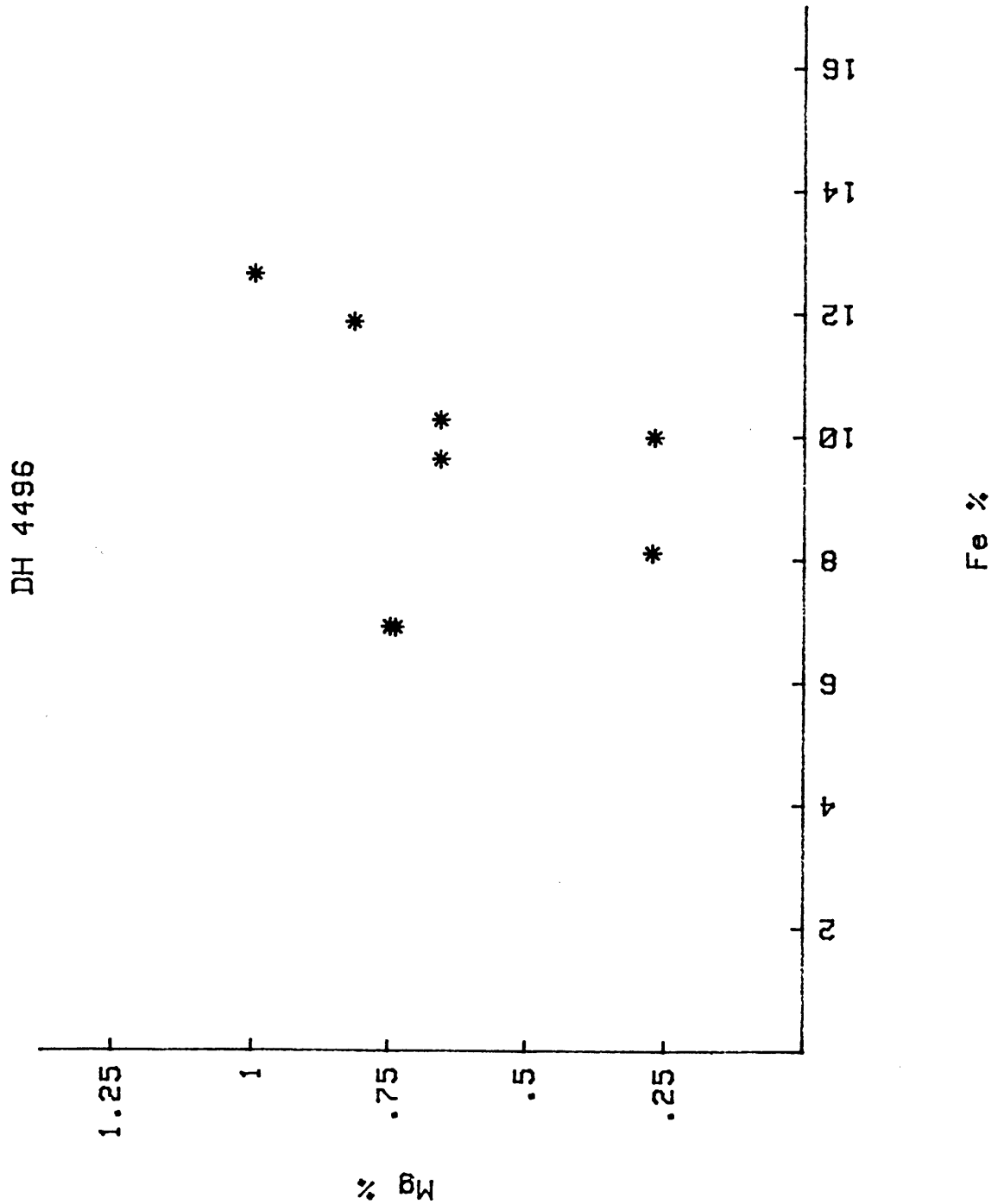

elsewhere (c.1% cf. c.0.1%). Mn is also enriched within the pyroxenoid - amphibole zone (c.5% cf. c.0.6%), but exhibits a greater halo. P and S are enriched only in the pyroxenoid subzone (c.0.2% and c.12%), have moderate values in most other lode rocks (c.0.015% and c.2%), and are very low in the sillimanite gneiss (c.0.005% and c.0.15%). The base metal variations are discussed in more detail in section 5.2.4.

Some elements show no distinct trends with respect to the centre of the WAL, and these include Fe (which is fairly constant - c.10%, Rb and Sr. Rb and Sr are both variable but show an overall decrease from east to west across the WAL (>95% significance: see Section 5.2.2). The Rb/Sr trend is on too small a scale (c.100 m) to exhibit the Rb/Sr trends of ore deposits noted by Plimer and Elliott (1977), which were based on a scale of about a kilometre.

The sillimanite gneisses which were analysed differ slightly in composition, with the lower gneiss having higher Si and lower K, Al and base metals than the upper gneiss. The two garnet quartzites are fairly equivalent in composition, although the upper one is higher in Pb and Al, and lower in S and Zn, than the lower garnet quartzite.

5.2.2. Correlation coefficient analysis.

Spearman and Kendall correlation coefficients were calculated using the SPSS statistical program at the University of NSW, and the results are summarised in Tables 5.2 and 5.3.

Most of the elements analysed fall within one of two groups. Group A includes most of the normal major elements enriched in detrital sediments, namely Ti, Al, Mg and K, as well as the minor elements Li, Ba and Ga. Group B elements are those more closely associated with the Broken Hill orebodies, specifically Ca, Mn, P, S, Pb, Zn, and Cu.

Table 5.2 Spearman Correlations

egree of onfidence:	90%	95%	99%
lement			
	Si, $\overline{\text{Na}}$	$\overline{\text{Sr}}$, $\overline{\text{Rb}}$	
i	d	$\overline{\text{Ca}}$, $\overline{\text{S}}$, $\overline{\text{P}}$, $\overline{\text{Pb}}$, $\overline{\text{Rb}}$, $\overline{\text{Sr}}$	
l	Mg, $\overline{\text{P}}$	$\overline{\text{Ca}}$, $\overline{\text{S}}$, $\overline{\text{Mn}}$, $\overline{\text{Zn}}$, $\overline{\text{Ga}}$	K, Ti, Ba, Li
e	Na, B		
g	Al, $\overline{\text{B}}$	$\overline{\text{Ca}}$, $\overline{\text{Ti}}$, Li	Ga
a	Mn, Pb, $\overline{\text{Ti}}$, Cu, $\overline{\text{Li}}$, $\overline{\text{B}}$	$\overline{\text{Si}}$, $\overline{\text{Al}}$, $\overline{\text{Mg}}$	P, S, Zn
a	d, K, Fe, $\overline{\text{Mn}}$, Rb, Sr	Ba, Li	B
	Na, B, Ga	Li	Al, $\overline{\text{Mn}}$, Ba
i	$\overline{\text{Ca}}$, $\overline{\text{P}}$, $\overline{\text{S}}$, $\overline{\text{Zn}}$, B	$\overline{\text{Mg}}$, Ba, Rb, Ga	Al, $\overline{\text{Mn}}$, Ba, Li
	$\overline{\text{Al}}$, $\overline{\text{Ti}}$, Mn, P, $\overline{\text{Ga}}$	$\overline{\text{Si}}$, $\overline{\text{Li}}$	Ca, S, Pb, Zn, Cu
n	Ca, $\overline{\text{Na}}$, P, Zn, $\overline{\text{B}}$	$\overline{\text{Al}}$, $\overline{\text{Li}}$	$\overline{\text{K}}$, $\overline{\text{Ti}}$
	$\overline{\text{Ti}}$	$\overline{\text{Al}}$, $\overline{\text{Si}}$, Zn, $\overline{\text{Li}}$, Pb, Cu	Ca, P, Zn
o	Ca	$\overline{\text{Si}}$, S	P, Zn
a	$\overline{\text{Si}}$, $\overline{\text{Ti}}$, Mn	$\overline{\text{Al}}$, S, $\overline{\text{Li}}$, Cu	Ca, P, S
a	Ca	S, Zn	P
a		Na, Ti, Li, Rb, B	Al, K, Ti
o	Na	$\overline{\text{d}}$, Ti, Ba	Sr
	Na	$\overline{\text{d}}$	Rb
	$\overline{\text{Ca}}$	Mg, Na, K, $\overline{\text{P}}$, $\overline{\text{Mn}}$, $\overline{\text{S}}$, Ba, $\overline{\text{Zn}}$, Ga	Al, Ti
	$\overline{\text{d}}$, Fe, $\overline{\text{Mg}}$, $\overline{\text{Ca}}$, K, Ti, $\overline{\text{Mn}}$	Ba	Na
a	K, $\overline{\text{P}}$	Al, Ti, Li	Mg

= depth down drillhole

ars above elements indicate negative correlations

Table 5.3 Kendall Correlations

egree of onfidence: lement	90%	95%	99%
		$\overline{Rb}$	$\overline{Sr}$
i	$\overline{Sr}$	$\overline{Ca}$, $\overline{S}$, $\overline{Zn}$	$\overline{P}$, $\overline{Pb}$
l	$\overline{P}$, $\overline{S}$	$\overline{Ca}$, $\overline{Zn}$, $\overline{Ga}$	K, Ti, $\overline{Mn}$, Li
e			
g	K	Al, $\overline{Ca}$, Ti, Li	
a	K, $\overline{Ga}$	$\overline{Si}$, $\overline{Al}$, $\overline{Mg}$, Mn, Cu, $\overline{Li}$	P, S, Zn
a	Ba		
	Mg, $\overline{Ca}$, Rb	Ga	Al, Ti, $\overline{Mn}$, Li
i	$\overline{P}$, $\overline{S}$, $\overline{Zn}$	Mg, $\overline{Ca}$, Ga	Al, K, $\overline{Mn}$, Li
	$\overline{Al}$, $\overline{Ti}$, Mn	Cu, $\overline{Li}$	$\overline{Si}$, Ca, S, Pb, Zn
n	P, S, Ga	Ca, $\overline{Li}$	$\overline{Al}$, $\overline{K}$, $\overline{Ti}$
	$\overline{Al}$, $\overline{Ti}$, Mn	$\overline{Si}$, Pb, Cu	Ca, P, Zn
b	Cu	Ca, S	$\overline{Si}$, P, Zn
n	$\overline{Ti}$	$\overline{Si}$, $\overline{Al}$, Cu, $\overline{Li}$	Ca, P, S, Pb
u	Pb	Ca, P, S, Zn	
i			
a	Na, Sr, B, Li	Rb	Al, K, Ti
b	K	Ba	Sr
r	$\overline{Si}$, Ba		$\overline{d}$, Rb
i	Ba	Mg, $\overline{Ca}$, $\overline{P}$, $\overline{Mn}$, $\overline{Zn}$, Ga	Al, K, Ti
	Ba		
a	$\overline{Ca}$, $\overline{Mn}$	Al, K, Ti, Li	Mg

= depth down drillhole

ars above elements indicate negative correlations

There is a strong positive correlation (usually >99% significance) between elements within the same group, and a negative correlation between elements from different groups.

Rb and Sr show a high correlation with each other, a moderate correlation with Ba and little correlation with any other elements.

Fe lacks any significant positive or negative correlation with any other elements, but correlations are negative for most group A elements and positive for most group B elements. This apparent independence is due to Fe being an important component in both the sulphides and silicates of the metasediments.

Si shows a negative correlation with many elements, but a positive correlation with none. This is due to other elements being swamped by the high abundance of quartz, and indicates that silica was a separate component in the original sediments, probably as chert.

Rb and Sr show a significant decrease with depth down the hole, and Si increases with depth.

Hawkins (1968b) and Stanton et al. (1978), have also noted the correlation of Ca, Mn, P and base metals in the Broken Hill lodes. The correlation of Fe with these, as noted by Hawkins (1968b), was not significant in this study.

5.2.3. Paleosalinity.

Degens et al. (1957a,b), found that the relation between Ga, Rb, and B provides a very useful geochemical method of discrimination between rocks thought to have been formed under conditions of differing salinity. This method has been succesfully applied to rocks of low metamorphic grade by Reynolds (1965a,b) and Davy (1980). A corresponding plot for WAL rocks indicates an extremely low salinity

(Figure 5.3), although the results could be complicated by post-depositional mobilisation of B. Harder (1974) noted than boron can be a very mobile element, although Reynolds (1965b) and Mehnert (1968) showed that while metamorphism may redistribute the boron somewhat, it is seldom lost from the rock (usually being removed from micas and stabilized in tourmaline, axinite and other borosilicates).

The rarity of these borosilicates in the Broken Hill lodes (Birch et al. 1982; Bottrill, 1983b), even in pegmatites and quartz veins, suggests that this process has not occurred in the Broken Hill lodes. Tourmaline - rich rocks found within the Willyama Complex, and recently in the North Mine lodes, are considered by Plimer (1983) and Slack et al. (in press) to represent original primary tourmaline precipitates. Ahmad and Wilson (1981) have inferred the presence of B-bearing retrograde fluids, but Stanton (1976d) and D. Milton (pers. comm.) argue against any significant large scale element movement in the Broken Hill lodes.

A comparison of some average analyses of marine and non-marine shales with sillimanite gneiss from Broken Hill is shown in Table 5.4. The high Ga, low S and Sr, relatively low Mn and very low Li in the sillimanite gneiss are indicative of low paleosalinity, according to the postulates of Keith & Degens (1959), and Wedepohl (1971).

Plimer (pers. comm.) suggested that the ore-forming fluids may have been essentially magmatic, and underwent limited mixing in a restricted basin. These fluids would have masked the paleosalinity indicators, and the hydrothermal wallrock alteration, resulting from their percolation through the sediments, may simply provide (useful) information regarding the composition of the fluids. In particular these solutions, poor in Mg, and high in K and Si, resulted in the Mg

Fig. 5.3 Relation between B, Ga and Rb in WAL whole-rock samples, showing the palaeosalinity fields of Degens et al. (1957).

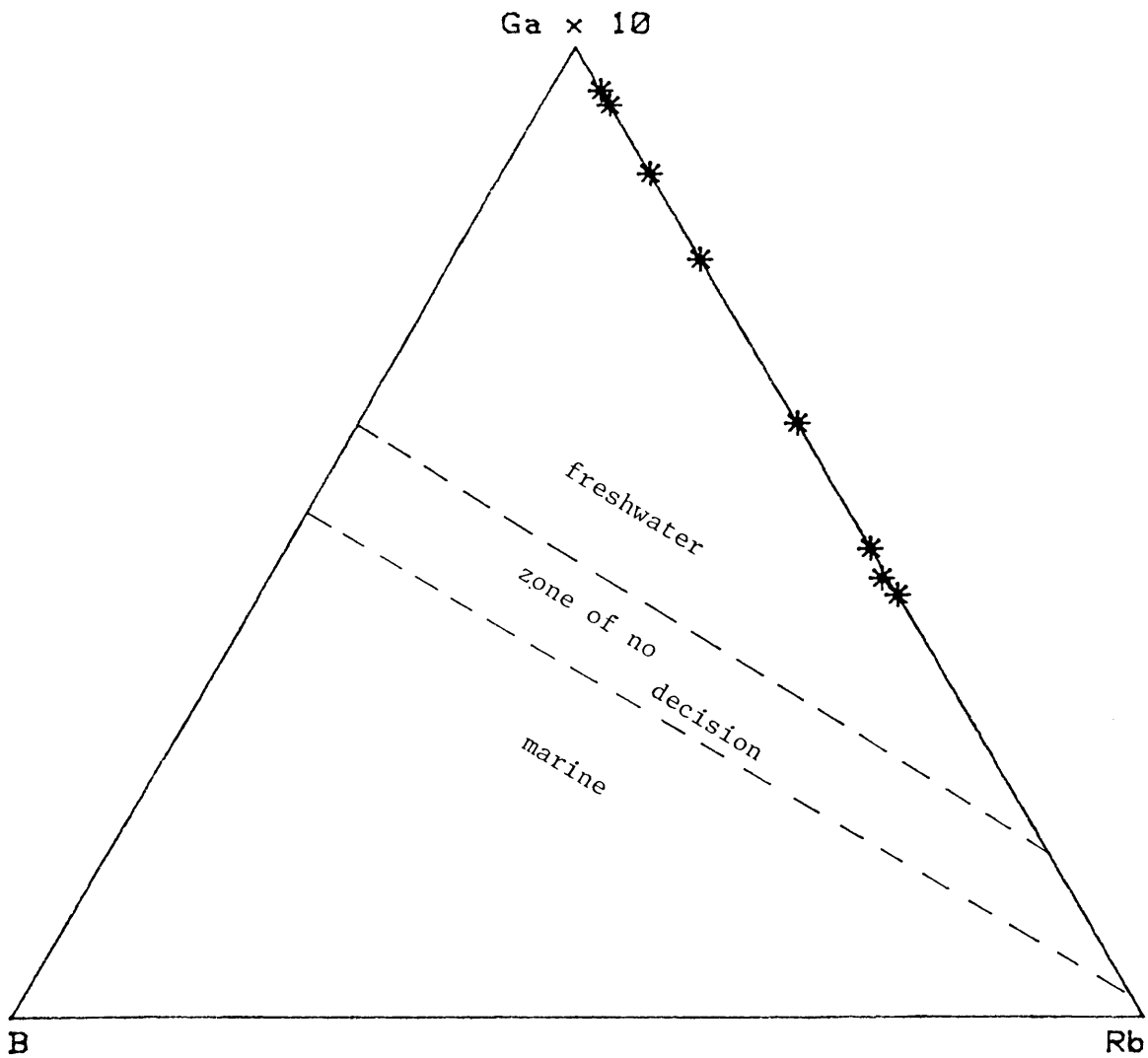

TABLE 5.4 : COMPARISON OF AVERAGE SILLIMANITE GNEISS, FRESHWATER SHALE & MARINE SHALE ANALYSES

	1	2	3	4	5
SiO_2 %	66.60	60.38	54.53	57.29	69.26
TiO_2	0.77	0.96	0.92	0.94	0.57
Al_2O_3	16.50	21.75	20.89	21.24	21.41
Fe_2O_3	0.54	1.22	*	*	*
FeO	6.97	7.01	8.58	7.49	8.90
MnO	0.30	0.26	0.80	0.12	0.61
MgO	1.48	1.83	1.65	1.73	1.23
CaO	1.14	0.63	0.54	0.31	0.16
Na_2O	0.99	0.44	0.22	0.21	0.15
K_2O	3.48	4.45	3.71	3.53	3.34
P_2O_5	0.15	0.14	0.23	0.17	n.d
S	n.d	n.d	0.92	0.15	0.152
B ppm	"	"	115	44	1.5
Ga	"	22	8	17	25
Li	"	n.d	159	92	23
Rb	"	172	n.d	n.d	185
F	"	n.d	817	642	n.d
Sr	"	55	250	205	13

1: Sillimanite gneiss (94 analyses) Plimer (1979). 2: Sillimanite gneiss (63 analyses) Shaw (1973). 3: Marine shale (15 analyses) Keith & Degens (1959). 4: Non-marine shale (15 analyses) Keith & Degens (1959). 5: Sillimanite gneiss (2 analyses). This study.

* = all iron as FeO n.d = not detected

- depletion, sericitization and silicification, as suggested by Plimer (1979).

Berner et al. (1979) noted that the presence of iron monosulphides other than pyrite in sediments is indicative of low salinity. Plimer (1981) noted the lack of evidence for any original pyrite within the Broken Hill lode, and postulated that an iron monosulphide (perhaps pyrrhotite), rather than pyrite, was the original iron sulphide in the Broken Hill lodes. This may then be taken as another indicator of low paleosalinity for these rocks, but is discussed in greater detail in section 6.2.

In conclusion, estimation of the paleosalinity is complicated by a number of unknown factors, but there is considerable evidence to indicate that the salinity of the depositional basin and/or ore-forming fluids was very low.

5.2.4. Base metal variations.

NBHC mine assay data for base metals were plotted as bar - graph plots (Appendix 4b), as the wide variation in sample lengths made comparisons of trends otherwise difficult, and are summarised in Figures 5.4 - 5.6.

The distribution of sulphides suggests the usual presence of three principle zones of enrichment:

I. A stratigraphically upper zone, within the gahnite - rich zone and high in the upper garnet quartzite.

II. A central zone, centred about the pyroxmangite subzone.

Fig. 5.4 Base metal variation in Drillhole 4496.

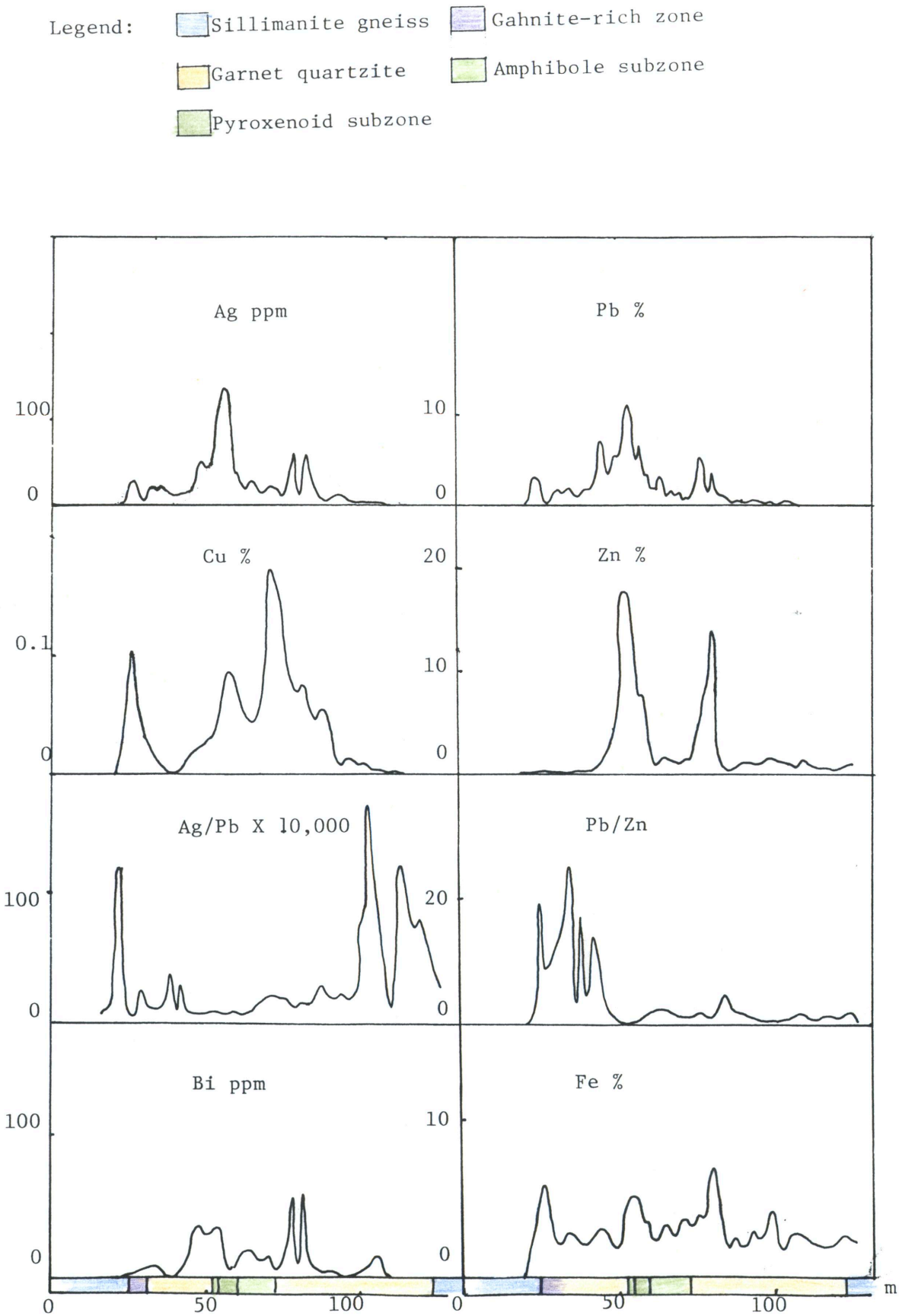

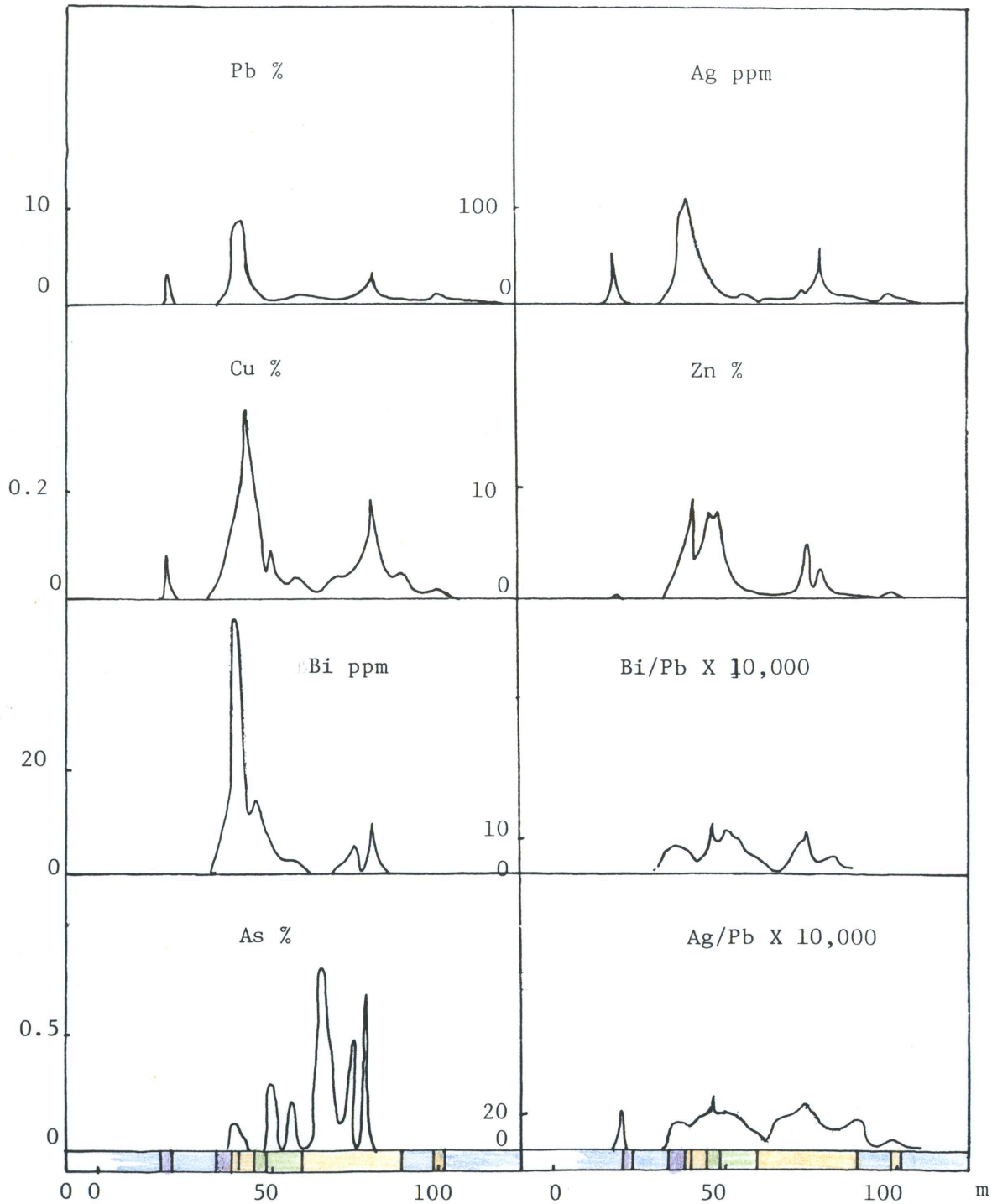

Fig. 5.5 Base metal variation in Drillhole 2682.

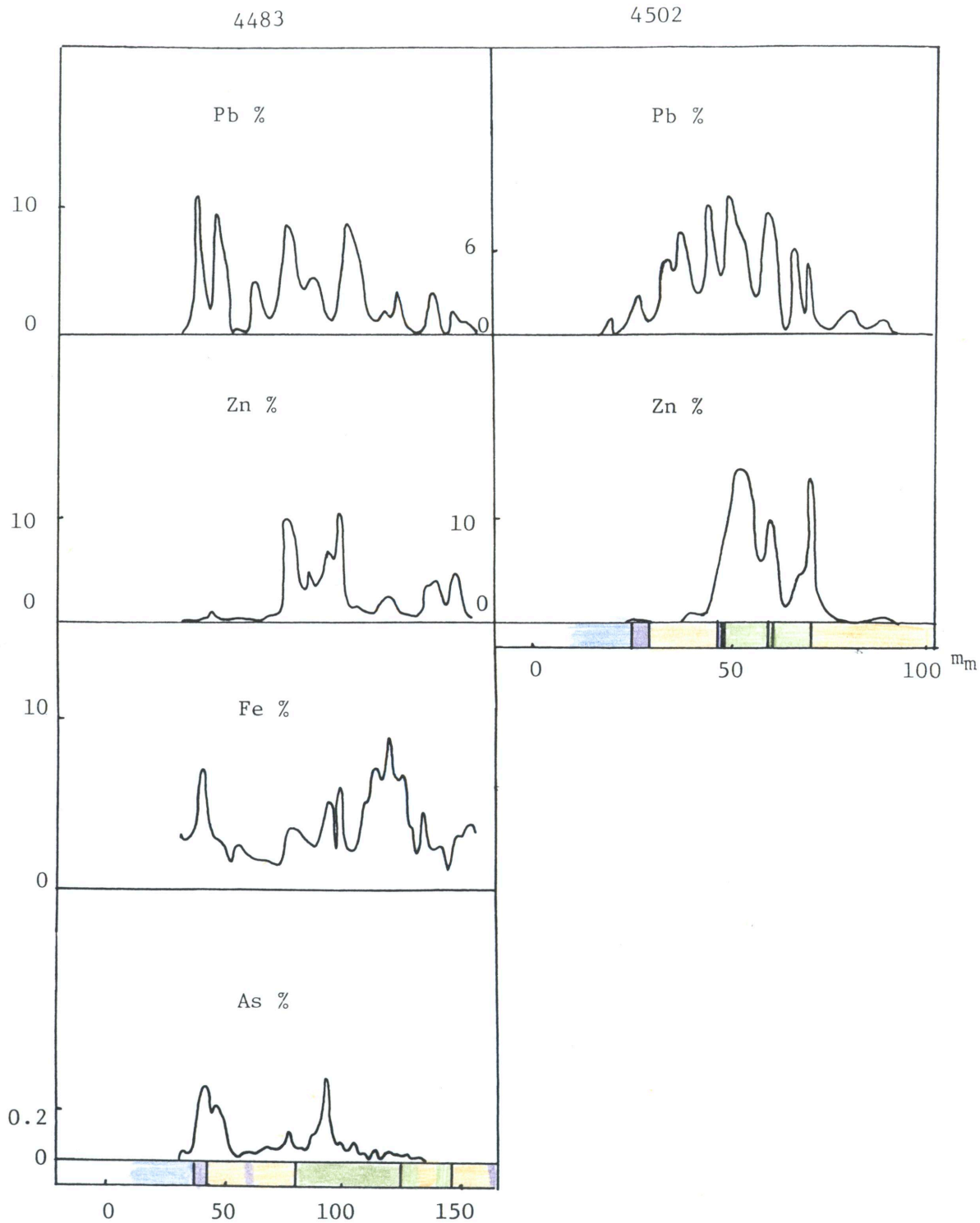

Fig. 5.6 Base metal variation in Drillholes 4483 and 4502.

III. A small, stratigraphically lower zone, within the lower garnet quartzite.

Pb is fairly well distributed throughout the WAL, but has peaks corresponding to the three sulphide-rich zones, and is richest within the central zone. The presence of several small galena-rich patches are also apparent. Zn is less widely distributed, and is relatively minor in the stratigraphically upper sulphide zone. Ag and Bi closely follow Pb in distribution, but minor fluctuations in the ratios Ag/Pb and Bi/Pb seem to occur (Figs. 5.5 - 5.6). High values of these ratios tend to be prevalent in low - Pb (and low Ag & Bi) areas, and may indicate either the presence of Bi - bearing minerals (other than galena) or, perhaps more likely, analytical errors as detection limits are approached and as such are not significant. Cu appears somewhat similar to Pb in distribution, but seems more widely dispersed. The distribution of Fe appears to be even more widespread, although still enriched in the principle sulphide zones. The generally high Fe values, even when pyrrhotite seems poor, suggests that part of the Fe determined in assays is derived from silicates, not just the sulphides as assumed by mine geologists (D. Milton, pers. comm.). Arsenic is very patchily distributed, usually being highest in sulphide zones, but can have high values elsewhere in the WAL.

5.3. Variations in Mineral chemistry.

Many of the mineral phases discussed in Chapter 3 show large variations in composition throughout the WAL and its wallrocks. This is most important for the phases that are principally prograde, e.g. garnet and biotite, but other minerals, including gahnite, chlorite, amphiboles and pyroxenes also show considerable chemical variations.

Fig. 5.7 Relation between Ag and Pb in Drillhole 4502.

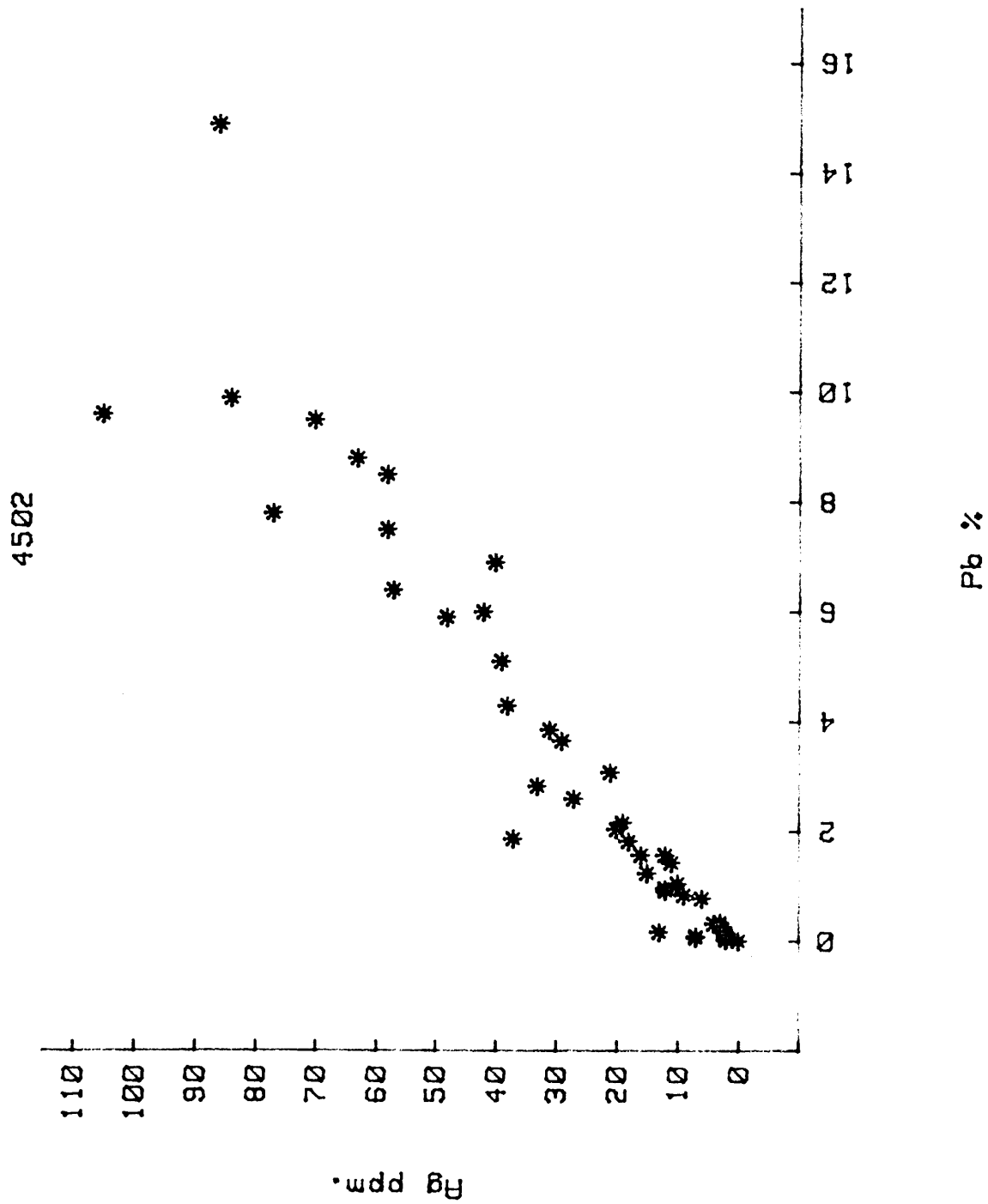

Fig. 5.8 Relation between Bi and Pb in Drillhole 4502.

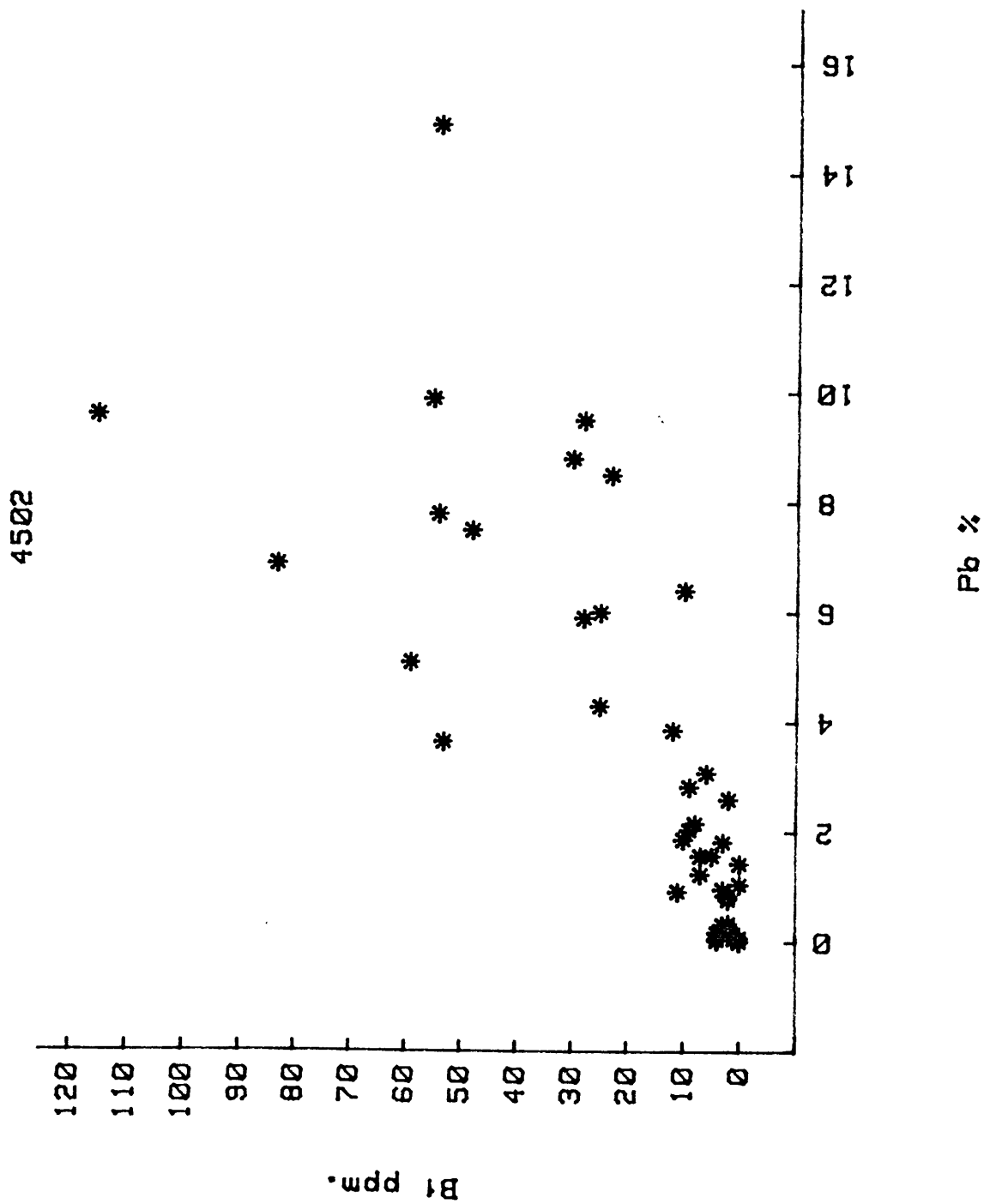

The pyroxenoids appear to have a relatively limited compositional range in the WAL (Figures 4.24 - 4.26), despite showing considerable chemical variation in nature (Brown et al. 1980). The plots are shown in Appendix 4c and are summarized in Figures 5.9 - 5.10.

5.3.1 Garnets

As discussed in section 4.3, WAL garnets vary from magnesian almandine to a Ca-Fe-rich spessartine. There is a general trend from low to high (Ca + Mn) /Mg towards the centre of the orebody. The low values around 65.2 m and 67.3 m in DH4502 occur in Mg-rich, chlorite and/or biotite-bearing samples; the trends can otherwise be related to the whole-rock Ca, Mn and Mg trends.

The Mg/(Mg + Fe) ratio is erratic with no obvious relationship to the whole rock trend (Figure 5.1), probably due to Fe contribution from the Ore-forming fluids as well as the detrital Fe influx. Re-equilibration of Fe-sulphides and Fe-silicates may have further complicated these trends (Mallio & Gheith, 1972). Some amphibole-rich samples have particularly low Mg/(Mg + Fe) (< 0.55), perhaps due to re-equilibration with amphiboles, or to Mn-metasomatism accompanying amphibole formation. The garnet at 26.9 m in DH4502 is associated with staurolite, and perhaps re-equilibrated with it, during retrograde metamorphism. The variation between other samples is usually smaller than their intergranular or intragranular variation.

5.3.2 Biotite

The biotites range in composition from near the phlogopite end-member to near the siderophyllite end-member (Figure 4.6 - 4.7). This Al variation in biotite is closely related to the whole rock Al

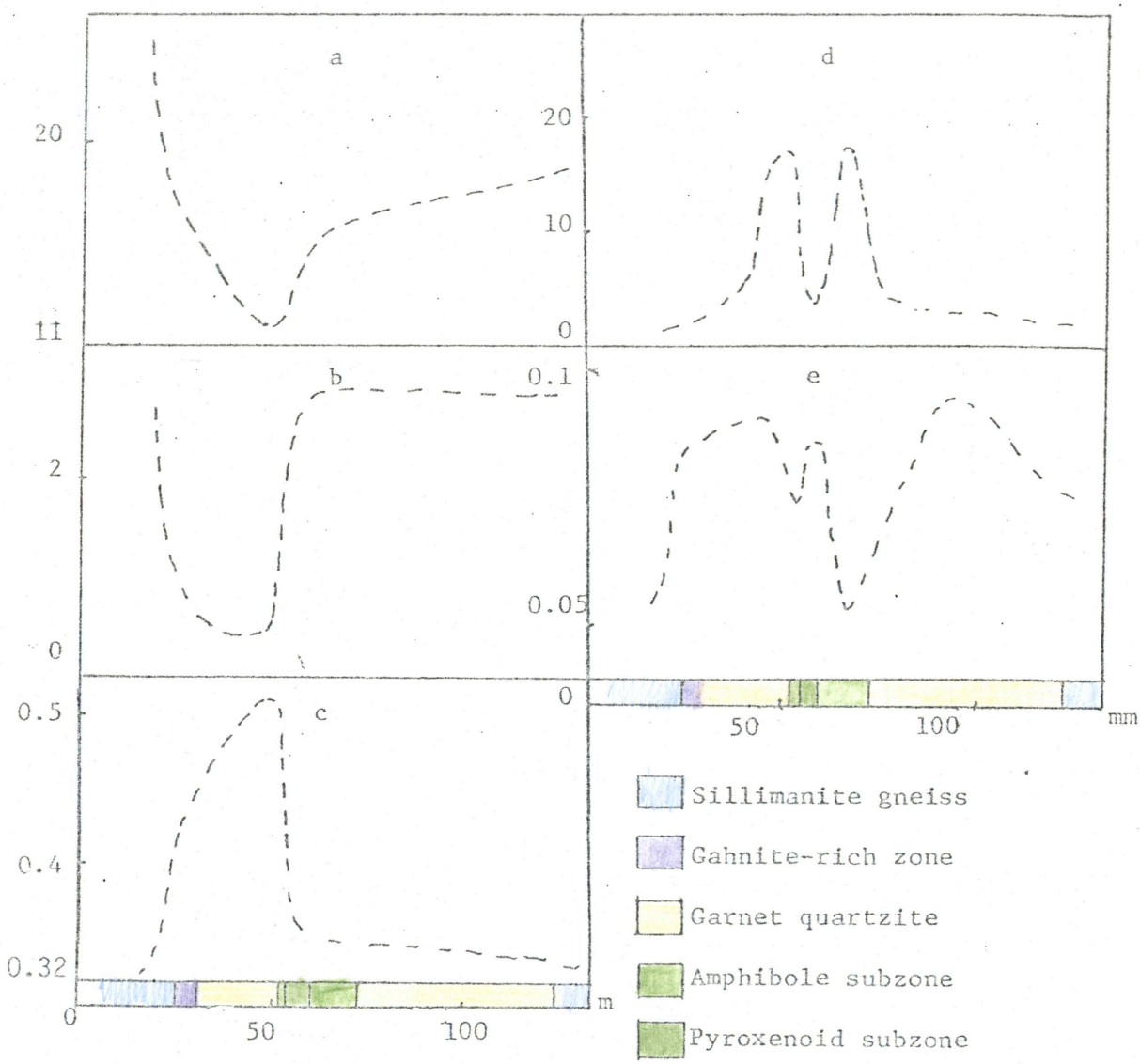

Fig. 5.09: Mineral chemistry variation in drillhole 4496.

a) % Al2O3 in biotite

b) TiO_2 % in biotite

c) Mg/Mg+Fe in biotite

d) CaO + MnO/MgO in garnet

e) MgO/MgO+FeO in garnet

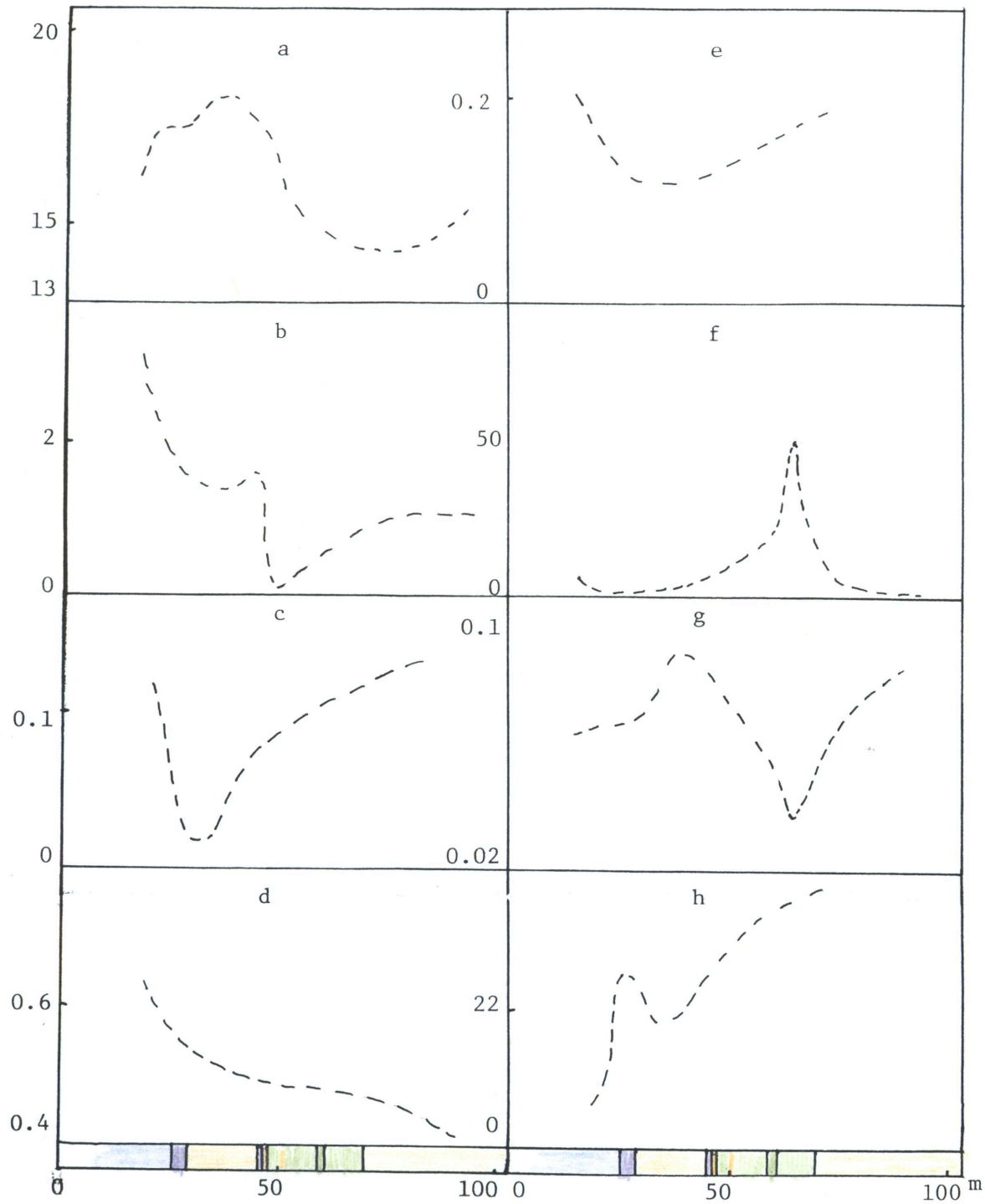

Fig. 5.10 Mineral chemistry variation in drillhole 4502

a) $\%Al_2O_3$ in biotite

b) $\%TiO_2$ in biotite

c) % MnO in biotite

d) Mg/Mg+Fe in biotite

e) %ZnO in biotite

f) (Ca+Mn)/Mg in garnet

g) MgO/MgO+FeO in garnet

h) Zn/Fe in gahnite

variation in DH4496 (compare Figs. 5.1 and 5.9), being highest outside the orebody and dropping steadily towards the centre of the orebody. The trend in DH4502, however, is not so simple, perhaps because most of the high - Al (>17wt.% Al_2O_3) biotites are associated with gahnite. This may be a sampling bias, as gahnite is not very abundant in the region where many of the samples were taken.

The Mg/Mg + Fe variation in biotite varies considerably between the two drillholes. High Mg/Mg + Fe values (>0.48) were recorded from biotite associated with amphiboles, and low values were recorded from biotite associated with zincian hercynite. Green biotite replacing gahnite has very low ratios (<0.15) but the other biotites have a relatively constant ratio of about 0.35.

Ti also shows a variable trend in the two holes. Drillhole DH4496 shows a strong trend of increasing Ti away from the centre of the WAL, but the most Ti - poor biotite (at 47.3m) is the green retrograde biotite. The two high Ti biotites (>2.5% TiO_2) coexist with feldspars (anorthite and orthoclase), but it is uncertain whether this has a direct relationship. The other samples in DH4496 show little variation, with approximately 1 - 2% TiO_2. Most biotites in DH4502 have between 1.1 and 1.3% TiO_2 while two samples have Ti - poor biotite (<0.8% TiO_2) - one of these is associated with amphiboles, the other with staurolite. Both samples may have re-equilibrated at low temperature, where Ti - biotite is less stable, although some biotites in association with staurolite do have a moderately high Ti content.

The sulphide-rich areas of the WAL are very low in Al and Ti, and thus any biotite present is likely to be poor in Al and Ti also. These biotites are relatively poor in Fe, as indicated by the close relation between Ti, Al and Fe / Fe + Mg in biotites (Figure 4.6 and 4.8),

although Fe is relatively constant throughout the lode, or is even enriched slightly in the (Ti and Al-poor) centre of the lode (c.f. Section 5.2.1). George (1969), Tso et al. (1977), Nesbitt and Kelly (1980) and Nesbitt (1982) have described similar Fe depletion in biotite in sulphide-rich rocks as resulting from sulphide-silicate reactions, and this applies also in the WAL. The most likely reaction to have occurred is:

Biotite + pyrite = Fe-depleted biotite + 2 pyrrhotite

There is evidence for slight enrichment of Zn and Mn in biotite in the outer parts of the WAL, although Mn-rich biotites occur rarely in the pyroxenoid subzone, and both Zn and Mn may approach their detection limits. Sulphide-silicate reactions are likely to deplete any Zn in biotite in sulphur-rich areas, and most Mn would preferentially partition into garnet or pyroxenoids rather than biotite under normal metamorphic conditions (Frondel and Ito, 1966).

5.3.3. Spinels.

Gahnite is seldom widespread enough to exhibit statistically significant trends, although an increase in Zn / Fe may occur towards the centre of the WAL, and zincian hercynite occurs near the edge of the WAL.

Chapter 6. Summary and Conclusions

6.1 Summary of zoning in WAL

It has been found that moderately well developed zoning exists between the country rocks and the lode rocks within the WAL, and is expressed in a number of ways. A whole-rock chemical trend is one of the most basic of these, and is clearly shown by an overall inverse relationship between Al, Ti, K and Mg / (Mg + Fe), all enriched in the detrital metasediments (sillimanite gneiss), and Mn, P, Ca, S, Pb, Zn and other base metals, all enriched towards the centre of the WAL.

These chemical variations are reflected in changes in the mineralogical constitution throughout the WAL (Figure 6.1 and Table 6.1). Passing from the sillimanite gneiss towards the centre of the WAL, the following series of assemblages are encountered:

Qtz - Bt - Sil ± Or ± Alm

→ Qtz - Bt ± Gah ± Alm ± Po ± Gn

→ Qtz - Alm - Bt ± Sl ± Po ± Gn

→ Qtz - Sps ± Amph ± Sl ± Po ± Gn

→ Pxn ± Qtz ± Sps ± Gn ± Sl ± Po

This results in five distinct mappable zones: sillimanite gneiss, a gahnite-rich zone, a garnet quartzite zone, an amphibole-bearing zone and a pyroxenoid-bearing zone. In detail, the zoning is considerably more complex, with interfingering of many of these zones, and abundance of minor rock types, including pegmatites, veins and remobilized sulphides, and small retrograde shear zones.

The distribution of sulphides is especially complex, but can generally be divided into three principal sections: i) The upper section (stratigraphic top of WAL) is relatively narrow, galena and

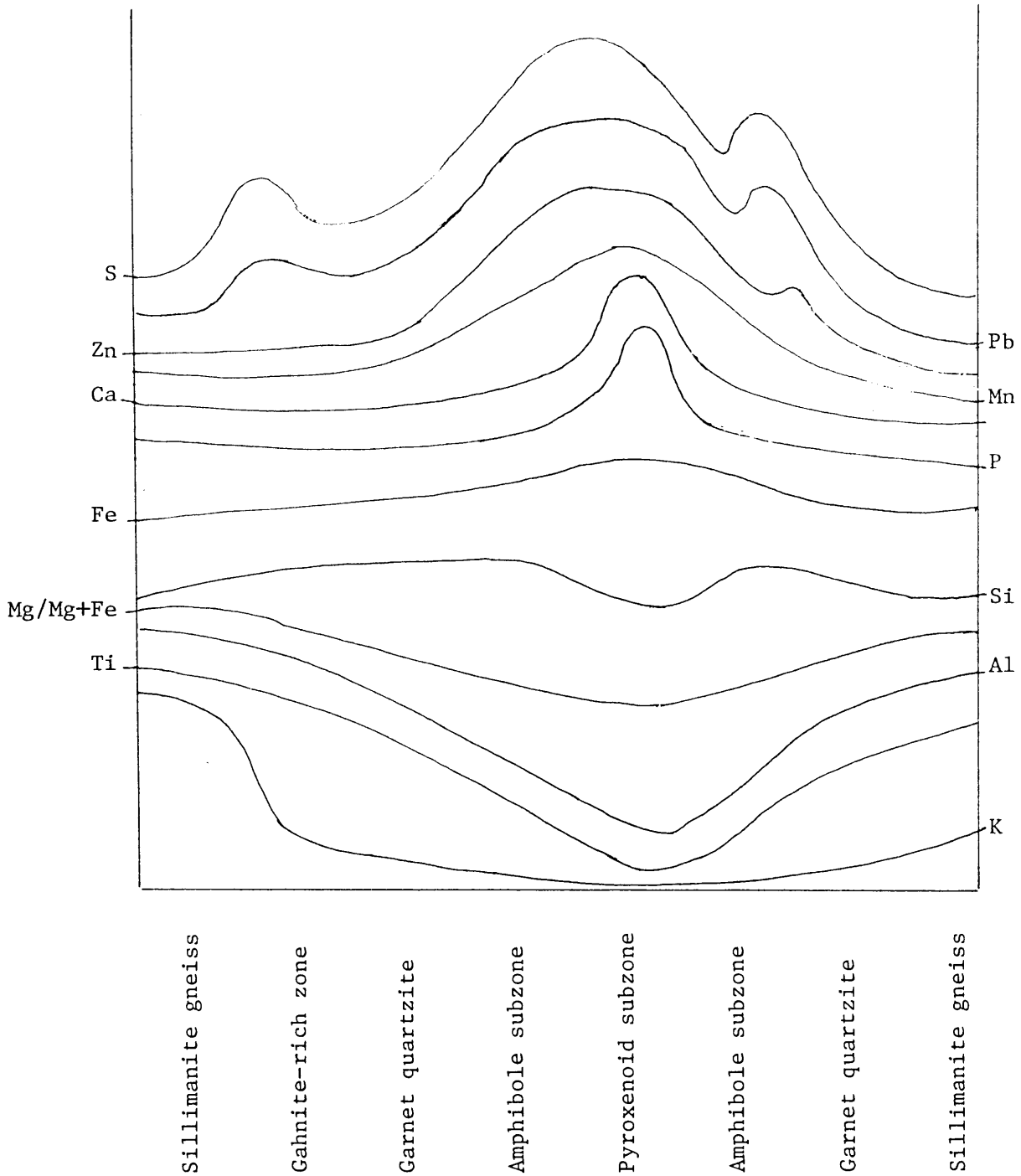

Fig. 6.1: Schematic summary of geochemical variation in the WAL.

Table 6.1: Summary of mineral distribution in the WAI.

	Quartz	Sillimanite	Garnet	Biotite	Principal Zinc Mineral	Retrograde Minerals	Total Sulphides	Galena/ Sphalerite
Sillimanite Gneiss		Major		Major			<1%	
Gahnite-rich Zone		Minor		Minor	Gahnite	Sericite	c.10%	>1
Garnet Quartzite	Major		Almandine	Minor			c.2%	
Amphibole-bearing Zone				Major		Amphiboles		
Pyroxenoid-bearing Zone	Minor	Absent	Spessar-tine	Minor	Absent	sphalerite	various Mn-silicates and amphiboles	c.10%
Amphibole-bearing Zone				Major		Minor	Amphiboles	
Garnet Quartzite	Major		Almandine	Minor			chlorite	c.2%
Sillimanite Gneiss		Major		Minor	Major	gahnite	sericite	<1%

Stratigraphic top

?

pyrrhotite - rich, and sphalerite poor, largely in the gahnite - rich section, ii) the central, most sulphide-rich section (generally around the pyroxenoid zone) and iii) the lower, narrow, less sulphide-rich section in the lower garnet - quartzite are richer in sphalerite and poorer in galena.

The distribution of retrograde minerals is asymmetric, with most chlorite appearing in the lower garnet - quartzite, most sericite in the upper part of the lode, and most cummingtonite around, but predominantly below, the pyroxenoid zone. Abundant sericite occurs around the pegmatite / sillimanite gneiss zone locally present in the upper garnet quartzite, while chlorite is related to a late-stage fracture zone in the lower garnet quartzite. Despite the widespread retrogression, well-defined RSZ cannot be distinguished within the WAL.

The whole-rock chemical variation is also expressed in the chemical variations of certain minerals, especially garnet. Mn and Ca increase, and Fe and Mg decrease in garnet towards the centre of the WAL, but Mg / Mg + Fe shows irregular trends and is complicated by partial retrograde re-equilibration of the Fe between amphiboles, sulphides and other minerals.

Biotite generally shows some correlation of Al, Ti and Mg / Mg + Fe between biotite and whole-rock compositions, although these trends are less regular than in garnet. Biotite formation or re-equilibration during retrogression, and the instability of the annite component, distort these trends.

Gahnite shows an irregular trend of increasing Zn / Fe towards the centre of the lode.

6.2 Origin of prograde mineral phases

Reactions 6.1 - 6.7 and 6.9 - 6.13 are derived principally from Helgeson et al. (1978) and Winkler (1974). Unless otherwise noted, the others are proposed by the author.

6.2.1 Sillimanite

Sillimanite may derive from metamorphism of a kaolinite group mineral or muscovite:

$$\text{kaolinite} \rightarrow \text{pyrophyllite} \rightarrow \text{andalusite} \rightarrow \text{sillimanite} \quad (6.1)$$

$$\text{quartz} + \text{muscovite} \rightarrow \text{sillimanite} + \text{K-feldspar} + H_2O \quad (6.2)$$

$$\text{muscovite} + H^+ \rightarrow \text{sillimanite} + \text{quartz} + K^+ + H_2O \quad (6.3)$$

$$\text{muscovite} + \text{chlorite} \rightarrow \text{sillimanite} + \text{biotite} + H_2O \quad (6.4)$$

Stanton et al. (1978) favoured direct derivation of sillimanite from a kaolinite type precursor.

6.2.2 Feldspars

K-feldspar may have originated as detrital, authigenetic or diagenetic feldspar, or by the dehydration of muscovite and/or biotite (reactions 6.2, and 6.5 - 6.7).

$$\text{muscovite} + \text{biotite} + \text{quartz} \rightarrow \text{garnet} + \text{K-feldspar} + H_2O \quad (6.5)$$

$$\text{quartz} + \text{biotite} \rightarrow \text{garnet} + \text{K-feldspar} + H_2O \quad (6.6)$$

$$\text{sillimanite} + \text{biotite} + \text{quartz} \rightarrow \text{garnet} + \text{K-feldspar} + H_2O \quad (6.7)$$

The Pb component of K-feldspar probably derived from desulphurization of galena by some of the following reactions:

muscovite + galena + quartz -> Pb-K feldspar + H_2S (6.8)

sillimanite + galena + quartz + H_2O -> Pb feldspar + H_2S (6.8a)

K-feldspar + galena + biotite + H^+ -> Pb-feldspar + K^+ + pyrrhotite (6.8b)

The anorthite found in the sillimanite gneiss is unlikely to be pre-metamorphic, due to its unusually high Ca content. It may have formed from one of the following reactions:

calcite + kaolinite -> anorthite + CO_2 + H_2O (6.9)

laumontite -> anorthite + quartz + H_2O (6.10)

heulandite -> laumotite -> wairakite -> anorthite + quartz + H_2O (6.10a)

6.2.3 Biotite.

Biotite forms by metamorphism of detrital or authigenitic or diagenetic ferromagnesian minerals and some important reactions are 6.4 and 6.11:

chlorite + muscovite -> garnet + biotite + H_2O (6.11)

6.2.4 Garnet.

Garnet may form from the reactions 6.5 - 6.7, 6.12 and 6.13:

chlorite + quartz -> garnet + H_2O (6.12)

Fe-chlorite + quartz -> Mg-chlorite + garnet + H_2O (6.13)

Much of the garnet probably formed quite early in the metamorphism, due to the high Mn and Fe/Mg in these rocks (Leake, 1972). The Mn-rich garnets formed principally by reaction of $MnCO_3$ with clays:

rhodochrosite + kaolinite + quartz -> spessartine + CO_2 + H_2O (6.14)

6.2.5 Spinels.

Gahnite is commonly thought to derive from reactions between sphalerite and aluminosilicates (Juve, 1967; Wall & England, 1979; Williams, 1983) but locally derives from prograde metamorphism of several silicates (Sundblad, 1982). These silicates include biotite (Dietvorst, 1980), staurolite (Atkin, 1978; Stoddard, 1979; Spry, 1982), and anthophyllite (Sundblad, 1982) - the first two of these being aluminosilicates which can be found naturally with high ZnO contents (Frondel & Ito, 1966; Griffen & Ribbe, 1973; Frondel & Ito, 1975; Griffen, 1981). Anthophyllites are unusual here in having low Al and Fe contents and no Zn has been recorded at all (although not commonly recorded in most analyses of rock forming minerals) (Robinson et al. 1982), but the gahnite - anthophyllite association could well have derived from a more Fe - Al - Zn - rich amphibole (Klein & Ito, 1968). Sundblad (1982) noted that gahnites were more iron - rich when

forming from silicate breakdown than when replacing sphalerite, and thus it is suggested that the ferroan gahnite/zincian hercynite of the WAL was formed largely by prograde breakdown of zincian ferroalumino - silicates. The large Zn / Fe range in gahnites from the WAL could indicate either a large Zn / Fe range in the precursor silicate, or zinc contribution from sphalerite breakdown.

The identity of the precursor to this Zn - Fe - Al silicate is another problem. The low temperature stability limits of Zn - chlorite (Radke et al. 1978) or Zn - biotites (Frondel and Ito, 1975) are unknown, but Zn - staurolite seems restricted to quite high metamorphic grades (Ashworth, 1975; Griffen, 1981). Chlorites may be authigenetic or diagenetic (Deer et al. 1966) and could conceivably have been original Zn - bearing phases (Frondel and Ito, 1975; Radke et al. 1978). Zinc bearing clays - sauconite ($Na_{0.33}Zn_3(Al,Si)_4O_{10}(OH)_2 .4H_2O$, a smectite) and fraipontite ($(Zn,Mg,Al)_3(Si,Al)_2O_5(OH)_4$, a septechlorite) are possible sedimentary components, but have not been found in marine sediments. R. Segnit (pers. comm.) noted that substantial absorptive zinc can be contained in opal - claystones (probable precursors to some of the siliceous rocks of the Broken Hill lodes) and Weber-Diefenbach (1977) observed the presence of substantial ZnO absorbed onto various amorphous hyroxides and silica in Red Sea metalliferous sediments (although it is very rapidly altered diagenetically to sphalerite there). Squiller and Sclar (1980) proposed that primary zinc - bearing carbonates were the progenitors of the zinc - rich minerals at Franklin, New Jersey (gahnite, franklinite, zincite, willemite, hendricksite, etc.) but the lack of most of these minerals at Broken Hill prevents direct comparison. Mossman & Heffernan (1978) found evidence for the presence

of zinc carbonate (smithsonite or hydrozincite) in metalliferous Red Sea sediments, and Bischoff (1969) found woodruffite ($(Zn,Mn)_2Mn_5O_{12}.4H_2O$) in the same deposits. Non - sulphide zinc in sediments may be present as either a carbonate, a clay mineral, a chlorite, absorbed ZnO, or a Zn-Mn oxide, and any combination of these may be a progenitor to gahnite.

A smithsonite - Fe sulphide assemblage is usually considered unstable with respect to a sphalerite - siderite assemblage (G.Moh, oral comm.; Brown, 1982) and we can thus assume that $ZnCO_3$ could only have been a minor constituent of the pyrrhotite and gahnite- rich rocks. Gahnite bearing rocks in the WAL are Mn-poor and of very low oxidation state, so an origin from Zn-Mn oxide is very unlikely. Most gahnite is closely associated with pyrrhotite and galena in the WAL, and this may indicate that either primary zincian clays can exist in equilibrium with Fe sulphides, or alternatively the assemblage re-equilibrated from an original sphalerite - ferroan silicate (e.g. chlorite) association, e.g.:

Fe-Al-rich chlorite + sphalerite -> gahnite + pyrrhotite + Fe-Al-poor chlorite (6.15)

Williams (1983) found evidence elsewhere for the reaction:

gedrite + sphalerite + O_2 -> gahnite+ quartz + S + H_2O (6.16)

An intermediate Zn-rich silicate, as discussed above, is probably involved in many cases.

The hercynite component of the spinels is probably formed from the metamorphism of Fe-rich silicates, in the reverse of reactions 4.1 -

4.4.

It seems unlikely that zincian clays would be stable at higher sulphur fugacities than smithsonite, as both are found in similar occurrences, i.e oxidized zones of zinc deposits (Fransolet et al., 1975; Ross, 1946). Zn carbonate in the Red Sea deposits was postulated to exist only in sediments where zinc is in greater amounts than necessary for stabilizing all S as sphalerite (Bischoff, 1969; Mossman & Heffernan, 1978). One or more of the following desulphurization reactions probably occurred:

$KAl_3Si_3O_{10}(OH)_2 + ZnS = ZnAl_2O_4 + KAlSi_2O_4 + H_2S$ (6.17)

muscovite sphalerite gahnite K-feldspar fluid

$Al_2SiO_5 + ZnS + H_2O = ZnAl_2O_4 + SiO_2 + H_2S$ (6.18)

sillimanite sphalerite fluid gahnite quartz fluid

6.2.6 Pyrrhotite and other sulphides.

With good evidence existing for sphalerite desulphurization, the possibility of desulphurization of other sulphides must be considered. Ferry (1981) has shown that, in contrast to pyrite, pyrrhotite is very rare as a primary phase in sedimentary rocks and its abundance in metamorphic rocks (Schneider, 1978) is mainly due to desulphurization. The most important reactions suggested by Ferry are:

$2FeS_2 + CH_4 = 2FeS + C + 2H_2S$ (6.19)

pyrite fluid pyrrhotite graphite fluid

$2FeS_2 + 2H_2O + C = 2FeS + 2H_2S + CO_2$ (6.19a)

pyrite fluid graphite pyrrhotite fluid

Ferry showed that when all pyrite has been converted to pyrrhotite, principally by the above reactions, further desulphurization can occur by sulphide-silicate reactions such as:

$$KAlSi_3O_8 + 3FeS + 4H_2O = KFe_3AlSi_3O_{10}(OH)_2 + 3H_2S \quad (6.20)$$

K-feldspar pyrrhotite fluid biotite fluid

This reaction results in iron-rich biotite, in contrast to the high Mg biotite in equilibrium with pyrite-pyrrhotite-biotite assemblages, which have low variance and a Mg/Mg + Fe about 0.95 (Ferry, 1981; Nesbitt, 1982; Robinson & Tracy, 1977). This may be partly responsible for the high Fe in many mineral phases of the WAL.

Plimer (1977a) found primary pyrite with no trace of pyrrhotite in quartz-albite rocks of lower granulite facies 30 km SW of Broken Hill, and inferred that desulphurization could not have taken place in the Willyama Complex. This may be an over-generalisation, however, as Rumble et al. (1982) noted that fluid flow is highly dependent upon individual rocktypes - BIF's, for example, being relatively impermeable, and Walther and Orville (1982) showed that volatile loss from well-foliated rocks would be relatively rapid due to their extremely small tensional strength.

Most other sulphides represent original primary precipitates, which have undergone recrystallization and some remobilization. Cubanite, however, is a high temperature phase formed from chalcopyrite and pyrrhotite:

$$\underset{\text{chalcopyrite}}{CuFeS_2} \quad \underset{\text{pyrrhotite}}{FeS} \rightarrow \underset{\text{cubanite}}{CuFe_2S_3} \qquad (6.21)$$

6.2.7 Pyroxenoids and pyroxenes

The pyroxenoids have range in composition of $Mn_{0.4-0.6}\ Fe_{0.3-0.4}\ Ca_{0.1-0.2}\ Mg_{0-0.1}\ Si_1\ O_3$, and the pyroxenes of $Mn_{0.2-0.3}\ Fe_{0.4-0.7}\ Ca_{0.5-0.9}\ Mg_{0.1-0.6}\ Si_2\ O_6$. The overlap in distribution of the pyroxenes and pyroxenoids, and the lack of local enrichment in Fe or Ca above that necessary for these phases, suggests that only one or two Mn-rich phases were originally present. The progenitors could be: i) a Mn-Fe-Ca oxide (Roy & Purkait, 1968), ii) a Mn-Fe-Ca carbonate (Peters, 1980; Winter et al., 1981), and iii) a Mn-Fe-Ca silicate (Stanton, 1983).

Neotocite/hisingerite/'sturtite'-type minerals have suitable compositions, except for lower Ca, for being precursors. Such phases, have however, only once been recorded as possible primary minerals in rocks of low metamorphic grade (Aleksiev & Bogdanov, 1974).

In contrast to the silicates, primary Mn oxides are common constituents of sediments but a homogenous phase (or even a mixture of common oxides) of appropriate composition is unknown. No indication of Fe-Mn separation, as in the natural oxides (Berger, 1968), can be detected in the WAL. Metamorphism can reduce Mn oxides to rhodonite and other silicates, but usually only partially (Siviprakash, 1980), and this is only minor with Fe (Klein, 1973). As no evidence exists for the presence of higher oxides of Mn or Fe in the WAL, they must have been insignificant primary phases.

Mn-Fe-Ca carbonates, in contrast to the silicates, are common primary phases in sediments (Curtis, 1967; Klein, 1973; Postma, 1977;

Berner, 1981a,b) and, in contrast to the oxides, occur with compositions quite compatable with the pyroxenoids and pyroxenes. Fe-Ca rhodochrosite and kutnahorite/ankerite type phases were considered as progenitors by Hodgson (1975b). Fe-rich carbonates are much more abundant in fresh water than marine sediments (Curtis, 1967; Postma, 1977; Berner et al. 1979) but manganoan siderite occurs in the Red Sea sediments (Bischoff, 1969) and siderite is postulated to have been a common primary phase in many Precambrian sedimentary Fe formations (Klein, 1973). Mn-Ca-Fe carbonates are rare in the WAL but some of that present could be relict primary carbonate. Carbonates of similar composition are very common in the more Ca-rich Pb lodes, where tephroite-fayalite series minerals are also locally common. Roy (1968) found that tephroite was diagnostic of a rhodochrosite precursor and thus the fayalite component presumably derives from siderite.

The breakdown temperature of $MnCO_3$ is less than that for $CaCO_3$ and thus the primary manganoan calcite now present in the WAL and the other Broken Hill lodes approaches the maximum stability limits of such carbonates under the prevailing metamorphic conditions (Winter et al. 1981). The Pb lodes are less siliceous overall, and more Ca-rich and Fe-poor, than the WAL and consequently Ca-rich, Fe-poor rhodonite and bustamite { $(Ca,Mn)SiO_3$ }. The lack of tephroite/fayalite minerals or abundant carbonates in the WAL is due to the higher Si content, forming more pyroxenoids by the reaction:

$$(Mn,Fe)_2SiO_4 + SiO_2 \rightarrow 2(Mn,Fe)SiO_3 \qquad (6.22)$$

6.3 Origin of principal rocktypes

6.3.1 Sillimanite gneiss (detrital facies).

This rocktype is similar in most components to an average marine shale, except for the following: i) The FeO/Fe_2O_3 ratio is very high, compatible with the euxinic basin necessary for deposition and preservation of sulphides (Large, 1980), ii) the Mg and Sr contents are low, particularly around the orebody, and this was considered by Plimer, (1979) to be due to pre-metamorphic hydrothermal alteration, iii) the B, Li and S contents are all low, indicating either low salinity or the mobility of these elements during metamorphism (Harder, 1974; Schneider, 1978).

The Mg depletion described by Plimer (1979) is very unusual for wallrock alteration and some possible explanations are : i) an influx of non-marine waters through Mg-poor basement, depleting Mg from solution prior to exhalation as hydrothermal metalliferous solutions ii) low temperature (<200 degrees C) authigenetic or diagenetic alteration of Mg-rich clays, releasing Mg in solution (Bohlke et al. 1980; Gelinas et al. 1982). Low temperature alteration of seafloor basalts may cause an increase in Fe/Mg (Gelinas et al. 1982) and a similar process is conceivable for pelitic sediments. Replacement of smectites by phillipsite or illite could also cause the potassic alteration at Broken Hill by Plimer (1979).

Gahnite and sulphide bearing rocks and garnet quartzites occur sporadically and indicate spasmodic exhalation of hydrothermal fluids (see below).

The pegmatites appear to have formed by remobilization of K-feldspar formed by the anatexis of micas.

6.3.2 Gahnite-rich zone.

The common association in the WAL of gahnite with galena and pyrrhotite but rarely with sphalerite provides good indirect evidence for the desulphurization of sphalerite. Direct evidence for desulphurization is rarely obvious but the general occurrence of most gahnite in a macroscopic selvage separating most sulphide-rich and Al -rich rocktypes is very significant. On a finer scale, a gahnite selvage can sometimes be seen bordering small quartz veins (with minor pyrrhotite in biotite-garnet quartzites, and this indicates some relation between gahnite and fluid activity - a high fluid flow being necessary to drive desulphurization reactions (Ferry, 1981). The high fluid flow possible in the well-foliated sillimanite gneiss may similarly drive the gahnite forming desulphurization reactions in the gahnite-bearing rocks by removing H2S (Walther and Orville, 1982).

6.3.3 Garnet quartzite.

This rock type is quite similar to the manganese silicate-rich rocks described as 'gondites' by Fermor (1909) and 'coticules' (Renard, 1878), although the latter name seems to be more particularly applied to mineralogically simple spessartine quartzites (Clifford, 1960). The garnet quartzites of the WAL are generally richer in sulphides and sometimes amphiboles than these, and the garnet is sometimes almandine not spessartine, but there is clearly a strong similarity between these rock types.

The origin of coticles has not been proven conclusively, although they are usually considered to be metasedimentary. The postulated origins include: i) Clifford (1960) described them as originating from Mn-rich sandy beds, ii) Schiller & Taylor (1965) concluded that they were originally chemically precipitated chert and Mn with detrital

clay, iii) Doyen (1971) found evidence for a rhodocrosite-rich parent rock to coticules, iv) Hodgson (1975b) thought that garnet quartzites at Broken Hill were formed by premetamorphic hydrothermal alteration (Mn metasomatism) of the pelitic wallrocks, v) Kramm (1976), postulated an origin from manganoan smectite, vi) Stanton et al. (1978) considered that a Mn-chamosite-rich sediment was a probable precursor to the garnet quartzites at Broken Hill, vii) but Spry (1978) showed how similar rocks can be formed by contact metamorphism of Mn-oxide rich clayey cherts.

Berger (1968), and Roy (1979) have noted the rarity of primary Mn silicates in unmetamorphosed sedimentary Mn deposits and normal sediments, where either carbonates (rhodochrosite) and/or higher oxides of Mn are present. Aleksiev and Bogdanov (1974),however, found apparently primary Mn hydrosilicates (neotocite to manganoan saponite in composition) in a hydrothermal Mn deposit. Although Roy and Purkait (1968) found evidence for partial reduction and conversion of Mn oxides to silicates at moderate metamorphic grades, Sivaprakash (1980) indicated the common stability of higher oxides of Mn at high metamorphic grades.

The presence of primary Mn oxides co-existing with sulphides is unlikely (although rare sulphides have been noted in ferro-manganese nodules (Muller, 1979)). Mn carbonates are assumed to be the most likely original Mn minerals as, in contrast to $MnCO_3$, there is a lack of evidence for the widespread occurrence of Mn silicates or oxides in sulphide-rich sediments or their former presence in the Broken Hill lodes (Section 6.3.4). Mg, K and Al show a negative correlation to Mn (Section 5.2.2), and presumably represent original clay minerals. The most Mn - rich, Mg - poor garnets contain considerable Ca and Fe, so

the original carbonate is suggested to be ferroan calcic rhodochrosite. The Fe could, however, have also been deposited as a K - Mg - Al poor phase like greenalite, as in the silicate-rich facies of other low metamorphic grade Fe formations most Ca and Mn are preferentially partioned into carbonates rather than silicates (Klein, 1973 and 1974; Floran and Papipke, 1977). The sulphides were probably deposited syngenetically, although there has been some metamorphic remobilization.

The presence of pyrrhotite may again indicate desulphurization, or alternatively it could be directly derived from iron monosulphides, indicative of low paleosalinity (Berner et al. 1979). It seems surprising that all prograde Fe sulphide at Broken Hill is pyrrhotite, while all Fe sulphides in rocks of similar metamorphic grade at Big Hill, 30km SW of Broken Hill, is pyrite. The quartz - albite rock at Big Hill seems unlikely to be much less permeable than the garnet - quartzite at Broken Hill, and Plimer & Finlow - Bates (1977) concluded that the pyrrhotite at Broken Hill was primary, originating from deep water hydrothermal exhalations, although the evidence for this is inconclusive. The original iron-sulphide phase remains unidentified but is considered to be principally pyrrhotite.

The progenitor to the garnet quartzite was a silica and manganese rich chemical sediment closely related to the ore rocks, and minor pyrrhotite and sphalerite are considered to have been original constituents. The rarity of manganese silicates in sedimentary rocks, and manganese oxides in sulphide-rich sediments, suggest that manganese carbonate was a major primary constituent. A variable detrital component and chemically precipitated chert were the other major phases.

6.3.4 Pyroxenoid - Amphibole zone.

The pyroxenoid-amphibole zone is considered to have originated by metamorphism of a mixed chemical precipitate of silica (chert), sulphides, and Mn-Fe-Ca minerals. The Mn/Fe/Ca/Mg ratios of WAL pyroxenes and pyroxenoids, lack of higher oxides of Mn or Fe in the WAL, and the rarity of primary Mn silicates in sediments indicates that carbonates were the most probable precursors for most of the Mn, Ca and Fe in this zone. Some of the Fe was, however, probably deposited as silicates.

The zone is extremely variable in mineral distribution, and it seems probable that this was largely due to remobilisation of sulphides and quartz from the more massive pyroxenoid 'boudins'.

The breakdown of the carbonates to pyroxenoids would have resulted in a high fCO_2, effectively flushing other fluids (H_2O,CH_4,H_2S,etc.) from the orebody. This would, in turn, have promoted the breakdown of hydrous silicates, sulphides and graphite in the vicinity of the orebody by buffering reactions. The metamorphogenic alteration zone noted about the Broken Hill lodes by Plimer (1975c & 1979) may partly result from this devolatilization.

6.4 Retrogression.

The retrogression in the WAL is widespread and extremely variable, but no clear relation to RSZ or other structures is apparent. The retrograde minerals present depend mainly on the composition and abundance of the prograde mineral phases.

6.4.1 Amphiboles

The amphiboles, as discussed in Section 4.8, are probably retrograde, replacing the pyroxenoids. The high Mg/Fe+Mg (and Fe/Fe+Mn) in amphiboles compared with the pyroxenoids resulted from limited re- equilibration, with preferential partitioning of Fe and Mg into amphiboles and Mn into pyroxenoids. The low variability in pyroxenoid compositions of the WAL, suggests that this re-equilibration was minor, although pyroxenoids richer in Fe and Mg (i.e. near pyroxferroite or orthopyroxene) would have been less stable during retrogression. The excess Mn from pyroxenoid breakdown could have been partitioned into garnet, which frequently shows high Mn/Mg + Fe rims, or could also have contributed to the secondary manganese minerals such as manganpyrosmalite, 'sturtite' and manganese carbonates, although these may all be formed during late stage retrogression. The presence of amphiboles in small shears, frequently intimately associated with sulphides, also suggests that there may have been some metasomatic movement, although this seldom appears to have involved distances of more than a few metres. The garnet quartzites are unlikely to be sufficiently permeable to such fluids, which would have travelled mainly along shears and fractures.

6.4.2 Other retrograde silicates

Pyrosmalite is an uncommon alteration product of the pyroxenoids and is commonly separated from them by a manganpyrosmalite-galena selvage, indicating some retrograde metasomatic remobilisation of Mn and galena.

Manganoan stilpnomelane is uncommon as inclusions within sulphides in relatively massive pyroxenoids, and may have a similar origin to the amphiboles and pyrosmalites. The Al and K appear to have been

introduced externally.

Staurolite is a not uncommon retrograde phase in the outer parts of the WAL, where it commonly appears to replace gahnite and can be quite zinc-rich.

Chlorites are common outside of the pyroxenoid-amphibole zone and result principally from alteration of biotite, but also from spinels and rarely garnet. There is some fine galena intergrown with some chlorite, again indicating metasomatic remobilization of sulphides.

Some very fine grained phases ('pug') of uncertain nature may be bethierine, greenalite and interlayered chlorite-illite and may partly recrystallise to chlorite or sericite.

Sericite can be formed from retrogression of gahnite, feldspars, sillimanite or rarely staurolite. Paragonite was identified only as an alteration of gahnite, but closely resembles sericite and may be more common than realised. The K in sericite may derive from the breakdown of biotite to chlorite (e.g. the reverse of reaction 6.4) or from fluids associated with migmatisation (Corbett & Phillips, 1981). Na is more difficult to account for, as it is low to very low in all other analysed phases of the WAL. It is possible that the K and Na are introduced in groundwater moving down shear zones (Etheridge & Cooper, 1981).

All the retrograde reactions involve addition of water. This could have the same origin as the K and Na, but the exsolution of water from quartz during the waning metamorphism (Spear and Selverstone, 1983) may have had an important contribution.

Some sulphurisation was associated with retrogression. The most important reactions are:

pyrrhotite + loellingite + H_2S -> arsenopyrite (6.23)

pyrrhotite + H_2S -> pyrite (6.24)

There is also some late stage sulphurisation of gahnite, producing a rim rich in fine pyrrhotite, presumably by the reaction:

Fe-rich gahnite + Al-poor biotite + H_2S -> Zn-rich gahnite + pyrrhotite + Al-rich biotite + H_2O (6.25)

These sulphurizaton reactions appear to be due to re-equilibration of H2S in the fluid phase (resulting from desulphurization during prograde reactions: Wall & England, 1979) with the various minerals. This H2S also precipitates the sphalerite in the alteration rim about gahnite.

The gudmundite-chalcopyrite assemblage is probably due to the breakdown of tetrahedrite (which is the most important phase with intrinsic Ag at Broken Hill, but was not identified in the WAL), and was previously noted from Broken Hill by Lawrence (1968).

6.5 Environment of Ore Deposition.

The structure of the sedimentary basin was not clearly defined in this study, but was certainly very elongate. The narrowing or 'necking' of the A lode between the WAL and the rest of the A lode could be taken to indicate a slight submarine rise separating the WAL from the major part of the basin, but tectonic thinning in the fold hinge could also be responsible. The western margin of the WAL has not been well defined but it seems to lens out quite rapidly, perhaps being controlled by penecontemporaneous faulting, The setting seems

quite compatible with the linear fault-bounded basin first postulated by McKenzie (1965) and, except for the abundance of volcanics in the sequence, fits the description of third-order sedimentary basins proposed by Large (1980) for sediment-hosted, submarine exhalative lead-zinc deposits.

The estimate of the paleosalinity is inconclusive, and the basin could have been normal marine or non-marine in character. Metal enrichment from hydrothermal solutions in the freshwater Lake Kivu of East Africa was found by Degens & Ross (1976), so a non-marine origin cannot be rejected outright.

The rate of detrital sedimentation seems to have been low, as little evidence for original rudites exists in the sillimanite gneiss, which is usually very pelitic. Graded bedding, found in nearby rocks by Glen & Laing (1975) and Willis et al. (1983), could indicate turbidite deposition, perhaps in deep water.

It may be inferred from the Al content of the pyroxenoid zone that, at the peak of chemical sedimentation, detrital sediments comprised < 10% of all sediments. Assuming that the rate of detrital sedimentation was constant then the ore body must have been deposited at >10 times the rate of detrital sedimentation. This high depositional rate could indicate either a very low rate of detrital sedimentation or possibly turbidite-type deposition of sulphides (B. Stevens, pers. comm.).

Calc-alkaline volcanism was certainly prevalent preceeding formation of the ore deposit, but had practically ceased by the time of ore deposition (Laing et al. 1978). The ore could have been deposited from fluids substantially comprising volcanic exhalations generated during cooling of shallow igneous intrusions or, alternatively, heating by igneous intrusions could have generated

hydrothermal convection systems in meteoric waters (Large, 1977) supplying the feeder system and leaching metals and other components from the volcano- sedimentary pile. Campbell et al. (1982) noted that stratabound ore deposits are commonly underlain by subvolcanic basaltic sills which may have instigated the convection systems - the basalts stratigraphically below the Broken Hill ore deposits may represent these sills.

6.6 Economic aspects of this thesis

This thesis has made several important contributions to the economic aspects of the WAL:

i) mappable chemical and mineralogical zones were identified in the WAL.

ii) a galena-rich, sphalerite-poor selvage is charactersistic of the stratigraphic top of the WAL, with a significant proportion of the whole-rock Zn being present as gahnite.

iii) a considerable amount of very fine grained sulphide is found, commonly intimately associated with retrograde silicates, and would be very difficult to recover efficiently and economically.

6.7 Summary of geological history

The Broken Hill ore deposit was deposited syngenetically in a euxinic, narrow tectonic basin, during the waning stages of early Proterozoic calc-alkaline volcanism. There were several exhalative pulses, producing mixed precipitates of chert, sulphides and Mn-Ca-Fe carbonates intercalated with shaley detrital sediments. The exhalation producing the WAL increased and decreased gradually, resulting in compositional zoning.

The sediments were subsequently buried, uplifted, and metamorphorsed to lower granulite facies, resulting in almost complete decarbonation of the WAL and most of the other lodes. The high CO_2 expelled probably instigated extensive dehydration, some desulphurization and perhaps the partial melting in the vicinity of the lodes. Some sulphide remobilisation also occurred at this stage.

This metamorphism was followed by variable retrogression, resulting in a complex series of mineral assemblages, further sulphide remobilisation, and some veining and brecciation.

7. Suggestions for further work

The author considers that the results of this thesis are worth following up and expanding upon. The study was necessarily limited in scope due to the large number, size and complexity of the Broken Hill lodes, but further examination of mineral variation in this and other lodes may confirm and enlarge upon the trends shown, and perhaps identify other less obvious trends. The whole-rock geochemical trends were indefinite due to the small number of analyses and further geochemical studies are similarly important to elaborate the known trends and identify others.

The variation in composition of sulphides could be important for metallurgical purposes by providing information on distribution of valuable and unfavourable elements - e.g. Ag, Bi in galena and Fe, Cd in sphalerite.

The nature and extent of retrogression is poorly understood but the evidence for mobilization of S suggests that further study of this would be of use.

The formation of gahnite is still a matter of some conjecture, and field and experimental studies should provide useful information on the thermodynamics of the sulphide - silicate - oxide system and the nature of the reactions and fluids.

8. Acknowledgements

I would like to thank my supervisors, Drs Peter Rickwood and Alaster Dunlop for their suggestions and criticisms of earlier versions of this thesis. I am indebted to innumerable other members of the University of NSW School of Geology and W.S. and L.B. Robinson University College, including most clerical, library and academic staff. In particular, Dr Kevin Tuckwell helped instigate the project and Dr Gerrit Neef showed me how to conduct research and set goals.

The NBHC Mines kindly gave permission to sample drillcore and underground exposures, and provided access to their mine plans and core logs. I am particularly indebted to Dave Milton for suggesting the project and following its progress with constant interest and encouragement. Most other Broken Hill mine geologists have contributed ideas to the project.

Among the geologists who have contributed valuable suggestions must be mentioned those of the Broken Hill mapping division, Geological Survey of New South Wales (especially Barney Stevens and Rob Barnes), Drs Ian Plimer (who read and criticized an earlier version of this thesis), Ralph Segnit, John Slack and Burton Murrell.

Nick Ware (ANU), Brendon Griffin (UA) and Peter Cheyne (MIM) assisted with electron microprobe analyses.

I would like to thank the Barrier Rangers' for their constant encouragement to complete this thesis, and anyone else who was involved in any way.

Last but not least I would like to thank the most important person of all: my wife, Sue, without who's tireless encouragement, support, patience, editing, technical and clerical assistance none of this would have been accomplished.

BIBLIOGRAPHY

ABRECHT, J and PETERS, Tj., 1975: Hydrothermal synthesis of pyroxenoids in the system $MnSiO_3$ at P_f = 2kb. Contrib. Mineral. Petrol. 50, p. 241 - 246.

ABRECHT, J and PETERS, Tj., 1980: The miscibility gap between rhodonite and bustamite along the join $MnSiO_3$ - $Ca_{0.6}Mn_{0.4}SiO_3$. Contrib. Mineral. Petrol. 74, p.261-269.

AHMAD, R. and WILSON, C.J.L. 1981: Uranium and Boron distributions related to metamorphic microstructure - evidence for metamorphic fluid activity. Contrib. Mineral. Petrol. 76, p. 24-32.

AHMAD, R. and WILSON, C.J.L. 1982: Microstructural relationships of sillimanite and "fibrolite" at Broken Hill, Australia. Lithos. 15, p. 49-58.

AIKAWA, N. 1979: Oriented intergrowth of rhodonite and pyroxmangite and their transformation mechanism. Mineral. J. 9, p. 255-269.

ALEKSIEV, B. and BOGDANOVA, K. 1974: The Obrochishte manganese deposit In DRAGOV, P. and KOLKOVSKI, B. (eds). Twelve ore deposits of Bulgaria. p.149-160. 4th IAGOD Symposium, Varna.

ANDREWS, E.C. 1922: The Geology of the Broken Hill district. NSW Geol. Survey. Mem. 8, 432 pp.

ASHWORTH, J.R. 1975: Staurolite at anomalously high grade. Contrib.

Mineral. Petrol., 53, p. 281-291.

ASHWORTH, J.R. 1976: Petrogenesis of migmatites in the Huntly-Portsoy area, Mineral. Mag., 40, p. 661-682.

ASHWORTH, J.R. and CHINNER, G.A. 1978: Coexisting garnet and cordierite in Scottish Caledonian migmatites. Contrib. Mineral. Petrol., 65, p. 379-394.

ATKIN, B.P. 1978: Hercynite as a breakdown produce of staurolite from within the aureole of the Ardara Pluton, Co. Donegal, Eire. Mineral. Mag., 42, p. 287-289.

BANERJEE, S. 1974: Tin in the the Base Metal Sulphide deposits at Geco, Manitouwadge, Ontario, Canada. Bull. Geol. Survey India, 40, 36 pp.

BARNES, R.G. 1980: Types of mineralisation in the Broken Hill block and their relationship to stratigraphy. In STEVENS, B.P.J. (ed.) A guide to stratigraphy and mineralization of the Broken Hill block, New South Wales. Records of the Geological Survey of N.S.W., 20(1), p. 33 - 70.

BARRON, L.M and BARNES, R.G. 1981: The mineral chemistry of some Corruga - type scheelite - bearing calc-silicate rocks and their comparison with other sulphide - bearing rocks, Broken Hill Block. Geol. Survey of NSW, Unpub. Petrol. Rept. 81/9, 42 pp.

BAYLISS, P. 1975: Nomenclature of the tri-octahedral chlorites. Can.

Mineral. 15, 178 - 180

BENTOR, Y.K., KASTNER, M., PERLMAN, I. and YELLIN, Y. 1981: Combustion metamorphism of bituminous sediments and the formation of melts of granitic and sedimentary composition. Geochim. Cosmochim. Acta, 45, p. 2229-2255.

BERGER, A., 1968: Zur Geochemie und Lagerstattenkunde des Mangans Gebruder Borntraeger, Berlin, Stuttgart, 216 p.

BERNER, R.A., 1964: Stability fields of iron minerals in anaerobic marine sediments. J. Geol. 71, p.826-834.

BERNER, R.A., 1970: Sedimentary pyrite formation, Amer. J. Sci., 268 p. 1-23.

BERNER, R.A., 1981a: Authigenic mineral formation resulting from organic matter decomposition in modern sediments. Fortschr. Mineral., 59, p. 117-135.

BERNER, R.A., 1981b: A new geochemical classification of sedimentary environments. J. Sed. Petrol. 51, p. 359-365.

BERNER, R.A., BALDWIN, T., HOLDREN, G.R., Jnr., 1979: Authigenic iron sulphides as palaeosalinity indicators, J. Sed. Petrol. 49, p. 1345 - 1350.

BETHUNE, P. de, LADURON, D. and BOCQUET, J., 1975: Diffusion processes

in resorbed garnets, Contrib. Mineral. Petrol. 50, p. 197-204.

BILLINGTON, L.G., 1979: The relationship of the Garnet Quartzite rocktypes to the orebodies in the Z.C.-N.B.H.C. Mines, Broken Hill, N.S.W., Australia, Unpublished MSc thesis, Univ. of N.S.W..

BINNS, R.A., 1962: Studies in metamorphism at Broken Hill, NSW. PhD thesis (unpub.). Univ. Cambridge.

BINNS, R.A., 1964: Zones of progressive regional metamorphism in the Willyama Complex, Broken Hill District, New South Wales. J. Geol. Soc. Aust., 11, p. 283-330.

BINNS, R.A., 1968b: Experimental studies of metamorphism at Broken Hill; In: RADMANOVICH, M. & WOODCOCK, J. (eds.)., Broken Hill mines - 1968. Austsn. Inst. Min. Metall. Monog. no. 3, Melb. p199-204.

BIRCH, W.D; CHAPMAN,A & PECOVER, S.R., 1983: The minerals. In: WORNER, H.K & MITCHELL, R.W., (eds.), Minerals of Broken Hill, Aust. Min. & Smelting, Melb. p. 68-195.

BISCHOFF, J.L., 1969: Red Sea geothermal brine deposits: their mineralogy, chemistry and genesis; In: DEGENS, E.T. and ROSS, D.A.(eds.), Hot brines and recent heavy metal deposits in the Red Sea. Springer-Verlag, New York, p. 386 - 401.

BLACKBURN, W.H., 1969: Zoned and unzoned garnets from the Grenville gneisses around Gannoque, Ontario. Canad. Mineral. 9, p. 691 - 698

BOHLKE, J.K, HONNOREZ, J & HONNOREZ-GUERSTEIN, B.M., 1980: Alteration of Basalts from site 396 B, DSDP: petrographic and mineralogical studies, Contrib. Mineral. Petrol., 73, p.341 - 364.

BORCHERT, H., 1970: On the ore deposition and geochemistry of manganese, Mineralium Deposita., 5, p. 300-314.

BOTH, R.A., 1970; Minor element geochemistry of sulphide minerals in the Broken Hill Lode, NSW. Unpub. PhD thesis, ANU.

BOTH, R.A. and RUTLAND, R.W.R., 1976: The problem of identifying and interpreting stratiform ore bodies in highly metamorphosed terrains: the Broken Hill example: In: WOLF, K.H. (ed.), Handbook of strata-bound and stratiform ore deposits. Elsevier, Amsterdam. Vol. 4, Ch. 6, p. 261 - 326.

BOTTRILL, R.S., 1983a: Zincian staurolite from Broken Hill, New South Wales. Aust. Miner., 44, p. 251-253.

BOTTRILL, R.S., 1983b: A manganaxinite-bearing assemblage from Broken Hill, New South Wales. Aust. Miner., 44, p.254-255.

BRIGATTI, A.F., 1982: Hisingerite: A review of its crystal chemistry In VAN OLPHEN, H. and VENIALE, F. (Eds.) "International Clay Conference 1981, Developments in Sedimentology 35, Elsevier, Amsterdam, p.97-110.

BROWN, A.C., 1982: Grenville iron - formations and associated stratiform zinc mineralization, Roddick Lake area, Mount Laurier Basin, Quebec. Can. J. Earth Sci., 19, p. 1670 - 1679.

BROWN, E.H., 1969: Some zoned garnets from the greenschist facies, Amer. Mineral., 54, p. 1662-1677.

BROWN, P.G., ESSENE, E.J. and PEACOR, D.R., 1980: Phase relations inferred from field data for Mn pyroxenes and pyroxenoids. Contrib. Mineral. Petrol., 74, p. 417-425.

BROWN, M., 1979: The petrogenesis of the St. Malo Migmatite Belt, Armorican Massif, France, with particular reference to the diatexites. N. Jb. Mineral. Abh., 135, p. 48-74.

BROWN, R.N., RILEY, J.F. and SCHULTZ, P.K., 1970: Contributions to Australian mineralogy : 1. A new zinc-bearing ilmenite from Broken Hill. AMDEL Bull., 10, p. 48-50.

BURFORD, B.J., 1972: Studies in Broken Hill Geology: A: Zoning in B lode, Broken Hill. Unpub. Hons. thesis, Adel. Uni.

BURRELL, H.C., 1942: A statistical and laboratory investigation of ore types at Broken Hill, New South Wales. PhD thesis (unpub.) Harvard Univ.

BUSCH, W., SCHNEIDER, G & MEHNERT, K.R., 1974: Initial melting at grain boundaries. Part II: Melting in rocks of granodiorite, quartz

dioritic and tonalitic compositions. Neues Jahrb.fur Mineral. Mh. 8, p. 345-370.

CALLENDER, E. and BOWSER, C.J., 1976: Freshwater manganese deposits. In: WOLF, K.H. (ed.) Handbook of stratabound and stratiform ore deposits. Elsevier, Amsterdam, 7, p. 341-389.

CALLENDER, E., and BOWSER, C.J., 1980: Manganese and copper geochemistry of interstitial fluids from manganese - nodule - rich pelagic sediments of the northeastern equatorial Pacific Ocean. Amer. J. Sci., 280, p. 1063-1096.

CALVERT, S.E. and PRICE, N.B., 1977: Shallow water, continental margin and lacustrine nodules: Distribution and geochemistry. In: GLASBY, G.P., (ed.) Marine manganese deposits. Elsevier, Amsterdam. Ch.3. p. 45 - 86.

CAMERON, K.L., 1975: An experimental study of actinolite-cummingtonite phase relations with notes on the synthesis of Fe-rich anthophyllite. Amer. Mineral., 60, p. 375-390.

CAMPBELL, I.H., FRANKLIN, J.M., GORTON, M.P., HART, T.R., and SCOTT, S.D., 1982: The role of subvolcanic sills in the generation of massive sulphide deposits. Econ. Geol., 77, p. 2248-2253.

CAMPBELL-SMITH, W., and BANNISTER, F.A., and HEY, M.H., 1946: Pennantite, a new manganese-rich chlorite from Benallt mine, Rhiw, Carnarvonshire. Mineral. Mag., 27, p. 217-220.

CARRUTHERS, D.S., and PRATTEN, R.D., 1961: The stratigraphic succession and stratigraphy in the Zinc Corporation and New Broken Hill Consolidated Ltd., Broken Hill, N.S.W. Econ. Geol., 56, p. 1088-1102.

ČECH, F., MISAŘ, Z. and POVONDRA, P., 1971: A green lead-containing orthoclase. Tschermaks Mineral. Petrol. Mitt., 15, p. 213-231.

CHENHALL, B.E., 1973: Some aspects of prograde and retrograde metamorphism at Broken Hill. Unpub. PhD, Univ. Syd.

CHENHALL, B.E., 1976: Chemical variation of almandine and biotite with progressive regional metamorphism of the Willyama Complex, Broken Hill, N.S.W. J. Geol. Soc. Aust., 23, p. 235-242.

CLARK, A.M., EASTON, A.J. & MOUNT, M., 1978: A study of the neotocite group. Mineral. Mag., 42, p. 279 (synopsis), Miniprint section. p. 26 - 30.

CLIFFORD, T.N., 1960: Spessartine and magnesian biotite in coticule-bearing rocks from Mill Hollow, Alstead Township, New Hampshire, U.S.A. A contribution to the petrology of metamorphosed manganiferous sediments. N. Jb. Mineral Abh., 94, p. 1369-1400.

COOMBS, D.S. NAKAMURA,Y & VUAGNAT, M., 1976: Pumpellyite-actinolite facies schists of the Taveyanne Formation near Loeche, Valais, Switzerland. J. Petrol., 17, p. 440-471.

CORBETT, G.J. and PHILLIPS, G.N., 1981: Regional retrograde metamorphism of a high grade terrain : The Willyama Complex,Broken Hill, Australia. Lithos, 14, p. 9-73.

CRERAR, D.A., CORMICK, R.K., and BARNES, H.L., 1980: Geochemistry of Manganese: An overview. In: VARENTSOV, I.M. and GRASSELLY, Gy. (eds.): Geology and Geochemistry of Manganese. Vol. 1. E. Schweizerbart'sche Verlagsbuchhandlung, Stuttgart, p. 293-334.

CROWLEY, M.S. and ROY, R., 1964: Crystalline solubility in the muscovite and phlogopite groups. Amer. Mineral., 49, p.348-362.

CURTIS, C.D., 1967: Diagenetic iron minerals in some British Carboniferous sediments. Geochim. Cosmochim. Acta., 31, p.2109-2123.

CURTIS, C.D. and SPEARS, D.A., 1968: The formation of sedimentary iron minerals. Econ. Geol., 63, p. 257-270.

DASGUPTA, H.C. and MANICKAVASAGAM, R.M., 1981: Regional metamorphism of non-calcareous, manganiferous sediments from India and the related petrogenic grid for a part of the system Mn-Fe-Si-O. J. Petrol., 22, p. 363-396.

DAVY, R., 1980: A chemical and mineralogical study of low-grade zinc mineralization at three localitites in the Proterozoic Banernall Basin of Western Australia. Geol. Survey of W.A. Report. 10, 70pp.

DE WAAL, S.A., 1981: Neoformed supergene sphalerite and possible precipitation control by gahnite. Bull. Minéral., 104, p. 732-736.

DEER, W.A., HOWIE, R.A & ZUSSMAN, J., 1966: Rock-forming minerals, (5 vols), Longman, London.

DEGENS, E.T. and ROSS, D.A., 1976: Stratabound metalliferous deposits found in or near active rifts: In: WOLF, K.H. (ed.) Handbook of Stratabound and Stratiform Ore Deposits, Vol. 4. p. 165-202. Elsevier, Amsterdam.

DEGENS, E.T., WILLIAMS, E.G. and KEITH, M.L., 1957: Environmental studies of carboniferous sediments. Bull. Amer. Assoc. Pet. Geol., 41, p. 2427-2455.

DEWAR, G.J.A., 1968: Detailed geological mapping north-east of No. 3 Shaft, North Broken Hill Limited In: RADMANOVICH, M. & WOODCOCK, J., Broken Hill Mines - 1968, Austsn. Inst. Min. Metall. Monog. No. 3, Melb. p. 137-154.

DIETRICH, R.V., 1971. Quartz - two new blues. Mineralogical Record, 2, p.79-82.

DIETVORST, E.J.L., 1980: Biotite breakdown and the formation of gahnite in metapelitic rocks from Kemio, S.W. Finland. Contrib. Miner. Petrol., 75,p. 327-337.

DONNAY, G., BETOURNAY, M. & HAMILL, G., 1980: McGillite, a new manganese hydroxychlorosilicate. Canad. Mineral. 18, p. 31-36.

DOYEN, L., 1971: The manganese ore deposit of Kisenge-Kamata (western Katanga) Mineralogical and sedimentological aspects of the primary ore

In: AMSUTZ, C.G & BERNARD, A.J., (eds.) Ores in sediments, Springer-Verlag, Berlin. p. 93 -100.

EDWARDS, A.C., 1977: Manganoan grunerites from Broken Hill, Aust. Mineral., No. 12, p. 61.

ELLIOTT, S.M., 1979: Geochemistry of the rocks enclosing Broken Hill-type deposits in the Broken Hill Block, Australia. Unpub. PhD Thesis, Uni. N.S.W.

ETHERIDGE, M.A. and COOPER, J.A., 1981: Rb/Sr isotopic and geochemical evolution of a recrystallized shear (mylonite) zone at Broken Hill. Contrib. Mineral. Petrol., 78, p. 74-84.

FAYE,G.H. and NICKEL,E.H., 1969: On the origin and colour and pleochrism of kyanite. Canad. Mineral. 10, p.35-46.

FERMOR, L.L., 1909: The manganese-ore deposits of India. Mem. Geol. Surv. India, 37. (Ref. In: Clifford (1960)).

FERRY, J.M., 1981: Petrology of graphitic sulphide-rich schists from south - central Maine: an example of desulphidation during prograde regional metamorphism. Amer. Mineral. 66, p.908-930.

FITZGERALD, J.D & McLAREN, A.C., 1982: The microstructures of microcline from some granitic rocks and pegmatites. Contrib. Mineral. Petrol., 80, p.219-229.

FLEISCHER,M., 1980: Glossary of Mineral species. Mineralogical Record, Tucson, Arizona. 192pp.

FLORAN, R.J. & PAPIKE, J.J., 1978: Mineralogy and petrology of the Gunflint Iron Formation, Minnesota-Ontario: Correlation of compositional and assemblage variations at low to moderate grade. J. Petrol., 19, p.215-288.

FOSTER, M.D., 1960: Interpretation of the composition of triocahedral micas. U.S. Geol. Survey. Prof. Papers,354-B, 48pp.

FOSTER, M.D., 1962: Interpretation of the composition and a classification of the chlorites. U.S. Geol. Survey Prof. Papers. 414-A, 33pp.

FRANSOLET, A-M. and BOURGUIGNON, P., 1975: Données nouvelles sur la fraipontite de Moresnet (Belgium). Bull. Soc. Fr. Minéral. Cristallogr., 98, p. 235-244.

FROESE, E., 1981: Applications of thermodynamics in the study of mineral deposits, Geol. Survey, Canada, Paper 80, 28 pp.

FRONDEL, C. and BAUER, L.H., 1953: Manganpyrosmalite and its polymorphic relation to friedelite and schallerite. Amer. Miner., 38, p.755-760.

FRONDEL, C. and BAUM, J.L., 1974: Structure and mineralogy of the Franklin Zinc-Iron-Manganese Deposit, New Jersey, Econ. Geol. 69, p.

157-180.

FRONDEL, C. and ITO, J., 1966: Hendricksite, a new species of mica, Amer. Mineral. 51, p. 1107-1123.

FRONDEL, C. and ITO, J., 1975: Zinc-rich chlorites from Franklin, New Jersey, with a note on chlorite nomenclature, N. Jb. Mineral Abh., 123, p. 111-115.

FROST, B.R., 1973: Ferroan gahnite from quartz-biotite-almandine schist, Wind River Mountains, Wyoming. Amer. Mineral. 58, p. 831-834.

GANGULY, J., 1972: Staurolite stability and related paragenesis. Theory, experiments and applications. J. Petrol., 13, p. 335-365.

GARRETTY, M.D., 1943: The mineralisation of the ore bodies at Broken Hill, N.S.W. D. Sc. thesis (unpub.) Univ. Sydney.

GELINAS, 1. MELLINGER, M. and TRUDEL, P., 1982: Archaean mafic metavolcanics from the Rouyn-Noranda district, Abitibi Greenstone Belt, Quebec. Mobility of the major elements. Can. J. Earth Sci., 19, p.2258-2275.

GEORGE, R. J., 1969: Sulphide-silicate reactions during metamorphism of the Nairne pyrite deposit. Proc. Austn. Inst. Min. Metall. 230, p.1 - 8.

GERMANN, K., 1971: Deposition of manganese and iron carbonates and

silicates in Liassic marl of the northern Limestone Alps (Kalkalpen). In: AMSTUTZ, G.C. & BERNARD, A.J. (eds.): Ores in Sediments. Springer-Verlag, Berlin. p. 129-138.

GLEN, R.A. & LAING, W.P., 1975: The significance of sedimentary structures in the Willyama Complex, New South Wales. Proc. Australas. Inst. Min. Metall., 256, p. 15-20.

GOLE, M.J., 1980: Low - temperature retrograde minerals in metamorphosed Archaean banded iron formations, Western Australia. Canad. Mineral., 18, p. 205-214.

GOLE, M.J., 1981: Archaean Banded Iron-Formations, Yilgarn Block, Western Australia, Eco. Geol., 75, p.1954-1974.

GRAMBLING, J.A., 1981: Pressures and temperatures in Precambrian metamorphic rocks, Earth & Planet. Sci. Lett., 53, p. 63-68.

GRANT, J.A. and WEIBLEN, P.W., 1971: Retrograde zoning in garnet near the second sillimanite isograd. Amer. J. Sci., 270, p.281-296.

GREW, C.S., 1981: Granulite-facies metamorphism at Molodezhnaya Station, East Antarctica, J. Petrol., 22, p. 297-336.

GRIFFEN, D.T., 1981: Synthetic Fe/Zn staurolites, and the ionic radius of $(IV)_{Zn}^{2+}$, Amer. Mineral., 66, p. 932-937.

GRIFFEN, D.T., GOSNEY, T.C. & PHILLIPS, W.R., 1982: The chemical

formula of natural staurolite, Amer. Mineral., 67, p. 292-297.

GRIFFEN, D.T & RIBBE, P.H., 1973: The crystal chemistry of staurolite. Amer. J. Sci., 273-A. p. 479-495.

GRIGGS, D., 1976: Hydrolytic weakening of quartz and other silicates, Geophys. J.R. Astr. Soc., 14, p. 19 - 31.

GUIDOTTI, C.V., 1969: The mineralogy and petrology of the transition from the lower to upper sillimanite zone in the Oquossoc Area, Maine, J. Petrol., 11, p. 277-336.

GULSON, B.L., 1983: Uranium-lead and lead. Lead investigations of minerals from the Broken Hill Lodes and mine sequence rocks and their implications for ore genesis, (abs.), In 7th Austn. Geol. Conv., Canberra. Geol. Soc. Aust. Abs. Ser. 9. p. 272-273.

GUSTAFSON, J.K., BURRELL, H.C. & GARRETTY, M.D., 1950: Geology of the Broken Hill Ore Deposit, Broken Hill, New South Wales, Australia, Bull. Geol. Soc. Amer., 61, p. 1369-1438.

HAASE,C.S., 1982: Metamorphic Petrology of the Negaunee Iron Formation, Marquette District, Northern Michigan: Mineralogy, metamorphic reactions, and phase equilibria. Econ. Geol., 77, p. 60 - 81

HARADA, K., SEKINO, H., NAGASHIMA, K., WATANABE, T. & MOMOI, H., 1974: High - iron bustamite and fluorapatite from the Broken Hill mine, NSW, Aust. Mineral. Mag., 39, p. 601-604.

HARDER, H., 1974: 5-N (Boron) Behaviour in metamorphic reactions. In: WEDEPOHL, K.H. (ed.) Handbook of Geochemistry, Springer - Verlag, Berlin, Vol. I. p. 5- N-1.

HARRISON, T.M & McDOUGALL, I., 1981: Excess Ar in metamorphic rocks from Broken Hill, New South Wales: implications for Ar40/ Ar39 age spectra and the thermal history of the region. Earth & Planet. Sci. Lett., 55. p. 123-149.

HAWKINS, B.W., 1968b: A quantitative chemical model of the Broken Hill Lead-Zinc deposit. Proc. Australis. Aust. Min. Metall., 227, p.11-15.

HEIER, K.S. & BILLINGS, G.K., 1970: 3-M-N (Lithium) abundance in common metamorphic processes In: WEDEPOHL, K.H. (ed.). Handbook of Geochemistry. Springer-Verlag, Berlin. II - 1 p.3-M-N-1.

HEWINS, R.H., 1975: Pyroxene geothermometry of some granulite facies rocks, Contrib. Mineral. Petrol., 90, p. 205-209.

HEY, M.H., 1954: A new review of chlorites. Min. Mag., 30. p. 277-292.

HODGE-SMITH, T., 1930: Sturtite - a new mineral. Broken Hill, N.S.W. Aust. Museum Records, 17. p.410-412.

HODGSON, C. J., 1975a: The geology and geological development of the Broken Hill Lode in the NBHC Mine, NSW, Part I: Structural Geology. J.Geol. Soc. Aust. 21, p.413-430.

HODGSON, C.J., 1975b: The geology and geological development of the Broken Hill Lode in the NBHC Mine, NSW. Part II: Mineralogy. J. Geol. Soc. Aust. 21. p.33-50.

HODGSON, C.J., 1975c: The geology and geological developent of the Broken Hill lode in the New Broken Hill Consolidated Mine, Australia, Part III: Petrology & Petrogenesis, J. Geol. Soc. Aust. 22, p.195-213.

HOLLISTER, L.S., 1966: Garnet zoning: An interpretation based on the Rayleigh fractionation model, Science, 154, p. 1647-1651.

HOPWOOD, D.T., 1978: Conformable elongate ore bodies & intrafolial folds parallel to a mineral streaking lineation In: VERWOERD, W.J. (ed.), Mineralization in metamorphic terrains, Geol. Soc. Sth. Africa. Sp. Publ., 4, p.41-51.

HUTTON, C.O., 1956: Manganpyrosmalite, bustamite and ferroan johannsenite from Broken Hill, NSW, Aust. Amer. Mineral. 41, p.581-591

IMMEGA, I.P. & KLEIN, C. Jr., 1976: Mineralogy and petrology of some metamorphic Precambrian iron-formations in Southwestern Montana. Amer. Mineral. 61, p.1117-1144.

JAYARAMAN, N., 1939: The cause of colour of the blue quartzes of the charnockites of South India and of the Champion gneiss and other related rocks of Mysore. Proc. Indian Acad. Sci., Sect A-9, p. 265-285.

JOHNSON, I.R. and GOW, N.N., 1975: Willyama inlier - mineralization In:KNIGHT, C.L. (Ed.) - Economic geology of Australia and Papua New Guinea. Australas. Inst. Min. Metall., Monograph 5. Vol. 1- Metals. p.495-498.

JOHNSON, I.R. & KLINGNER, G.D., 1975: Broken Hill ore deposit and its environment. In: KNIGHT, C.L.(ed.) Economic geology of Australia and Papua-New Guinea, 1: metals. Aust. Inst, Min.Metall., Parkville, Vic. (Monog. series no.5). p 476-492.

JONES, T.R., 1968: Garnet sandstone and garnet rims at orebody contacts, Broken Hill. In: RADMANOVICH, M. & WOODCOCK, J. (eds.) Broken Hill Mines - 1968, Australas. Instn. Min. Metall. Monog. no. 3, Melb. . p 171-178.

JUVE, G., 1967: Zinc and lead deposits in the Håfjell syncline, Ofoten, Northern Norway. Norges Geologiske Undersøkelse, 244, p. 1-54.

KATZ, M.B., 1976: Broken Hill - A Precambrian hot spot?, Precambrian Research, 3, p. 91-106.

KEITH, M.C. & DEGENS, E.T., 1959: Geochemical indicators of marine and fresh-water sediments In:ABELSON, P.H. (ed.) Researches in Geochemistry: Wiley, N.Y. p. 38-61.

KING, H.F. & O'DRISCOLL, E.S., 1953: The Broken Hill Lode. In: EDWARDS, A. B. (ed.) Geology of Australian ore deposits. 5th Empire

Mining and Metallurgical Congress, 1953. p.578-600.

KLEIN, C., 1974: Greenalite, stilpnomelane, minnesotaite, crocidolite and carbonates in a very low-grade metamorphic Precambrian iron-formation. Can. Mineral., 12, p. 475-498.

KLEIN, C., 1973: Changes in mineral assemblages with metamorphism of some banded Precambrian iron-formations. Econ.Geol., 68, p. 1075-1088.

KLEIN, C., 1978: Regional metamorphism of Proterozoic iron-formation, Labrador Trough, Canada, Amer. Mineral., 63, p. 898-912.

KLEIN, C., & ITO, J., 1968: Zincian and manganoan amphiboles from Franklin, New Jersey. Amer. Mineral., 53 p. 264-265.

KLUG, H.P. & ALEXANDER, L.E, 1969: X-ray diffraction procedures. Wiley, New York.

KRAMM, V., 1976: The coticule rocks (spessartine quartzites) of the Venn-Stavelot Massif, Ardennes, a volcanoclastic metasediment?, Contrib. Mineral. Petrol., 56, p. 135-155.

KRETZ, R., 1983: Symbols for rock-forming minerals. Amer. Miner., 68. p.277-279.

KWAK, T.A.P., 1974: Natural staurolite breakdown reactions at moderate to high pressures, Contrib. Mineral. Petrol., 44, p. 57-80.

LAING, W.P., MARJORIBANK, R.W., and RUTLAND, R.W.R., 1978: Structure of the Broken Hill mine area and its significance for the genesis of the orebodies, Econ. Geol., 73, p. 1112-1136.

LARGE, D.E., 1980: Geological parameters associated with sediment - hosted, submarine exhalative Pb-Zn deposits: An empirical model for exploration. Geol. Jb., D40, p.59-129.

LARGE, R.R., 1977: Chemical evolution and zonation of massive sulphide deposits in volcanic terrains. Econ. Geol., 72, 549-572

LAWRENCE, L.J., 1968: The minerals of the Broken Hill district In: RADMANOVICH, M., & WOODCOCK, J. (eds.) Broken Hill mines - 1968, AIMM monog. no.3, Melb. p.103-136.

LAWRENCE, L.J., 1967: Sulphide neomagmas and highly metamorphosed sulphide deposits, Mineralium Deposita, 2, p. 5-10.

LAWRENCE, L.J., 1973: Polymetamorphism of the sulphide ores of Broken Hill, N.S.W., Australia, Mineralium Deposita, 8, p. 211-236.

LAYTON, W. & PHILLIPS, R., 1960: The cummingtonite problem. Mineral. Mag., 32, p. 659-663.

LEAKE, B.E., 1972: Garnetiferous striped amphibolites from Connemara, Western Ireland. Mineral. Mag., 38, p. 649-665.

LEAKE, B.E., 1978: Nomenclature of Amphiboles, Can. Mineral., 16, p.

501-520.

LE MAITRE, R.W., 1973: Partially fused granite blocks from Mt. Elephant, Victoria. J. Pet., 15, p.403-412.

LEYH, W.R., 1980: The structural and metaorphic geology of the Springs Area, Broken Hill, NSW. MSc thesis, Uni. NSW (unpub.)

LEYH, W.R. & LARSEN, D.F., 1983: Iron formation related base metal prospects, Broken Hill, NSW. In: Broken Hill Conference, 1983. Aust. Inst. Min. Met., Parkville, Vic. p. 133-156.

LINDQVIST, B. & JANSSON, S., 1962: On the crystal chemistry of hisingerite. Amer. Mineral., 47, p.1356-1362.

MacKENZIE, D.H., 1968: Lead lode at New Broken Hill Consolidated Limited. In: RADMANOVICH, M. & WOODCOCK, J. (eds.) Broken Hill Mines - 1968, Australas. Instn. Min. Metall. Monog. no. 3, Melb. p. 161-169.

MacKENZIE, D.H. & GOW, N., 1975: Relationships between ore, banded iron formation and Potosi gneiss at Broken Hill. 1st. Aust. Geol. Conv. on Proterozoic Geol. p. 51 (abs.).

MacKENZIE, K.J.D. & BEREZOWSKI, R.M., 1980: Thermal and mossbauer studies of iron - containing hydrous silicates. II. Hisingerite. Thermochem. Acta., 41, p. 335-355.

MAIDEN, K.J., 1975: High grade metamorphic structures in the Broken

Hill orebody, Proc. Australas. Inst. Min. Metall., 254, p. 19-27.

MAIDEN, K.J., 1976: Piercement structures formed by metamorphic mobilization of the Broken Hill orebody, Proc. Australas. Inst. Min. Metall., 257, p. 1-8.

MAISONEUVE, J. 1981: The composition of the Precambrian ocean waters. Sed. Geol., 31. p. 1-11.

MALLIO, W.J. & GHEITH, M.A., 1972: Textural and chemical evidence bearing on sulfide-silicate reactions in metasediments, Mineralium Deposita. 7, p. 13-17.

MARESCH, W.V., MOTTANA, A., 1976: The pyroxmangite-rhodonite transformation for the MnSiO3 composition, Contrib. Mineral. Petrol., 55, p. 69-79.

MARJORIBANKS, R.W., RUTLAND, R.W.R., GLEN, R.A. & LAING, W.P., 1980: The structure and tectonic evolution of the Broken Hill region, Australia, Precambrian Research, 13, p. 209-240.

MASON, B., 1973: Manganese silicate minerals from Broken Hill, New South Wales, J. Geol. Soc. Aust., 20, p. 397-404.

MATTHIAS, I.G., 1973: The geology of the B-lode complex, Broken Hill, N.S.W., Unpub. Ph.D., University of New England.

MATTHIAS, I.G., 1974: High Grade regional metamorphism of the B-lode

complex, Broken Hill, New South Wales, Trans. Inst. Min. Metall. (Sect. B: Appl. Earth Sci.), 83, p. 875-80.

MEHNERT, K.R.., 1968: Composition and abundance of common metamorphic rock types. In: WEDEPOHL, K.H. (ed.) Handbook of Geochemistry, Springer-Verlag, Berlin. Vol. 1., p.272-296.

MOHR, D.W & NEWTON, R.C., 1983: Kyanite - staurolite metamorphism in sulphide schists of the Anakesta formation, Great Smokey Mountains, North Carolina, Amer. J. Sci., 283. p. 97-134.

MOINE, B., SAUVAN, P. & JAROUSSE, J., 1981: Geochemistry of evaporite-bearing series: A tentative guide for the identification of meta-evaporites, Contrib. Mineral. Petrol., 76, p. 401-412.

MOOKHERJEE, A., 1976: Ores and metamorphism: Temporal and genetic relationships, In: WOLF, K.H. (Ed.) Handbook of strata-bound and stratiform ore deposits, Elsevier, Amsterdam. Vol. 4. p. 203-260.

MOSSMAN, D.J. & HEFFERNAN, K.J., 1978: Simulated low-grade metamorphism of metalliferous mud from the Red Sea Atlantis II geothermal deep, Econ. Geol., 73, p. 1150-1189.

MUAN, A., 1959: Stability relations among some manganese minerals, Amer. Mineral., 44, p. 946-959.

MUELLER, R.F., 1961: Oxidation in high temperature petrogenesis, Amer. J. Sci., 259, p. 460-480.

MUELLER, R.F., 1967: Mobility of the elements in metamorphism, J. Geol., 75, p. 565- 582.

MÜLLER, D., 1979: Sulphide Inclusions in manganese nodules of the northern Pacific, Mineralium Deposita., 14, p. 375-380.

NEDELEC, A: & PAQUET, J., 1981: Biotite melting in high-grade metamorphic gneisses from the Haut Allier (French Massif Central), Contrib. Mineral. Petrol., 77, p. 1-10.

NEMEC, Von D., 1980: Zinkhaltiger staurolith aus den Leptynitten der Blanicer Furche und aus übrigen Moldanubikum der Böhmisch-Mährischen Hohe (ČSSR), Chem. Erde, 39, p. 311-320.

NESBITT, E.B. & KELLY, W.C., 1980: Metamorphic zonation of sulphides, oxides and graphite in and around the orebodies at Ducktown, Tennessee, Econ. Geol., 75, p. 1010-1021.

NESBITT, B.G., 1982: Metamorphic sulfide-silicate equilibria in the massive sulfide deposits at Ducktown, Tennessee, Econ. Geol., 77, p. 364-378.

NORRISH, K. & CHAPPELL, B.W., 1967: X-ray fluorescence Spectroscopy, In: ZUSSMAN, J. (ed.). Physical methods in determinative Mineralogy. Academic Press, London. p. 161-214.

O'DRISCOLL, E.S.T., 1983: Broken Hill at the cross - roads In: Broken

Hill Conference, 1983, Aust. Inst. Min. Metall., Melb. p. 29-48.

PEACOR, D.R., ESSENE, E.J., SIMMONS, W.B., BIGELOW, W.C., 1974: Kellyite, a new Mn-Al member of the Serpentine Group from Bald Knob, North Carolina, and new data on grovesite, Amer. Mineral., 59, p. 1153-1156.

PEDERSEN, F.D., 1980: Remobilization of the massive sulphide ore of the Black Angel Mine, Central West Greenland, Econ. Geol., 75, p. 1022-1041.

PEDERSEN, T.F. & PRICE, N.B., 1982: The geochemistry of manganese carbonate in Panama Basin sediments, Geochim. Cosmochim. Acta., 46, p. 59-68.

PETERS, T.J. 1980: Progressive metamorphism of manganese carbonates and cherts in the Alps. In: VARENTSOV, I.M. & GRASSELLY, GY. (eds.), Geology & Geochemistry of Manganese, E. Schweizerbartsche Verlagsbuchhandlung, Stuttgart, Vol. 1 p. 271-283.

PETERSEN, E.V., ESSENE, E.J., PEACOR, D.R., & VALLEY, J.W., 1982: Fluorine end - member micas and amphiboles. Amer. Miner. 67, p. 538-544.

PHILLIPS, E.R., RANSOM, D.M. & VERNON, R.H., 1972: Myrmetite and muscovite developed by retrograde metamorphism at Broken Hill, NSW, Mineral. Mag. 38, p. 570 - 578.

PHILLIPS, G.N., 1978: Metamorphism and geochemistry, Willyama Complex, Broken Hill, Unpub. Ph.D. Thesis, Monash Uni., p. 452.

PHILLIPS, G.N., 1980: Water activity changes across an amphibolite-granulite facies transition, Broken Hill, Australia, Contrib. Mineral. Petrol., 75, p. 377-386.

PHILLIPS, G.N. & WALL, V.J., 1981: Evaluation of prograde regional metamorphic conditions: their implications for the heat source and water activity during metamorphism in the Willyama Complex, Broken Hill, Australia, Bull. Minér., 104, p. 801-810.

PHILLIPS, G.N., WALL, V.J. & ARCHIBALD, N.J., 1980: Metamorphosed Fe-rich tholeiites and their relationship to sulphide mineralization, Broken Hill, N.S.W., 5th Aust. Geol. Conv., Hobart. (Abs.). p. 47.

PIDGEON, R.T., 1967: A rubidium-Strontium geochronological study of the Willyama Complex, Broken Hill, Aust. J. Pet., 8, p.283-324.

PLIMER, I.R., 1968: Variability in the Broken Hill lode, North Broken Hill Mine, N.S.W., B.Sc. Hons. Thesis (unpubl.) - U.N.S.W.

PLIMER, I.R., 1975a: The geochemistry of amphibolite retrogression at Broken Hill, Australia, N.Jb Mineral. Mh., p. 431-482.

PLIMER, I.R., 1975b: Geochemistry of hydrothermal alteration around the Broken Hill orebodies, Unpubl. Rept. to Broken Hill M.M.A. 43 pp.

PLIMER, I.R., 1975c: A metamorphogenic alteration zone around the stratiform Broken Hill ore deposits, Australia, Geochemical Journal, 9, p. 211-220.

PLIMER, I.R., 1976a: A plumbian feldspar pegmatite associated with the Broken Hill orebodies, Australia, N. Jb. Mineral Mh, p. 272-288.

PLIMER, I.R., 1976b: Garnet-biotite relationships in high grade metamorphic rocks at Broken Hill, Australia, Geol. Mag., 113(3), p. 263-270.

PLIMER, I.R., 1977a: The mineralogy of the high grade metamorphic rocks enclosing the Broken Hill orebodies, Australia, N. Jb. Mineral Abh., 131, p. 115-139.

PLIMER, I.R., 1978a: Proximal and distal stratabound ore deposits, Mineralium Deposita, 13, p. 345-353.

PLIMER, I.R., 1978b: The origin of the albite-rich rocks enclosing the cobaltian pyrite deposit at Thackaringa, N.S.W., Australia, Mineral. Deposita, 12, p. 175-187.

PLIMER, I.R., 1979: Sulphide rock zonation and hydrothermal alteration at Broken Hill, Australia, Trans. Instn. Min. Metall., (Sect. B: Appl. Earth Sci.), 88, p. 237-241.

PLIMER, I.R., 1980a: A discussion of the paper by E.F. Stumpfl "Manganese haloes surrounding metamorphic stratabound base metal

deposits", Mineralium Deposita, 15, p. 237-241.

PLIMER, I.R., 1980c: Hydrothermal mobilization of silver during retrograde metamorphism at Broken Hill, Australia, N. Jb. Miner. Mh, 1980, p. 433-437.

PLIMER, I.R., 1981: Water depth - a critical factor for exhalative ore deposits. BMR. J. Aust. Geol. & Geophys., 6, p. 293-300.

PLIMER, I.R., 1982a: Fluorine-bearing minerals from Broken Hill, N.S.W., Aust. Miner., 29, 214-215.

PLIMER, I.R., 1983: The association of tourmaline - bearing rocks with mineralisation at Broken Hill, NSW. In: Broken Hill Conference, 1983. AIMM, Melb. p. 157-176.

PLIMER, I.R. & ELLIOTT, S.M., 1979: The use of Rb/Sr ratios as a guide to mineralization, J. Geochem. Explor., 12, p. 21-34.

PLIMER, I.R., & FINLOW-BATES, T., 1978: Relationship between primary iron sulphide species, sulphur source, depth of formation and age of submarine exhalative sulphide deposits, Mineralium Deposita, 13, p. 399-410.

PORRENGA, D.H., 1966: Clay minerals in recent sediments of the Niger Delta. Proc. 14th Natnl. Conference on Clay minerals. Oxford press, p. 221-223.

PORTNOV, A.M., VAINTRUB, B.G., SOLNTSEVA, L.S. & DUBAKINA, L.S., 1978: Sturtite, a hydrous silicate of manganese with the structure of trioctahedral mica, Dokl. Akad. Nauk. SSSR 243, p. 1292-1294.

POSTMA, D., 1977: The occurrence and chemistry of recent iron-rich mixed carbonates in a river bog, J. Sed. Petrol., 47, p. 1089-1098.

PUCHELT, H., 1971: Recent iron sediment formation at the Kameni Islands, Santorini (Greece). In: AMSTUTZ,CG & BERNARD,A.J. (eds.) 1971: Ores in sediments, Springer-Verlag, Berlin. p. 227-245.

PYZIK, A.J. & SOMMER, S.E., 1981: Sedimentary iron monosulphides: kinetics and mechanisms, Geochim. Cosmochim. Acta, 45, p. 687-698.

RADKE, F., SCHULTZ, P.K. & BROWN, R.N., 1978: Contributions to Australian mineralogy 9. Zinc-rich chlorite from Chillagoe, Queensland. Aust. Mineral. Devt. Labs. Bull. 23, p. 25-28.

RAMDOHR, P., 1950: The ore deposit of Broken Hill, in N.S.W., Australia, in the light of new geological investigations and ore-microscopy investigations, Hiedelberger Beitrage zur Mineralogie and Petrographie (Bd. 2). 25pp.

RAMDOHR, P., 1969: The ore minerals and their intergrowths. Pergammon press, Oxford. 3rd Ed., English translation, 1174pp.

RAMDOHR, P., 1972: Minerals and structures of the Broken Hill orebody. Summary by H.F. KING, Zinc Corp. Ltd., Broken Hill, from literal

translation by Dr. R.O. BRUNNSCHWEILER of the BMR. Copy held at MMA Lib., Broken Hill. 6 pp.

REED, S.J.B. & WARE, N.G., 1975: Quantitative electron microprobe analysis of silicates using energy-dispersive electron microprobe spectrometry. J. Pet. 16, p. 499-519.

RENARD, A., 1878: Sur la structure et la composition minéralogique du coticule. Mém. Cour. et Mém. des Sav. Étr. Acad. Roy. de Belg., Tome XLI, Bruxelles. (Ref. in CLIFFORD (1960))

REYNOLDS, R.C. Jr. 1965a: The concentration of Boron in Precambrian seas. Geochem. Cosmochem. Acta, 29, p.1-16.

REYNOLDS, R.C., Jr. 1965b: Geochemical behaviour of boron during the metamorphism of carbonate rocks. Geochim. Cosmochim. Acta, 29, p.1101-1114.

REYNOLDS, P.H., 1971: A U-Th-Pb isotope study of rocks and ores from Broken Hill, Aust., Earth, Planet. Sci. Lett., 12, p.215-223.

RICE, J.M. & FERRY, J.M., 1982: Buffering, infiltration, and the control of intensive variables during metamorphism. In: FERRY, J.M (ed) Characterization of metamorphism through chemical equilibria. Reviews in Mineralogy vol. 10, p.267-326. Mineral. Soc. Amer., Washington.

RICKWOOD, P.C., 1968: On recasting analyses of garnet into end member molecules, Contrib. Mineral. Petrol., 18, p. 175-198.

ROBERTS, W.L., RAPP, E.R & WEBER, J., 1974: Encyclopedia of minerals, Van Nostrand, New York. 693p.

ROBINSON, P. & TRACY, R.J., 1977: Sulphide-silicate-oxide equilibria in sillimanite-K-feldspar grade pelitic schists, central Massachusetts: EOS, 58, p.73-524.

ROBINSON, P., SPEAR, F.S., SCHUMACHER, J.C., LAIRD, J., KLEIN, C., EVANS, B.W., DOOLAN, B.L., 1982. Phase relations of metamorphic amphiboles: natural occurrence and theory In: VEBLEN,D.R & RIBBE, P.H (eds.). Reviews in mineralogy vol. 9B; Amphiboles: Petrology and experimental phase relations. Ch.1. Mineral. Soc. Amer., Washington. p. 1-228.

ROSS, C.S., 1946: Sauconite - a clay mineral of the montmorillonite group, Amer. Mineral., 31, p. 411-424.

ROSSMAN, G.R., GREW, E.S. & DOUASE, W.A., 1982: The colours of sillimanite, Amer. Mineral., 67, p. 749-761.

ROY, S., 1968: Mineralogy of the different genetic types of manganese deposits, Econ. Geol., 63, p. 760-786.

ROY, S., 1976: Ancient manganese deposits, In: WOLF, K.H. (Ed.) Handbook of stratabound and stratiform ore deposits, Elsevier, Amsterdam. Vol.7 p. 395-476.

ROY, S. & PURKAIT, P.K., 1968: Mineralogy and genesis of the metamorphosed manganese silicate rocks (gondites) of Gowari Wadhono,

Madhya Pradesh, India, Contr. Mineral. Petrol., 20, p. 86-114.

RUI, I.J. & BAKKE, I., 1975: Stratabound sulphide mineralisation in the Kjøli area, Røros district, Norwegian Caledonides. Norsk Geologisk Tidsskrift, 55 p. 51-75.

RUMBLE, D.I., FERRY, J.M., HOERING, T.C. & BOUCOT, A.J., 1982: Fluid flow during metamorphism at the Beaver Brook Fossil Locality, New Hampshire, Amer. J. Sci., 282, p. 886-919.

RUSSELL, M.J., SOLOMON, M. & WALSHE, J.L., 1981: The genesis of sediment-hosted, exhalative zinc + lead deposits, Mineralium Deposita, 16, p. 113-127.

RUTLAND, R.W.R., MARJORIBANKS, R.W., LAING, W.P. & GLEN, R.A., 1978: Tectonic deformations at Broken Hill, New South Wales, Australia, and their significance for interpretations of ore environment, Trans. Instn. Min. Metall. (Sect. B: Appl. Earth Sci.) 87, p. B172-B176.

RYALL, W.R., 1979: Mercury in the Broken Hill (N.S.W., Australia) lead-zinc-silver bodies, J. Geochem. Expl., 11, p. 175-194.

RYALL, W.R., 1981: The forms of mercury in some Australian stratiform Pb-Zn-Ag deposits of different regional metamorphic grades, Mineral. Deposita, 16, p. 425-435.

SAMSONOVA, N.S., ZHABIN, A.G., SEREEVA, T.A., BOGOMODOVA, V.D., 1982: Zinciferous chlorite from the Kvaisi lead-zinc deposit. Doklady Acad.

Nauk. SSSR., 226, p. 1458-1462.

SANFORD, R.F., 1981: Mineralogical and chemical effects of hydration reactions and application to serpentinization, Amer. Mineral., 66, 290-297.

SAXBY, J.D., 1981: Organic matter in ancient ores and sediments. BMR. J. of Aust. Geol. & Geophys., 6, p. 287-291.

SCHILLER, E.A. & TAYLOR, F.C., 1965: Spessartine-quartz rocks (coticles) from Nova Scotia, Amer. Mineral., 50, p. 1477-1481.

SCHNIEDER, A., 1978: Abundance in common metamorphic rocks. In: WEDEPOHL, K.H. (ed). Handbook of Geochemistry. Springer - Verlag, Berlin. 16-M-1-5,16-N-1-3. Vol. 2 pt.16 (sulphur).

SCOTT, S.D., BOTH, R.A. & KISSIN, S.A., 1977: Sulphide petrology of the Broken Hill region, New South Wales, Econ. Geol. 72, p. 1410-1425.

SEGNIT, E.R., 1961: Petrology of the zinc lode, N.B.H.C. Ltd., Broken Hill, N.S.W., Proc. Australas. Inst. Min. Metall., 199, p. 87-112.

SEGNIT, E.R., 1977: Jacobsite and magnetite from Broken Hill, New South Wales. Aust. Mineral., 9, p.37-39.

Serdyuchenko, D.P., 1948: On the crystallochemical role of Ti in micas. Doklady Akad. Nauk SSSR., 59, p.739. (Ref. in Deer et al., 1966).

SHARMA, R.S. & MacRAE, N.D., 1981: Paragenetic relations in gedrite-cordierite-staurolite-biotite-sillimanite-kyanite gneisses at Ajitpura, Rajasthan, India, Contrib. Mineral Petrol., 78, p. 48-60.

SHAW, S.E., 1968: Rb-Sr isotopic studies of the mine sequence rocks at Broken Hill. In; RADMANOVICH, M. & WOODCOCK, J. (eds.) Broken Hill Mines - 1968, Australas. Instn. Min. Metall. Monog. no. 3, Melb. p. 185-198.

SHAW, S.E., 1973: Geochemistry of the mine sequence rocks, Broken Hill, Unpub. Report, Macquarie University. (in MMA Library, Broken Hill).

SIVAPRAKASH, C., 1980: Mineralogy of manganese deposits of Koduru and Garbham, Andhra Pradesh, India, Econ. Geol. 75, p. 1083-1104.

SMELLIE, J.A.T., 1974: Formation of atoll garnets from the aureole of the Ardara Pluton, Co. Donegal, Ireland, Mineral. Mag., 39, p. 878-888.

SMITH, D.C., 1980: Highly aluminouus sphene (titanite) in natural high - pressure hydrous-eclogite-facies rocks from Norway and Italy, and in experimental runs at high pressure. 26th International Geological Congress (1980). Mineralogy Section 2 p. 145 (Abstract).

SPEAR, F.S. & SELVERSTONE, J., 1983: Water exsolution from quartz: implications for the generation of retrograde metamorphic fluids. Geology, 11, p.82-85.

SPEER, J.A. 1981: The nature and magnetic expression of isograds in the contact aureole of the Liberty Hill pluton, South Carolina : a summary. Geol. Soc. Amer. Bull., 92, p.603-609.

SPRY, A. 1969: Metamorphic textures, Oxford Press.

SPRY, P.G., 1978: The geochemistry of garnet-rich lithologies associated with the Broken Hill orebody, N.S.W., Australia, Unpub. M.Sc. thesis, Uni. of Adelaide.

SPRY, P.G., 1982: An unusual gahnite-forming reaction, Geco Base metal deposit, Mamtouwadge, Ontario. Can. Min., 20, p.549-553.

SQUILLER, S.F. & SCLAR, C.B., 1980: Genesis of the Sterling Hill zinc deposit, Sussex Co., New Jersey, In: RIDGE, J.D. (Ed.), Proceedings of the fifth quadrennial IAGOD symposium, Vol. 1, p. 759-766.

STANTON, R.L., 1964: Mineral interfaces in stratiform ores, Trans. Instn. Min. & Metall. (Sect. B: Appl. Earth Sci.),74, p. B45-B79.

STANTON, R.L., 1966: Compositions of stratiform ores as evidence of depositional processes, Trans. Instn. Min. Metall., (Sect. B: Applied Earth Sci.) 75, p. B75-B84.

STANTON, R.L., 1972: A preliminary account of chemical relationships between sulphide lode and "banded iron formation" at Broken Hill, N.S.W., Econ. Geol. 67, p. 1128-1145.

STANTON, R.L., 1976a: Petrochemical studies of the ore environment at Broken Hill, New South Wales: 1 - Constitution of "banded iron formation", Trans. Instn. Min. Metall.(Sect. B: Appl. Earth Sci.) 85, p. B33-B46.

STANTON, R.L., 1976b: Petrochemical studies of the ore environment at Broken Hill, New South Wales: 2 - Regional metamorphism of banded iron formations and their immediate associates, Trans. Instn. Min. Metall., Sect. B, 85, Appl. Earth Sci.) 85, p. B118-B131.

STANTON, R.L., 1976c: Petrochemical studies of the ore environment at Broken Hill, N.S.W: 3 - banded iron formations and sulphide orebodies: constitutional and genetic ties, Trans. Inst. Min. Metall.,(Sect. B, Appl. Earth Sci.) 85, p. B132-B141.

STANTON, R.L., 1976d: Petrochemical studies of the ore environment at Broken Hill, New South Wales: 4 - environmental synthesis, Trans. Instn. Min. Metall. (Sect. B: Appl. Earth Sci.), 85, p. B221-B233.

STANTON, R.L., 1977: Discussion on papers (1976 a, b, c, d), Trans. Instn. Min. Metall. (Sect. B: Appl. Earth Sci.), 86, p. B111-B114.

STANTON, R.L., 1978a: Tectonic deformations at Broken Hill, New South Wales, Australia, and their significance for interpretations of ore environment: Authors reply, Trans. Instn. Min. Metall.(Sect. B: Appl. Earth Sci.) 87, p. B176-B180.

STANTON, R.L., 1982: Metamorphism of a stratiform sulfide orebody at Mount Misery, Einasleigh, Queensland, Australia: 1 - Observations & 2 - Implications, Trans. Instn. Min. Metall. (Sect. B: Appl. Earth Sci.), 91, p. B47-71 & B72-80.

STANTON, R.L., 1983: Stratiform ores and metamorphic processes - some thoughts arising from Broken Hill. In: Broken Hill Conference, 1983. Aust. Inst. Min. Metall., Melb. p. 11-28.

STANTON, R.L. & RICHARDS, S.M., 1961: The abundances of lead, zinc copper and silver at Broken Hill, Proc. Australas. Inst. Min. Metall., 198, p. 309-367.

STANTON, R.L., ROBERTS, W.P.H. & CHANT, R.A., 1978: Petrochemical studies of the ore environment at Broken Hill, N.S.W: 5 - Major element constitution of the lode and its interpretation, Proc. Australas. Inst. Min. Metall., 266, p. 51-78.

STANTON, R.L. & VAUGHAN, J.P., 1979: Facies of ore formation: A preliminary account of the Pegmont deposit as an example of potential relations between small "iron formations" and stratiform sulphide ores, Proc. Australas. Inst. Min. Metall. 270, p. 25-38.

STANTON, R.L. & WILLIAMS, K.L., 1978: Garnet compositions at Broken Hill, N.S.W., as indicators of metamorphic processes, J. Petrol., 19, p. 514-529.

STEVENS, B.P.J., STROUD, W.J., WILLIS, I.L., BROWN, R.E., & BARNES,

R.G., 1980: A stratigraphic interpretation of the Broken Hill Block In: STEVENS, B.P.J (ed) A guide to the stratigraphy and mineralization of the Broken Hill Block, NSW. Records of the Geol. Survey of NSW, 20. p. 9-32.

STILLWELL, F.L., 1959: Petrology of the Broken Hill lode and its bearing on ore genesis, Proc. Australas. Inst. Min. Metall., 190, p. 1-84.

STILLWELL, F.L. & EDWARDS, A.B., 1939: Note on lollingite and the occurence of cobalt and nickel in the Broken Hill Lode. Proc. Australas. Inst. Min. Metall., 114, p.111-124.

STILLWELL, F.L. & EDWARDS, A.B., 1956: Uralite dolerite dykes in relation to the Broken Hill lode, Proc. Australas. Inst. Min. Met., 178, p. 213-232.

STODDARD, E.F., 1979: Zinc-rich hercynite in high-grade metamorphic rocks: a product of dehydration of staurolite, Amer. Mineral., 84, p. 736-741.

STUMPFL, E.F., 1979: Manganese haloes surrounding metamorphic stratabound base metal deposits, Mineralium Deposita., 14, p. 207-217.

SUESS, E., 1978: Mineral phases formed in anoxic sediments by microbial decomposition of organic matter, Geochim. Cosmochim. Acta, 43, p. 339-352.

SUNDBLAD, K., 1981: Chemical evidence for, and implications of, a primary FeS phase in the Ankarvatlnet Zn-Cu-Pb massive sulphide deposit, Central Swedish Caledonides, Mineralium Deposita, 16, p. 129-146.

SUNDBLAD, K., 1982: Distribution of gahnite-bearing sulphidic deposits in the Scandinavian Caledonides. Trans. Instn. Min. Metall. (Sect. B - Appl. Earth Sci.), 91, p. B214-B218.

TAYLOR, G.H., 1971: Carbonaceous Matter: A guide to the genesis and history of ores, Soc. Mining. Geol. Japan, Spec. Issue, 3, p. 283-288. (Proc. IMA-IAGOD Meetings '70, IAGOD Vol.).

THOMAS, W.N., 1960: Notes on facies variation in rocks of the Willyama Series; Report to the Zinc Corporation Ltd., Ref. No. N.S.W. 103/38, 10th June, 1960. M.M.A. Library, Broken Hill.

TRACY, R.J., 1982: Compositional zoning and inclusions in metamorphic minerals In: FERRY, J.M. (ed.) Characteristics of metamorphism through mineral equilibria: Reviews in mineralogy. 10, p.355-397.

TRACY, R.J. & DIETSCH, C.W. 1982: High-temperature retrograde reactions in pelitic gneiss, central Massachusettes, Can. Mineral., 20, p. 425-437.

TSO, J.L., GILBERT, M.C. & CRAIG, J.R., 1979: Sulphidation of synthetic biotites. Amer. Mineral., 64, p.304-316.

TURNER, W.J., 1927: Notes on the geology of the Pinnacles Mine and District. Proc. Aus. Inst. Min. Metall., 68. p. 299-312.

VERNON, R.H., 1962: Co-existing cummingtonite and hornblende in an amphibolite from Duchess, Queensland, Aust. Amer. Mineral., 47, p. 360-370.

VERNON, R.H. & RANSOM, D.M., 1971: Retrograde schists of the amphibolite facies at Broken Hill, New South Wales, J. Geol. Soc. Aust. 18, p. 267-277.

VOKES, F.M., 1968: Regional metamorphism of the Palaeozoic geosynclinal sulphide ore deposits of Norway, Trans. Instn. Min. Metall., (Sect. B: Appl. Earth Sci.) B77, p. 53-80.

VOKES, F.M., 1971: Some aspects of the regional metamorphic mobilization of pre-existing sulphide deposits, Mineralium Deposita, 6, p. 122-129.

WALKER, J.L., 1964: Primary geochemical dispersion in relation to the mineralization at Broken Hill, N.S.W., Unpub. Ph.D., Imperial College, London.

WALL, V.J. & ENGLAND, R.N., 1979: Zn-Fe Spinel-Silicate-Sulphide reactions as sensors of metamorphic intensive variables and processes.

Geol. Soc. Amer. Ann. Meet. (abstracts with programs) 11, p.534.

WALTHER, J.V. and ORVILLE, P.M., 1982: Volatile production and transport in regional metamorphism. Contrib. Mineral. Petrol., 79, 252-257.

WEBER-DIEFENBACH, K., 1977: Geochemistry and diagenesis of recent heavy metal ore deposits of the Atlantis - II - Deep (Red Sea). In: KLEMM, D.D., & SCHNEIDER, H-J.(eds.). Time and stratabound ore deposits. Springer- Verlag. New York., p. 419-436.

WEDEPOHL, K.H., 1971: Environmental influences on the chemical composition of shales and clays IN: AHRENS, L.H., PRESS, F., RUNCORN S.K. and UREY, H.C. (Eds.). Physics and Chemistry of the Earth, Pergammon Press, Oxford. Vol. 8, p. 307-333.

WEDEPOHL, K.H., 1972: Abundance in rock-forming minerals, phase equilibria, zinc minerals. (Zinc, 30-D) in WEDEPOHL, K.H., (ed.) Handbook of geochemistry, Springer-Verlag, Berlin-Heidelberg. II-3, p.30-D-1-12.

WEDEPOHL, K.H., 1980: Geochemical behaviour of manganese In: VARENSTOV, I.M., and GRASSELLY, Gy. (Eds.), Geology and Geochemistry of Manganese, Stuttgart., E. Schweigerbart'sche Verlagbuchhardlung. Vol. 1., p.335-352.

WENDLANDT, R.F., 1981: Influence of CO2 on melting of model granulite facies assemblages: a model for the genesis of charnockites, Amer.

Mineral., 66, p. 1164-1174.

WHELAN, J.A. & GOLDICH, S.S., 1961: New data for hisingerite and neotocite. Amer. Mineral., 46, p.1412-1423.

WHITE, D.E., 1968: Environments of generation of some base metal ore deposits, Econ. Geol., 63, p. 301-335.

WILKINS, R.W.T., 1977: Fluid inclusion assemblages of the stratiform Broken Hill ore deposit, N.S.W., Australia, Science, 198, p. 185-187.

WILLIAMS, P., 1983: A metamorphic sulphide-silicate reaction producing gahnite from the Fornas Cu mine, NW Spain. (Abstr.& programme)."Sulphide mineralogy and petrology with special reference to metamorphic rocks". Mineral. Soc. Ann. Meet. Mineral. Soc. Bull. No. 57, p. 8-9.

WILLIS, I.L., BROWN, R.E., STROUD, W.J. & STEVENS,B.P.J., 1983: The early Proterozoic Willyama Supergroup: stratigraphic subdivision and interpretation of high to low-grade metamorphic rocks in the Broken Hill Block, NSW. J. Geol. Soc. Aust., 30, p.195-224.

WILLIS, I.L., STEVENS, B.P.J., STROUD, W.J., BROWN, R.E., BRADLEY, G.M. & BARNES, R.G., 1983: Metasediments, composite gneisses, and migmatites In: STEVENS, B.D.J. & STROUD, W.J. (eds.). Rocks of the Broken Hill Block: Their classification, nature, stratigraphic distributrion and origin. Records of the Geol. Surv. NSW., 21(1). p.57-126.

WINTER, G.A., ESSENE, E.J., & PEACOR, D.R., 1981: Carbonates and Pyroxenoids from the manganese deposit near Bald Knob, North Carolina, Amer. Mineral., 66, p. 278-289.

WINTSCH,R.P., 1981: Syntectonic Oxidation. Amer.J. Sci., 281, p.1223-1239

WISE, M.A., 1981, Blue quartz in Virginia, Virginia Minerals, 27, p. 9-13.

WONES, D.R., FAHEY, J.J. & AYUSO, R.A., 1977: A search for "annite"(abstract). EOS, 58, p.525.

WRIGHT, T.L., 1968: X - ray and optical studies of alkali feldspars: II An X - ray method for determining the composition and structural state from measurement of 20 values for three reflections. Amer. Miner., 53, p. 88-104.

YARDLEY, B.W.D., 1981: A note on the composition and stability of Fe-staurolite, N Jahrb. Mineral Mh., p. 127-132.

Addendum to Bibliography

HAWKINS, B.W., 1968a: The Zinc Lode Orebodies of the Broken Hill Lode. in RADMANOVICH, M. & WOODCOCK, J. (eds.) Broken Hill Mines - 1968. Australas. Inst. Min. Met. Mon. 3, p. 151-159

HOBBS, B.E., 1966: The structural environment of the northern part of the Broken Hill orebody. Jnl. Geol. Soc. Aust., 13, p. 315-318

HELGESON, H.C., DELANEY, J.M., NESBITT, H.W. & BIRD, D.K., 1978: Summary and critique of the thermodynamic properties of rock-forming minerals. Amer. J. Sci., 278-A, p. 1-229

WINKLER, H.G.F., 1974: Petrogenesis of metamorphic rocks. Springer-Verlag, Berlin. pp. 334

BACHINSKI, S.W. & SIMPSON, E.L., 1984: Ti-phlogopites of the Shaw's Cove minette: a comparison with other micas of other lamprophyres, potassic rocks, Kimberlites and mantle xenoliths. Amer. Miner., 69, p. 41-56

PETERSEN, E.U., ANOVITZ, L.M. & ESSENE, E.J., 1984: Donpeacorite, $(Mn,Mg)MgSi_2O_6$, a new orthopyroxene and its proposed phase relations in the system $MnSiO_3$-$MgSiO_3$-$FeSiO_3$. Amer. Miner., 69, p. 472-480

APPENDIX I : ANALYTICAL METHODS

1. Electron Microprobe Analysis

These analyses were conducted at the Research School of Earth Sciences, Australian National University, Canberra, and on the Jeol 733 microprobes in the Electron Optical Centre, Adelaide University and Mineral Services, Mount Isa Mines Limited, Mount Isa. The Jeol 733 microprobes utilise both wavelength and energy dispersive spectrometers, while the ANU microprobe uses the energy dispersive system of Reed & Ware (1975). Both systems gave detection limits of about 0.05 wt.% oxide.

2. X-Ray Fluorescence

These analyses were determined on whole-rock samples for Si, Ti, Al, Fe, Mn, Mg, Ca, Na, K, Pb, Zn, S, P, Ba, Rb and Sr by the Zinc Corporation Assay Office at Broken Hill, NSW. The samples were prepared in a Lithium Borate Glass, using the standard methods of Norrish & Chappel (1967).

3. Emission Spectroscopy

Ga, Li and B were determined at the Australian Mineral Development Laboratories, Frewville, South Australia, by standard emission spectroscopic methods.

4. Atomic Absorption Spectroscopy

Analyses for Pb, Ag, Zn, Cu, Fe, As and Bi were conducted by the Zinc Corporation Assay Office by Atomic Absorption Spectroscopy. Samples were digested in HCl and HNO_3.

APPENDIX I (a)

5. X-Ray Diffraction Analysis

Samples were handpicked, finely crushed and spread on glass slides prior to analysis in a Phillips Norelco X-Ray Diffractometer. Normally Ni-filtered Cu radiation was used, at 40 kV and 20 mA, and the scan speed varied between 1^0 and $\frac{1}{4}^0$ per minute, depending on the precision required. Where high precision was necessary, about 10-20% of A.R. Si or $KBrO_3$ were mixed with the samples for calibration. $KBrO_3$ was used for the X-Ray Diffraction determination of structural states of the potash feldspars, and the relevant peaks ($CuK\alpha_1$) were assumed to be 21.12^0, 41.17^0 and 31.56^0, for the method of Wright (1968).

APPENDIX II : MINERAL ANALYSES

These analyses were conducted at the Electron Optical Centre, Adelaide University (AU), the Research School of Earth Sciences, Australian National University (ANU), and the Mineral Services laboratories, Mount Isa Mines Pty Ltd (MIM). Further details of the microprobe techniques are provided in Appendix 1.

Detection Limits

The detection limits for most elements is about 0.05 wt%. The analyses are recorded here to four decimal places because that is how they are output from the AU microprobe. The last two decimal places, at least, are insignificant. Similarly, the last decimal place in the calculated formula is insignificant.

Sample Localities

Large numbers such as 4502/16.6 represent drillhole samples, in this example a sample from 16.6 m in DDH4502. Most of these drillholes are shown in Figures 2.1 to 2.10. Small numbers such as 3/4 are samples collected from underground exposures of the WAL in the NBHC Mine, and have no real locality significance. The underlying codes, e.g. G1 RIM, represent specific points analysed on the polished section.

CONTENTS

SELECTED ANALYSES FROM :JAN82 : 1, 2, 5, 8, 14, 15, 17, 18, 20, 26, 27, 30, 32, 33, 35, 36, 39, 41, 42, 51-54, 56-58, 62-64, -89, 93-95, 98-102, 104, 107-109, 113-114, 127-128, 134-135, 144, 153-154, 158, 160-161, 165-167, 171-177, 181-185, 192-196

GARNETS (ANU)
****

	2/1B. G1.	2/1B. G1RIM.	2/1B. G2.	2/1B. G3.	2/4A. G1CORE.	2/4A. G1RIM.	2/4A. G2CORE.	2/4A. G2RIM.
SIO2	36.6600	36.5600	36.4200	36.5800	37.0600	36.9800	36.7700	36.7500
TIO2	.1300	.1800	.1900	.1300	0.0000	0.0000	0.0000	0.0000
AL2O3	20.7700	20.9900	20.8500	20.7800	21.0200	20.9700	20.7600	20.8200
FEO	12.4000	12.0400	12.3800	12.2700	24.2400	23.7500	24.3700	24.3500
MNO	25.4200	25.5400	25.2000	25.5500	14.7500	14.9100	14.9000	14.8100
MGO	1.2700	1.3200	1.3600	1.2600	2.1900	2.1200	2.1500	2.1000
CAO	4.0500	3.8700	4.0500	3.9400	1.5000	1.5000	1.4100	1.2500
K2O	0.0000	0.0000	0.0000	0.0000	0.0000	0.0000	0.0000	0.0000
NA2O	0.0000	0.0000	0.0000	0.0000	0.0000	0.0000	0.0000	0.0000
CL	0.0000	0.0000	0.0000	0.0000	0.0000	0.0000	0.0000	0.0000
	100.7000	100.5000	100.4500	100.5100	100.7600	100.2300	100.3600	100.0800
O=F,CL	0.0000	0.0000	0.0000	0.0000	0.0000	0.0000	0.0000	0.0000
TOTAL	100.7000	100.5000	100.4500	100.5100	100.7600	100.2300	100.3600	100.0800
SI	2.9648	2.9578	2.9517	2.9638	2.9861	2.9923	2.9820	2.9859
TI	.0079	.0110	.0116	.0079	0.0000	0.0000	0.0000	0.0000
AL	1.9803	2.0020	1.9922	1.9849	1.9967	2.0004	1.9848	1.9942
FE	.8387	.8146	.8391	.8314	1.6335	1.6072	1.6529	1.6546
MN	1.7414	1.7502	1.7300	1.7535	1.0067	1.0219	1.0235	1.0192
MG	.1531	.1592	.1643	.1521	.2630	.2557	.2599	.2543
CA	.3510	.3355	.3517	.3421	.1295	.1301	.1225	.1088
K	0.0000	0.0000	0.0000	0.0000	0.0000	0.0000	0.0000	0.0000
NA	0.0000	0.0000	0.0000	0.0000	0.0000	0.0000	0.0000	0.0000
CL	0.0000	0.0000	0.0000	0.0000	0.0000	0.0000	0.0000	0.0000
O,OH,CL,F	12.0000	12.0000	12.0000	12.0000	12.0000	12.0000	12.0000	12.0000
No. atoms	20.0371	20.0303	20.0406	20.0358	20.0155	20.0075	20.0256	20.0170

	2/4A. G3.	2/5A-I. G1.	2/5A-I. G1RIM.	2/5A-I. G2.	2/5A-I. G3 CORE.	2/5A-I. G3 RIM.	2/7A. G1 CORE.	2/7A. G1 RIM.
SIO2	37.1700	36.3700	36.3800	36.3700	36.0400	36.4700	36.7600	36.8100
TIO2	0.0000	0.0000	0.0000	0.0000	.1300	0.0000	0.0000	0.0000
AL2O3	20.9200	20.4600	20.5300	20.6000	20.4500	20.8100	21.3900	21.1600
FEO	24.0800	11.3000	10.9500	11.0500	12.0700	11.8800	31.8500	32.2800
MNO	15.1300	28.8900	29.2800	29.1500	28.4400	28.9500	5.8800	5.9000
MGO	1.9700	.3200	0.0000	.3300	0.0000	0.0000	2.7800	2.5200
CAO	1.6800	3.1700	3.1200	2.9900	3.1700	2.6800	1.8300	1.9000
K2O	0.0000	0.0000	0.0000	0.0000	0.0000	0.0000	0.0000	0.0000
NA2O	0.0000	0.0000	0.0000	0.0000	0.0000	0.0000	0.0000	0.0000
CL	0.0000	0.0000	0.0000	0.0000	0.0000	0.0000	0.0000	0.0000
	100.9500	100.5100	100.2600	100.4900	100.3000	100.7900	100.4900	100.5700
O=F,CL	0.0000	0.0000	0.0000	0.0000	0.0000	0.0000	0.0000	0.0000
TOTAL	100.9500	100.5100	100.2600	100.4900	100.3000	100.7900	100.4900	100.5700
SI	2.9930	2.9747	2.9826	2.9731	2.9618	2.9757	2.9592	2.9681
TI	0.0000	0.0000	0.0000	0.0000	.0080	0.0000	0.0000	0.0000
AL	1.9860	1.9729	1.9843	1.9853	1.9813	2.0018	2.0300	2.0114
FE	1.6216	.7730	.7508	.7554	.8296	.8107	2.1443	2.1768
MN	1.0320	2.0015	2.0334	2.0184	1.9797	2.0009	.4009	.4030
MG	.2364	.0390	0.0000	.0402	0.0000	0.0000	.3335	.3028
CA	.1450	.2778	.2741	.2619	.2791	.2343	.1578	.1642
K	0.0000	0.0000	0.0000	0.0000	0.0000	0.0000	0.0000	0.0000
NA	0.0000	0.0000	0.0000	0.0000	0.0000	0.0000	0.0000	0.0000
CL	0.0000	0.0000	0.0000	0.0000	0.0000	0.0000	0.0000	0.0000
O,OH,CL,F	12.0000	12.0000	12.0000	12.0000	12.0000	12.0000	12.0000	12.0000
No. atoms	20.0140	20.0388	20.0253	20.0343	20.0396	20.0234	20.0258	20.0262

	2/7A. G2.	2/7A. G3 CORE.	2/7A. G3 RIM.	4496/53.6. G1 CORE.	4496/53.6. G1 RIM.	4496/53.6. G1 INT.	4496/53.6. G1 INT2.	4496/53.6. G1 RIM 2.
SIO2	36.8000	36.5000	36.7100	37.1100	37.0300	36.9300	37.0700	36.6300
TIO2	0.0000	0.0000	0.0000	0.0000	0.0000	0.0000	0.0000	.1400
AL2O3	21.1300	21.3000	21.2300	21.0100	20.4900	21.2300	20.9100	20.9600
FEO	32.2800	32.0500	32.3300	23.5600	22.3400	23.6900	23.2800	23.3100
MNO	6.0800	6.1500	5.8200	14.6400	17.5700	14.4100	15.3800	15.7800
MGO	2.6700	2.6500	2.5500	2.6700	1.7000	2.7600	2.3400	2.3300
CAO	1.9400	1.8500	1.8700	1.5100	1.3700	1.4700	1.5200	1.5900
K2O	0.0000	0.0000	0.0000	0.0000	0.0000	0.0000	0.0000	0.0000
NA2O	0.0000	0.0000	0.0000	0.0000	0.0000	0.0000	0.0000	0.0000
CL	0.0000	0.0000	0.0000	0.0000	0.0000	0.0000	0.0000	0.0000
	100.9000	100.5000	100.5100	100.5000	100.5000	100.4900	100.5000	100.7400
O=F,CL	0.0000	0.0000	0.0000	0.0000	0.0000	0.0000	0.0000	0.0000
TOTAL	100.9000	100.5000	100.5100	100.5000	100.5000	100.4900	100.5000	100.7400
SI	2.9604	2.9473	2.9618	2.9872	3.0052	2.9720	2.9909	2.9585
TI	0.0000	0.0000	0.0000	0.0000	0.0000	0.0000	0.0000	.0085
AL	2.0039	2.0277	2.0193	1.9938	1.9604	2.0142	1.9889	1.9958
FE	2.1717	2.1644	2.1815	1.5861	1.5163	1.5945	1.5709	1.5746
MN	.4143	.4206	.3977	.9982	1.2078	.9823	1.0511	1.0796
MG	.3201	.3189	.3066	.3203	.2056	.3310	.2814	.2805
CA	.1672	.1601	.1617	.1302	.1191	.1268	.1314	.1376
K	0.0000	0.0000	0.0000	0.0000	0.0000	0.0000	0.0000	0.0000
NA	0.0000	0.0000	0.0000	0.0000	0.0000	0.0000	0.0000	0.0000
CL	0.0000	0.0000	0.0000	0.0000	0.0000	0.0000	0.0000	0.0000
O,OH,CL,F	12.0000	12.0000	12.0000	12.0000	12.0000	12.0000	12.0000	12.0000
No. atoms	20.0377	20.0389	20.0285	20.0159	20.0146	20.0208	20.0145	20.0350

	4496/53.6. G2 CORE.	4496/53.6. G2 RIM.	4496/53.6. G3 RIM.	4496/53.6. G3 CORE.	4496/60.1. G2.	4496/60.1. G1 CORE.	4496/60.1. G3.	4496/60.1. G1 RIM.
SIO2	36.1700	35.5100	36.3500	36.8500	36.7500	36.6800	36.8700	36.1300
TIO2	0.0000	0.0000	.1600	0.0000	.2400	.1400	0.0000	.1900
AL2O3	21.1100	24.1400	21.0500	21.2000	20.9900	20.7100	20.9200	20.6200
FEO	22.8300	22.7000	17.7400	23.5200	17.6600	17.1600	17.5300	16.7500
MNO	16.9100	14.4000	21.0000	15.2100	20.5300	21.8300	21.2400	22.5600
MGO	2.0100	2.3200	.9200	2.6500	1.6000	1.3100	1.5800	1.2200
CAO	1.4600	1.4400	3.2700	1.5100	2.2300	2.1700	1.8600	2.1400
K2O	0.0000	0.0000	0.0000	0.0000	0.0000	0.0000	0.0000	0.0000
NA2O	0.0000	0.0000	0.0000	0.0000	0.0000	0.0000	0.0000	.3300
CL	0.0000	0.0000	0.0000	0.0000	0.0000	0.0000	0.0000	.0600
	100.4900	100.5100	100.4900	100.9400	100.0000	100.0000	100.0000	99.7473
O=F,CL	0.0000	0.0000	0.0000	0.0000	0.0000	0.0000	0.0000	.0253
TOTAL	100.4900	100.5100	100.4900	100.9400	100.0000	100.0000	100.0000	99.7473
SI	2.9397	2.8429	2.9540	2.9616	2.9815	2.9879	2.9948	2.9592
TI	0.0000	0.0000	.0098	0.0000	.0146	.0086	0.0000	.0117
AL	2.0227	2.2784	2.0167	2.0087	2.0076	1.9889	2.0033	1.9910
FE	1.5518	1.5199	1.2057	1.5809	1.1982	1.1690	1.1908	1.1473
MN	1.1642	.9765	1.4456	1.0354	1.4108	1.5063	1.4614	1.5651
MG	.2435	.2768	.1114	.3174	.1935	.1590	.1913	.1489
CA	.1271	.1235	.2847	.1300	.1939	.1894	.1619	.1878
K	0.0000	0.0000	0.0000	0.0000	0.0000	0.0000	0.0000	0.0000
NA	0.0000	0.0000	0.0000	0.0000	0.0000	0.0000	0.0000	.0533
CL	0.0000	0.0000	0.0000	0.0000	0.0000	0.0000	0.0000	.0000
O,OH,CL,F	12.0000	12.0000	12.0000	12.0000	12.0000	12.0000	12.0000	12.0000
No. atoms	20.0489	20.0179	20.0279	20.0341	20.0001	20.0091	20.0036	20.0643

	4496/67.3. G?.	4496/67.3. G1 CORE.	4496/67.3. G1 RIM.	4496/67.3. G2 CORE.	4496/67.3. G2 RIM.	4496/67.3. G3PINKCORE.	4496/67.3. G3PALERIM.	4496/67.3. G4palecore.
SIO2	34.3900	36.5500	36.5400	36.4300	36.3200	36.4300	36.3500	36.3600
TIO2	0.0000	0.0000	0.0000	0.0000	0.0000	.1200	0.0000	.1100
AL2O3	20.0300	20.8600	20.9300	20.9800	20.7600	20.7100	21.0600	20.8100
FEO	27.8400	29.1100	28.7700	29.1000	29.0600	29.3900	29.4800	29.1500
MNO	11.0300	10.4000	11.1600	10.6900	11.4500	10.5100	10.8500	10.5200
MGO	1.9200	2.6900	2.1400	2.4200	2.0000	2.4700	1.9400	2.7100
CAO	.8400	.8800	.9100	.8800	.9100	.8600	.8200	.8400
K2O	0.0000	0.0000	0.0000	0.0000	0.0000	0.0000	0.0000	0.0000
NA2O	.2000	0.0000	0.0000	0.0000	0.0000	0.0000	0.0000	0.0000
CL	0.0000	0.0000	0.0000	0.0000	0.0000	0.0000	0.0000	0.0000
	96.2500	100.4900	100.4500	100.5000	100.5000	100.4900	100.5000	100.5000
O=F,CL	0.0000	0.0000	0.0000	0.0000	0.0000	0.0000	0.0000	0.0000
TOTAL	96.2500	100.4900	100.4500	100.5000	100.5000	100.4900	100.5000	100.5000
SI	2.9313	2.9616	2.9673	2.9557	2.9587	2.9588	2.9561	2.9498
TI	0.0000	0.0000	0.0000	0.0000	0.0000	.0073	0.0000	.0067
AL	2.0128	1.9927	2.0038	2.0068	1.9937	1.9830	2.0191	1.9904
FE	1.9846	1.9727	1.9539	1.9746	1.9798	1.9963	2.0050	1.9778
MN	.7964	.7138	.7677	.7347	.7901	.7231	.7474	.7229
MG	.2439	.3248	.2590	.2926	.2428	.2990	.2351	.3277
CA	.0767	.0764	.0792	.0765	.0794	.0748	.0715	.0730
K	0.0000	0.0000	0.0000	0.0000	0.0000	0.0000	0.0000	0.0000
NA	.0336	0.0000	0.0000	0.0000	0.0000	0.0000	0.0000	0.0000
CL	0.0000	0.0000	0.0000	0.0000	0.0000	0.0000	0.0000	0.0000
O,OH,CL,F	12.0000	12.0000	12.0000	12.0000	12.0000	12.0000	12.0000	12.0000
No. atoms	20.0791	20.0421	20.0308	20.0408	20.0445	20.0424	20.0343	20.0483

	4496/67.3. G4pinkint.	4496/67.3. G4palerim.	4496/72.3. G1 CORE.	4496/72.3. G1 RIM.	4496/72.3. G2 CORE.	4496/72.3. G2 RIM.	4496/72.3. G3.	4496/125.8. G1 CORE.
SIO2	36.8000	36.7600	36.4700	36.1600	36.4700	36.2300	36.3300	37.5100
TIO2	0.0000	0.0000	0.0000	.1400	.1300	0.0000	0.0000	.1500
AL2O3	20.7800	21.1400	20.7600	20.5700	20.6900	20.9400	20.8700	21.0500
FEO	29.0200	28.6100	19.6700	18.9500	19.5500	18.3400	19.8200	36.1300
MNO	10.3300	11.0000	20.6500	21.8900	20.5200	21.7100	20.0200	3.1200
MGO	2.7400	2.1500	1.2200	.8100	1.1400	.9300	1.3700	2.9800
CAO	.8300	.8500	2.3400	2.3200	2.3700	2.3300	2.3600	.2000
K2O	0.0000	0.0000	0.0000	0.0000	0.0000	0.0000	0.0000	0.0000
NA2O	0.0000	0.0000	0.0000	0.0000	0.0000	.2600	0.0000	0.0000
CL	0.0000	0.0000	0.0000	0.0000	0.0000	0.0000	0.0000	0.0000
	100.5000	100.5100	101.1100	100.8400	100.8700	100.7400	100.7700	101.1400
O=F,CL	0.0000	0.0000	0.0000	0.0000	0.0000	0.0000	0.0000	0.0000
TOTAL	100.5000	100.5100	101.1100	100.8400	100.8700	100.7400	100.7700	101.1400
SI	2.9769	2.9752	2.9586	2.9520	2.9632	2.9504	2.9522	3.0011
TI	0.0000	0.0000	0.0000	.0086	.0079	0.0000	0.0000	.0090
AL	1.9818	2.0172	1.9855	1.9798	1.9818	2.0104	1.9994	1.9855
FE	1.9633	1.9366	1.3346	1.2938	1.3284	1.2491	1.3470	2.4176
MN	.7078	.7541	1.4190	1.5137	1.4122	1.4976	1.3780	.2114
MG	.3303	.2593	.1475	.0986	.1380	.1129	.1659	.3553
CA	.0719	.0737	.2034	.2029	.2063	.2033	.2055	.0171
K	0.0000	0.0000	0.0000	0.0000	0.0000	0.0000	0.0000	0.0000
NA	0.0000	0.0000	0.0000	0.0000	0.0000	.0417	0.0000	0.0000
CL	0.0000	0.0000	0.0000	0.0000	0.0000	0.0000	0.0000	0.0000
O,OH,CL,F	12.0000	12.0000	12.0000	12.0000	12.0000	12.0000	12.0000	12.0000
No. atoms	20.0323	20.0162	20.0486	20.0495	20.0381	20.0652	20.0481	19.9972

	4496/125.8. G1 CORE.	4496/125.8. G1 RIM.	4496/125.8. G2 CORE.	4496/125.8. G2 RIM.	4496/125.8. G3.	4502/19.3. G 1.	4502/19.3. G2 CORE.	4502/19.3. G2 RIM.
SIO2	37.2700	37.1000	37.2900	37.2600	36.8600	36.5100	36.7900	36.7200
TIO2	.1500	0.0000	.1000	0.0000	0.0000	.1000	0.0000	0.0000
AL2O3	20.9100	21.1600	21.4200	21.1600	20.9900	21.4000	21.3800	21.2900
FEO	35.9100	36.1200	35.6500	36.2400	36.1300	35.3600	35.1800	34.6500
MNO	3.1000	3.4300	3.2100	3.2300	3.3300	2.8000	2.8600	2.8000
MGO	2.9600	2.5700	3.3900	2.7800	2.6700	2.5400	2.6500	2.5400
CAO	.2000	.2400	.3100	.1800	.2600	1.2700	1.2600	1.2100
K2O	0.0000	0.0000	0.0000	0.0000	0.0000	0.0000	0.0000	0.0000
NA2O	0.0000	0.0000	0.0000	0.0000	0.0000	0.0000	0.0000	0.0000
CL	0.0000	0.0000	0.0000	0.0000	0.0000	0.0000	0.0000	0.0000
	100.5000	100.6200	101.3700	100.8500	100.2400	99.9800	100.1200	99.2100
O=F,CL	0.0000	0.0000	0.0000	0.0000	0.0000	0.0000	0.0000	0.0000
TOTAL	100.5000	100.6200	101.3700	100.8500	100.2400	99.9800	100.1200	99.2100
SI	3.0011	2.9915	2.9727	2.9944	2.9860	2.9582	2.9723	2.9870
TI	.0091	0.0000	.0060	0.0000	0.0000	.0061	0.0000	0.0000
AL	1.9850	2.0115	2.0131	2.0048	2.0046	2.0442	2.0364	2.0417
FE	2.4183	2.4358	2.3768	2.4357	2.4478	2.3961	2.3770	2.3572
MN	.2114	.2343	.2168	.2199	.2285	.1922	.1957	.1929
MG	.3552	.3088	.4028	.3330	.3223	.3067	.3191	.3079
CA	.0173	.0207	.0265	.0155	.0226	.1103	.1091	.1055
K	0.0000	0.0000	0.0000	0.0000	0.0000	0.0000	0.0000	0.0000
NA	0.0000	0.0000	0.0000	0.0000	0.0000	0.0000	0.0000	0.0000
CL	0.0000	0.0000	0.0000	0.0000	0.0000	0.0000	0.0000	0.0000
O,OH,CL,F	12.0000	12.0000	12.0000	12.0000	12.0000	12.0000	12.0000	12.0000
No. atoms	19.9973	20.0027	20.0147	20.0032	20.0117	20.0136	20.0095	19.9922

	4502/19.3. G3 RIM.	4502/19.3. G3 CORE.	4502/19.3. G3 CORE.	4502/19.3. G4 RIM.	4502/37.3. G1 CORE.	4502/37.3. G1 RIM.	4502/37.3. G 3.	4502/56.9. G CORE.
SIO2	36.5000	36.3500	36.5400	36.3500	36.2500	36.0500	36.5700	36.4500
TIO2	0.0000	0.0000	0.0000	0.0000	0.0000	0.0000	.1000	0.0000
AL2O3	21.4900	21.2200	21.3900	21.2200	21.3900	20.9400	21.3200	20.6600
FEO	35.6100	35.4100	35.1400	34.8800	32.1400	31.9600	31.0000	21.3100
MNO	3.0300	2.8800	2.9800	2.8400	6.3400	6.4200	6.1300	16.0800
MGO	2.2100	2.2500	2.6100	2.6200	2.9000	2.3500	3.6200	1.7000
CAO	1.1500	1.2600	1.3400	1.2800	.9300	.9100	1.1300	3.8100
K2O	0.0000	0.0000	0.0000	0.0000	0.0000	0.0000	0.0000	0.0000
NA2O	0.0000	0.0000	0.0000	.2800	0.0000	0.0000	0.0000	0.0000
CL	0.0000	0.0000	0.0000	0.0000	0.0000	0.0000	.1300	0.0000
	99.9900	99.3700	100.0000	99.4700	99.9500	98.6300	99.4526	100.0100
O=F,CL	0.0000	0.0000	0.0000	0.0000	0.0000	0.0000	.0547	0.0000
TOTAL	99.9900	99.3700	100.0000	99.4700	99.9500	98.6300	99.4526	100.0100
SI	2.9619	2.9677	2.9598	2.9602	2.9413	2.9676	2.9530	2.9655
TI	0.0000	0.0000	0.0000	0.0000	0.0000	0.0000	.0061	0.0000
AL	2.0559	2.0424	2.0427	2.0373	2.0461	2.0322	2.0296	1.9816
FE	2.4167	2.4178	2.3805	2.3756	2.1810	2.2003	2.0935	1.4500
MN	.2083	.1992	.2045	.1959	.4357	.4477	.4193	1.1082
MG	.2673	.2738	.3151	.3180	.3507	.2883	.4356	.2061
CA	.1000	.1102	.1163	.1117	.0809	.0803	.0978	.3321
K	0.0000	0.0000	0.0000	0.0000	0.0000	0.0000	0.0000	0.0000
NA	0.0000	0.0000	0.0000	.0449	0.0000	0.0000	0.0000	0.0000
CL	0.0000	0.0000	0.0000	0.0000	0.0000	0.0000	.0000	0.0000
O,OH,CL,F	12.0000	12.0000	12.0000	12.0000	12.0000	12.0000	12.0000	12.0000
No. atoms	20.0101	20.0111	20.0189	20.0437	20.0357	20.0163	20.0350	20.0437

	4502/56.9. GARNET.	4502/56.9. G3 CORE.	4502/65.1A. G1 CORE.	4502/65.1A. G1 RIM.	4502/65.1A. G2 RIM.	4502/65.1A. G2 CORE.	4502/65.1A. G2 INT.	4502/65.1A. G 3A(rim).
SIO2	36.3000	36.4600	36.5000	36.0200	36.4600	36.4600	36.3800	36.7800
TIO2	0.0000	0.0000	0.0000	0.0000	0.0000	0.0000	.1400	0.0000
AL2O3	20.9500	21.1000	20.6600	20.4700	20.2500	20.6300	20.4600	20.6000
FEO	20.2100	20.9800	16.9800	19.8200	17.4800	18.6900	18.2600	17.5100
MNO	17.1300	16.5200	23.2500	20.7200	23.6600	21.8700	22.5000	23.1700
MGO	1.5200	1.6200	.5900	.9300	.5400	.6100	.6300	.4700
CAO	3.9000	3.9400	2.0300	2.0900	2.0500	1.9200	1.9600	1.9700
K2O	0.0000	0.0000	0.0000	0.0000	0.0000	0.0000	0.0000	0.0000
NA2O	0.0000	0.0000	0.0000	0.0000	0.0000	0.0000	0.0000	0.0000
CL	0.0000	0.0000	0.0000	0.0000	0.0000	0.0000	0.0000	0.0000
	100.0100	100.6200	100.0100	100.0500	100.4400	100.1800	100.3300	100.5000
O=F,CL	0.0000	0.0000	0.0000	0.0000	0.0000	0.0000	0.0000	0.0000
TOTAL	100.0100	100.6200	100.0100	100.0500	100.4400	100.1800	100.3300	100.5000
SI	2.9531	2.9481	2.9901	2.9607	2.9887	2.9860	2.9795	3.0010
TI	0.0000	0.0000	0.0000	0.0000	0.0000	0.0000	.0086	0.0000
AL	2.0093	2.0114	1.9953	1.9836	1.9569	1.9919	1.9755	1.9816
FE	1.3751	1.4187	1.1633	1.3625	1.1983	1.2801	1.2507	1.1949
MN	1.1804	1.1315	1.6133	1.4426	1.6428	1.5172	1.5609	1.6014
MG	.1843	.1952	.0720	.1139	.0660	.0745	.0769	.0572
CA	.3400	.3414	.1782	.1841	.1801	.1685	.1720	.1722
K	0.0000	0.0000	0.0000	0.0000	0.0000	0.0000	0.0000	0.0000
NA	0.0000	0.0000	0.0000	0.0000	0.0000	0.0000	0.0000	0.0000
CL	0.0000	0.0000	0.0000	0.0000	0.0000	0.0000	0.0000	0.0000
O,OH,CL,F	12.0000	12.0000	12.0000	12.0000	12.0000	12.0000	12.0000	12.0000
No. atoms	20.0422	20.0462	20.0124	20.0474	20.0327	20.0181	20.0241	20.0082

	4502/65.1A. G 3B.	4502/65.1A. G 3C.	4502/65.1A. G 3D(core).	4502/65.1A. G 3E.	4502/65.1A. G 3F.	4502/65.1A. G 3G(rim).	4502/65.1B. GI CORE.	4502/65.1B. GI RIM.
SIO2	36.5200	36.7800	36.6000	36.6700	36.5800	36.6200	36.5300	36.4700
TIO2	0.0000	0.0000	0.0000	0.0000	0.0000	0.0000	0.0000	.1600
AL2O3	20.6600	20.5300	20.4600	20.4700	20.4200	20.3200	20.4400	20.5500
FEO	18.9800	18.7100	18.8900	18.2700	18.1900	18.0700	20.4100	18.3800
MNO	21.4400	21.7000	21.6700	22.3300	22.6700	22.5800	20.0300	21.8700
MGO	.8000	.7400	.8000	.6900	.5700	.6300	.8100	.7100
CAO	2.1000	2.0200	2.0700	2.0700	2.0800	2.0500	2.2800	2.3600
K2O	0.0000	0.0000	0.0000	0.0000	0.0000	0.0000	0.0000	0.0000
NA2O	0.0000	0.0000	0.0000	0.0000	0.0000	0.0000	0.0000	0.0000
CL	0.0000	0.0000	0.0000	0.0000	0.0000	0.0000	0.0000	0.0000
	100.5000	100.4800	100.4900	100.5000	100.5100	100.2700	100.5000	100.5000
O=F,CL	0.0000	0.0000	0.0000	0.0000	0.0000	0.0000	0.0000	0.0000
TOTAL	100.5000	100.4800	100.4900	100.5000	100.5100	100.2700	100.5000	100.5000
SI	2.9802	2.9992	2.9889	2.9939	2.9909	2.9986	2.9842	2.9770
TI	0.0000	0.0000	0.0000	0.0000	0.0000	0.0000	0.0000	.0098
AL	1.9876	1.9736	1.9698	1.9703	1.9684	1.9616	1.9686	1.9776
FE	1.2953	1.2760	1.2901	1.2475	1.2439	1.2375	1.3944	1.2548
MN	1.4820	1.4989	1.4990	1.5443	1.5701	1.5662	1.3860	1.5122
MG	.0973	.0899	.0974	.0840	.0695	.0769	.0986	.0864
CA	.1836	.1765	.1811	.1811	.1822	.1799	.1996	.2064
K	0.0000	0.0000	0.0000	0.0000	0.0000	0.0000	0.0000	0.0000
NA	0.0000	0.0000	0.0000	0.0000	0.0000	0.0000	0.0000	0.0000
CL	0.0000	0.0000	0.0000	0.0000	0.0000	0.0000	0.0000	0.0000
O,OH,CL,F	12.0000	12.0000	12.0000	12.0000	12.0000	12.0000	12.0000	12.0000
No. atoms	20.0260	20.0141	20.0263	20.0210	20.0250	20.0205	20.0315	20.0243

	4502/65.1B. G2.	4502/65.1B. G3.	4502/65.1B. G3 RIM.	4502/66.0. G1 CORE.	4502/66.0. G2 RIM.	4502/66.0. G2 CORE.	4502/66.0. G3 CORE.	4502/66.0. G3 RIM.
SIO2	36.7200	36.1800	36.2500	36.2200	36.3600	36.5100	36.9100	36.3800
TIO2	.1100	.1000	0.0000	.1100	0.0000	0.0000	.1600	0.0000
AL2O3	20.6400	20.5400	20.6400	20.4100	20.9200	20.7900	20.8600	20.8300
FEO	18.6200	17.3400	16.1800	21.2100	22.0100	22.9800	22.3800	21.9900
MNO	21.4500	23.1900	24.8100	16.3000	17.3300	16.3700	16.9900	17.0100
MGO	.6400	.5200	.3500	.7800	1.0500	1.2400	1.1300	.8400
CAO	2.3200	2.3600	2.2600	3.5500	3.1600	3.0600	3.2200	3.2400
K2O	0.0000	0.0000	0.0000	0.0000	0.0000	0.0000	0.0000	0.0000
NA2O	0.0000	0.0000	0.0000	0.0000	0.0000	0.0000	0.0000	0.0000
CL	0.0000	0.0000	0.0000	0.0000	0.0000	0.0000	0.0000	0.0000
	100.5000	100.2300	100.4900	98.5800	100.8300	100.9500	101.6500	100.2900
O=F,CL	0.0000	0.0000	0.0000	0.0000	0.0000	0.0000	0.0000	0.0000
TOTAL	100.5000	100.2300	100.4900	98.5800	100.8300	100.9500	101.6500	100.2900
SI	2.9917	2.9680	2.9695	2.9932	2.9530	2.9603	2.9688	2.9674
TI	.0067	.0062	0.0000	.0068	0.0000	0.0000	.0097	0.0000
AL	1.9825	1.9865	1.9933	1.9885	2.0031	1.9873	1.9781	2.0030
FE	1.2687	1.1896	1.1085	1.4659	1.4950	1.5583	1.5055	1.5001
MN	1.4803	1.6114	1.7215	1.1410	1.1922	1.1243	1.1576	1.1752
MG	.0777	.0636	.0427	.0961	.1271	.1498	.1355	.1021
CA	.2025	.2074	.1984	.3143	.2750	.2659	.2775	.2832
K	0.0000	0.0000	0.0000	0.0000	0.0000	0.0000	0.0000	0.0000
NA	0.0000	0.0000	0.0000	0.0000	0.0000	0.0000	0.0000	0.0000
CL	0.0000	0.0000	0.0000	0.0000	0.0000	0.0000	0.0000	0.0000
O,OH,CL,F	12.0000	12.0000	12.0000	12.0000	12.0000	12.0000	12.0000	12.0000
No. atoms	20.0103	20.0326	20.0339	20.0058	20.0454	20.0459	20.0324	20.0310

SELECTED ANALYSES FROM :SEP82 : 1-4, 9, 16-17

	4502/66.0A. GAR1 CORE.	4502/66.0A. GAR1 RIM.	4502/66.0A. G1 MID PT.	4502/66.0A. G1 Opp Rim.	4502/66.0A. GAR2.	4496/29.6. GAR CORE.	4496/29.6. GAR RIM.
SIO2	38.0614	36.3370	37.4754	37.8320	37.8839	34.3672	37.0771
TIO2	.0596	.0333	.0040	.0229	0.0000	.0072	.0080
AL2O3	20.2008	19.7428	20.0181	20.4812	20.4107	19.4526	20.4457
FEO	22.3199	22.9655	22.6553	21.8367	21.7996	29.0627	32.5043
MNO	16.0457	16.5562	15.7412	16.5229	17.0419	3.2450	3.6089
MGO	1.0422	.5267	.9828	.7224	.7342	2.3561	2.1664
CAO	3.1408	2.4450	3.1629	3.1703	3.3842	.3004	.3450
NA2O	.0066	.0145	0.0000	.0003	0.0000	.0100	.0250
K2O	.0101	.0119	0.0000	.0125	0.0000	.0059	.0013
ZNO	.0291	0.0000	0.0000	.0780	0.0000	0.0000	.0423
TOTAL	100.9162	98.6329	100.0397	100.6792	101.2545	88.8071	96.2240
SI	3.0623	3.0219	3.0490	3.0527	3.0460	3.0766	3.0851
TI	.0036	.0021	.0002	.0014	0.0000	.0005	.0005
AL	1.9161	1.9357	1.9201	1.9484	1.9347	2.0530	2.0056
FE	1.5019	1.5973	1.5416	1.4736	1.4659	2.1759	2.2619
MN	1.0935	1.1663	1.0848	1.1293	1.1606	.2461	.2544
MG	.1250	.0653	.1192	.0869	.0880	.3143	.2686
CA	.2708	.2179	.2757	.2741	.2916	.0288	.0308
NA	.0010	.0024	0.0000	.0000	0.0000	.0018	.0041
K	.0010	.0013	0.0000	.0013	0.0000	.0007	.0001
ZN	.0017	0.0000	0.0000	.0047	0.0000	0.0000	.0026
Oxygen	12.0000	12.0000	12.0000	12.0000	12.0000	12.0000	12.0000
No. atoms	19.9771	20.0101	19.9907	19.9724	19.9867	19.8976	19.9136

SELECTED ANALYSES FROM :JAN83 : 1, 7-8, 12, 16, 25, 29, 34, 43, 63, 69, 73, 119-120, 135, 143-144, 160-162, 169, 174, 178, 1
220, 224

GARNETS (AU)
****

	4502/16.6. GARNET.	4502/75.9. G1.	4502/75.9. G2.	4502/44.3. GARNET.	4502/91.6. GARNET 1.	4502/29.9. GARNET 1.	4502/29.9. GNT 2.	4502/48.6. GARNET.
SIO2	36.3236	33.4291	36.8788	35.0525	36.4634	34.2827	37.0715	36.5717
TIO2	0.0000	.0102	.0499	0.0000	.0008	0.0000	.0201	.0130
AL2O3	20.4089	18.8544	20.5366	19.8440	20.4369	19.4240	20.4393	20.2086
FEO	30.1262	34.5195	34.4595	33.7483	36.4907	36.8315	37.1032	23.6349
MNO	8.0624	4.7459	4.9134	5.4483	2.6851	2.3293	2.3209	15.2310
MGO	2.1881	2.3966	2.4216	2.3264	3.3231	2.5238	2.7016	1.6167
CAO	1.8981	.5210	.5137	.8653	.1945	.2197	.2319	1.5410
NA2O	0.0000	.0141	.0293	0.0000	.0037	.0082	.0003	.0058
K2O	0.0000	.0063	.0017	.0204	.0043	.0115	0.0000	.0136
ZNO	.0817	0.0000	.0184	.0633	.0647	.0641	.0493	.0645
TOTAL	99.0890	94.4971	99.8229	97.3685	99.6672	95.6948	99.9381	98.9008
SI	2.9831	2.9227	3.0037	2.9520	2.9751	2.9438	3.0134	3.0123
TI	0.0000	.0007	.0031	0.0000	.0000	0.0000	.0012	.0008
AL	1.9760	1.9434	1.9719	1.9702	1.9658	1.9663	1.9587	1.9623
FE	2.0692	2.5241	2.3473	2.3770	2.4900	2.6450	2.5224	1.6281
MN	.5609	.3515	.3390	.3887	.1856	.1694	.1598	1.0626
MG	.2678	.3123	.2939	.2920	.4041	.3230	.3273	.1985
CA	.1670	.0488	.0448	.0781	.0170	.0202	.0202	.1360
NA	0.0000	.0024	.0047	0.0000	.0006	.0014	.0000	.0009
K	0.0000	.0007	.0002	.0022	.0004	.0013	0.0000	.0014
ZN	.0050	0.0000	.0011	.0039	.0039	.0041	.0030	.0039
Oxygen	12.0000	12.0000	12.0000	12.0000	12.0000	12.0000	12.0000	12.0000
No. atoms	20.0289	20.1064	20.0098	20.0641	20.0426	20.0743	20.0060	20.0069

	4502/47.1C. GARNET.	2/9A. GNT.	4545/42.8. GNT.	1/2. GARNET.	4478/85.8. GNT COR.	4478/85.8. GNT RIM.	4478/68.1. GNT.	2/9B. GNT 1.
SIO2	36.1811	36.2925	36.4886	37.1376	38.1725	38.4741	37.5602	36.9348
TIO2	0.0000	.0163	.0211	0.0000	.0595	.0287	.0650	0.0000
AL2O3	21.1615	20.1072	21.3212	21.2901	21.2354	21.3887	20.5684	20.9173
FEO	29.0193	12.1783	15.9212	30.6845	19.9173	19.6325	10.3753	12.7188
MNO	7.7396	24.9680	19.8358	7.9578	14.1178	14.1367	23.5057	26.5348
MGO	2.8239	.2006	1.6785	1.9109	1.6538	1.6091	.1417	.2707
CAO	2.2074	3.4266	4.5488	1.7400	5.9982	5.8708	8.1791	3.1526
NA2O	.0073	0.0000	.0276	.0034	0.0000	0.0000	.0087	.4473
K2O	0.0000	0.0000	.0032	0.0000	.0155	0.0000	0.0000	.0035
ZNO	.1338	0.0000	.1309	0.0000	.0441	.0007	0.0000	.0380
TOTAL	99.2739	97.1895	99.9769	100.7243	101.2141	101.1413	100.4041	101.0178
SI	2.9478	3.0355	2.9519	2.9901	3.0228	3.0395	3.0217	2.9902
TI	0.0000	.0010	.0013	0.0000	.0035	.0017	.0039	0.0000
AL	2.0326	1.9827	2.0335	2.0209	1.9825	1.9921	1.9508	1.9964
FE	1.9773	.8519	1.0772	2.0662	1.3191	1.2971	.6981	.8612
MN	.5341	1.7689	1.3593	.5427	.9470	.9460	1.6018	1.8196
MG	.3429	.0250	.2024	.2293	.1952	.1894	.0170	.0327
CA	.1927	.3071	.3943	.1501	.5090	.4970	.7051	.2735
NA	.0012	0.0000	.0044	.0005	0.0000	0.0000	.0014	.0714
K	0.0000	0.0000	.0003	0.0000	.0016	0.0000	0.0000	.0004
ZN	.0081	0.0000	.0078	0.0000	.0026	.0000	0.0000	.0023
Oxygen	12.0000	12.0000	12.0000	12.0000	12.0000	12.0000	12.0000	12.0000
No. atoms	20.0366	19.9722	20.0324	19.9997	19.9832	19.9628	19.9997	20.0475

	2/9B. GNT 2.	4483/143.6. G 1.	4483/143.6. G2.	4483/143.6. G3.	4478/62.8. G1.	4483/116.1. G1.	2/13d. G1.	Sturtite. coarse G 1.
SIO2	38.1391	34.2692	36.7439	36.9363	36.7663	38.3267	39.3972	38.1738
TIO2	.0537	.0880	.0679	.0623	.0612	.0567	.0868	0.0000
AL2O3	19.5584	20.2248	20.6084	21.0220	20.5882	19.5594	20.5766	20.0563
FEO	11.4197	15.5115	15.1987	15.5720	11.1001	11.3044	12.2583	25.8887
MNO	27.7622	19.9370	20.8584	20.4296	23.0840	28.4989	22.3527	10.3909
MGO	.2193	.5317	.2391	.5025	.2322	.1462	.5639	2.0740
CAO	3.6387	6.2950	6.0497	6.1955	8.0431	3.2454	7.2642	3.0832
NA2O	.0183	.0155	.0087	0.0000	.0246	.0270	.0140	0.0000
K2O	.0388	0.0000	0.0000	0.0000	.0118	.0043	0.0000	.0052
ZNO	0.0000	.0548	.0193	.0445	.0586	.0670	.0385	.0281
TOTAL	100.8482	96.9275	99.7941	100.7647	99.9701	101.2360	102.5522	99.7002
SI	3.0865	2.8982	2.9939	2.9769	2.9829	3.0930	3.0867	3.0809
TI	.0033	.0056	.0042	.0038	.0037	.0034	.0051	0.0000
AL	1.8660	2.0165	1.9796	1.9975	1.9692	1.8609	1.9006	1.9083
FE	.7729	1.0971	1.0357	1.0496	.7532	.7630	.8032	1.7474
MN	1.9031	1.4282	1.4396	1.3947	1.5864	1.9481	1.4834	.7104
MG	.0264	.0670	.0290	.0604	.0281	.0176	.0658	.2495
CA	.3155	.5705	.5282	.5350	.6992	.2806	.6098	.2666
NA	.0029	.0026	.0014	0.0000	.0039	.0043	.0022	0.0000
K	.0040	0.0000	0.0000	0.0000	.0012	.0004	0.0000	.0005
ZN	0.0000	.0034	.0012	.0027	.0035	.0040	.0022	.0017
Oxygen	12.0000	12.0000	12.0000	12.0000	12.0000	12.0000	12.0000	12.0000
No. atoms	19.9807	20.0893	20.0128	20.0206	20.0313	19.9755	19.9589	19.9653

	Sturtite. G 2 fine.	4496/65.2. G1.	4496/65.2. G 2.	4496/98.4. G1.	4496/32.. G.	4496/85.7. G.	4496/26.9. G.	4483/143.6. G4.
SIO2	38.5888	35.9825	38.7475	39.3177	36.4691	39.5589	38.3758	36.5076
TIO2	.0288	0.0000	.0365	.0100	.0213	0.0000	0.0000	.0654
AL2O3	20.4360	19.2273	20.7084	21.0889	19.4181	20.8862	20.2979	21.0531
FEO	26.3924	27.6622	34.0363	30.3634	34.6767	31.8958	37.1568	15.5987
MNO	10.6143	4.2316	4.0877	7.7050	2.8334	6.4258	2.6709	20.7491
MGO	2.0904	2.6857	3.0859	3.1981	3.2924	2.6929	2.1794	.4671
CAO	3.1181	.2512	.2464	.4964	.2090	.9925	.2240	6.1381
NA2O	.0183	.0399	.0278	.0205	0.0000	.0212	.0202	.0054
K2O	.0140	.0122	0.0000	.0047	0.0000	0.0000	0.0000	0.0000
ZNO	.0725	.0401	.0096	.1253	0.0000	.0457	0.0000	0.0000
TOTAL	101.3736	90.1327	100.9861	102.3300	96.9200	102.5190	100.9250	100.5845
SI	3.0675	3.1510	3.0794	3.0781	3.0425	3.0965	3.0805	2.9552
TI	.0017	0.0000	.0022	.0006	.0013	0.0000	0.0000	.0040
AL	1.9151	1.9850	1.9402	1.9464	1.9098	1.9274	1.9209	2.0091
FE	1.7546	2.0259	2.2622	1.9880	2.4194	2.0880	2.4945	1.0560
MN	.7147	.3139	.2752	.5110	.2002	.4261	.1816	1.4227
MG	.2476	.3505	.3655	.3731	.4093	.3141	.2607	.0564
CA	.2656	.0236	.0210	.0416	.0187	.0832	.0193	.5324
NA	.0029	.0069	.0044	.0032	0.0000	.0033	.0032	.0009
K	.0014	.0014	0.0000	.0005	0.0000	0.0000	0.0000	0.0000
ZN	.0043	.0026	.0006	.0072	0.0000	.0026	0.0000	0.0000
Oxygen	12.0000	12.0000	12.0000	12.0000	12.0000	12.0000	12.0000	12.0000
No. atoms	19.9754	19.8606	19.9504	19.9498	20.0013	19.9414	19.9605	20.0366

BIOTITES (AU)

	4502/29.9. BI 2.	4502/47.1C. GN BI.	4502/47.1C. GN BI 2.	4545/42.8. BI 2.	1/2. BIOTITE.	4526/90.6. BI 1.
SIO2	36.8366	29.1763	30.2828	41.2224	36.4138	39.0799
TIO2	1.3721	0.0000	.0146	.7477	2.8676	.5124
AL2O3	18.2696	19.7722	18.7345	11.4166	19.1213	10.8520
FEO	21.1237	31.6884	27.7952	17.1100	19.7112	17.2305
MNO	.0278	.4151	.3849	1.4605	.1288	2.1587
MGO	9.4375	4.5193	4.2222	15.8973	8.7581	15.1799
CAO	0.0000	.0092	0.0000	0.0000	0.0000	0.0000
NA2O	.2256	.0071	.0889	.0169	.0287	.0246
K2O	9.4973	4.3009	8.3258	9.1848	8.9408	9.8069
ZNO	.0744	.3286	.0933	.1966	.1113	.0881
TOTAL	96.8646	90.2171	89.9422	97.2528	96.0816	94.9330
SI	5.5456	4.9410	5.1625	6.0858	5.4715	5.9985
TI	.1553	0.0000	.0019	.0830	.3240	.0592
AL	3.2425	3.9475	3.7653	1.9870	3.3872	1.9638
FE	2.6596	4.4880	3.9629	2.1126	2.4770	2.2119
MN	.0035	.0595	.0556	.1826	.0164	.2807
MG	2.1174	1.1406	1.0727	3.4977	1.9612	3.4725
CA	0.0000	.0017	0.0000	0.0000	0.0000	0.0000
NA	.0669	.0024	.0299	.0049	.0085	.0074
K	1.8241	.9292	1.8108	1.7300	1.7139	1.9205
ZN	.0083	.0411	.0118	.0214	.0124	.0100
Oxygen	22.0000	22.0000	22.0000	22.0000	22.0000	22.0000
No. atoms	37.6233	37.5511	37.8733	37.7052	37.3721	37.9245

	4526/90.6. BI 2.	4496/65.2. BI 1.	4496/98.4. BI 1.	4526/89.2. Mn-Bi 1.	4526/89.2. Mn-Bi 2.	4496/32.. Bi.
SIO2	39.0978	37.1701	37.5759	39.5427	39.6521	37.1896
TIO2	.3640	1.2553	1.2489	1.1467	1.0860	.6485
AL2O3	10.5975	15.8941	17.3594	10.8184	10.5227	16.5427
FEO	13.2392	19.0310	18.8310	21.4921	22.1454	15.5932
MNO	2.0453	.1111	.0925	2.4462	2.4133	.0441
MGO	17.5294	10.1866	9.9669	10.9339	10.9560	11.0128
CAO	0.0000	0.0000	0.0000	0.0000	.0006	.0184
NA2O	.0487	.2650	.1732	.0197	.0073	.2415
K2O	9.9829	9.2014	9.7573	9.8556	9.7205	8.3648
ZNO	.0122	.0850	.1391	.0344	0.0000	.0718
TOTAL	92.9170	93.1996	95.1442	96.2897	96.5039	89.7274
SI	6.0219	5.7701	5.7048	6.0999	6.1154	5.8547
TI	.0422	.1466	.1426	.1330	.1260	.0768
AL	1.9243	2.9088	3.1071	1.9675	1.9133	3.0703
FE	1.7054	2.4707	2.3910	2.7728	2.8564	2.0530
MN	.2668	.0146	.0119	.3196	.3153	.0059
MG	4.0237	2.3567	2.2551	2.5137	2.5182	2.5838
CA	0.0000	0.0000	0.0000	0.0000	.0001	.0031
NA	.0148	.0811	.0518	.0060	.0022	.0749
K	1.9616	1.8223	1.8899	1.9396	1.9126	1.6800
ZN	.0014	.0098	.0156	.0039	0.0000	.0084
Oxygen	22.0000	22.0000	22.0000	22.0000	22.0000	22.0000
No. atoms	37.9620	37.5807	37.5699	37.7561	37.7593	37.4109

SELECTED ANALYSES FROM :JAN83 : 2, 4, 9-10, 13, 15, 26, 46-47, 70, 74, 82-83, 193, 195, 203-204, 211

BIOTITE (AU)
****

	4502/16.6. BI 1.	4502/16.6. BI 2.	4502/75.9. BIOT 1.	4502/75.9. BIOT 2.	4502/44.3. BIOTITE.	4502/91.6. BI 1.
SIO2	34.5352	35.2726	34.4696	37.2328	35.5935	36.7750
TIO2	2.9055	2.8712	1.0302	.9721	1.6758	1.0758
AL2O3	16.2475	16.6040	13.9688	14.9380	17.2283	15.5652
FEO	18.4424	18.3870	19.0084	18.9859	19.9249	16.0773
MNO	.1202	.1196	.1636	.0878	.1040	.1079
MGO	9.8991	9.8373	12.2079	12.5298	9.1965	13.1391
CAO	.0547	.0518	0.0000	.0119	0.0000	0.0000
NA2O	.0849	.0914	.1869	.1779	.1920	.2625
K2O	9.0107	9.2734	8.5079	8.5326	9.4395	9.2565
ZNO	.1987	.2200	.2336	.0889	.1681	.2182
TOTAL	91.4989	92.7283	89.7769	93.5577	93.5226	92.4775
SI	5.4862	5.5196	5.6088	5.7415	5.5549	5.6920
TI	.3471	.3379	.1261	.1127	.1967	.1252
AL	3.0429	3.0632	2.6796	2.7157	3.1698	2.8403
FE	2.4502	2.4063	2.5867	2.4485	2.6006	2.0812
MN	.0162	.0159	.0225	.0115	.0137	.0141
MG	2.3436	2.2942	2.9604	2.8796	2.1390	3.0308
CA	.0093	.0087	0.0000	.0020	0.0000	0.0000
NA	.0266	.0282	.0599	.0541	.0591	.0801
K	1.8262	1.8514	1.7662	1.6787	1.8795	1.8279
ZN	.0233	.0254	.0281	.0101	.0194	.0250
Oxygen	22.0000	22.0000	22.0000	22.0000	22.0000	22.0000
No. atoms	37.5716	37.5508	37.8384	37.6543	37.6328	37.7165

SELECTED ANALYSES FROM :JAN82 : 16, 34, 38, 40, 43-44, 46-48, 59-60, 96-97, 103, 105-106, 110-112, 115-116, 122, 130, 137

BIOTITE (ANU)
****

	2/4A. BI1.	2/7A. BI1.	2/7A. BI c Ilm.	2/7A. BI 3.	2/7A. BI 4.	4496/53.6. BI 1.	4496/53.6. BI 2.
SIO2	36.5900	36.3200	34.2400	35.8800	35.9000	37.7800	38.6200
TIO2	1.7700	1.1500	1.0900	1.0700	1.1200	.7100	.4300
AL2O3	15.5200	17.8700	17.8300	17.9800	18.0200	12.0000	11.6600
FEO	17.4200	17.9300	20.0100	18.4200	18.1000	15.7600	15.4900
MNO	.3300	0.0000	.1800	0.0000	0.0000	.7200	.7200
MGO	11.1000	11.6800	11.4700	11.5100	11.4100	15.6900	16.2100
CAO	0.0000	0.0000	0.0000	0.0000	0.0000	.1200	0.0000
K2O	9.5900	9.5200	8.0300	9.6700	9.5100	9.3200	9.4300
NA2O	.2500	.2400	.2200	.2100	0.0000	.3100	.2900
CL	.3300	.1300	.0500	.1200	0.0000	.2200	.1500
	91.5104	94.2926	92.9095	94.3547	94.0600	91.7036	92.3684
O=F,CL	.1390	.0547	.0211	.0505	0.0000	.0926	.0632
TOTAL	91.5104	94.2926	92.9095	94.3547	94.0600	91.7036	92.3684
SI	5.7187	5.5269	5.3451	5.4818	5.5015	5.8858	5.9664
TI	.2080	.1316	.1280	.1229	.1291	.0832	.0500
AL	2.8596	3.2059	3.2814	3.2385	3.2556	2.2040	2.1237
FE	2.2770	2.2819	2.6124	2.3536	2.3198	2.0534	2.0014
MN	.0437	0.0000	.0238	0.0000	0.0000	.0950	.0942
MG	2.5855	2.6489	2.6685	2.6207	2.6059	3.6429	3.7322
CA	0.0000	0.0000	0.0000	0.0000	0.0000	.0200	0.0000
K	1.9122	1.8482	1.5993	1.8848	1.8593	1.8524	1.8586
NA	.0770	.0720	.0677	.0632	0.0000	.0952	.0883
CL	.0000	.0000	.0000	.0000	0.0000	.0000	.0000
O,OH,CL,F	22.0000	22.0000	22.0000	22.0000	22.0000	22.0000	22.0000
No. atoms	37.6815	37.7153	37.7262	37.7657	37.6711	37.9320	37.9148

BIOTITES (ANU)

	4496/53.6. BI 3.	4496/53.6. BI 3A.	4496/53.6. BI4/G2.	4496/53.6. BI 4/K.	4496/125.8. BI 1.	4496/125.8. BI 2.	4496/125.8. BI 3.
SIO2	38.0900	38.8800	38.1000	39.5900	35.4600	35.9200	34.9400
TIO2	.5900	.6400	.3000	.5300	1.2100	1.3000	1.1900
AL2O3	11.3400	11.3800	11.8000	11.9800	19.0700	18.8400	18.4800
FEO	14.6800	15.2300	15.7300	17.2000	19.1000	19.0600	19.2800
MNO	.6400	.7700	.6900	.9100	0.0000	0.0000	0.0000
MGO	16.0300	15.9400	16.2400	16.3300	9.6100	9.7100	9.5800
CAO	.1500	.1500	0.0000	.0900	0.0000	0.0000	0.0000
K2O	8.8900	9.2300	9.5700	9.9200	9.4800	9.5100	9.4300
NA2O	.2400	0.0000	.2600	.1800	.2000	.2400	.2000
CL	.1900	.2300	.1700	.2200	0.0000	.1000	0.0000
	90.0399	91.4815	92.1441	96.0236	94.1300	94.2589	93.1000
O=F,CL	.0800	.0969	.0716	.0926	0.0000	.0421	0.0000
TOTAL	90.0399	91.4815	92.1441	96.0236	94.1300	94.2589	93.1000
SI	5.9968	6.0302	5.9162	5.9222	5.4553	5.4976	5.4530
TI	.0699	.0747	.0350	.0596	.1400	.1496	.1397
AL	2.1048	2.0808	2.1602	2.1127	3.4587	3.3994	3.4002
FE	1.9329	1.9755	2.0428	2.1518	2.4575	2.4397	2.5165
MN	.0853	.1012	.0908	.1153	0.0000	0.0000	0.0000
MG	3.7612	3.6845	3.7583	3.6405	2.2033	2.2148	2.2282
CA	.0253	.0249	0.0000	.0144	0.0000	0.0000	0.0000
K	1.7856	1.8264	1.8959	1.8932	1.8607	1.8570	1.8776
NA	.0745	0.0000	.0796	.0531	.0606	.0724	.0615
CL	.0000	.0000	.0000	.0000	0.0000	.0000	0.0000
O,OH,CL,F	22.0000	22.0000	22.0000	22.0000	22.0000	22.0000	22.0000
No. atoms	37.8363	37.7982	37.9787	37.9629	37.6362	37.6305	37.6768

	4502/19.3. BI2.	4502/19.3. BI 3.	4502/19.3. BI 4.	4502/19.3. BI 5.	4502/19.3. BI 1.	4502/19.3. BI 6.	4502/19.3. BI 7.
SIO2	34.2300	33.5400	32.6200	33.9200	33.6600	33.9400	33.6400
TIO2	3.1900	3.0900	3.0000	3.1300	2.8600	3.1100	3.0700
AL2O3	18.1600	17.8600	18.2700	18.6400	18.8300	18.4400	18.7900
FEO	22.6300	22.2400	20.7700	21.6700	22.2400	21.8300	21.8400
MNO	0.0000	0.0000	0.0000	0.0000	0.0000	0.0000	0.0000
MGO	6.9000	6.6700	6.3600	6.8700	6.6300	6.7100	6.6700
CAO	.0900	.1000	.1200	0.0000	.1100	0.0000	0.0000
K2O	9.5500	9.4300	9.4000	9.6300	9.0500	9.7300	9.6500
NA2O	.1500	0.0000	.1300	.1300	.1800	.1500	.2700
CL	.0900	.0800	.1000	0.0000	.0500	.0700	.0700
	94.6110	92.6731	90.3489	93.9900	93.3995	93.6852	93.7052
O=F,CL	.0379	.0337	.0421	0.0000	.0211	.0295	.0295
TOTAL	94.6110	92.6731	90.3489	93.9900	93.3995	93.6852	93.7052
SI	5.3469	5.3506	5.3128	5.3248	5.3112	5.3441	5.2979
TI	.3747	.3707	.3675	.3695	.3394	.3683	.3636
AL	3.3442	3.3590	3.5080	3.4497	3.5028	3.4231	3.4887
FE	2.9563	2.9672	2.8291	2.8450	2.9348	2.8747	2.8766
MN	0.0000	0.0000	0.0000	0.0000	0.0000	0.0000	0.0000
MG	1.6063	1.5858	1.5437	1.6073	1.5591	1.5746	1.5655
CA	.0151	.0171	.0209	0.0000	.0186	0.0000	0.0000
K	1.9032	1.9192	1.9532	1.9287	1.8218	1.9546	1.9389
NA	.0462	0.0000	.0417	.0402	.0560	.0465	.0838
CL	.0000	.0000	.0000	0.0000	.0000	.0000	.0000
O,OH,CL,F	22.0000	22.0000	22.0000	22.0000	22.0000	22.0000	22.0000
No. atoms	37.5928	37.5697	37.5770	37.5652	37.5437	37.5858	37.6149

	4502/19.3. BI+spl.	4502/37.3. BI 1.	4502/37.3. BI 2.	4502/37.3. BI 4.	4502/37.3. BI 5.	4502/37.3. Bi 3.
SIO2	33.6400	35.0300	35.5800	33.8500	36.2300	38.2400
TIO2	2.8800	1.1100	1.3900	1.3500	1.1700	1.3100
AL2O3	18.8000	18.4900	18.6200	17.6600	18.9000	19.5300
FEO	22.3200	20.1700	17.1100	18.1500	17.5000	18.8300
MNO	0.0000	0.0000	0.0000	0.0000	0.0000	0.0000
MGO	6.2300	9.9900	10.4100	10.3300	10.8300	11.6200
CAO	0.0000	.1400	0.0000	.1000	0.0000	0.0000
K2O	9.4700	9.0000	9.2800	8.4000	9.7500	10.0300
NA2O	.1900	.1300	.1500	.1700	.2700	.2100
CL	.1100	.2300	.1600	.2000	.1500	.2300
	93.1768	93.3215	92.0262	89.3678	94.1684	99.0315
O=F,CL	.0463	.0969	.0674	.0842	.0632	.0969
TOTAL	93.1768	93.3215	92.0262	89.3678	94.1684	99.0315
SI	5.3265	5.4268	5.5150	5.4358	5.5054	5.5179
TI	.3429	.1293	.1620	.1630	.1337	.1422
AL	3.5094	3.3770	3.4025	3.3434	3.3859	3.3224
FE	2.9556	2.6133	2.2180	2.4376	2.2240	2.2724
MN	0.0000	0.0000	0.0000	0.0000	0.0000	0.0000
MG	1.4701	2.3065	2.4047	2.4722	2.4526	2.4989
CA	0.0000	.0232	0.0000	.0172	0.0000	0.0000
K	1.9130	1.7788	1.8351	1.7209	1.8902	1.8465
NA	.0593	.0397	.0458	.0538	.0809	.0597
CL	.0000	.0000	.0000	.0000	.0000	.0000
O,OH,CL,F	22.0000	22.0000	22.0000	22.0000	22.0000	22.0000
No. atoms	37.5768	37.6946	37.5832	37.6440	37.6727	37.6600

SELECTED ANALYSES FROM :SEP82 : 15, 22, 25

BIOTITE (AU)
****

	4496/29.6. BI 1.	4502/25.4. #2 BI1.	4502/25.4. BI 2.
SIO2	36.4308	37.0379	36.2698
TIO2	1.2924	1.7536	1.6013
AL2O3	18.0743	17.0963	17.0649
FEO	16.4039	17.6918	17.7048
MNO	.0811	.1043	.1223
MGO	9.4449	9.7020	9.6694
CAO	0.0000	0.0000	0.0000
NA2O	.1958	.1027	.0920
K2O	9.1204	8.8239	9.1029
ZNO	.1224	.0646	.0238
TOTAL	91.1660	92.3771	91.6512
SI	5.6950	5.7355	5.6849
TI	.1519	.2042	.1888
AL	3.3310	3.1212	3.1533
FE	2.1446	2.2913	2.3208
MN	.0107	.0137	.0162
MG	2.2004	2.2391	2.2587
CA	0.0000	0.0000	0.0000
NA	.0603	.0313	.0284
K	1.8190	1.7433	1.8203
ZN	.0141	.0074	.0028
Oxygen	22.0000	22.0000	22.0000
No. atoms	37.4271	37.3870	37.4741

SELECTED ANALYSES FROM :SEP82 : 14

SILLIMANITE (AU)
****

	4496/29.6. SILL.
SIO2	34.5212
TIO2	0.0000
AL2O3	55.1664
FEO	.1799
MNO	.0161
MGO	.0078
CAO	0.0000
NA2O	.0021
K2O	.0009
ZNO	.0553
TOTAL	89.9497
SI	1.0347
TI	0.0000
AL	1.9494
FE	.0045
MN	.0004
MG	.0003
CA	0.0000
NA	.0001
K	.0000
ZN	.0012
Oxygen	5.0000
No. atoms	7.9907

SELECTED ANALYSES FROM :GAHNT : 1-31

SPINELS (AU&ANU) ANU: 1-18, AU: 19-31
****

	4502/19.3. J1.	4502/19.3. J2 CORE.	4502/19.3. J2 RIM.	4502/19.3. J3 RIM.	4502/19.3. J3 CORE.	4502/37.3. J1CORE.	4502/37.3. J1 RIM.	4502/37.3. J2.
SIO2	0.0000	.3500	0.0000	0.0000	0.0000	0.0000	0.0000	0.0000
TIO2	0.0000	0.0000	0.0000	0.0000	0.0000	0.0000	.2200	0.0000
AL203	55.5000	52.7600	54.7000	55.0600	55.7000	53.4100	53.6700	54.0000
FEO	23.0200	20.8000	22.4500	22.2700	22.4300	11.4200	11.4800	11.7300
MNO	.2900	.1900	.2500	.1600	.1800	.2400	.2000	.2300
MGO	1.3000	1.1700	1.1200	1.0400	1.2100	1.2000	1.0700	1.1400
CAO	0.0000	0.0000	0.0000	0.0000	0.0000	0.0000	0.0000	0.0000
NA2O	0.0000	0.0000	0.0000	0.0000	0.0000	0.0000	0.0000	0.0000
ZNO	17.4000	16.0800	17.1700	17.3400	17.7000	27.5800	28.0900	26.9600
TOTAL	97.5100	91.3500	95.6900	95.8700	97.2200	93.8500	94.7300	94.0600
SI	0.0000	.0112	0.0000	0.0000	0.0000	0.0000	0.0000	0.0000
TI	0.0000	0.0000	0.0000	0.0000	0.0000	0.0000	.0052	0.0000
AL	1.9762	1.9875	1.9831	1.9897	1.9855	1.9930	1.9871	2.0032
FE	.5815	.5558	.5774	.5709	.5672	.3023	.3015	.3087
MN	.0074	.0051	.0065	.0042	.0046	.0064	.0053	.0061
MG	.0585	.0557	.0513	.0475	.0545	.0566	.0501	.0535
CA	0.0000	0.0000	0.0000	0.0000	0.0000	0.0000	0.0000	0.0000
NA	0.0000	0.0000	0.0000	0.0000	0.0000	0.0000	0.0000	0.0000
ZN	.3884	.3797	.3902	.3928	.3955	.6451	.6520	.6269
Oxygen	4.0000	4.0000	4.0000	4.0000	4.0000	4.0000	4.0000	4.0000
No. atoms	7.0119	6.9951	7.0085	7.0051	7.0073	7.0035	7.0012	6.9984

	4502/37.3. J3 RIM.	4502/37.3. J4.	4502/37.3. J5.	4502/37.3. J 6.	4502/37.3. J 7.	4502/37.3. J 8.	4502/37.3. J 3 CORE.	4502/42.1. J (corr.).
SIO2	0.0000	0.0000	.2400	0.0000	0.0000	0.0000	0.0000	0.0000
TIO2	0.0000	.1200	0.0000	.1400	.1400	0.0000	0.0000	.1200
AL203	53.2000	54.0200	53.4000	59.4600	55.1400	62.6800	53.7100	53.0900
FEO	11.4600	11.5500	11.2600	12.8500	11.7400	13.3900	11.5400	12.3500
MNO	.2900	.2800	.1600	0.0000	.1500	.1900	.2500	.1500
MGO	1.2000	1.1600	.9800	1.1800	1.1900	1.2600	1.1000	.8700
CAO	0.0000	0.0000	0.0000	0.0000	0.0000	0.0000	0.0000	0.0000
NA2O	0.0000	0.0000	0.0000	0.0000	0.0000	0.0000	0.0000	0.0000
ZNO	27.1900	27.0300	29.4400	29.4400	27.8000	32.3200	27.0700	26.8000
TOTAL	93.3400	94.1600	95.4800	103.0700	96.1600	109.8400	93.6700	93.3800
SI	0.0000	0.0000	.0075	0.0000	0.0000	0.0000	0.0000	0.0000
TI	0.0000	.0028	0.0000	.0030	.0032	0.0000	0.0000	.0029
AL	1.9944	2.0010	1.9722	2.0083	2.0004	1.9976	2.0024	1.9929
FE	.3048	.3035	.2950	.3079	.3021	.3027	.3052	.3289
MN	.0078	.0075	.0042	0.0000	.0039	.0044	.0067	.0040
MG	.0569	.0543	.0458	.0504	.0546	.0508	.0518	.0413
CA	0.0000	0.0000	0.0000	0.0000	0.0000	0.0000	0.0000	0.0000
NA	0.0000	0.0000	0.0000	0.0000	0.0000	0.0000	0.0000	0.0000
ZN	.6390	.6276	.6816	.6233	.6322	.6457	.6326	.6306
Oxygen	4.0000	4.0000	4.0000	4.0000	4.0000	4.0000	4.0000	4.0000
No. atoms	7.0028	6.9967	7.0064	6.9929	6.9965	7.0012	6.9988	7.0007

	4502/42.1. J2.	4502/25.4. SPIN. CORE.	4502/25.4. SPN RIM1.	4502/25.4. SPN RIM2.	4502/25.4. J 1.	4502/91.6. GAHNITE 1.	4502/29.9. GAHNITE 1.	4502/48.6. GAHNITE.
SIO2	0.0000	.0163	.0225	.0145	.0324	.0104	.0110	.0320
TIO2	.1200	0.0000	0.0000	.0126	.0444	0.0000	0.0000	0.0000
AL203	53.2500	59.2065	58.8150	59.2990	56.7236	58.5463	54.5901	54.8462
FEO	12.2100	11.2751	10.0208	10.4514	9.8453	8.4861	16.9902	12.5851
MNO	.1700	.1184	.1104	.1318	.1371	.0611	.0785	.6044
MGO	.7100	1.3815	1.1343	1.3404	1.2812	1.2517	1.7669	1.5969
CAO	0.0000	0.0000	0.0000	0.0000	0.0000	0.0000	0.0000	0.0000
NA2O	0.0000	.6338	.6648	.6457	.5721	.8628	.5832	.7401
ZNO	26.8500	32.2244	33.2335	32.2681	24.3204	35.2693	23.9343	29.5371
TOTAL	93.3100	104.8560	104.0013	104.1635	92.9565	104.4877	97.9542	99.9418
SI	0.0000	.0005	.0006	.0004	.0010	.0003	.0003	.0010
TI	.0029	0.0000	0.0000	.0003	.0010	0.0000	0.0000	0.0000
AL	1.9992	1.9835	1.9892	1.9939	2.0698	1.9794	1.9542	1.9442
FE	.3252	.2680	.2404	.2493	.2548	.2035	.4315	.3165
MN	.0046	.0028	.0027	.0032	.0036	.0015	.0020	.0154
MG	.0337	.0585	.0485	.0570	.0591	.0535	.0800	.0716
CA	0.0000	0.0000	0.0000	0.0000	0.0000	0.0000	0.0000	0.0000
NA	0.0000	.0355	.0376	.0363	.0349	.0488	.0349	.0439
ZN	.6319	.6767	.7046	.6801	.5563	.7475	.5371	.6564
Oxygen	4.0000	4.0000	4.0000	4.0000	4.0000	4.0000	4.0000	4.0000
No. atoms	6.9975	7.0255	7.0236	7.0205	6.9805	7.0344	7.0400	7.0489

	4502/47.1C. GAHNITE.	1/2. GAHNITE.	1/2.4483 J2 COR 2.	149.1. J.	4496/98.4. J.	4496/26.9. J core.	4496/26.9. J rim.
SIO2	.0234	0.0000	.0116	.0585	0.0000	.0123	.0251
TIO2	0.0000	.0065	0.0000	0.0000	0.0000	.0460	0.0000
AL203	57.4798	60.0157	60.1833	59.3466	58.5106	56.8408	56.9228
FEO	7.7183	18.6766	18.7545	8.3069	11.0871	14.5972	13.2665
MNO	.1073	.2537	.2790	.1791	.0942	.0359	.0601
MGO	.4530	2.2832	2.2880	1.3200	1.6077	1.6595	1.4549
CAO	0.0000	0.0000	0.0000	.0030	0.0000	0.0000	0.0000
NA2O	.8018	.5867	.5489	.8411	.9149	.8137	.8654
ZNO	37.1460	22.1463	21.8581	33.5283	31.1367	27.4651	28.7181
TOTAL	103.7296	103.9687	103.9234	103.5835	103.3512	101.4705	101.3129
SI	.0007	0.0000	.0003	.0017	0.0000	.0004	.0007
TI	0.0000	.0001	0.0000	0.0000	0.0000	.0010	0.0000
AL	1.9763	1.9886	1.9920	2.0027	1.9832	1.9648	1.9723
FE	.1883	.4390	.4403	.1989	.2666	.3579	.3261
MN	.0027	.0060	.0066	.0043	.0023	.0009	.0015
MG	.0197	.0956	.0957	.0563	.0689	.0725	.0637
CA	0.0000	0.0000	0.0000	.0001	0.0000	0.0000	0.0000
NA	.0461	.0325	.0304	.0474	.0518	.0470	.0501
ZN	.8006	.4600	.4535	.7093	.6616	.5951	.6237
Oxygen	4.0000	4.0000	4.0000	4.0000	4.0000	4.0000	4.0000
No. atoms	7.0342	7.0219	7.0189	7.0207	7.0343	7.0397	7.0382

SELECTED ANALYSES FROM :JAN82 : 3-4, 6, 9, 13, 19, 21, 45

CUMMINGTONITE-GRUNERITE (ANU)
****

	2/1B. K1.	2/1B. K2.	2/1B. K3.	2/1B. K4.	2/4A. K1.	2/4A. K2.	2/4A. K3.	4496/53.6. K1.
SIO2	49.9900	49.4900	50.2100	49.5700	50.7000	51.0600	50.3900	51.1400
TIO2	0.0000	.1500	0.0000	.1500	0.0000	.1000	.1100	0.0000
AL2O3	.2400	.2600	.3800	0.0000	.1900	.3200	.2100	.3000
FEO	26.3600	25.4300	26.1100	26.3300	29.6700	29.8100	30.0000	25.4700
MNO	11.5700	11.1000	11.5600	11.6100	5.3500	5.5200	5.3500	5.4400
MGO	8.2700	8.5600	8.2200	7.9400	10.0100	9.7700	9.7500	13.2100
CAO	1.0800	1.1400	1.1700	1.0700	.4000	.5600	.4900	.3200
K2O	0.0000	0.0000	0.0000	0.0000	0.0000	0.0000	0.0000	0.0000
NA2O	.2200	.3100	.2200	0.0000	0.0000	.1700	.2300	.2800
CL	.0600	.0600	.0900	0.0000	0.0000	0.0000	0.0000	0.0000
	97.5373	96.2473	97.5810	96.6700	96.3200	97.3100	96.5300	96.1600
O=F,CL	.0253	.0253	.0379	0.0000	0.0000	0.0000	0.0000	0.0000
TOTAL	97.5373	96.2473	97.5810	96.6700	96.3200	97.3100	96.5300	96.1600
SI	7.8806	7.8735	7.8901	7.9064	7.9636	7.9473	7.9262	7.8927
TI	0.0000	.0179	0.0000	.0180	0.0000	.0117	.0130	0.0000
AL	.0446	.0488	.0704	0.0000	.0352	.0587	.0389	.0546
FE	3.4753	3.3836	3.4314	3.5123	3.8976	3.8804	3.9465	3.2875
MN	1.5450	1.4958	1.5387	1.5686	.7118	.7278	.7128	.7112
MG	1.9430	2.0296	1.9251	1.8874	2.3432	2.2663	2.2856	3.0384
CA	.1824	.1943	.1970	.1829	.0673	.0934	.0826	.0529
K	0.0000	0.0000	0.0000	0.0000	0.0000	0.0000	0.0000	0.0000
NA	.0684	.0972	.0681	0.0000	0.0000	.0521	.0713	.0852
CL	.0000	.0000	.0000	0.0000	0.0000	0.0000	0.0000	0.0000
O,OH,CL,F	23.0000	23.0000	23.0000	23.0000	23.0000	23.0000	23.0000	23.0000
No. atoms	38.1392	38.1407	38.1207	38.0756	38.0188	38.0377	38.0772	38.1226

	4496/53.6. K2.	4496/53.6. K2A.	4496/53.6. K3.	4496/53.6. K4.	4496/60.1. K1.	4496/60.1. K2.	4496/60.1. K3.	4496/60.1. K4.
SIO2	49.7100	51.5900	51.4800	51.1300	51.5100	47.4100	51.3400	51.5900
TIO2	0.0000	0.0000	.1300	0.0000	.1200	0.0000	0.0000	0.0000
AL2O3	.3500	.4200	.4600	.4000	.3800	.1900	.2000	.2400
FEO	23.9700	25.0800	25.5700	25.1800	30.6700	27.9500	30.7700	31.0300
MNO	5.3600	5.7500	5.6800	6.0300	10.3400	9.1800	10.6500	10.8200
MGO	12.4100	12.9300	12.9700	12.9200	6.8300	6.3200	6.5200	6.7300
CAO	.5600	.4600	.3600	.6000	.5500	.5000	.5300	.5000
K2O	0.0000	0.0000	0.0000	0.0000	0.0000	0.0000	0.0000	0.0000
NA2O	.3900	.2500	.2700	.2500	.2000	.2200	0.0000	.3300
CL	0.0000	.0500	0.0000	0.0000	.1200	.0900	0.0000	.0700
	92.7500	96.3195	96.9200	96.5100	100.2147	91.4810	100.0100	101.0152
O=F,CL	0.0000	.0211	0.0000	0.0000	.0505	.0379	0.0000	.0295
TOTAL	92,7500	96.3195	96.9200	96.5100	100.2147	91.4810	100.0100	101.0152
SI	7.9340	7.9245	7.8859	7.8778	7.9435	7.9942	7.9746	7.9341
TI	0.0000	0.0000	.0150	0.0000	.0139	0.0000	0.0000	0.0000
AL	.0659	.0761	.0831	.0727	.0691	.0378	.0366	.0435
FE	3.1996	3.2219	3.2758	3.2446	3.9556	3.9415	3.9972	3.9911
MN	.7246	.7481	.7370	.7870	1.3507	1.3112	1.4012	1.4095
MG	2.9519	2.9599	2.9610	2.9667	1.5697	1.5882	1.5093	1.5425
CA	.0958	.0757	.0591	.0991	.0909	.0903	.0882	.0824
K	0.0000	0.0000	0.0000	0.0000	0.0000	0.0000	0.0000	0.0000
NA	.1227	.0757	.0815	.0759	.0608	.0731	0.0000	.1000
CL	0.0000	.0000	0.0000	0.0000	.0000	.0000	0.0000	.0000
O,OH,CL,F	23.0000	23.0000	23.0000	23.0000	23.0000	23.0000	23.0000	23.0000
No. atoms	38.0943	38.0818	38.0983	38.1236	38.0541	38.0363	38.0072	38.1032

	4496/67.3. K1.	4496/67.3. K2.	4496/67.3. K3.	4496/72.3. K1.	4496/72.3. K2(poik.).	4496/72.3. K3.	4502/56.9. K1.	4502/56.9. K2.
SIO2	48.4400	49.5400	49.6100	48.9500	49.0000	48.9100	50.7700	50.6200
TIO2	0.0000	0.0000	0.0000	0.0000	.1000	0.0000	0.0000	0.0000
AL2O3	.4100	.5500	.3200	.2100	.2300	.2400	.3700	.3300
FEO	28.9800	29.7400	29.4500	35.3000	35.3300	36.0500	30.0500	28.9600
MNO	2.3000	2.3200	2.2400	6.9900	6.8300	7.1000	6.8300	7.0300
MGO	11.4400	11.7900	11.6500	5.7200	5.6800	5.6000	8.4100	8.7600
CAO	.2200	.2200	.2400	.2800	.3700	.3600	1.2600	1.2200
K2O	0.0000	0.0000	0.0000	0.0000	0.0000	0.0000	0.0000	0.0000
NA2O	.2300	.3700	.2500	0.0000	.1900	.2000	.3700	.2500
CL	.0500	0.0000	0.0000	.0700	.1000	.0800	0.0000	.0800
	91.8595	94.5300	93.7600	97.2252	97.4089	98.2031	98.0600	96.9131
O=F,CL	.0211	0.0000	0.0000	.0295	.0421	.0337	0.0000	.0337
TOTAL	91.8595	94.5300	93.7600	97.2252	97.4089	98.2031	98.0600	96.9131
SI	7.8871	7.8547	7.9140	7.9018	7.8892	7.8519	7.9242	7.9450
TI	0.0000	0.0000	0.0000	0.0000	.0121	0.0000	0.0000	0.0000
AL	.0787	.1028	.0602	.0400	.0437	.0454	.0681	.0611
FE	3.9462	3.9436	3.9290	4.7657	4.7572	4.8401	3.9226	3.8014
MN	.3172	.3116	.3027	.9558	.9315	.9655	.9030	.9346
MG	2.7760	2.7859	2.7697	1.3761	1.3629	1.3398	1.9563	2.0491
CA	.0384	.0374	.0410	.0484	.0638	.0619	.2107	.2052
K	0.0000	0.0000	0.0000	0.0000	0.0000	0.0000	0.0000	0.0000
NA	.0738	.1156	.0786	0.0000	.0603	.0633	.1138	.0773
CL	.0000	0.0000	0.0000	.0000	.0000	.0000	0.0000	.0000
O,OH,CL,F	23.0000	23.0000	23.0000	23.0000	23.0000	23.0000	23.0000	23.0000
No. atoms	38.1175	38.1517	38.0953	38.0877	38.1206	38.1679	38.0986	38.0740

	4502/56.9. K3.	4502/65.1A. K 1.	4502/65.1A. K2.	4502/65.1A. K3.	4502/65.1A. K4.	4502/65.1A. K5.	4502/65.1A. FIB K.	4502/65.1B. K1.
SIO2	50.4600	51.7100	48.5800	48.7300	48.5400	48.3700	48.0800	47.6300
TIO2	0.0000	0.0000	0.0000	.1600	0.0000	0.0000	0.0000	0.0000
AL2O3	.1600	.3800	.3800	.2400	.1900	.1700	.2400	.2100
FEO	29.5200	34.6800	36.3400	36.4900	36.3800	36.3000	36.0700	35.4900
MNO	6.9600	7.7100	8.0300	8.1500	7.9400	7.9000	7.9800	7.7000
MGO	8.0900	3.6400	3.7300	3.8000	3.6200	3.7100	3.6900	3.6000
CAO	1.1400	.3300	.3700	.4100	.4100	.3400	.3200	.4100
K2O	0.0000	0.0000	0.0000	0.0000	0.0000	0.0000	0.0000	0.0000
NA2O	.1600	0.0000	.2400	.2400	.2200	.2300	.3400	.3000
CL	0.0000	0.0000	.1300	.1200	0.0000	.1000	.0700	.0500
	96.4900	98.4500	97.2526	97.8347	97.3000	96.6989	96.4952	95.1795
O=F,CL	0.0000	0.0000	.0547	.0505	0.0000	.0421	.0295	.0211
TOTAL	96.4900	98.4500	97.2526	97.8347	97.3000	96.6989	96.4952	95.1795
SI	7.9917	8.1794	7.9183	7.9049	7.9394	7.9393	7.9199	7.9445
TI	0.0000	0.0000	0.0000	.0195	0.0000	0.0000	0.0000	0.0000
AL	.0299	.0709	.0730	.0459	.0366	.0329	.0466	.0413
FE	3.9101	4.5878	4.9538	4.9505	4.9765	4.9830	4.9691	4.9507
MN	.9337	1.0330	1.1087	1.1199	1.1001	1.0984	1.1134	1.0879
MG	1.9095	.8581	.9061	.9187	.8824	.9075	.9059	.8949
CA	.1935	.0559	.0646	.0713	.0719	.0598	.0565	.0733
K	0.0000	0.0000	0.0000	0.0000	0.0000	0.0000	0.0000	0.0000
NA	.0499	0.0000	.0771	.0767	.0709	.0744	.1104	.0986
CL	0.0000	0.0000	.0000	.0000	0.0000	.0000	.0000	.0000
O,OH,CL,F	23.0000	23.0000	23.0000	23.0000	23.0000	23.0000	23.0000	23.0000
No. atoms	38.0183	37.7853	38.1016	38.1074	38.0777	38.0953	38.1218	38.0911

	4502/65.1B. K2 2ry.	4502/65.1B. K3.	4502/65.1B. K4.	4502/65.1B. K5 (2ry?).	4502/65.1B. K6.	4502/65.1B. K7 2ry?.	4502/66.0. K1.	4502/66.0. K1 CORE.
SIO2	48.0200	48.2000	48.3200	48.4100	48.3400	48.5800	49.3900	50.0600
TIO2	0.0000	0.0000	0.0000	0.0000	0.0000	0.0000	0.0000	0.0000
AL2O3	.2900	.3800	.1900	.2600	.1400	.2700	.3700	.2200
FEO	35.8900	36.6200	37.1200	36.9500	36.6600	36.8500	32.1000	33.3600
MNO	7.7100	8.1400	8.2300	8.0400	8.0700	8.0600	3.8500	4.0600
MGO	3.6000	3.5300	3.7300	3.6500	3.6900	3.7000	8.3900	8.5900
CAO	.4100	.4300	.4400	.3800	.3000	.4400	.2900	.2800
K2O	0.0000	0.0000	0.0000	0.0000	0.0000	0.0000	0.0000	0.0000
NA2O	.1300	.2600	.2300	.3400	.2000	.3000	.3300	.3100
CL	.1000	.0800	.0900	.0900	.0600	.1100	.0600	.0500
	95.7289	97.3031	97.9710	97.7410	97.2073	97.8468	94.5273	96.7195
O=F,CL	.0421	.0337	.0379	.0379	.0253	.0463	.0253	.0211
TOTAL	95.7289	97.3031	97.9710	97.7410	97.2073	97.8468	94.5273	96.7195
SI	7.9488	7.8902	7.8724	7.8912	7.9195	7.8980	7.9644	7.9289
TI	0.0000	0.0000	0.0000	0.0000	0.0000	0.0000	0.0000	0.0000
AL	.0566	.0733	.0365	.0500	.0270	.0517	.0703	.0411
FE	4.9685	5.0134	5.0578	5.0373	5.0230	5.0104	4.3291	4.4190
MN	1.0810	1.1287	1.1358	1.1101	1.1199	1.1100	.5259	.5447
MG	.8881	.8612	.9057	.8867	.9009	.8965	2.0163	2.0277
CA	.0727	.0754	.0768	.0664	.0527	.0766	.0501	.0475
K	0.0000	0.0000	0.0000	0.0000	0.0000	0.0000	0.0000	0.0000
NA	.0424	.0839	.0738	.1092	.0646	.0961	.1049	.0968
CL	.0000	.0000	.0000	.0000	.0000	.0000	.0000	.0000
O,OH,CL,F	23.0000	23.0000	23.0000	23.0000	23.0000	23.0000	23.0000	23.0000
No. atoms	38.0581	38.1261	38.1587	38.1508	38.1076	38.1395	38.0611	38.1056

	4502/66.0. K2.	4502/66.0. K3.	4502/66.0. K4.	4502/66.0. K5.	4502/66.0. K6.	4502/66.0. K7.	AVERAGE . of 46.
SIO2	49.7200	49.7100	49.1000	50.2500	49.0300	49.8100	49.6346
TIO2	.1800	0.0000	0.0000	0.0000	0.0000	0.0000	.0261
AL2O3	.2900	.2900	.2900	.3000	.2600	.3500	.2841
FEO	33.6100	33.6000	33.2200	33.6500	32.0800	32.9300	31.7211
MNO	3.9000	3.8900	3.8500	3.9000	3.7700	3.8600	6.8402
MGO	8.2000	8.2600	8.1600	8.3700	8.0000	8.6000	7.4948
CAO	.3700	.2800	.2800	.2800	.2800	.2800	.4985
K2O	0.0000	0.0000	0.0000	0.0000	0.0000	0.0000	0.0000
NA2O	.1700	.2500	.2500	.2500	.2300	.2500	.2267
CL	.0900	0.0000	0.0000	0.0000	.1200	0.0000	.0487
	96.1510	96.2800	95.1500	97.0000	93.2647	96.0800	96.5697
O=F,CL	.0379	0.0000	0.0000	0.0000	.0505	0.0000	.0205
TOTAL	96.1510	96.2800	95.1500	97.0000	93.2647	96.0800	96.5697
SI	7.9224	7.9296	7.9269	7.9435	8.0040	7.9331	7.9267
TI	.0216	0.0000	0.0000	0.0000	0.0000	0.0000	.0031
AL	.0545	.0545	.0552	.0559	.0500	.0657	.0534
FE	4.4789	4.4825	4.4854	4.4487	4.3798	4.3862	4.2467
MN	.5264	.5256	.5265	.5222	.5213	.5207	.9260
MG	1.9473	1.9637	1.9633	1.9719	1.9463	2.0413	1.7736
CA	.0632	.0479	.0484	.0474	.0490	.0478	.0850
K	0.0000	0.0000	0.0000	0.0000	0.0000	0.0000	0.0000
NA	.0534	.0786	.0795	.0779	.0740	.0785	.0714
CL	.0000	0.0000	0.0000	0.0000	.0000	0.0000	.0000
O,OH,CL,F	23.0000	23.0000	23.0000	23.0000	23.0000	23.0000	23.0000
No. atoms	38.0676	38.0824	38.0853	38.0675	38.0246	38.0734	38.0859

SELECTED ANALYSES FROM :JAN83 : 61-62, 68, 130-131, 158-159, 165-168, 179, 183, 199-200

CUMMINGTONITE - GRUNERITE SERIES (AU)
****

	2/9A. AMPH 1.	2/9A. AMPH 2.	4545/42.8. AMPH.	2/9B. DANN 1.	2/9B. DANN 2.	4483/143.6. P/A ? 3.	4483/143.6. P/A ? 4.	4483/143.6. P/A?6.
SIO2	48.0288	48.0693	53.5728	49.4152	48.4304	44.3967	45.5436	45.2369
TIO2	0.0000	.0175	.0121	.0578	0.0000	.0235	0.0000	.0064
AL2O3	.0825	.1386	.3281	.0876	.0784	.1107	.0956	.1103
FEO	32.4453	30.2935	17.5749	25.1066	24.9139	32.7859	33.1937	33.1246
MNO	10.7091	11.1747	4.4094	9.3409	9.6059	8.6433	8.6497	7.9564
MGO	2.5850	3.9151	12.5366	5.2981	5.2671	4.3654	4.6532	5.1954
CAO	.1452	.2759	9.2899	5.7061	5.2541	1.2810	1.1612	1.1473
NA2O	.0400	.0269	.0365	.0413	.1275	.0497	.0438	.0389
K2O	.0198	0.0000	.0920	.1006	.1060	.0151	.0013	.0146
ZNO	.1081	.1852	.1046	.1345	0.0000	.2368	.1821	.1550
TOTAL	94.1638	94.0967	97.9569	95.2887	93.7833	91.9081	93.5242	92.9858
SI	8.0898	8.0404	7.9502	7.9928	7.9766	7.7430	7.7765	7.7498
TI	0.0000	.0022	.0014	.0070	0.0000	.0031	0.0000	.0008
AL	.0164	.0273	.0574	.0167	.0152	.0228	.0192	.0223
FE	4.5705	4.2378	2.1812	3.3963	3.4318	4.7821	4.7401	4.7459
MN	1.5279	1.5833	.5543	1.2798	1.3401	1.2769	1.2510	1.1546
MG	.6489	.9760	2.7726	1.2772	1.2929	1.1347	1.1841	1.3265
CA	.0262	.0494	1.4772	.9889	.9272	.2394	.2125	.2106
NA	.0133	.0089	.0107	.0132	.0414	.0171	.0147	.0131
K	.0043	0.0000	.0174	.0208	.0223	.0034	.0003	.0032
ZN	.0135	.0229	.0115	.0161	0.0000	.0305	.0230	.0196
Oxygen	23.0000	23.0000	23.0000	23.0000	23.0000	23.0000	23.0000	23.0000
No. atoms	37.9107	37.9481	38.0338	38.0088	38.0476	38.2526	38.2214	38.2464

	4483/143.6. P/A?7.	4483/143.6. P/A?8.	4483/143.6. P/A?9.	2/13d. K1.	4526/89.2. P/K.	4526/89.2. P/K?1.	4526/89.2. P/K?2.
SIO2	44.7078	44.5015	43.1500	53.1773	53.5533	54.9452	54.6872
TIO2	.0680	.0384	0.0000	.0032	0.0000	.0033	.0271
AL2O3	.1204	.0831	.0768	.1003	.1111	.0869	.0992
FEO	32.4695	32.6469	32.2081	27.3644	21.6421	22.6694	22.7029
MNO	8.1027	7.7619	7.8722	9.3145	10.3583	10.7418	10.4373
MGO	4.6829	5.1493	5.0467	7.2680	10.4094	9.6400	9.9607
CAO	1.1966	1.4317	1.7720	2.4845	1.7205	1.9071	1.9722
NA2O	.0081	.0459	.0374	.0438	.0544	.0107	.0062
K2O	.0121	0.0000	0.0000	0.0000	.0301	.0114	.0269
ZNO	.1424	.1735	.1055	.1374	.1821	0.0000	.1306
TOTAL	91.5105	91.8322	90.2687	99.8934	98.0613	100.0158	100.0503
SI	7.7822	7.7267	7.6593	8.1025	8.1173	8.1777	8.1413
TI	.0089	.0050	0.0000	.0004	0.0000	.0004	.0030
AL	.0247	.0170	.0161	.0180	.0199	.0152	.0174
FE	4.7269	4.7406	4.7813	3.4870	2.7435	2.8217	2.8266
MN	1.1947	1.1416	1.1836	1.2022	1.3299	1.3542	1.3162
MG	1.2148	1.3324	1.3350	1.6504	2.3514	2.1383	2.2099
CA	.2232	.2664	.3370	.4056	.2794	.3041	.3146
NA	.0028	.0157	.0131	.0132	.0163	.0031	.0018
K	.0027	0.0000	0.0000	0.0000	.0058	.0022	.0051
ZN	.0183	.0223	.0138	.0155	.0204	0.0000	.0144
Oxygen	23.0000	23.0000	23.0000	23.0000	23.0000	23.0000	23.0000
No. atoms	38.1992	38.2676	38.3393	37.8946	37.8838	37.8169	37.8503

SELECTED ANALYSES FROM :SEP82 : 5-8, 29-30

CUMMINGTONITE - GRUNERITE SERIES (AU)
****

	4502/66.0A. AMPH1.	4502/66.0A. AMPH2.	4502/66.0A. AMPH3.	4502/66.0A. AMPH4.	2/9BA. UNKSIL 1.	2/9BA. UNKSIL 2.
SIO2	36.1731	47.4385	47.5718	50.9544	51.2203	50.7360
TIO2	.0436	.0140	.0192	.0215	.0042	.0032
AL2O3	.1347	.3745	.1289	.1551	.0547	.0312
FEO	30.9884	35.0563	33.5596	34.0786	31.3479	26.9377
MNO	3.1387	3.6569	3.9833	3.6812	11.4116	11.5545
MGO	7.4103	7.5143	8.2479	8.3963	4.3045	4.9997
CAO	.2441	.4537	.2567	.2570	.6800	3.7853
NA2O	.0220	.0233	.0323	.0315	.1800	.0376
K2O	0.0000	.0177	0.0000	0.0000	.0190	.0153
ZNO	.1529	.1986	.1040	.1386	.1049	.0985
TOTAL	78.3078	94.7478	93.9037	97.7142	99.3271	98.1990
SI	7.3846	7.8023	7.8424	7.9857	8.0779	8.0215
TI	.0067	.0017	.0024	.0025	.0005	.0004
AL	.0324	.0726	.0251	.0287	.0102	.0058
FE	5.2907	4.8220	4.6269	4.4667	4.1347	3.5619
MN	.5427	.5095	.5562	.4887	1.5245	1.5474
MG	2.2545	1.8419	2.0264	1.9611	1.0117	1.1781
CA	.0534	.0800	.0453	.0432	.1149	.6413
NA	.0089	.0076	.0105	.0097	.0559	.0117
K	0.0000	.0037	0.0000	0.0000	.0038	.0031
ZN	.0231	.0241	.0127	.0161	.0122	.0115
Oxygen	23.0000	23.0000	23.0000	23.0000	23.0000	23.0000
No. atoms	38.5970	38.1653	38.1479	38.0023	37.9463	37.9825

SELECTED ANALYSES FROM :JAN83 : 68, 121-124, 142, 156, 164

ACTINOLITE (AU)
****

	4545/42.8. AMPH.	4478/85.8. HBD NPK.	4478/85.8. HBD POIK.	4478/85.8. HBD 3.	4478/85.8. HBD 4.	2/9B. MN-ACTIN.	4483/143.6. P/A ? 1.	4483/143.6. P/A?5.
SIO2	53.5728	51.7275	51.6746	50.9627	51.9444	50.9427	47.5912	48.2146
TIO2	.0121	.3504	.0467	.1598	.0374	.0033	0.0000	.0329
AL2O3	.3281	3.2773	.9874	2.3743	.9246	.2804	.3328	.3442
FEO	17.5749	17.9882	18.7898	18.2565	19.1744	23.8463	27.3259	26.1673
MNO	4.4094	1.7065	1.0778	1.0345	1.1365	5.6751	3.8908	3.6499
MGO	12.5366	12.1372	11.3228	11.2894	11.3643	5.7337	4.9890	5.5931
CAO	9.2899	10.4409	11.2989	11.3713	11.5564	9.8170	9.9204	10.1929
NA2O	.0365	.1258	.0601	.0925	.0441	.0449	.0107	.0517
K2O	.0920	.4464	.0327	.2732	.0148	.0654	0.0000	.0124
ZNO	.1046	.2720	.6495	.1902	.2241	.0278	.1076	.1278
TOTAL	97.9569	98.4722	95.9403	96.0044	96.4210	96.4366	94.1684	94.3868
SI	7.9502	7.6190	7.8536	7.7153	7.8540	8.0084	7.8144	7.8384
TI	.0014	.0388	.0053	.0182	.0043	.0004	0.0000	.0040
AL	.0574	.5691	.1769	.4238	.1648	.0520	.0644	.0660
FE	2.1812	2.2159	2.3883	2.3115	2.4246	3.1352	3.7525	3.5578
MN	.5543	.2129	.1388	.1327	.1456	.7557	.5411	.5026
MG	2.7726	2.6643	2.5646	2.5471	2.5608	1.3433	1.2208	1.3551
CA	1.4772	1.6478	1.8400	1.8446	1.8723	1.6536	1.7454	1.7756
NA	.0107	.0365	.0180	.0276	.0131	.0139	.0035	.0166
K	.0174	.0839	.0063	.0528	.0029	.0131	0.0000	.0026
ZN	.0115	.0296	.0730	.0213	.0250	.0032	.0131	.0154
Oxygen	23.0000	23.0000	23.0000	23.0000	23.0000	23.0000	23.0000	23.0000
No. atoms	38.0338	38.1176	38.0648	38.0949	38.0673	37.9788	38.1552	38.1341

SELECTED ANALYSES FROM :JAN83 : 80-81, 84, 87, 95-97

TIRODITE (AU)
****

	4526/90.6. AMPH 1.	4526/90.6. AMPH 2.	4526/90.6. P INT(1).	4526/90.6. P INT(4).	4526/90.6. DARK 2.	4526/90.6. DKMATRIX 1.	4526/90.6. DKMATRIX 2.
SIO2	53.5422	52.9589	51.3411	50.7837	53.7800	53.1299	54.1229
TIO2	.0155	.0044	0.0000	.0011	.0220	0.0000	0.0000
AL2O3	.2818	.1779	.3245	.1298	.1062	.1139	.0980
FEO	17.9319	18.2347	17.5250	15.6142	17.7680	16.6898	17.2004
MNO	8.8151	10.0266	11.6129	10.4546	11.0619	10.7372	11.0366
MGO	12.6592	13.2104	12.9704	12.4719	13.3378	13.0329	13.4379
CAO	4.5070	2.5802	1.9179	5.4725	2.0208	4.2847	2.1379
NA2O	.0801	.0550	.0998	.0534	.0547	.0460	.0368
K2O	.0568	.0283	.0100	.0226	.0036	.0129	.0126
ZNO	.2074	.2004	.2694	.1430	.2160	.1294	.0708
TOTAL	98.0970	97.4768	96.0710	95.1468	98.3710	98.1767	98.1539
SI	7.9948	7.9791	7.9019	7.8742	8.0180	7.9516	8.0536
TI	.0017	.0005	0.0000	.0001	.0025	0.0000	0.0000
AL	.0496	.0316	.0589	.0237	.0187	.0201	.0172
FE	2.2393	2.2977	2.2558	2.0248	2.2154	2.0890	2.1405
MN	1.1149	1.2796	1.5140	1.3731	1.3970	1.3612	1.3911
MG	2.8171	2.9663	2.9751	2.8820	2.9636	2.9070	2.9801
CA	.7211	.4165	.3163	.9092	.3228	.6871	.3409
NA	.0236	.0163	.0303	.0163	.0161	.0136	.0108
K	.0108	.0054	.0020	.0045	.0007	.0025	.0024
ZN	.0229	.0223	.0306	.0164	.0238	.0143	.0078
Oxygen	23.0000	23.0000	23.0000	23.0000	23.0000	23.0000	23.0000
No. atoms	37.9959	38.0155	38.0848	38.1243	37.9784	38.0463	37.9444

SELECTED ANALYSES FROM :JAN83 : 64-66, 132-133, 137, 139, 172-173, 17

RHODONITE (AU)
****

	2/9A. P2(A).	2/9A. P1(B).	2/9A. P3.	4478/68.1. P ?1.	4478/68.1. P ? 2.
SIO2	45.2469	45.5706	47.3195	46.2650	45.3998
TIO2	0.0000	.0188	.0055	0.0000	.0201
AL2O3	.0031	.0157	0.0000	.0114	.0118
FEO	17.9518	17.9518	17.8025	16.4226	16.4569
MNO	27.2267	26.5880	27.6047	27.7733	27.8989
MGO	.7724	.7852	.7699	.5153	.5627
CAO	5.3792	5.9759	6.1043	7.5195	7.5121
NA2O	.0026	.0050	.0095	0.0000	.0265
K2O	.0008	.0059	0.0000	.0152	.0230
ZNO	.1821	.2361	.1512	.1770	.3226
TOTAL	96.7656	97.1530	99.7671	98.6993	98.2344
SI	1.0008	1.0016	1.0087	1.0001	.9912
TI	0.0000	.0003	.0001	0.0000	.0003
AL	.0001	.0004	0.0000	.0003	.0003
FE	.3321	.3300	.3174	.2969	.3005
MN	.5101	.4950	.4985	.5086	.5159
MG	.0255	.0257	.0245	.0166	.0183
CA	.1275	.1407	.1394	.1742	.1757
NA	.0001	.0002	.0004	0.0000	.0011
K	.0000	.0002	0.0000	.0004	.0006
ZN	.0030	.0038	.0024	.0028	.0052
Oxygen	3.0000	3.0000	3.0000	3.0000	3.0000
No. atoms	4.9992	4.9980	4.9914	4.9999	5.0092

SELECTED ANALYSES FROM :SEP82 : 33

ACTINOLITE (AU)
****

	2/9BA. K1.
SIO2	52.4173
TIO2	.0063
AL2O3	.3493
FEO	23.4745
MNO	5.2669
MGO	6.4662
CAO	10.8098
NA2O	.0418
K2O	.0780
ZNO	.0668
TOTAL	98.9769
SI	7.9886
TI	.0007
AL	.0628
FE	2.9920
MN	.6799
MG	1.4687
CA	1.7653
NA	.0126
K	.0152
ZN	.0075
Oxygen	23.0000
No. atoms	37.9930

RHODONITES (AU)

	4478/68.1. P 7 3.	4478/68.1. P 7 4.	4478/62.8. Pb 1.	4478/62.8. Pb 2.	4483/116.1. P1.
SIO2	45.6893	47.2935	46.5254	46.6346	49.4976
TIO2	.0371	0.0000	0.0000	.0249	0.0000
AL2O3	.0029	.0142	.0022	.0154	.0048
FEO	16.5107	16.3634	16.2566	16.4612	17.1914
MNO	28.0632	27.7888	27.5235	27.3470	30.2349
MGO	.5118	.5388	.7162	.7644	.5842
CAO	7.1591	7.7386	7.5416	7.5370	5.7590
NA2O	.0107	.0079	.0307	.0112	.0194
K2O	0.0000	.0010	.0058	0.0000	.0260
ZNO	.1639	.2592	.2391	.1430	.1161
TOTAL	98.1487	100.0054	98.8411	98.9387	103.4334
SI	.9962	1.0053	1.0018	1.0022	1.0160
TI	.0006	0.0000	0.0000	.0004	0.0000
AL	.0001	.0004	.0001	.0004	.0001
FE	.3011	.2909	.2928	.2959	.2951
MN	.5183	.5004	.5020	.4978	.5257
MG	.0166	.0171	.0230	.0245	.0179
CA	.1673	.1763	.1740	.1736	.1267
NA	.0005	.0003	.0013	.0005	.0008
K	0.0000	.0000	.0002	0.0000	.0007
ZN	.0026	.0041	.0038	.0023	.0018
Oxygen	3.0000	3.0000	3.0000	3.0000	3.0000
No. atoms	5.0034	4.9947	4.9989	4.9974	4.9847

RHODONITE (AU)
****

	2/5A-1. PXM2.
SIO2	46.5300
TIO2	0.0000
AL2O3	.2100
FEO	18.0700
MNO	30.4200
MGO	0.0000
CAO	4.7800
K2O	0.0000
NA2O	0.0000
CL	0.0000
	100.0100
O=F,CL	0.0000
TOTAL	100.0100
SI	1.0011
TI	0.0000
AL	.0053
FE	.3252
MN	.5544
MG	0.0000
CA	.1102
K	0.0000
NA	0.0000
CL	0.0000
O,OH,CL,F	3.0000
No. atoms	4.9962

SELECTED ANALYSES FROM :JAN83 : 78-79, 88-89, 98-99, 146-149, 151, 180-181, 186, 201-202

PYROXMANGITE (AU)
****

	4526/90.6. P1.	4526/90.6. P1(2).	4526/90.6. P INT(5).	4526/90.6. P INT(6).	4526/90.6. BRITE A 1.	4526/90.6. BRITE A 2.	2/9B. P1(PRIM)2.
SIO2	47.9037	47.7686	44.5233	44.1271	48.6032	48.6983	46.5767
TIO2	0.0000	.0089	0.0000	.0195	0.0000	0.0000	.0261
AL2O3	0.0000	.0219	.0036	.0200	.0278	.0086	.0056
FEO	17.2238	17.8564	14.6516	14.8152	14.9009	15.0380	21.7786
MNO	27.0903	27.2098	29.1463	29.1000	30.7981	30.5211	26.4441
MGO	3.2347	3.4889	3.5007	3.4690	3.0377	3.0865	1.2606
CAO	4.0524	3.5973	3.8367	3.7689	3.8975	4.0979	3.1708
NA2O	.0085	.0224	.0239	0.0000	0.0000	.0092	.0287
K2O	.0053	0.0000	.0073	.0076	0.0000	0.0000	0.0000
ZNO	.3204	.1954	.1958	.1924	.2100	.1434	.1625
TOTAL	99.8391	100.1696	95.8892	95.5197	101.4752	101.6030	99.4537
SI	1.0080	1.0036	.9858	.9827	1.0079	1.0079	1.0035
TI	0.0000	.0001	0.0000	.0003	0.0000	0.0000	.0004
AL	0.0000	.0005	.0001	.0005	.0007	.0002	.0001
FE	.3031	.3138	.2713	.2759	.2584	.2603	.3924
MN	.4829	.4842	.5466	.5489	.5410	.5351	.4826
MG	.1014	.1092	.1155	.1151	.0939	.0952	.0405
CA	.0914	.0810	.0910	.0899	.0866	.0909	.0732
NA	.0004	.0009	.0010	0.0000	0.0000	.0004	.0012
K	.0001	0.0000	.0002	.0002	0.0000	0.0000	0.0000
ZN	.0050	.0030	.0032	.0032	.0032	.0022	.0026
Oxygen	3.0000	3.0000	3.0000	3.0000	3.0000	3.0000	3.0000
No. atoms	4.9922	4.9965	5.0148	5.0168	4.9918	4.9922	4.9966

PYROXMANGITE (AU)

	2/9B. P2A.	2/9B. P2B.	2/9B. P2C.	2/9B. MNPYROS?2.	2/13d. P1.	2/13d. P2.	Sturtite. P 1.
SIO2	47.0623	46.5978	47.7582	47.9134	48.4870	48.3842	47.7142
TIO2	0.0000	0.0000	0.0000	0.0000	0.0000	.0087	0.0000
AL2O3	.0008	0.0000	.0063	.0677	.0091	.0178	.2986
FEO	22.0544	21.5457	20.4061	24.2101	20.5455	20.4836	22.7769
MNO	26.9676	25.9070	27.9736	16.9664	24.7025	24.8012	24.9780
MGO	1.2911	1.2526	1.1102	1.4379	1.8881	1.8476	1.3225
CAO	2.9467	3.0237	3.2395	.5896	5.1054	5.2156	3.1941
NA2O	.0298	.0323	.0376	.0657	.0196	0.0000	.0083
K2O	.0027	.0081	.0164	.0683	0.0000	0.0000	.1362
ZNO	.2570	.2010	.0540	.1845	.2475	.2883	.1663
TOTAL	100.6124	98.5682	100.6019	91.5036	101.0047	101.0470	100.5951
SI	1.0033	1.0097	1.0125	1.0760	1.0131	1.0115	1.0097
TI	0.0000	0.0000	0.0000	0.0000	0.0000	.0001	0.0000
AL	.0000	0.0000	.0002	.0018	.0002	.0004	.0074
FE	.3932	.3904	.3618	.4547	.3590	.3581	.4031
MN	.4870	.4755	.5024	.3227	.4372	.4392	.4477
MG	.0410	.0404	.0351	.0481	.0588	.0576	.0417
CA	.0673	.0702	.0736	.0142	.1143	.1168	.0724
NA	.0013	.0014	.0016	.0029	.0008	0.0000	.0003
K	.0001	.0002	.0004	.0020	0.0000	0.0000	.0037
ZN	.0040	.0032	.0008	.0031	.0038	.0045	.0026
Oxygen	3.0000	3.0000	3.0000	3.0000	3.0000	3.0000	3.0000
No. atoms	4.9973	4.9911	4.9884	4.9255	4.9872	4.9882	4.9886

	4526/89.2. P/R?1.	4526/89.2. P/R?2.
SIO2	49.8494	49.5233
TIO2	0.0000	0.0000
AL2O3	.0261	.0198
FEO	18.2466	17.8806
MNO	26.8728	27.0886
MGO	2.5295	2.4189
CAO	4.7235	4.6207
NA2O	.0063	.0026
K2O	.0048	0.0000
ZNO	.1583	.2724
TOTAL	102.4173	101.8269
SI	1.0192	1.0194
TI	0.0000	0.0000
AL	.0006	.0005
FE	.3120	.3078
MN	.4654	.4723
MG	.0771	.0742
CA	.1035	.1019
NA	.0003	.0001
K	.0001	0.0000
ZN	.0024	.0041
Oxygen	3.0000	3.0000
No. atoms	4.9806	4.9804

SELECTED ANALYSES FROM :SEP82 : 32, 38

PYROXMANGITE (AU)
****

	2/9BA. PXM 1.	2/9BA. PXM 2.
SIO2	47.4453	46.8969
TIO2	0.0000	.0062
AL2O3	.0166	.0056
FEO	21.3954	21.2515
MNO	27.2372	27.1671
MGO	1.1265	1.2670
CAO	3.3941	3.2321
NA2O	.0054	.0245
K2O	.0260	0.0000
ZNO	.1660	.1623
TOTAL	100.8125	100.0132
SI	1.0070	1.0043
TI	0.0000	.0001
AL	.0004	.0001
FE	.3798	.3806
MN	.4897	.4928
MG	.0356	.0404
CA	.0772	.0742
NA	.0002	.0010
K	.0007	0.0000
ZN	.0026	.0026
Oxygen	3.0000	3.0000
No. atoms	4.9933	4.9961

SELECTED ANALYSES FROM :JAN82 : 7, 10-12, 22-25, 28, 31

PYROXMANGITE (ANU)
****

	2/1B. PXM1.	2/1B. PXM2.	2/1B. PXM3.	2/1B. PXM4.	2/5A. PXM1.
SIO2	46.0100	46.3900	46.1100	46.3700	45.6600
TIO2	.1400	.2000	.2000	.1400	0.0000
AL2O3	.1800	.1100	0.0000	0.0000	.1200
FEO	19.9300	20.2300	19.0200	19.6500	21.2000
MNO	27.9900	28.5300	28.6900	28.1500	28.4100
MGO	2.1200	2.1600	2.0500	2.0600	1.3600
CAO	3.4100	3.3700	3.8100	3.3500	2.6000
K2O	0.0000	0.0000	0.0000	0.0000	0.0000
NA2O	.2500	.3700	.2200	.3000	.3500
CL	0.0000	0.0000	0.0000	0.0000	0.0000
	100.0300	101.3600	100.1000	100.0200	99.7000
O=F,CL	0.0000	0.0000	0.0000	0.0000	0.0000
TOTAL	100.0300	101.3600	100.1000	100.0200	99.7000
SI	.9860	.9831	.9875	.9923	.9891
TI	.0023	.0032	.0032	.0023	0.0000
AL	.0045	.0027	0.0000	0.0000	.0031
FE	.3572	.3586	.3407	.3517	.3841
MN	.5081	.5122	.5204	.5103	.5213
MG	.0677	.0682	.0654	.0657	.0439
CA	.0783	.0765	.0874	.0768	.0604
K	0.0000	0.0000	0.0000	0.0000	0.0000
NA	.0106	.0155	.0093	.0127	.0149
CL	0.0000	0.0000	0.0000	0.0000	0.0000
O,OH,CL,F	3.0000	3.0000	3.0000	3.0000	3.0000
No. atoms	5.0147	5.0200	5.0140	5.0117	5.0168

	2/5A. PXM2.	2/5A. PXM3.	2/5A. PXM4.	2/5A-I. PXM1.	2/5A-I. PXM3.
SIO2	45.9200	45.7000	45.5500	46.1300	46.3000
TIO2	0.0000	0.0000	0.0000	0.0000	0.0000
AL2O3	0.0000	0.0000	.2000	0.0000	.1100
FEO	20.1500	20.2300	20.6200	21.3300	20.4700
MNO	29.6800	29.1800	29.0500	29.1400	28.9600
MGO	1.2900	1.3500	1.3600	1.4500	1.3000
CAO	2.8400	2.8000	2.7500	2.6500	2.8700
K2O	0.0000	0.0000	0.0000	0.0000	0.0000
NA2O	.2000	.3600	.3100	0.0000	0.0000
CL	0.0000	0.0000	0.0000	0.0000	0.0000
	100.0800	99.6200	99.8400	100.7000	100.0100
O=F,CL	0.0000	0.0000	0.0000	0.0000	0.0000
TOTAL	100.0800	99.6200	99.8400	100.7000	100.0100
SI	.9911	.9906	.9860	.9900	.9960
TI	0.0000	0.0000	0.0000	0.0000	0.0000
AL	0.0000	0.0000	.0051	0.0000	.0028
FE	.3637	.3667	.3733	.3829	.3683
MN	.5426	.5358	.5327	.5297	.5277
MG	.0415	.0436	.0439	.0464	.0417
CA	.0657	.0650	.0638	.0609	.0662
K	0.0000	0.0000	0.0000	0.0000	0.0000
NA	.0085	.0154	.0132	0.0000	0.0000
CL	0.0000	0.0000	0.0000	0.0000	0.0000
O,OH,CL,F	3.0000	3.0000	3.0000	3.0000	3.0000
No. atoms	5.0131	5.0171	5.0180	5.0100	5.0026

SELECTED ANALYSES FROM :JAN83 : 94, 134, 138, 140, 170-171, 205-209

HEDENBERGITE (AU)
****

	4526/90.6. DARK 1.	4478/68.1. HED ? 1.	4478/68.1. HED 2.	4478/68.1. H3.	4478/62.8. Hed 1.	4478/62.8. Hed 2.
SIO2	52.3226	49.1032	47.2935	46.8996	48.7712	48.6145
TIO2	.0194	.0244	0.0000	0.0000	.0090	.0230
AL2O3	.1739	.1108	.1136	.0661	.0899	.1696
FEO	12.2383	18.5682	18.8675	19.4766	18.3321	17.5578
MNO	8.8494	8.6804	8.7151	9.0490	8.7145	8.9159
MGO	9.7934	2.4767	2.2476	1.8668	2.8725	3.2750
CAO	15.7314	19.5319	19.8099	19.9954	20.4583	20.0684
NA2O	.0223	.0220	.0366	.0212	.0376	.0186
K2O	0.0000	.0021	0.0000	0.0000	0.0000	0.0000
ZNO	0.0000	.0762	.0636	.1349	.1710	.3026
TOTAL	99.1507	98.5959	97.1474	97.5096	99.4561	98.9454
SI	2.0361	2.0177	1.9898	1.9789	1.9935	1.9920
TI	.0006	.0008	0.0000	0.0000	.0003	.0007
AL	.0080	.0054	.0056	.0033	.0043	.0082
FE	.3983	.6381	.6639	.6873	.6267	.6017
MN	.2917	.3021	.3106	.3234	.3017	.3095
MG	.5680	.1517	.1409	.1174	.1750	.2000
CA	.6559	.8600	.8931	.9040	.8960	.8811
NA	.0017	.0018	.0030	.0018	.0030	.0015
K	0.0000	.0001	0.0000	0.0000	0.0000	0.0000
ZN	0.0000	.0023	.0020	.0042	.0052	.0092
Oxygen	6.0000	6.0000	6.0000	6.0000	6.0000	6.0000
No. atoms	9.9602	9.9799	10.0090	10.0202	10.0056	10.0039

	4526/89.2. Hed 1.	4526/89.2. H 2.	4526/89.2. H 3.	4526/89.2. H 4.	4526/89.2. H 5.
SIO2	54.5386	51.1835	52.0753	51.3192	51.3301
TIO2	0.0000	0.0000	0.0000	0.0000	.0322
AL2O3	.1776	.0447	.1209	.0463	.1839
FEO	16.6904	18.4906	15.1460	14.2346	15.4085
MNO	8.1320	9.2193	6.6290	7.4644	8.3000
MGO	8.3680	7.9197	7.6504	6.7705	6.8419
CAO	15.6484	11.1780	18.1219	20.3172	17.4620
NA2O	.0321	.0545	.0840	.0711	0.0000
K2O	.0380	.0003	.0376	0.0000	.0019
ZNO	.0338	.1427	0.0000	.1553	.0300
TOTAL	103.6589	98.2333	99.8651	100.3786	99.5905
SI	2.0509	2.0520	2.0346	2.0126	2.0278
TI	0.0000	0.0000	0.0000	0.0000	.0010
AL	.0079	.0021	.0056	.0021	.0086
FE	.5249	.6200	.4949	.4669	.5091
MN	.2590	.3131	.2194	.2480	.2777
MG	.4690	.4732	.4455	.3957	.4028
CA	.6305	.4802	.7586	.8538	.7392
NA	.0024	.0043	.0065	.0055	0.0000
K	.0018	.0000	.0019	0.0000	.0001
ZN	.0009	.0042	0.0000	.0045	.0009
Oxygen	6.0000	6.0000	6.0000	6.0000	6.0000
No. atoms	9.9473	9.9491	9.9668	9.9891	9.9670

SELECTED ANALYSES FROM :JAN83 : 85-86, 93, 100-102

KANOITE (AU)
****

	4526/90.6. P INT(2).	4526/90.6. P INT(3).	4526/90.6. BRIGHT 2.GY	4526/90.6. EXSLN 1.GY	4526/90.6. EXSLN 2.GY	4526/90.6. EXSLN 3.
SIO2	48.3558	47.6038	50.7323	50.7245	50.3369	49.8629
TIO2	.0189	.0163	0.0000	.0205	0.0000	0.0000
AL2O3	.0916	.0850	.0807	.0880	.1025	.1170
FEO	17.4441	16.9876	17.3954	18.5433	18.8297	17.5292
MNO	20.1532	19.2389	20.3722	19.3913	18.6970	19.8394
MGO	9.9446	10.2838	9.3757	9.9400	10.2340	10.2328
CAO	2.5831	2.6327	2.6616	2.2711	2.2186	3.2816
NA2O	.0408	.0339	.0437	.0268	.0417	.0306
K2O	.0134	.0082	.0159	.0105	0.0000	0.0000
ZNO	.2776	.1462	.1994	.3559	.4031	.2385
TOTAL	98.9231	97.0364	100.8769	101.3719	100.8635	101.1320
SI	1.9817	1.9810	2.0234	2.0140	2.0080	1.9896
TI	.0006	.0005	0.0000	.0006	0.0000	0.0000
AL	.0044	.0042	.0038	.0041	.0048	.0055
FE	.5979	.5912	.5802	.6158	.6282	.5850
MN	.6996	.6782	.6882	.6522	.6318	.6705
MG	.6074	.6378	.5573	.5882	.6084	.6085
CA	.1134	.1174	.1137	.0966	.0948	.1403
NA	.0033	.0028	.0034	.0021	.0033	.0024
K	.0007	.0004	.0008	.0005	0.0000	0.0000
ZN	.0084	.0045	.0059	.0104	.0119	.0070
Oxygen	6.0000	6.0000	6.0000	6.0000	6.0000	6.0000
No. atoms	10.0174	10.0181	9.9768	9.9846	9.9912	10.0089

SELECTED ANALYSES FROM :SEP82 : 10-12, 18

STAUROLITE (AU)
****

	4496/29.6. STT 1 CORE.	4496/29.6. STT RIM 1.	4496/29.6. STT RIM 2.	4496/29.6. STT COR 1.
SIO2	27.2693	27.0031	27.0498	27.8439
TIO2	.1777	.4917	.2007	.5177
AL2O3	51.6105	51.4754	50.5348	52.8197
FEO	10.5636	10.0956	10.6611	11.5894
MNO	.1452	.1466	.1207	.1453
MGO	1.4018	1.2831	1.3269	1.4107
CAO	0.0000	0.0000	0.0000	0.0000
NA2O	.0979	.0823	.0701	.0875
K2O	0.0000	.0189	0.0000	0.0000
ZNO	3.5808	3.4102	3.6204	3.6654
TOTAL	94.8468	94.0069	93.5845	98.0796
SI	7.8466	7.8187	7.8999	7.7821
TI	.0385	.1071	.0441	.1088
AL	17.5080	17.5715	17.3994	17.4040
FE	2.5421	2.4447	2.6040	2.7090
MN	.0354	.0360	.0299	.0344
MG	.6011	.5537	.5775	.5876
CA	0.0000	0.0000	0.0000	0.0000
NA	.0555	.0470	.0403	.0482
K	0.0000	.0070	0.0000	0.0000
ZN	.7615	.7297	.7814	.7571
Oxygen	46.0000	46.0000	46.0000	46.0000
No. atoms	75.3888	75.3155	75.3765	75.4313

SELECTED ANALYSES FROM :JAN83 : 27, 30, 222-223, 210

STAUROLITE (AU)
****

	4502/29.9. STT 1.	4502/29.9. STT 2.	4496/26.9. Staur 1.	4496/26.9. Staur 2.	4496/32.. Staurolite.
SIO2	24.5022	27.4175	28.5552	28.4720	29.6031
TIO2	.5070	.4668	.1049	.1516	.3879
AL2O3	46.9727	51.6854	51.9024	51.2780	53.3757
FEO	11.8344	11.8342	11.9947	11.9430	11.6472
MNO	.1154	.1022	.0977	.1506	.1500
MGO	1.2127	1.2934	1.4066	1.3282	1.5822
CAO	0.0000	0.0000	0.0000	0.0000	0.0000
NA2O	.0982	.0940	.1266	.1180	.1115
K2O	.0143	0.0000	.0045	0.0000	0.0000
ZNO	3.0652	3.2315	4.2672	4.0210	2.5219
TOTAL	88.3221	96.1250	98.4598	97.4624	99.3795
SI	7.6670	7.8176	7.9829	8.0333	8.0874
TI	.1193	.1001	.0221	.0322	.0797
AL	17.3282	17.3740	17.1061	17.0567	17.1911
FE	3.0970	2.8220	2.8044	2.8182	2.6611
MN	.0306	.0247	.0231	.0360	.0347
MG	.5655	.5496	.5860	.5585	.6442
CA	0.0000	0.0000	0.0000	0.0000	0.0000
NA	.0606	.0528	.0698	.0656	.0600
K	.0057	0.0000	.0016	0.0000	0.0000
ZN	.7088	.6809	.8816	.8384	.5092
Oxygen	46.0000	46.0000	46.0000	46.0000	46.0000
No. atoms	75.5827	75.4217	75.4777	75.4390	75.2673

SELECTED ANALYSES FROM :JAN83 : 20, 21, 23, 154, 198, 213-214, 216

CHLORITES (AU)
****

	4502/91.6. UNK3.	4502/91.6. YELL CHL.	4502/91.6. CHL spot1.	4483/149.1. CHL?.	4496/98.4. CHL 1.	4496/32.. Chl.	4496/85.7. Chl.	4496/85.7. Chl.
SIO2	25.2080	24.8648	21.9214	20.7613	25.4498	23.8958	25.9184	24.9618
TIO2	.0143	.0395	0.0000	.0112	.0622	.0199	.0747	.0523
AL2O3	20.7537	24.2633	22.5508	22.0478	21.4939	20.2024	20.9598	19.1001
FEO	35.1549	37.7737	40.6648	41.1754	23.0228	22.1197	31.9802	33.1143
MNO	.9660	.1111	.1295	1.1349	.2506	.0907	1.1460	1.4253
MGO	4.2342	7.7270	2.7947	.5266	14.0196	13.9512	8.4692	5.4584
CAO	0.0000	.0623	0.0000	0.0000	0.0000	0.0000	0.0000	.0556
NA2O	.0168	.0548	.0020	0.0000	0.0000	0.0000	.0499	.0435
K2O	.8775	.0090	0.0000	.0286	0.0000	.0132	0.0000	.0711
ZNO	.1123	.2947	.1831	.2376	.4082	.0819	.5526	.1923
TOTAL	87.3377	95.2002	88.2463	85.9234	84.7071	80.3748	89.1508	84.4747
SI	5.6772	5.1102	5.0253	4.9726	5.4957	5.4404	5.5906	5.7713
TI	.0024	.0061	0.0000	.0020	.0101	.0034	.0121	.0091
AL	5.5103	5.8788	6.0945	6.2256	5.4719	5.4225	5.3300	5.2062
FE	6.6215	6.4925	7.7962	8.2478	4.1578	4.2118	5.7691	6.4030
MN	.1843	.0193	.0251	.2302	.0458	.0175	.2094	.2791
MG	1.4212	2.3667	.9548	.1880	4.5118	4.7337	2.7225	1.8808
CA	0.0000	.0137	0.0000	0.0000	0.0000	0.0000	0.0000	.0138
NA	.0075	.0222	.0009	0.0000	0.0000	0.0000	.0212	.0198
K	.2521	.0024	0.0000	.0087	0.0000	.0038	0.0000	.0210
ZN	.0187	.0448	.0310	.0421	.0651	.0138	.0881	.0329
Oxygen	28.0000	28.0000	28.0000	28.0000	28.0000	28.0000	28.0000	28.0000
No. atoms	47.6952	47.9566	47.9279	47.9170	47.7583	47.8469	47.7430	47.6369

SELECTED ANALYSES FROM :JAN82 : 73-75, 139, 149-150, 205

CHLORITES (ANU)
****

	4496/67.3. CHL2.	4496/67.3. CHL 3.	4496/67.3. CHL 1A.	4502/37.3. CHL.	4502/42.1. CHL 1.	4502/42.1. CHL2.	4502/42.1. CHL 3.
SIO2	20.8900	21.1700	22.7500	24.5600	24.5800	25.1500	23.9900
TIO2	.2800	0.0000	.1300	.2300	.3500	.1200	.2000
AL2O3	16.5100	16.6000	18.7100	19.4600	20.1400	18.1400	20.6100
FEO	26.1500	27.2600	28.5500	37.9600	33.9200	40.9500	34.0500
MNO	.6100	.7600	.6600	.4800	.4000	.5900	.4100
MGO	9.5300	9.1400	11.0700	4.8400	7.4200	4.1500	7.2000
CAO	.1200	.1000	.0700	0.0000	0.0000	.1800	0.0000
K2O	.0700	0.0000	0.0000	.0900	.1900	0.0000	0.0000
NA2O	.4000	.4900	.3600	.1300	.3200	.2900	.1800
CL	.1600	.1800	.0800	0.0000	0.0000	.0600	0.0000
	74.0462	74.9420	82.0431	87.7500	87.3200	89.3773	86.6400
O=F,CL	.0674	.0758	.0337	0.0000	0.0000	.0253	0.0000
TOTAL	74.0462	74.9420	82.0431	87.7500	87.3200	89.3773	86.6400
SI	5.3950	5.4284	5.3049	5.5714	5.4838	5.6827	5.3971
TI	.0544	0.0000	.0228	.0392	.0587	.0204	.0338
AL	5.0268	5.0182	5.1435	5.2043	5.2972	4.8322	5.4663
FE	5.6481	5.8459	5.5677	7.2017	6.3290	7.7384	6.4065
MN	.1334	.1651	.1304	.0922	.0756	.1129	.0781
MG	3.6680	3.4928	3.8470	1.6363	2.4671	1.3975	2.4140
CA	.0332	.0275	.0175	0.0000	0.0000	.0436	0.0000
K	.0231	0.0000	0.0000	.0260	.0541	0.0000	0.0000
NA	.2036	.2476	.1654	.0581	.1407	.1291	.0798
CL	.0000	.0000	.0000	0.0000	0.0000	.0000	0.0000
O,OH,CL,F	28.0000	28.0000	28.0000	28.0000	28.0000	28.0000	28.0000
No. atoms	48.1856	48.2254	48.1991	47.8294	47.9063	47.9568	47.8758

SELECTED ANALYSES FROM :JAN83 : 127-129, 145, 152

PYROSMALITE (AU)
****

	2/9B. PYROS 1.	2/9B. PYROS 2.	2/9B. PYROS 3.	2/9B. Pl(PRIM)PS.	2/9A. PYROS-CL.
SIO2	34.2335	34.9515	34.1265	34.7858	33.6036
TIO2	0.0000	0.0000	0.0000	.0056	0.0000
AL2O3	.0175	.0223	.0149	.0093	.0162
FEO	29.0049	28.5247	28.7450	26.9088	28.0356
MNO	22.2800	22.6585	22.9390	24.6293	23.8507
MGO	.4721	.5155	.4472	.4092	.4594
CAO	.0977	.0895	.0477	.1139	.0752
NA2O	.0212	.0359	.0751	.0121	.0368
K2O	.0169	.0076	.0105	0.0000	0.0000
ZNO	0.0000	0.0000	0.0000	.0342	0.0000
TOTAL	86.1438	86.8055	86.4059	86.9082	86.0775
SI	6.0877	6.1375	6.0643	6.1171	6.0175
TI	0.0000	0.0000	0.0000	.0007	0.0000
AL	.0037	.0046	.0031	.0019	.0034
FE	4.3137	4.1891	4.2720	3.9575	4.1987
MN	3.3560	3.3703	3.4528	3.6687	3.6178
MG	.1251	.1349	.1184	.1072	.1226
CA	.0186	.0168	.0091	.0215	.0144
NA	.0074	.0124	.0263	.0042	.0130
K	.0038	.0017	.0024	0.0000	0.0000
ZN	0.0000	0.0000	0.0000	.0044	0.0000
Oxygen	20.0000	20.0000	20.0000	20.0000	20.0000
No. atoms	33.9161	33.8673	33.9486	33.8832	33.9875

SELECTED ANALYSES FROM :SEP82 : 23,

CHLORITE (AU)
****

	4502/25.4. CHL 1.	4502/25.4. CHL2.
SIO2	23.9330	20.1177
TIO2	.1112	0.0000
AL2O3	20.6840	20.0489
FEO	33.8951	32.1169
MNO	.2491	.1780
MGO	5.3478	3.7087
CAO	0.0000	0.0000
NA2O	.0080	.0237
K2O	.1536	0.0000
ZNO	.0848	.8763
TOTAL	84.4666	77.0702
SI	5.5242	5.1727
TI	.0193	0.0000
AL	5.6285	6.0773
FE	6.5431	6.9063
MN	.0487	.0388
MG	1.8396	1.4211
CA	0.0000	0.0000
NA	.0036	.0120
K	.0452	0.0000
ZN	.0145	.1665
Oxygen	28.0000	28.0000
No. atoms	47.6666	47.7946

SELECTED ANALYSES FROM :JAN83 : 136, 150

MANGANPYROSMALITE (AU)
****

	4478/68.1. MN-PYROS.	2/9B. MNPYROS?.
SIO2	32.9609	31.1433
TIO2	.0047	0.0000
AL2O3	.0401	.0240
FEO	26.0845	19.1962
MNO	25.8192	27.9390
MGO	.1224	.3762
CAO	.1098	.1756
NA2O	0.0000	.0072
K2O	0.0000	0.0000
ZNO	.0256	0.0000
TOTAL	85.1672	78.8615
SI	5.9927	6.0587
TI	.0006	0.0000
AL	.0086	.0055
FE	3.9662	3.1232
MN	3.9763	4.6040
MG	.0332	.1091
CA	.0214	.0366
NA	0.0000	.0028
K	0.0000	0.0000
ZN	.0034	0.0000
Oxygen	20.0000	20.0000
No. atoms	34.0024	33.9398

SELECTED ANALYSES FROM :SEP82 : 28, 31, 34

PYROSMALITE (AU)
****

	2/9BA. K?1.	2/9BA. UNK 3.	2/9BA. 2/K2.
SIO2	35.3907	34.9783	35.0887
TIO2	0.0000	.0303	0.0000
AL2O3	0.0000	.0194	.0622
FEO	28.7605	29.1218	28.7380
MNO	23.0740	23.5382	23.2096
MGO	.4502	.4126	.4538
CAO	.1449	.0663	.1003
NA2O	.0361	0.0000	.0172
K2O	.0018	0.0000	0.0000
ZNO	.0793	.0840	.0431
TOTAL	87.9375	88.2509	87.7129
SI	6.1388	6.0791	6.1123
TI	0.0000	.0040	0.0000
AL	0.0000	.0040	.0128
FE	4.1722	4.2328	4.1867
MN	3.3902	3.4652	3.4246
MG	.1164	.1069	.1178
CA	.0269	.0123	.0187
NA	.0123	0.0000	.0059
K	.0004	0.0000	0.0000
ZN	.0102	.0108	.0055
Oxygen	20.0000	20.0000	20.0000
No. atoms	33.8676	33.9150	33.8843

SELECTED ANALYSES FROM :JAN83 : 3, 72, 45, 155

SERICITE (AU)
****

	4502/16.6. Mu/Ser.	1/2.4502/47.1C. SERICITE.	4483/149.1. SER.	SER.
SIO2	45.5379	52.1609	46.4457	46.4143
TIO2	.6015	.0625	0.0000	.0112
AL2O3	31.7494	38.2515	33.8315	27.3933
FEO	.8360	.9810	2.6466	7.0587
MNO	.0109	.0333	.0417	.2615
MGO	.8725	.7757	.6371	.7769
CAO	.0280	.0177	0.0000	0.0000
NA2O	.1705	.1036	.1891	.0199
K2O	11.3353	8.6093	11.4489	10.7301
ZNO	.0265	.1637	.1564	.2753
TOTAL	91.1685	101.1592	95.3970	92.9412
SI	6.3575	6.3824	6.2487	6.5608
TI	.0632	.0058	0.0000	.0012
AL	5.2256	5.5179	5.3661	4.5650
FE	.0976	.1004	.2978	.8345
MN	.0013	.0035	.0048	.0313
MG	.1815	.1415	.1277	.1637
CA	.0042	.0023	0.0000	0.0000
NA	.0469	.0250	.0501	.0055
K	2.0190	1.3440	1.9651	1.9350
ZN	.0027	.0148	.0156	.0288
Oxygen	22.0000	22.0000	22.0000	22.0000
No. atoms	35.9996	35.5373	36.0759	36.1257

SELECTED ANALYSES FROM :JAN82 : 123-124

SERICITE (ANU)
****

	4502/19.3. SER 1.	4502/19.3. SER 2.
SIO2	42.9800	45.8500
TIO2	.2500	.1800
AL2O3	33.6600	35.8500
FEO	.9400	.9500
MNO	0.0000	0.0000
MGO	.4700	.8300
CAO	.1400	0.0000
K2O	10.7900	9.7900
NA2O	.1100	.3700
CL	0.0000	.0500
	89.3400	93.6595
O=F,CL	0.0000	.0211
TOTAL	89.3400	93.6595
SI	6.1206	6.1519
TI	.0268	.0182
AL	5.6511	5.6708
FE	.1120	.1066
MN	0.0000	0.0000
MG	.0997	.1660
CA	.0214	0.0000
K	1.9603	1.6758
NA	.0309	.0978
CL	0.0000	.0000
O,OH,CL,F	22.0000	22.0000
No. atoms	36.0226	35.8871

SELECTED ANALYSES FROM :JAN83 : 22, 24

PARAGONITE, (AU)
****

	4502/91.6. PARAG 1.	4502/91.6. PARAG 2.
SIO2	46.5704	45.1989
TIO2	.0012	.0161
AL2O3	36.8154	36.5285
FEO	3.5986	1.2355
MNO	.2746	.0929
MGO	.2542	.0923
CAO	.1809	.1798
NA2O	6.7632	6.2487
K2O	.9082	1.8796
ZNO	.0813	.1123
TOTAL	95.4480	91.5846
SI	6.0493	6.0670
TI	.0001	.0016
AL	5.6379	5.7805
FE	.3909	.1387
MN	.0302	.0106
MG	.0492	.0185
CA	.0252	.0259
NA	1.7314	1.6530
K	.1505	.3219
ZN	.0078	.0111
Oxygen	22.0000	22.0000
No. atoms	36.0727	36.0286

SELECTED ANALYSES FROM :JAN83 : 176-177

STILPNOMELANE (AU)
****

	4483/116.1. Mn-Bi?.	4483/116.1. Bi 2 ?.
SIO2	46.0775	45.2867
TIO2	.0693	0.0000
AL2O3	4.7113	4.6021
FEO	30.9691	30.4896
MNO	9.7477	10.0140
MGO	1.1393	1.0930
CAO	0.0000	0.0000
NA2O	.0325	.0488
K2O	4.1196	4.1862
ZNO	.0669	.0154
TOTAL	96.9332	95.7358
SI	11.9204	11.8956
TI	.0135	0.0000
AL	1.4369	1.4251
FE	6.7005	6.6980
MN	2.1361	2.2281
MG	.4393	.4279
CA	0.0000	0.0000
NA	.0166	.0253
K	1.3597	1.4029
ZN	.0128	.0030
Oxygen	36.0000	36.0000
No. atoms	60.0357	60.1060

SELECTED ANALYSES FROM :JAN83 : 217

BERTHIERINE (AU)
****

	4496/85.7. Berth?.
SIO2	19.3294
TIO2	.0073
AL2O3	14.5851
FEO	34.3367
MNO	1.5545
MGO	3.5905
CAO	0.0000
NA2O	.0261
K2O	.0420
ZNO	.1249
TOTAL	73.5965
SI	2.7064
TI	.0008
AL	2.4075
FE	4.0207
MN	.1844
MG	.7492
CA	0.0000
NA	.0072
K	.0075
ZN	.0129
Oxygen	14.0000
No. atoms	24.0965

SELECTED ANALYSES FROM :JAN83 : 184-185, 187-188

'STURTITE'- HISINGERITE
****

	Sturtite. His 1.	Sturtite. HIS 2.	Sturtite. HIS 3.	Sturtite. HIS 4.
SIO2	27.7137	45.0424	43.6524	44.9521
TIO2	.0076	0.0000	0.0000	.0141
AL2O3	.1318	.0867	.0809	.1003
FEO	17.7986	24.7893	22.1536	24.8574
MNO	11.4449	21.6812	21.1920	21.2419
MGO	.5628	.2511	.2002	.2262
CAO	.2425	.7348	.3600	.3888
NA2O	1.0109	3.9034	13.2101	.3380
K2O	.0407	.0361	.3099	.1031
ZNO	.0438	0.0000	.0668	0.0000
TOTAL	58.9973	96.5250	101.2259	92.2219
SI	1.0089	1.0057	.9498	1.0371
TI	.0002	0.0000	0.0000	.0002
AL	.0057	.0023	.0021	.0027
FE	.5419	.4629	.4031	.4796
MN	.3529	.4100	.3906	.4151
MG	.0305	.0084	.0065	.0078
CA	.0095	.0176	.0084	.0096
NA	.0725	.1718	.5665	.0154
K	.0019	.0010	.0086	.0030
ZN	.0012	0.0000	.0011	0.0000
Oxygen	3.0000	3.0000	3.0000	3.0000
No. atoms	5.0252	5.0796	5.3367	4.9705

SELECTED ANALYSES FROM :JAN83 : 31

GREENALITE? (AU)
****

	4502/48.6. BN PUG.
SIO2	29.3517
TIO2	0.0000
AL2O3	8.9074
FEO	35.9028
MNO	.8951
MGO	3.9686
CAO	.5257
NA2O	.0217
K2O	.1008
ZNO	.0514
TOTAL	79.7252
SI	3.6742
TI	0.0000
AL	1.3145
FE	3.7586
MN	.0949
MG	.7404
CA	.0705
NA	.0054
K	.0161
ZN	.0048
Oxygen	14.0000
No. atoms	23.6792

SELECTED ANALYSES FROM :JAN83 : 32, 48, 49

"PUG" (AU)
****

	4502/48.6. WHITE PUG.	4502/48.6. BN PUG 2.	4502/48.6. CLEARPUG2.
SIO2	26.7766	28.0915	26.6304
TIO2	0.0000	0.0000	.0109
AL2O3	20.7263	16.1344	19.3879
FEO	29.7996	33.4389	31.0567
MNO	.4248	.7365	.5244
MGO	8.6957	6.8408	7.7205
CAO	.0025	.1634	.0838
NA2O	.0153	.0279	.0351
K2O	.0202	.0684	.0518
ZNO	0.0000	.1265	0.0000
TOTAL	86.4610	85.6283	85.5015
SI	2.9178	3.1757	2.9673
TI	0.0000	0.0000	.0009
AL	2.6626	2.1504	2.5469
FE	2.7157	3.1615	2.8941
MN	.0392	.0705	.0495
MG	1.4122	1.1525	1.2821
CA	.0003	.0198	.0100
NA	.0033	.0062	.0077
K	.0028	.0099	.0074
ZN	0.0000	.0106	0.0000
Oxygen	14.0000	14.0000	14.0000
No. atoms	23.7539	23.7572	23.7660

SELECTED ANALYSES FROM :JAN83 : 125-126

SPHENE (AU)
****

	2/9B. SPHENE 1.	2/9B. SPHENE 2.
SIO2	31.6320	31.5876
TIO2	32.8558	32.4145
AL2O3	2.4317	2.0507
FEO	2.4302	2.8351
MNO	.7269	1.0300
MGO	.3046	.2671
CAO	26.4980	25.9735
NA2O	.0564	.0040
K2O	.0437	.0008
ZNO	.1554	.0821
TOTAL	97.1347	96.2454
SI	1.0638	1.0737
TI	.8310	.8286
AL	.0964	.0822
FE	.0684	.0806
MN	.0207	.0297
MG	.0153	.0135
CA	.9548	.9460
NA	.0037	.0003
K	.0019	.0000
ZN	.0039	.0021
Oxygen	5.0000	5.0000
No. atoms	8.0598	8.0567

SELECTED ANALYSES FROM :JAN82 : 37, 145-146

ILMENITE (ANU)
****

	2/7A. ILM 1.	4502/37.3. ILM 1.	4502/37.3. ILM 2.
SIO2	0.0000	0.0000	0.0000
TIO2	52.4400	50.3600	44.9300
AL2O3	0.0000	0.0000	0.0000
FEO	44.9900	43.7200	39.0200
MNO	3.3100	4.4200	3.9100
MGO	0.0000	1.3200	1.1800
CAO	0.0000	0.0000	0.0000
K2O	0.0000	0.0000	0.0000
NA2O	0.0000	.1900	.1800
CL	0.0000	0.0000	0.0000
	100.7400	100.0100	89.2200
O=F,CL	0.0000	0.0000	0.0000
TOTAL	100.7400	100.0100	89.2200
SI	0.0000	0.0000	0.0000
TI	.9917	.9612	.9612
AL	0.0000	0.0000	0.0000
FE	.9461	.9279	.9283
MN	.0705	.0950	.0942
MG	0.0000	.0499	.0500
CA	0.0000	0.0000	0.0000
K	0.0000	0.0000	0.0000
NA	0.0000	.0095	.0101
CL	0.0000	0.0000	0.0000
O,OH,CL,F	3.0000	3.0000	3.0000
No. atoms	5.0083	5.0436	5.0438

SELECTED ANALYSES FROM :SEP82 : 13, 24, 39

ILMENITE (AU)
****

	4496/29.6. ILM 1.	4502/25.4. ILM 1.	4496/29.6. ILM 2.
SIO2	.0274	.0268	.0387
TIO2	51.9244	51.2718	52.7263
AL2O3	.0432	.0073	.0108
FEO	36.4796	38.7767	37.1466
MNO	.6212	2.0296	.6135
MGO	.2100	.0313	.2028
CAO	0.0000	0.0000	0.0000
NA2O	0.0000	.0023	0.0000
K2O	.0061	.0305	.0014
ZNO	.0540	0.0000	.0419
TOTAL	89.3659	92.1763	90.7820
SI	.0007	.0007	.0010
TI	1.0687	1.0384	1.0686
AL	.0014	.0002	.0003
FE	.8349	.8733	.8372
MN	.0144	.0463	.0140
MG	.0086	.0013	.0081
CA	0.0000	0.0000	0.0000
NA	0.0000	.0001	0.0000
K	.0002	.0010	.0000
ZN	.0011	0.0000	.0008
Oxygen	3.0000	3.0000	3.0000
No. atoms	4.9300	4.9614	4.9302

SELECTED ANALYSES FROM :JAN83 : 163, 37-38

CALCITE
****

	4483/143.6. MnCcl.	4502/48.6. CO3.	4502/48.6. CO3 (#1).
SIO2	.0191	.0542	.0155
TIO2	0.0000	0.0000	.0163
AL2O3	.0145	.0093	.0098
FEO	1.1065	1.4560	.5410
MNO	3.4170	9.0311	8.4969
MGO	.1578	.0658	.0088
CAO	48.9382	46.3622	23.6379
NA2O	0.0000	.0171	.0249
K2O	0.0000	0.0000	.0114
ZNO	0.0000	.0138	.0943
TOTAL	53.6531	57.0095	32.8568
SI	.0003	.0009	.0005
TI	0.0000	0.0000	.0004
AL	.0003	.0002	.0003
FE	.0164	.0207	.0136
MN	.0512	.1301	.2170
MG	.0042	.0017	.0004
CA	.9272	.8449	.7637
NA	0.0000	.0006	.0015
K	0.0000	0.0000	.0004
ZN	0.0000	.0002	.0021
Oxygen	1.0000	1.0000	1.0000
No. atoms	1.9995	1.9993	2.0000

SELECTED ANALYSES FROM :JAN83 : 11, 75

ILMENITE (AU)
****

	4502/75.9. ILM 1.	1/2. ILMENITE.
SIO2	.0130	.0321
TIO2	52.9409	52.0602
AL2O3	0.0000	0.0000
FEO	45.2022	44.2791
MNO	1.4236	1.6498
MGO	.1046	.2149
CAO	0.0000	0.0000
NA2O	0.0000	.0195
K2O	0.0000	0.0000
ZNO	.0419	.0259
TOTAL	99.7262	98.2815
SI	.0003	.0008
TI	1.0050	1.0026
AL	0.0000	0.0000
FE	.9542	.9483
MN	.0304	.0358
MG	.0039	.0082
CA	0.0000	0.0000
NA	0.0000	.0010
K	0.0000	0.0000
ZN	.0008	.0005
Oxygen	3.0000	3.0000
No. atoms	4.9947	4.9971

SELECTED ANALYSES FROM :JAN83 : 5, 6

ANORTHITE (AU)
****

	4502/16.6. PLAG 1.	4502/16.6. PLAG 2.
SIO2	42.9317	42.5554
TIO2	0.0000	.0212
AL2O3	32.7135	32.2777
FEO	.0634	.0353
MNO	.0443	.0007
MGO	.0046	0.0000
CAO	19.7715	19.8508
NA2O	.3199	.3158
K2O	.0219	.0062
ZNO	.0150	.0152
TOTAL	95.8858	95.0783
SI	2.0773	2.0778
TI	0.0000	.0008
AL	1.8661	1.8580
FE	.0026	.0014
MN	.0018	.0000
MG	.0003	0.0000
CA	1.0251	1.0385
NA	.0305	.0304
K	.0014	.0004
ZN	.0005	.0005
Oxygen	8.0000	8.0000
No. atoms	13.0055	13.0080

SELECTED ANALYSES FROM :J

ORTHOCLASE (AU)
****

	1/2. ORTHOCLASE.
SIO2	63.6080
TIO2	.0173
AL2O3	18.4817
FEO	.0341
MNO	0.0000
MGO	0.0000
CAO	.0378
NA2O	.6819
K2O	15.5612
ZNO	.0646
TOTAL	98.4866
SI	2.9821
TI	.0006
AL	1.0215
FE	.0013
MN	0.0000
MG	0.0000
CA	.0019
NA	.0630
K	.9308
ZN	.0022
Oxygen	8.0000
No. atoms	13.0034

SELECTED ANALYSES FROM :JAN82 : 125, 126, 129

ORTHOCLASE (ANU)
****

	4502/19.3. FSPR 1.	4502/19.3. FSPR 2.	4502/19.3. FSPR 3.
SIO2	61.8500	61.8600	63.0300
TIO2	0.0000	0.0000	0.0000
AL2O3	18.4000	18.4600	18.5700
FEO	0.0000	0.0000	0.0000
MNO	0.0000	0.0000	0.0000
MGO	0.0000	0.0000	0.0000
CAO	.1100	.1400	.1600
K2O	15.8800	15.8600	16.2300
NA2O	.2400	.2300	.3300
CL	0.0000	0.0000	0.0000
	96.4800	96.5500	98.3200
O=F,CL	0.0000	0.0000	0.0000
TOTAL	96.4800	96.5500	98.3200
SI	2.9678	2.9659	2.9705
TI	0.0000	0.0000	0.0000
AL	1.0409	1.0434	1.0318
FE	0.0000	0.0000	0.0000
MN	0.0000	0.0000	0.0000
MG	0.0000	0.0000	0.0000
CA	.0057	.0072	.0081
K	.9721	.9701	.9759
NA	.0227	.0217	.0307
CL	0.0000	0.0000	0.0000
O,OH,CL,F	8.0000	8.0000	8.0000
No. atoms	13.0091	13.0084	13.0169

PLAGIOCLASE (M.I.M.)

	4502/16.6 An 1	4502/16.6 An 2	4502/16.6 An 9	4502/16.6 An 4	4502/16.6 An 14
SiO_2	43.30	43.72	44.05	43.10	43.03
TiO_2	0.00	0.08	0.03	0.00	0.05
Al_2O_3	35.55	35.75	34.56	35.46	35.61
FeO	0.03	0.07	0.00	0.01	0.00
MgO	0.22	0.07	0.12	0.00	0.00
CaO	19.95	20.56	19.13	20.08	20.10
Na_2O	0.25	0.26	0.98	0.19	0.24
K_2O	0.00	0.04	0.20	0.00	0.00
TOTAL	99.30	100.55	99.07	98.84	99.03
Si	2.021	2.023	2.061	2.021	2.015
Ti	0.000	0.003	0.001	0.000	0.002
Al	1.955	1.946	1.906	1.960	1.965
Fe	0.001	0.003	0.000	0.001	0.000
Mg	0.015	0.005	0.009	0.000	0.000
Ca	0.998	1.004	0.959	1.009	1.008
Na	0.023	0.024	0.089	0.018	0.021
K	0.000	0.002	0.012	0.000	0.000
Oxygen	8	8	8	8	8

ORTHOCLASE (M.I.M.)

	4502/19.3 KF 1	4502/19.3 KF 2	4502/19.3 KF 3	4502/19.3 KF 4	4502/19.3 KF 5
SiO_2	63.73	63.55	63.82	64.07	62.69
Al_2O_3	19.66	19.67	19.64	19.60	19.30
FeO	.06	0.00	0.00	0.00	0.03
CaO	.02	0.00	0.03	0.16	0.00
Na_2O	0.46	0.48	0.46	0.41	0.45
K_2O	15.59	15.75	15.65	15.40	15.58
PbO	1.84	2.29	1.71	1.68	1.22
TOTAL	101.37	101.74	101.30	101.32	99.27
Si	2.944	2.939	2.947	2.952	2.946
Al	1.071	1.072	1.069	1.064	1.069
Fe	0.002	0.000	0.000	0.000	0.001
Ca	0.001	0.000	0.001	0.008	0.000
Na	0.042	0.043	0.041	0.037	0.041
K	0.919	0.929	0.922	0.905	0.934
Pb	0.023	0.029	0.021	0.021	0.015
Oxygen	8	8	8	8	8

GAHNITE (M.I.M.)

	4502/47.1c GAH 1	4502/47.1c GAH 2	4502/47.1c GAH 3	4502/47.1c GAH 4
SiO_2	0.21	0.39	0.25	0.03
Al_2O_3	56.89	57.06	56.60	56.36
FeO	6.41	6.58	7.52	7.84
MnO	0.09	0.04	0.20	0.15
MgO	0.00	0.00	0.00	0.00
ZnO	36.50	36.66	36.35	35.32
TOTAL	100.13	100.74	100.92	99.70
Si	0.006	0.011	0.008	0.001
Al	2.010	2.003	1.994	2.006
Fe	0.161	0.164	0.188	0.198
Mn	0.003	0.001	0.005	0.004
Mg	0.000	0.000	0.000	0.000
Zn	0.808	0.806	0.802	0.788
Oxygen	4	4	4	4

HERCYNITE (M.I.M.)

	4502/19.3 Hc 1	4502/19.3 Hc 2	4502/19.3 Hc 3	4502/19.3 Hc 4	4502/19.3 Hc 5
SiO_2	0.05	0.03	0.02	0.03	0.02
TiO_2	0.00	0.00	0.00	0.01	0.00
Al_2O_3	57.26	57.65	57.60	57.71	57.03
FeO	22.25	22.22	22.62	21.78	22.07
MnO	0.18	0.10	0.13	0.14	0.14
MgO	1.51	1.46	1.48	1.39	1.38
CaO	0.01	0.00	0.00	0.00	0.00
Na_2O	0.59*	0.54	0.55	0.59	0.59
K_2O	0.01	0.02	0.00	0.00	0.01
Cr_2O_3	0.15	0.11	0.15	0.10	0.11
ZnO	17.98	17.80	17.90	18.30	18.11
TOTAL	99.97	99.92	100.45	100.08	99.47
Si	0.001	0.001	0.001	0.001	0.001
Ti	0.000	0.000	0.000	0.000	0.000
Al	1.980	1.989	1.982	1.990	1.983
Fe	0.546	0.544	0.552	0.545	0.545
Mn	0.004	0.003	0.003	0.004	0.004
Mg	0.066	0.064	0.064	0.061	0.061
Ca	0.000	0.000	0.000	0.000	0.000
Na	0.033	0.030	0.031	0.034	0.034
K	0.000	0.001	0.000	0.000	0.001
Cr	0.004	0.003	0.003	0.002	0.003
Zn	0.389	0.385	0.386	0.395	0.395
Oxygen	4	4	4	4	4

* These high Na values are probably due to peak overlap with Zn.

	GREEN BIOTITES (M.I.M.) CON'T	BROWN BIOTITE (M.I.M.)	SERICITE (M.I.M.)			
	4502 /47.1c Bt 7-Gn	4502 /19.3 Bt 2-Bn	4502 /47.1c Ser 1	4502 /47.1c Ser 2	4502 /16.6 Ser 2	4502 /16.6 Ser 3
SiO_2	32.85	34.96	45.73	45.47	45.96	48.85
TiO_2	0.07	2.87	0.00	0.00	0.11	0.06
Al_2O_3	18.35	19.41	33.50	34.53	35.83	31.63
FeO	27.01	21.17	2.17	2.13	0.81	1.52
MnO	0.28	0.08	0.00	0.02	n.a.*	n.a.*
MgO	5.28	6.38	0.51	0.55	0.59	1.72
CaO	0.03	0.00	0.01	0.00	0.26	0.08
Na_2O	0.12	0.17	0.17	0.18	0.15	0.14
K_2O	8.45	9.53	10.22	10.47	11.36	11.34
Cl_2O	0.84	0.15	0.00	0.00	0.01	0.10
F_2O	0.74	0.00	0.00	2.31	n.a.*	n.a.*
TOTAL	94.02	94.66	92.31	95.15	95.08	95.44
Si	5.318	5.411	6.290	6.111	6.140	6.511
Ti	0.009	0.334	0.000	0.000	0.011	0.006
Al	3.501	3.542	5.430	5.469	5.642	4.968
Fe	3.657	2.734	0.249	0.239	0.090	0.170
Mn	0.039	0.010	0.000	0.019	-	-
Mg	1.275	1.472	0.105	0.111	0.118	0.342
Ca	0.005	0.000	0.002	0.000	0.038	0.012
Na	0.036	0.052	0.045	0.048	0.039	0.037
K	1.745	1.881	1.794	1.708	1.937	1.928
Cl	0.189	0.033	0.000	0.000	0.001	0.018
F	0.268	0.000	0.000	0.691	-	-
Oxygen	22	22	22	22	22	22

N.A. Not Analysed

GREEN BIOTITES (M.I.M.)

	4502/47.1c Bt 1-Gn	4502/47.1c Bt 2-Gn	4502/47.1c Bt 3-Gn	4502/47.1c Bt 4-Gn	4502/47.1c Bt 5-Gn
SiO_2	33.23	33.49	32.99	34.04	32.81
TiO_2	0.11	0.10	0.09	0.11	0.07
Al_2O_3	18.34	18.14	18.35	18.12	18.28
FeO	25.39	25.18	26.40	26.18	26.74
MnO	0.21	0.20	0.29	0.25	0.29
MgO	5.93	6.00	5.52	5.69	5.31
CaO	0.00	0.00	0.00	0.00	0.00
Na_2O	0.10	0.02	0.15	0.12	0.10
K_2O	9.03	8.89	8.80	9.14	8.50
Cl_2O	0.67	0.67	0.74	0.73	0.79
F_2O	0.00	1.20	0.00	0.00	1.52
TOTAL	92.99	93.91	93.33	94.38	94.42
Si	5.391	5.383	5.361	5.454	5.294
Ti	0.014	0.012	0.011	0.013	0.009
Al	3.506	3.437	3.515	3.421	3.477
Fe	3.445	3.385	3.587	3.508	3.608
Mn	0.028	0.028	0.040	0.035	0.040
Mg	1.433	1.437	1.337	1.360	1.278
Ca	0.000	0.000	0.000	0.000	0.000
Na	0.033	0.007	0.048	0.037	0.033
K	1.868	1.823	1.823	1.869	1.751
Cl	0.151	0.149	0.166	0.162	0.177
F	0.000	0.430	0.000	0.000	0.547
Oxygen	22	22	22	22	22

ILMENITE (M.I.M.)

	4502/19.3 Ilm 1	4502/19.3 Ilm 2	4502/19.3 Ilm 3	4502/19.3 Ilm 4	4502/19.3 Ilm 5	4502/19.3 Ilm 8	4502/19.3 Ilm 10	4502/19.3 Ilm 11	4502/19.3 Ilm 12
SiO_2	0.03	0.01	0.01	0.02	0.01	0.07	0.01	0.04	0.00
TiO_2	50.84	51.45	51.84	51.23	50.77	51.11	51.10	31.03	51.34
Al_2O_3	0.02	0.01	0.00	0.00	0.01	0.00	0.01	0.01	0.01
FeO	44.79	45.09	45.31	44.79	44.92	44.74	44.98	44.99	45.05
MnO	0.82	0.83	0.80	0.86	0.79	0.83	0.83	0.90	0.85
MgO	0.07	0.07	0.07	0.06	0.06	0.08	0.05	0.07	0.06
CaO	0.01	0.00	0.00	0.00	0.00	0.00	0.01	0.01	0.00
Na_2O	0.00	0.01	0.02	0.02	0.01	0.01	0.02	0.01	0.00
Cr_2O_3	0.00	0.03	0.00	0.00	0.00	0.00	0.04	0.02	0.03
ZnO	0.02	0.00	0.00	0.07	0.08	0.03	0.08	0.00	0.12
TOTAL	96.59	97.50	98.05	97.07	96.65	96.88	97.13	97.09	97.46
Si	0.001	0.000	0.000	0.001	0.000	0.002	0.000	0.001	0.000
Ti	0.999	1.001	1.002	1.001	0.998	1.000	0.998	0.997	1.000
Al	0.001	0.000	0.000	0.000	0.000	0.005	0.000	0.000	0.000
Fe	0.979	0.975	0.974	0.973	0.982	0.973	0.978	0.978	0.976
Mn	0.018	0.018	0.018	0.019	0.018	0.018	0.019	0.020	0.018
Mg	0.003	0.003	0.003	0.003	0.002	0.003	0.002	0.003	0.002
Ca	0.000	0.000	0.000	0.000	0.000	0.000	0.000	0.000	0.000
Na	0.000	0.000	0.001	0.001	0.000	0.006	0.001	0.000	0.000
Cr	0.000	0.001	0.000	0.000	0.000	0.000	0.001	0.000	0.000
Zn	0.000	0.000	0.000	0.002	0.002	0.001	0.001	0.000	0.001
Oxygen	3	3	3	3	3	3	3	3	3

SILLIMANITE (M.I.M.)

	4502/19.3 Sil 1	4502/19.3 Sil 2	4502/19.3 Sil 3	4502/19.3 Sil 4	4502/19.3 Sil 5
SiO_2	37.29	37.37	37.30	37.38	37.42
TiO_2	0.19	0.30	0.05	0.03	0.05
Al_2O_3	61.80	61.88	61.67	61.82	61.96
FeO	0.44	0.63	0.27	0.27	0.23
Cr_2O_3	0.00	0.02	0.03	0.02	0.03
ZnO	0.06	0.01	0.00	0.04	0.00
TOTAL					
Si	1.010	1.009	1.014	1.013	1.013
Ti	0.004	0.000	0.001	0.001	0.001
Al	1.973	1.969	1.975	1.976	1.977
Fe	0.010	0.014	0.006	0.006	0.005
Cr	0.000	0.001	0.001	0.000	0.001
Zn	0.001	0.000	0.000	0.001	0.000
Oxygen	5	5	5	5	5

FLUORAPATITE (ANU)

	4502/53.6 Ap 1	4502/56.9 Ap 2
P_2O_5	37.19	40.74
SiO_2	0.48	0.99
TiO_2	0.00	0.00
Al_2O_3	0.00	0.00
FeO	0.00	0.00
MnO	0.99	0.13
MgO	0.41	0.23
CaO	48.78	55.28
Na_2O	0.38	0.23
Cl	0.08	0.05
TOTAL	88.31	97.65
P	2.824	2.794
Si	0.043	0.080
Ti	0.000	0.000
Al	0.000	0.000
Fe	0.000	0.000
Mn	0.075	0.009
Mg	0.055	0.028
Ca	4.689	4.799
Na	0.066	0.036
Cl	0.012	0.007
Oxygen	12	12
TOTAL ATOMS	19.765	19.781

SPHENE (M.I.M.)

	2/9B Sphn 2-1	2/9B Sphn 2-2	2/9B Sphn 2-4	2/9B Sphn 3-3	2/9B Sphn 4-4
SiO_2	31.83	30.94	30.62	30.51	30.19
TiO_2	31.87	33.47	35.28	34.75	34.24
Al_2O_3	2.12	2.13	2.17	2.65	3.18
FeO	3.71	2.86	1.71	1.45	1.48
MnO	1.42	1.07	0.35	0.54	0.32
MgO	0.65	0.36	0.13	0.07	0.14
CaO	25.79	26.93	28.56	28.36	28.42
Na_2O	0.17	0.10	0.10	0.07	0.06
K_2O	0.00	0.00	0.03	0.00	0.00
ZnO	0.06	0.00	0.00	0.00	0.00
Cl_2O	0.03	0.01	0.01	0.05	0.01
Total	97.75	97.87	98.96	98.45	98.04
Si	1.064	1.046	1.013	1.012	1.006
Ti	0.801	0.835	0.878	0.867	0.858
Al	0.084	0.083	0.085	0.103	0.125
Fe	0.014	0.079	0.047	0.040	0.041
Mn	0.040	0.030	0.010	0.009	0.009
Mg	0.032	0.018	0.006	0.000	0.007
Ca	0.924	0.957	1.012	1.008	1.015
Na	0.011	0.006	0.006	0.015	0.004
K	0.000	0.000	0.001	0.000	0.000
Zn	0.001	0.000	0.000	0.000	0.000
Cl	0.001	0.000	0.000	0.002	0.000
Oxygens	5	5	5	5	5

APPENDIX III : ASSAY DATA

Drillhole locations:

1) DH 4502 - See Fig. 2.4

2) DH 4496 - See Fig. 2.4

3) DH 4483 - See Fig. 2.4

4) DZ 2682 - See Fig. 2.1

APPENDIX III: ASSAY DATA

DH4502

INTERVAL	METRES FROM	TO	Pb %	Ag ppm	Zn %	Cu %	Bi ppm	Fe %	As %
1	4.80	16.70	0.00	0	0.00	0.00	0	0.00	0.000
2	16.70	17.10	.08	7	.04	0.00	0	1.20	0.000
3	17.10	19.50	.06	7	.09	.02	4	3.40	0.000
4	19.50	20.70	1.86	37	.10	.06	10	4.00	0.000
5	20.70	22.60	.07	2	.05	.01	0	2.50	0.000
6	22.60	24.00	.11	2	.08	.02	2	2.60	0.000
7	24.00	27.00	1.23	15	.43	.04	7	4.00	0.000
8	27.00	28.00	2.59	27	.21	.14	2	5.70	0.000
9	28.00	28.90	1.81	18	.04	.02	3	2.30	0.000
10	28.90	29.40	.16	13	.69	.04	1	2.10	0.000
11	29.40	32.40	.91	12	.03	.02	11	2.40	0.000
12	32.40	35.40	4.29	38	.04	.02	25	2.30	0.000
13	35.40	36.50	1.56	16	.05	.06	7	3.50	0.000
14	36.50	38.30	6.40	57	.15	.30	10	10.70	0.000
15	38.30	41.30	3.85	31	1.12	.08	12	4.20	0.000
16	41.30	44.30	2.15	19	.51	.08	8	5.00	0.000
17	44.30	44.50	9.90	84	16.80	.06	55	9.20	0.000
18	44.50	47.00	7.80	77	3.60	.04	54	2.60	0.000
19	47.00	49.30	2.82	33	7.50	.08	9	3.00	0.000
20	49.30	50.70	9.50	70	9.90	.10	28	4.20	0.000
21	50.70	52.90	7.50	58	16.30	.06	48	5.30	0.000
22	52.90	55.30	5.90	48	13.20	.04	28	4.90	0.000
23	55.30	56.10	3.07	21	13.50	.10	6	5.00	0.000
24	56.10	59.00	2.03	20	5.70	.06	9	2.60	0.000
25	59.00	60.30	8.80	63	12.30	.08	30	5.40	0.000
26	60.30	60.80	.83	9	1.75	.06	2	2.30	0.000
27	60.80	61.40	8.50	58	10.00	.08	23	3.80	0.000
28	61.40	61.80	14.90	86	22.40	.14	54	7.50	0.000
29	61.80	63.70	6.00	42	5.90	.08	25	3.00	0.000
30	63.70	66.40	.34	3	1.64	.06	2	2.10	0.000
31	66.40	67.10	5.10	39	4.50	.12	59	4.30	0.000
32	67.10	67.50	9.60	105	18.70	.16	115	8.00	0.000
33	67.50	69.10	3.65	29	4.60	.08	53	3.20	0.000
34	69.10	69.60	1.42	11	19.00	.04	0	8.10	0.000
35	69.60	70.10	1.04	10	2.10	.02	0	1.40	0.000
36	70.10	71.80	6.90	40	27.20	.04	83	4.20	0.000
37	71.80	74.80	.31	4	.65	.04	3	3.00	0.000
38	74.80	77.80	.02	2	.21	.08	0	3.40	0.000
39	77.80	80.80	.77	6	.21	.06	2	1.90	0.000
40	80.80	83.80	1.56	12	.06	.04	5	2.30	0.000
41	83.80	86.60	.16	2	.11	.04	4	4.00	0.000
42	86.60	87.50	.29	3	.05	.03	2	14.20	0.000
43	87.50	89.00	.03	2	.22	.02	4	1.50	0.000
44	89.00	91.70	.95	12	.52	.04	3	1.70	0.000

0 = NOT DETERMINED OR BELOW DETECTION LIMITS

APPENDIX IIIA: ASSAY DATA

DH4496

INTERVAL	METRES FROM	TO	Pb %	Ag ppm	Zn %	Cu %	Bi ppm	Fe %	As %
1	19.80	21.70	0.00	0	0.00	0.00	0	0.00	0.000
2	21.70	24.70	.05	6	.05	.02	0	2.30	0.000
3	24.70	27.10	3.09	31	.11	.10	1	5.30	0.000
4	27.10	27.80	1.44	23	.22	.22	2	10.40	0.000
5	27.80	30.80	.43	13	.04	.04	3	2.60	0.000
6	30.80	33.80	1.76	22	.15	.02	6	2.00	0.000
7	33.80	36.80	1.90	25	.05	.02	10	2.80	0.000
8	36.80	38.70	.11	5	.10	.02	0	2.20	0.000
9	38.70	40.60	1.46	19	.06	0.00	0	2.00	0.000
10	40.60	42.00	.15	5	.07	0.00	0	2.60	0.000
11	42.00	45.00	2.08	19	.10	.02	14	2.60	0.000
12	45.00	47.20	8.10	59	2.40	.02	49	3.50	0.000
13	47.20	48.40	2.43	22	1.59	.02	28	2.30	0.000
14	48.40	51.20	5.30	53	3.90	.04	36	1.70	0.000
15	51.20	53.60	5.40	52	20.00	.02	25	4.60	0.000
16	53.60	56.50	12.10	136	16.90	.08	44	5.20	0.000
17	56.50	58.00	5.30	37	7.20	.16	7	3.20	0.000
18	58.00	58.80	8.00	54	14.30	.08	4	6.00	0.000
19	58.80	59.80	4.10	28	7.10	.08	2	3.20	0.000
20	59.80	60.30	4.31	41	2.30	.04	28	1.50	0.000
21	60.30	60.70	28.30	215	13.30	.08	176	5.20	0.000
22	60.70	63.70	1.87	15	.75	.06	17	2.20	0.000
23	63.70	66.70	3.09	35	1.29	.04	17	3.20	0.000
24	66.70	69.20	1.02	21	1.11	.08	11	2.40	0.000
25	69.20	72.20	1.29	34	1.27	.20	16	3.70	0.000
26	72.20	73.50	.64	13	1.11	.12	4	3.10	0.000
27	73.50	75.70	.57	12	.83	.10	5	3.00	0.000
28	75.70	77.20	1.62	26	1.30	.08	20	3.90	0.000
29	77.20	79.00	5.50	69	5.60	.07	65	3.60	0.000
30	79.00	80.40	.57	9	7.90	.19	9	7.20	0.000
31	80.40	81.20	3.73	56	10.80	.07	44	5.60	0.000
32	81.20	81.80	9.10	106	24.10	.08	74	10.60	0.000
33	81.80	82.10	.93	36	.87	0.00	3	1.80	0.000
34	82.10	82.50	23.20	311	6.70	.15	177	3.40	0.000
35	82.50	83.20	4.16	50	2.50	.04	32	1.60	0.000
36	83.20	83.70	9.10	129	16.60	.10	62	14.20	0.000
37	83.70	86.10	1.20	23	.15	.05	7	1.50	0.000
38	86.10	89.10	.20	7	.13	.06	2	2.10	0.000
39	89.10	92.10	.60	12	.54	.01	4	1.50	0.000
40	92.10	95.10	.54	18	.70	.03	2	2.70	0.000
41	95.10	98.10	.29	6	.78	.01	0	2.20	0.000
42	98.10	100.70	.07	6	.78	.02	0	4.20	0.000
43	100.70	101.20	.10	7	19.00	.01	0	6.20	0.000
44	101.20	104.20	.01	2	.56	0.00	0	1.50	0.000
45	104.20	107.20	.11	7	.57	.01	18	2.40	0.000
46	107.20	110.20	.27	3	.15	0.00	0	2.10	0.000
47	110.20	112.20	.08	3	1.96	.01	0	2.20	0.000
48	112.20	115.20	.03	4	.10	0.00	0	1.70	0.000
49	115.20	118.20	.04	3	.06	0.00	0	1.50	0.000
50	118.20	120.20	.04	4	.04	0.00	0	1.70	0.000
51	120.20	121.80	.05	4	.16	0.00	1	1.50	0.000
52	121.80	123.40	.07	4	.17	0.00	3	2.40	0.000
53	123.40	123.70	.07	3	.10	.04	0	2.30	0.000

54	123.70	124.30	.03	1	.03	.02	0	3.80	0.000
55	124.30	125.90	.08	3	.04	0.00	0	1.80	0.000
56	125.90	127.10	.17	0	.14	0.00	0	2.00	0.000

0 = NOT DETERMINED OR BELOW DETECTION LIMITS

APPENDIX IIIB: ASSAY DATA

DH4483

INTERVAL	METRES FROM	TO	Pb %	Ag ppm	Zn %	Cu %	Bi ppm	Fe %	As %
1	5.40	32.00	0.00	0	0.00	0.00	0	0.00	0.000
2	32.00	33.10	.67	17	.14	.07	12	3.90	.062
3	33.10	35.50	.25	2	.04	.01	2	2.80	.024
4	35.50	36.30	1.21	12	.10	.01	10	3.20	.028
5	36.30	38.00	5.30	48	.07	.07	35	3.60	.042
6	38.00	38.80	8.90	67	.26	.26	39	11.10	.720
7	38.80	41.10	4.25	31	.39	.17	24	7.30	.245
8	41.10	43.40	1.69	11	.05	.10	14	5.40	.335
9	43.40	44.50	.56	3	.36	.04	9	3.00	.186
10	44.50	45.40	10.60	75	2.80	.07	59	3.40	.064
11	45.40	48.40	4.10	28	.03	.05	11	3.00	.270
12	48.40	51.40	2.94	24	.03	.05	15	2.80	.152
13	51.40	53.00	.14	0	.05	0.00	0	1.70	.048
14	53.00	53.80	.53	4	.09	0.00	0	.40	0.000
15	53.80	54.30	.09	1	.05	.03	0	1.90	0.000
16	54.30	55.00	3.11	79	.08	.10	24	3.30	.042
17	55.00	56.50	.22	1	.03	.01	0	2.20	.012
18	56.50	57.40	.54	7	.11	.01	0	3.60	.008
19	57.40	60.20	.16	1	.09	0.00	0	1.90	.026
20	60.20	61.60	9.60	142	.06	.09	97	2.10	.042
21	61.60	64.60	1.94	31	.03	.02	26	1.50	.036
22	64.60	67.60	.79	19	.18	.05	0	1.60	.048
23	67.60	70.60	.72	9	.55	0.00	0	1.50	.060
24	70.60	73.40	1.19	19	.53	.02	2	1.30	.052
25	73.40	73.90	4.23	57	.69	.06	19	.10	.054
26	73.90	75.70	7.20	80	11.40	.10	48	3.90	.052
27	75.70	76.30	1.33	17	2.40	.08	7	1.60	.054
28	76.30	78.30	4.40	45	9.70	.08	51	3.70	.225
29	78.30	80.40	1.79	30	8.40	.14	16	3.60	.058
30	80.40	81.10	1.39	25	8.70	.08	8	3.80	.375
31	81.10	84.10	1.76	33	2.90	.14	14	3.00	.040
32	84.10	87.10	2.21	30	5.10	.06	13	2.80	.052
33	87.10	90.10	2.22	36	3.30	.10	9	2.50	.116
34	90.10	92.20	1.52	30	3.90	.18	20	3.40	.114
35	92.20	94.20	.50	10	6.70	.16	2	5.00	1.040
36	94.20	95.40	.52	11	13.80	.12	0	5.80	.178
37	95.40	97.30	1.80	35	5.70	.10	8	2.30	.106
38	97.30	98.20	.22	9	26.00	.34	0	11.20	.050
39	98.20	100.80	2.33	54	10.40	.28	10	6.10	.084
40	100.80	103.80	5.80	69	.89	.12	23	2.00	.046
41	103.80	106.80	2.38	36	1.41	.12	13	2.20	.098
42	106.80	107.50	.82	23	1.11	.14	0	5.30	.014
43	107.50	110.00	.62	11	1.06	.14	0	5.10	.038
44	110.00	112.20	.55	12	.65	.20	0	4.50	.010
45	112.20	113.80	.62	10	1.25	.52	0	6.90	.066
46	113.80	115.40	.45	8	.76	.24	0	7.10	.014
47	115.40	115.70	.29	7	28.00	.08	3	15.20	0.000
48	115.70	118.50	.97	17	2.10	.38	4	6.20	.028
49	118.50	120.60	.57	17	2.10	1.32	0	10.70	.044
50	120.60	123.20	2.76	62	1.56	.38	14	6.90	.024
51	123.20	124.20	2.49	39	.26	.10	15	2.80	.062
52	124.20	126.00	1.07	20	1.06	.30	2	6.30	0.000
53	126.00	127.40	.09	9	.32	.50	0	15.00	.030

54	127.40	130.40	.18	9	.32	.06	0	3.50	.016
55	130.40	133.40	.19	20	.46	.02	3	2.10	.022
56	133.40	135.30	.03	3	.38	.08	2	5.20	.010
57	135.30	136.60	1.60	41	5.70	.10	0	3.90	0.000
58	136.60	139.60	2.16	42	3.20	.02	9	2.10	0.000
59	139.60	141.60	.40	9	6.40	.10	0	2.50	0.000
60	141.60	143.40	.09	15	3.10	.06	9	2.50	0.000
61	143.40	144.70	1.00	30	.96	.17	14	1.10	0.000
62	144.70	146.40	1.36	42	4.00	.08	15	1.60	0.000
63	146.40	149.40	.59	16	13.80	.06	18	3.00	0.000
64	149.40	150.90	.70	18	3.90	.04	12	2.70	0.000
65	150.90	153.90	.56	15	.14	.14	2	3.70	0.000

0 = NOT DETERMINED OR BELOW DETECTION LIMITS

APPENDIX IIIC: ASSAY DATA

DZ2682

INTERVAL	METRES FROM	TO	Pb %	Ag ppm	Zn %	Cu %	Bi ppm	Fe %	As %
1	8.40	18.30	0.00	0	0.00	0.00	0	0.00	0.000
2	18.30	19.20	4.20	138	.40	.13	0	0.00	0.000
3	19.20	20.70	.60	14	.20	.04	0	0.00	0.000
4	20.70	34.10	0.00	0	0.00	0.00	0	0.00	0.000
5	34.10	37.50	1.20	16	1.80	.07	9	0.00	0.000
6	37.50	39.90	8.00	90	4.00	.15	51	0.00	.013
7	39.90	41.30	9.60	125	25.00	.25	41	0.00	.006
8	41.30	42.10	1.60	22	2.40	.03	9	0.00	.006
9	42.10	43.40	3.20	74	5.40	.51	11	0.00	0.000
10	43.40	45.70	2.00	40	4.60	.23	15	0.00	0.000
11	45.70	46.30	.20	36	11.00	.11	16	0.00	0.000
12	46.30	48.20	.80	14	6.80	.04	9	0.00	0.000
13	48.20	49.10	.60	12	10.20	.10	4	0.00	.033
14	49.10	50.70	.60	14	5.80	.08	9	0.00	.026
15	50.70	53.80	.20	4	1.80	.02	2	0.00	0.000
16	53.80	56.80	.40	4	.80	.03	3	0.00	.030
17	56.80	59.90	.60	6	.40	.04	2	0.00	0.000
18	59.90	62.90	.20	0	.20	.01	0	0.00	0.000
19	62.90	66.00	.20	4	.40	.01	0	0.00	.127
20	66.00	69.00	.20	4	.20	.04	0	0.00	.050
21	69.00	72.10	.20	4	.20	.04	2	0.00	.010
22	72.10	73.50	.20	6	1.00	.03	2	0.00	.013
23	73.50	74.70	.80	16	5.40	.08	12	0.00	.080
24	74.70	75.30	.40	8	14.40	.08	3	0.00	0.000
25	75.30	76.70	.40	8	.80	.04	1	0.00	0.000
26	76.70	78.80	1.20	16	2.20	.08	2	0.00	.130
27	78.80	79.40	31.40	288	6.40	.36	48	0.00	0.000
28	79.40	80.20	2.20	36	.40	.24	7	0.00	.026
29	80.20	83.40	.40	4	.40	.07	2	0.00	0.000
30	83.40	86.40	.40	4	.40	.03	0	0.00	0.000
31	86.40	89.50	.20	4	.20	.04	0	0.00	0.000
32	89.50	91.40	.20	4	.20	.04	0	0.00	0.000
33	91.40	97.50	0.00	0	0.00	0.00	0	0.00	0.000
34	97.50	100.60	.60	6	.20	.01	0	0.00	0.000
35	100.60	101.20	.40	4	.20	.01	0	0.00	0.000
36	101.20	119.80	0.00	0	0.00	0.00	0	0.00	0.000

0 = NOT DETERMINED OR BELOW DETECTION LIMITS

Appendix 4.

A) Whole rock geochemical trends
B) Base metal trends
C) Mineral composition trends

Legend

S : Sillimanite gneiss
J : gahnite - rich rocks
G : garnet quartzite
A : amphibole subzone
P : pyroxenoid subzone

Circles represent green biotite.
On the gahnite plot the inverted triangles represent rim compositions, while the normal triangles represent core compositions.
Triangles represent core compositions on (CaO + MnO/MgO) versus distance for garnet plots, and rim compsitions on (MgO/MgO + FeO) versus distance garnet plots.

CONTENTS

Diamond drill holes prefixed DZ are on the Zinc Corporation Lease; those prefixed DH or with no prefix are from the NBHC Leases.

Appendix 4A: Wholerock Geochemical Trends

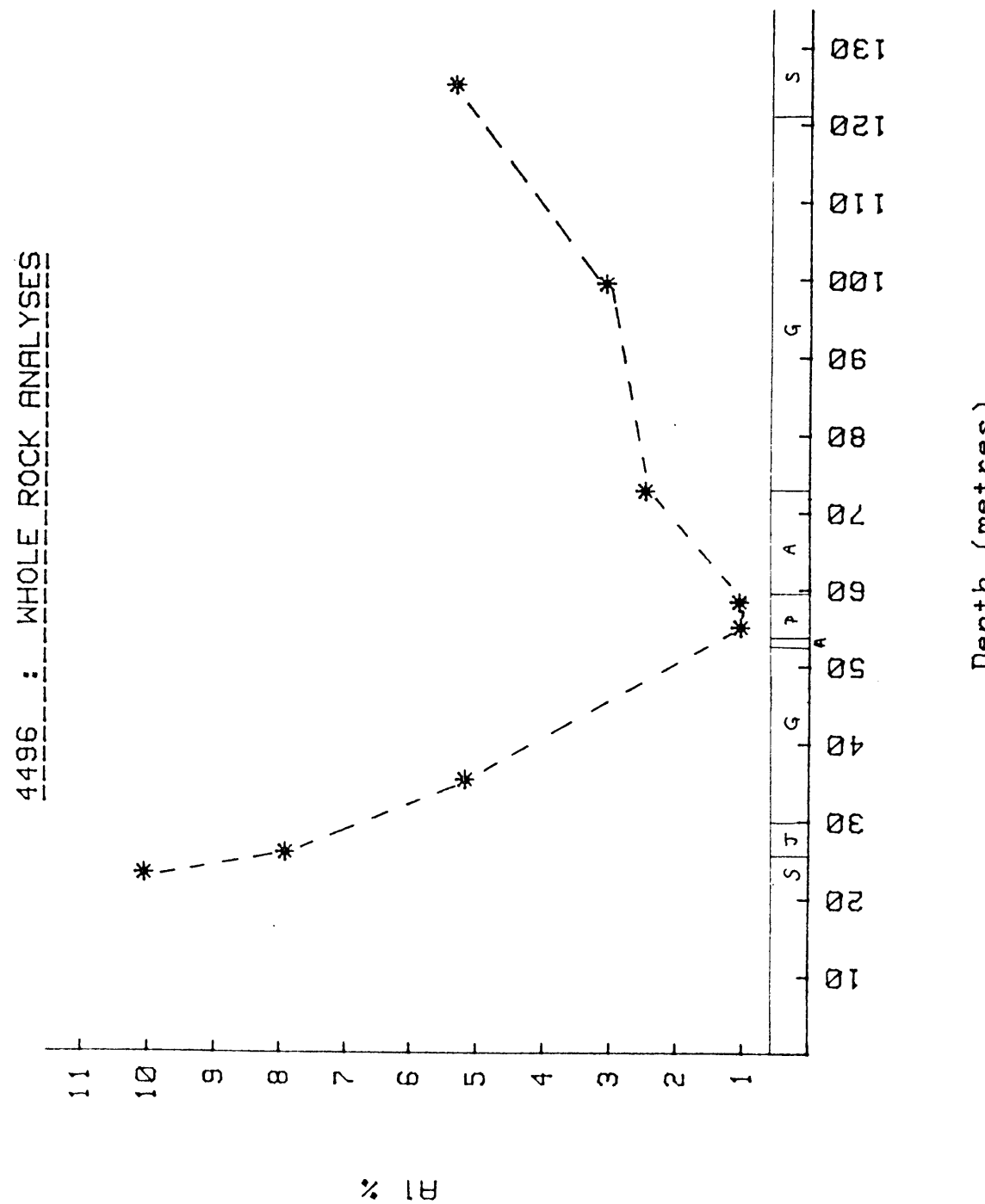

Appendix 4A cont.

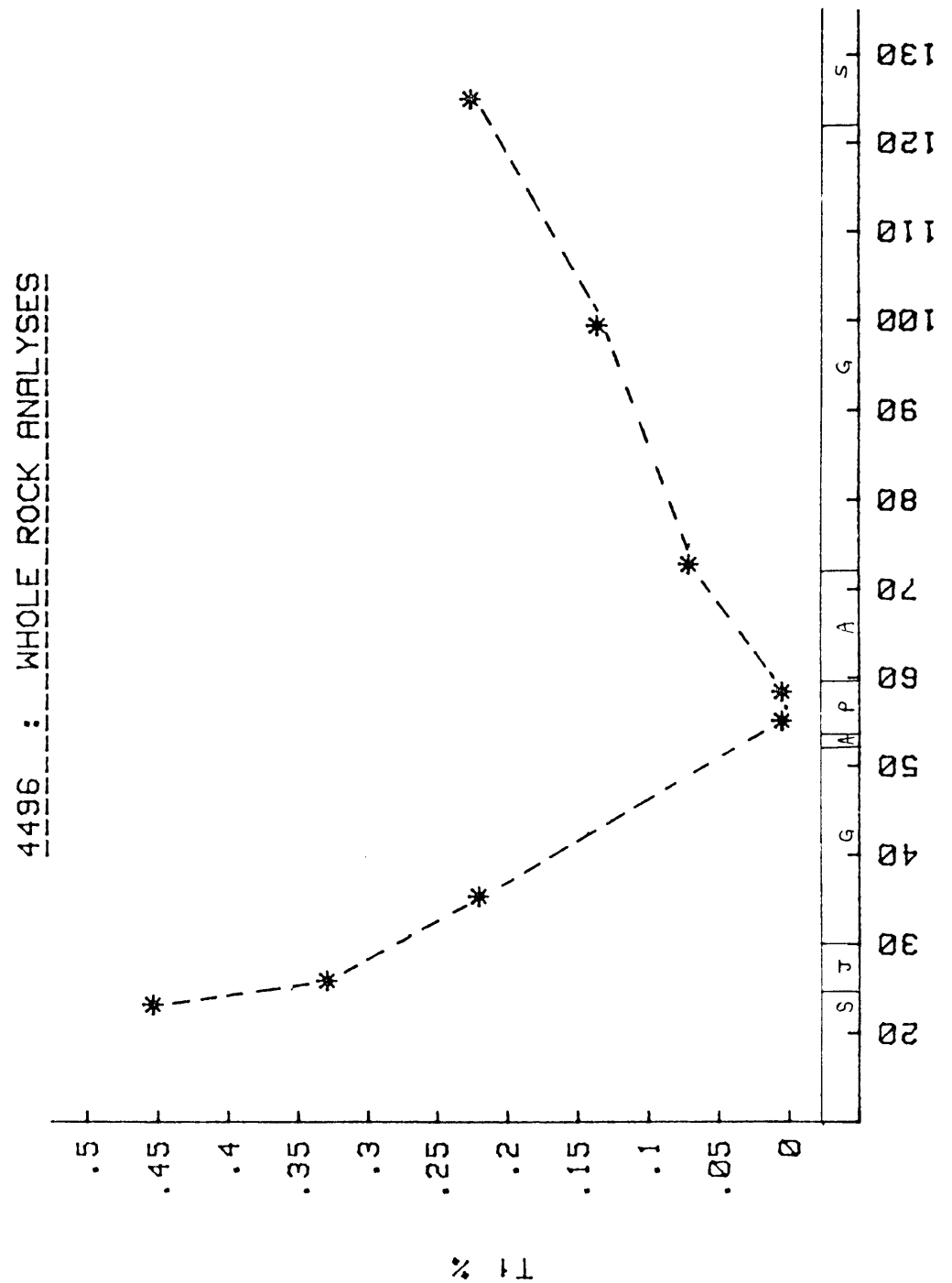

Appendix 4A cont.

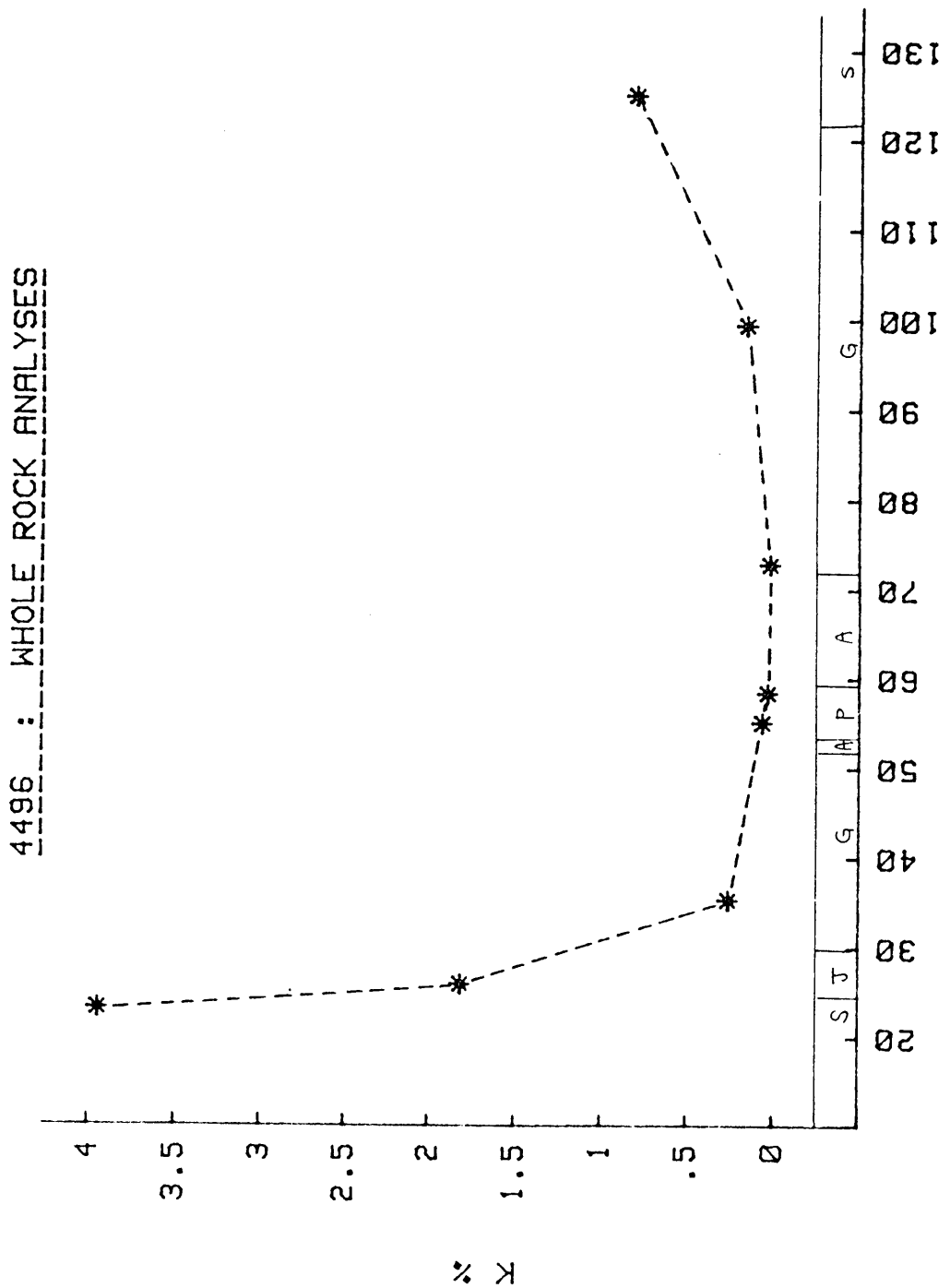

Appendix 4A cont.

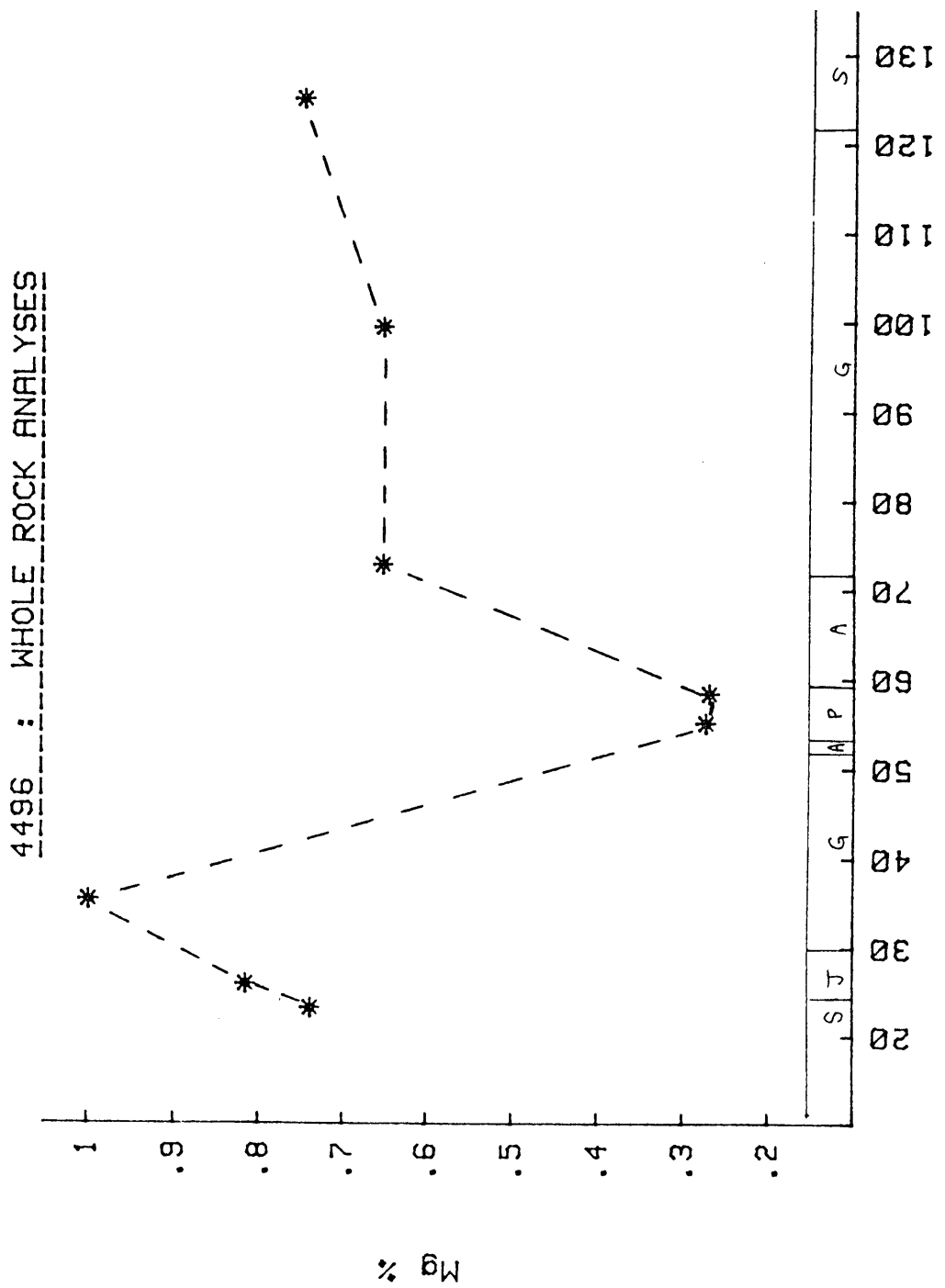

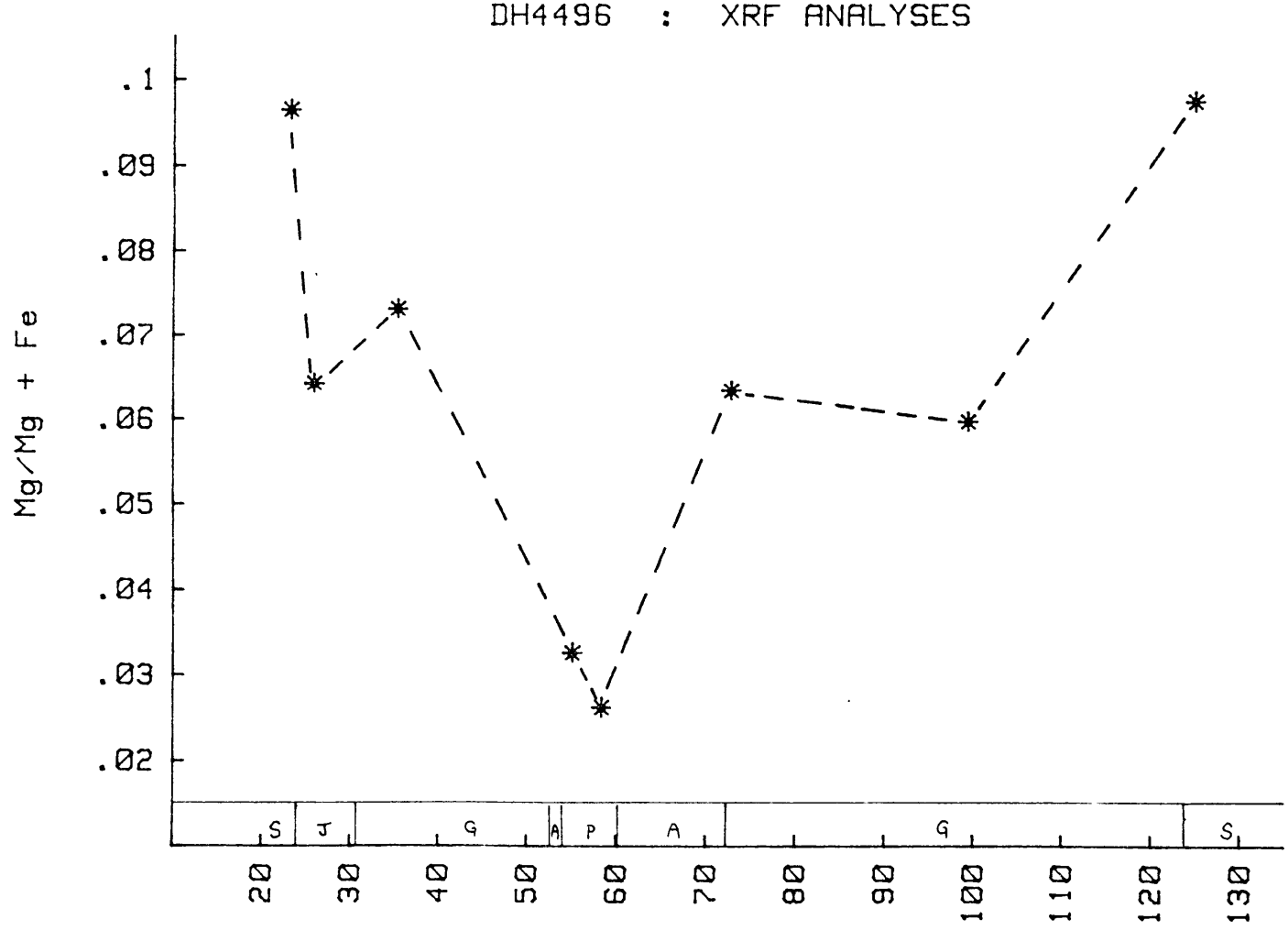
DH4496 : XRF ANALYSES
Mg/Mg + Fe
.1
.09
.08
.07
.06
.05
.04
.03
.02
S
J
G
A
P
A
G
S
20
30
40
50
60
70
80
90
100
110
120
130
Depth (metres)

Appendix 4A cont.

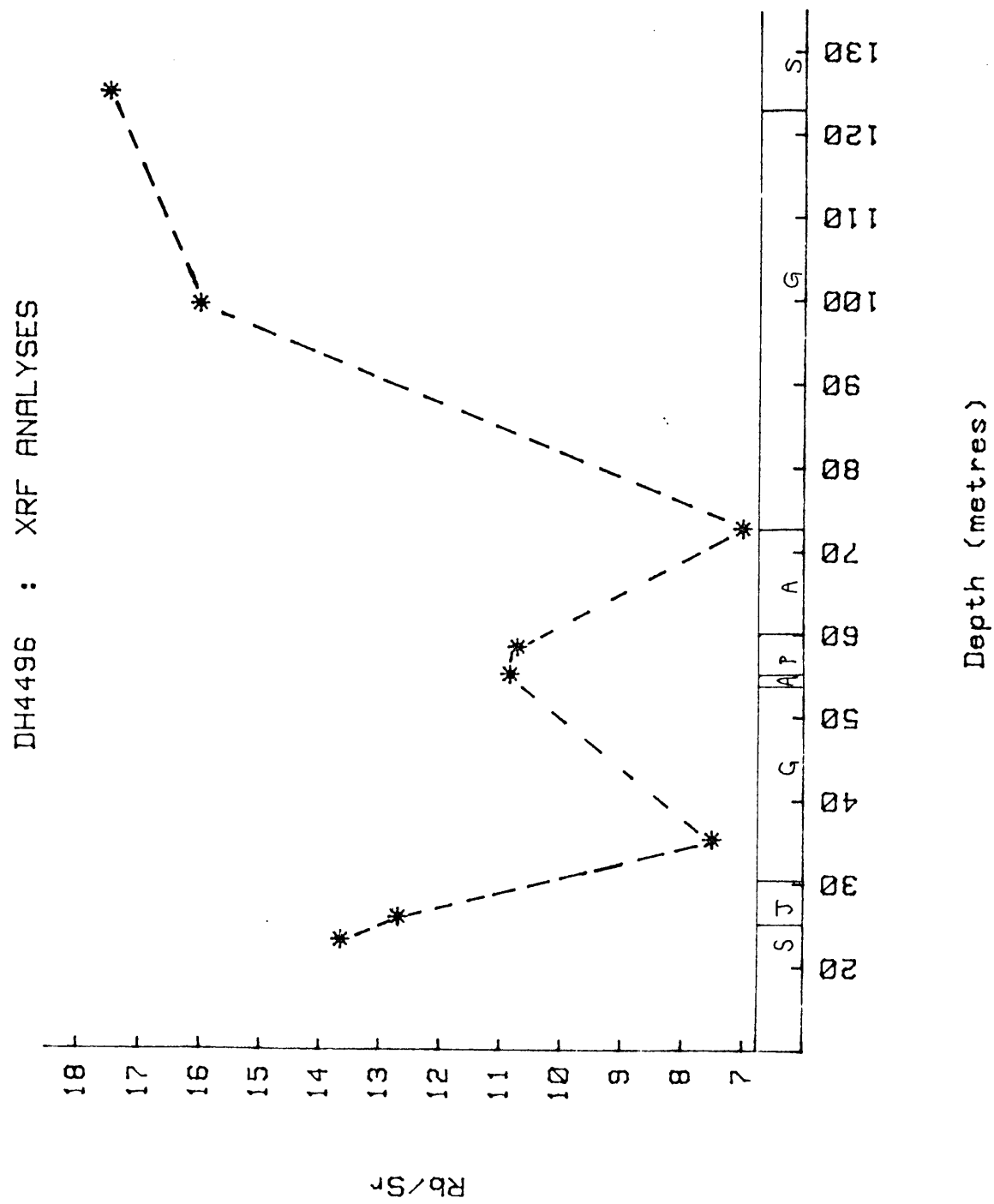

Appendix 4A cont.

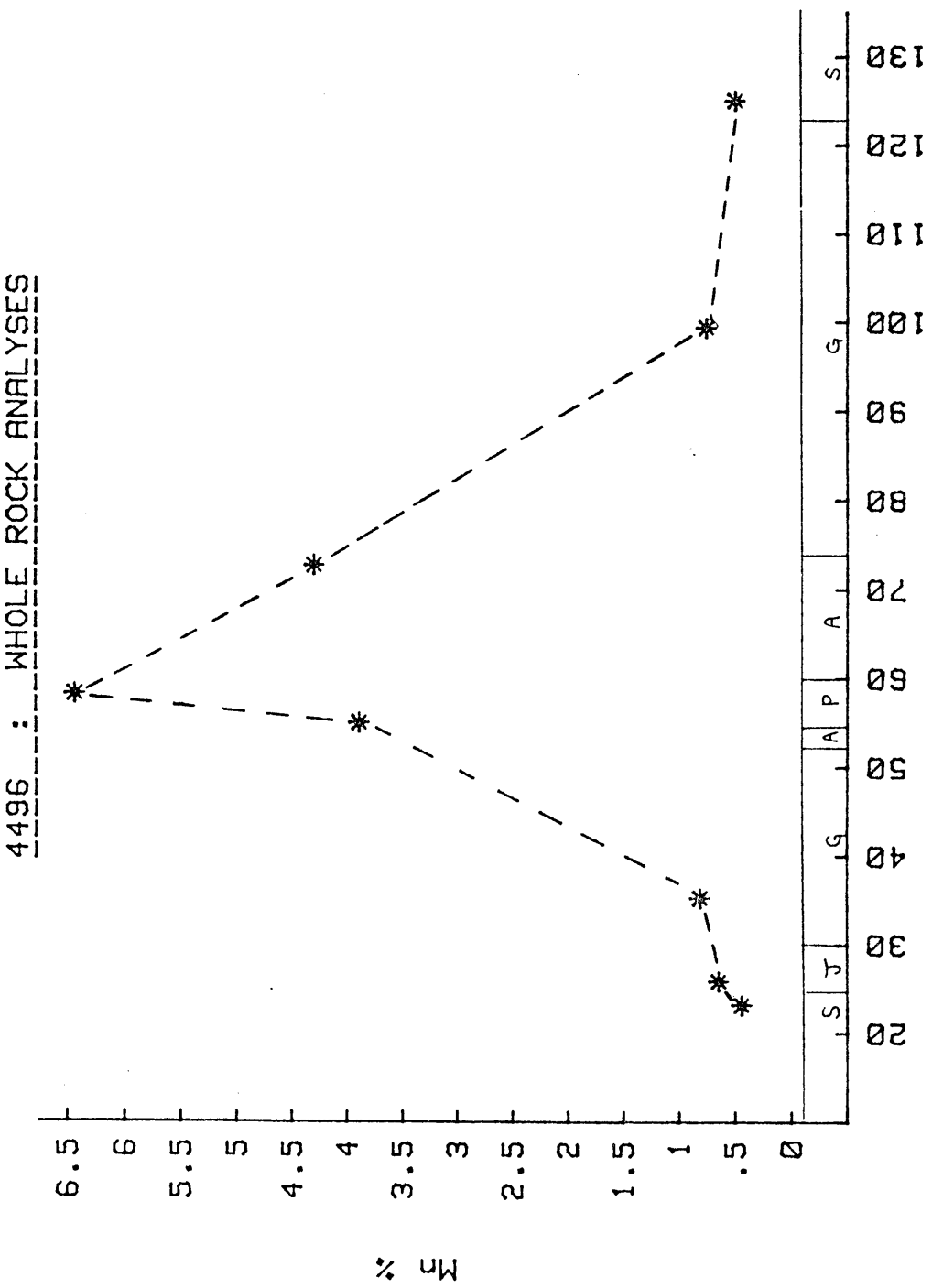

Appendix 4A cont.

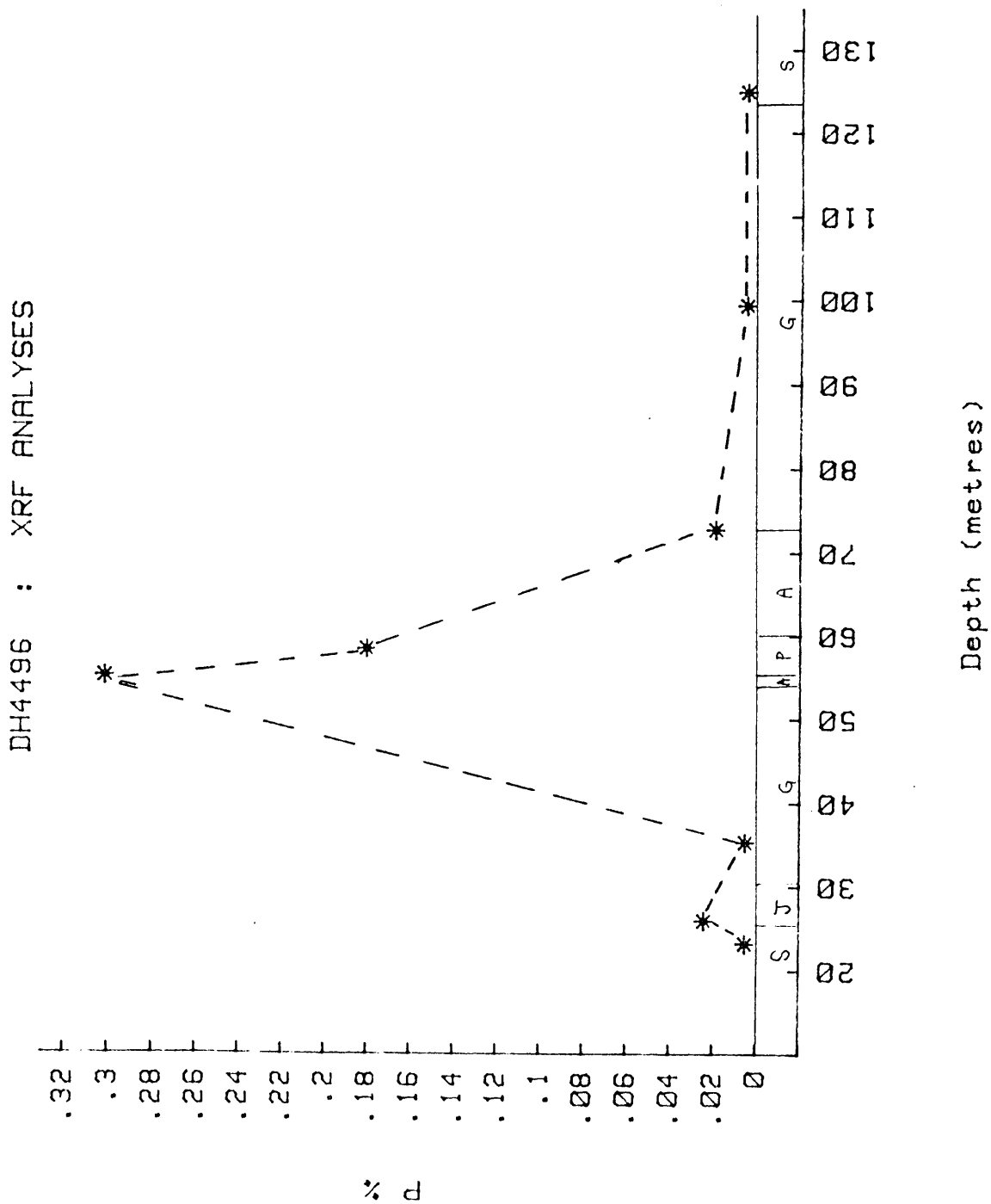

Appendix 4A cont.

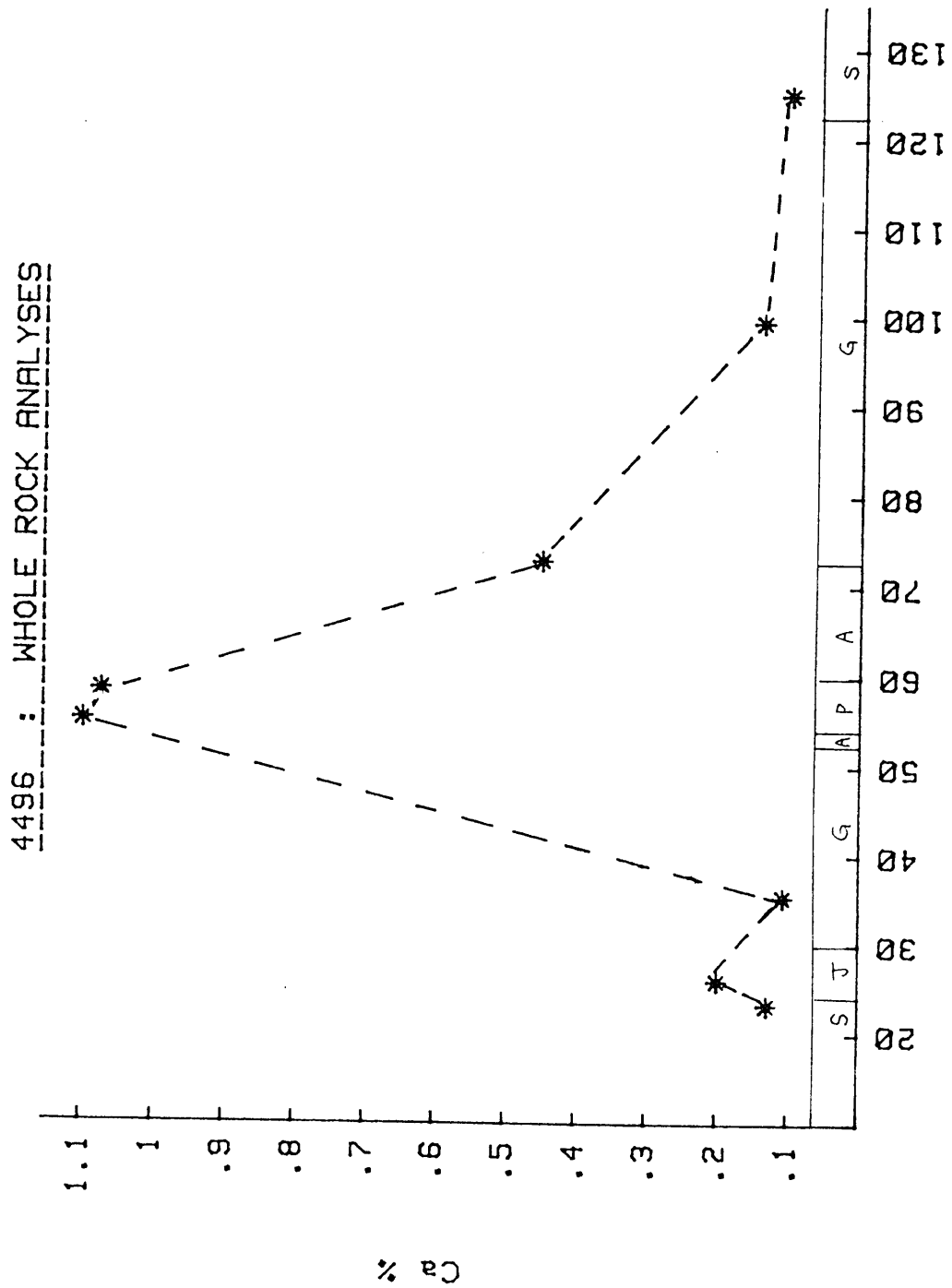

Appendix 4A cont.

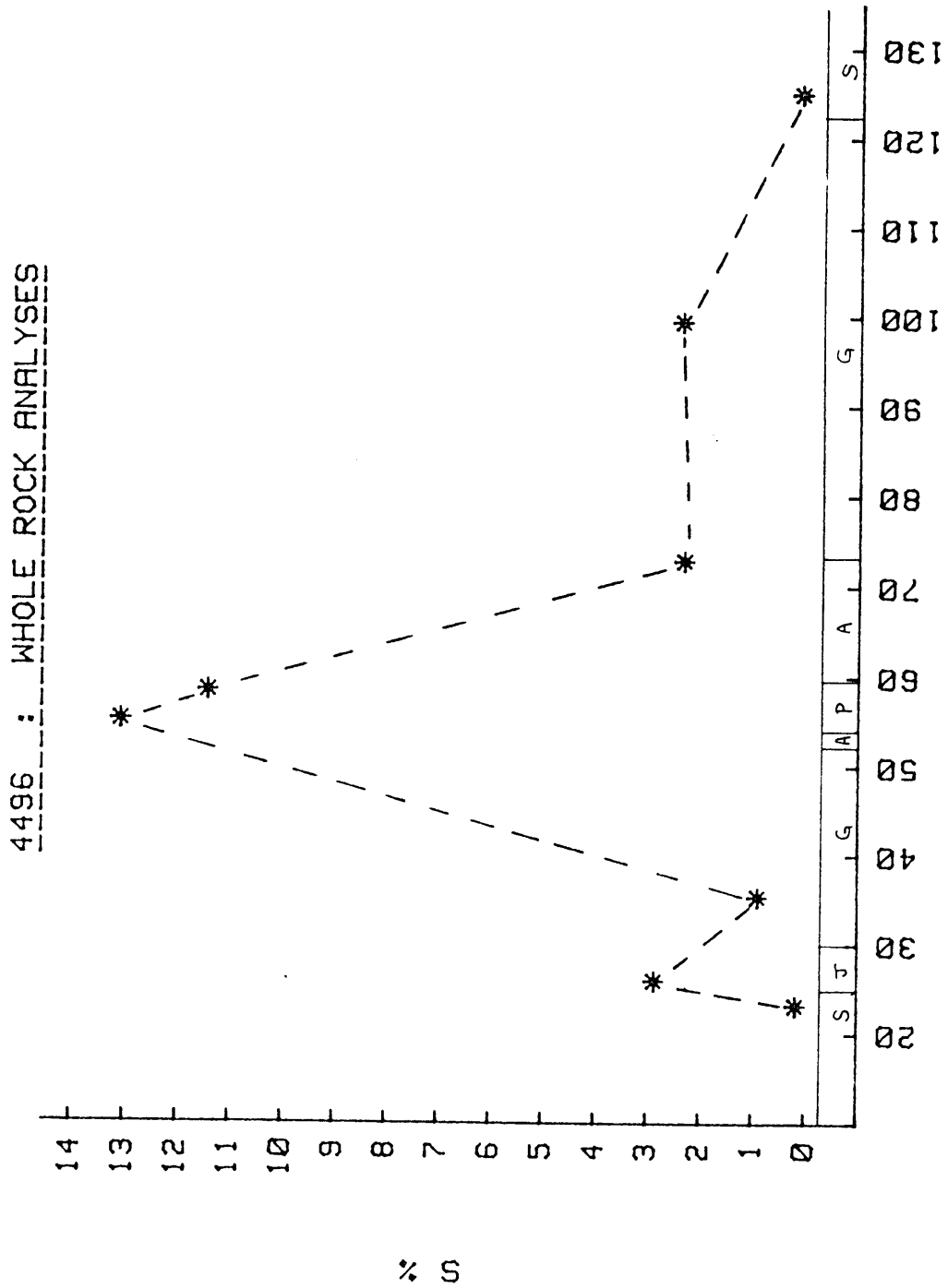

Appendix 4A cont.

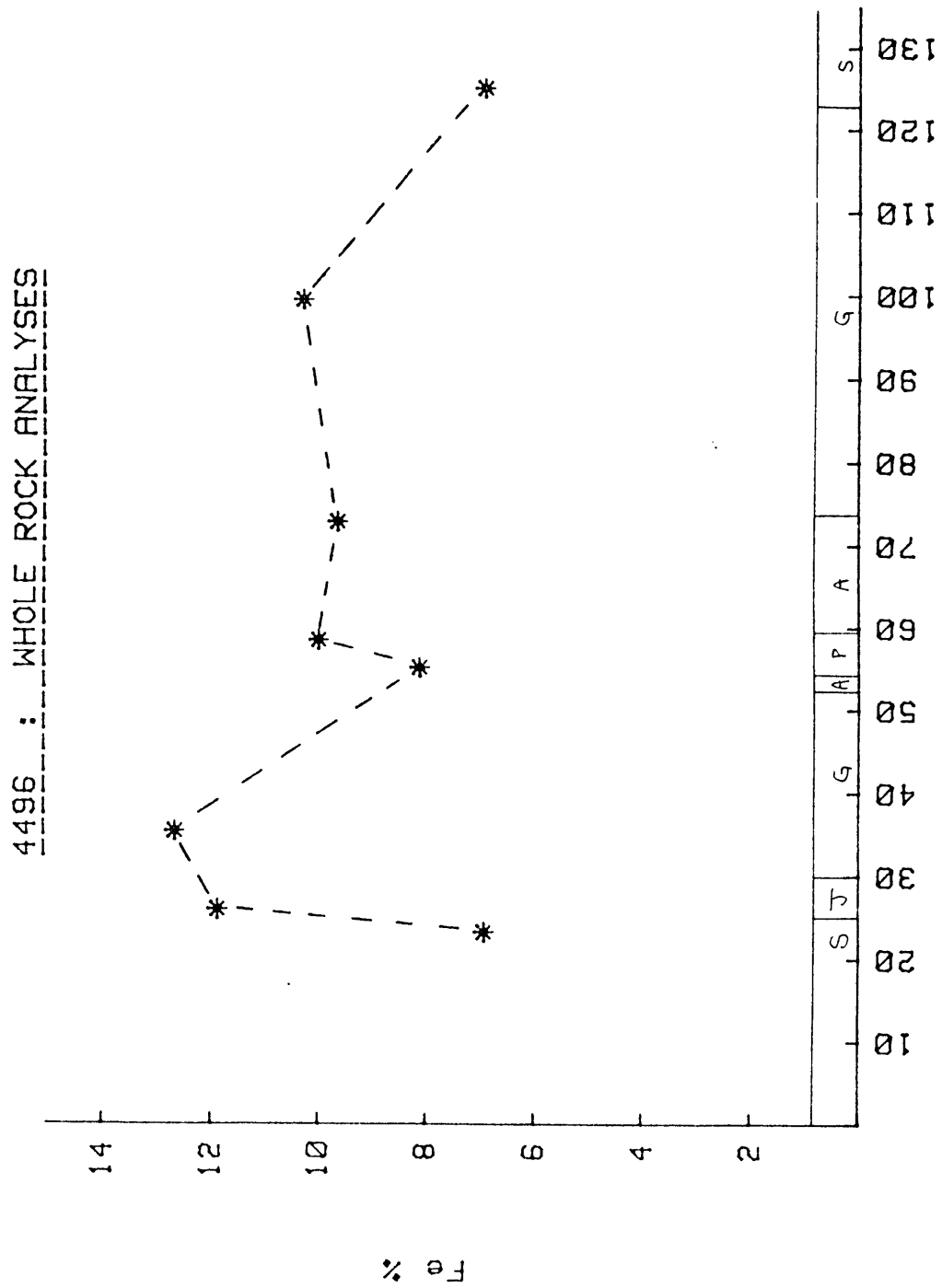

Appendix 4A cont.

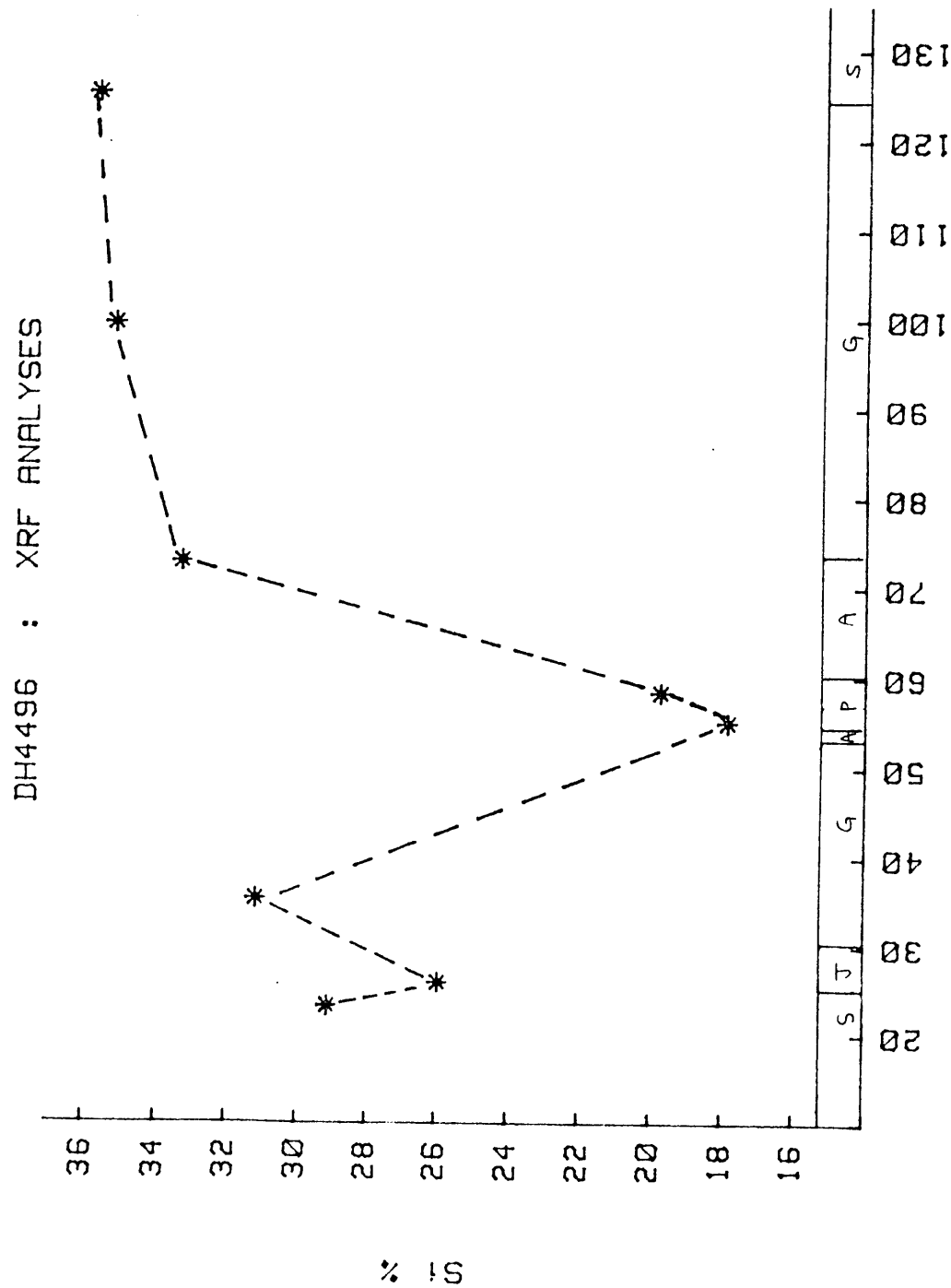

Appendix 4B: Base Metal Trends

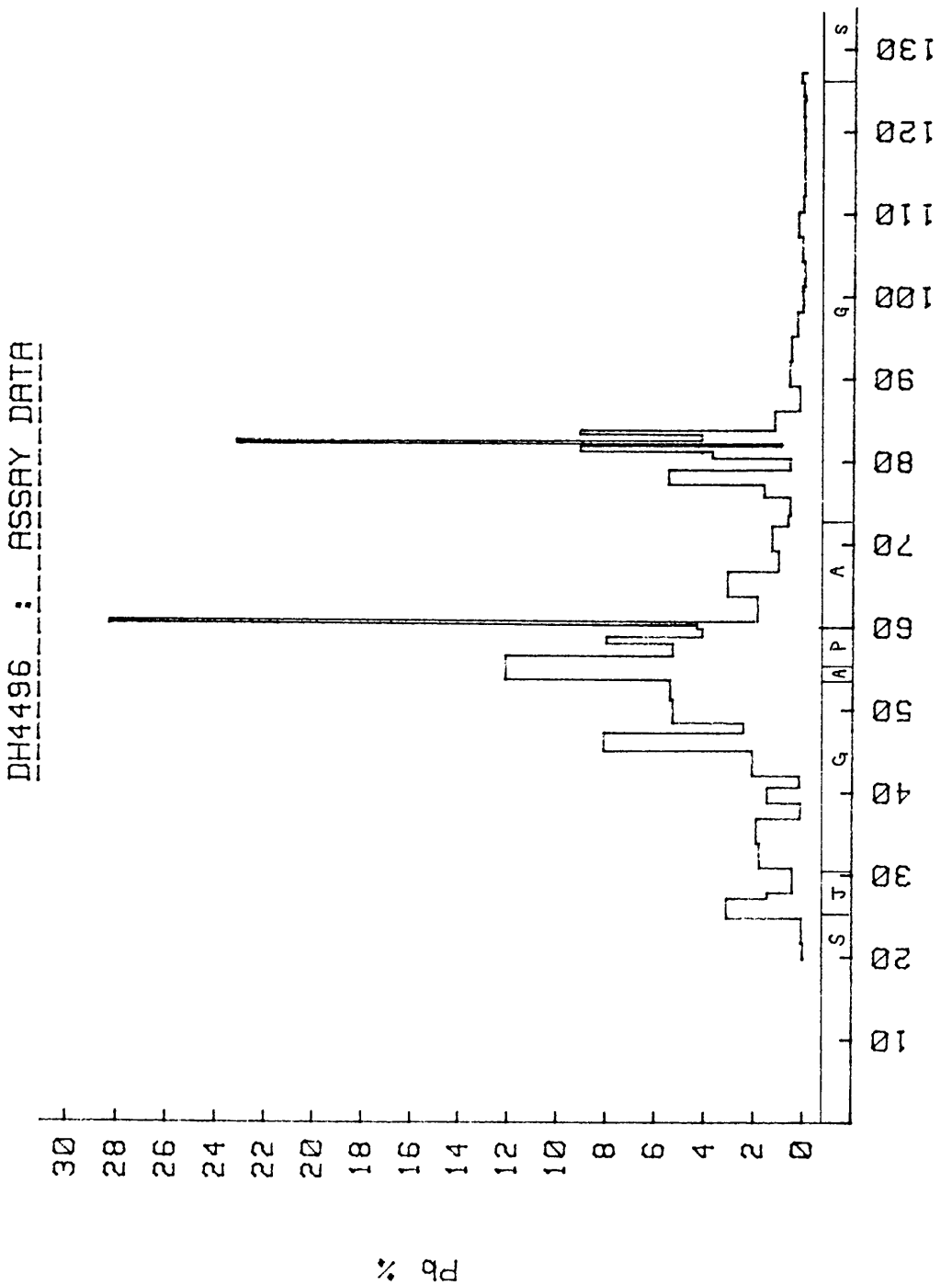

Appendix 4B cont.

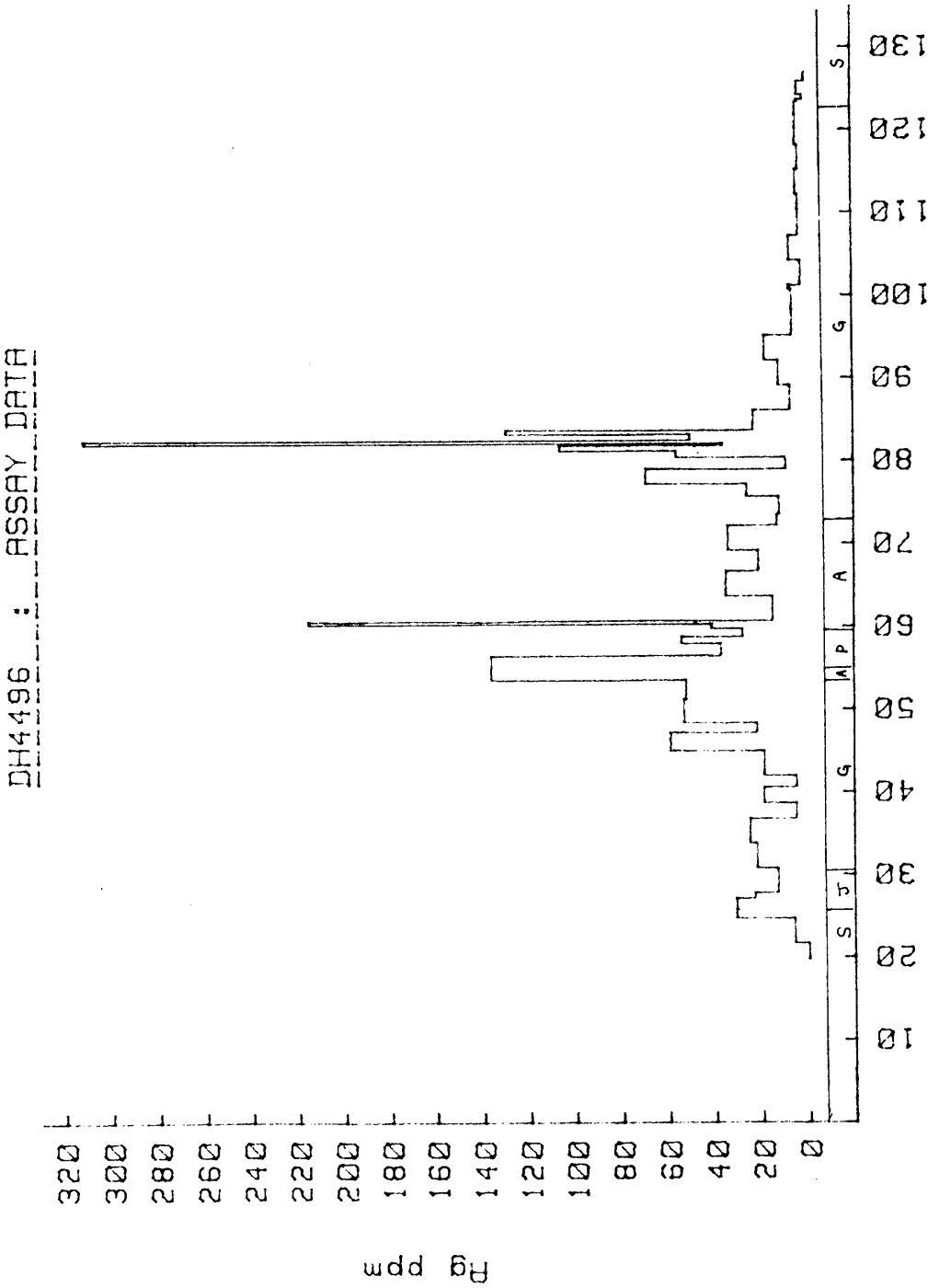

Appendix 4B cont.

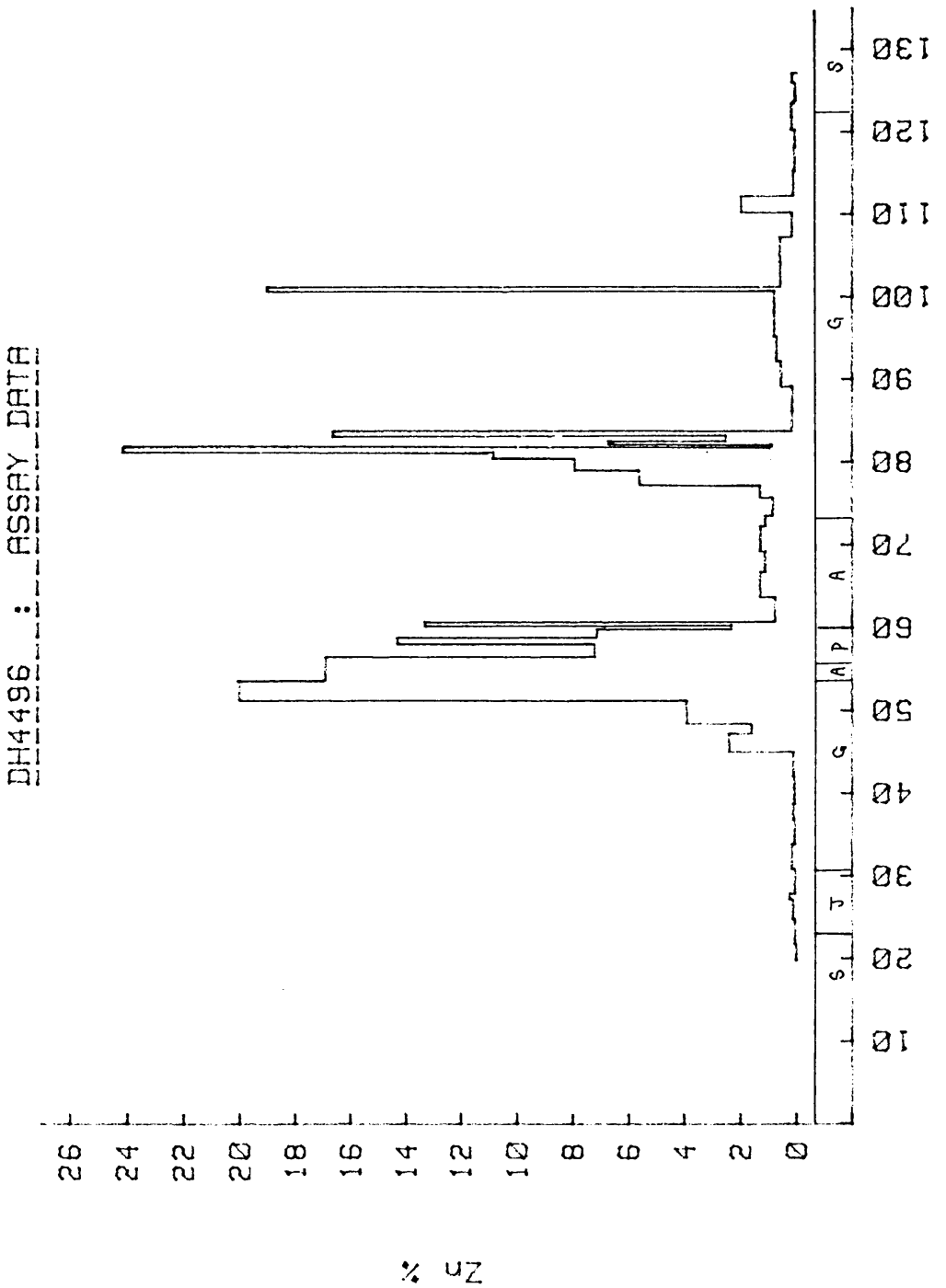

Appendix 4B cont.

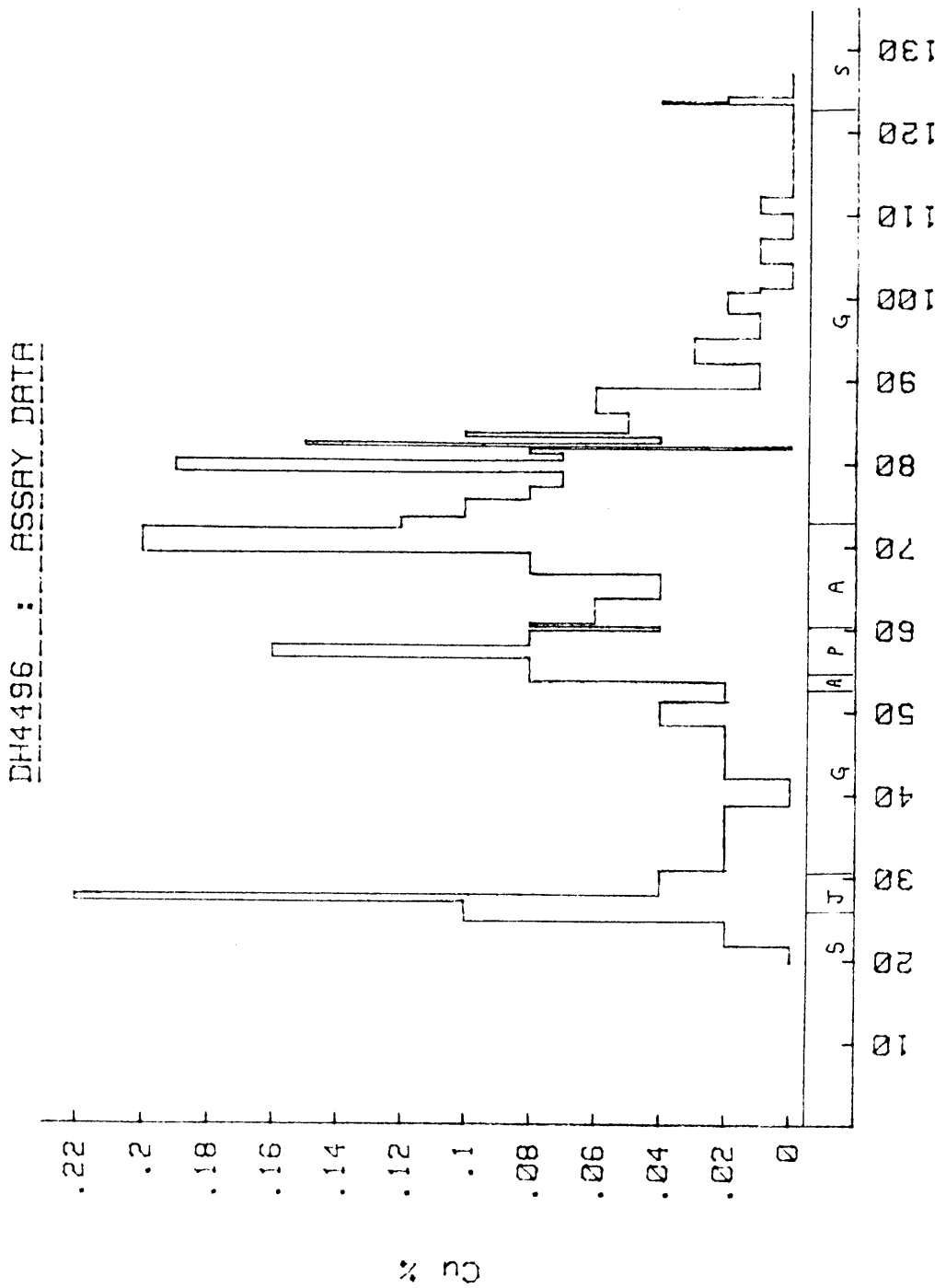

Appendix 4B cont.

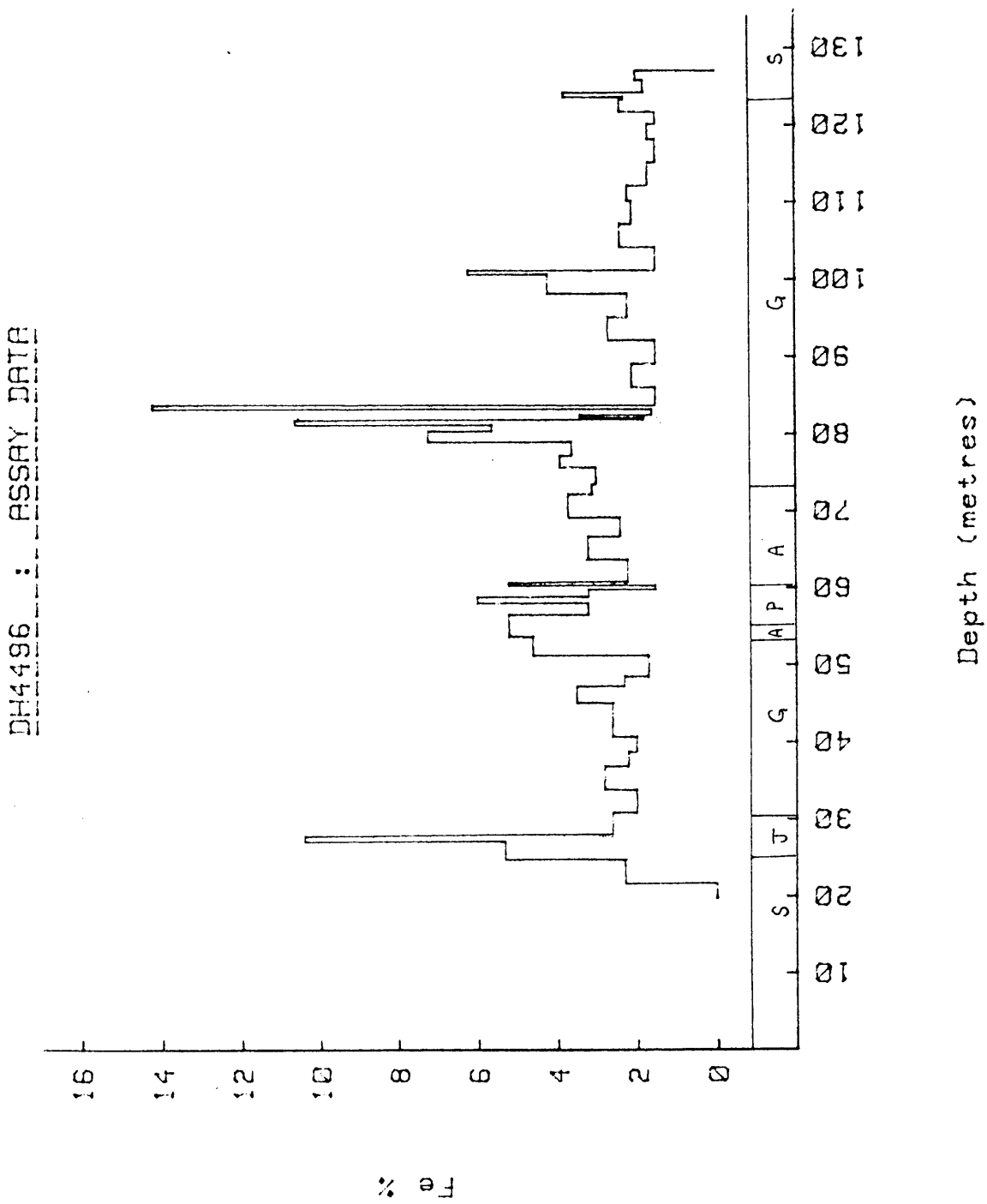

Appendix 4B cont.

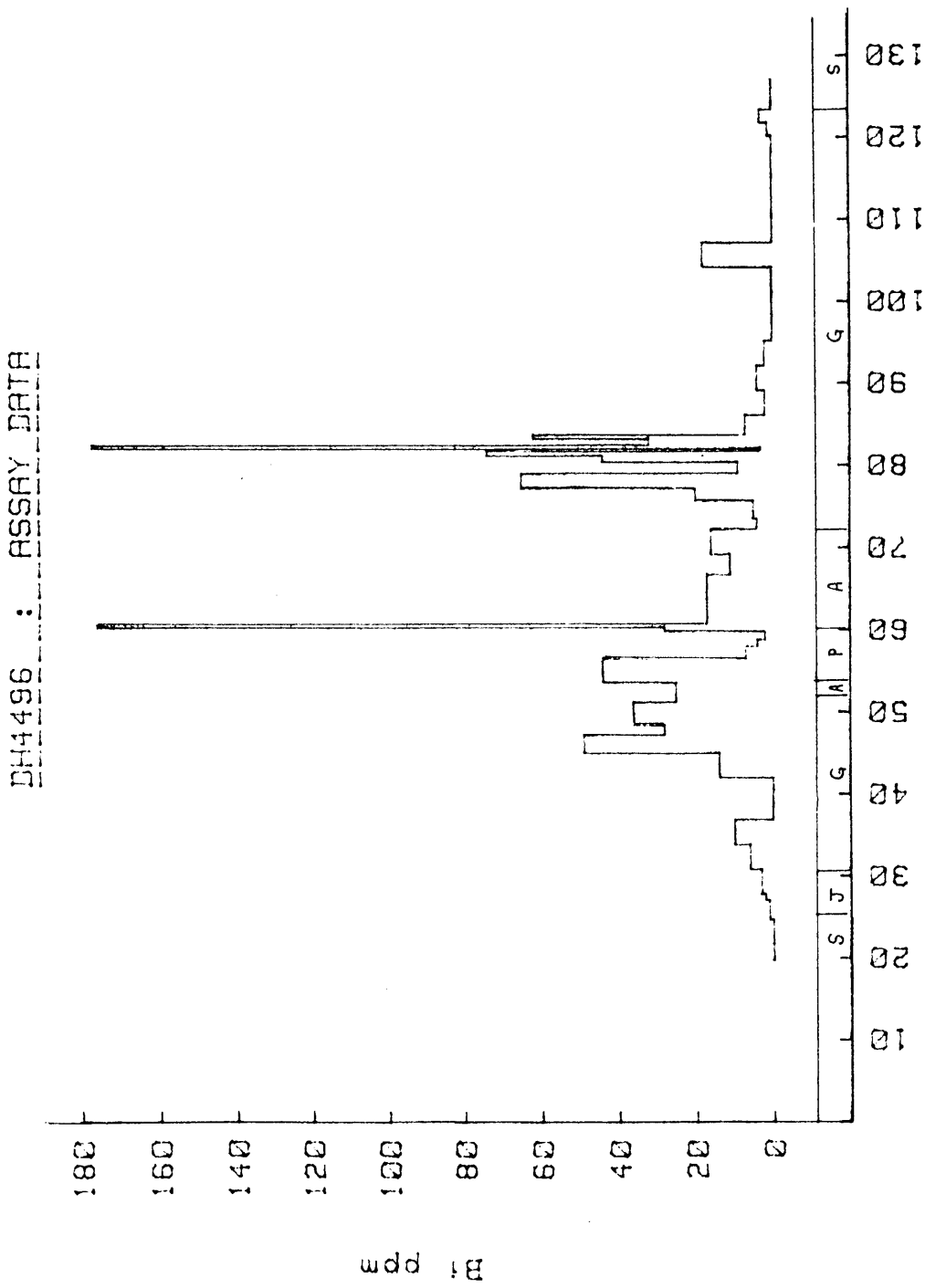

Appendix 4B cont.

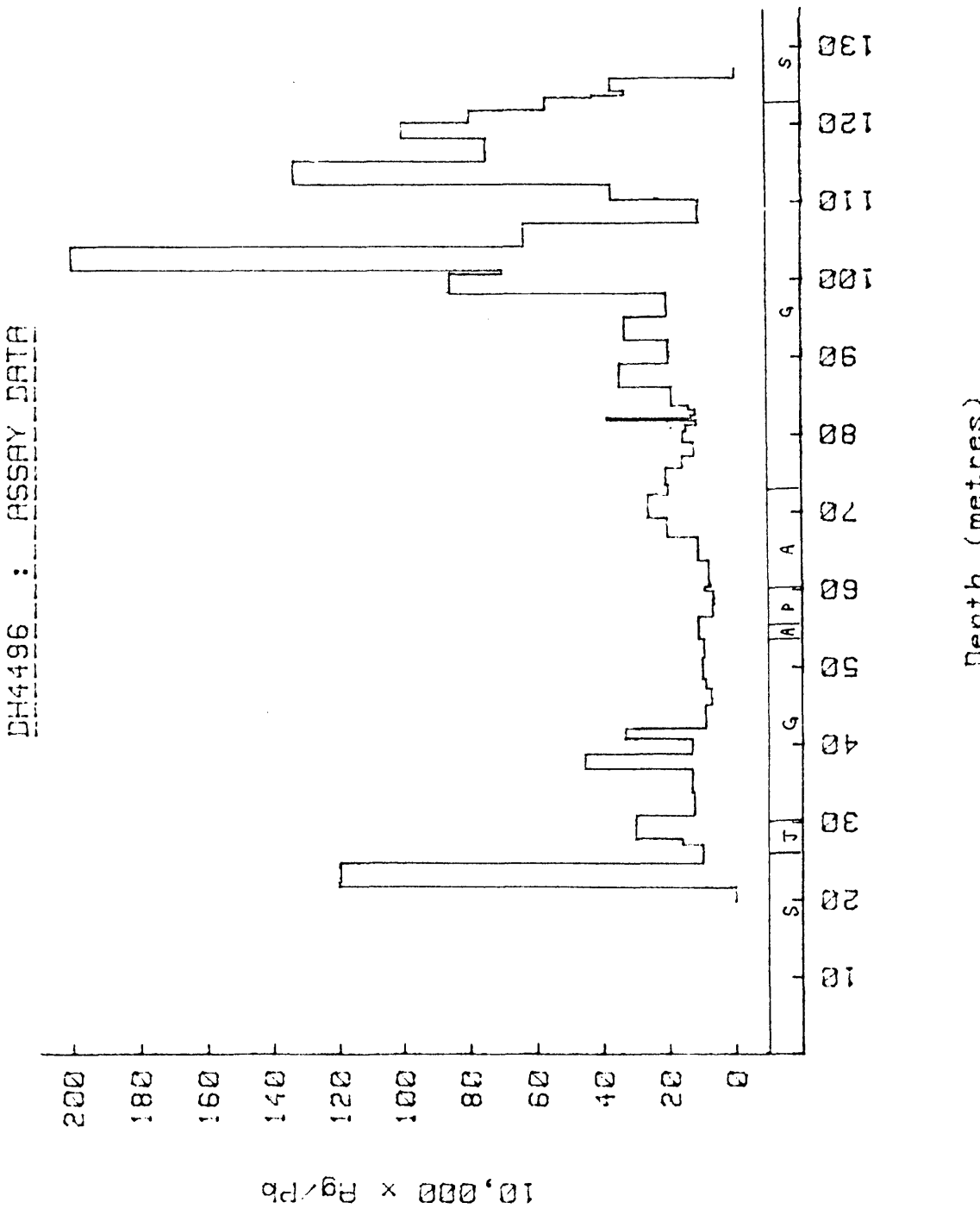

Appendix 4B cont.

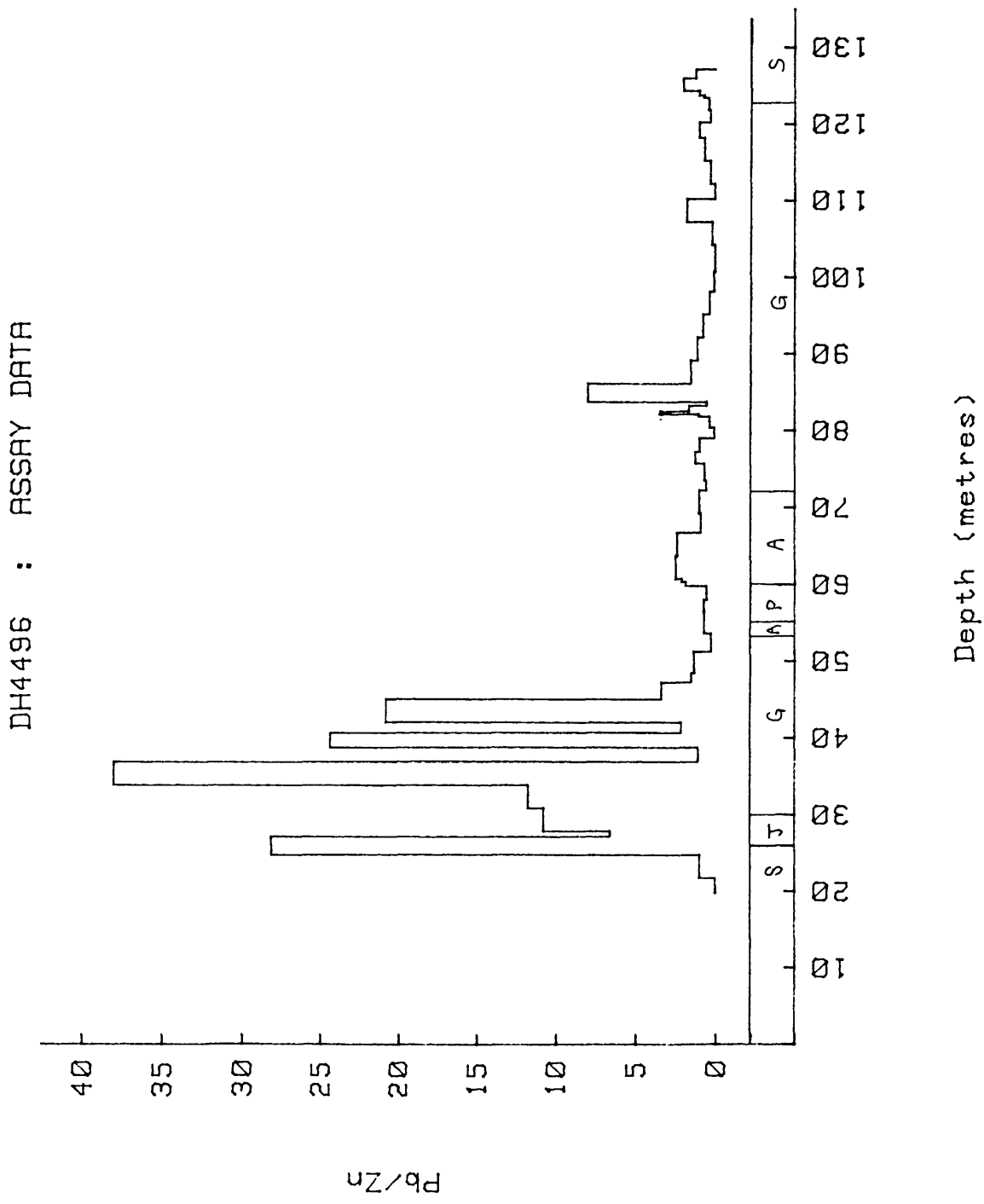

Appendix 4B cont.

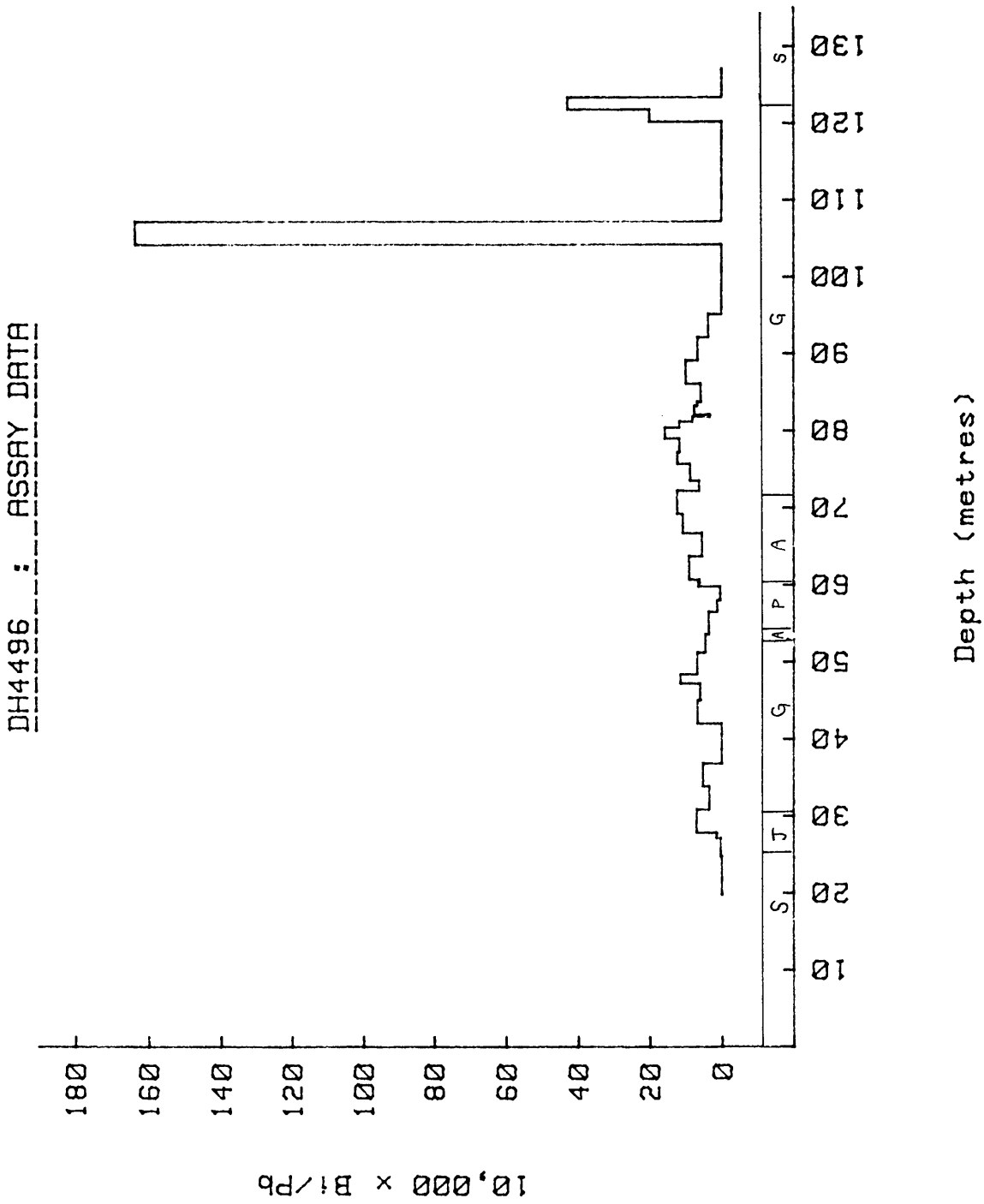

Appendix 4B cont.

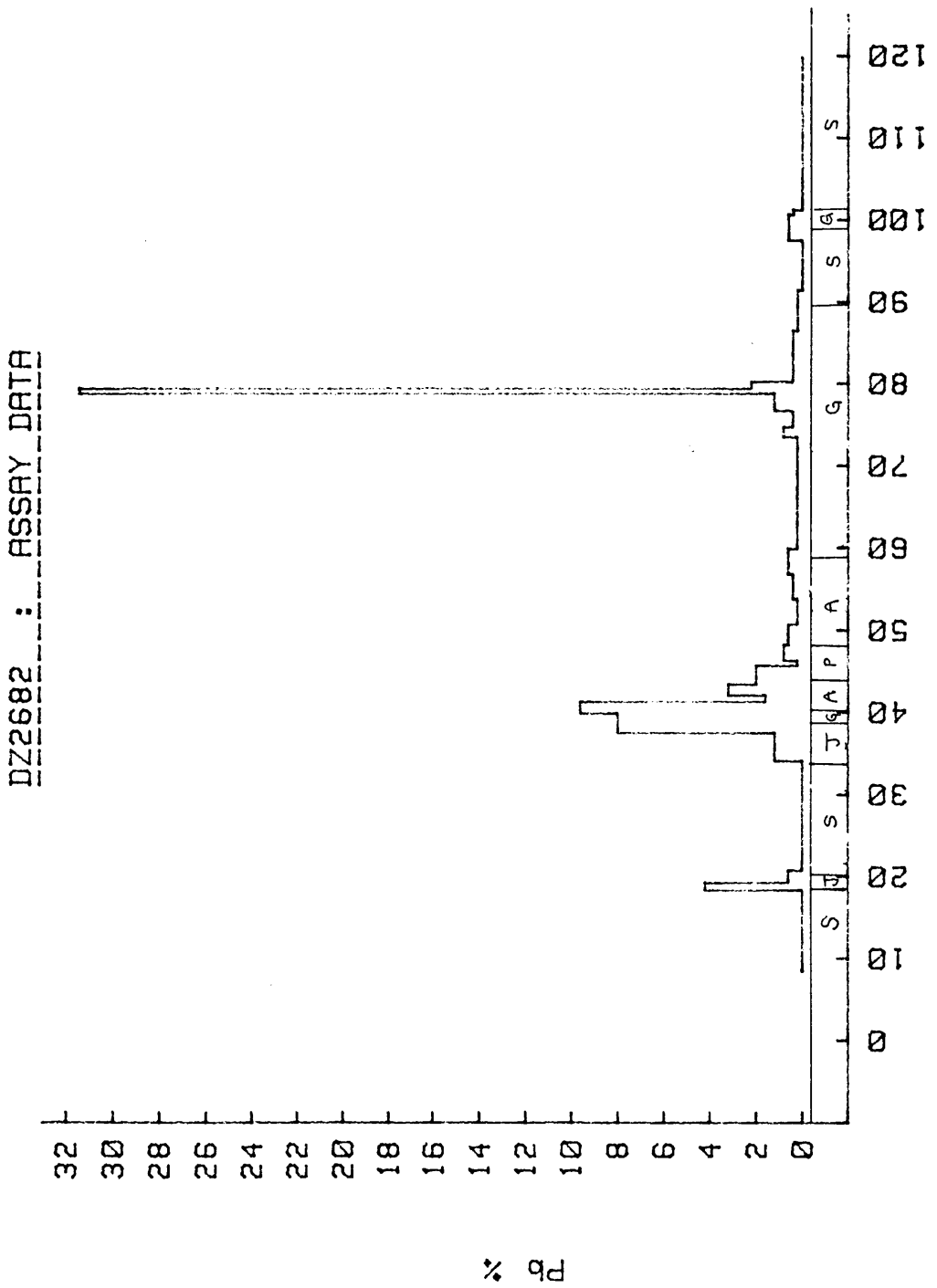

Appendix 4B cont.

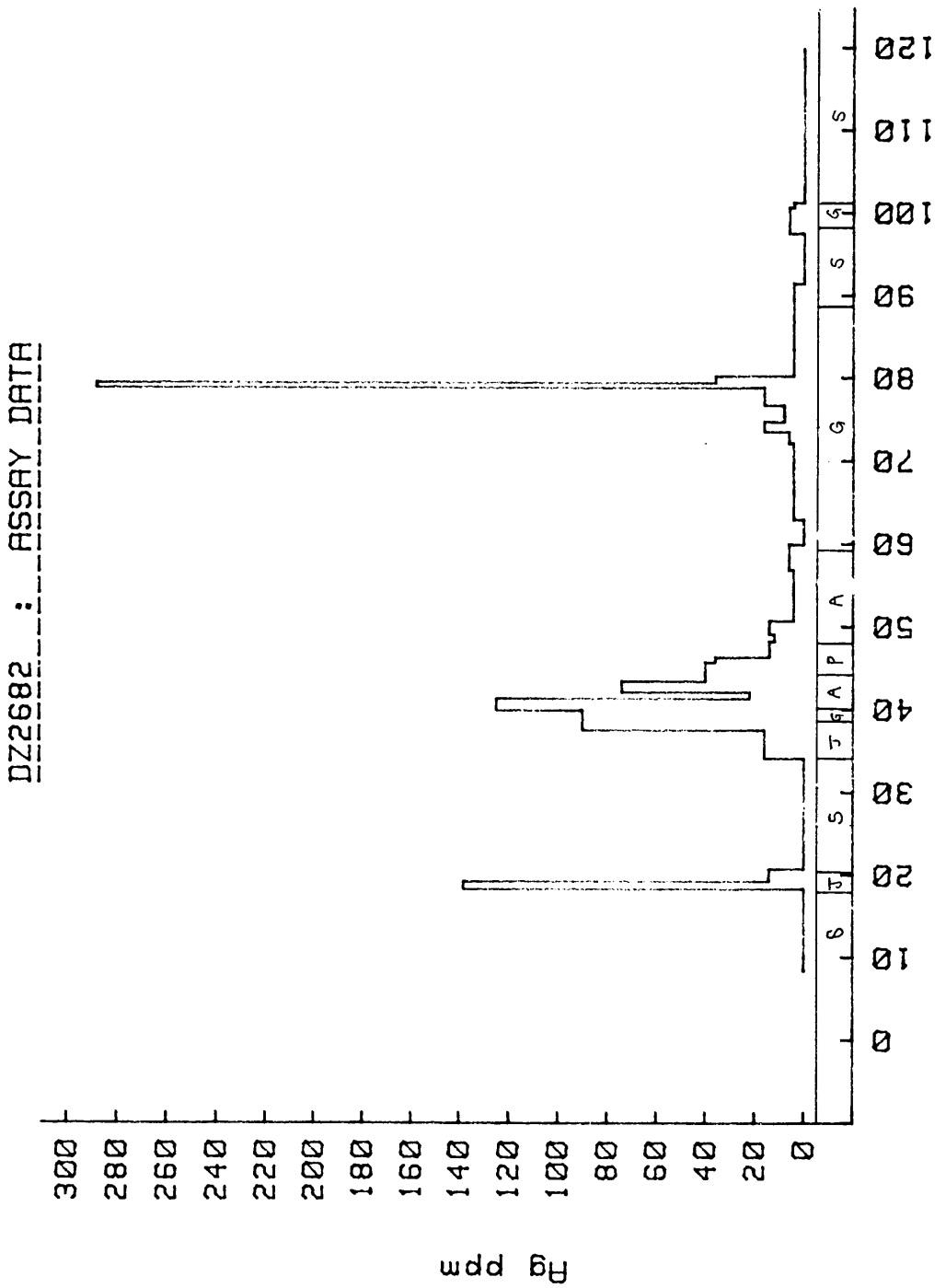

Appendix 4B cont.

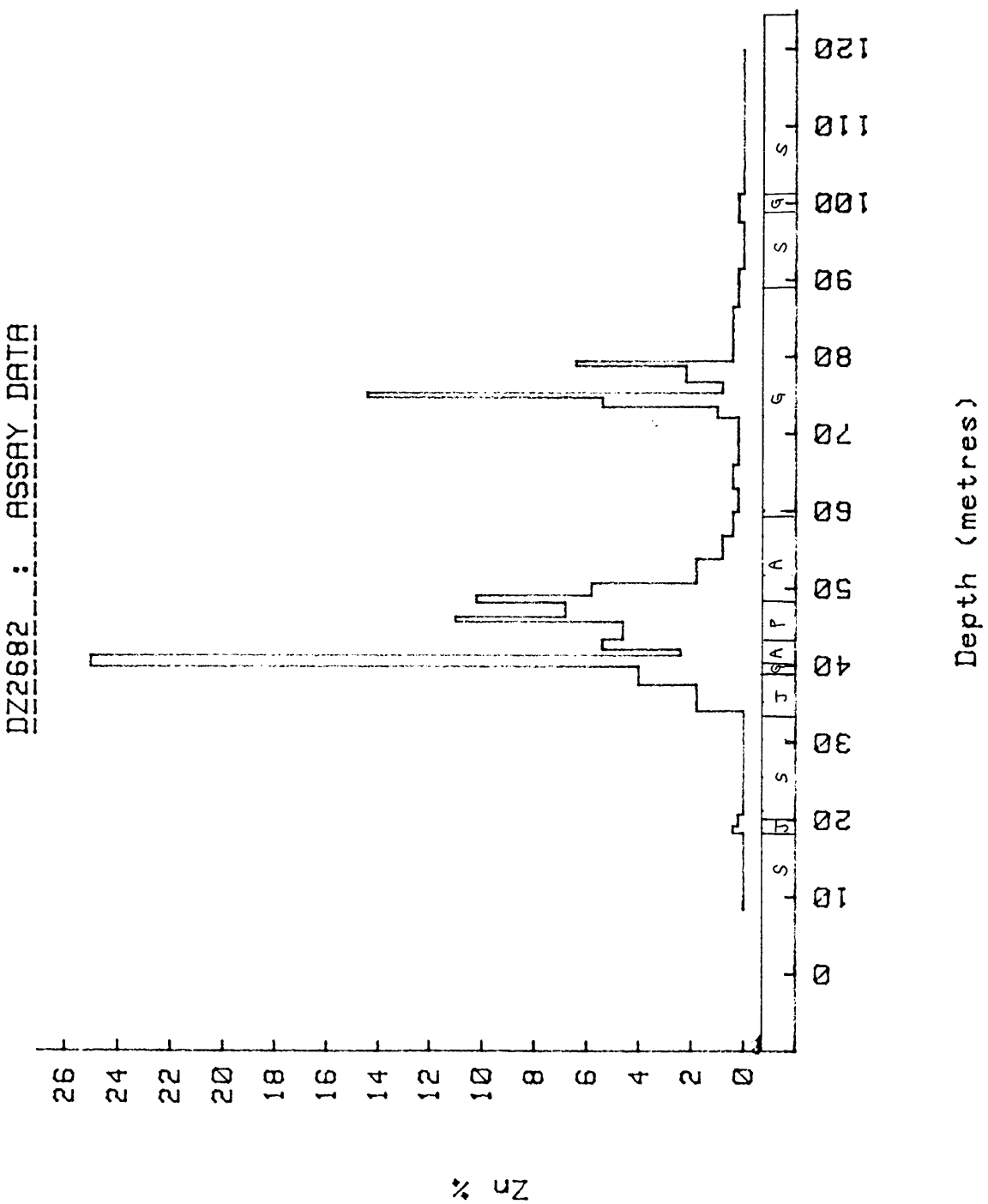

Appendix 4B cont.

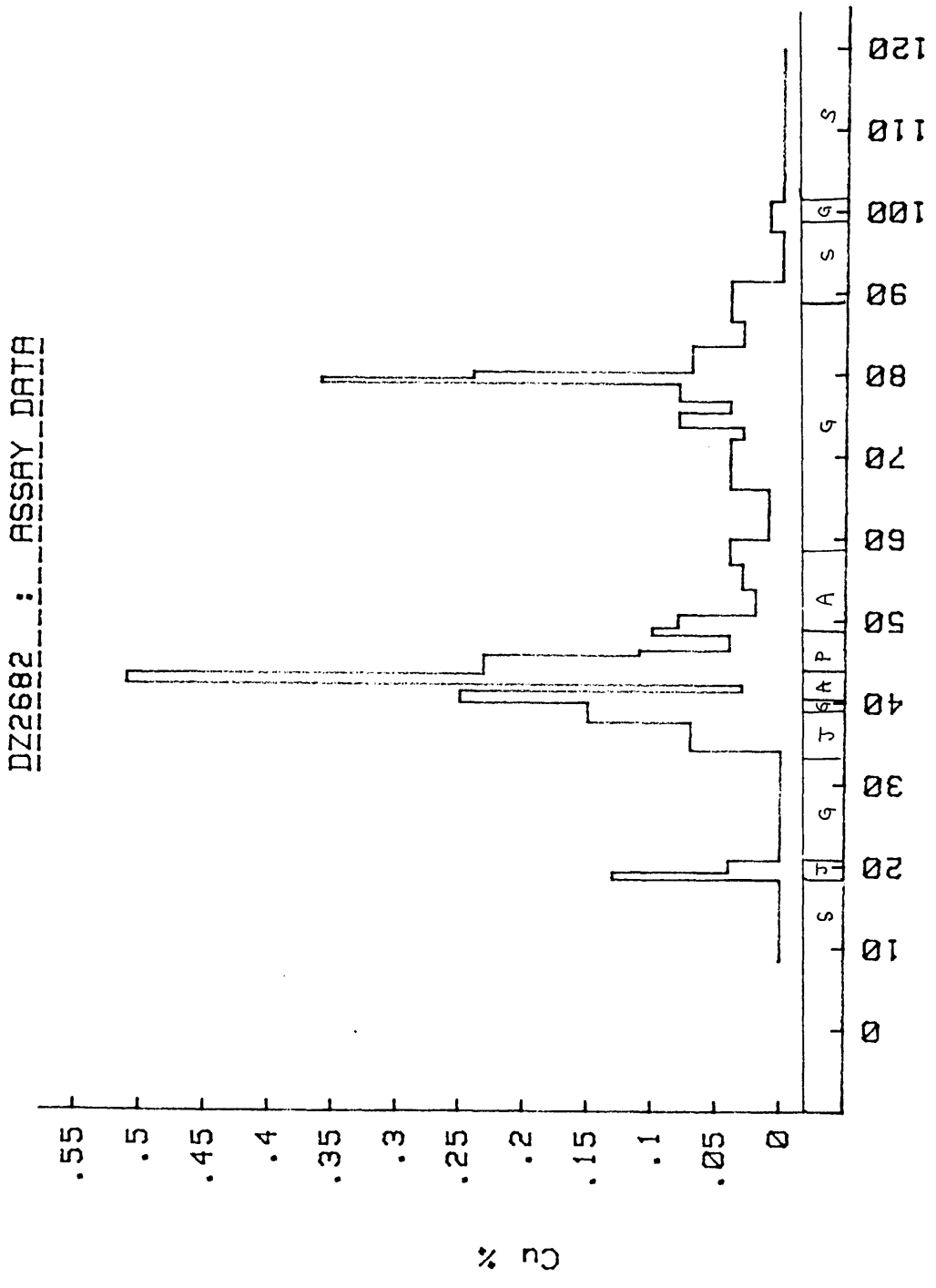

Appendix 4B cont.

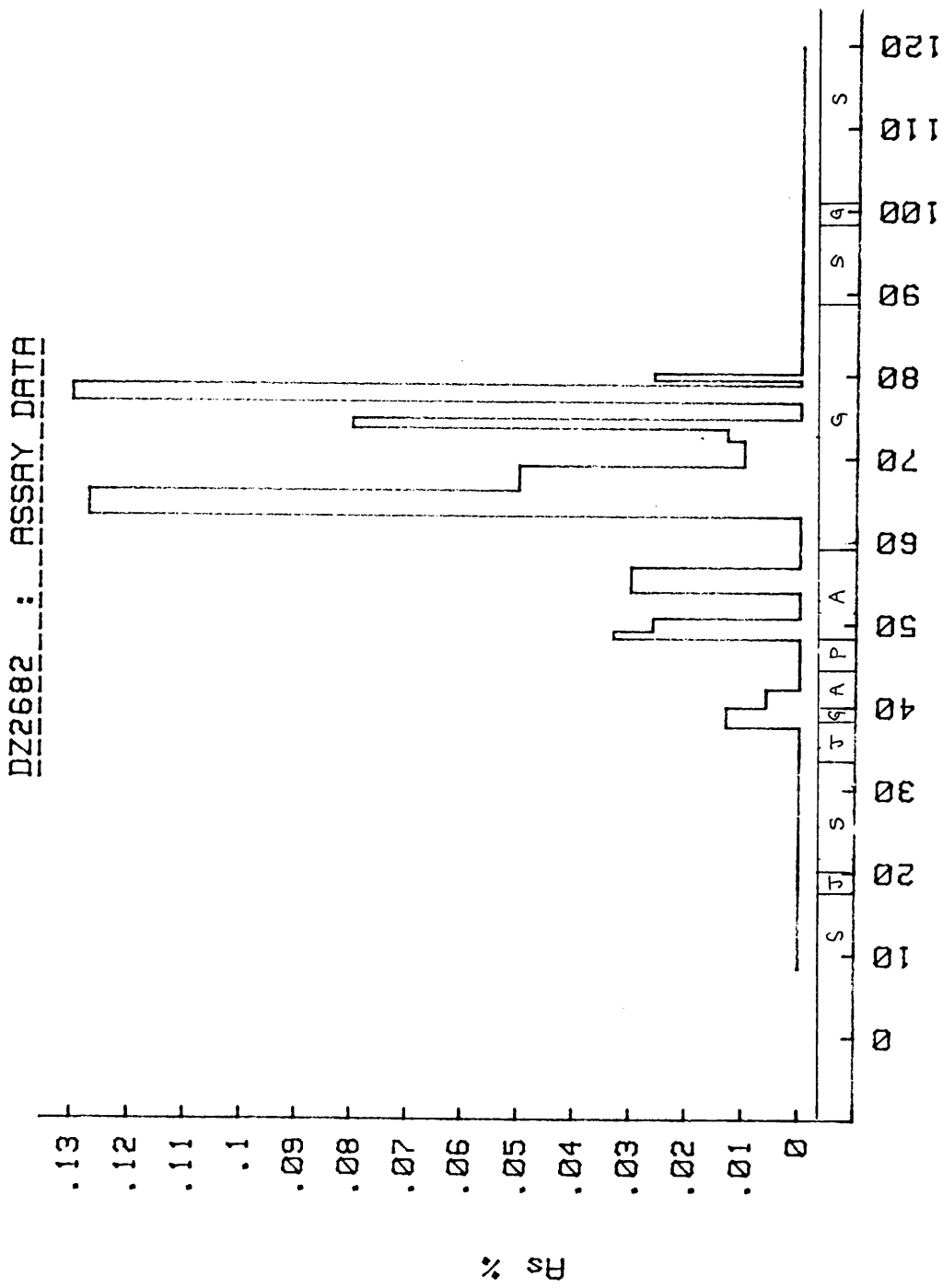

Appendix 4B cont.

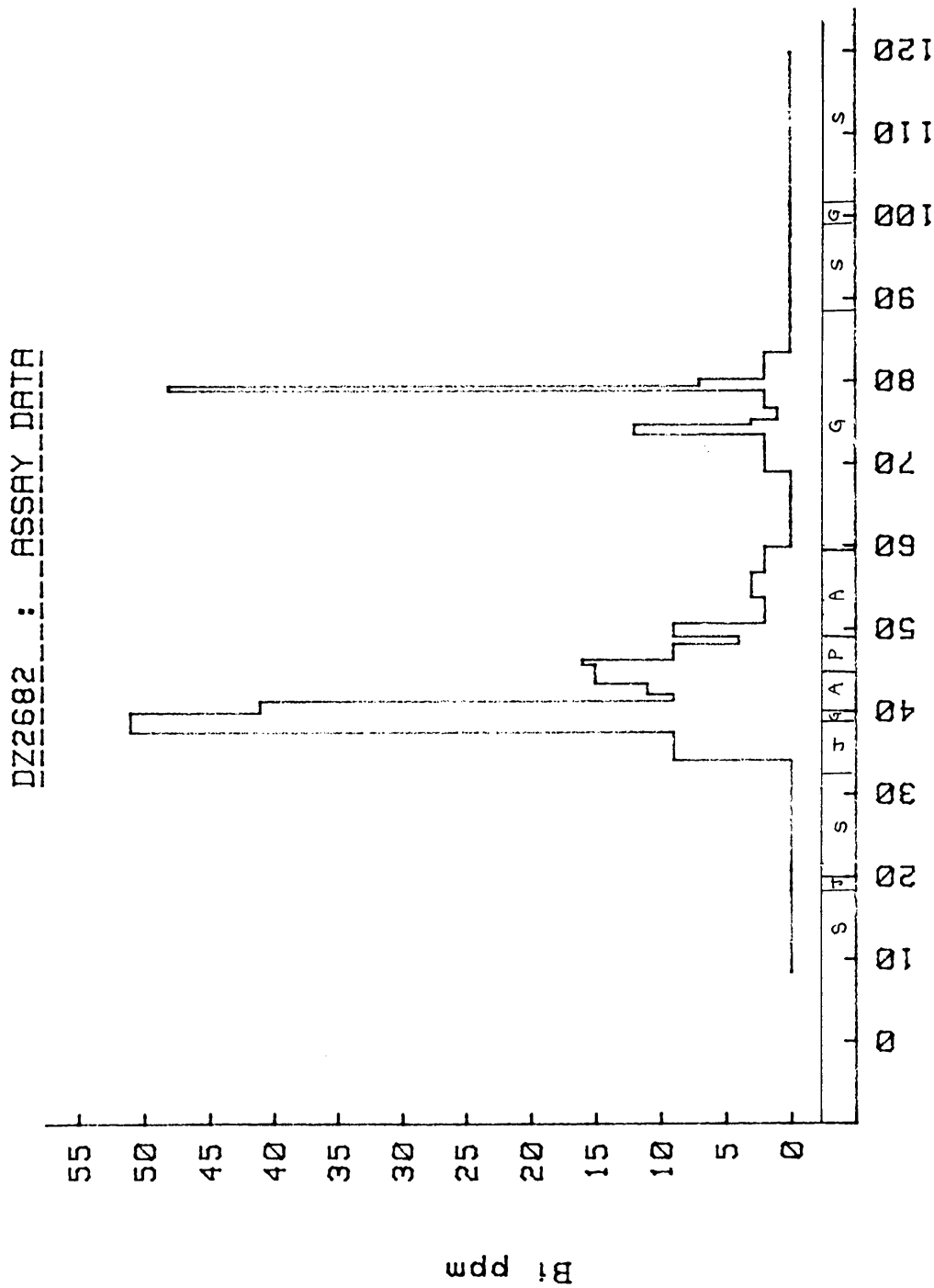

Appendix 4B cont.

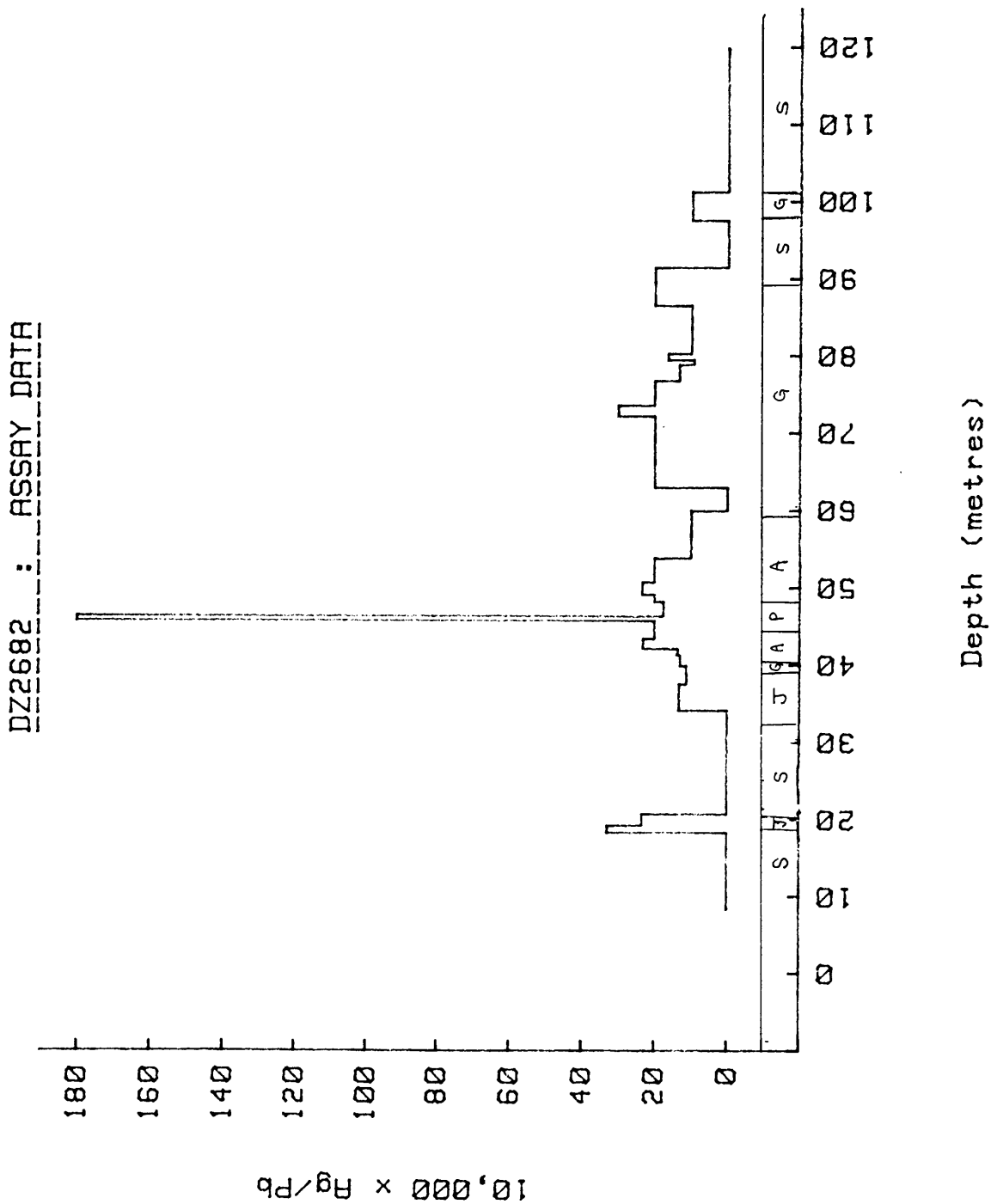

Appendix 4B cont.

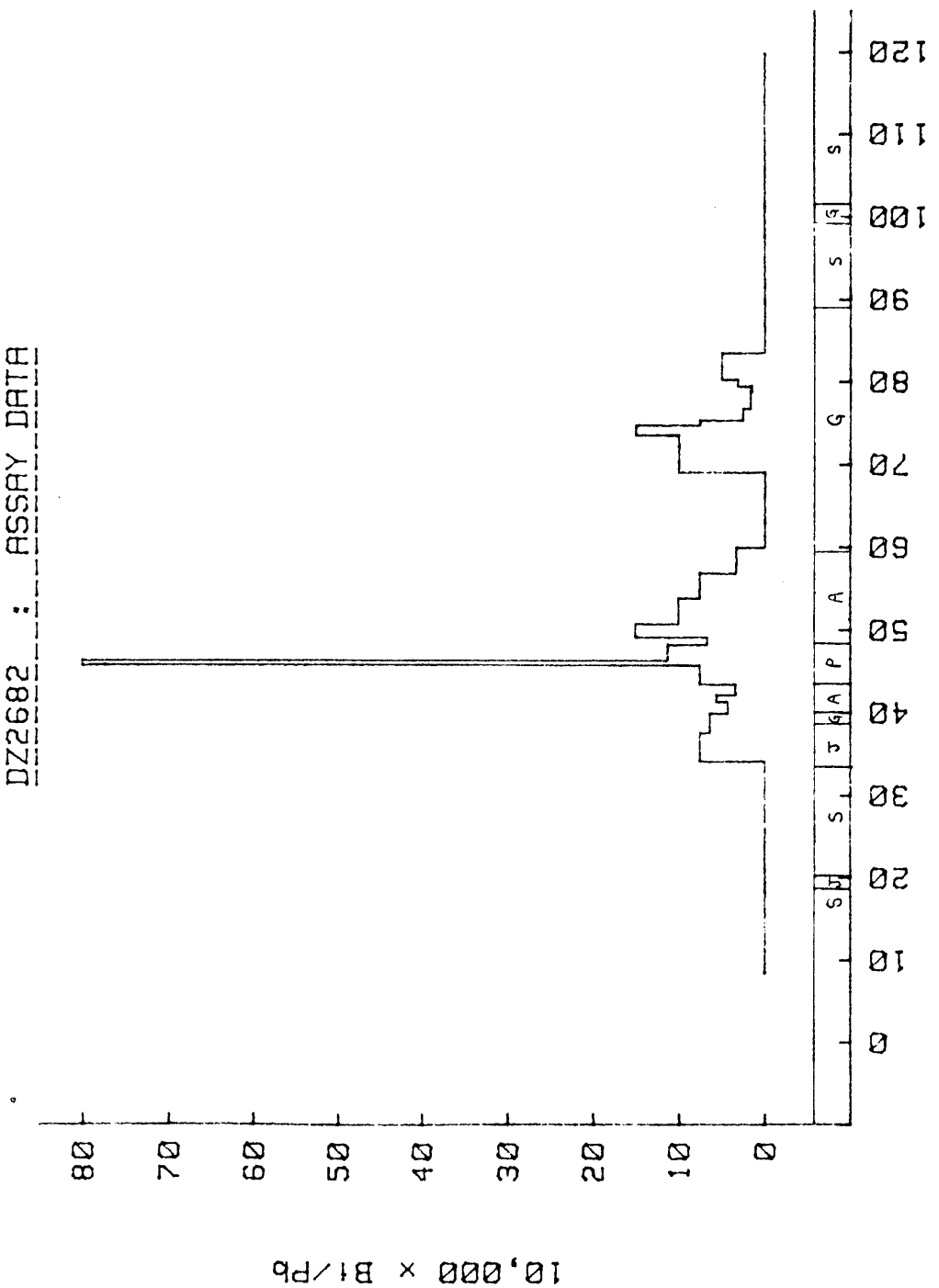

Appendix 4B cont.

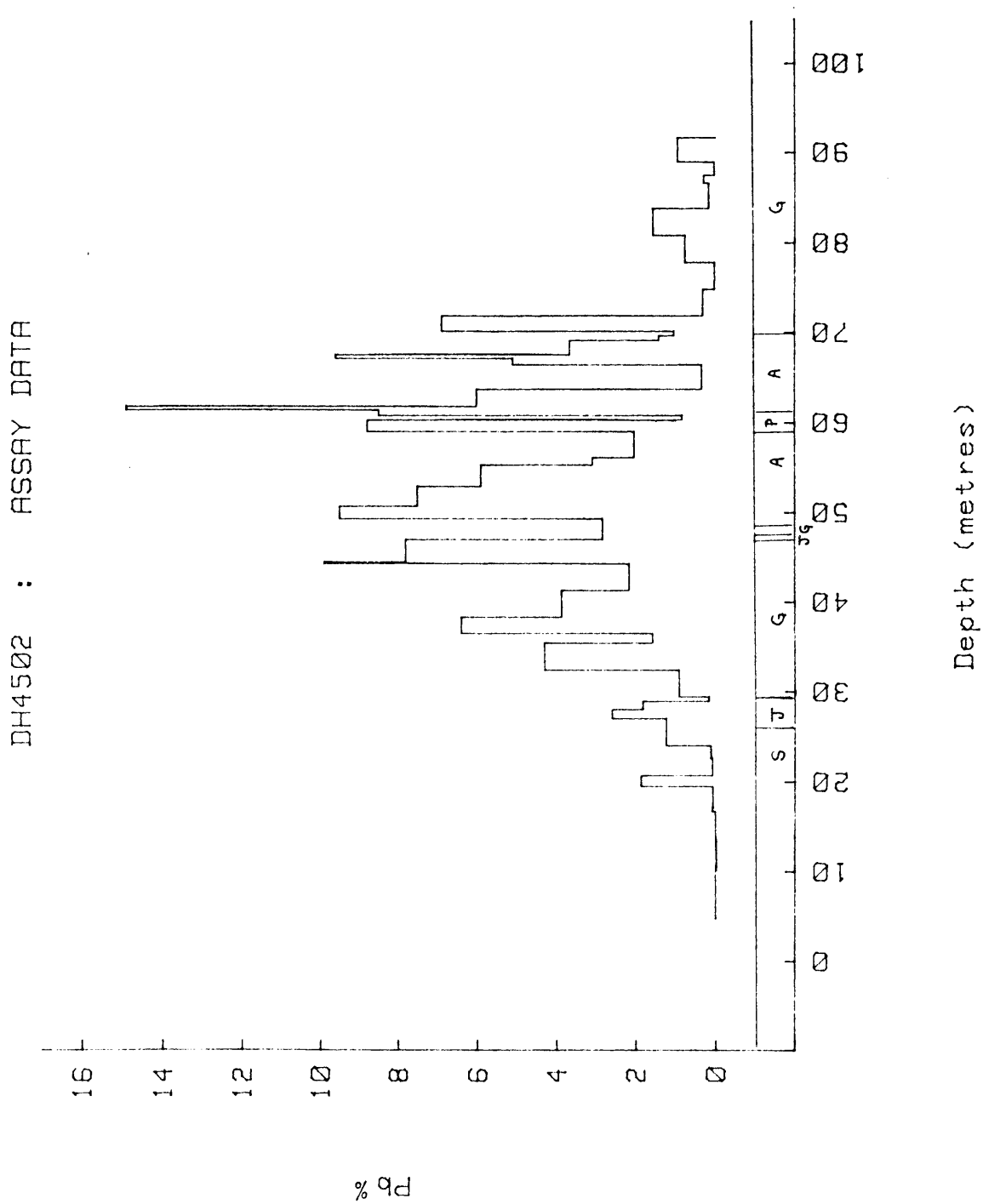

Appendix 4B cont.

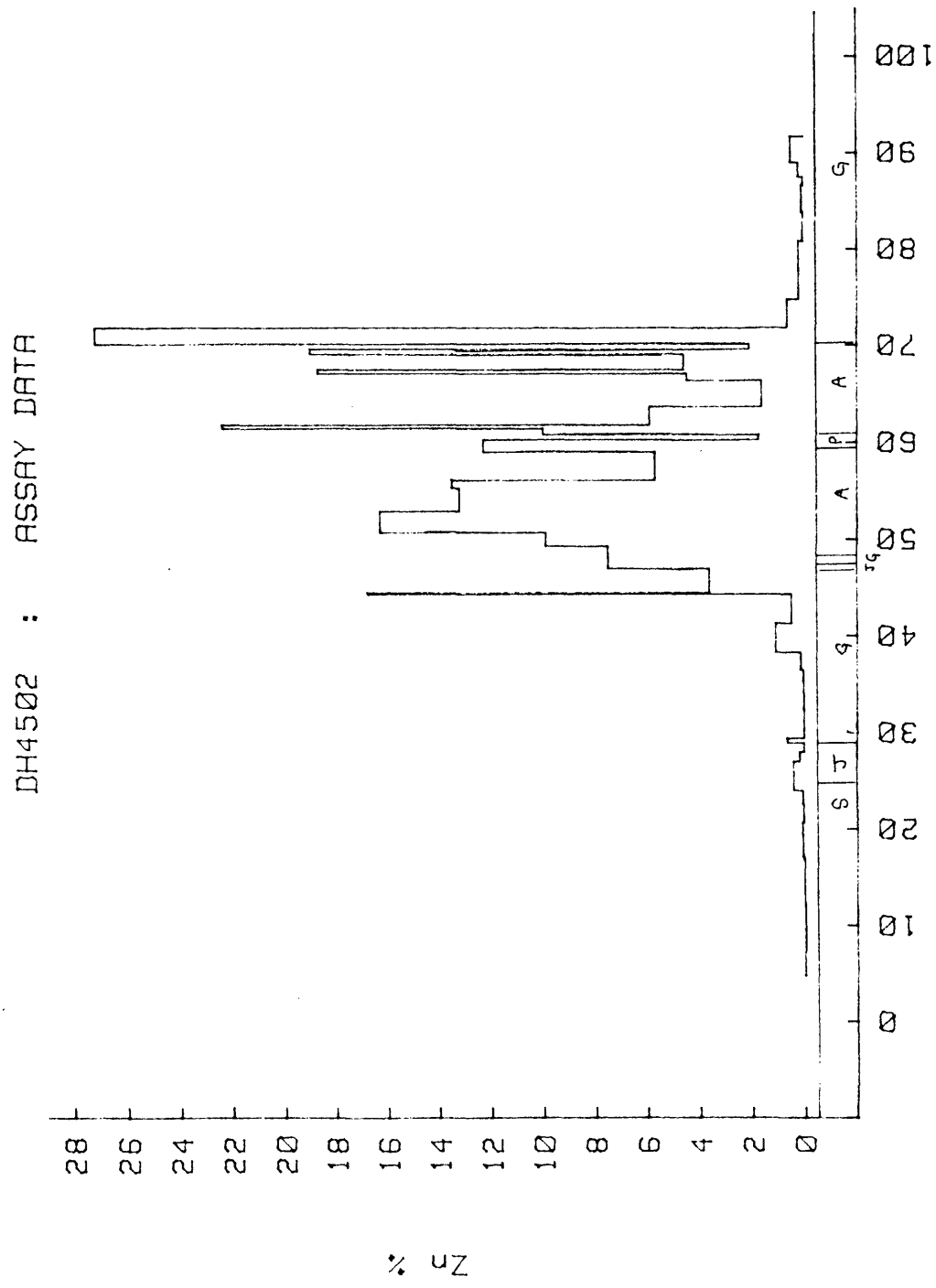

Appendix 4B cont.

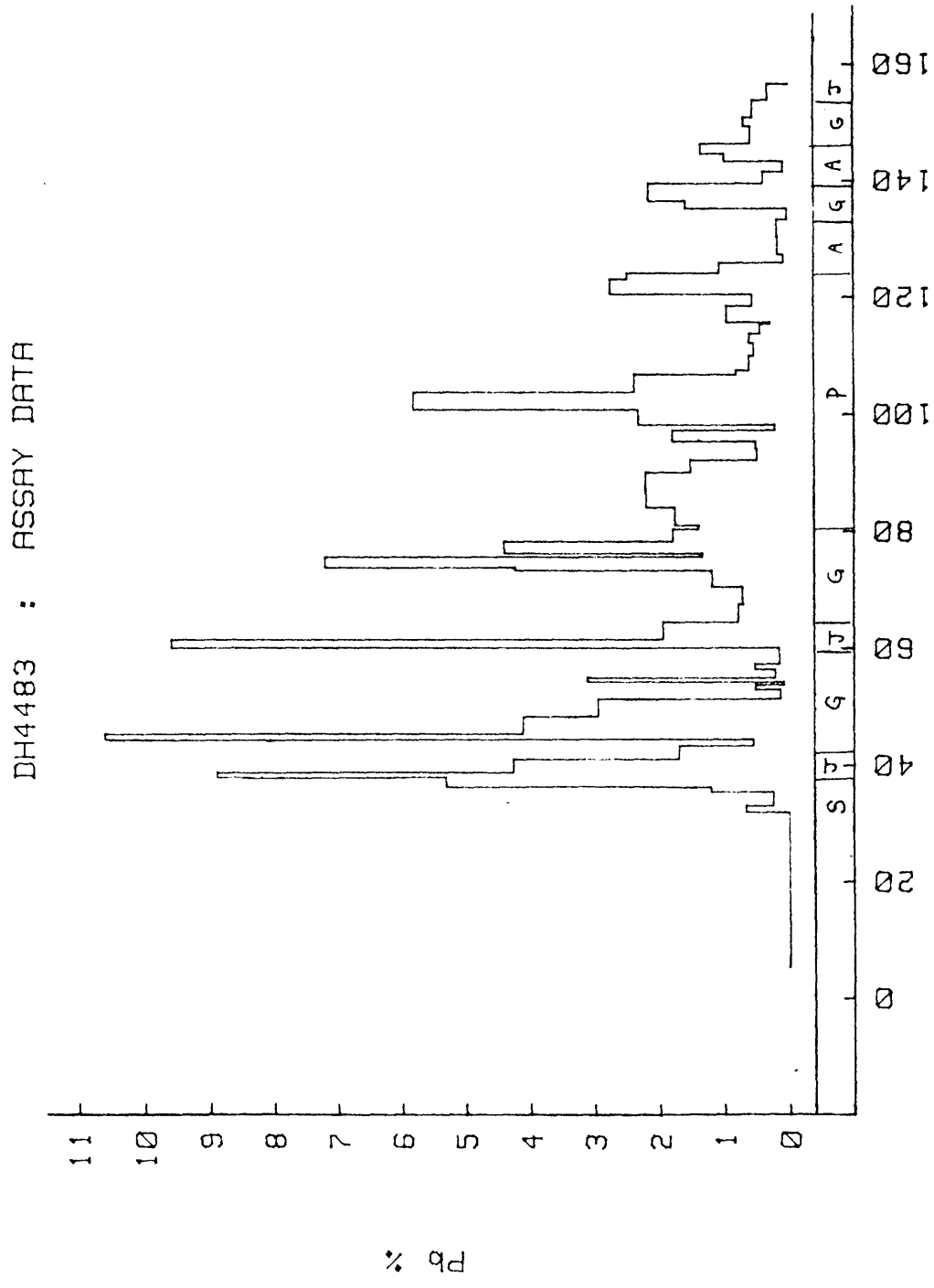

Appendix 4B cont.

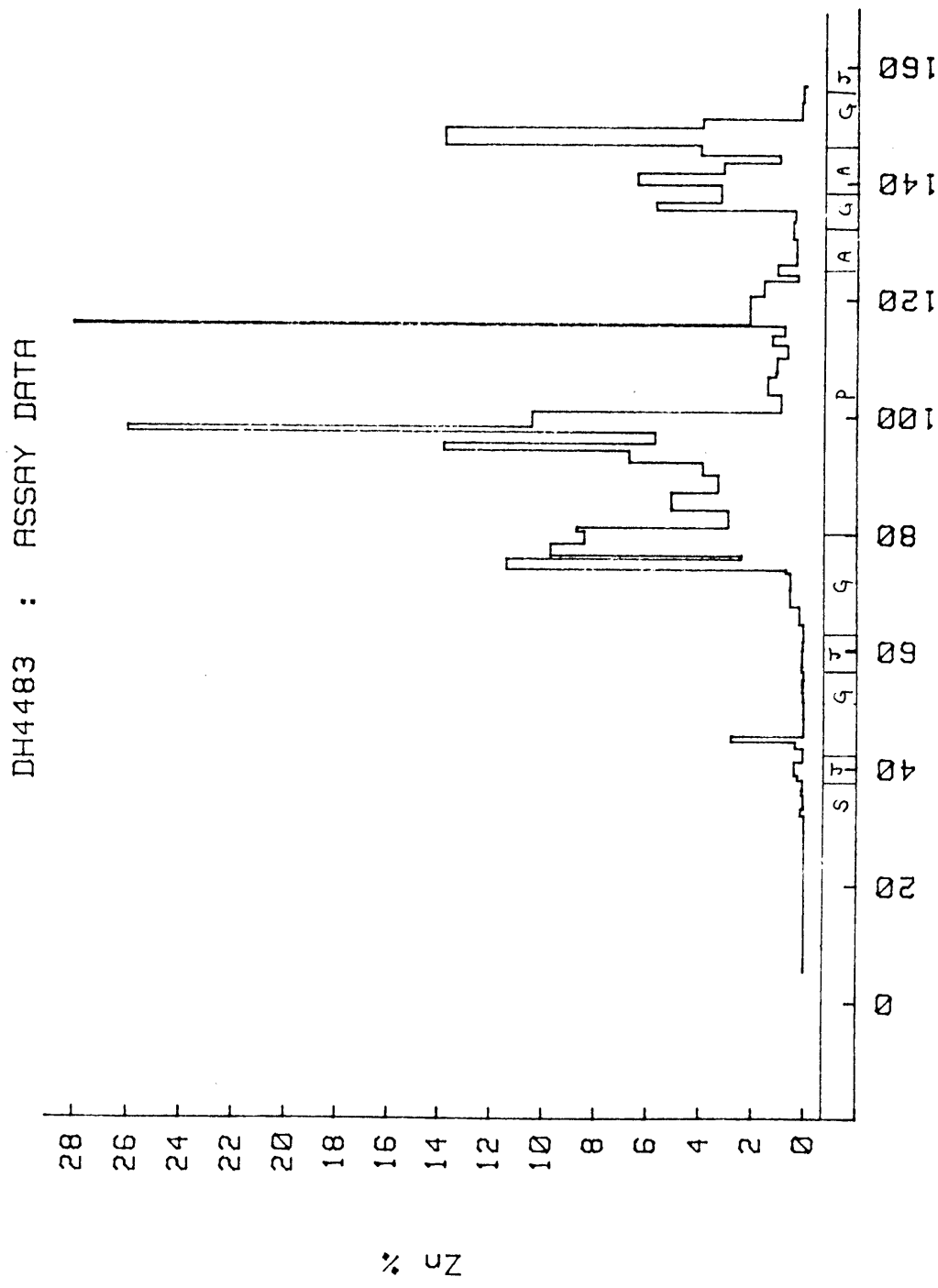

Appendix 4B cont.

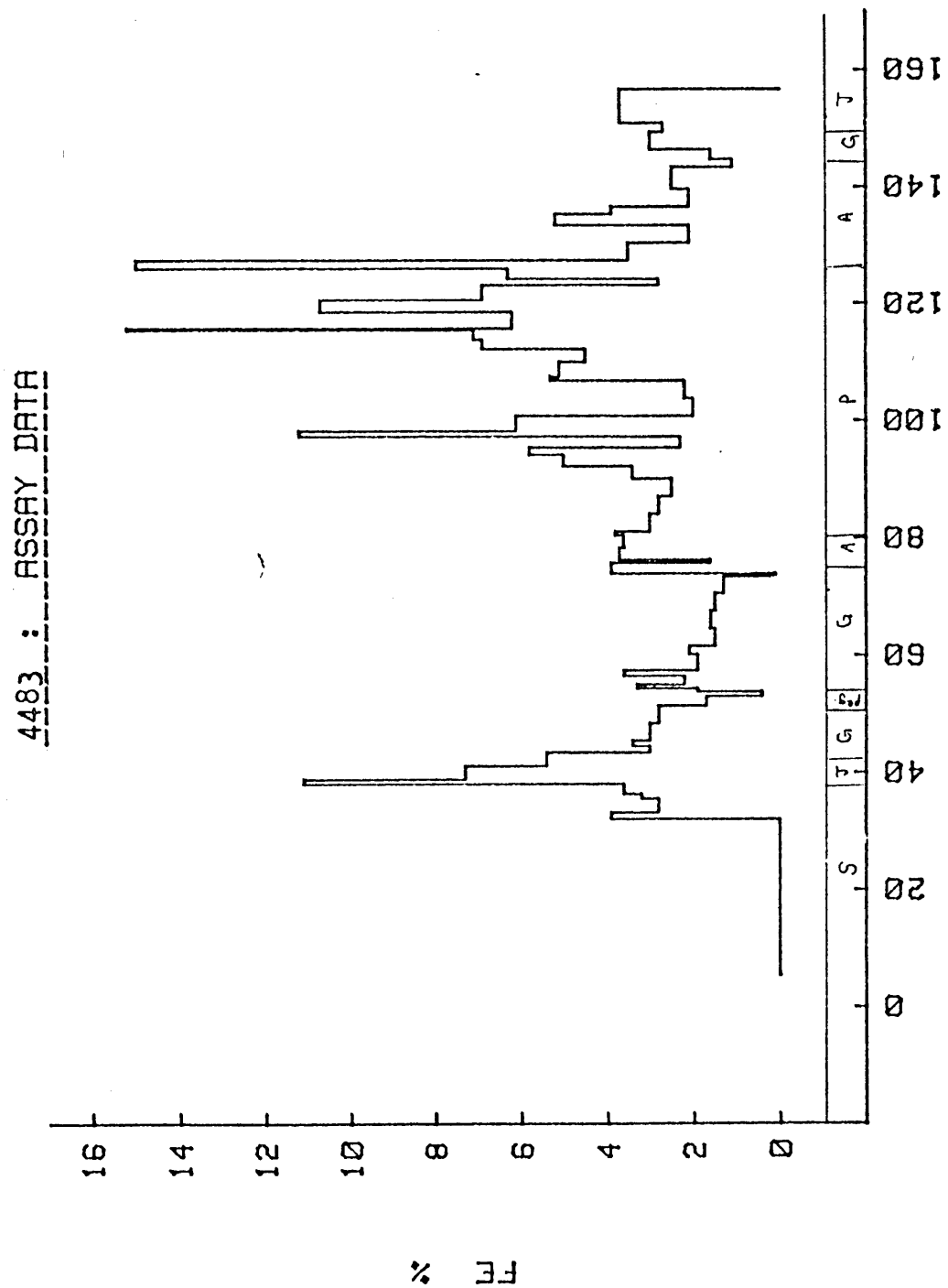

Appendix 4B cont.

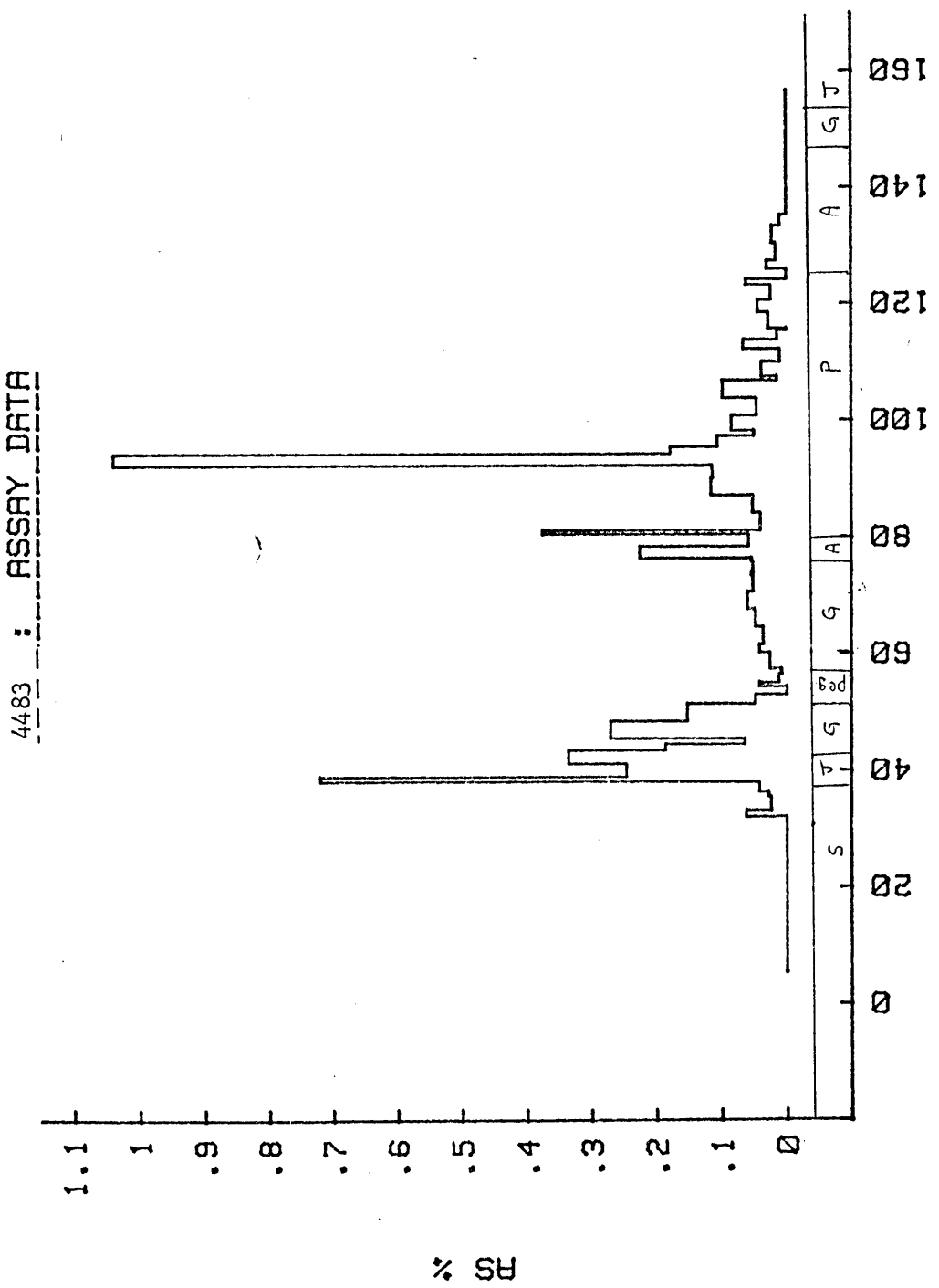

Appendix 4C: Mineral Chemistry Trends

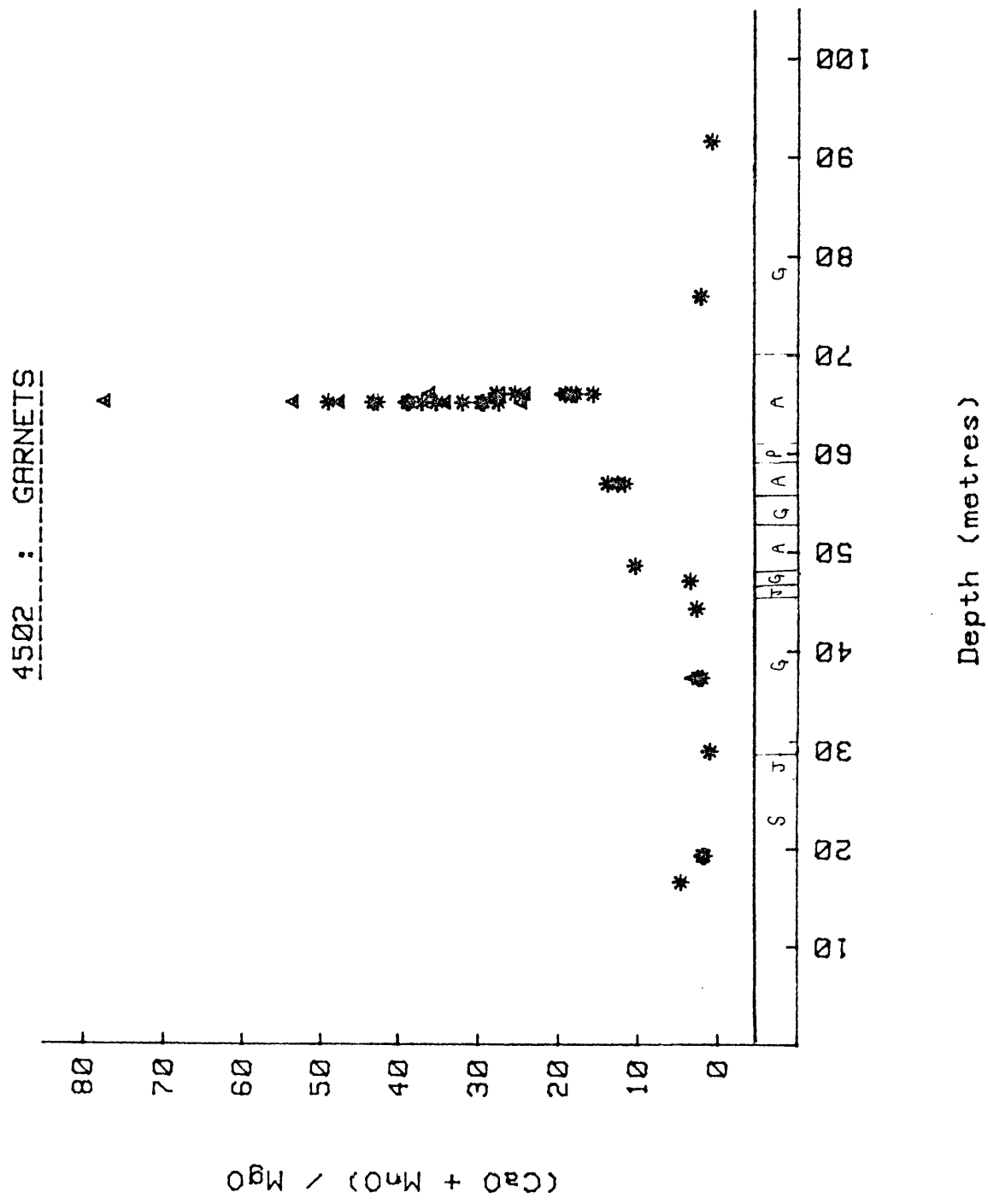

Appendix 4C cont.

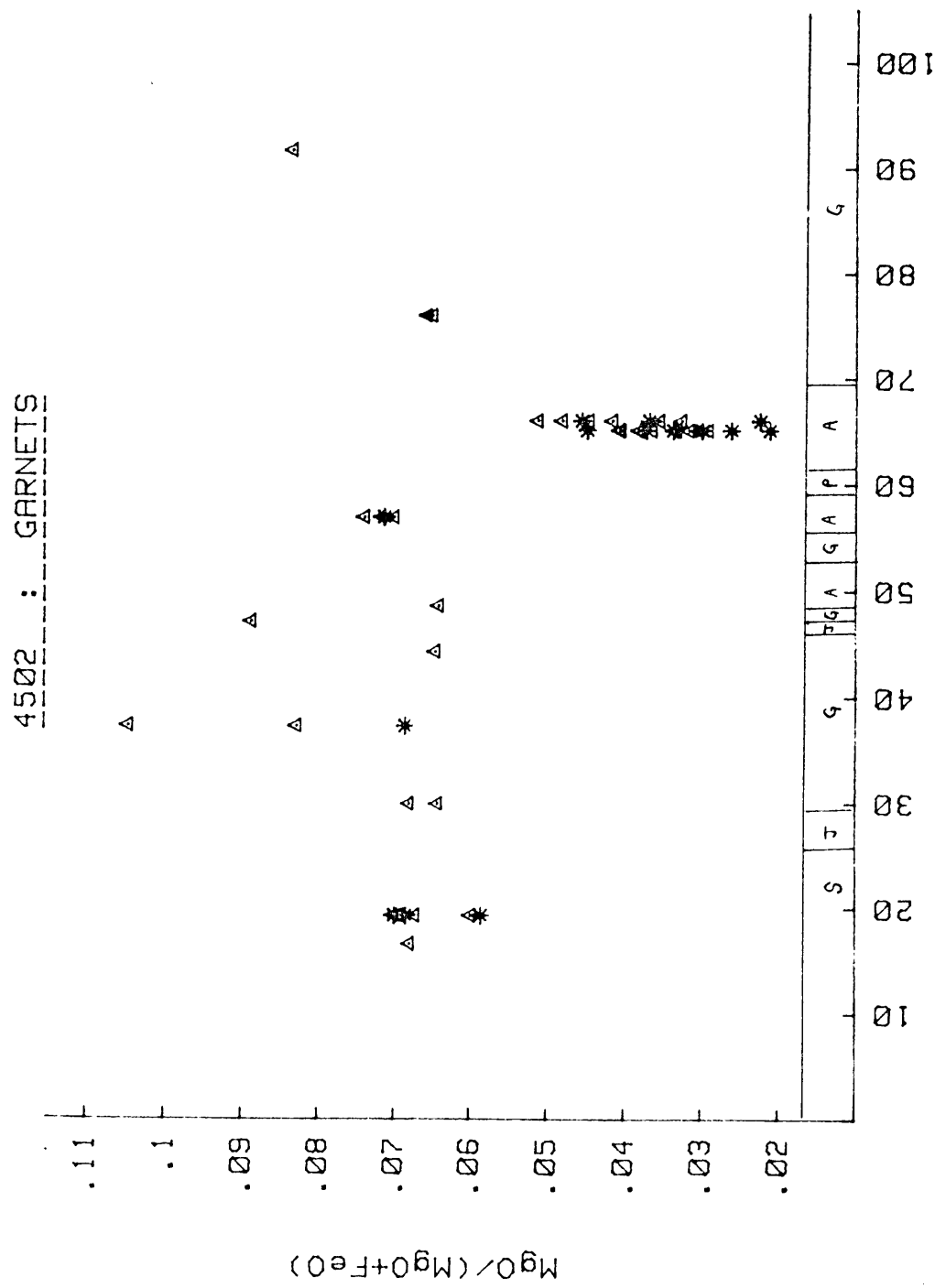

Appendix 4C cont.

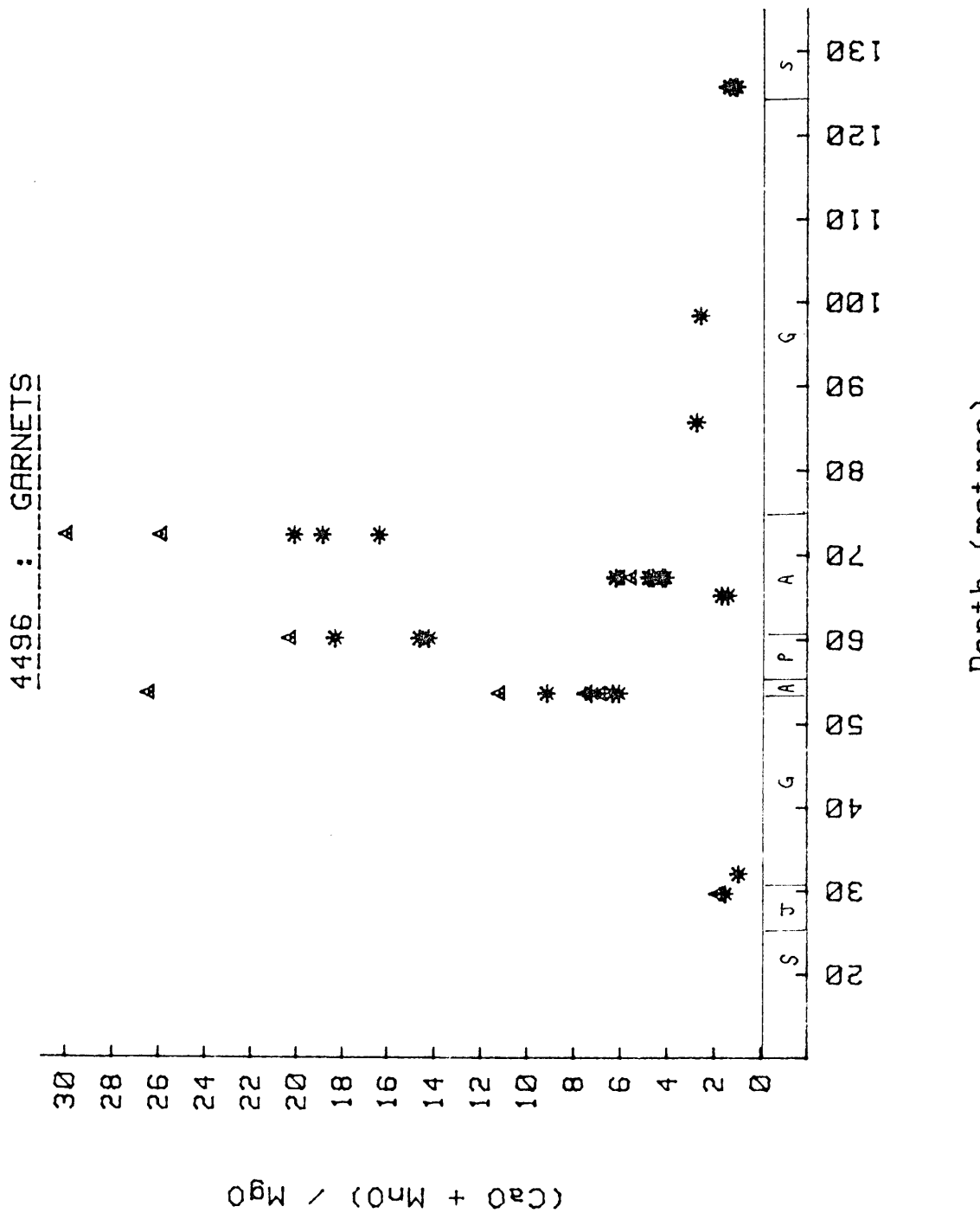

Appendix 4C cont.

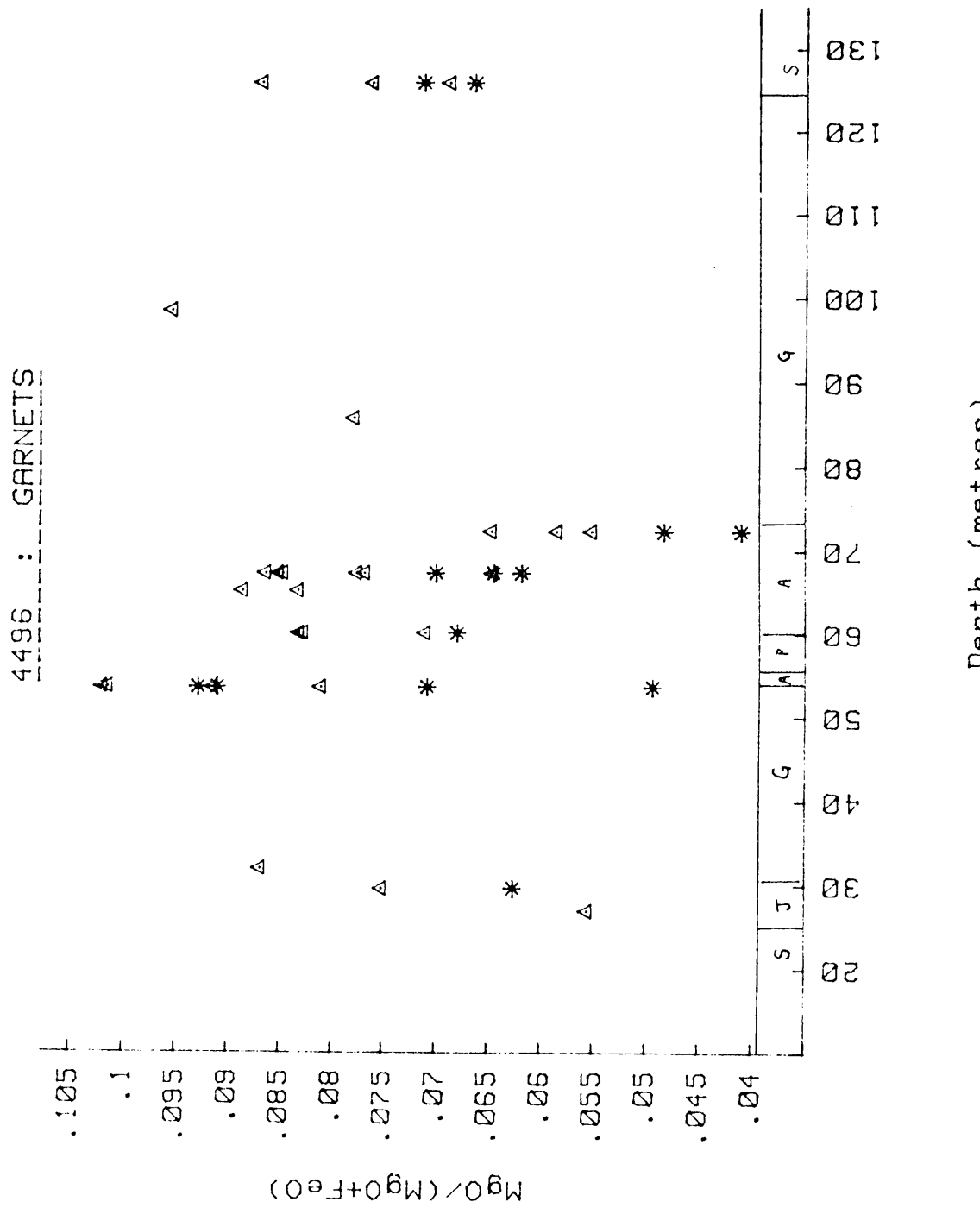

Appendix 4C cont.

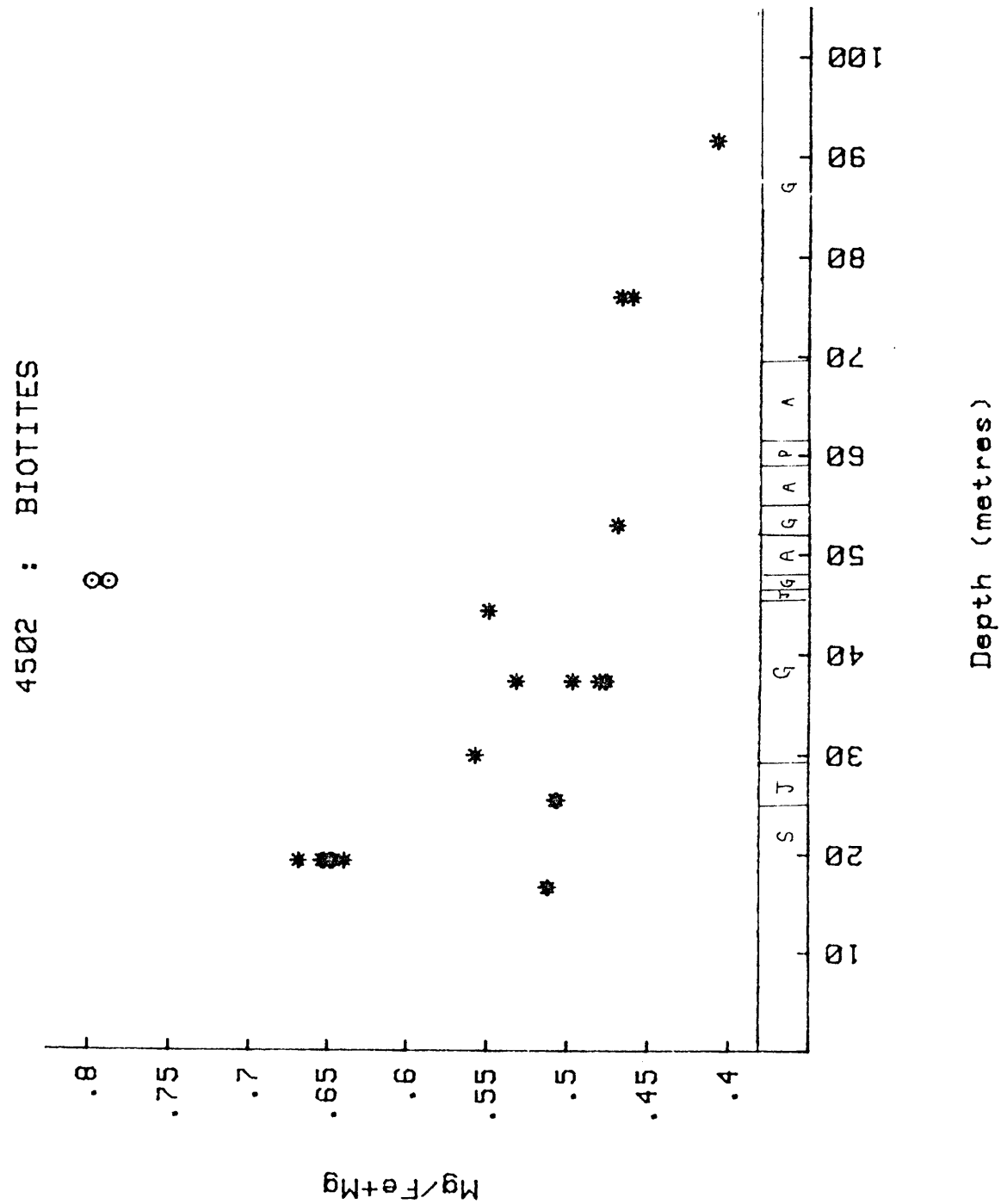

Appendix 4C cont.

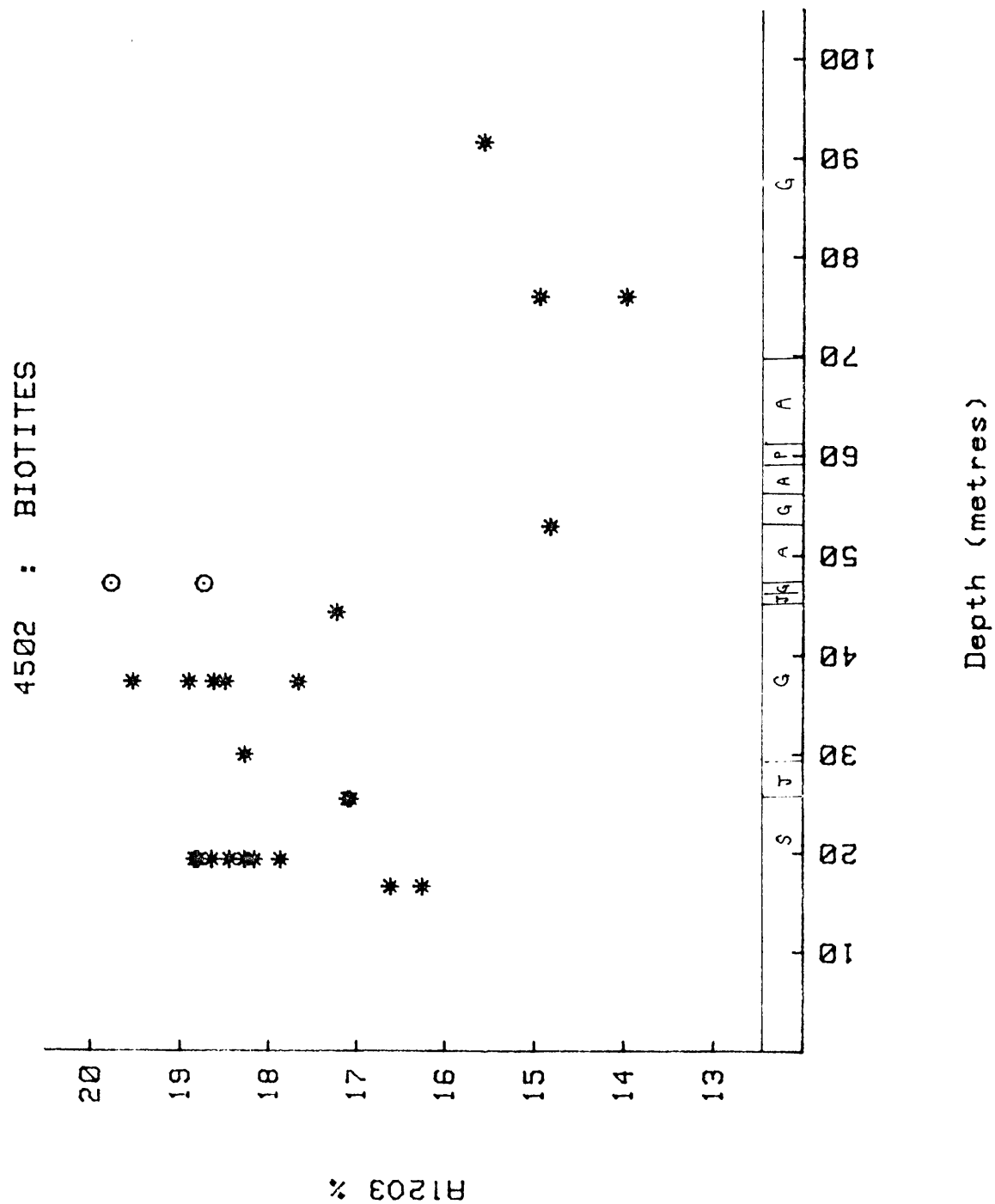

Appendix 4C cont.

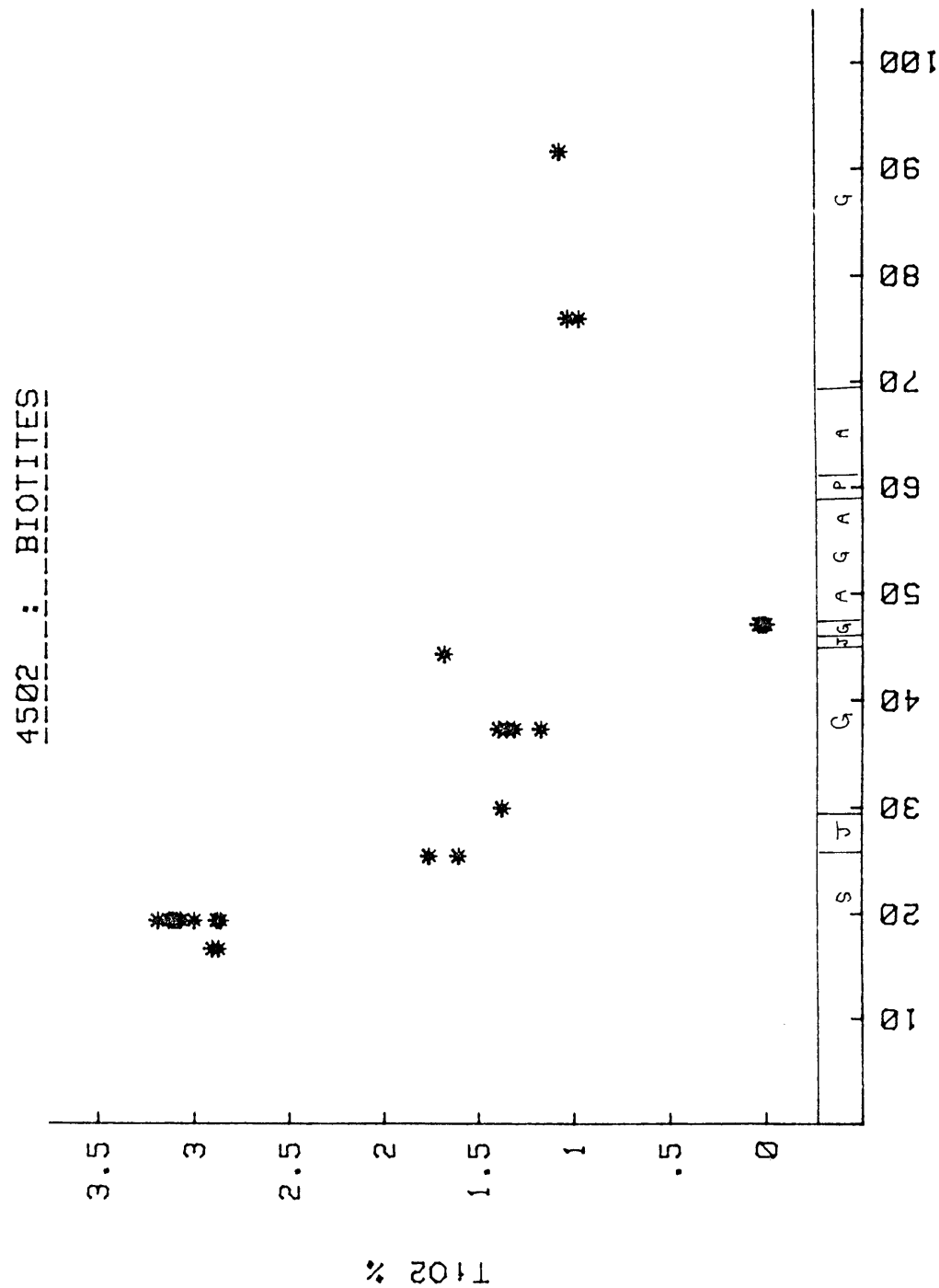

Appendix 4C cont.

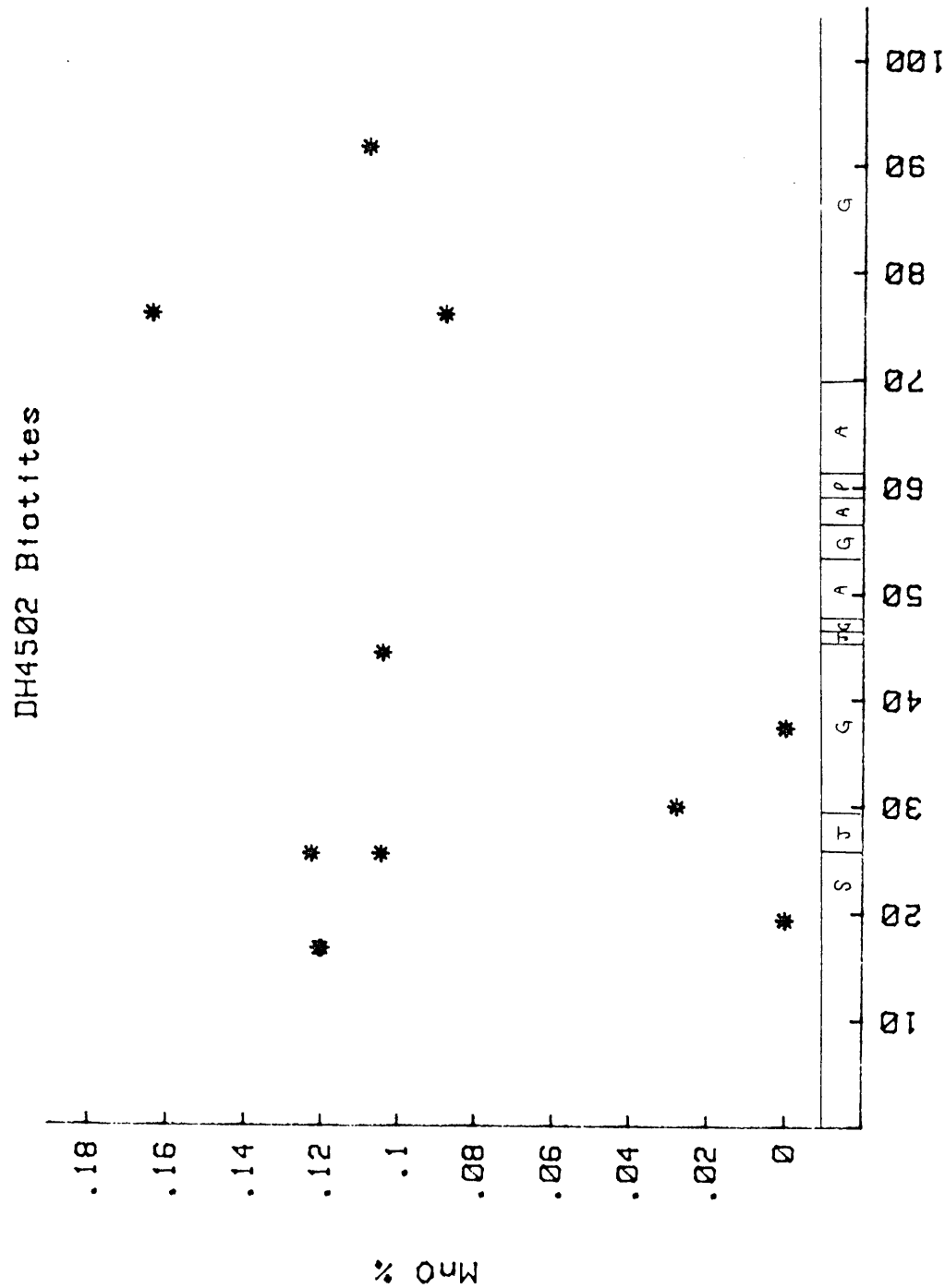

Appendix 4C cont.

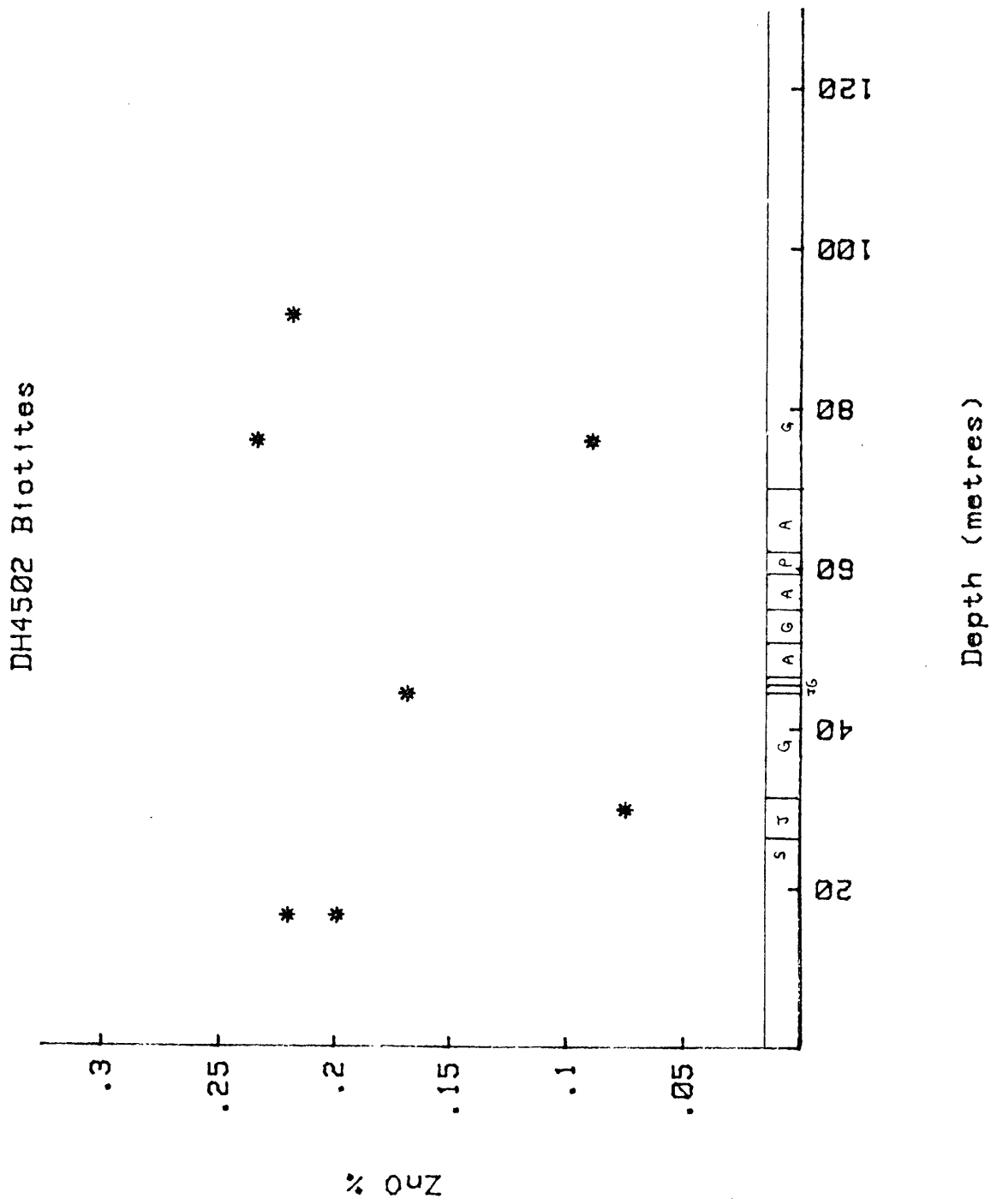

Appendix 4C cont.

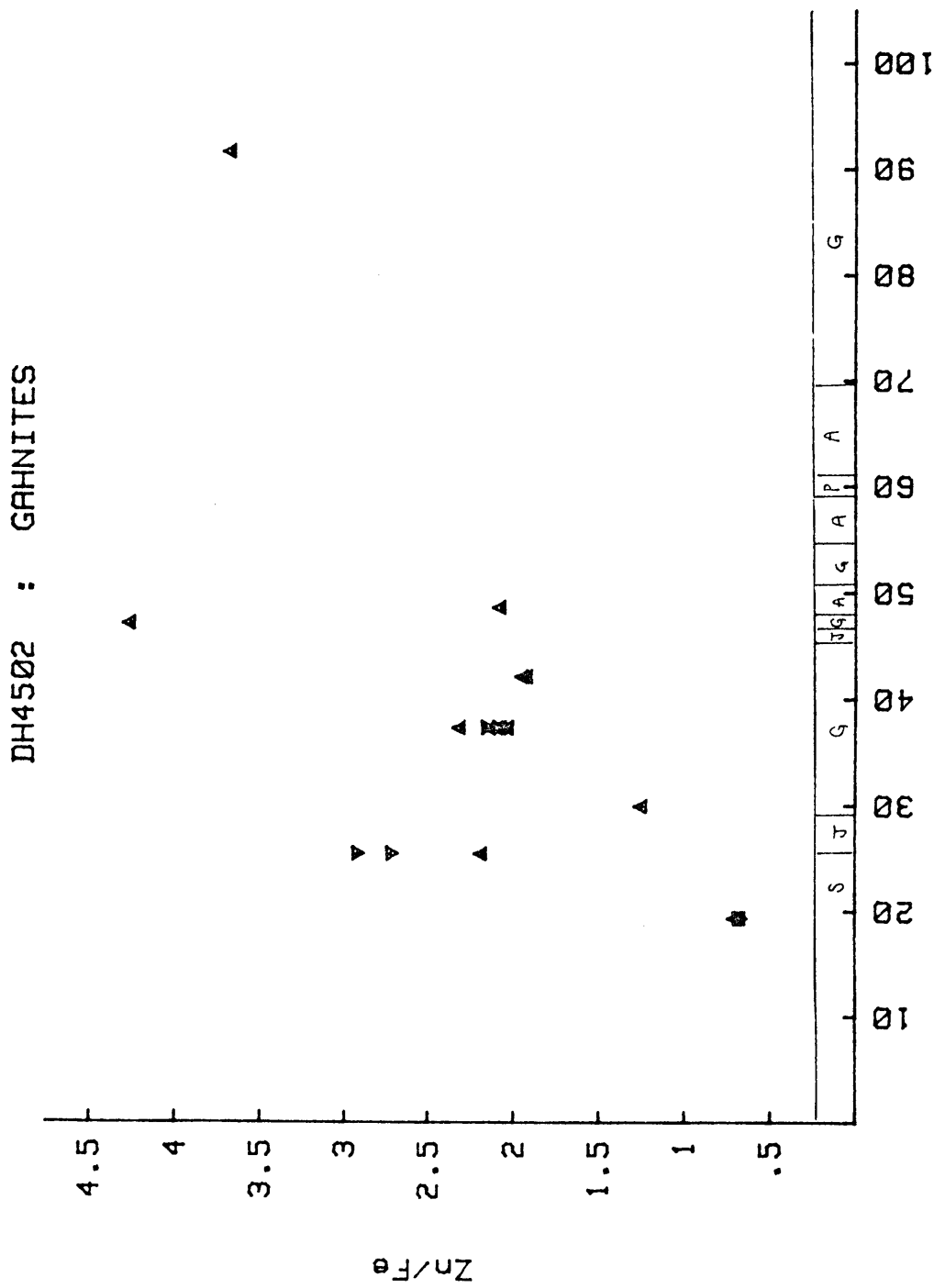

Appendix 4C cont.

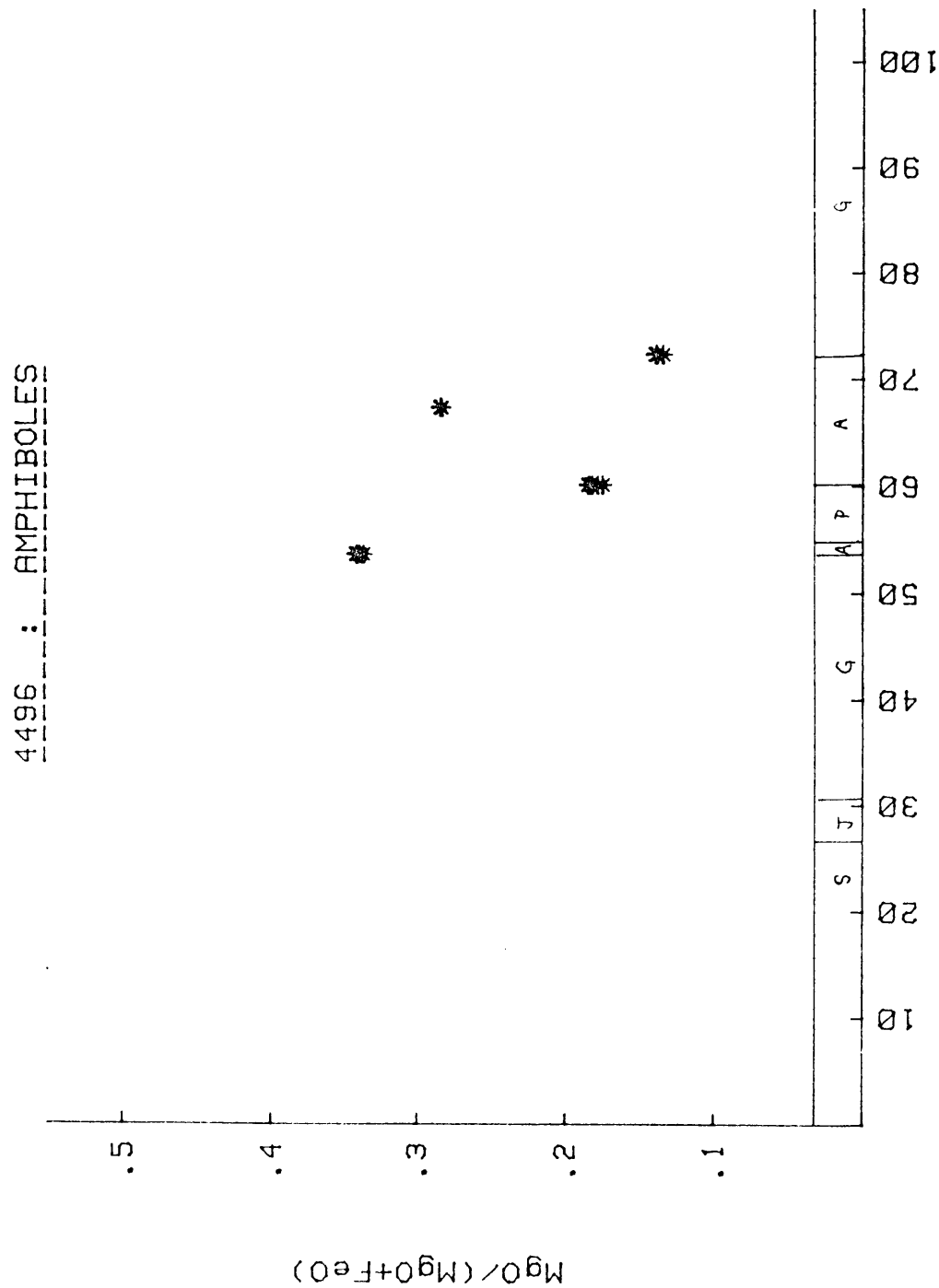

APPENDIX V : RESULTS OF X-RAY DIFFRACTION ANALYSES OF PYROXENOIDS FROM VARIOUS PARTS OF THE WAL.

17 pyroxenoid-bearing samples from various parts of the WAL were analysed by X-ray Diffraction to determine the relative abundance of rhodonite and pyroxmangite in the WAL. The results are shown below. The XRD methods are described in Appendix 1, and the sample locations are discussed in Appendix II.

Sample No.	Pyroxenoid
1/7	Pyroxmangite
2/1	Pyroxmangite
2/1A	Pyroxmangite + rhodonite
2/5A	Pyroxmangite
2/9A	Pyroxmangite
2/9A (different part of sample)	Pyroxmangite + rhodonite
2/9B	Pyroxmangite + rhodonite
4478/62.8	Rhodonite
4478/68.1	Rhodonite
4483/116.1	Rhodonite + minor pyroxmangite
4483/117.2	Pyroxmangite & minor rhodonite
4526/89.2	Pyroxmangite & minor rhodonite
4526/89.9	Rhodonite
4526/90.6	Pyroxmangite
4543/76.0	Rhodonite
4543/76.0 (different part of)	Pyroxmangite
4610/68.1	Rhodonite

In summary:

8 analyses indicate dominant pyroxmangite
6 analyses indicate dominant rhodonite
3 analyses indicate approximately equal amounts of rhodonite and pyroxmangite

APPENDIX VI: PUBLICATIONS AND SUPPORTING DOCUMENTS

A. BOTTRILL, R.S. 1983; Zincian staurolite from Broken Hill, N.S.W., Aust Mineral., 44, p.251-3.

B. BOTTRILL, R.S. 1983; A manganaxinite-bearing assemblage from Broken Hill, N.S.W., Aust. Mineral., 44. p.254-255.

C. Contributions to "Minerals of Broken Hill", H.K. WORNER and R.W. MITCHELL (eds.), 1983.

THE AUSTRALIAN MINERALOGIST

Number 44
December, 1983

ZINCIAN STAUROLITE FROM BROKEN HILL, NEW SOUTH WALES

R. S. Bottrill

W. S. & L. B. Robinson College,
Broken Hill, N.S.W.

ABSTRACT

Zinc-rich staurolite has been found in the Fe-Al-rich wallrocks of the Western A lode, Broken Hill, N.S.W. It appears to be restricted to retrograde shear zones of lower to middle amphibolite grade which transect the lower granulite facies ore-bearing metasediments. The staurolite largely drives from retrogressive breakdown of ferroan gahnite, a previously undescribed reaction, but biotite is also involved in the reaction. The zinc content of staurolite does not extend its stability range into the lower granulite facies.

INTRODUCTION

The lead-silver-zinc deposits at Broken Hill, New South Wales lie within a sequence of volcano-sedimentary rocks, metamorphosed to the lower granulite facies (Plimer, 1979; Phillips, 1980). The metamorphism was complex, with at least two major prograde events and a prolonged retrogressive episode of amphibolite to greenschist grades (Harrison & McDougall, 1981; Phillips, 1980).

Staurolite has been noted previously from retrograde shear zones of the district (Vernon & Ransom, 1971; Corbett & Phillips, 1981) and recently also from the lode rocks (Spry, 1978; Birch et al., 1982). Although staurolite is a typical mineral in lower amphibolite grade rocks, zincian varities have been described from lower granulite facies assemblages (Nemec, 1980; Ashworth, 1975). As the P-T dependence of zinc in staurolite is unknown (Griffen, 1981), the Broken Hill occurrence is of considerable interest.

OCCURRENCE

Staurolite is uncommon in the lode rocks, but is moderately abundant within retrograde shear zones intersecting the relatively iron and aluminium-rich wallrocks of the Western A lode, New Broken Hill Consolidated Mine (NBHC) from where specimens were obtained for this study. The wallrocks are gneisses and quartzites containing almandine ± biotite ± gahnite ± sillimanite ± orthoclase ± sulphides. Local small sericite ± chlorite-rich zones occur within both lode and wallrocks.

Staurolite in these rocks occurs as yellow-brown to red-brown, euhedral, slightly poikiloblastic and commonly twinned crystals from 0.01 to 2mm in size. Most coexisting phases have similar grainsize, but gahnite is usually coarser, ranging from about 0.2 to 4mm in diameter.

EDITORIAL

The centenary of the Broken Hill mines in 1983 has been marked by a number of major events, notably the holding of the Gemboree in that city over Easter and the Australasian Institute of Mining & Metallurgy Conference in July. In the publishing area, the highlight has undoubtedly been *'Minerals of Broken Hill'*, a book which has received widespread praise.

Six years ago, the Australian Mineralogist devoted an issue to minerals from Broken Hill, as a memorial to the late Sir Maurice Mawby, whose devotion to their study was probably unsurpassed. The Editorial Board felt it was appropriate to mark the 100 year celebrations of Broken Hill in a similar way. This issue is again devoted to aspects of the orebodies' mineralogy, in particular to some new discoveries. We hope it will be a stimulus to other mineralogists to continue expanding the knowledge of Broken Hill minerals.

Fig. 1

A euhedral staurolite crystal (0.5 x 0.2 mm) containing relict gahnite (dark grey) in a matrix of garnet (mid grey, high relief), biotite (mid grey, mottled, with fine ilmenite) and quartz (light grey to white). Cross polarised light.

Fig. 2

A gahnite porphyroblast (1.4x1.8mm) containing a garnet inclusion, with a replacement rim of fine to medium grained staurolite, in a matrix of gahnite (dark grey), garnet (mid grey), fine biotite (mottled grey), quartz (light grey to white) and galena (black). Party crossed polars.

The staurolite appears to be in equilibrium with all phases except gahnite, and a typical assemblage is staurolite — quartz — almandine — biotite ± sillimanite ± muscovite. Pyrrhotite, sphalerite and arsenopyrite may also be present in minor amounts. Gahnite, when present, usually shows some replacement by staurolite (Figs 1 & 2) and gahnite-free staurolite bearing assemblages are, in part, due to complete replacement of gahnite by staurolite.

CHEMISTRY, X-RAY DIFFRACTION AND OPTICS

The compositions of several staurolites and coexisting minerals from the Western A lode were determined by electron microprobe and are shown in Table 1.

The staurolites contain small, but significant amounts of zinc, with a maximum of 4.27 wt. % ZnO. The average staurolite formula is $(Fe_{2.7}Zn_{0.7}Mg_{0.6})_{4.0}Al_{17.3}Si_{7.9}O_{46}$, which is closer to that of Griffen (1981) than that of Yardley (1981).

The gahnite is quite iron-rich, and iron may occasionally exceed zinc in some spinels of the Western A lode. The rim of gahnite shows Zn-enrichment and depletion in Fe and Mg. This is probably due to partial re-equilibration of gahnite and staurolite during retrogression, with preferential partitioning of Zn into gahnite, and Fe and Mg into staurolite.

Although trioctahedral micas may accommodate up to 23wt% ZnO (in hendricksite, Frondel & Ito, 1966), the biotites in these assemblages contain only .33wt% ZnO. Similarly, up to 10wt% ZnO has been found in chlorites (Frondel & Ito, 1975), but *< 0.42wt% ZnO* was found in chlorites of the Western A lode. One optically homogenous, low-alkali (1.3 K atoms / 22 oxygens) biotite in an NBHC sample contains 1.3wt% ZnO (Table 1). This may be a mixed layer chlorite-biotite, as described by Mohr & Newton (1981).

The X-ray powder diffraction pattern for staurolite from sample No. 4496/29.6 was recorded on a Phillips Norelco diffractometer, using Cu/Ni radiation and calibrated with a silicon external standard. The lattice parameters, refined from 18 lines and indexed on a monoclinic lattice with reference to ASTM file No. 15-397 using the method of Griffen (1981) are: a = 7.870A, b = 16.602A, c = 5.657A, B = 90.0° and V = 739.1A^3. These unit cell dimensions are similar to other zincian staurolites (Griffen & Ribbe, 1973), but, as noted by Griffen (1981), other elemental substitutions prevent strictly linear correlation with the zinc contents. Electron microprobe analysis of staurolite from this sample indicates a range from 3.41 to 3.67wt% ZnO.

In this section, the staurolite appears biaxial positive, with a very large 2V. The pleochroism is $\alpha = \beta$ = colourless, γ = straw yellow, and refractive indices are α = 1.740(5), β = 1.746(5) and γ = 1.735(5).

TABLE 1: COMPOSITIONS AND STRUCTURAL FORMULAE OF COEXISTING ZINC-RICH MINERALS

	1	2	3	4	5
SiO_2	28.56	27.52	.03	.01	36.77
TiO_2	.10	.33	.00	.05	1.10
Al_2O_3	51.90	51.30	56.92	56.84	25.01
FeO	11.99	11.35	13.27	14.60	17.78
MnO	.10	.13	.06	.04	.02
MgO	1.41	1.36	1.45	1.66	8.82
Na_2O	.13	.10	.87	.81	.21
K_2O	—	—	—	—	7.06
ZnO	4.27	3.49	28.72	27.47	1.27
Total	98.46	95.58	101.32	101.48	98.04
Si	7.983	7.877	.000	.000	5.283
Ti	.022	.072	.000	.001	.119
Al	17.106	17.316	1.972	1.965	4.237
Fe	2.804	2.721	.326	.358	2.137
Mn	.023	.032	.002	.001	.003
Mg	.586	.580	.064	.073	1.888
Na	.070	.028	.050	.047	.059
K	.000	.000	.000	.000	1.295
Zn	.882	.738	.624	.595	.135
Oxygen	46.	46.	4.	4.	22.
No. atoms	75.48	75.36	7.04	7.04	37.16

1 : Most zinc-rich staurolite analysed, sample 4496/26.9

2 : Average of nine staurolites, samples 4496/26.9,29.6,32.0 and 4502/29.9

3 : Gahnite rim, sample 4496/26.9

4 : Gahnite core, sample 4496/26.9

5 : Low-alkali or partly chloritized biotite, sample 4496/26.9

(Samples from NBHC drill hole No. 4496 at depth in metres indicated after /)

DISCUSSION

Naturally occurring staurolites are frequently found to contain significant zinc (Griffen & Ribbe, 1973) and a complete series to the zincian end member was synthesized by Griffen (1981). The maximum ZnO content found in naturally occurring staurolite is, however, only 7wt.% (Griffen & Ribbe, 1973), and is rarely > 1 wt.%.

It has been suggested (Guidotti, 1970; Ashworth, 1975;) that zinc may stabilize staurolite to higher temperature and pressure, but there is no experimental evidence to confirm this. The partial to complete replacement of gahnite by staurolite (sometimes with coexisting muscovite) at Broken Hill indicates re-equilibration at T and P well below those of the original granulite conditions, due to locally high a_{H_2O} and suitable chemical conditions in the retrograde shear zones.

The breakdown of gahnite to staurolite has not been previously described, although illustrated by Spry (1978) in an unpublished thesis. The breakdown of zincian staurolite to gahnite or zincian hercynite during prograde metamorphism has, however, been noted by Stoddard (1979) and Spry (1978).

The actual reaction is uncertain and complex. Biotite is a common associate of staurolite and would balance the equation by the coupled reaction : $FeSi \rightleftharpoons Al_2$. The reaction could thus be represented as:

Fe-gahnite + Fe-Si-biotite = Zn-staurolite + Al-biotite with preferential partitioning of Fe into staurolite and Zn preferentially remaining in gahnite.

ACKNOWLEDGEMENTS

The NBHC Mine kindly permitted collection and donated additional samples for this study. Dr. B. Griffen & Ms. S. Phillips provided invaluable assistance with electron microprobe analyses. Valuable discussions were contributed by Mr. D. Milton (NBHC Mines) and Dr. W.D. Birch is particularly thanked for the encouragement and review of this manuscript.

REFERENCES

Ashworth, J.R., 1975: Staurolite at anomalously high grade. *Contrib. Mineral. Petrol., 53*, 281-291.

Birch, W.D., Chapman, A. & Pecover, S.R., 1982: The Minerals *in* Worner, H.K. & Mitchell, R.W. (Eds.) *Minerals of Broken Hill*, 68-195, Australian Mining and Smelting Ltd., Melbourne.

Corbett, G.J. & Phillips, G.N., 1981: Regional retrograde metamorphism of a high grade terrain: The Willyama Complex, Broken Hill, Australia. *Lithos, 14*, 59-73.

Frondel, C. & Ito, J., 1966: Hendricksite, a new species of mica. *Amer. Mineral, 51*, 1107-1123.

Frondel, C. & Ito, J., 1975: Zinc-rich chlorites from Franklin, New Jersey, with a note on chlorite nomenclature. *Neues Jahrb. Mineral Abh., 123*, 111-115.

Griffen, D.T., 1981: Synthetic Fe/Zn staurolites, and the ionic radius of IV Zn^{2+}. *Amer. Mineral., 66*, 932-937.

Griffen, D.T. & Ribbe, P.H., 1973: The crystal chemistry of staurolite. *Amer. J. Sci. 273-A*, 479-495.

Guidotti, C.V., 1970: The mineralogy and petrology of the transition from the lower to upper sillimanite zone in the Oquossoc area, Maine. *J. Petrol., 11*, 277-336.

Harrison, T.M. & McDougall, I., 1981: Excess ^{40}Ar in metamorphic rocks from Broken Hill, NSW: implications for $^{40}Ar/^{39}Ar$ age spectra and the thermal history of the region. *Earth Planet. Sci. Lett., 55*, 123-149.

Mohr, D.W. & Newton, R.C., 1983: Kyanite — staurolite metamorphism in sulphide schists of the Anakeesta formation, Great Smokey Mountains, North Carolina. *Amer. J. Sci., 283*, 57-134.

Nemec, Von D., 1980: Zinkhaltinger staurolith aus den Leptyniten der Bianicer Furche und aus ubrigen Moldanubikum der Bohmisch — Mahrischen Hohe (CSSR). *Chem. Erde., 39*, 311-320.

Phillips, G.N., 1980: Water activity changes across an amphibolite — granulite facies transition, Broken Hill, Australia. *Contrib. Mineral. Petrol., 75*, 377-386.

Plimer, I.R., 1979: Sulphide rock zonation and hydrothermal alteration at Broken Hill, Australia. *Trans. Inst. Mining Met., Sect. B., 88*, 161-176.

Spry, P.G. 1978: The geochemistry of garnet-rich lithologies associated with the Broken Hill orebody, NSW, Australia. MSc thesis, Univ. Adelaide (unpub.).

Stoddard, E.F., 1979: Zinc-rich hercynite in high-grade metamorphic rocks: a product of dehydration of staurolite. *Amer. Mineral., 64*, 736-741.

Vernon, R.H. & Ransom, D.M., 1971: Retrograde schists of the amphibolite facies at Broken Hill, New South Wales. *J. geol. Soc. Aust., 18*, 267-277.

A NOTE ON VESUVIANITE FROM THE ZINC CORPORATION MINE, BROKEN HILL, NEW SOUTH WALES

W. D. Birch

Department of Mineralogy & Petrology

National Museum of Victoria
285 Russell Street, Melbourne,
Victoria, 3000

ABSTRACT

Rounded greenish brown grains of vesuvianite up to 6mm across have recently been found in calcite-rich ore from the Zinc Corporation Mine. The occurrence of this vesuvianite as a prograde gangue mineral contrasts with previously recorded vesuvianite from Broken Hill, which was regarded as having crystallized under late-state retrograde conditions. Microprobe analyses of both types are presented.

Vesuvianite was first reported from No. 2 lens ore at Broken Hill by Stillwell (1959), but without description. Since then, specimens have been collected occasionally, usually as brownish bladed masses (Plimer, 1982; Birch et at, 1982) associated with coarse-grained sulphides.

Amongst a large collection of Broken Hill minerals recently donated to the National Museum of Victoria by Dr. Ian Plimer was a small specimen of calcite-rich ore from No. 2 lens, on 20 level of the Zinc Corporation Mine. The piece consisted of an aggregate of polygonal white calcite grains containing scattered rounded grains up to 6mm across of a greenish-brown vitreous mineral, which was identified by X-ray diffraction as vesuvianite. Small grains of sphalerite were also present.

A second specimen in the same Broken Hill collection consisted of a bladed mass of dark reddish brown vesuvianite crystals up to 7cm long, associated with a compact hedenbergite-quartz-vesuvianite rock. This was collected from the 19 level of the Zinc Corporation Mine. A small area of euhedral green hedenbergite crystals with a thin 'sturtite' crust occurred on this specimen.

Both vesuvianite specimens were analysed by electron microprobe (Table 1). The greenish-brown vesuvianite in the calcitic ore has a lower Fe/Mg ratio, and negligible Ti, in contrast to the reddish brown variety, which has 1.0% TiO_2. Both these factors may be responsible for the colour difference. Fluorine contents are similar in both (1.8% F), but Cl is absent from the greenish brown vesuvianite. The hedenbergite crystals coexisting with the reddish brown vesuvianite contain only 2.0% MnO (less Mn than Mg on a cation percent basis). The 'sturtite' is Fe-rich. Previous analyses of vesuvianite (Plimer 1982) show similar Fe, Mg, Mn and F contents to those of the reddish brown crystals described here.

Vesuvianite may be more widespread in the calcite-rich No. 2 lens ore in the Zinc Corporation than previously thought and may have some importance as a primary, i.e. prograde fluorine-rich mineral. All previously described vesuvianite has been regarded as having crystallized during late-stage retrograde metamorphism (e.g. Plimer, 1982) in the presence of fluorine-enriched fluids.

Localized higher fluorine activities may have determined whether vesuvianite formed in preference to grossular as a prograde mineral in the calcitic ore in No. 2 lens.

ACKNOWLEDGEMENTS

The microprobe analyses were carried out in the Geology Department, University of Melbourne.

Appendix VI-c

To whom it may concern,

I acknowledge that Ralph Bottrill has contributed significantly to the chapters of the book 'Minerals of Broken Hill', edited by H.K. Worner & R.W. Mitchell, that I was a principal author to; in particular to the following sections:

Albite p. 72
Algodonite p. 72
Ankerite p. 78
Aurichalcite p. 81
Axinite p. 82
Birnessite p. 88
Cryptomelane p. 112
Hollandite p. 130
Hydrozincite p. 130
Jacobsite p. 133
Monazite p. 146
Prehnite p. 148
Psilomelane p. 148
Romanechite p. 171
Seligmannite p. 171
Sphalerite p. 184
Wurtzite p. 194

and was also joint author of the addendum (following page).

Signed:

Dr. W.D. Birch,
Curator of Minerals, rocks and meteorites,
National Museum of Victoria.

ADDENDUM

Bill Birch, Ralph Bottrill, Ian Plimer

ADDITIONAL MINERAL DESCRIPTIONS

Since publication of the first edition of 'Minerals of Broken Hill', new mineralogical data have been accumulated, including evidence to support the finding of at least five species previously unrecorded at Broken Hill. Much of the new information reported here has been gathered by Ralph Bottrill during studies on the western A lode ore, NBHC. The following notes should be read in conjunction with Chapter 8.

ACTINOLITE, manganoan

Dark green actinolite crystals from the western part of A lode, NBHC, contain up to 5.7% MnO. The mineral is a product of the breakdown of pyroxmangite.

BINDHEIMITE

Bindheimite is a lead-antimony hydroxy oxide not a hydrous lead sulphate as stated in Chapter 8.

BISMUTH

Rounded inclusions of bismuth, up to 0.1 mm across, occur rarely in galena grains from 21 level of the NBHC Mine. The mineral was identified recently in drill core from within 100 metres of the southern extremity of the lead lode (Milton, pers. comm., 1983).

BOLEITE

The reference by Winchell & Rouse (1974) to an old Broken Hill specimen labelled percylite and subsequently identified as boleite, is in error, as is the reference to the American Museum of Natural History in Washington. The actual mine, according to the original label with the specimen, is the Beltana Broken Hill Mine, South Australia and the specimen in question is in the collection of the National Museum of Natural History - Smithsonian Institution (Mason, pers. comm., 1983).

DIOPSIDE, manganoan (see also schefferite)

Recent microprobe analyses of dark green to near black pyroxenes from western A lode ore, NBHC, reveal unusually high magnesium contents for Broken Hill pyroxenes. The compositions range from magnesian manganoan hedenbergite to manganoan diopside close to $Ca_{0.6}Mg_{0.3}Mn_{0.4}Fe_{0.3}Si_2O_6$.

GRUNERITE

A recent microprobe analysis of an cummingtonite-group amphibole from western A lode ore in NBHC plots in the grunerite field (see Fig. 8.4). The mineral was associated with sulphides and chlorite.

HERCYNITE

Dark green to black spinel crystals from wall rocks within western A lode, NBHC Mine, contain up to 63 mol % of the hercynite end member.

ORTHOCLASE-MICROCLINE

Additional X-ray diffraction analysis on green lode feldspar from NBHC indicates that some is orthoclase. This suggests there may be a continuous series of structural states between orthoclase and minimum microcline in these feldspars at Broken Hill.

PARAGONITE

Some of the fine-grained alteration products around gahnite crystals from western A lode rocks in NBHC have been shown by microprobe analysis to be paragonite, not sericite.

PERCYLITE (see BOLEITE*)*

Roepperite

Microprobe analysis of the 'type' specimen of Broken Hill roepperite (Birch, in press) gave a maximum ZnO content of 0.34 wt%. Seven other specimens of so-called roepperite from the ZC & NBHC Mines have also been analysed, with only small amounts of zinc (< 0.5% ZnO) detected. Roepperite can therefore be regarded as unsubstantiated at Broken Hill

RHODOCHROSITE, zincian

Microprobe and X-ray diffraction analysis have recently been carried out on NMV specimens consisting of fawn to yellowish and honey-brown botryoidal carbonate minerals on concretionary goethite. The compositions lie in the range zincian rhodocrosite (Mn/Zn = 7) to manganoan smithsonite (Mn/Zn = 0.6). Small amounts of Pb and Cu are present and only traces of Ca and Mg; Fe is absent (Birch, unpub. data).

SAFFLORITE

X-ray diffraction and microprobe analysis of a number of specimens labelled safflorite reveal them to loellingite (Birch, unpub. data). The status of safflorite is now in doubt at Broken Hill.

SCHEELITE

Recent observations have shown that the spessartine-grossular garnet 'sandstone' on the edge of the lead lode, 20 level, NBHC Mine, contains up to 2% of Mo-poor scheelite as tension gash fillings up to 3mm wide and 15 cm long (Plimer, unpub. data).

Schefferite

A dark red-brown cleavage block labelled schefferite (i.e. manganoan diopside) from the Australian Museum collection has been determined as bustamite by electron microprobe analysis and X-ray diffraction (Plimer, unpub. data).

SMITHSONITE, manganoan (see RHODOCHROSITE, zincian)

STAUROLITE, zincian

Staurolite crystals up to 2 mm across and yellowish to reddish brown in colour are associated with garnet, biotite and occasional sulphides in marginal western A lode rocks in the NBHC. The staurolites contain up to 4.5% ZnO (Bottrill, in press).

TIRODITE

Additional microprobe analyses of cummingtonite series amphiboles in western A lode ore from NBHC has extended the known composition range (see Fig. 8.4) to the tirodite field.

UNKNOWN Cu, Zn, Ca SULPHATES

Rare small, pale blue, hexagonal (?) platy crystals and deeper bluish green transparent prisms, have recently been found encrusting leached galena from outcrops in the old Block 10 leases. They contain major Cu, Zn, Ca, and S and may be related to devilline and ktenasite

ERRATA

Page 29, line 33 second column: Ecandrewsite is a zinc analogue of ilmenite, not a zinc spinel.

Page 33, fifth last line, first column: 'purchased by' should read 'donated to'.

Page 34, line 18, first column: Albert Campbell should read Arthur Campbell.

Page 35, line 13, second column: Gordon Campbell and Geoff Lithglow of Broken Hill should be added to the list of important collectors

APPENDIX VII : ABBREVIATIONS

a_{H2O}	:	Water activity
BIF	:	Banded iron-formation
NBHC	:	New Broken Hill Consolidated Mine
P_{H2O}	:	Partial pressure of water
PPL	:	Plane - polarised light
P_T	:	Total pressure
PXPL	:	Partly-crossed polarised light
RSZ	:	Retrograde shear zone
WAL	:	Western A-Lode
XPL	:	Cross-polarised light
ZC	:	Zinc Corporation

Mineral Symbols (largely from Kretz (]983)

Alm	:	Almandine
Amph	:	Amphibole
Bt	:	Biotite
Gah	:	Gahnite
Gn	:	Galena
Po	:	Pyrrhotite
Pxn	:	Pyroxenoid
Q	:	Quartz
Sil	:	Sillimanite
Sl	:	Sphalerite
Sps	:	Spessartine

```
10    !
20    !            "SELXP:H9"        R.BOTTRILL
30    !
40    !              REVISED FROM "SELECT" :16/11/83
50    !
60    !   PROGRAM TO SELECT PROBE DATA & PRINT MINERAL COMPOSITION AND FORMULA
70    !   (up to 10 Files, 200 analyses and 15 elements)
80    !
90    OPTION BASE 1
100   DIM Item$(15)[6],Heading$[80],Elv(30,200),Value(15),Tot(13),Mwgt(15),Oxrat
(15),Mole(15),Oxprop(15),Ncations(15),Nanions(15),Element$(15)[9]
110   DIM Cations(15),Anions(15),Elvt(34),Sample$(200)[12],Mineral$(200)[12],Fa$
(10,200)[8],Fyl(10),Ja(10),V(12)
120   SHORT Atomsum
130   INTEGER I,N,Ne,Nel,Ne2,Ne3,Ne4,An,Nj,N5,Neav,Ij,Aj,F,A,Fi,Aji
140   PRINT "SELXP : SELECTS PROBE ANALYSES AND CALCULATES FORMULAE & AVERAGES
"
150   PRINT "(up to 10 Files, 200 analyses and 15 elements)"
160   PRINT "ASSUMES 1st 7 elements are: Si, Ti, Al, Fe2+, Mn2+, Mg, Ca"
170   PRINT "Any others may follow."
180   !
190 Rerun:LINPUT "HEADING ?",Heading$
200   An=0
210   Anal$=""
220   Set=0
230   FOR Fi=1 TO F
240    FOR Aji=1 TO Ja(F)
250     Fa$(Fi,Aji)=""
260    NEXT Aji
270   NEXT Fi
280   F=0
290   MAT Elv=ZER(30,200)
300   PRINTER IS 16
310   GOTO Linpf
320   !
330   !                    LOAD FILE
340   !
350 Linpf:  LINPUT "FILE NAME ?, CONT for same, OR 0 TO STOP ?",File$
360   IF File$="" THEN File$=Oldfile$
370   IF File$="0" THEN File
380   IF Anal$="N" THEN Ja(F)=Aj
390   F=F+1
400   Fyl$(F)=File$
410   Aj=0
420   ON ERROR GOSUB Error
430   ASSIGN #1 TO File$&"A:H9"                          ! MAIN DATA FILE
440   ASSIGN #2 TO File$&"B:H9"                          ! INFO FILE
450   READ #2;Ni,Nemax,Unf
460   REDIM Item$(Nemax),Value(Nemax)
470   READ #2;Item$(*)
480   OFF ERROR
490   IF Anal$<>"N" THEN Singl
500   FOR Nx=1 TO Nemax
510     IF Lastitems$(Nx)<>Item$(Nx) THEN Incomp
520   NEXT Nx
530   GOTO Forsets
540   !
550 Incomp:  PRINT "THIS FILE IS INCOMPATIBLE WITH ";Oldfile$
560   INPUT "YOU MAY EITHER: try to continue anyway (1); select another file (2)
; or stop and print (3)",Inc
```

```
570   ON Inc GOTO Forsets,Linpf,File
580   !
590   !                    SINGLE ANALYSES
600   !
610 Singl:   INPUT "Press CONT for a single analysis, or 1CONT for a series
of analyses",Set
620   IF NOT Set THEN Notset
630   Av=0
640   INPUT "CALCULATE AVERAGE OF SERIES ? ( CONT /N)",Cas$
650   IF Cas$<>"N" THEN Av=1
660   IF File$=Oldfile$ THEN Oxno  !!!!!
670   IF Oldfile$<>"" THEN De=8
680   IF Oldfile$<>"" THEN Ifde
690   GOTO Dataline
700   !
710   !                   SINGLE ANALYSES
720   !
730 Notset:   An=An+1
740 Ian:  INPUT "ANALYSIS No. ?",I
750   GOSUB Reads
760   IF File$=Oldfile$ THEN Oxno!!!!!     STILL PROBLEMS
770   IF Newf$<>"" THEN De=8
780   IF Newf$<>"" THEN Ifde
790   !
800   !        *****    DATA ON ATOMIC WEIGHTS, etc    *****
810   !
820 Dataline:   DATA 60.09,1,2,79.9,1,2,101.94,2,3,71.85,1,1,70.94,1,1,40.32,1,
,56.08,1,1,0,0,0,0,0,0,0,0,0,0,0,0,0,0
830   De=1
840 Ifde:   IF (Item$(1)="DEPTH") OR (Item$(1)="Depth") THEN De=De+1
850   FOR Nj=De TO Nemax                  !   DETERMINE MOLECULAR WEIGHTS ETC.
860      IF Newf$<>"" THEN Ifmw
870      READ Mwgt(Nj)
880      READ Cations(Nj),Anions(Nj)
890 Ifmw:      IF Mwgt(Nj)<>0 THEN Ornj
900      IF Item$(Nj)="NA2O" THEN Na
910      IF (Item$(Nj)="K2O") OR (Item$(Nj)="K2O") THEN K
920      IF Item$(Nj)="ZNO" THEN Zn
930      IF Item$(Nj)="CL" THEN Cl
940      IF Item$(Nj)="F" THEN F
950      GOTO Inputmwgt
960 Na:  Mwgt(Nj)=60.98
970      Anions(Nj)=1
980      Cations(Nj)=2
990      GOTO Ornj
1000 K:  Mwgt(Nj)=94.2
1010     Anions(Nj)=1
1020     Cations(Nj)=2
1030     GOTO Ornj
1040 Zn: Mwgt(Nj)=81.31
1050     Anions(Nj)=1
1060     Cations(Nj)=1
1070     GOTO Ornj
1080 Cl: Mwgt(Nj)=35.5
1090     Anions(Nj)=-.5
1100     Cations(Nj)=1E-20
1110     GOTO Ornj
1120 F:  Mwgt(Nj)=19.00
1130     Anions(Nj)=-.5
1140     Cations(Nj)=1E-20
```

```
1150     GOTO Ornj
1160     !
1170 Inputmwgt:PRINT "MOL. WGT., No. CATIONS and No. ANIONS IN "&Item$(Nj)&" ?"
1180     INPUT "?",Mwgt(Nj),Cations(Nj),Anions(Nj)
1190 Ornj:   Oxrat(Nj)=Anions(Nj)/Cations(Nj)
1200  NEXT Nj
1210  !
1220  ! LABEL ELEMENTS
1230  !
1240  De=1
1250  IF (Item$(1)="DEPTH") OR (Item$(1)="Depth") THEN De=2
1260  FOR Ne3=De TO Nemax
1270    Pos2=POS(Item$(Ne3),"2")
1280    Element$(Ne3)=Item$(Ne3)[1,2]
1290    IF Pos2=2 THEN Element$(Ne3)=Item$(Ne3)[1;1]
1300  NEXT Ne3
1310  !
1320  !
1330  IF Item$(5)<>"FE2O3" THEN Oxno !!!!!!
1340  Mwgt(5)=159.70
1350  Cations(5)=2
1360  Anions(5)=3
1370  Oxrat(5)=1.5
1380  !
1390 Oxno:INPUT "No. OF OXYGENS IN MINERAL FORMULA ?",Nox
1400 Forsets:  IF Set THEN GOSUB Sets
1410  IF Set THEN GOTO File
1420  GOSUB Ratios
1430  GOTO Display
1440  !
1450  !      CALCULATE ELEMENT RATIOS
1460  !
1470 Ratios:  Oxsum=0
1480  FOR Nel=De TO Nemax
1490    Mole(Nel)=Value(Nel)/Mwgt(Nel)      ! MOLECULAR PROPORTIONS OF CATIONS
1500    Oxprop(Nel)=Mole(Nel)*Anions(Nel)   ! MOLECULAR PROPORTIONS OF ANIONS
1510    Oxsum=Oxsum+Oxprop(Nel)
1520  NEXT Nel
1530  Factor=Nox/Oxsum
1540  Atomsum=0
1550  FOR N=De TO Nemax                    ! CALCULATE FORMULA
1560    Nanions(N)=Factor*Oxprop(N)
1570    Ncations(N)=Nanions(N)/Oxrat(N)
1580    N2=Nemax+N
1590    Elv(N2,An)=Ncations(N)
1600    Atomsum=Atomsum+Nanions(N)+Ncations(N)
1610  NEXT N
1620  Nfinal=N2+1
1630  Elv(Nfinal,An)=Nox
1640  Elv(Nfinal+1,An)=Atomsum
1650  Element$(Nemax+1)="Oxygen    "
1660  Element$(Nemax+2)="No. atoms"
1670  Hcl=Hf=0
1680  FOR H=1 TO Nemax
1690    IF Item$(H)="CL" THEN Hcl=H
1700    IF Item$(H)="F" THEN Hf=H
1710  NEXT H
1720  IF (An<>1) AND NOT Set THEN Display
1730  RETURN
1740  !
```

```
1750  !  DISPLAY FOR CHECKING
1760  !
1770 Display:PRINT LIN(1);SPA(12);Sample$(An);LIN(1);SPA(12);Mineral$(An);LIN(1
1780  FOR Ne4=De TO Nemax
1790    PRINT USING "9A,4D.4D";Item$(Ne4);Elv(Ne4,An)
1800  NEXT Ne4
1810  PRINT LIN(1);"TOTAL ";SPA(3);Total;LIN(1);RPT$("_",18);LIN(1)
1820  FOR Ne2=De TO Nemax
1830    PRINT USING "9A,4D.4D";Element$(Ne2);Elv(Ne2+Nemax,An)
1840  NEXT Ne2
1850  PRINT LIN(1);"Oxygens   ";Nox;LIN(2);"No. atoms ";Atomsum;LIN(1)
1860  Oxch$=""
1870  INPUT "CHANGE OX. NO. ? (Y/ )",Oxch$
1880  IF Oxch$="Y" THEN GOTO Oxno
1890  !
1900  !       NEW RUN
1910  !
1920 Oldfil: Oldfile$=File$          !!!!!!!!!!!!!!!!!!
1930  Newf$=""
1940  INPUT "Continue with this File or Stop ? ( /0) ",Newf$
1950 !  INPUT "New File / Same or Stop ? (N/ /0) ",Newf$
1960  IF Newf$="" THEN GOTO Ian
1970  IF Newf$="N" THEN GOTO Linpf
1980  !
1990  !       ** FILE **
2000  !
2010 File:   Oldfile$=File$
2020  IF NOT Set THEN Gsp
2030  Ja(F)=Aj
2040  Ff=F
2050  IF Av THEN GOSUB Average
2060 Gsp: GOSUB Printing
2070  Rerun$=""
2080  INPUT "Another run ? (Y/N)",Rerun$
2090  IF Rerun$="Y" THEN GOTO Rerun
2100  GOTO Optout
2110  !
2120  !     *****   PRINTING SUBROUTINES   *****
2130  !
2140 Printing:  Noc=6
2150  Hcopy=16
2160  PRINT LIN(4)
2170  GOSUB Printout
2180  Tp$=""
2190  INPUT "PAPER PRINT ? : Thermal or 2601A or CONT (T/2/ )",Tp$
2200  INPUT "Number of columns / page ? (up to 7 on Thermal Printer, or 12 on Da
isywheel).",Nocp
2210  Noc=Nocp
2220  IF Nocp=0 THEN Noc=6
2230  IF Tp$="" THEN RETURN
2240  IF Tp$="T" THEN Hcopy=0
2250  IF Tp$="2" THEN Hcopy=11
2260  IF Hcopy THEN Pr11
2270  PRINTER IS Hcopy,WIDTH(80)
2280  GOTO Printout
2290 Pr11:  PRINTER IS Hcopy,WIDTH(156)
2300  !
2310  !              PRINTOUT
2320  !
2330 Printout:  J=An
```

```
2340  IF Av THEN J=J+1
2350 ! IF Hcopy=11 THEN PRINT PAGE
2360 ! IF Hcopy=0 THEN PRINT LIN(6)
2370  PRINT "SELECTED ANALYSES FROM :"; !! ;SPA(32);RPT$("*",17),LIN(1)
2380  FOR F=1 TO Ff
2390    PRINT Fyl$(F);" : ";
2400    FOR A=1 TO Ja(F)-1
2410     PRINT Fa$(F,A);", ";
2420    NEXT A
2430    PRINT Fa$(F,Ja(F))
2440    PRINT SPA(24);
2450  NEXT F
2460  PRINT LIN(1)
2470  PRINT Heading$;LIN(1);RPT$("*",LEN(Heading$))
2480  FOR Ij=1 TO J STEP Noc
2490   PRINT LIN(1);SPA(10);
2500   FOR Jno=Ij TO Ij+Noc-1                    !  Print headings to columns
2510     IF Jno>J THEN Nxtjno
2520     PRINT SPA(10-LEN(Sample$(Jno)));Sample$(Jno);".";
2530 Nxtjno: NEXT Jno
2540   PRINT LIN(1);SPA(10);
2550   FOR Jno=Ij TO Ij+Noc-1
2560     IF Jno>J THEN Nextjno
2570     Mineral$(Jno)=TRIM$(Mineral$(Jno))
2580     PRINT SPA(10-LEN(Mineral$(Jno)));Mineral$(Jno);".";
2590 Nextjno: NEXT Jno
2600   PRINT LIN(1)
2610   MAT Tot=ZER
2620   FOR Ne=De TO Nemax
2630      PRINT USING "#,9A";Item$(Ne)
2640      FOR Ino=Ij TO Ij+Noc-1
2650          IF Ino>J THEN Nextino
2660          Colum=Ino-Ij+1
2670          PRINT USING "#,6D.4D";Elv(Ne,Ino)
2680          Tot(Colum)=Tot(Colum)+Elv(Ne,Ino)
2690    IF NOT Hcl THEN Fv
2700    Vcl=.4211*Elv(Hcl,Ino)
2710    Tot(Colum)=Tot(Colum)-Vcl
2720 Fv: IF NOT Hf THEN Plt
2730    Vf=.2256*Elv(Hf,Ino)
2740    Tot(Colum)=Tot(Colum)-Vcl
2750 Plt: V(Colum)=Vf+Vcl
2760          IF Ne=1 THEN Tot(Colum)=0
2770 Nextino: NEXT Ino
2780    PRINT
2790    NEXT Ne
2800    IF Hf OR Hcl THEN Fcl
2810    PRINT LIN(1);"TOTAL    ";
2820    FOR Colm=1 TO Colum
2830      PRINT USING "#,6D.4D";Tot(Colm)
2840    NEXT Colm
2850    PRINT LIN(2)
2860    GOTO Forne4
2870 Fcl:    PRINT LIN(1),SPA(9);
2880    FOR Colm=1 TO Colum
2890      PRINT USING "#,6D.4D";Tot(Colm)
2900    NEXT Colm
2910    PRINT LIN(1);"O=F,CL   ";
2920    FOR Colm=1 TO Colum
2930    IF Hf OR Hcl THEN PRINT USING "#,6D.4D";V(Colm)
```

```
2940     NEXT Colm
2950     PRINT
2960     PRINT SPA(12);RPT$(" _______    ",Colum)
2970     PRINT LIN(1);"TOTAL     ";
2980     FOR Colm=1 TO Colum
2990       PRINT USING "#,6D.4D";Tot(Colm)
3000     NEXT Colm
3010     PRINT LIN(2)
3020     ! lllllllllllllllllllllllllllllll
3030 Forne4:     FOR Ne4=De TO Nemax+2
3040     IF Hcl OR Hf THEN Element$(Nemax+1)="O,OH,CL,F"
3050       PRINT USING "#,9A";Element$(Ne4)
3060       FOR Ano=Ij TO Ij+Noc-1
3070         IF Ano>J THEN Nextano
3080         PRINT USING "#,6D.4D";Elv(Ne4+Nemax,Ano)
3090 Nextano:NEXT Ano
3100         IF (Ne4=Nemax) OR (Ne4=Nemax+1) THEN PRINT LIN(1)
3110       PRINT
3120     NEXT Ne4
3130      IF Hcopy=11 THEN PRINT PAGE
3140   NEXT Ij
3150   Jf=J
3160   PRINTER IS 16
3170   RETURN
3180   !
3190   !       ****************** ERROR TRAPS ********************
3200   !
3210 Error: ! Check for errors 56,59,80,& 89
3220         BEEP
3230         IF ERRN=56 THEN E56
3240         IF ERRN=59 THEN E59
3250         IF ERRN=80 THEN E80
3260         IF ERRN=89 THEN E89
3270 Ex:     PRINT ERRM$
3280         BEEP
3290         PRINT "PROGRAM TERMINATED"
3300         BEEP
3310         STOP
3320 E56:    DISP "File not yet created. Try again."
3330         WAIT 3000
3340         GOTO Linpf
3350 E59:    PRINTER IS 16
3360         GOTO Ex
3370 E80:    DISP "Disc NOT in. Put it in then ";
3380         GOTO Ex1
3390 E89:    DISP "CHECK READ error. ";
3400         Try=Try+1
3410         IF Try>3 THEN E89a
3420         DISP "Try again ";
3430         GOTO Ex1
3440 E89a:   DISP "Try another tape ";
3450 Ex1:    BEEP
3460         DISP "press CONT"
3470         PAUSE
3480         RETURN
3490   !
3500   !            SUBROUTINE SETS
3510   !            ***************
3520   !
3530   !
```

```
3540  !      READS ANALYSES (a series of numbers may be read)
3550  !
3560 Sets: IF NOT Aj THEN PRINT LIN(2);"   NEXT ANALYSIS No.?";LIN(2);"OR first
and last of SERIES (separated by -)"
3570  IF NOT Aj THEN PRINT "OR CONT to STOP";LIN(1);"OR N to change file ?"
3580  Anal$=""
3590  BEEP
3600  INPUT "    ? ",Anal$
3610  IF Anal$="N" THEN Chf
3620  IF Anal$="" THEN RETURN
3630  Pos=POS(Anal$,"-")
3640  Aj=Aj+1
3650  Fa$(F,Aj)=Anal$
3660  IF Pos THEN Block
3670  I=VAL(Anal$)
3680  An=An+1
3690  GOSUB Reads
3700  GOSUB Ratios
3710  GOTO Sets
3720 Block: Start=VAL(Anal$[1,Pos-1])
3730  End=VAL(Anal$[Pos+1])
3740  IF Start>End THEN Backwards
3750  FOR I=Start TO End
3760    An=An+1
3770    GOSUB Reads
3780    GOSUB Ratios
3790  NEXT I
3800  OFF END #1
3810  OFF END #4
3820  Anal$=""
3830  GOTO Sets
3840 Backwards:DISP "FIRST NO. > SECOND NO.! - RE-ENTER!"
3850  BEEP
3860  WAIT 3000
3870  GOTO Sets
3880 Chf: ASSIGN #1 TO *
3890  ASSIGN #2 TO *
3900  FOR Nz=1 TO Nemax
3910      Lastitems$(Nz)=Item$(Nz)
3920  NEXT Nz
3930  Oldfile$=File$           !!!!!!!!!!!!!!!!!
3940  GOTO Linpf
3950  ! !
3960  !    READING ANALYSIS
3970  !
3980 Reads:  READ #1,I;Sample$(An),Mineral$(An),Value(*)        ! READ ANALYSIS
3990  Total=0
4000  De=1
4010  IF (Item$(1)="DEPTH") OR (Item$(1)="Depth") THEN De=2
4020  FOR Ne=De TO Nemax
4030    Elv(Ne,An)=Value(Ne)     !! ??????????????????????
4040    Total=Total+Value(Ne)
4050  NEXT Ne
4060  Elv(Ne,An)=Total  !!??
4070  RETURN
4080  !
4090  !      ******    AVERAGE OF SET OF ANALYSES   ******
4100  !
4110 Average:  N5=2+2*Nemax
4120  MAT Elvt=RSUM(Elv)
```

```
4130  FOR Neav=1 TO N5
4140    Elv(Neav,An+1)=Elvt(Neav)/An
4150  NEXT Neav
4160  Sample$(An+1)="  AVERAGE "
4170  Mineral$(An+1)="  of "&VAL$(An)
4180  RETURN
4190  !
4200  !          FINISH
4210  !
4220 Optout:  PRINT LIN(12),SPA(36),"          ",LIN(1),SPA(36)," THE END ",L
IN(1),SPA(36),"          "
4230  STOP
4240  END
```

N.B. This computer program is written in the 'enhanced' form of Basic used by Hewlett-Packard computers.

L